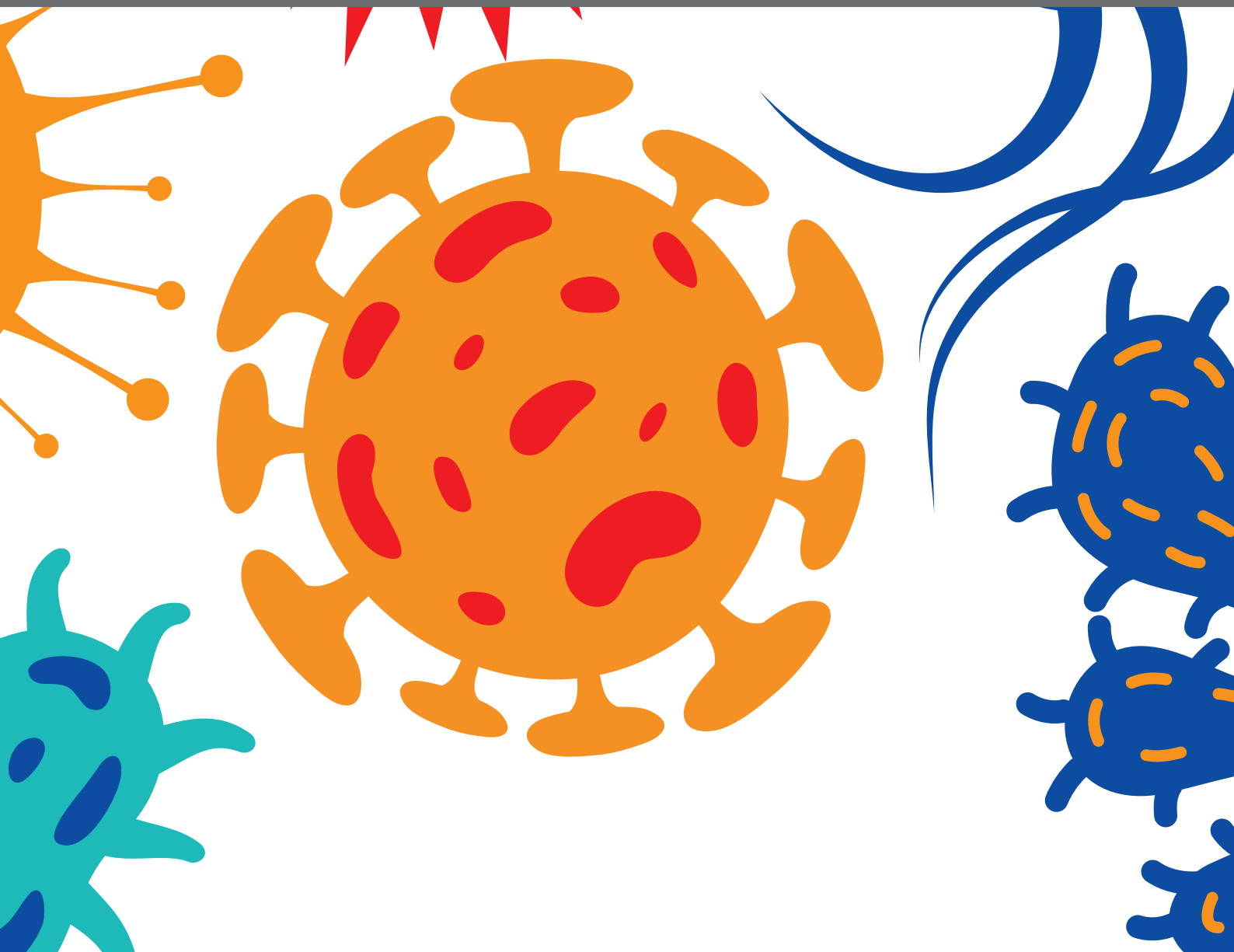




UNRAVELLING T. CRUZI BIOLOGY

EDITED BY: Nobuko Yoshida, Martin Craig Taylor and Noelia Lander
PUBLISHED IN: Frontiers in Cellular and Infection Microbiology





frontiers

Frontiers eBook Copyright Statement

The copyright in the text of individual articles in this eBook is the property of their respective authors or their respective institutions or funders. The copyright in graphics and images within each article may be subject to copyright of other parties. In both cases this is subject to a license granted to Frontiers.

The compilation of articles constituting this eBook is the property of Frontiers.

Each article within this eBook, and the eBook itself, are published under the most recent version of the Creative Commons CC-BY licence.

The version current at the date of publication of this eBook is CC-BY 4.0. If the CC-BY licence is updated, the licence granted by Frontiers is automatically updated to the new version.

When exercising any right under the CC-BY licence, Frontiers must be attributed as the original publisher of the article or eBook, as applicable.

Authors have the responsibility of ensuring that any graphics or other materials which are the property of others may be included in the CC-BY licence, but this should be checked before relying on the CC-BY licence to reproduce those materials. Any copyright notices relating to those materials must be complied with.

Copyright and source acknowledgement notices may not be removed and must be displayed in any copy, derivative work or partial copy which includes the elements in question.

All copyright, and all rights therein, are protected by national and international copyright laws. The above represents a summary only. For further information please read Frontiers' Conditions for Website Use and Copyright Statement, and the applicable CC-BY licence.

ISSN 1664-8714

ISBN 978-2-88966-013-1

DOI 10.3389/978-2-88966-013-1

About Frontiers

Frontiers is more than just an open-access publisher of scholarly articles: it is a pioneering approach to the world of academia, radically improving the way scholarly research is managed. The grand vision of Frontiers is a world where all people have an equal opportunity to seek, share and generate knowledge. Frontiers provides immediate and permanent online open access to all its publications, but this alone is not enough to realize our grand goals.

Frontiers Journal Series

The Frontiers Journal Series is a multi-tier and interdisciplinary set of open-access, online journals, promising a paradigm shift from the current review, selection and dissemination processes in academic publishing. All Frontiers journals are driven by researchers for researchers; therefore, they constitute a service to the scholarly community. At the same time, the Frontiers Journal Series operates on a revolutionary invention, the tiered publishing system, initially addressing specific communities of scholars, and gradually climbing up to broader public understanding, thus serving the interests of the lay society, too.

Dedication to Quality

Each Frontiers article is a landmark of the highest quality, thanks to genuinely collaborative interactions between authors and review editors, who include some of the world's best academicians. Research must be certified by peers before entering a stream of knowledge that may eventually reach the public - and shape society; therefore, Frontiers only applies the most rigorous and unbiased reviews.

Frontiers revolutionizes research publishing by freely delivering the most outstanding research, evaluated with no bias from both the academic and social point of view. By applying the most advanced information technologies, Frontiers is catapulting scholarly publishing into a new generation.

What are Frontiers Research Topics?

Frontiers Research Topics are very popular trademarks of the Frontiers Journals Series: they are collections of at least ten articles, all centered on a particular subject. With their unique mix of varied contributions from Original Research to Review Articles, Frontiers Research Topics unify the most influential researchers, the latest key findings and historical advances in a hot research area! Find out more on how to host your own Frontiers Research Topic or contribute to one as an author by contacting the Frontiers Editorial Office: researchtopics@frontiersin.org

UNRAVELLING T. CRUZI BIOLOGY

Topic Editors:

Nobuko Yoshida, Federal University of São Paulo, Brazil

Martin Craig Taylor, University of London, United Kingdom

Noelia Lander, University of Georgia, United States

Citation: Yoshida, N., Taylor, M. C., Lander, N., eds. (2020). Unravelling T. cruzi Biology. Lausanne: Frontiers Media SA. doi: 10.3389/978-2-88966-013-1

Table of Contents

- 05 Editorial: Unravelling *T. cruzi* Biology**
Martin Craig Taylor, Noelia Lander and Nobuko Yoshida
- 08 Echocardiographic Measurements in a Preclinical Model of Chronic Chagasic Cardiomyopathy in Dogs: Validation and Reproducibility**
Eduardo B. Carvalho, Isalira P. R. Ramos, Alvaro F. S. Nascimento, Guilherme V. Brasil, Debora B. Mello, Martin Oti, Michael Sammeth, Maria T. Bahia, Antonio C. Campos de Carvalho and Adriana B. Carvalho
- 16 Redox Balance Keepers and Possible Cell Functions Managed by Redox Homeostasis in *Trypanosoma cruzi***
Andrea C. Mesías, Nisha J. Garg and M. Paola Zago
- 36 An Evolutionary View of *Trypanosoma cruzi* Telomeres**
Jose Luis Ramirez
- 43 A Novel Calcium-Activated Potassium Channel Controls Membrane Potential and Intracellular pH in *Trypanosoma cruzi***
Patricia Barrera, Christopher Skorka, Michael Boktor, Noopur Dave and Veronica Jimenez
- 60 Identification and Localization of the First Known Proteins of the *Trypanosoma cruzi* Cytostome Cytopharynx Endocytic Complex**
Nathan Michael Chasen, Isabelle Coppens and Ronald Drew Etheridge
- 75 The Influence of Recombinational Processes to Induce Dormancy in *Trypanosoma cruzi***
Bruno Carvalho Resende, Anny Caroline Silva Oliveira, Anna Carolina Paganini Guañabens, Bruno Marçal Repolês, Verônica Santana, Priscila Mazzochi Hiraiwa, Sérgio Danilo Junho Pena, Glória Regina Franco, Andrea Mara Macedo, Erich Birelli Tahara, Stênio Perdigão Frago, Luciana Oliveira Andrade and Carlos Renato Machado
- 88 Structure, Properties, and Function of Glycosomes in *Trypanosoma cruzi***
Wilfredo Quiñones, Héctor Acosta, Camila Silva Gonçalves, Maria Cristina M. Motta, Melisa Gualdrón-López and Paul A. M. Michels
- 99 Landmarks of the Knowledge and *Trypanosoma cruzi* Biology in the Wild Environment**
Ana Maria Jansen, Samanta Cristina das Chagas Xavier and André Luiz R. Roque
- 114 Disruption of Intracellular Calcium Homeostasis as a Therapeutic Target Against *Trypanosoma cruzi***
Gustavo Benaim, Alberto E. Paniz-Mondolfi, Emilia Mia Sordillo and Nathalia Martinez-Sotillo
- 129 RNA Binding Proteins and Gene Expression Regulation in *Trypanosoma cruzi***
Bruno A. A. Romagnoli, Fabiola B. Holetz, Lysangela R. Alves and Samuel Goldenberg

- 146 ***The Influence of Environmental Cues on the Development of Trypanosoma cruzi in Triatominae Vector***
Raíssa de Fátima Pimentel Melo, Alessandra Aparecida Guarneri and Ariel Mariano Silber
- 155 ***A CRISPR/Cas9-riboswitch-Based Method for Downregulation of Gene Expression in Trypanosoma cruzi***
Noelia Lander, Teresa Cruz-Bustos and Roberto Docampo
- 165 ***Trypanosoma cruzi-Infected Human Macrophages Shed Proinflammatory Extracellular Vesicles That Enhance Host-Cell Invasion via Toll-Like Receptor 2***
André Cronemberger-Andrade, Patrícia Xander, Rodrigo Pedro Soares, Natália Lima Pessoa, Marco Antônio Campos, Cameron C. Ellis, Brian Grajeda, Yifat Ofir-Birin, Igor Correia Almeida, Neta Regev-Rudzki and Ana Claudia Torrecilhas
- 180 ***Trypanosoma brucei and Trypanosoma cruzi DNA Mismatch Repair Proteins Act Differently in the Response to DNA Damage Caused by Oxidative Stress***
Viviane Grazielle-Silva, Tehseen Fatima Zeb, Richard Burchmore, Carlos Renato Machado, Richard McCulloch and Santuza M. R. Teixeira
- 194 ***GCN2-Like Kinase Modulates Stress Granule Formation During Nutritional Stress in Trypanosoma cruzi***
Amaranta Muniz Malvezzi, Mirella Aricó, Normanda Souza-Melo, Gregory Pedroso dos Santos, Paula Bittencourt-Cunha, Fabiola Barbieri Holetz and Sergio Schenkman
- 209 ***Precision Health for Chagas Disease: Integrating Parasite and Host Factors to Predict Outcome of Infection and Response to Therapy***
Santiago J. Martinez, Patricia S. Romano and David M. Engman
- 220 ***Trypanosoma cruzi Promotes Transcriptomic Remodeling of the JAK/STAT Signaling and Cell Cycle Pathways in Myoblasts***
Lindice M. Nisimura, Laura L. Coelho, Tatiana G. de Melo, Paloma de Carvalho Vieira, Pedro H. Victorino, Luciana R. Garzoni, David C. Spray, Dumitru A. Iacobas, Sanda Iacobas, Herbert B. Tanowitz and Daniel Adesse



Editorial: Unravelling *T. cruzi* Biology

Martin Craig Taylor¹, Noelia Lander² and Nobuko Yoshida^{3*}

¹ Faculty of Infectious and Tropical Diseases, London School of Hygiene and Tropical Medicine, London, United Kingdom,

² Center for Tropical and Emerging Global Diseases, University of Georgia, Athens, GA, United States, ³ Departamento de Microbiologia, Imunologia e Parasitologia, Escola Paulista de Medicina, Universidade Federal de São Paulo, São Paulo, Brazil

Keywords: *Trypanosoma cruzi*, Chagas disease, parasite-host interaction, gene function, CRISPR/Cas9 technique

Editorial on the Research Topic

Unravelling *T. cruzi* Biology

Trypanosoma cruzi, a protozoan parasite that causes Chagas disease, affects an estimated 8 million people, mainly in Latin America, but also in many developed countries where the disease is not endemic. Options for drug treatment are limited and not fully effective, especially in the chronic phase of the disease. The genetic complexity of *T. cruzi*, with a number of gene families with hundreds of members and genes of unknown function, in addition to the absence of efficient techniques for genetic manipulation before the CRISPR era, have contributed to the slow progress in understanding the biology of this parasite. The aim of this Research Topic is to provide an overview of the current knowledge on diverse aspects of *T. cruzi* biology. We received contributions ranging from molecular and cellular approaches to evaluate gene function and analyze parasite organelles, to studies on parasite-host interactions, signal transduction during infection, alternative pathways for identification of new drug targets, pathology of Chagas disease in animal model and *T. cruzi* biology in the wild environment, as well as in different stages of the parasite's life cycle.

Several studies in this topic assessed *T. cruzi* gene functions using the CRISPR/Cas9 system. Using a CRISPR/Cas9-riboswitch-based method, Lander et al. succeeded in the downregulation at the mRNA level of genes encoding glycoprotein 72 (*TcGP72*) and vacuolar proton pyrophosphatase (*TcVP1*), as proof of concept. They found that *TcVP1* is not essential for the viability of epimastigotes or the infective stages of *T. cruzi*, although it is important for normal growth of epimastigotes in rich medium, and for trypomastigote invasion of host cells. Also using CRISPR/Cas9, Malvezzi et al. generated *T. cruzi* devoid of *TcK1*, an ortholog of the protein kinase named general control non-repressible 2 (*GCN2*) that phosphorylates the eukaryotic initiation factor 2 alpha subunit (*eIF2α*). Under starvation, *TcK1* depleted cells showed reduced accumulation of stress RNA granules, independently of *eIF2α* phosphorylation. In absence of *TcK1*, metacyclogenesis increased, but the trypomastigotes were less infective to mammalian host cells. Regarding *T. cruzi* structure, Chasen et al. used a combination of CRISPR/Cas9-mediated endogenous tagging, fluorescently labeled overexpression constructs and endocytic assays, to identify the first known cytosome-cytopharynx complex (SPC) targeted protein (CP1), which co-localizes with endocytosed protein and disassembles in infective forms of *T. cruzi*. Two additional proteins that target to SPC (CP2 and CP3) were also identified. In addition, they defined the location of a region adjacent to the SPC entrance, known as the pre-oral ridge (POR), which lies between the entrance of the flagellar pocket and the cytosome. CRISPR/Cas9 technology was also used by Grazielle-Silva et al. to investigate the involvement of DNA mismatch repair (MMR) component MSH6 in the oxidative stress response in *T. cruzi*, by generating MSH6 null mutants. The loss of one or two alleles of *T. cruzi msh6* resulted in increased susceptibility to H₂O₂ exposure, besides impaired MMR. They confirmed that MSH2 associated with MSH6 is a central component of the MMR pathway responsible for the recognition and correction of base mismatches that occur during DNA replication and recombination. In their review on RNA binding proteins (RBPs)

OPEN ACCESS

Edited and reviewed by:

Jeroen P. J. Saeij,
University of California, Davis,
United States

*Correspondence:

Nobuko Yoshida
nyoshida@unifesp.br

Specialty section:

This article was submitted to
Parasite and Host,
a section of the journal
Frontiers in Cellular and Infection
Microbiology

Received: 01 June 2020

Accepted: 22 June 2020

Published: 28 July 2020

Citation:

Taylor MC, Lander N and Yoshida N
(2020) Editorial: Unravelling
T. cruzi Biology.
Front. Cell. Infect. Microbiol. 10:382.
doi: 10.3389/fcimb.2020.00382

and gene expression regulation in *T. cruzi*. Romagnoli et al. also presented data on downregulation of three RBPs, by using the CRISPR/Cas9 technique. RBP silencing affected cell division. References were made to the characterization of messenger ribonucleoprotein (mRNP) particles, which can be organized into larger complexes forming stress RNA granules, depending on RBPs. They suggest that protein composition of the mRNPs as well as the localization and fate of mRNAs, and consequently of the genes expressed, depend on RBPs, which allow the coordinated expression of mRNAs encoding proteins that are related in function, resulting in the formation of post-transcriptional operons. All of these studies highlight the impact that CRISPR/Cas9 technology has had on *T. cruzi* research.

Ramirez discussed the co-evolution of telomeres, subtelomeres, and the trans-sialidase type II (TSII) family, and the role that these regions may have played in shaping *T. cruzi*'s genome. It is suggested that these regions, together with retrotransposon elements, promote the generation of genetic variability, and that members of the TS II family positioned at the subtelomeres co-evolved to be part of the transition to the telomeric repeat. This review also proposed that double strand breaks introduced in the subtelomeres by retrotransposon nucleases are repaired by homologous recombination, and when the repair includes non-homologous chromatids there is a possibility to generate gene variants.

To survive the inimical conditions *T. cruzi* encounters in the insect vector and the mammalian host, the parasite has to adapt to distinct microenvironments, where nutrient availability, osmolarity, ionic concentrations, and pH vary significantly. Mesías et al. reviewed the current knowledge of the oxidant environment experienced by *T. cruzi* in the insect and mammalian hosts, and the molecular strategies exploited by the parasite to deal with oxidative stress. *T. cruzi* utilizes a network of antioxidant enzymes to control the cytotoxic effects of reactive oxygen species (ROS) and reactive nitrogen species (RNS) to which they are exposed in the triatomine and the mammalian hosts. In their review, Melo et al. discussed how environmental factors, such as temperature, availability of nutrients and consequent oxidative and osmotic stresses may alter *T. cruzi* development in the triatomine insect. Replication of epimastigotes and differentiation into metacyclic trypomastigotes are affected by these factors. Another study in this Research Topic investigated *T. cruzi* adaptation to different environments. Barrera et al. aimed at characterizing an ion channel that plays a critical role in parasite survival. They identified and characterized the expression pattern and function of a novel calcium-activated potassium channel (TcCAKC), which resides in the plasma membrane of all three life stages of *T. cruzi*. They generated TcCAKC null parasites, which showed impaired growth, decreased production of trypomastigotes and slower intracellular replication. Epimastigotes lacking the channel had significantly lower cytosolic calcium, hyperpolarization, changes in intracellular pH, and increased proton extrusion rate.

Trypanosoma cruzi infection may induce the inflammatory process that ultimately lead to myocardiopathy. Extracellular vesicles (EVs) shed by trypomastigote forms of *T. cruzi* could

be involved in promoting inflammation. Cronemberger-Andrade et al. have found that *T. cruzi*-infected macrophages shed EVs that interact with Toll-like-receptor 2 (TLR2) and stimulate the translocation of NF- κ B, inducing expression of proinflammatory cytokines (TNF- α , IL-6, and IL-1 β), and STAT-1 and STAT-3 signaling pathways. In addition, EVs from parasites or from *T. cruzi*-infected macrophages enhanced host cell invasion. Nisimura et al. re-analyzed previous microarray dataset from four different *T. cruzi* strains, in order to better understand the transcriptomic impact that each strain has on JAK-STAT signaling and cell cycle pathways. They reported that *T. cruzi* strains differentially alter the expression of JAK-STAT signaling, whose activation may lead to muscle cell hypertrophy, and distinctly modulate cell cycle pathways.

Identification of targets for new drugs to treat Chagas disease is an important issue. Moreover, the ability of *T. cruzi* to establish dormancy associated with resistance to drug treatment has been recently reported. Using different *T. cruzi* DTUs during their replicative epimastigote and amastigote stages, Resende et al. investigated the influence of recombinational processes to induce dormancy in *T. cruzi*. For both epimastigote and amastigote forms, the number of dormant cells was higher in hybrid than in non-hybrid strains. Treatment of *T. cruzi* with gamma radiation, which generates DNA lesions repaired by homologous recombination, resulted in increased percentage of dormancy. In parasites harboring single knockout for RAD51, there was a significant reduction in the number of dormant cells. Altogether, these data suggest the existence of an adaptive difference among *T. cruzi* strains to generate dormant cells, and that homologous recombination could be important for dormancy in this parasite.

Potential therapeutic targets for treatment of *T. cruzi* infection have been identified by exploiting the differences between the mechanisms involved in intracellular Ca²⁺ signaling in humans and trypanosomatids. Benaïm et al. reviewed data that support targeting Ca²⁺ homeostasis as a strategy against Chagas disease by giving examples of reported drugs with trypanocidal effects. In another review, Quiñones et al. discussed the potential of glycosomal enzymes, which are essential for the trypanosomatid viability, as drug targets. Biochemical and proteomic analysis of glycosomes have revealed the integration of glycosomes in overall *T. cruzi* metabolism. In these authors' view, the differences in human and trypanosomatid proteins make a variety of glycosomal enzymes promising drug targets. It is also referred that selective, potent inhibitors of some glycosomal proteins have been demonstrated to interfere with metabolic processes.

Carvalho et al. conducted a robust echocardiographic evaluation of left ventricular (LV) function in dogs chronically infected with *T. cruzi*. Parameters analyzed included end-systolic volume (ESV), end-diastolic volume (EDV), ejection fraction (EF), and fractional shortening (FS). A significant LVEF and FS reduction was observed in infected animals compared to controls. The authors concluded that the canine model of chronic chagasic cardiomyopathy (CCC) mimics human disease, reproducing the percentage of individuals that develop heart failure during the chronic infection.

In an integrative review, Martinez et al. discussed the current state of diagnosis and prognosis of Chagas disease, the treatment

for the disease, approaches to improve treatment, as well as host factors and parasite susceptibility and resistance to drug. Prediction of disease outcome and determining whether and when treatment of infection may be necessary, still remains as a prospect to be fulfilled.

T. cruzi is primarily a parasite of wild mammals. Jansen et al. reviewed *T. cruzi* biology in the natural environment. They discussed among other topics: *T. cruzi* genotypes and ecology, transmission in nature, *T. cruzi* biology in opossums, mixed infections and the recent outbreaks of acute Chagas disease by oral infection.

Overall, this Research Topic brings together an important collection of articles focused on fundamental aspects of *T. cruzi* biology, using state-of-the-art technology to elucidate the function of proteins and the metabolic pathways to which they belong; as well as reviewing the current literature involving the main features of the parasite that causes Chagas disease.

AUTHOR CONTRIBUTIONS

All authors listed have made a substantial, direct and intellectual contribution to the work, and approved it for publication.

ACKNOWLEDGMENTS

We thank all the contributors of this Research Topic.

Conflict of Interest: The authors declare that the research was conducted in the absence of any commercial or financial relationships that could be construed as a potential conflict of interest.

Copyright © 2020 Taylor, Lander and Yoshida. This is an open-access article distributed under the terms of the Creative Commons Attribution License (CC BY). The use, distribution or reproduction in other forums is permitted, provided the original author(s) and the copyright owner(s) are credited and that the original publication in this journal is cited, in accordance with accepted academic practice. No use, distribution or reproduction is permitted which does not comply with these terms.



Echocardiographic Measurements in a Preclinical Model of Chronic Chagasic Cardiomyopathy in Dogs: Validation and Reproducibility

OPEN ACCESS

Edited by:

Nobuko Yoshida,
Federal University of São Paulo, Brazil

Reviewed by:

Veronica Jimenez,
California State University, Fullerton,
United States
Paulo Marcos Matta Guedes,
Federal University of Rio Grande do
Norte, Brazil

*Correspondence:

Adriana B. Carvalho
carvalhoab@biof.ufrj.br

[†]These authors have contributed
equally to this work

Specialty section:

This article was submitted to
Parasite and Host,
a section of the journal
Frontiers in Cellular and Infection
Microbiology

Received: 01 July 2019

Accepted: 10 September 2019

Published: 24 September 2019

Citation:

Carvalho EB, Ramos IPR,
Nascimento AFS, Brasil GV, Mello DB,
Oti M, Sammeth M, Bahia MT,
Campos de Carvalho AC and
Carvalho AB (2019)
Echocardiographic Measurements in a
Preclinical Model of Chronic Chagasic
Cardiomyopathy in Dogs: Validation
and Reproducibility.
Front. Cell. Infect. Microbiol. 9:332.
doi: 10.3389/fcimb.2019.00332

Eduardo B. Carvalho^{1†}, **Isalira P. R. Ramos**^{2†}, **Alvaro F. S. Nascimento**³,
Guilherme V. Brasil¹, **Debora B. Mello**², **Martin Oti**¹, **Michael Sammeth**¹, **Maria T. Bahia**³,
Antonio C. Campos de Carvalho^{1,2,4} and **Adriana B. Carvalho**^{1,2,4*}

¹ Carlos Chagas Filho Institute of Biophysics, Federal University of Rio de Janeiro, Rio de Janeiro, Brazil, ² National Center for Structural Biology and Bioimaging, Federal University of Rio de Janeiro, Rio de Janeiro, Brazil, ³ School of Medicine, Federal University of Ouro Preto, Ouro Preto, Brazil, ⁴ National Institute for Science and Technology in Regenerative Medicine, Federal University of Rio de Janeiro, Rio de Janeiro, Brazil

Background: The failure to translate preclinical results to the clinical setting is the rule, not the exception. One reason that is frequently overlooked is whether the animal model reproduces distinctive features of human disease. Another is the reproducibility of the method used to measure treatment effects in preclinical studies. Left ventricular (LV) function improvement is the most common endpoint in preclinical cardiovascular disease studies, while echocardiography is the most frequently used method to evaluate LV function. In this work, we conducted a robust echocardiographic evaluation of LV size and function in dogs chronically infected by *Trypanosoma cruzi*.

Methods and Results: Echocardiography was performed blindly by two distinct observers in mongrel dogs before and between 6 and 9 months post infection. Parameters analyzed included end-systolic volume (ESV), end-diastolic volume (EDV), ejection fraction (EF), and fractional shortening (FS). We observed a significant LVEF and FS reduction in infected animals compared to controls, with no significant variation in volumes. However, the effect of chronic infection in systolic function was quite variable, with EF ranging from 17 to 66%. Using the cut-off value of $EF \leq 40\%$, established for dilated cardiomyopathy (DCM) in dogs, only 28% of the infected dogs were affected by the chronic infection.

Conclusions: The canine model of CCC mimics human disease, reproducing the percentage of individuals that develop heart failure during the chronic infection. It is thus mandatory to establish inclusion criteria in the experimental design of canine preclinical studies to account for the variable effect that chronic infection has on systolic function.

Keywords: Chagas disease, chagasic cardiomyopathy, canine model, dogs, systolic dysfunction

INTRODUCTION

Chagas disease is caused by the protozoan parasite *Trypanosoma cruzi*. This parasite can be transmitted to humans, domestic, or wild mammals and the infection is very difficult to cure. It is endemic in Latin America and has been spreading to non-endemic regions due to the migration of infected individuals. The estimated number of infected immigrants is over 300,000 in the United States and 80,000 in Europe (Rassi et al., 2010; Steverding, 2014). The classic mode of transmission involves *Triatomine* insects known as kissing bugs, but several other modes exist, such as blood transfusions, congenital, solid organ or bone marrow transplantation, and food-borne. After an acute phase characterized by non-specific symptoms, patients enter the chronic phase and can remain asymptomatic for the rest of their lives. However, ~30% of infected individuals will develop chronic chagasic cardiomyopathy (CCC), which is characterized by episodes of sudden cardiac death (SCD) due to complex ventricular arrhythmias, cardiac dilation and heart failure (HF). Survival is highly dependent on New York Heart Association (NYHA) functional class and on the presence of systolic dysfunction: 5-year mortality is over 80% in class III–IV patients (Rassi et al., 2006). The reason why only a subset of patients develop CCC remains unknown.

Current treatment recommendations for HF due to Chagas disease are identical to the ones given for other causes of HF (Rassi et al., 2006; de Andrade et al., 2011). Cardiac transplantation is further complicated in these patients by the possibility of parasite reactivation caused by immunosuppression. Large clinical trials have been conducted to investigate the efficacy of antiparasitic drugs (Rassi et al., 2006; de Andrade et al., 2011; Morillo et al., 2015) and cell therapy (dos Santos et al., 2012) for the treatment of CCC. Despite the evidence of beneficial effects available from small animal models (Garcia et al., 2005; Guarita-Souza, 2006; Goldenberg et al., 2008; Soares et al., 2011), both treatments were ineffective in human trials. The failure to translate preclinical results to the clinical setting is not new and the reasons are many, ranging from poor training in experimental design to the difficulty in publishing negative data (Collins and Tabak, 2014). However, one reason that is frequently overlooked is whether the animal model reproduces distinctive clinical and pathological features of human disease (Houser et al., 2012). Unfortunately, this is a major issue in rodent models of Chagas disease. Even though mice and rats usually respond to *T. cruzi* infection with cardiac inflammation and fibrosis, which are important hallmarks of CCC, they do not develop left ventricular dysfunction (Goldenberg et al., 2008; Soares et al., 2011; Jasmin et al., 2014; Mello et al., 2015). On the other hand, improvement of left ventricular function is commonly used as the primary endpoint in clinical trials of cardiac diseases. Therefore, in order to test the efficacy of alternative therapies for CCC, we need to find an animal model that reproduces this critical feature of human disease.

Dogs chronically infected by *T. cruzi* present cardiac inflammation, fibrosis, electrocardiographic alterations, and autoantibody production (de Lana et al., 1992; Guedes et al.,

2009; Caldas et al., 2013; Daliry et al., 2014), which are all important characteristics of human CCC. However, data on left ventricular dysfunction are not robust. The literature reports a total of 16 dogs that were chronically infected by *T. cruzi* and had their cardiac function evaluated by echocardiography (Pascon et al., 2010; Sousa et al., 2011; Santos et al., 2012). The number of animals is too small to draw conclusions on this model's potential to reproduce human systolic dysfunction, a matter further aggravated by the large variance in ejection fraction (EF) reported in these publications. Nonetheless, the canine model is promising because dogs can naturally develop a form of dilated cardiomyopathy (DCM) that bears resemblance with human disease, including severe systolic dysfunction (Dukes-McEwan et al., 2003; Wess et al., 2017). We hypothesize the same could be true for CCC. Therefore, the objective of this work was to conduct a robust echocardiographic evaluation of left ventricular size and function in dogs chronically infected by *T. cruzi*.

MATERIALS AND METHODS

A more detailed version of these methods can be found in the **Supplementary Material**.

Animals and Infection

Four month-old mongrel dogs ($n = 78$) were submitted to intraperitoneal inoculation of the VL-10 strain of *Trypanosoma cruzi* (discrete typing unit TcII isolated from human hosts in the State of Minas Gerais, Brazil) at a dose of 2,000 trypomastigotes/kg (Caldas et al., 2013, 2017). The VL-10 *T. cruzi* strain induces progressive heart fibrosis in dogs correlated with electrocardiographic alterations similar to those detected in humans (Caldas et al., 2013). Ten age-matched dogs were used as non-infected controls. Animals were fed commercial dog food and water *ad libitum*. All experiments were performed in conformity with the guidelines of the National Council for the Control of Animal Experimentation (Brazil) and the National Institutes of Health guide for the care and use of Laboratory animals (NIH Publications No. 8023, revised 1978). This study was approved by the local Committee on the Ethics of Animal Use of the Federal University of Ouro Preto under numbers 2012/18 and 2015/48.

Parasitemia was verified from the 10th day post infection by fresh blood examination in samples collected from the marginal ear vein. Additionally, anti-*T. cruzi* IgG antibodies were quantified in serum samples before, 30 and 180 days after *T. cruzi* infection by ELISA, as previously reported (Guedes et al., 2002).

Echocardiography

Images were acquired before infection and between 6 and 9 months post infection. Dogs were anesthetized with intravenous sodium thiopental (15 mg/kg) and the precordial area was shaved. Data were collected with Esaote MyLab™30 Gold Cardiovascular or GE Healthcare Vivid i echocardiography equipment and analyzed with EchoPAC PC version 112 software. Images were measured independently by two blinded examiners. Left ventricular EF, end-systolic volume (ESV), and

end-diastolic volume (EDV) were determined using the area-length (or bullet) method in two-dimensional mode images. Volumes were indexed by body surface area (BSA). Left ventricular fractional shortening (FS) was also determined in two-dimensional images.

Statistics

Statistical analyses were conducted using R version 3.5.2 (R Core Team, 2017) with RStudio version 1.1.463 (RStudio Team, 2016) as a visual interface. Raw data, R packages and code used for analyses are provided in **Supplementary Material**. Correlation and level of agreement between echocardiographic measurements were determined by intraclass correlation coefficients (ICC) and Bland-Altman analysis (Giavarina, 2015), respectively. Interobserver reproducibility was determined by calculating percent differences between examiners (absolute difference between 2 measurements from the same image, divided by the mean of the 2 measurements). Volumes and systolic function were compared using Two-way ANOVA followed by Tukey's post-test to correct for multiple comparisons. Data were considered statistically significant if *p*-value was below 0.05.

RESULTS AND DISCUSSION

Mortality of Experimental *T. cruzi* Infection in Dogs

All infected animals had trypomastigotes upon fresh blood examination between 10 and 20 days after inoculation. Accordingly, *T. cruzi*-specific IgG antibodies were detected in serum samples obtained from all infected dogs, remaining at high levels during the follow-up period (**Supplementary Figure 1a**).

Out of 78 dogs initially infected for this study, 25 animals died during the acute phase of infection, resulting in a mortality rate of 32%. The time period in which the animal deaths occurred varied from 1 to 6 months post infection (median 3, 1st Q 2.5, 3rd Q 5.5). Seven animals were excluded: 4 due to aggressive behavior, 2 in which the "post infection" echocardiographic exam was not conducted, and 1 was found to be pregnant after the study was initiated. The remaining 46 infected animals were used in this study (**Supplementary Figure 1b**). The observed mortality rate was much higher than expected for the acute phase of Chagas disease transmitted by insect vectors in humans, in which 0.25% of infected individuals die of severe myocarditis or meningoencephalitis (Rassi et al., 2010). However, mortality is dependent on transmission routes. For instance, food-borne transmission is reported to be more severe and to have mortality rates up to 35% in humans (Rassi et al., 2010). This is also the case in rodent animal models (Barreto-de-Albuquerque et al., 2015). In addition, mortality correlates to the dose of trypomastigotes administered at infection (Borges et al., 2013) and VL-10 strain is known to be aggressive and unresponsive to antiparasitic drugs even during the acute phase (Caldas et al., 2008, 2017), further contributing to the mortality observed in our dogs. The reason for using such an aggressive strain was to maximize cardiac tissue damage, as previous work by our group has shown that a smaller inoculum (<2,000

trypomastigotes/kg) or other inoculation routes would result in less tissue damage (Bahia et al., 2002).

Alterations of Left Ventricular Size and Function in Canine Chronic Chagasic Cardiomyopathy

Our approach to minimize echocardiographic variability was to average the data analyzed by both examiners before comparing non-infected controls to *T. cruzi*-infected animals. Descriptive statistics are shown in **Table 1**.

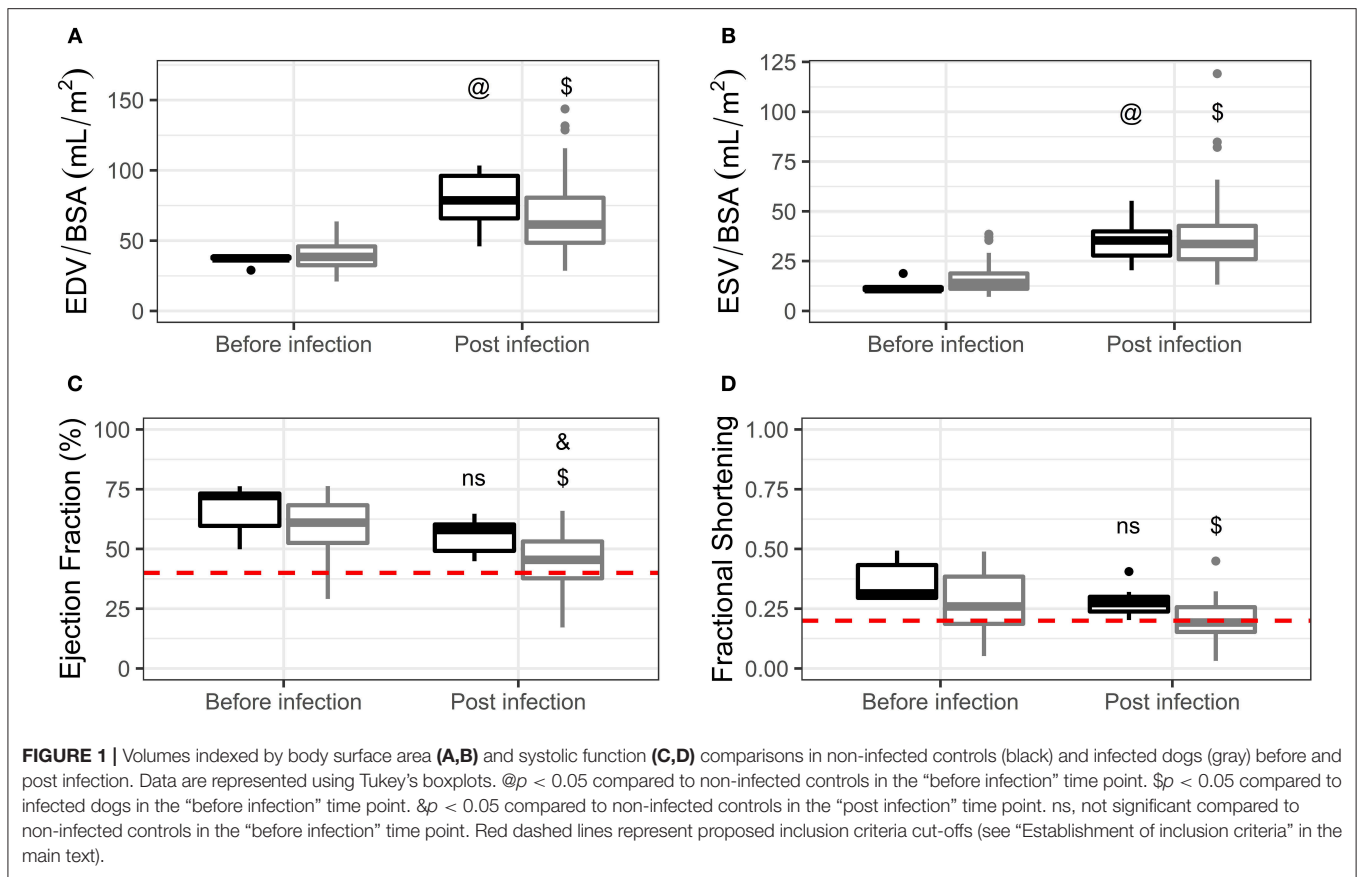
No differences were found between experimental groups in the before infection time point in EDV, ESV, EF, or FS (**Figures 1A–D**, respectively). Both groups, infected and non-infected, exhibited a significant increase in EDV and ESV when compared to baseline, even after indexing for BSA. No differences were present in EDV (**Figure 1A**) or ESV (**Figure 1B**) when comparing infected and non-infected dogs in the post infection time point. On the other hand, infected animals exhibited a significant decrease in EF when compared to baseline and to non-infected controls in the post infection time point (**Figure 1C**). Non-infected dogs did not show a significant decrease in EF when compared to baseline. FS was significantly decreased in infected dogs when compared to baseline, although no differences were present between this group and non-infected controls in the post infection time point (**Figure 1D**).

Even though we observed an overall EF reduction in infected animals, it is important to note that EF values ranged from 17.14 to 65.95% (**Table 1**). Therefore, the effect of chronic *T. cruzi* infection in systolic function can be quite diverse in dogs, varying from normal to severe dysfunction. Although this may be interpreted as a weakness of the model, one needs to remember that the same is observed in humans. Some patients remain

TABLE 1 | Descriptive statistics for volumes and systolic function.

Parameter	Group	Time point	Min	1st Q	Median	Mean	3rd Q	Max
EDV*	NI	BI	29.02	37.28	37.44	36.32	38.57	39.32
		PI	45.89	65.86	78.69	78.21	69.13	103.39
	Inf	BI	20.95	32.51	38.45	39.50	45.91	63.64
		PI	28.57	48.47	61.45	67.44	80.57	143.72
ESV*	NI	BI	9.07	10.47	10.96	12.23	11.83	18.83
		PI	20.42	27.83	35.41	34.95	39.93	55.30
	Inf	BI	7.04	11.10	14.09	16.35	18.85	38.53
		PI	13.20	25.99	33.64	37.56	42.76	119.17
EF	NI	BI	49.88	59.67	72.14	66.22	73.19	76.22
		PI	44.88	49.22	57.94	55.30	60.28	64.70
	Inf	BI	29.07	52.52	61.05	58.96	68.28	76.27
		PI	17.14	37.71	45.48	45.11	53.12	65.95
FS	NI	BI	0.291	0.295	0.314	0.365	0.433	0.493
		PI	0.202	0.238	0.273	0.277	0.300	0.405
	Inf	BI	0.051	0.186	0.259	0.277	0.384	0.488
		PI	0.031	0.152	0.192	0.202	0.256	0.449

*Corrected for body surface area. PI, post infection; BI, before infection; Inf, infected; NI, non-infected.



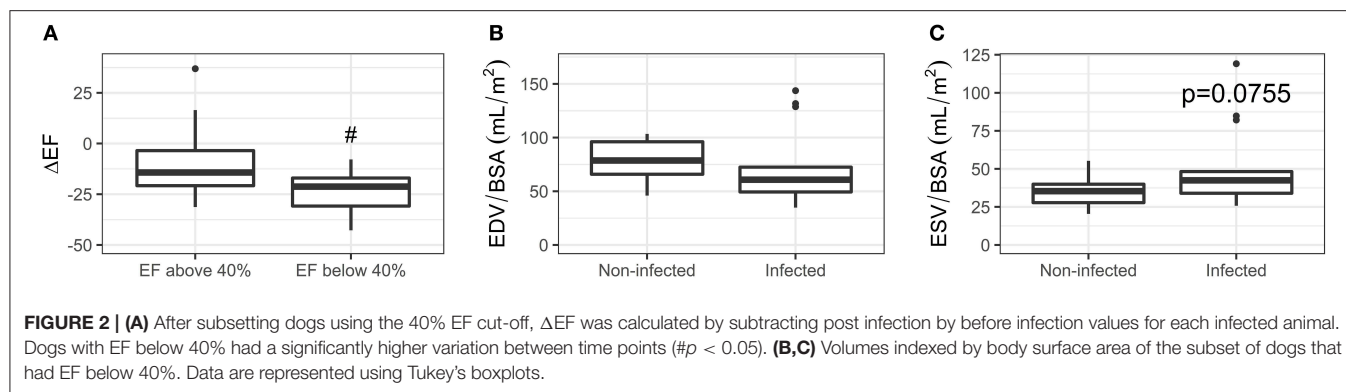
asymptomatic for the rest of their lives while, for unknown reasons, ~30% develop CCC. In this context, one of the proposed criteria for the diagnosis of canine idiopathic DCM uses the EF cut-off value of 40% (Dukes-McEwan et al., 2003). Applying this cut-off to our data, CCC would be present in 28.2% of the infected dogs, which is very similar to the proportion of patients that develop the disease. Importantly, this subset of dogs had a significantly higher reduction in EF ($\Delta EF = EF \text{ post infection} - EF \text{ before infection}$) when compared to dogs that fall above the cut-off (**Figure 2A**). In addition, reference values (mean \pm 2 SD) for our 10 age-matched non-infected dogs range from 41.01 to 69.57%, further supporting the 40% EF cut-off. Finally, this number falls well within the established criteria for cardiac dysfunction in humans (Lang et al., 2015) and children (Lopez et al., 2010).

FS has a much more robust dataset available for dogs in the literature. A meta-analysis of 1,152 normal adult animals (including 22 different breeds and mongrels) reports FS of 0.34 ± 0.051 (Hall et al., 2008). Assuming a normal distribution, reference values (mean \pm 2 SD) would range from 0.238 to 0.442. Our subset of dogs with EF below 40% also falls below the FS 0.238 cut-off, with values ranging from 0.031 to 0.194.

Cardiac dilation is another important aspect of CCC. We observed an increase in EDV comparing 4 month-old (before infection) to 10–13 month-old (post infection) dogs, even after indexing for BSA. Since, this is observed in both non-infected

and infected animals, we believe it is due to a larger physiological growth rate of the heart in relation to the body in pups transitioning to adulthood (Northup et al., 1957). Moreover, volumes can be lower in pups due to the higher heart rates at this age (Bayón et al., 1994). Therefore, comparisons between non-infected controls and infected dogs in the post infection time point (when all dogs are adults) are more valuable to evaluate cardiac dilation in our model.

Chronic infection did not lead to overall cardiac dilation in adult dogs (**Figure 1A**). One could expect that our animals with EF below 40% would have higher EDV and/or ESV values. However, there were no differences between this subset of infected dogs in comparison to non-infected controls (**Figures 2B,C**), although we did observe a borderline p -value for ESV (0.0755). Severe cardiomegaly and systolic dysfunction tend to co-exist in stage 4 chagasic cardiomyopathy patients (Rassi et al., 2010). Nevertheless, this does not happen in earlier stages, especially stage 3, in which patients can present diffuse LV wall motion abnormalities but only mild to moderate cardiomegaly (Rassi et al., 2010). In fact, cardiac dilation and systolic dysfunction are considered independent risk factors in the prognostic evaluation of CCC (Rassi et al., 2006), underscoring the heterogeneous presentation of the disease. Thus, the presence of systolic dysfunction but not overt cardiac dilation in our model is compatible with the clinical characteristics described for stage 3 CCC.



Reproducibility of Echocardiography in Canine Chronic Chagasic Cardiomyopathy

LV function improvement is the most common endpoint in cardiovascular disease studies, while echocardiography is the most frequently used method to evaluate LV function (Lang et al., 2015). Therefore, reproducibility is crucial not only in clinical trials but also in preclinical studies to increase the likelihood that treatment effects are translatable to the clinical setting. Unfortunately, this type of analysis is rare in preclinical models and there are no studies in the literature investigating echocardiographic reproducibility in dogs. For this reason, we compared our data to the human pediatric population, which is more similar to dogs at least in weight, size, and heart rate. Moreover, our dogs were infected at a young age, thus, the effects of physiological growth must be taken into consideration, as in children.

Echocardiographic images were independently measured by two blinded examiners. ICC and Bland-Altman analyses for long axis length (Supplementary Figures 2a–d), short axis area (Supplementary Figures 2e–h), and short axis length (Supplementary Figures 2i–l) in systole and diastole were conducted. We observed a high correlation ($0.85 < \text{ICC} < 0.97$, Supplementary Table 1 and Supplementary Figure 3a) between examiners for all measurements. Bland-Altman plots show an average difference between examiners below 0.21 mm for length and 0.45 mm^2 for area (Supplementary Table 1 and Supplementary Figure 3b).

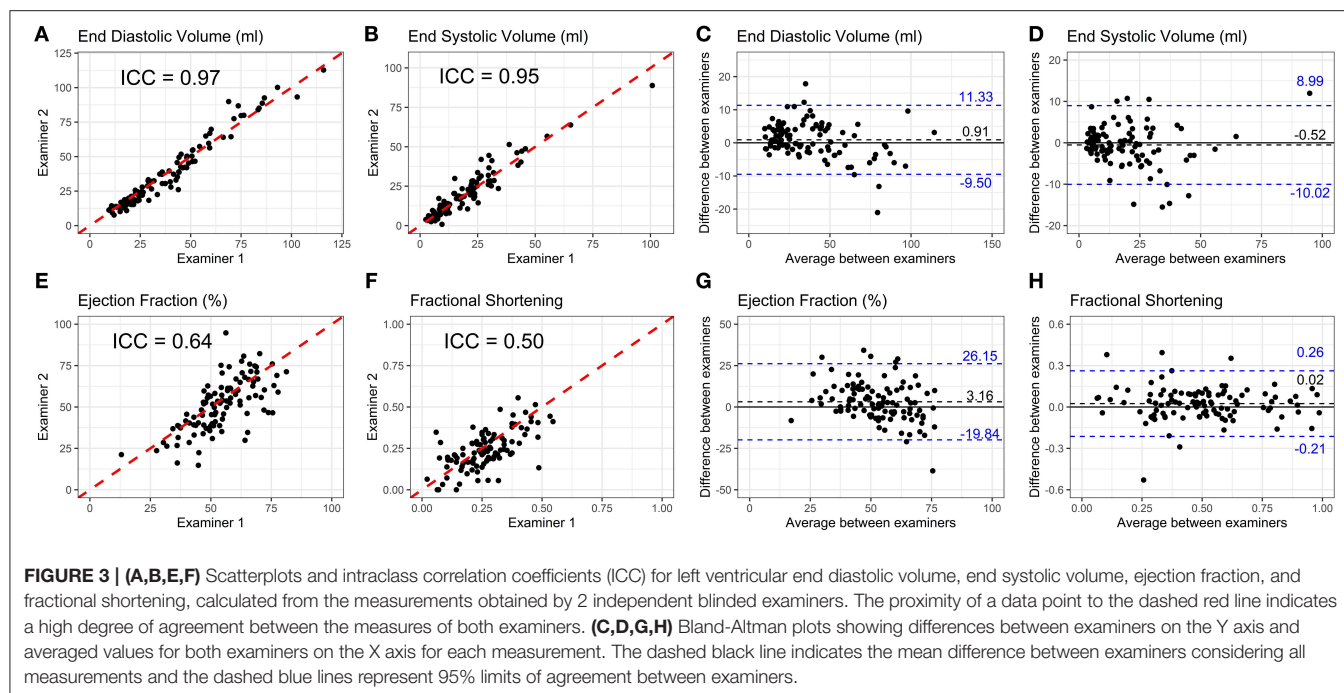
The ventricular volume variability (VVV) study from the Pediatric Heart Network reported mean percent differences between examiners for length measurements between 5 and 7% (Colan et al., 2012). In our case, this range was from 6 to 11% (Supplementary Table 1 and Supplementary Figure 3c). Anatomic differences between dogs and humans might account for this small increase in variability: the larger antero-posterior thoracic diameter in dogs makes it more challenging to obtain high quality echocardiographic images. Area measurements had mean percent differences between 11 and 19% (Supplementary Table 1 and Supplementary Figure 3c), higher than the differences in length. This was also observed in the pediatric population (Selamet Tierney et al., 2017).

ICC and Bland-Altman plots for volume extrapolations using the area-length method are illustrated in Figure 3. This method was chosen because it has been demonstrated to have higher reproducibility in children (Margossian et al., 2015). There was a high correlation and low mean difference between examiners for EDV (ICC = 0.97, difference = 0.93 mL, Figures 3A,C) and ESV (ICC = 0.95, difference = -0.49 mL, Figures 3B,D). EF had lower correlation between examiners (ICC = 0.64, Figure 3E), while the mean difference was higher (3.16, Figure 3G). Variability between examiners in ejection fraction estimations is a known issue in echocardiography (Cantinotti and Koestenberger, 2017). The VVV study reported that, together with slopes, variables that are extrapolated from direct measurements have the highest percent differences among 119 echocardiography variables examined (Colan et al., 2012). If calculated from 2 measures, as is the case for volumes, the interobserver mean percent difference was 13.6%. If calculated from 4 measures, the case of ejection fraction, the interobserver mean percent difference was 22.2%. In another study, the Pediatric Heart Network reported mean percent differences between examiners for EDV and EF to be 10.3 and 12.8%, respectively (Selamet Tierney et al., 2017). Data for ESV were not available. In our study, mean percent differences for EDV and EF were 12.79 and 18.47%, respectively (Supplementary Table 1 and Supplementary Figure 3c), within the range of values reported for the pediatric population.

FS had lower correlation (ICC = 0.50, Figure 3F) and higher mean percent difference (26.3%, Supplementary Table 1 and Supplementary Figure 3c) than EF, but we kept this parameter in our study because it is the most frequently used for the evaluation of cardiac function in dogs.

The Need for Establishment of Inclusion Criteria

Given the results reported above, we consider that our canine model of CCC is a viable option for preclinical testing of new therapies. However, if the endpoint involves improvement of systolic function, inclusion criteria are mandatory. We propose that the cut-off value of 40% EF be used to include animals in treatment groups (red dashed line in Figure 1C). This cut-off value is also a major criteria for the diagnosis of idiopathic DCM



proposed by the European Society of Veterinary Cardiology (Dukes-McEwan et al., 2003). Dogs with EF between 40 and 50% might be used as a separate group to evaluate treatment effects in a mild systolic dysfunction scenario. The use of EF is recommended over FS due to the lower interobserver variability. If only FS is available, the 0.238 value might be adopted based on the robust metaanalysis published by Hall (Hall et al., 2008). But we advise caution in this case since such a cut-off would lead to the inclusion of 63% of our infected animals. FS values below 0.25 may be considered abnormally low. However, this is highly breed specific. We suggest the more stringent value of 0.20 (red dashed line in **Figure 1D**), in agreement with the value recommended by the canine idiopathic DCM guidelines (Dukes-McEwan et al., 2003). The use of EF is also recommended over volumes, especially if dogs are to be infected at a young age.

Limitations

The inclusion criteria proposed create operational concerns for the model. If only ~30% of infected animals are included, there will be considerable increases in cost and space requirements to reach a sufficient number of animals for preclinical testing, but studies will gain translational robustness. Echocardiography interobserver variability, another limitation, could still be reduced using multibeat averages as opposed to single beat measurements (Colan et al., 2012). Reducing variability can impact sample size requirements and improve the cost and space concerns raised above. Finally, we cannot rule out that longer periods of observation of chronic infection could increase the proportion of dogs with systolic dysfunction. Further studies need to be conducted to address this possibility.

CONCLUSIONS

The dog model of CCC reproduces most of the features of the human disease, including the low percentage of animals (~30%) that develop LV dysfunction post infection. But, if therapies are to be tested in this model, and improvement in LVEF is the target endpoint, inclusion criteria are mandatory and LVEF by echocardiography must be below 40%.

DATA AVAILABILITY STATEMENT

The datasets generated for this study can be found in the **Supplementary Material**.

ETHICS STATEMENT

The animal study was reviewed and approved by Committee on the Ethics of Animal Use of the Federal University of Ouro Preto.

AUTHOR CONTRIBUTIONS

EC and IR conducted echocardiography image acquisition and analysis. AN conducted animal infection and helped with echocardiography image acquisition. GB conducted echocardiography image acquisition. DM conducted data analysis and helped with echocardiography image acquisition. MO and MS conducted data analysis. MB participated in the conception and design, and provided funding for the study. ACC participated in the conception and design, provided funding for the study, and wrote the

manuscript. ABC participated in the conception, design and data analysis, provided funding for the study, and wrote the manuscript.

FUNDING

This study was funded by the following agencies: Conselho Nacional de Desenvolvimento Científico e Tecnológico (CNPq) (Grant No. 466550/2014-6 awarded to MTB, 465656/2014-5 and 404598/2012-9 awarded to ACC, 446362/2014-0 awarded to ABC), Fundação Carlos Chagas Filho de Amparo à Pesquisa

do Estado do Rio de Janeiro (FAPERJ), Coordenação de Aperfeiçoamento de Pessoal de Nível Superior (CAPES) and DECIT—Ministério da Saúde. The funders had no role in study design, data collection and analysis, decision to publish, or preparation of the manuscript.

SUPPLEMENTARY MATERIAL

The Supplementary Material for this article can be found online at: <https://www.frontiersin.org/articles/10.3389/fcimb.2019.00332/full#supplementary-material>

REFERENCES

- Bahia, M. T., Tafuri, W. L., Caliani, M. V., Veloso, V. M., Carneiro, C. M., Coelho, G. L. L. M., et al. (2002). Comparison of *Trypanosoma cruzi* infection in dogs inoculated with blood or metacyclic trypomastigotes of Berenice-62 and Berenice-78 strains via intraperitoneal and conjunctival routes. *Rev. Soc. Bras. Med. Trop.* 35, 339–345. doi: 10.1590/S0037-86822002000400010
- Barreto-de-Albuquerque, J., Silva-dos-Santos, D., Pérez, A. R., Berbert, L. R., de Santana-van-Vliet, E., Farias-de-Oliveira, D. A., et al. (2015). *Trypanosoma cruzi* infection through the oral route promotes a severe infection in mice: new disease form from an old infection? *PLoS Negl. Trop. Dis.* 9:e0003849. doi: 10.1371/journal.pntd.0003849
- Bayón, A., Fernández Palacio, M. J., Montes, A. M., and Gutiérrez Panizo, C. (1994). M-mode echocardiography study in growing Spanish mastiffs. *J. Small Anim. Pract.* 35, 473–479. doi: 10.1111/j.1748-5827.1994.tb03953.x
- Borges, D. C., Araújo, N. M., Cardoso, C. R., and Lazo Chica, J. E. (2013). Different parasite inocula determine the modulation of the immune response and outcome of experimental *Trypanosoma cruzi* infection. *Immunology* 138, 145–156. doi: 10.1111/imm.12022
- Caldas, I. S., da Matta Guedes, P. M., dos Santos, F. M., de Figueiredo Diniz, L., Martins, T. A. F., do Nascimento, A. F., et al. (2013). Myocardial scars correlate with eletrocardiographic changes in chronic *Trypanosoma cruzi* infection for dogs treated with Benznidazole. *Trop. Med. Int. Health* 18, 75–84. doi: 10.1111/tmi.12002
- Caldas, I. S., de Figueiredo Diniz, L., da Matta Guedes, P. M., da Nascimento, Á. F. S., da Cunha Galvão, L. M., Lima, W. G., et al. (2017). Myocarditis in different experimental models infected by *Trypanosoma cruzi* is correlated with the production of IgG1 isotype. *Acta Trop.* 167, 40–49. doi: 10.1016/j.actatropica.2016.12.015
- Caldas, I. S., Talvani, A., Caldas, S., Carneiro, C. M., de Lana, M., da Matta Guedes, P. M., et al. (2008). Benznidazole therapy during acute phase of Chagas disease reduces parasite load but does not prevent chronic cardiac lesions. *Parasitol. Res.* 103, 413–421. doi: 10.1007/s00436-008-0992-6
- Cantinotti, M., and Koestenberger, M. (2017). Quantification of left ventricular size and function by 2-dimensional echocardiography: so basic and so difficult: how to increase the accuracy and reproducibility in children? *Circ. Cardiovasc. Imaging* 10:e007165. doi: 10.1161/CIRCIMAGING.117.007165
- Colan, S. D., Shirali, G., Margossian, R., Gallagher, D., Altmann, K., Canter, C., et al. (2012). The ventricular volume variability study of the Pediatric Heart Network: study design and impact of beat averaging and variable type on the reproducibility of echocardiographic measurements in children with chronic dilated cardiomyopathy. *J. Am. Soc. Echocardiogr.* 25, 842–854.e6. doi: 10.1016/j.echo.2012.05.004
- Collins, F. S., and Tabak, L. A. (2014). Policy: NIH plans to enhance reproducibility. *Nature* 505, 612–613. doi: 10.1038/505612a
- Daliry, A., Caldas, I. S., de Figueiredo Diniz, L., Torres, R. M., Talvani, A., Bahia, M. T., et al. (2014). Anti-adrenergic and muscarinic receptor autoantibodies in a canine model of Chagas disease and their modulation by benznidazole. *Int. J. Cardiol.* 170, e66–e67. doi: 10.1016/j.ijcard.2013.11.022
- de Andrade, J. P., Neto, J. A. M., de Paola, A. A. V., Vilas-Boas, F., and Oliveira, G. M. M., Bacal, F., et al. (2011). I Diretriz Latino-Americana para o diagnóstico e tratamento da cardiopatia chagásica: resumo executivo. *Arq. Bras. Cardiol.* 96, 434–442. doi: 10.1590/S0066-782X2011000600002
- de Lana, M., Chiari, E., and Tafuri, W. L. (1992). Experimental Chagas' disease in dogs. *Mem. Inst. Oswaldo Cruz* 87, 59–71. doi: 10.1590/S0074-02761992000100011
- dos Santos, R. R., Rassi, S., Feitosa, G., Grecco, O. T., Rassi, A., da Cunha, A. B., et al. (2012). Cell therapy in Chagas cardiomyopathy (Chagas arm of the multicenter randomized trial of cell therapy in cardiopathies study). *Circulation* 125, 2454–2461. doi: 10.1161/CIRCULATIONAHA.111.067785
- Dukes-McEwan, J., Borgarelli, M., Tidholm, A., Vollmar, A. C., and Häggström, J. (2003). Proposed guidelines for the diagnosis of canine idiopathic dilated cardiomyopathy. *J. Vet. Cardiol.* 5, 7–19. doi: 10.1016/S1760-2734(06)70047-9
- Garcia, S., Ramos, C. O., Senra, J. F. V., Vilas-Boas, F., Rodrigues, M. M., Campos-de-Carvalho, A. C., et al. (2005). Treatment with benznidazole during the chronic phase of experimental Chagas' disease decreases cardiac alterations. *Antimicrob. Agents Chemother.* 49, 1521–1528. doi: 10.1128/AAC.49.4.1521-1528.2005
- Giavarina, D. (2015). Understanding Bland Altman analysis. *Biochem. Med.* 25, 141–151. doi: 10.11613/BM.2015.015
- Goldenberg, R. C. S., Jelicks, L. A., Fortes, F. S. A., Weiss, L. M., Rocha, L. L., Zhao, D., et al. (2008). Bone marrow cell therapy ameliorates and reverses Chagasic cardiomyopathy in a mouse model. *J. Infect. Dis.* 197, 544–547. doi: 10.1086/526793
- Guarita-Souza, L. C. (2006). Simultaneous autologous transplantation of cocultured mesenchymal stem cells and skeletal myoblasts improves ventricular function in a murine model of chagas disease. *Circulation* 114, 1–120. doi: 10.1161/CIRCULATIONAHA.105.000646
- Guedes, P. M. M., Veloso, V. M., Afonso, L. C. C., Caliani, M. V., Carneiro, C. M., Diniz, L. F., et al. (2009). Development of chronic cardiomyopathy in canine Chagas disease correlates with high IFN- γ , TNF- α , and low IL-10 production during the acute infection phase. *Vet. Immunol. Immunopathol.* 130, 43–52. doi: 10.1016/j.vetimm.2009.01.004
- Guedes, P. M. M., Veloso, V. M., Tafuri, W. L., da Galvão, L. M. C., Carneiro, C. M., de Lana, M., et al. (2002). The dog as model for chemotherapy of the Chagas' disease. *Acta Trop.* 84, 9–17. doi: 10.1016/S0001-706X(02)00139-0
- Hall, D. J., Cornell, C. C., Crawford, S., and Brown, D. J. (2008). Meta-analysis of normal canine echocardiographic dimensional data using ratio indices. *J. Vet. Cardiol.* 10, 11–23. doi: 10.1016/j.jvc.2008.03.001
- Houser, S. R., Margulies, K. B., Murphy, A. M., Spinale, F. G., Francis, G. S., Prabhu, S. D., et al. (2012). Animal models of heart failure. *Circ. Res.* 111, 131–150. doi: 10.1161/RES.0b013e3182582523
- Jasmin, Jelicks, L. A., Tanowitz, H. B., Peters, V. M., Mendez-Otero, R., de Carvalho, A. C. C., et al. (2014). Molecular imaging, biodistribution and efficacy of mesenchymal bone marrow cell therapy in a mouse model of Chagas disease. *Microbes Infect.* 16, 923–935. doi: 10.1016/j.micinf.2014.08.016
- Lang, R. M., Badano, L. P., Mor-Avi, V., Afilalo, J., Armstrong, A., Ernande, L., et al. (2015). Recommendations for cardiac chamber quantification by echocardiography in adults: an update from the American Society of

- Echocardiography and the European Association of Cardiovascular Imaging. *Eur. Heart J. Cardiovasc. Imaging* 16, 233–270. doi: 10.1093/ehjci/jev014
- Lopez, L., Colan, S. D., Frommelt, P. C., Ensing, G. J., Kendall, K., Younoszai, A. K., et al. (2010). Recommendations for quantification methods during the performance of a pediatric echocardiogram: a report from the Pediatric Measurements Writing Group of the American Society of Echocardiography Pediatric and Congenital Heart Disease Council. *J. Am. Soc. Echocardiogr.* 23, 465–95; quiz 576–7. doi: 10.1016/j.echo.2010.03.019
- Margossian, R., Chen, S., Sleeper, L. A., Tani, L. Y., Shirali, G., Golding, F., et al. (2015). The reproducibility and absolute values of echocardiographic measurements of left ventricular size and function in children are algorithm dependent. *J. Am. Soc. Echocardiogr.* 28, 549–558.e1. doi: 10.1016/j.echo.2015.01.014
- Morillo, C. A., Ramos, I. P., Mesquita, F. C. P., Brasil, G. V., Rocha, N. N., Takiya, C. M., et al. (2015). Adipose tissue-derived mesenchymal stromal cells protect mice infected with *Trypanosoma cruzi* from cardiac damage through modulation of anti-parasite immunity. *PLoS Negl. Trop. Dis.* 9:e0003945. doi: 10.1371/journal.pntd.0003945
- Morillo, C. A., Marin-Neto, J. A., Avezum, A., Sosa-Estani, S., Rassi, A., Rosas, F., et al. (2015). Randomized trial of benznidazole for chronic Chagas' cardiomyopathy. *N. Engl. J. Med.* 373, 1295–1306. doi: 10.1056/NEJMoa1507574
- Northup, D. W., van Lier, E. J., and Clifford Stickney, J. (1957). The effect of age, sex, and body size on the heart weight-body weight ratio in the dog. *Anat. Rec.* 128, 411–417. doi: 10.1002/ar.1091280305
- Pascon, J. P. E., Pereira Neto, G. B., Sousa, M. G., Júnior, D. P., and Camacho, A. A. (2010). Clinical characterization of chronic chagasic cardiomyopathy in dogs. *Pesqui. Vet. Bras.* 30, 115–120. doi: 10.1590/S0100-736X2010000200003
- R Core Team (2017). *R: A Language and Environment for Statistical Computing*. R Foundation for Statistical Computing, Vienna, Austria. Available online at: <https://www.R-project.org/> (accessed August 15, 2019).
- Rassi, A., Rassi, A., Little, W. C., Xavier, S. S., Rassi, S. G., Rassi, A. G., et al. (2006). Development and validation of a risk score for predicting death in Chagas' heart disease. *N. Engl. J. Med.* 355, 799–808. doi: 10.1056/NEJMoa053241
- Rassi, A., Rassi, A., and Marin-Neto, J. A. (2010). Chagas disease. *Lancet* 375, 1388–1402. doi: 10.1016/S.0140-6736(10)60061-X
- RStudio Team (2016). *RStudio: Integrated Development for R*. RStudio, Inc., Boston, MA. Available online at: <http://www.rstudio.com/> (accessed August 15, 2019).
- Santos, F. M., Lima, W. G., Gravel, A. S., Martins, T. A. F., Talvani, A., Torres, R. M., et al. (2012). Cardiomyopathy prognosis after benznidazole treatment in chronic canine Chagas' disease. *J. Antimicrob. Chemother.* 67, 1987–1995. doi: 10.1093/jac/dks135
- Selamet Tierney, E. S., Hollenbeck-Pringle, D., Lee, C. K., Altmann, K., Dunbar-Masterson, C., Golding, F., et al. (2017). Reproducibility of left ventricular dimension versus area versus volume measurements in pediatric patients with dilated cardiomyopathy. *Circ. Cardiovasc. Imaging* 10:e006007. doi: 10.1161/CIRCIMAGING.116.006007
- Soares, M. B. P., Lima, R. S., Souza, B. S. F., Vasconcelos, J. F., Rocha, L. L., dos Santos, R. R., et al. (2011). Reversion of gene expression alterations in hearts of mice with chronic chagasic cardiomyopathy after transplantation of bone marrow cells. *Cell Cycle* 10, 1448–1455. doi: 10.4161/cc.10.9.15487
- Sousa, M. G., Paulino-Junior, D., Pascon, J. P. E., Pereira-Neto, G. B., Carareto, R., Champion, T., et al. (2011). Cardiac function in dogs with chronic Chagas cardiomyopathy undergoing autologous stem cell transplantation into the coronary arteries. *Can. Vet. J.* 52, 869–874.
- Steverding, D. (2014). The history of Chagas disease. *Parasit. Vectors* 7:317. doi: 10.1186/1756-3305-7-317
- Wess, G., Domenech, O., Dukes-McEwan, J., Häggström, J., and Gordon, S. (2017). European Society of Veterinary Cardiology screening guidelines for dilated cardiomyopathy in Doberman Pinschers. *J. Vet. Cardiol.* 19, 405–415. doi: 10.1016/j.jvc.2017.08.006

Conflict of Interest: The authors declare that the research was conducted in the absence of any commercial or financial relationships that could be construed as a potential conflict of interest.

Copyright © 2019 Carvalho, Ramos, Nascimento, Brasil, Mello, Oti, Sammeth, Bahia, Campos de Carvalho and Carvalho. This is an open-access article distributed under the terms of the Creative Commons Attribution License (CC BY). The use, distribution or reproduction in other forums is permitted, provided the original author(s) and the copyright owner(s) are credited and that the original publication in this journal is cited, in accordance with accepted academic practice. No use, distribution or reproduction is permitted which does not comply with these terms.



Redox Balance Keepers and Possible Cell Functions Managed by Redox Homeostasis in *Trypanosoma cruzi*

Andrea C. Mesías¹, Nisha J. Garg^{2*} and M. Paola Zago^{1*}

¹ Instituto de Patología Experimental, Consejo Nacional de Investigaciones Científicas y Técnicas (CONICET) - Universidad Nacional de Salta, Salta, Argentina, ² Department of Microbiology and Immunology, Institute for Human Infections and Immunity, University of Texas Medical Branch, Galveston, TX, United States

OPEN ACCESS

Edited by:

Martin Craig Taylor,
University of London, United Kingdom

Reviewed by:

Fernanda Ramos Gadelha,
Campinas State University, Brazil
Sergio Schenkman,
Federal University of São Paulo, Brazil
Ana Maria Tomás,
University of Porto, Portugal

*Correspondence:

Nisha J. Garg
nigarg@utmb.edu
M. Paola Zago
mpzago@conicet.gov.ar

Specialty section:

This article was submitted to
Parasite and Host,
a section of the journal
Frontiers in Cellular and Infection
Microbiology

Received: 20 August 2019

Accepted: 05 December 2019

Published: 20 December 2019

Citation:

Mesías AC, Garg NJ and Zago MP
(2019) Redox Balance Keepers and
Possible Cell Functions Managed by
Redox Homeostasis in
Trypanosoma cruzi.
Front. Cell. Infect. Microbiol. 9:435.
doi: 10.3389/fcimb.2019.00435

The toxicity of oxygen and nitrogen reactive species appears to be merely the tip of the iceberg in the world of redox homeostasis. Now, oxidative stress can be seen as a two-sided process; at high concentrations, it causes damage to biomolecules, and thus, trypanosomes have evolved a strong antioxidant defense system to cope with these stressors. At low concentrations, oxidants are essential for cell signaling, and in fact, the oxidants/antioxidants balance may be able to trigger different cell fates. In this comprehensive review, we discuss the current knowledge of the oxidant environment experienced by *T. cruzi* along the different phases of its life cycle, and the molecular tools exploited by this pathogen to deal with oxidative stress, for better or worse. Further, we discuss the possible redox-regulated processes that could be governed by this oxidative context. Most of the current research has addressed the importance of the trypanosomes' antioxidant network based on its detox activity of harmful species; however, new efforts are necessary to highlight other functions of this network and the mechanisms underlying the fine regulation of the defense machinery, as this represents a master key to hinder crucial pathogen functions. Understanding the relevance of this balance keeper program in parasite biology will give us new perspectives to delineate improved treatment strategies.

Keywords: *Trypanosoma cruzi*, stage-specific oxidants, antioxidant network, regulation, redox-dependent mechanisms

INTRODUCTION

Chagas disease (ChD) is one of the most important neglected tropical diseases in South and Central America and in Mexico. It is estimated that 6–7 million people are infected with *Trypanosoma cruzi* (*T. cruzi*), and ~300,000 new cases of ChD emerge each year that account for >10,000 deaths per year¹. During last two decades, ChD cases have also been reported in non-endemic countries (e.g., United States and Canada), Western Pacific region, and Europe (reviewed in Schmunis, 2007; Albajar-Vinas and Jannin, 2011; Tanowitz et al., 2011), primarily due to immigration of seropositive individuals from endemic countries. However, in the Southern US, the natural cycle of *T. cruzi* transmission is evidenced with the detection of high rate of infection in dogs (Curtis-Robles et al., 2017, 2018) and autochthonous cases of ChD in humans (Garcia et al., 2017).

¹ World Health Organization (WHO) | Epidemiology, <http://www.who.int/chagas/epidemiology/en/>

Two drugs, benznidazole and nifurtimox, are currently available for the treatment of patients diagnosed early after *T. cruzi* infection, but these drugs have limited efficacy in the chronic disease phase (Morillo et al., 2015). Further, these drugs have several side effects, and are not recommended for persons with neurological and psychiatric disorders or some degree of kidney failure, and for pregnant women (reviewed in Patterson and Wyllie, 2014). Several vaccines are in the experimental stage (reviewed in Rodríguez-Morales et al., 2015; Rios et al., 2019) even though none of these are yet available to prevent or control human *T. cruzi* infection. Thus, new prophylactic and therapeutic strategies for control of *T. cruzi* infection and chronic ChD are urgently needed.

T. cruzi is an intracellular kinetoplastid parasite with a complex life cycle that goes through several biochemical and morphological changes during its transit through the vector and mammalian host. Remarkably, *T. cruzi* can potentially infect 1000's of vertebrate species, and at least 40 invertebrate species (Teixeira et al., 2009). This parasite's tremendous adaptability to infect a wide variety of hosts ensures its survival in the sylvatic and domestic cycles. An example of the pathogen's plasticity can be found in the reactive species management system used by *T. cruzi* to keep homeostasis and ensure redox-dependent pathways.

T. CRUZI EXPOSURE TO OXIDANTS IN INSECT VECTORS

Oxidant Stressors in the Triatomine Vectors

T. cruzi faces a variety of oxidative stressors of internal and external origin during its replication and differentiation in the insect (Figure 1). Briefly, after being ingested by triatomines with a blood meal, parasite goes through an active binary division as an epimastigote in the insect gut. Once the nutrients available for parasite proliferation become limited, epimastigote forms move to the posterior midgut, adhere to the wax cover of the rectal cuticle by hydrophobic interactions, and undergo metacyclogenesis. During parasite's replication and passage through the vector's intestinal tube, significant amount of oxidants are produced by the triatomine's immune system (Figure 1A) (Ursic-Bedoya and Lowenberger, 2007). It is suggested that triatomine recognition of pathogen-associated molecular patterns (PAMPs) triggers innate immunity as well as humoral and cellular protection (reviewed in Azambuja et al., 2016). Briefly, the gut lumen is a prime site for the production of immune effectors including reactive oxygen species (ROS) and reactive nitrogen species (RNS) (Garcia et al., 2007, 2010; Genta et al., 2010) by a pool of enzymes. Nitric oxide synthase (NOS) was firstly identified through its cross-reaction with human NADPH oxidase p67^{phox} antibody (Whitten et al., 2001), and its expression and activity in *R. prolixus* was later confirmed by 2,3-diaminonaphthalene fluorescence-based assay that detects NO (Whitten et al., 2007). Other enzymes, namely dual oxidase (DUOX) and NADPH oxidase (NOX), produce superoxide radical ($O_2^{\bullet-}$), and the latter can dismutate to hydrogen

peroxide (H_2O_2) or react with nitric oxide (NO) to produce peroxynitrite ($ONOO^-$) (Ha et al., 2005; Azambuja et al., 2016). The phenoloxidase (PO) cascade, a hallmark immune component of insects, is also present in triatomines leading to the production of toxic quinones, melanin, and some intermediates of reactive oxygen species (ROS) and reactive nitrogen species (RNS) to encapsulate and kill the pathogens (reviewed in Flores-Villegas et al., 2015). PO activity was increased after vector infection with *T. cruzi* Dm28c strain though it had no effect on parasite viability (Castro et al., 2012), and therefore, its function as a driver of innate immunity against *T. cruzi* was not established. Moreover, these authors postulated that parasite-induced PO modifies vector immune responses to decrease the gut microbiota and favor parasite development in the insect gut.

In addition to vectorial oxidants, epimastigotes and metacyclic trypomastigotes are exposed to other compounds like heme (ferriprotoporphyrin-IX) and heme breakdown products in the midgut of the insect; produced by degradation of hemoglobin that is the most abundant protein in mammalian blood. At an estimated concentration of 10 mM blood heme (bound to hemoglobin), triatomine midgut is believed to carry toxic amounts of heme during digestion of a single blood meal (Graça-Souza et al., 2006). Free heme, even at 50–100 μ M concentration, is a toxic molecule due to its ability to generate ROS (Gutteridge and Smith, 1988) catalyzing the oxidation of proteins, the formation of cytotoxic lipid peroxides via lipid peroxidation and damaging DNA (reviewed in Kumar and Bandyopadhyay, 2005). Nevertheless, triatomine vectors exploit heme crystallization into hemozoin as a prime redox regulator mechanism that protects the insect itself, but also promotes parasite infection (Ferreira et al., 2018). Therefore, in this context, free heme toxicity would be mitigated. *T. cruzi* genome lacks the genes/proteins required for the biosynthesis of heme (El-Sayed et al., 2005); however, it is an essential cofactor that *T. cruzi* must intake from the host. It was demonstrated that heme and its breakdown products promote proliferation in *T. cruzi* epimastigotes (Lara et al., 2007). Strikingly, *T. cruzi* insect stage is able to withstand 1 mM hemin—a concentration known to disrupt phospholipid membranes—without any obvious toxic effect (Lara et al., 2007). Nogueira et al., also described that heme proliferative phenomenon was accompanied by a marked increase in ROS formation in epimastigotes (Nogueira et al., 2011, 2015). It was proposed that heme-induce transient oxidative stress drives the epimastigote proliferation through activation of calcium-calmodulin-dependent kinase II (CaMKII) (Souza et al., 2009; Nogueira et al., 2011). Thus, *T. cruzi* epimastigote can avoid heme toxicity, and instead use it as a signaling molecule for its proliferation in the insect midgut (Lara et al., 2007; Paes et al., 2011; Nogueira et al., 2017).

Oxidants Produced by Insect Stage Parasite

T. cruzi also produces oxidants during its replication and differentiation in the insect midgut. ROS production in *T. cruzi*,

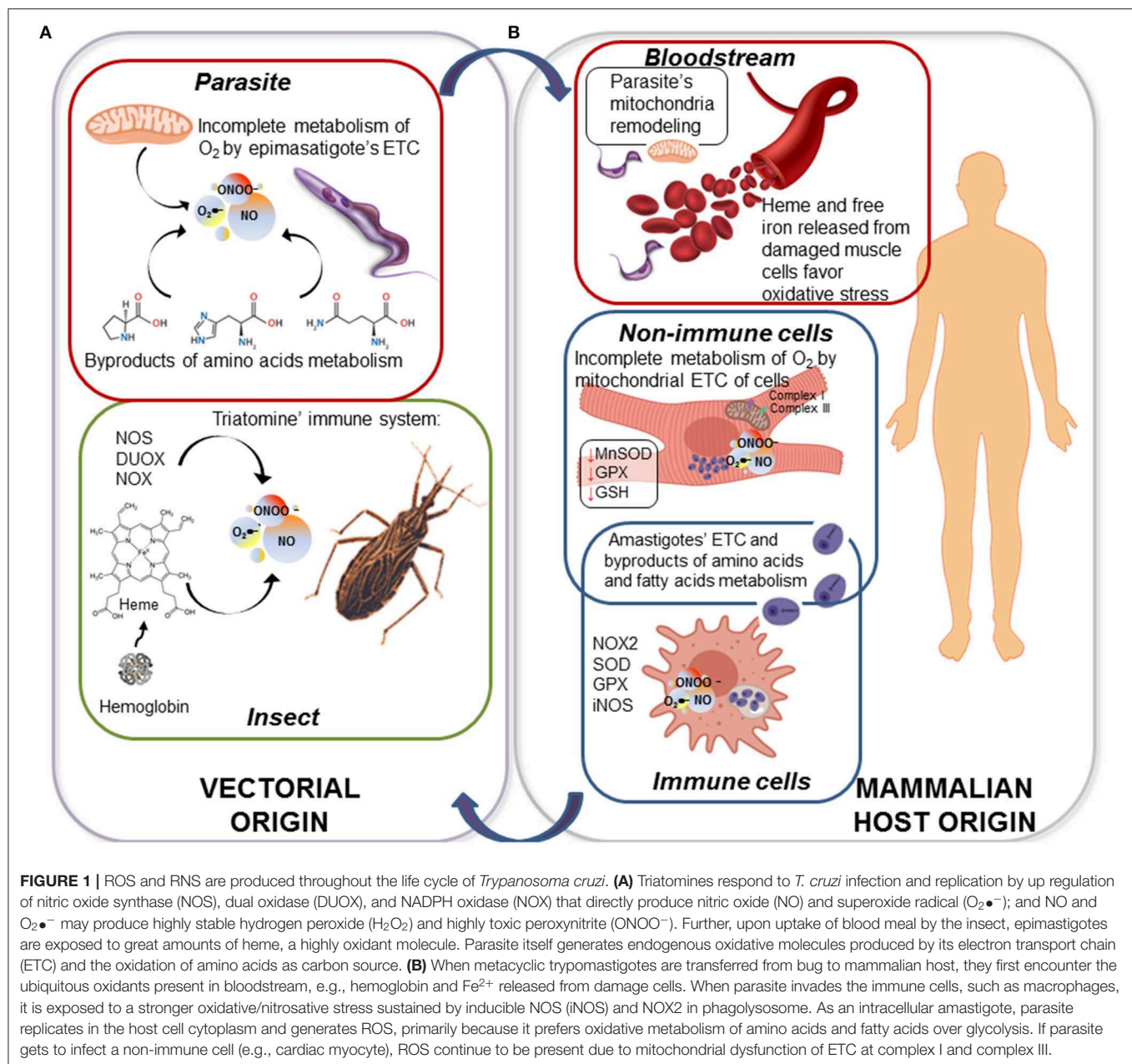


FIGURE 1 | ROS and RNS are produced throughout the life cycle of *Trypanosoma cruzi*. **(A)** Triatomines respond to *T. cruzi* infection and replication by up regulation of nitric oxide synthase (NOS), dual oxidase (DUOX), and NADPH oxidase (NOX) that directly produce nitric oxide (NO) and superoxide radical ($O_2^{\bullet-}$); and NO and $O_2^{\bullet-}$ may produce highly stable hydrogen peroxide (H_2O_2) and highly toxic peroxynitrite ($ONOO^-$). Further, upon uptake of blood meal by the insect, epimastigotes are exposed to great amounts of heme, a highly oxidant molecule. Parasite itself generates endogenous oxidative molecules produced by its electron transport chain (ETC) and the oxidation of amino acids as carbon source. **(B)** When metacyclic trypomastigotes are transferred from bug to mammalian host, they first encounter the ubiquitous oxidants present in bloodstream, e.g., hemoglobin and Fe^{2+} released from damage cells. When parasite invades the immune cells, such as macrophages, it is exposed to a stronger oxidative/nitrosative stress sustained by inducible NOS (iNOS) and NOX2 in phagolysosome. As an intracellular amastigote, parasite replicates in the host cell cytoplasm and generates ROS, primarily because it prefers oxidative metabolism of amino acids and fatty acids over glycolysis. If parasite gets to infect a non-immune cell (e.g., cardiac myocyte), ROS continue to be present due to mitochondrial dysfunction of ETC at complex I and complex III.

in general, is closely related to nutrients metabolism in each developmental stage. The epimastigote stage relies on oxidation of L-proline, L-histidine, and L-glutamine for energy supply. These amino acids are released from digestion of blood proteins being abundantly present in the hemolymph and tissue fluids of the hematophagous vectors (Cazzulo, 1984; Bringaud et al., 2006). L-alanine, is produced as a metabolic end product by *T. cruzi* when it grows in a medium rich in glucose and amino acids, but it can also be taken up and oxidized to CO_2 delivering electrons to electron transport chain (ETC) (Girard et al., 2018). Thus, amino acids oxidation fuels respiratory complexes and oxidative phosphorylation for ATP generation; however, during this

process, electron leakage to O_2 can also result in $O_2^{\bullet-}$ formation, possibly supporting an oxidative environment (Figure 1A). Further, Nogueira et al. (2017) showed that presence of heme during *in vitro* culture of *T. cruzi*, induced mitochondrial membrane hyperpolarization and an increase in endogenous $O_2^{\bullet-}$ production. As we mentioned previously, the heme-induced mitochondrial ROS were beneficial in promoting epimastigote survival and proliferation. Conversely, urate-like antioxidants produced in the hemolymph were found to arrest epimastigotes' growth and promote differentiation of epimastigotes to metacyclic infective form (Nogueira et al., 2015). To sum up, *T. cruzi* epimastigotes appear to utilize the components of oxidative stress for their growth in the insect

gut, and then for switching to metacyclogenesis and be ready for transition to mammalian infective stage.

T. CRUZI EXPOSURE TO OXIDANTS IN THE MAMMALIAN HOST

Exposure to Oxidative and Nitrosative Stress in Immune Cells

Triatomines release infective, non-replicative, metacyclic trypomastigotes in feces while taking the next blood meal on a mammalian host. Once trypomastigotes enter the blood stream of the vertebrate host, they quickly infect a variety of cells and differentiate to the replicative amastigote stage. During this process, the parasite has to deal with a second wave of oxidative stress. Studies in mice and humans show that innate and adaptive immune responses, involving macrophages, neutrophils, natural killer cells, B and T lymphocytes, should control the parasite through the production of ROS/RNS, proinflammatory T_H1 cytokines, trypanolytic antibodies, and cytotoxic T lymphocytes' activity; readers are referred to excellent reviews on this topic (Junqueira et al., 2010; Machado et al., 2012; Cardillo et al., 2015; Bonney et al., 2019). A thorough analysis of all the components of natural and experimental innate and adaptive immunity against *T. cruzi* infection is beyond the scope of this article. Herein, we will focus on macrophages that offer the first line of defense upon parasite engulfment (discussed in Lopez et al., 2018).

T. cruzi (metacyclics and trypomastigotes) can actively invade a variety of non-immune and immune cells and also may be phagocytosed by macrophages and dendritic cells (reviewed in Walker et al., 2013). The parasite uptake triggers an almost immediate increase in the expression of inflammatory cytokines followed by delayed and subpar production of $O_2^{\bullet-}$ and NO in macrophages (Koo et al., 2018). As in the vector host, in infected macrophages also, inducible NADPH oxidase (NOX2) produces $O_2^{\bullet-}$ that can be transformed spontaneously or enzymatically by superoxide dismutases (SODs) to H_2O_2 , and the latter is dismutated by GPx and catalase (Figure 1B) (Gupta et al., 2011). Likewise, inducible nitric oxide synthetase (iNOS) produces NO that can react with $O_2^{\bullet-}$ and generate $ONOO^-$ in infected macrophages. Although $ONOO^-$ has a short life, it is the most powerful cytotoxic effector produced by macrophages for parasite killing (Alvarez et al., 2011). Yet, it must be mentioned that the proinflammatory cytokines and the oxidative and nitrosative stress are capable of controlling, but not preventing the dissemination of virulent parasite strains from macrophages (reviewed in Lopez et al., 2018; Koo and Garg, 2019). This is, in part, attributed to the ability of the virulent isolates of *T. cruzi* to orchestrate their antioxidant system and allow sub-par and delayed activation of oxidative/nitrosative burst in the host immune cells (Piacenza et al., 2009b; Zago et al., 2016). Others have indicated that oxidative stress produced in response to *T. cruzi* infection correlates with higher parasite burden in an animal infection model, pointing to oxidative environment as an enhancer of infection (Paiva et al., 2012).

In agreement with this finding, treatment with compounds, such as iron chelator desferrioxamine and melatonin that also have antioxidant capacity reduced the parasite proliferation (Arantes et al., 2007; Santello et al., 2007). However, it was a correlative observation, and authors did not clarify if the observed proliferative effects on the parasite were indeed due to antioxidant nature of these drugs. Regardless, the current literature indicates a dual role of ROS/RNS in parasite control vs. parasite proliferation and spreading in the mammalian host. Immune oxidative response can, in fact, control parasite infection whereas at lower levels, an oxidant environment may promote pathogen replication.

Exposure to Oxidative Stress in Non-immune Cells

Parasite is also exposed to cytotoxic molecules in non-immune cells, primarily because a wide variety of ROS and RNS are continuously formed as byproducts of aerobic metabolism. In general terms, mitochondrial ETC coupled with oxidative phosphorylation accounts for 85–90% of the O_2 consumed in a cell. Up to 3% of the consumed O_2 is incompletely metabolized, and results in $O_2^{\bullet-}$ release (Silva et al., 2011; Wang and Hai, 2016). The heart is particularly dependent on mitochondria to produce the energy required for its contractile activity, and mitochondria represent up to 30% of the total volume of cardiomyocytes, providing 90% of the cellular ATP energy through oxidative phosphorylation. In cardiomyocytes infected by *T. cruzi*, and in the myocardium of chronically infected animals (Mukherjee et al., 2003; Wen and Garg, 2004) and ChD clinically symptomatic patients (Cunha-Neto et al., 2005; Wen et al., 2006; Wan et al., 2012; Dhiman et al., 2013), mitochondrial dysfunction was well-documented by us and other researchers. Specifically, activities of the respiratory complex I and complex III were compromised and resulted in a significant increase in electron leakage to O_2 and $O_2^{\bullet-}$ production in mitochondria of infected cardiomyocytes and ChD hearts (Vyatkina et al., 2004; Gupta et al., 2009). *In vivo* studies in mice and rats showed that mitochondrial defects persisted beyond the acute phase of infection, correlating with high mitochondrial ROS (mtROS) levels during chronic disease phase (Wen et al., 2008, 2017; Wan et al., 2016). Further, the increase in mtROS production correlated with a decline in the expression and activity of the mitochondrial antioxidant enzyme Mn^{+2} superoxide dismutase (MnSOD), and a decline in the cytosolic glutathione peroxidase (GPx) activity and GSH content in the myocardium of chronically infected animals (Wen and Garg, 2004) and in ChD patients (Pérez-Fuentes et al., 2003; Wen et al., 2006; de Oliveira et al., 2007; Wan et al., 2012; Dhiman et al., 2013), thus revealing the persistence of a pro-oxidant milieu along the infection process. These studies point to the role of ETC as an important source of oxidant species in non-immune cells, especially in cardiomyocytes that are one of the main target cells invaded by *T. cruzi* (Figure 1B). Garg and co-workers have proposed that a lack of appropriate antioxidant and repair response result in self-perpetuating mitochondrial dysfunction and ROS production

in the heart (reviewed in Lopez et al., 2018; Bonney et al., 2019). This mtROS production in Chagas heart can provide a defense against parasite persistence; however, it also signals the fibrotic gene expression and contribute to evolution of chronic cardiomyopathy (Wan et al., 2012; Wen et al., 2017).

Non-enzymatic Oxidative Stress

As in the insect stage, *T. cruzi* is also exposed to the non-enzymatic oxidative species in the mammalian host. For example, essential metals, such as iron, zinc, and copper play a critical role in many biological processes. The $\text{Fe}^{+2}/\text{Fe}^{+3}$ and $\text{Cu}^{+2}/\text{Cu}^{+3}$ act as electron donor/acceptor and play a vital role in catalysis of a variety of enzymatic reactions that involve an electron transfer. Specifically, up to 70% of the body iron is present in red blood cells (RBCs) in the form of hemoglobin and in muscle cells as a component of myoglobin (Winter et al., 2014). In these tissues, iron is also present in iron-sulfur (Fe-S) clusters, and it serves as a cofactor to support ETC, respiration, and oxygen transport (reviewed in Rouault, 2012). Likewise, copper is the cofactor of metabolic enzymes (e.g., cytochrome c oxidase in mitochondria, CuZnSOD in cytosol) and it catalyzes the enzymatic activity of key enzymes of the secretory pathway (reviewed in Polishchuk and Lutsenko, 2013; Baker et al., 2017). However, these metals are redox active, and in an oxidative environment undergo redox-cycling reactions leading to exacerbated production of free radical species. The toxicity of iron, and, by association, of copper, is driven by their ability to reduce peroxides, via Fenton chemistry, into highly reactive hydroxyl radical that subsequently reacts at diffusion-limited rates with various biomolecules (Valko et al., 2016; Sánchez et al., 2017). Further, Fe-S clusters are preferred targets of $\text{O}_2\bullet^-$, and their oxidation leads to Fe^{+2} release that then can feed Fenton reaction and ROS production (Fridovich, 1995).

Heme and free iron released by dying RBCs and damaged muscle cells may also generate oxidative stress (Beard, 2001; McCord, 2004). Thus, it could be speculated that the breakdown of metal ion homeostasis can expose *T. cruzi* to iron (and up to some extent copper) in the blood stream as well as in muscle cells and tissues that are the preferred site of *T. cruzi* replication. Skeletal muscle and heart may also accumulate considerable amounts of iron as is noted in brain, liver and other tissues, and there is evidence that increased iron storage correlates with ROS formation in tissues (Yoshiji et al., 1992; Barollo et al., 2004; Shoham and Youdim, 2004; Sullivan, 2004). Cytosolic ferritin (binds up to 4,500 iron atoms for storage) may be a source of free iron when it undergoes degradation in response to stress (reviewed in Philpott et al., 2017). Thus, we propose that endogenous iron storage in muscle cells and tissues may also expose intracellular amastigotes to oxidative stress. Still, many reports describe the requirement for a mild oxidizing environment for the efficient iron mobilization, which in turn enhances intracellular parasite growth. Hence, it is suggested that depletion of intracellular iron stores in host cells could impair *T. cruzi* replication. Conversely, host responses transferring iron to the intracellular sites of *T. cruzi* replication may enhance parasite pathogenicity (reviewed in Andrews, 2012; Paiva et al.,

2018). Future studies are needed to clearly define the role of iron metabolism and redox signaling in parasite proliferation.

ROS as a Byproduct of Trypomastigote/Amastigote Metabolism

ROS generation within *T. cruzi* is closely related to available energy sources. In contrast to epimastigote forms of *T. cruzi* that rely on amino acids metabolism in the vector host, infective trypomastigotes have access to abundant glucose (up to 5 mM) in bloodstream of the vertebrate host. Not surprisingly then, trypomastigotes utilize glucose as a preferred carbon source for their energy requirement in the mammalian host (Silber et al., 2009). Glucose fermentation in trypomastigotes' glycosome—a peroxisome-like organelle—produces CO_2 , succinate, and acetate (reviewed in Bringaud et al., 2006; Michels et al., 2006), and provides substrates for oxidative phosphorylation. The bioenergetics metabolism in the intracellular, replicative, amastigote stage remains controversial. Some investigators have indicated that the intracellular form of the parasite arrests the expression of glucose transporters (Silber et al., 2009), and utilizes fatty acids and amino acids taken from the cell cytosol to satisfy its energy needs (Engel et al., 1987; Silber et al., 2009). Indeed, expression of enzymes needed for fatty acids oxidation are increased in amastigote form of the parasite (Atwood et al., 2005), thus suggesting a metabolic shift. However, recent studies have employed a metabolic labeling approach to show that *T. cruzi* infection modulates host cell metabolism and stimulates cellular glucose uptake that can then be utilized by parasite for its own replication in the host cytosol (Shah-Simpson et al., 2017). These seemingly contradictory results could simply suggest that intracellular parasites fuel their metabolism in a flexible manner. Thus, while epimastigotes rely on amino acids catabolism and mitochondrial respiration, trypomastigote—and likely amastigote—parasite forms depend mostly on glycolysis but sparingly use fatty acids or other sources of energy. If such is the case, then they do not need to face a strong endogenous ROS stress that otherwise is associated with high mitochondrial activity.

Nevertheless, from a different line of evidence, Gonçalves et al. (2011) have shown, through functional assessment of mitochondrial metabolism, an increased generation of H_2O_2 in the bloodstream trypomastigotes compared to the epimastigote stage (Gonçalves et al., 2011). According to these authors, during the parasite transformation from the insect to infective trypomastigote form, mitochondrial organelle undergoes remodeling that results in (a) increased activities of the respiratory complex II and complex III facilitating electrons' entrance to the ETC, and (b) decreased expression and activity of complex IV. This would promote the generation of an "electron bottleneck," favoring $\text{O}_2\bullet^-$ and H_2O_2 formation (Gonçalves et al., 2011). In this scenario, it is argued that even if trypomastigotes are more dependent on glycolysis than oxidative phosphorylation for their energy need (Bringaud et al., 2006; Silber et al., 2009), they may still be exposed to excessive oxidative stress due to mitochondrial remodeling and increased ROS production (Gonçalves et al., 2011).

Drugs-Derived Oxidative Stress

Treatment with anti-parasite drugs, benznidazole (BZ) and nifurtimox (NFX), also exposes the parasite to oxidative stress. BZ is the preferred drug for the treatment of acute ChD. In this sense, it is worthy of note that several BZ delivery platforms and formulations have been assayed in pre-clinical studies (Scalise et al., 2016; Santos Souza et al., 2017; García et al., 2018) and a pediatric formulation of BZ is available since 2011², improving dosing accuracy, safety, and adherence to treatment. Both BZ and NFX are pro-drugs that are cleaved to their active form in the parasite by nitroreductase type I (NTR-I) (Hall et al., 2011; Hall and Wilkinson, 2012). It is suggested that the activated BZ and NFX (and their metabolites), through direct binding to trypanothione (T[SH]₂, N¹,N⁸-bisglutathionylspermidine) and GSH, make these antioxidants unavailable for the parasite's defense (Maya et al., 1997; Trochine et al., 2014). Thus, BZ/NFX, at appropriate concentration, would decrease the availability of low MW thiols such that oxygen redox cycling-derived free radicals, drug-derived free radicals, and reduced electrophilic metabolites are accumulated and cause cytotoxic effects on the parasite biomolecules (Maya et al., 1997). The activation of BZ by NTR-I also generates DNA-toxic glyoxal adducts in an oxygen-insensitive reaction (Hall and Wilkinson, 2012). In the host, BZ promotes an adaptive response to oxidative injury activating the nuclear factor-erythroid 2-related factor-2 (Nrf2) and multidrug resistance associated protein 2 (MRP2) (Rigalli et al., 2016). However, anti-parasite therapy is not always successful because of varying degrees of susceptibility of different parasite strains. This is probably, due to diverse mechanisms such as differences in the thiol content, NTR-I downregulation (Wilkinson et al., 2008), or deletion of copies of the gene encoding prostaglandin F_{2α} synthase (referred as old yellow enzyme) that is involved in activating the anti-parasite drugs (Murta et al., 2006). Nevertheless, at present, there are no drugs clinically superior to NFX or BZ.

THE COMPLEXITY OF ROS AND RNS CYTOTOXIC EFFECTS ON *T. CRUZI*

Before we discuss the cytotoxic effects of oxidative stress on parasite, it should be mentioned that ROS and RNS are broad terms that include free radical and non-radical active species with different levels of toxicity. Effect of each active molecule depends on its amount, reactivity, half-life, diffusion properties, and biological interactions. Furthermore, it is well-established that many of these species can give rise to secondary oxidants with different reactivity and lifespan than the initial ones (reviewed in Halliwell and Gutteridge, 2015). Overall, high concentrations of reactive species produced by immune response, oxidative metabolism, and other environmental factors create a complex landscape of oxidative stress that the parasite has to deal with to maintain redox homeostasis for its survival in diverse hosts.

One of the main targets of ROS is DNA. There are many types of oxidative modifications noted in the sugar-phosphate

backbone and nitrogenous bases of DNA, and considering the low reduction coefficient of guanine, this base is recognized as the most susceptible nucleotide (David et al., 2007). Once guanine is oxidized, it assumes a *syn* conformation called 8-oxoguanine (8-oxoG) that mimics thymine, and thereby exerts a strong mutagenic effect by transversion. Oxidized DNA is also susceptible to nicks, and introduces single and double strand DNA breaks (Cheng et al., 1992; Aguiar et al., 2013). While double strand breaks are lethal if left unrepaired, oxidized bases may be mutagenic, cytotoxic or both. Indeed, recent studies have shown that exposure to H₂O₂ caused a 2-fold increase in the frequency of mutations to *T. cruzi* DNA (Torres-Silva et al., 2018), and it turned out to be cytotoxic to the pathogen (Zago et al., 2016; Mesias et al., 2018). However, others have proposed that oxidative DNA damage, along with the recently documented 8-oxoG lesion repair system in *T. cruzi* (Machado-silva et al., 2016), were beneficial in enhancing the genetic diversity and favored the selection of parasites capable of evading immune system and develop drug resistance (Torres-Silva et al., 2018). Further studies will be necessary to elucidate the levels and types of oxidative DNA modifications that are cytotoxic to *T. cruzi* vs. those that offer survival advantages to the parasite.

Reactive lipid species (RLS) within the membranes can be formed enzymatically (e.g., by lipoxygenase and cyclooxygenase) or through non-enzymatic lipid peroxidation and nitration pathways (Gaschler and Stockwell, 2017). Major classes of RLS include lipid aldehydes, α,β -unsaturated carbonyls, and nitroalkenes (discussed in Esterbauer et al., 1991; Ayala et al., 2014; Gaschler and Stockwell, 2017). Some of these are stable, and can diffuse through cell membrane affecting membrane functions, such as lipid-lipid interactions, ion gradients, fluidity and permeability, thus, causing a major issue for cell homeostasis (Skouta et al., 2014; Van der Paal et al., 2016; Agmon and Stockwell, 2017; Agmon et al., 2018). Other RLS, e.g., 5-deoxy-delta-12,14-prostaglandin J₂ (15d-PGJ₂), signal intracellular receptor PPAR- γ to mediate resolution of inflammation (Agmon and Stockwell, 2017). There is scarce evidence regarding the generation of RLS and their role in *T. cruzi*; though some investigators have reported that heme-induced ROS elicited lipid peroxidation, 4-hydroxy-2-nonenal (4-HNE) adducts, and yet it supported epimastigotes' proliferation (Nogueira et al., 2011).

Proteins are also major targets of oxidation due to their high concentration and reactivity with multiple oxidants (reviewed in Davies, 2016). Proteins may undergo oxidative modifications that are reversible (e.g., sulfenylation, nitrosylation, or S-glutathionylation of cysteine residue) or irreversible (e.g., protein carbonylation and 3-nitrotyrosine formation); and these oxidative modifications can affect protein function or protein-protein interaction (Cai and Yan, 2013). Alternatively, self-protein oxidative modifications could be exploited by the parasite for signaling various pathways. Indeed, it was shown that in presence of extracellular matrix that constitute the cell surrounding layer crossed by the parasite for invasion of host cells, pathogen undergoes selective S-nitrosylation and tyrosine nitration (Pereira et al., 2015). These authors proposed that *T. cruzi* actively modulates its nitrosylation allowing its internalization into host cells.

²Drugs for Neglected Diseases initiative (DNDi); <https://www.dndi.org/achievements/paediatric-benznidazole/>

In summary, the complete extent of the effects of ROS/RNS on *T. cruzi* is not fully disclosed. Yet, the killing of *T. cruzi* by oxidative stress in immune cells and the generation of DNA-toxic glyoxal and oxidative adducts by BZ are well-documented (Maya et al., 2003; Wilkinson et al., 2011). Thus, the antioxidant enzymes expressed by *T. cruzi* are essential for providing defense against oxidative damage and allow the parasite to thrive in oxidative conditions, discussed below.

A DISTINCTIVE ANTIOXIDANT SYSTEM IN PARASITIC PROTOZOANS

Trypanothione (T[SH]₂), a Unique Derivative of Glutathione

T. cruzi antioxidant machinery relies on a low molecular weight diglutathionyl-spermidine conjugate named T[SH]₂ that is analogous to glutathione (GSH) in most eukaryotes (Manta et al., 2013) (Table 1). The production and consumption of T[SH]₂ antioxidant is increased in bloodstream and intracellular stages of the parasite (Ariyanayagam and Fairlamb, 2001; Ariyanayagam et al., 2003). Firstly, biosynthesis of GSH substrate in protozoan parasites is catalyzed by two enzymes. Gamma-glutamylcysteine synthetase (GshA) ligates L-glutamate and L-cysteine to form γ -glutamylcysteine; and in a second step glutathione synthetase (GshB) forms a C-N bond between γ -glutamylcysteine and L-glycine to produce GSH. The fluctuating concentrations of GSH in human patient's plasma and the significant decrease in plasma GSH levels in seropositive patients (Dhiman et al., 2013) suggest that *T. cruzi* synthesizes its own GSH as well as utilizes host's GSH to supply the needed substrate for T[SH]₂ production. Next, the trypanothione synthetase (TryS) enzyme catalyzes an ATP-dependent two-step reaction in which two GSH molecules and a polyamine (spermidine) are used to synthesize T[SH]₂ in cytosol of the parasite (Oza et al., 2002). The T[SH]₂ molecules deliver reducing equivalents to peroxidases and other enzymes responsible for neutralizing ROS, and the oxidized form of trypanothione is reduced by trypanothione reductase (TryR) in presence of NADPH produced by the pentose phosphate pathway (PPP) (discussed below and reviewed in Irigoín et al., 2008). Considering their essential function in maintaining reduced T[SH]₂, TryS, and TryR are attractive drug targets for control of trypanosomes.

The redox potentials of T[SH]₂ (2,242 mV) and GSH (2,230 mV) are very similar, though T[SH]₂ (pKa 7.4) and GSH (pKa 8.7) exhibit dramatic differences in their pKa values (Moutiez et al., 1994). Since rate constants for thiol-disulfide exchange is optimal when the thiol pKa value is equal to the solution pH value, T[SH]₂ is more reactive than GSH under physiological conditions. Furthermore, dithiols are kinetically superior than the monothiol (Dormeyer et al., 2001) in reducing intramolecular disulfides (Table 1). Thus, it is believed that T[SH]₂ serves as a major antioxidant molecule in trypanosomes and GSH is primarily consumed to produce T[SH]₂ in *T. cruzi* (Olin-Sandoval et al., 2012).

Besides T[SH]₂ and GSH, insect stage epimastigotes utilize a significant amount of N1-methyl-4-mercaptosthistidine or ovothiol A as antioxidant. Ovothiol A has non-enzymatic

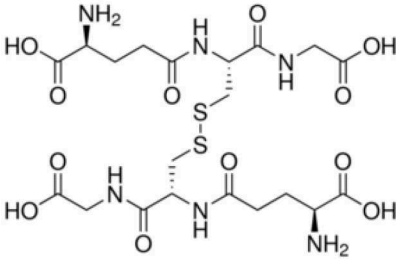
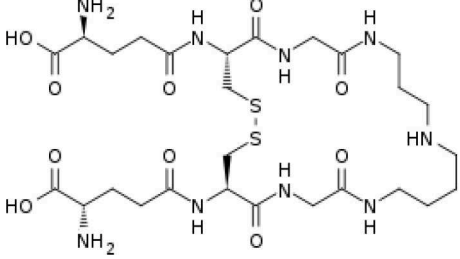
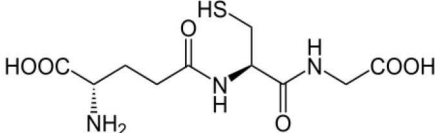
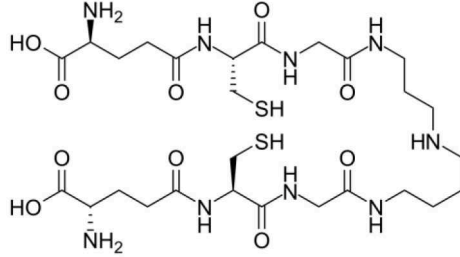
reactivity with H₂O₂; yet its neutralizing activity is considerably less than that of T[SH]₂. Therefore, under physiological conditions, it is unlikely that ovothiol A plays a major role in the metabolism of hydrogen peroxide (Ariyanayagam and Fairlamb, 2001). *T. cruzi* also possesses significant levels of vitamin C (ascorbate) antioxidant. Unlike humans and other vertebrates, parasite genome encodes for complete ascorbate biosynthesis pathway, and it is speculated to be localized in glycosome (Wilkinson et al., 2005) and serve as an alternative ROS scavenger in *T. cruzi* and other trypanosomes (Wilkinson et al., 2002a).

A Network of Antioxidant Enzymes in *T. cruzi*

Trypanosomes utilize a highly developed network of peroxidases and superoxide dismutases to control ROS and RNS (reviewed in Irigoín et al., 2008; Piacenza et al., 2009a; Machado-silva et al., 2016). Briefly, trypanosomes have equipped their mitochondria, the site of electron release to oxygen and O₂•⁻ formation, with a solid antioxidant defense. These include (a) two iron-dependent, superoxide dismutases (FeSODA and FeSODC) that convert O₂•⁻ into H₂O₂; and (b) a two-cysteine mitochondrial tryparedoxin peroxidase (mTXNPx) capable of rapidly detoxifying H₂O₂ and ONOO⁻ (Ismail et al., 1997; Piñeyro et al., 2011a; Phan et al., 2015). The endoplasmic reticulum (ER) utilizes oxidizing environment for the formation of the disulfide bonds required for the folding of proteins into functionally active forms (Malhotra and Kaufman, 2007). Persistent oxidative stress can result in protein unfolding and cell death (Sano and Reed, 2013). Whether trypanosomes face excessive oxidative stress in the ER is not experimentally documented, yet two distinct peroxidases are localized in the ER in *T. cruzi*, namely, ascorbate peroxidase (APx) that utilizes ascorbate to remove H₂O₂, and non-selenium glutathione peroxidase II (nsGPx-II) that detoxifies hydroperoxides (Wilkinson et al., 2002c). Others have shown that APx is localized on the ER and mitochondrial membranes in all parasites stages but also on plasma membrane in infective stages (Hugo et al., 2017), thus implying that APx may play a role during parasite invasion. Similarly, trypanosomes utilize a highly specialized peroxisome, labeled as glycosome, for important metabolic functions, including glycolytic pathway, pentose-phosphate pathway, β -oxidation of fatty acids, purine salvage, and biosynthetic pathways for pyrimidines, ether-lipids and squalenes (Haanstra et al., 2016). Accordingly, *T. cruzi* has evolved to localize FeSODB2 and nsGPx-I antioxidant enzymes in the glycosomal compartment (Wilkinson et al., 2000, 2002b; Patel et al., 2010). It was demonstrated that nsGPxs do not metabolize H₂O₂, yet, nsGPx-I and -II overexpression in trypanosomes conferred protection from exogenous H₂O₂, thus suggesting their role in detoxifying the secondary products of lipid peroxidation reactions (Wilkinson and Kelly, 2003). However, the relevance of nsGPx in the infective stage of *T. cruzi* is unknown.

Finally, cytosolic tryparedoxin peroxidase (cTXNPx), FeSODB1, and GPx-I maintain the redox balance in parasite's cytoplasm. Experiments with recombinant enzyme and FeSOD-overexpressing parasites revealed its importance in virulence and pathogenicity, safeguarding the parasite from host-derived

TABLE 1 | Trypanothione and glutathione are the major, low MW thiols utilized by *T. cruzi* to keep redox homeostasis.

	Glutathione	Trypanothione
A. Chemical structure		
Oxidized state:		
Reduced state:		
B. Enzymes involved	GshA and GshB	TryS
C. Substrates	ATP L-Glutamate L-Cysteine L-Glycine	ATP Spermidine GSH (*possibly synthesized by parasite)
D. Reduction coefficient (Fairlamb and Cerami, 1992)	$E_o = -0.230$	$E_o = -0.242 \text{ V}$
E. pKa (Moutiez et al., 1994)	8.7	7.4
F. Concentration	1 mM in blood (Richie et al., 1996). 6.9 mM in intracellular milieu of HeLa cells (Montero et al., 2013)	0.12–0.64 nmol/10 ⁸ epimastigotes; 0.25–0.95 nmol/10 ⁸ bloodstream trypomastigotes; 0.12 nmol/10 ⁸ amastigotes (Ariyanayagam and Fairlamb, 2001; Ariyanayagam et al., 2003)

Glutathione (ubiquitous monothiol among eukaryotes) and trypanothione (a kinetoplastid-specific dithiol) are synthesized by parasites' antioxidant machinery, and these molecules play a key role in distribution of reducing equivalents along the antioxidant network. Even when they have similar characteristics, $T[SH]_2$ is considered a kinetically superior antioxidant.

cytotoxic oxidants (Piacenza et al., 2008; Arias et al., 2013; Martínez et al., 2019). The expression levels of cTXNPx as well as of mTXNPx are increased in infective and intracellular stages of the parasite (Zago et al., 2016); these two enzymes work in concert to control the cytosolic and mitochondrial oxidative stress (De Figueiredo Peloso et al., 2011), and are extensively studied for the design of anti-parasite therapies. Lastly, annotation of the parasite genome has revealed that *T. cruzi* lacks catalase, glutathione reductase, thioredoxin reductase, and selenium-dependent glutathione peroxidases (El-Sayed et al., 2005).

Tryparedoxin Intermediates

An important mediator for the $T[SH]_2$ -fuelled redox reactions is the dithiol protein and oxidoreductase named tryparedoxin

(TXN) (Lopez et al., 2000). In *T. cruzi*, two isoforms TXN-I and TXN-II, have been identified. TXNs are considered members of the thioredoxin family of proteins based on the comparative sequence analysis, presence of common motif WCPPC of the oxidoreductase superfamily in their catalytic center and some other features that are conserved throughout this type of oxidoreductases. However, TXNs display many differences from the host thioredoxins, and are considered to be unique proteins of trypanosomatids and appropriate targets for anti-parasite drug design (Comini et al., 2007). TXNs transfer reducing equivalents from $T[SH]_2$ to redox pathway that include cTXNPx, mTXNPx, and nsGPx-I involving thiol/disulfide exchange (reviewed in Arias et al., 2013). In *T. cruzi*, TXN-I is localized in cytosol, and TXN-II is anchored to outer membrane of mitochondria, ER, and glycosomes via a C-terminal hydrophobic tail (Arias et al., 2013). TXN-II is also

able to transfer reducing equivalents to low molecular weight disulfides (e.g., GSSG, cystine, dehydroascorbate) and catalyze the reduction of S-nitrosoglutathione and S-nitrosocysteine, and thus, regenerate the reduced form of key metabolites in *T. cruzi* (Arias et al., 2013).

Besides their role in oxidant recycling, new possible functions of TXNs were delineated by interactomics. For example, TXN-I was predicted to interact with other oxidative metabolism components, cysteine and methionine related pathways, as well as protein translation and degradation partners (Piñeyro et al., 2011b). For TXN-II, different interactors were identified under physiological and oxidative stress conditions, and it was suggested to influence the proteins involved in energy metabolism and cytoskeleton and protein translation (Arias et al., 2015; Dias et al., 2018). Further studies will be required to demonstrate the biological significance of TXNs in *T. cruzi* adaptation to different environmental conditions imposed by its life cycle.

REDOX-DEPENDENT PROCESSES

In recent years, several scientists have identified new roles of redox homeostasis. It is suggested that ROS (e.g., H_2O_2) at low levels serve as second messenger, and low MW thiols monitor the cellular redox state and play a decisive role in triggering physiological pathways like programmed cell death and DNA replication (Remacle et al., 1995; Gonzalez-Gonzalez et al., 2017; Lorenzen et al., 2017; Phull et al., 2018). Besides, thiol peroxidases appear to be important players in redox signaling processes. In yeast, it is further demonstrated that these enzymes are involved in active peroxide signal distribution via disulfide exchange (Delaunay et al., 2002; Veal et al., 2004; Okazaki et al., 2005; Iwai et al., 2010). Similarly, in mammals, there are several examples showing that peroxiredoxins (PRDXs) function as peroxide receptors and transduce signal to target protein circuits involved in cell growth, differentiation, apoptosis, and carcinogenesis (Neumann et al., 2003; Han et al., 2005; Edgar et al., 2012; Jarvis et al., 2012; Kil et al., 2012; Sharapov and Novoselov, 2019). Yet, it is not fully elucidated how peroxidase-dependent mechanisms would operate in *T. cruzi*. Despite the knowledge gaps, antioxidant network not only protects the parasite from ROS and RNS, but also supports cellular redox-regulated processes (Figure 2).

Programmed Cell Death (PCD)

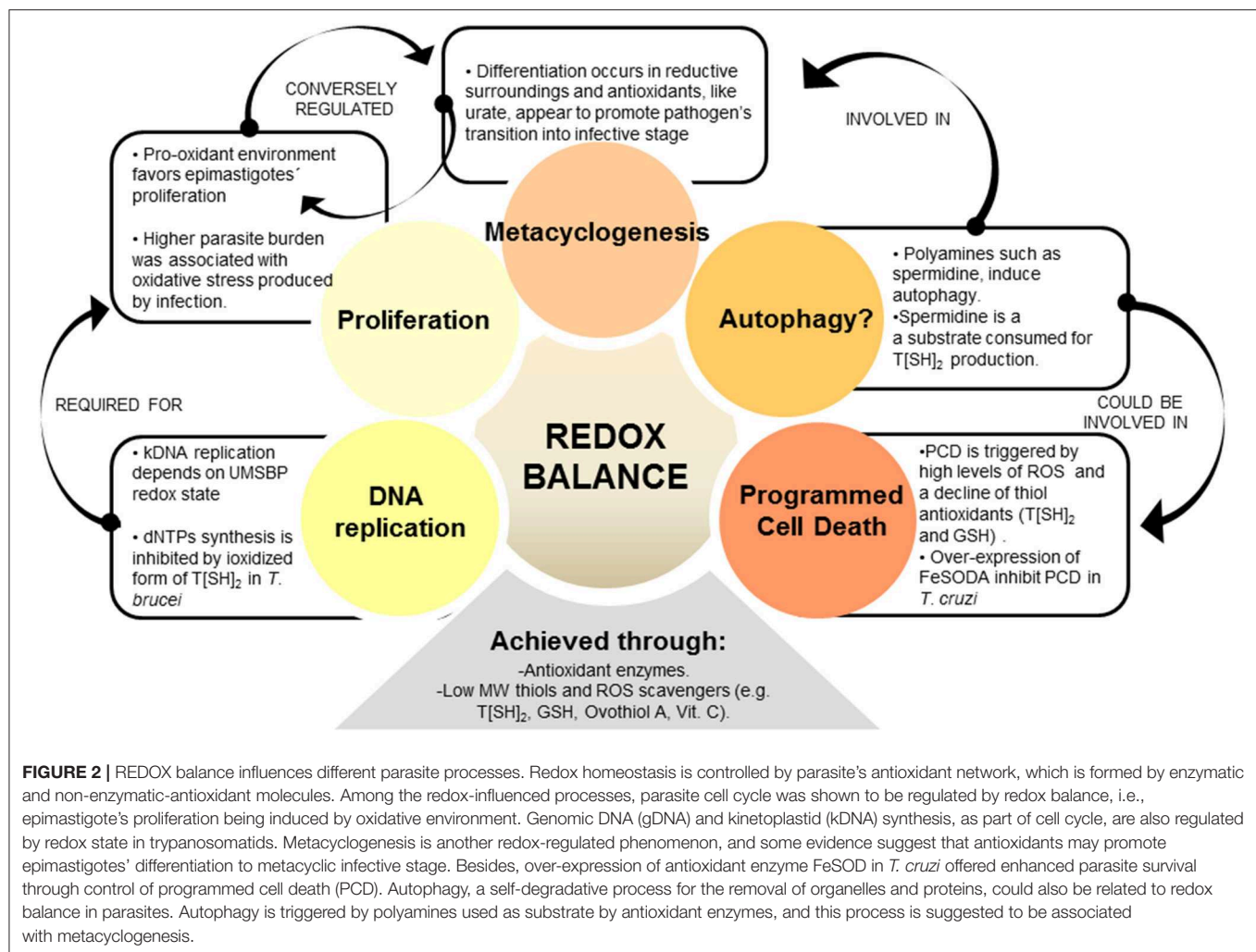
Readers are referred to excellent recent reviews describing the signaling events and methods of cell death in higher eukaryotes (Green and Llamby, 2015; Weinlich et al., 2017; D'Arcy, 2019). Briefly, cell death/cell removal occurs by three main modes: apoptosis (type I), autophagy (type II), and necrosis (type III) (Green and Llamby, 2015). In particular, apoptosis describes the death of a cell mediated by an intracellular program that can be triggered by exogenous or endogenous stimuli. Some common features of apoptosis include (a) translocation of phosphatidylserine to outer side of the plasma membrane, (b) annexin and calreticulin exposure on the cell surface, and (c) morphological changes, including condensation of the cell

cytoplasm, nuclear DNA fragmentation, dissociation of cell organelles, and disruption of the cell plasma membrane. The boundary between type I and type II cell death is not entirely clear; apoptosis may begin with autophagy (or *vice versa*), and blockage of caspase activity may lead to cell death by type II mode than the type I mode. The switch between type I and type III modes of cell death is determined by a variety of factors, discussed elsewhere (Elmore, 2007; Weinlich et al., 2017). Other types of regulated cell death include necroptosis, pyroptosis, ferroptosis, phagoptosis, and entosis (reviewed in D'Arcy, 2019). Moreover, new insights into these processes show that the border between life and death is so tight that some of these unconventional pathways can in fact promote survival. Remarkably, it was also recently described that cells can recover from the brink of apoptosis or necroptosis through new pathways defined as resuscitation and anastasis (Gudipaty et al., 2018).

Trypanosomes exhibit several features of eukaryotic cell apoptosis, including loss of mitochondrial membrane potential, cytochrome c release, cell shrinkage, and DNA fragmentation, although the exact mechanisms involved in PCD of trypanosomatids and its biological relevance is still under debate (De Souza et al., 2010; Dos Anjos et al., 2016; Menna-Barreto, 2019). The classical caspases and Bcl-2 homologs were not found in trypanosomes, but meta-caspases (TcMCA3 and TcMCA5) were described in *T. cruzi* (Laverriere et al., 2012). TcMCA5-overexpressing *T. cruzi* epimastigotes exhibited apoptosis-like phenotype in presence of fresh human serum (Kosec et al., 2006). Further, *T. cruzi* epimastigotes incubated in fresh human serum exhibited a decline in T[SH]₂ and GSH levels, decreased mitochondrial aconitase activity, and increased ROS levels (Piacenza et al., 2007). Others have suggested that complement deposition on parasite membranes leads to assembly of membrane attack complex (MAC) that triggers Ca^{2+} influx/overload, disruption of mitochondrial membrane potential, increase in mtROS production, and release of mitochondrial molecules into cytosol, thus signaling apoptosis and parasite death (Irigoin et al., 2009). Further, a recent study showed that cardiomyocytes produce diffusible redox mediators (e.g., H_2O_2) that promote PCD in amastigotes and control intracellular proliferation of parasite (Estrada et al., 2018). However, the expression of FeSODA antioxidant is increased in infective trypomastigote and replicative amastigote forms (Atwood et al., 2005), and it is possible that parasite utilizes these antioxidants to evade death in the host cells. Indeed, experimental overexpression of FeSODA arrested PCD in *T. cruzi* (Piacenza et al., 2007), thus providing an experimental proof for the relationship between PCD and antioxidant status in *T. cruzi*. Summarizing, these studies suggest that parasite utilizes antioxidant system to survive in the bloodstream and increase its chances to invade and replicate in the cells of a vertebrate host. Future studies will reveal the mechanistic utilization of antioxidant network by *T. cruzi* to prevent its own death in bloodstream and/or in phagocytes and non-immune cells.

Degradation Machineries

Eukaryotic cells utilize autophagy to degrade unwanted, aged or damaged cellular material and release the nutrients (e.g.,



amino acids and nucleotides) for self-preservation. Currently, >40 AuTophagy-related (ATG) proteins and other proteins that participate in autophagy are known (Xie and Klionsky, 2007; Inoue and Klionsky, 2010; Jin and Klionsky, 2014; Kuma et al., 2017). The autophagy pathway involves several steps including, (1) autophagy induction, (2) cargo selection and package, (3) vesicle nucleation, (4) vesicle expansion and completion, (5) retrieval, (6) fusion of the autophagosome with lysosome vacuole, and (7) vesicle breakdown (Zhao and Zhang, 2018). The readers are referred to excellent reviews for further details of this pathway (Xie and Klionsky, 2007; Chun et al., 2018).

In trypanosomes, though genes involved in cargo packaging are not identified, homologs, or orthologs of >50% of the ATG genes have been predicted by genomic searches (Brennand et al., 2012). Several of these, including TOR1 and TOR2 involved in first step of autophagy (Barquilla and Navarro, 2009) and ATG3, ATG4, ATG5, ATG7, ATG10, and ATG12 involved in vesicle expansion and completion step were characterized in trypanosomatids by a gene knock-out approach (reviewed in Brennand et al., 2012). *T. cruzi* epimastigotes subjected to serum deprivation showed autophagic characteristics such as accumulation of monodansylcadaverine-labeled vesicles

and redistribution of TcATG8 (Jimenez et al., 2008). Of the two isoforms of TcATG8 (TcATG8.1 and TcATG8.2), only TcATG8.1 was a *bona fide* ATG8/LC3 homolog that localized in autophagosome-like vesicles in nutrient-starved *T. cruzi* (Alvarez et al., 2008). Vanrell et al. (2017) found that TcATG8.1 expression and mTOR-dependent autophagy were induced during early stages of metacyclogenesis and showed that spermidine and related polyamines positively regulated autophagy and differentiation of epimastigote to metacyclic trypomastigote form (Vanrell et al., 2017). Spermidine is essential for parasite proliferation (González et al., 2001) and it is also a key metabolite used for T[SH]₂ synthesis. Others have shown the peroxide concentrations (vs. antioxidant status) direct the parasite differentiation and metacyclogenesis (Nogueira et al., 2015). Together, these findings suggest that oxidants/antioxidants balance and nutrients availability guide the parasite to induce autophagy and metacyclogenesis, the two closely related processes. Specifically, a fine balance of intracellular spermidine and ROS levels likely determine proliferation, autophagy, differentiation to metacyclic trypomastigote form, as well as antioxidant capacity while the parasite gets ready to enter the mammalian host. How parasite senses spermidine

and ROS levels for such a fine-tuned cell cycle control is still unknown.

Eukaryotic cells also utilize several additional approaches, including ER-associated degradation (ERAD), lysosomal proteases, and 20S proteasome complex to remove the oxidized/degraded proteins (reviewed in Korovila et al., 2017; Hwang and Qi, 2018). Trypanosomes lack an elaborated ERAD network to recycle their proteins (Harbut et al., 2012). Ubiquitin proteasome pathway (UPP)—an alternative system for the turnover of damaged proteins—is expected to be present based on the finding of 269 putative components of the UPP pathway in *T. cruzi* proteome (Gupta et al., 2018). Some of the UPP components are unique to *T. cruzi*, and are proposed to be potential drug targets (Gupta et al., 2018). Specifically, proteasome activity is detected in all life cycle stages of *T. cruzi*, and its inhibition increased the carbonylated protein content, resulting from formation of covalent, non-reversible lipid aldehyde adducts on side chain of cysteine, histidine, and lysine residues. Others have shown that treatment with specific proteasome inhibitors blocked *T. cruzi* growth, metacyclogenesis (Cardoso et al., 2008), and intracellular amastigote-to-trypomastigote differentiation (González et al., 1996). Indeed, proteasome-dependent proteolysis of carbonylated proteins that were extensively present in late log phase epimastigote cultures was suggested to signal metacyclogenesis (Cardoso et al., 2011). Thus, it appears that ROS induction of protein damage and protein degradation machinery might play an important role in parasite development, though further in-depth studies are needed to delineate the mechanistic role of ROS in regulating protein degradation machineries in trypanosomes.

Nucleotides Synthesis and DNA Replication

Cellular DNA synthesis and proliferation, as well as DNA repair mechanisms depend on the production of a balanced supply of deoxyribonucleotides (dNTPs). Ribonucleotide reductases (RNRs) catalyze the *de novo* synthesis of dNTPs from the corresponding ribonucleotides. Though RNRs are highly diverse, their catalytic activity requires peptides harboring a free radical, redox-active thiols, and proteins of the thioredoxin family, and, therefore they are directly influenced by cell redox environment. Indeed, a tight relationship between ROS level and DNA replication is described in higher eukaryotes (Shackelford et al., 2000; Burhans and Heintz, 2009). Macrophage production of NO and NO donors inhibited DNA synthesis, likely through NO-mediated inactivation of critical thiols on R1 subunit and destruction of tyrosyl radical on the R2 subunit of RNRs (Holmgren and Sengupta, 2010). Others showed that increased levels of ROS dissociate replication accelerator-component from the replisome complex and slow down DNA synthesis as a safeguard for genome stability (Somyajit et al., 2017). Importantly, it was shown that peroxiredoxin-2 (PRDX2), an antioxidant enzyme, forms a replisome-associated ROS sensor to regulate the replication machinery (Somyajit et al., 2017), pointing out the relevance of the redox signaling/antioxidant status in dNTP synthesis and DNA replication.

The finding of an inhibitory effect of oxidized forms of T[SH]₂ and tryparedoxin on dNTP synthesis in *T. brucei* (Dormeyer

et al., 2001) offered the initial evidence for a relationship between *de novo* nucleotide synthesis and redox status in trypanosomes. Authors noted that tryparedoxins transfer the reducing energy from T[SH]₂ to RNR enzyme (Dormeyer et al., 2001). In *T. cruzi*, we observed a direct correlation between the intracellular T[SH]₂ content and replication of epimastigotes (Mesias et al., 2018). These observations suggest that T[SH]_{2-red}/T[SH]_{2-ox} ratio, at least partially, regulates the DNA synthesis during parasite proliferation. How the oxidant/antioxidant balance could modulate genomic DNA replication inside parasite nucleus remains to be understood in future studies.

Replication of parasite's kinetoplast DNA (kDNA) is also dependent on redox status. Kinetoplast is a unique DNA structure present in a single large mitochondrion located close to the nucleus of trypanosomatids. Each kinetoplast consists of 10–20 copies of maxicircle DNA (20,000–40,000 bp) and 10,000 or more copies of topologically interlocked minicircle DNA (<1,000 bp). Like mtDNA, maxicircles encode rRNAs and components of the respiratory complexes. The heterogeneous sequences of minicircle DNA encodes guide RNAs that function in mRNA editing process (reviewed in Cavalcanti and De Souza, 2018). The replication of minicircle DNA is a complex mechanism that begins with the attachment of the universal minicircle sequence (UMS), located at the origin of replication of minicircle DNA, with the UMS binding protein (UMSBP), firstly identified in *Crithidia fasciculata* (a related, non-pathogenic trypanosome) (Tzfati et al., 1992) and more recently in *T. cruzi* (Coelho et al., 2003). Recent studies showed that USBBP affinity for target kDNA and oligomerization was sensitive to redox potential in *C. fasciculata* and *Leishmania donovani* (Onn et al., 2004; Singh et al., 2016), and the reduction of USBBP activates its binding to the minicircle DNA origin site, whereas USBBP oxidation impaired this activity. Molecules of the antioxidant network, TXN-II and TXNPx, were found to be involved in governing the oxidized/reduced state of the USBBP in *C. fasciculata* (Sela et al., 2008). Further, deletion of USBBP in *Leishmania* resulted in decreased ATP production associated with reduced complex III activity (Singh et al., 2016), an event that also results in increased electron leakage and superoxide generation in mitochondria (Wong et al., 2017).

Thus, parasite's redox environment, modulated by its antioxidant machinery, regulates dNTP synthesis, kDNA replication, and oxidative phosphorylation that are necessary for trypanosomes proliferation.

POSSIBLE FINE-TUNING MECHANISMS OF *T. CRUZI* ANTIOXIDANT SYSTEM

As discussed above, *T. cruzi* is constantly exposed to ROS and RNS throughout its life cycle and needs to effectively coordinate the antioxidant and repair systems to overcome the toxic effects of oxidative stress. These responses ought to be precise enough to control the effects of the exogenous insult without altering the cellular environment in the parasite, as this can affect other cell signaling pathways. Even more, parasite has to assemble specific responses according to the type of oxidative insult. This section is focused on what we know, and mostly, what we do

not know about how trypanosomes achieve fine-tuning of the antioxidant system.

The unbiased transcriptomic and proteomic approaches have shown that the expression and activity of the enzymes of the antioxidant network are up-regulated in the infective and intracellular stages of *T. cruzi* (Atwood et al., 2005; Parodi-Talice et al., 2007; Zago et al., 2016). At least partly, one regulation layer should reside on stage-specific mechanisms. Ribosome profiling studies have indicated that *T. cruzi*, during the infective metacyclic stage, exerts a translational control through down-regulation of ribosomal components and up-regulation of virulence factors (e.g., trans-sialidases) (Smircich et al., 2015). Recent advances in chromatin proteomics have revealed a substantial association between histone post-translational modifications (PTMs) and stage-specific transition in *T. cruzi* (De Jesus et al., 2016; Picchi et al., 2017) (**Figure 3**). What is more interesting, some of the PTMs of histones were not only novel and unusual, such as alternative lysine acetylation, serine/threonine acetylation, and N-terminal methylation, but also some of these PTMs were unique to *T. cruzi* and other trypanosomes (De Jesus et al., 2016; Picchi et al., 2017). Thus, it is likely that as *T. cruzi* undergoes stage-specific transitions in multiple hosts, it employs histone's modifications to organize chromatin along with the traditional post-transcriptional and translational mechanisms to drive the expression and activity of its antioxidant network. This hypothesis remains to be experimentally proven.

In trypanosomatids, gene expression is not regulated at the transcription initiation level (reviewed in Teixeira and DaRocha, 2003; Martínez-Calvillo et al., 2010; De Gaudenzi et al., 2011). Instead, RNA-binding proteins (RBPs) that associate with mRNAs and other regulatory proteins to form ribonucleoprotein complexes (mRNPs) are suggested to exert post-transcriptional regulation in trypanosomes. There are a wide variety of RBPs, displaying different RNA binding domains, e.g., RNA-recognition motif (RRM), pumilio and Fem-3-binding factor (PUF), as well as zinc fingers (CCCH). Several RBPs were described in *T. cruzi* (Alves and Goldenberg, 2016; Romaniuk et al., 2016), and some were suggested to be involved in stabilization (or destabilization) of mRNA in response to extracellular stimuli (Fernández-Moya et al., 2012; Alves and Goldenberg, 2016). Specifically, RBSR1 and the nuclear SR protein TRRM1 were identified as nutritional stress-related RBPs in *T. cruzi* (Wippel et al., 2018). *T. cruzi* may also employ RBPs to form active or repressive mRNP complexes for post-transcriptional regulation of antioxidant machinery in response to other stress sources.

Other regulation layers may involve the microenvironment within the parasite and the exogenous stimuli present in the host environment. For example, RNA stress granules (SGs) were proposed to regulate gene expression in response to local stress (Protter and Parker, 2016; Khong et al., 2017). SGs are ribonucleoprotein assemblies that incorporate different components depending on the stimuli present (e.g., heat shock, starvation, oxidative stress, etc.) to regulate the post-transcriptional fate of mRNAs (Chen and Liu, 2017; Harvey et al., 2017). These cytoplasmic foci act as traps for dispensable mRNAs, and thereby, prevent new translation initiation until

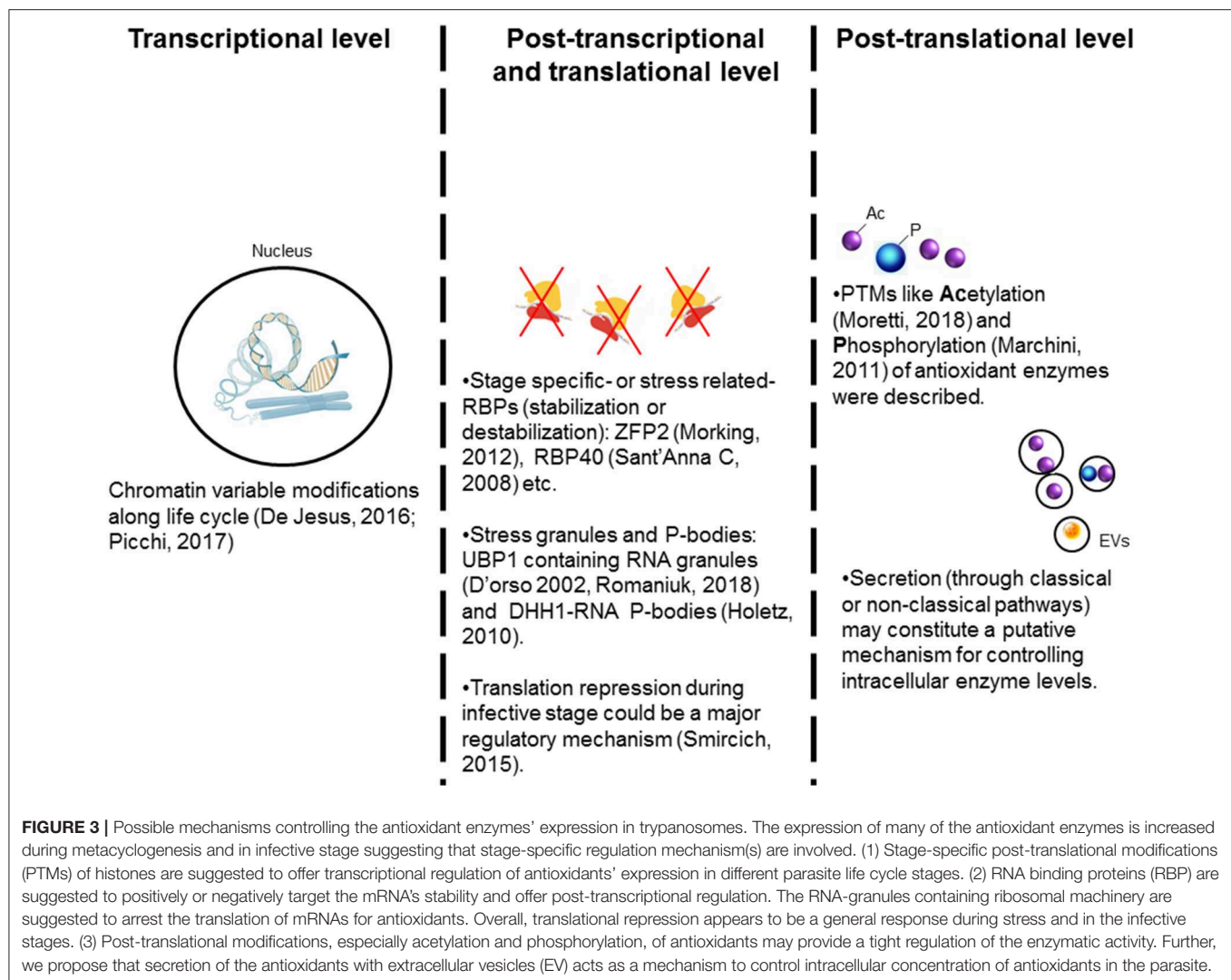
the stress factor(s) have been removed (Rodrigues et al., 2010). The occurrence of mammalian-like SGs and protein synthesis arrest by eIF2 α phosphorylation in response to stress was described in *T. cruzi* (Tonelli et al., 2011). Further, uridine-binding protein 1 and 2 (UBP1 and UB2) that are present in the nucleus in small amounts under normal conditions, may accumulate in the cytoplasm under oxidative stress to form RNA SGs and affect mRNA translation (Cassola et al., 2007). Recent studies have demonstrated UB1-dependent translational repression as a mechanism for stage-specific regulation of gene expression in *T. cruzi* (Romaniuk et al., 2018) (**Figure 3**). DHH1, a DEAD box RNA helicase, is a common component of both SGs and processing bodies (P-bodies, constitutive RNA-granules); and it was described in *T. cruzi* (Holetz et al., 2007). Interestingly, DHH1-containing granules in *T. cruzi* were found to comprise a putative TryS-coding transcript (Holetz et al., 2010), thus indicating that SGs (and P-bodies) may also regulate the antioxidant response in *T. cruzi*.

In higher eukaryotes, phosphorylation, acetylation, and ubiquitination are usually ROS-sensitive PTMs (Liu et al., 2013; Tseng et al., 2014). In *T. cruzi* and other trypanosomatids, PTM-dependent regulation of signaling mechanisms is not studied in detail. Schenkman and co-workers have recently developed the acetylome of *T. cruzi*, and showed that some cytosolic enzymes including antioxidant effectors were continuously acetylated and deacetylated; presumably as a control system for their enzymatic activity or protein-protein interaction (Moretti et al., 2018). Further, a large-scale phosphoproteome analysis study showed that antioxidant enzymes, TryR, TryS, and thiol-dependent reductase 1, are major targets of phosphorylation during the metacyclogenesis transition process (Marchini et al., 2011; Amorim et al., 2017). Thus, PTMs could have a key role in achieving a rapid regulation of antioxidants enzymatic activity as well as in stage-specific modulation of antioxidants expression. Additionally, some antioxidant enzymes are actively secreted by the infective stages of *T. cruzi* (Bayer-santos et al., 2013; Gadelha et al., 2013), and parasite may utilize this secretory pathway to regulate the intracellular protein contents.

To sum up, parasite must elicit a rapid and precise response toward oxidative stress and maintain redox homeostasis. It appears that diverse mechanisms (i.e., chromatin modification, RBPs, and PTMs) are involved in stage-specific regulation of antioxidant gene expression during metacyclogenesis and in infective/replicative forms of *T. cruzi* (Atwood et al., 2005; Parodi-Talice et al., 2007; Zago et al., 2016). In addition, control strategies (RBPs, stress granules conformation, PTMs) may also be employed to fine-tune the adaptation to microenvironment. Future research will provide precise information regarding the specific regulation processes acting over antioxidant components in each situation.

CONCLUSIONS AND REMARKS

In this review, we have discussed the different oxidative challenges that parasite has to face throughout its life stages, the mechanism(s) employed for controlling this condition, and the



cellular processes influenced by the parasite's intracellular redox environment. Further analysis of the interacting partners of the antioxidant components could give us a deeper knowledge of the pathways depending on redox balance. If we consider the available interactomes in trypanosomes (Piñeyro et al., 2011b; Arias et al., 2015; Peloso et al., 2016), it is clear that antioxidant system is linked to many cellular pathways. It is our hope that future investigations will focus on understanding the crosstalk between antioxidants and other cellular processes and enhance our understanding of the influence of redox balance on *T. cruzi* biology.

Different drugs are assayed for the treatment of ChD and sometimes their trypanocidal activity relies on their ability to produce a redox imbalance over the parasite cell. Indeed, nifurtimox and benznidazole, current drugs administered to treat acute ChD, generate a non-specific oxidative effect over pathogen macromolecules. Conversely, several naturally produced antioxidant compounds (e.g., vitamins B12, C, K3, and catechin) were also shown to have a degree of anti-parasitic effect

(Paveto et al., 2004; Ciccarelli et al., 2012; Desoti et al., 2015). In some cases, the toxic effects of antioxidants were explained as a consequence of ROS increase, produced by the redox cycling process. In other words, antioxidant administration, like pro-oxidants, may lead to a compromising cell redox imbalance controlling parasite spread.

There is no doubt about the relevance of the antioxidant network for rational drug design against trypanosomatids (Piacenza et al., 2009b; Flohé, 2012; Talevi et al., 2018). The deeper knowledge of the mechanisms involved in the regulation of antioxidant responses in the different life cycle stages of the parasite will provide better opportunities for designing new, multi-component, parasite control strategies.

AUTHOR CONTRIBUTIONS

AM conceptualized the study. AM, MZ, and NG searched for literature, wrote the manuscript, reviewed and edited the manuscript.

FUNDING

This work was supported in part by grants from the National Institute of Allergy and Infectious Diseases (R01AI054578; R01AI136031) of the National

Institutes of Health to NG and from National Agency for Scientific and Technological Promotion (ANPYCT) award (PICT 2012-1423) to MZ. AM is the recipient of a postdoctoral fellowship from CONICET.

REFERENCES

- Agmon, E., Solon, J., Bassereau, P., and Stockwell, B. R. (2018). Modeling the effects of lipid peroxidation during ferroptosis on membrane properties. *Sci. Rep.* 8:5155. doi: 10.1038/s41598-018-23408-0
- Agmon, E., and Stockwell, B. R. (2017). Lipid homeostasis and regulated cell death. *Curr. Opin. Chem. Biol.* 39, 83–89. doi: 10.1016/j.cbpa.2017.06.002
- Aguiar, P. H. N., Furtado, C., Repolês, B. M., Ribeiro, G. A., Mendes, I. C., Peloso, E. F., et al. (2013). Oxidative stress and DNA lesions: the role of 8-oxoguanine lesions in *Trypanosoma cruzi* cell viability. *PLoS Negl. Trop. Dis.* 7:e2279. doi: 10.1371/journal.pntd.0002279
- Albajar-Vinas, P., and Jannin, J. (2011). The hidden Chagas disease burden in Europe. *Euro Surveill.* 16:19975. doi: 10.2807/ese.16.38.19975-en
- Alvarez, M. N., Peluffo, G., Piacenza, L., and Radi, R. (2011). Intraphagosomal peroxynitrite as a macrophage-derived cytotoxin against internalized *Trypanosoma cruzi*: consequences for oxidative killing and role of microbial peroxiredoxins in infectivity. *J. Biol. Chem.* 286, 6627–6640. doi: 10.1074/jbc.M110.167247
- Alvarez, V. E., Kosec, G., Sant'Anna, C., Turk, V., Cazzulo, J. J., and Turk, B. (2008). Autophagy is involved in nutritional stress response and differentiation in *Trypanosoma cruzi*. *J. Biol. Chem.* 283, 3454–3464. doi: 10.1074/jbc.M708474200
- Alves, L. R., and Goldenberg, S. (2016). RNA-binding proteins related to stress response and differentiation in protozoa. *World J. Biol. Chem.* 7:78–87. doi: 10.4331/wjbc.v7.i1.78
- Amorim, J. C., Batista, M., Da Cunha, E. S., Lucena, A. C. R., Lima, C. V. D. P., Sousa, K., et al. (2017). Quantitative proteome and phosphoproteome analyses highlight the adherent population during *Trypanosoma cruzi* metacyclogenesis. *Sci. Rep.* 7:9899. doi: 10.1038/s41598-017-10292-3
- Andrews, N. W. (2012). Oxidative stress and intracellular infections: more iron to the fire. *J. Clin. Invest.* 122, 2352–2354. doi: 10.1172/JCI64239
- Arantes, J. M., Pedrosa, M. L., Martins, H. R., Veloso, V. M., de Lana, M., Bahia, M. T., et al. (2007). *Trypanosoma cruzi*: treatment with the iron chelator desferrioxamine reduces parasitemia and mortality in experimentally infected mice. *Exp. Parasitol.* 117, 43–50. doi: 10.1016/j.exppara.2007.03.006
- Arias, D. G., Marquez, V. E., Chiribao, M. L., Gadelha, F. R., Robello, C., Iglesias, A. A., et al. (2013). Redox metabolism in *Trypanosoma cruzi*: functional characterization of trypanodioxins revisited. *Free Radic. Biol. Med.* 63, 65–77. doi: 10.1016/j.freeradbiomed.2013.04.036
- Arias, D. G., Piñeyro, M. D., Iglesias, A. A., Guerrero, S. A., and Robello, C. (2015). Molecular characterization and interactome analysis of *Trypanosoma cruzi* trypanodioxin II. *J. Proteomics* 120, 95–104. doi: 10.1016/j.jprot.2015.03.001
- Ariyanayagam, M. R., and Fairlamb, A. H. (2001). Ovotiol and trypanothione as antioxidants in trypanosomatids. *Mol. Biochem. Parasitol.* 115, 189–198. doi: 10.1016/S0166-6851(01)00285-7
- Ariyanayagam, M. R., Oza, S. L., Mehlert, A., and Fairlamb, A. H. (2003). Bis(glutathionyl)spermine and other novel trypanothione analogues in *Trypanosoma cruzi*. *J. Biol. Chem.* 278, 27612–27619. doi: 10.1074/jbc.M302750200
- Atwood, J. A., Weatherly, D. B., Minning, T. A., Bundy, B., Cavola, C., Oppendoes, F. R., et al. (2005). The *Trypanosoma cruzi* proteome. *Science* 309, 473–476. doi: 10.1126/science.1110289
- Ayala, A., Muñoz, M. F., and Argüelles, S. (2014). Lipid peroxidation: production, metabolism, and signaling mechanisms of malondialdehyde and 4-hydroxy-2-nonenal. *Oxid. Med. Cell. Longev.* 2014:360438. doi: 10.1155/2014/360438
- Azambuja, P., Garcia, E. S., Waniek, P. J., Vieira, C. S., Figueiredo, M. B., Gonzalez, M. S., et al. (2016). *Rhodnius prolixus*: from physiology by Wigglesworth to recent studies of immune system modulation by
- Trypanosoma cruzi* and *Trypanosoma rangeli*. *J. Insect Physiol.* 97, 45–65. doi: 10.1016/j.jinsphys.2016.11.006
- Baker, Z. N., Cobine, P. A., and Leary, S. C. (2017). The mitochondrion: a central architect of copper homeostasis. *Metalomics* 9, 1501–1512. doi: 10.1039/C7MT00221A
- Barollo, M., D'Inca, R., Scarpa, M., Medici, V., Cardin, R., Fries, W., et al. (2004). Effects of iron deprivation or chelation on DNA damage in experimental colitis. *Int. J. Colorectal Dis.* 19, 461–466. doi: 10.1007/s00384-004-0588-2
- Barquilla, A., and Navarro, M. (2009). Trypanosome TOR as a major regulator of cell growth and autophagy. *Autophagy* 5, 256–258. doi: 10.4161/auto.5.2.7591
- Bayer-santos, E., Aguilar-bonavides, C., Rodrigues, S. P., Maur, E., Marques, A. F., Varela-ramirez, A., et al. (2013). Proteomic analysis of *Trypanosoma cruzi* secretome: characterization of two populations of extracellular vesicles and soluble proteins. *J. Proteome Res.* 12, 883–897. doi: 10.1021/pr300947g
- Beard, J. L. (2001). Iron biology in immune function, muscle metabolism and neuronal functioning. *J. Nutr.* 131, 568S–579S. doi: 10.1093/jn/131.2.568S
- Bonney, K. M., Luthringer, D. J., Kim, S. A., Garg, N. J., and Engman, D. M. (2019). Pathology and pathogenesis of Chagas heart disease. *Annu. Rev. Pathol. Mech. Dis.* 14, 020117–043711. doi: 10.1146/annurev-pathol-020117-043711
- Brennand, A., Rico, E., and Michels, P. A. M. (2012). Autophagy in trypanosomatids. *Cells* 1, 346–371. doi: 10.3390/cells1030346
- Bringaud, F., Rivière, L., and Coustou, V. (2006). Energy metabolism of trypanosomatids: adaptation to available carbon sources. *Mol. Biochem. Parasitol.* 149, 1–9. doi: 10.1016/j.molbiopara.2006.03.017
- Burhans, W. C., and Heintz, N. H. (2009). The cell cycle is a redox cycle: linking phase-specific targets to cell fate. *Free Radic. Biol. Med.* 47, 1282–1293. doi: 10.1016/j.freeradbiomed.2009.05.026
- Cai, Z., and Yan, L. J. (2013). Protein oxidative modifications: beneficial roles in disease and health. *J. Biochem. Pharmacol. Res.* 1, 15–26.
- Cardillo, F., De Pinho, R. T., Antas, P. R. Z., and Mengel, J. (2015). Immunity and immune modulation in *Trypanosoma cruzi* infection. *Pathog. Dis.* 73:ftv082. doi: 10.1093/femspd/ftv082
- Cardoso, J., de Paula Lima, C., Leal, T., Gradia, D. F., Fragosio, S. P., Goldenberg, S., et al. (2011). Analysis of proteasomal proteolysis during the *in vitro* metacyclogenesis of *Trypanosoma cruzi*. *PLoS ONE* 6:e21027. doi: 10.1371/journal.pone.0021027
- Cardoso, J., Soares, M. J., Menna-Barreto, R. F. S., Le Bloas, R., Sotomaior, V., Goldenberg, S., et al. (2008). Inhibition of proteasome activity blocks *Trypanosoma cruzi* growth and metacyclogenesis. *Parasitol. Res.* 103, 941–951. doi: 10.1007/s00436-008-1081-6
- Cassola, A., De Gaudenzi, J. G., and Frasch, A. C. (2007). Recruitment of mRNAs to cytoplasmic ribonucleoprotein granules in trypanosomes. *Mol. Microbiol.* 65, 655–670. doi: 10.1111/j.1365-2958.2007.05833.x
- Castro, D. P., Moraes, C. S., Gonzalez, M. S., Ratcliffe, N. A., Azambuja, P., and Garcia, E. S. (2012). *Trypanosoma cruzi* immune response modulation decreases microbiota in *Rhodnius prolixus* gut and is crucial for parasite survival and development. *PLoS ONE* 7:e36591. doi: 10.1371/journal.pone.0036591
- Cavalcanti, D. P., and De Souza, W. (2018). The kinetoplast of trypanosomatids: from early studies of electron microscopy to recent advances in atomic force microscopy. *Scanning* 2018:9603051. doi: 10.1155/2018/9603051
- Cazzulo, J. J. (1984). Protein and amino acid catabolism in *Trypanosoma cruzi*. *Comp. Biochem. Physiol. B* 79, 309–320. doi: 10.1016/0305-0491(84)90381-X
- Chen, L., and Liu, B. (2017). Relationships between stress granules, oxidative stress, and neurodegenerative diseases. *Oxid. Med. Cell. Longev.* 2017, 1–10. doi: 10.1155/2017/1809592

- Cheng, K., Cahill, D., Kasai, H., Nishimura, S., and Loeb, L. (1992). 8-Hydroxyguanine, an abundant form of oxidative DNA damage, causes G—T and A—C substitutions. *J. Biol. Chem.* 267, 166–172.
- Chun, Y., Kim, J., Chun, Y., and Kim, J. (2018). Autophagy: an essential eegradation program for cellular homeostasis and life. *Cells* 7:278. doi: 10.3390/cells7120278
- Ciccarelli, A. B., Frank, F. M., Puente, V., Malchiodi, E. L., Batlle, A., and Lombardo, M. E. (2012). Antiparasitic effect of vitamin B12 on *Trypanosoma cruzi*. *Antimicrob. Agents Chemother.* 56, 5315–5320. doi: 10.1128/AAC.00481-12
- Coelho, E. R., Ürményi, T. P., Da Silveira, J. F., Rondinelli, E., and Silva, R. (2003). Identification of PDZ5, a candidate universal minicircle sequence binding protein of *Trypanosoma cruzi*. *Int. J. Parasitol.* 33, 853–858. doi: 10.1016/S0020-7519(03)00107-3
- Comini, M. A., Krauth-Siegel, R. L., and Flohé, L. (2007). Depletion of the thioredoxin homologue tryparedoxin impairs antioxidative defence in African trypanosomes. *Biochem. J.* 402, 43–49. doi: 10.1042/BJ20061341
- Cunha-Neto, E., Dzau, V. J., Allen, P. D., Stamatiou, D., Benvenuti, L., Higuchi, M. L., et al. (2005). Cardiac gene expression profiling provides evidence for cytokinopathy as a molecular mechanism in Chagas' disease cardiomyopathy. *Am. J. Pathol.* 167, 305–313. doi: 10.1016/S0002-9440(10)62976-8
- Curtis-Robles, R., Meyers, A. C., Auckland, L. D., Zecca, I. B., Skiles, R., and Hamer, S. A. (2018). Parasitic interactions among *Trypanosoma cruzi*, triatomine vectors, domestic animals, and wildlife in Big Bend National Park along the Texas-Mexico border. *Acta Trop.* 188, 225–233. doi: 10.1016/j.actatropica.2018.09.002
- Curtis-Robles, R., Snowden, K. F., Dominguez, B., Dinges, L., Rodgers, S., Mays, G., et al. (2017). Epidemiology and molecular typing of *Trypanosoma cruzi* in naturally-infected hound dogs and associated triatomine vectors in Texas, USA. *PLoS Negl. Trop. Dis.* 11:e0005298. doi: 10.1371/journal.pntd.0005298
- D'Arcy, M. S. (2019). Cell death: a review of the major forms of apoptosis, necrosis and autophagy. *Cell Biol. Int.* 43, 582–592. doi: 10.1002/cbin.11137
- David, S. S., O'Shea, V. L., and Kundu, S. (2007). Base excision repair of oxidative DNA damage. *Nature* 447, 941–950. doi: 10.1038/nature05978
- Davies, M. J. (2016). Protein oxidation and peroxidation. *Biochem. J.* 473, 805–825. doi: 10.1042/BJ20151227
- De Figueiredo Peloso, E., Vitor, S. C., Ribeiro, L. H. G., Piñeyro, M. D., Robello, C., and Gadelha, F. R. (2011). Role of *Trypanosoma cruzi* peroxiredoxins in mitochondrial bioenergetics. *J. Bioenerg. Biomembr.* 43, 419–424. doi: 10.1007/s10863-011-9365-4
- De Gaudenzi, J. G., Noé, G., Campo, V. A., Frasch, A. C., and Cassola, A. (2011). Gene expression regulation in trypanosomatids. *Essays Biochem.* 51, 31–46. doi: 10.1042/bse0510031
- De Jesus, T. C. L., Nunes, V. S., Lopes, M. D. C., Martil, D. E., Iwai, L. K., Moretti, N. S., et al. (2016). Chromatin proteomics reveals variable histone modifications during the life cycle of *Trypanosoma cruzi*. *J. Proteome Res.* 15, 2039–2051. doi: 10.1021/acs.jproteome.6b00208
- de Oliveira, T. B., Pedrosa, R. C., and Filho, D. W. (2007). Oxidative stress in chronic cardiopathy associated with Chagas disease. *Int. J. Cardiol.* 116, 357–363. doi: 10.1016/j.ijcard.2006.04.046
- De Souza, E. M., Nefertiti, A. S. G., Bailly, C., Lansiaux, A., and Soeiro, M. N. C. (2010). Differential apoptosis-like cell death in amastigote and trypomastigote forms from *Trypanosoma cruzi*-infected heart cells *in vitro*. *Cell Tissue Res.* 341, 173–180. doi: 10.1007/s00441-010-0985-5
- Delaunay, A., Pflieger, D., Barrault, M. B., Vinh, J., and Toledano, M. B. (2002). A thiol peroxidase is an H₂O₂ receptor and redox-transducer in gene activation. *Cell* 111, 471–481. doi: 10.1016/S0092-8674(02)01048-6
- Desoti, V. C., Lazarin-Bidóia, D., Ribeiro, F. M., Martins, S. C., Da Silva Rodrigues, J. H., Ueda-Nakamura, T., et al. (2015). The combination of vitamin K3 and vitamin C has synergic activity against forms of *Trypanosoma cruzi* through a redox imbalance process. *PLoS ONE* 10:e0144033. doi: 10.1371/journal.pone.0144033
- Dhiman, M., Coronado, Y. A., Vallejo, C. K., Petersen, J. R., Ejilemele, A., Nuñez, S., et al. (2013). Innate immune responses and antioxidant/oxidant imbalance are major determinants of human Chagas disease. *PLoS Negl. Trop. Dis.* 7:e2364. doi: 10.1371/journal.pntd.0002364
- Dias, L., Peloso, E. F., Leme, A. F. P., Carnielli, C. M., Pereira, C. N., Werneck, C. C., et al. (2018). *Trypanosoma cruzi* tryparedoxin II interacts with different peroxiredoxins under physiological and oxidative stress conditions. *Exp. Parasitol.* 184, 1–10. doi: 10.1016/j.exppara.2017.10.015
- Dormeyer, M., Reckenfelderbäumer, N., Lüdemann, H., and Krauth-Siegel, R. L. (2001). Trypanothione-dependent synthesis of deoxyribonucleotides by *Trypanosoma brucei* ribonucleotide reductase. *J. Biol. Chem.* 276, 10602–10606. doi: 10.1074/jbc.M010352200
- Dos Anjos, D. O., Sobral Alves, E. S., Gonçalves, V. T., Fontes, S. S., Nogueira, M. L., Suarez-Fontes, A. M., et al. (2016). Effects of a novel β -lapachone derivative on *Trypanosoma cruzi*: parasite death involving apoptosis, autophagy and necrosis. *Int. J. Parasitol. Drugs Drug Resist.* 6, 207–219. doi: 10.1016/j.ijpddr.2016.10.003
- Edgar, R. S., Green, E. W., Zhao, Y., Van Ooijen, G., Olmedo, M., Qin, X., et al. (2012). Peroxiredoxins are conserved markers of circadian rhythms. *Nature* 485, 459–464. doi: 10.1038/nature11088
- Elmore, S. (2007). Apoptosis: a review of programmed cell death. *Toxicol. Pathol.* 35, 495–516. doi: 10.1080/01926230701320337
- El-Sayed, N. M., Myler, P. J., Bartholomeu, D. C., Nilsson, D., Aggarwal, G., Tran, A. N., et al. (2005). The genome sequence of *Trypanosoma cruzi*, etiologic agent of Chagas disease. *Science* 309, 409–415. doi: 10.1126/science.1112631
- Engel, J. C., Franke de Cazzulo, B. M., Stoppani, A. O., Cannata, J. J., and Cazzulo, J. J. (1987). Aerobic glucose fermentation by *Trypanosoma cruzi* axenic culture amastigote-like forms during growth and differentiation to epimastigotes. *Mol. Biochem. Parasitol.* 26, 1–10. doi: 10.1016/0166-6851(87)90123-X
- Esterbauer, H., Schaur, R. J., and Zollner, H. (1991). Chemistry and biochemistry of 4-hydroxynonenal, malonaldehyde and related aldehydes. *Free Radic. Biol. Med.* 11, 81–128. doi: 10.1016/0891-5849(91)90192-6
- Estrada, D., Specker, G., Martínez, A., Dias, P. P., Hissa, B., Andrade, L. O., et al. (2018). Cardiomyocyte diffusible redox mediators control *Trypanosoma cruzi* infection: role of parasite mitochondrial iron superoxide dismutase. *Biochem. J.* 475, 1235–1251. doi: 10.1042/BCJ20170698
- Fairlamb, A. H., and Cerami, A. (1992). Metabolism and functions of trypanothione in the *Kinetoplastida*. *Annu. Rev. Microbiol.* 46, 695–729. doi: 10.1146/annurev.mi.46.100192.003403
- Fernández-Moya, S. M., García-Pérez, A., Kramer, S., Carrington, M., and Estévez, A. M. (2012). Alterations in DRBD3 ribonucleoprotein complexes in response to stress in *Trypanosoma brucei*. *PLoS ONE* 7:e48870. doi: 10.1371/journal.pone.0048870
- Ferreira, C. M., Stiebler, R., Saraiva, F. M., Lechuga, G. C., Walter-Nuno, A. B., Bourguignon, S. C., et al. (2018). Heme crystallization in a Chagas disease vector acts as a redox-protective mechanism to allow insect reproduction and parasite infection. *PLoS Negl. Trop. Dis.* 12:e0006661. doi: 10.1371/journal.pntd.0006661
- Flohé, L. (2012). The trypanothione system and its implications in the therapy of trypanosomatid diseases. *Int. J. Med. Microbiol.* 302, 216–220. doi: 10.1016/j.ijmm.2012.07.008
- Flores-Villegas, A. L., Salazar-Schettino, P. M., Córdoba-Aguilar, A., Gutiérrez-Cabrera, A. E., Rojas-Wastavino, G. E., Bucio-Torres, M. I., et al. (2015). Immune defence mechanisms of triatomines against bacteria, viruses, fungi and parasites. *Bull. Entomol. Res.* 105, 523–532. doi: 10.1017/S0007485315000504
- Fridovich, I. (1995). Superoxide radical and superoxide dismutases. *Annu. Rev. Biochem.* 64, 97–112. doi: 10.1146/annurev.bi.64.070195.000525
- Gadelha, F. R., Gonçalves, C. C., Mattos, E. C., Alves, M. J. M., Piñeyro, M. D., Robello, C., et al. (2013). Release of the cytosolic tryparedoxin peroxidase into the incubation medium and a different profile of cytosolic and mitochondrial peroxiredoxin expression in H₂O₂-treated *Trypanosoma cruzi* tissue culture-derived trypomastigotes. *Exp. Parasitol.* 133, 287–293. doi: 10.1016/j.exppara.2012.12.007
- García, E. S., Genta, F. A., de Azambuja, P., and Schaub, G. A. (2010). Interactions between intestinal compounds of triatomines and *Trypanosoma cruzi*. *Trends Parasitol.* 26, 499–505. doi: 10.1016/j.pt.2010.07.003
- García, E. S., Ratcliffe, N. A., Whitten, M. M., Gonzalez, M. S., and Azambuja, P. (2007). Exploring the role of insect host factors in the dynamics of *Trypanosoma cruzi*-*Rhodnius prolixus* interactions. *J. Insect Physiol.* 53, 11–21. doi: 10.1016/j.jinsphys.2006.10.006

- García, M. C., Guzman, M. L., Himelfarb, M. A., Litterio, N. J., Olivera, M. E., and Jimenez-Kairuz, A. (2018). Preclinical pharmacokinetics of benzimidazole-loaded interpolyelectrolyte complex-based delivery systems. *Eur. J. Pharm. Sci.* 122, 281–291. doi: 10.1016/j.ejps.2018.07.005
- García, M. N., Burroughs, H., Gorchakov, R., Gunter, S. M., Dumonteil, E., Murray, K. O., et al. (2017). Molecular identification and genotyping of *Trypanosoma cruzi* DNA in autochthonous Chagas disease patients from Texas, USA. *Infect. Genet. Evol.* 49, 151–156. doi: 10.1016/j.meegid.2017.01.016
- Gaschler, M. M., and Stockwell, B. R. (2017). Lipid peroxidation in cell death. *Biochem. Biophys. Res. Commun.* 482, 419–425. doi: 10.1016/j.bbrc.2016.10.086
- Genta, F. A., Souza, R. S., Garcia, E. S., and Azambuja, P. (2010). Phenol oxidases from *Rhodnius prolixus*: temporal and tissue expression pattern and regulation by ecdysone. *J. Insect Physiol.* 56, 1253–1259. doi: 10.1016/j.jinsphys.2010.03.027
- Girard, R. M. B. M., Crispim, M., Alencar, M. B., Silber, A. M., Burchmore, R., Schnauffer, A., et al. (2018). Uptake of L-Alanine and its distinct roles in the bioenergetics of *Trypanosoma cruzi*. *mSphere* 3, e00338–18. doi: 10.1128/mSphereDirect.00338-18
- Gonçalves, R. L. S., Barreto, R. F. S. M., Polycarpo, C. R., Gadelha, F. R., Castro, S. L., and Oliveira, M. F. (2011). A comparative assessment of mitochondrial function in epimastigotes and bloodstream trypomastigotes of *Trypanosoma cruzi*. *J. Bioenerg. Biomembr.* 43, 651–661. doi: 10.1007/s10863-011-9398-8
- González, J., Ramalho-Pinto, F. J., Frevert, U., Ghiso, J., Tomlinson, S., Scharfstein, J., et al. (1996). Proteasome activity is required for the stage-specific transformation of a protozoan parasite. *J. Exp. Med.* 184, 1909–1918. doi: 10.1084/jem.184.5.1909
- González, N. S., Huber, A., and Algranati, I. D. (2001). Spermidine is essential for normal proliferation of trypanosomatid protozoa. *FEBS Lett.* 508, 323–326. doi: 10.1016/S0014-5793(01)03091-5
- Gonzalez-Gonzalez, F. J., Chandel, N. S., Jain, M., and Budinger, G. R. S. (2017). Reactive oxygen species as signaling molecules in the development of lung fibrosis. *Transl. Res.* 190, 61–68. doi: 10.1016/j.trsl.2017.09.005
- Graça-Souza, A. V., Maya-Monteiro, C., Paiva-Silva, G. O., Braz, G. R. C., Paes, M. C., Sorgine, M. H. F., et al. (2006). Adaptations against heme toxicity in blood-feeding arthropods. *Insect Biochem. Mol. Biol.* 36, 322–335. doi: 10.1016/j.ibmb.2006.01.009
- Green, D. R., and Llambi, F. (2015). Cell death signaling. *Cold Spring Harb. Perspect. Biol.* 7:a006080. doi: 10.1101/cshperspect.a006080
- Gudipaty, S. A., Conner, C. M., Rosenblatt, J., and Montell, D. J. (2018). Unconventional ways to live and die: cell death and survival in development, homeostasis, and disease. *Annu. Rev. Cell Dev. Biol.* 34, 311–332. doi: 10.1146/annurev-cellbio-100616-060748
- Gupta, I., Aggarwal, S., Singh, K., Yadav, A., and Khan, S. (2018). Ubiquitin Proteasome pathway proteins as potential drug targets in parasite *Trypanosoma cruzi*. *Sci. Rep.* 8:8399. doi: 10.1038/s41598-018-26532-z
- Gupta, S., Bhatia, V., Wen, J., Wu, Y., Huang, M. H., and Garg, N. J. (2009). *Trypanosoma cruzi* infection disturbs mitochondrial membrane potential and ROS production rate in cardiomyocytes. *Free Radic. Biol. Med.* 47, 1414–1421. doi: 10.1016/j.freeradbiomed.2009.08.008
- Gupta, S., Dhiman, M., Wen, J. J., and Garg, N. J. (2011). ROS signalling of inflammatory cytokines during *Trypanosoma cruzi* infection. *Adv. Parasitol.* 76, 153–170. doi: 10.1016/B978-0-12-385895-5.00007-4
- Gutteridge, J. M., and Smith, A. (1988). Antioxidant protection by haemopexin of haem-stimulated lipid peroxidation. *Biochem. J.* 256, 861–5. doi: 10.1042/bj2560861
- Ha, E. M., Oh, C. T., Bae, Y. S., and Lee, W. J. (2005). A direct role for dual oxidase in *Drosophila* gut immunity. *Science* 310, 847–850. doi: 10.1126/science.1117311
- Haanstra, J. R., González-Marciano, E. B., Gualdrón-López, M., and Michels, P. A. M. (2016). Biogenesis, maintenance and dynamics of glycosomes in trypanosomatid parasites. *Biochim. Biophys. Acta* 1863, 1038–1048. doi: 10.1016/j.bbamcr.2015.09.015
- Hall, B. S., Bot, C., and Wilkinson, S. R. (2011). Nifurtimox activation by trypanosomal type I nitroreductases generates cytotoxic nitrile metabolites. *J. Biol. Chem.* 286, 13088–13095. doi: 10.1074/jbc.M111.230847
- Hall, B. S., and Wilkinson, S. R. (2012). Activation of benzimidazole by trypanosomal type I nitroreductases results in glyoxal formation. *Antimicrob. Agents Chemother.* 56, 115–123. doi: 10.1128/AAC.05135-11
- Halliwell, B., and Gutteridge, J. (2015). *Free Radicals in Biology and Medicine*. New York, NY: Oxford University Press.
- Han, Y. H., Kim, H. S., Kim, J. M., Kim, S. K., Yu, D. Y., and Moon, E. Y. (2005). Inhibitory role of peroxiredoxin II (Prx II) on cellular senescence. *FEBS Lett.* 579, 4897–4902. doi: 10.1016/j.febslet.2005.07.049
- Harbut, M. B., Patel, B. A., Yeung, B. K. S., McNamara, C. W., Bright, A. T., Ballard, J., et al. (2012). Targeting the ERAD pathway via inhibition of signal peptide peptidase for antiparasitic therapeutic design. *Proc. Natl. Acad. Sci. U.S.A.* 109, 21486–21491. doi: 10.1073/pnas.1216016110
- Harvey, R., Dezi, V., Pizzinga, M., and Willis, A. E. (2017). Post-transcriptional control of gene expression following stress: the role of RNA-binding proteins. *Biochem. Soc. Trans.* 45, 1007–1014. doi: 10.1042/BST20160364
- Holetz, F. B., Alves, L. R., Probst, C. M., Dallagiovanna, B., Marchini, F. K., Manque, P., et al. (2010). Protein and mRNA content of TcDHH1-containing mRNPs in *Trypanosoma cruzi*. *FEBS J.* 277, 3415–3426. doi: 10.1111/j.1742-4658.2010.07747.x
- Holetz, F. B., Correa, A., Ávila, A. R., Nakamura, C. V., Krieger, M. A., and Goldenberg, S. (2007). Evidence of P-body-like structures in *Trypanosoma cruzi*. *Biochem. Biophys. Res. Commun.* 356, 1062–1067. doi: 10.1016/j.bbrc.2007.03.104
- Holmgren, A., and Sengupta, R. (2010). The use of thiols by ribonucleotide reductase. *Free Radic. Biol. Med.* 49, 1617–1628. doi: 10.1016/j.freeradbiomed.2010.09.005
- Hugo, M., Martínez, A., Trujillo, M., Estrada, D., Mastrogiovanni, M., Linares, E., et al. (2017). Kinetics, subcellular localization, and contribution to parasite virulence of a *Trypanosoma cruzi* hybrid type A heme peroxidase (TcAPx-CcP). *Proc. Natl. Acad. Sci. U.S.A.* 114, E1326–E1335. doi: 10.1073/pnas.1618611114
- Hwang, J., and Qi, L. (2018). Quality control in the endoplasmic reticulum: crosstalk between ERAD and UPR pathways. *Trends Biochem. Sci.* 43, 593–605. doi: 10.1016/j.tibs.2018.06.005
- Inoue, Y., and Klionsky, D. J. (2010). Regulation of macroautophagy in *Saccharomyces cerevisiae*. *Semin. Cell Dev. Biol.* 21, 664–670. doi: 10.1016/j.semcdb.2010.03.009
- Irigoin, F., Cibils, L., Comini, M. A., Wilkinson, S. R., Flohé, L., and Radi, R. (2008). Insights into the redox biology of *Trypanosoma cruzi*: trypanothione metabolism and oxidant detoxification. *Free Radic. Biol. Med.* 45, 733–742. doi: 10.1016/j.freeradbiomed.2008.05.028
- Irigoin, F., Inada, N. M., Fernandes, M. P., Piacenza, L., Gadelha, F. R., Vercesi, A. E., et al. (2009). Mitochondrial calcium overload triggers complement-dependent superoxide-mediated programmed cell death in *Trypanosoma cruzi*. *Biochem. J.* 418, 595–604. doi: 10.1042/BJ20081981
- Ismail, S. O., Paramchuk, W., Skeiky, Y. A. W., Reed, S. G., Bhatia, A., and Gedamu, L. (1997). Molecular cloning and characterization of two iron superoxide dismutase cDNAs from *Trypanosoma cruzi*. *Mol. Biochem. Parasitol.* 86, 187–197. doi: 10.1016/S0166-6851(97)00032-7
- Iwai, K., Naganuma, A., and Kuge, S. (2010). Peroxiredoxin Ahp1 acts as a receptor for alkylhydroperoxides to induce disulfide bond formation in the Cad1 transcription factor. *J. Biol. Chem.* 285, 10597–10604. doi: 10.1074/jbc.M109.090142
- Jarvis, R. M., Hughes, S. M., and Ledgerwood, E. C. (2012). Peroxiredoxin 1 functions as a signal peroxidase to receive, transduce, and transmit peroxide signals in mammalian cells. *Free Radic. Biol. Med.* 53, 1522–1530. doi: 10.1016/j.freeradbiomed.2012.08.001
- Jimenez, V., Paredes, R., Sosa, M. A. M., and Galanti, N. (2008). Natural programmed cell death in *T. cruzi* epimastigotes maintained in axenic cultures. *J. Cell. Biochem.* 105, 688–698. doi: 10.1002/jcb.21864
- Jin, M., and Klionsky, D. J. (2014). Transcriptional regulation of ATG9 by the Pho23-Rpd3 complex modulates the frequency of autophagosome formation. *Autophagy* 10, 1681–1682. doi: 10.4161/autophagy.29641
- Junqueira, C., Caetano, B., Bartholomeu, D., Melo, M., Ropert, C., Rodrigues, M., et al. (2010). The endless race between *Trypanosoma cruzi* and host immunity: lessons for and beyond Chagas disease. *Expert Rev. Mol. Med.* 12:e29. doi: 10.1017/S1462399410001560

- Khong, A., Matheny, T., Jain, S., Mitchell, S. F., Wheeler, J. R., and Parker, R. (2017). The stress granule transcriptome reveals principles of mRNA accumulation in stress granules. *Mol. Cell* 68, 808–820.e5. doi: 10.1016/j.molcel.2017.10.015
- Kil, I. S., Lee, S. K., Ryu, K. W., Woo, H. A., Hu, M. C., Bae, S. H., et al. (2012). Feedback control of adrenal steroidogenesis via H₂O₂-dependent, reversible inactivation of peroxiredoxin III in mitochondria. *Mol. Cell* 46, 584–594. doi: 10.1016/j.molcel.2012.05.030
- Koo, S. J., and Garg, N. J. (2019). Metabolic programming of macrophage functions and pathogens control. *Redox Biol.* 24:101198. doi: 10.1016/j.redox.2019.101198
- Koo, S. J., Szczesny, B., Wan, X., Putluri, N., and Garg, N. J. (2018). Pentose phosphate shunt modulates reactive oxygen species and nitric oxide production controlling *Trypanosoma cruzi* in macrophages. *Front. Immunol.* 9:202. doi: 10.3389/fimmu.2018.00202
- Korovila, I., Hugo, M., Castro, J. P., Weber, D., Höhn, A., Grune, T., et al. (2017). Proteostasis, oxidative stress and aging. *Redox Biol.* 13, 550–567. doi: 10.1016/j.redox.2017.07.008
- Kosec, G., Alvarez, V. E., Agüero, F., Sánchez, D., Dolinar, M., Turk, B., et al. (2006). Metacaspases of *Trypanosoma cruzi*: possible candidates for programmed cell death mediators. *Mol. Biochem. Parasitol.* 145, 18–28. doi: 10.1016/j.molbiopara.2005.09.001
- Kuma, A., Komatsu, M., and Mizushima, N. (2017). Autophagy-monitoring and autophagy-deficient mice. *Autophagy* 13, 1619–1628. doi: 10.1080/15548627.2017.1343770
- Kumar, S., and Bandyopadhyay, U. (2005). Free heme toxicity and its detoxification systems in human. *Toxicol. Lett.* 157, 175–188. doi: 10.1016/j.toxlet.2005.03.004
- Lara, F. A., Sant'Anna, C., Lemos, D., Laranja, G. A. T., Coelho, M. G. P., Reis Salles, I., et al. (2007). Heme requirement and intracellular trafficking in *Trypanosoma cruzi* epimastigotes. *Biochem. Biophys. Res. Commun.* 355, 16–22. doi: 10.1016/j.bbrc.2006.12.238
- Laverrière, M., Cazzulo, J., and Alvarez, V. (2012). Antagonistic activities of *Trypanosoma cruzi* metacaspases affect the balance between cell proliferation, death and differentiation. *Cell Death Differ.* 19, 1358–1369. doi: 10.1038/cdd.2012.12
- Liu, Y. B., Gao, X., Deeb, D., Arbab, A. S., and Gautam, S. C. (2013). Pristimerin induces apoptosis in prostate cancer cells by down-regulating Bcl-2 through ROS-dependent ubiquitin-proteasomal degradation pathway. *J. Carcinog. Mutagen. Suppl.* 6:005. doi: 10.4172/2157-2518.S6-005
- Lopez, J. A., Carvalho, T. U., de Souza, W., Flohé, L., Guerrero, S. A., Montemartini, M., et al. (2000). Evidence for a trypanothione-dependent peroxidase system in *Trypanosoma cruzi*. *Free Radic. Biol. Med.* 28, 767–772. doi: 10.1016/S0891-5849(00)00159-3
- Lopez, M., Tanowitz, H. B., and Garg, N. J. (2018). Pathogenesis of chronic Chagas disease: macrophages, mitochondria, and oxidative stress. *Curr. Clin. Microbiol. Rep.* 5, 45–54. doi: 10.1007/s40588-018-0081-2
- Lorenzen, I., Mullen, L., Bekeschus, S., and Hanschmann, E. M. (2017). Redox regulation of inflammatory processes is enzymatically controlled. *Oxid. Med. Cell. Longev.* 2017:8459402. doi: 10.1155/2017/8459402
- Machado, F. S., Dutra, W. O., Esper, L., Gollob, K. J., Teixeira, M. M., Factor, S. M., et al. (2012). Current understanding of immunity to *Trypanosoma cruzi* infection and pathogenesis of Chagas disease. *Semin. Immunopathol.* 34, 753–770. doi: 10.1007/s00281-012-0351-7
- Machado-silva, A., Cerqueira, P. G., Grazielle-silva, V., Gadelha, F. R., de Peloso, E. F., Teixeira, S. M., et al. (2016). How *Trypanosoma cruzi* deals with oxidative stress: antioxidant defence and DNA repair pathways. *Mutat. Res. Rev. Mutat. Res.* 767, 8–22. doi: 10.1016/j.mrrev.2015.12.003
- Malhotra, J. D., and Kaufman, R. J. (2007). Endoplasmic reticulum stress and oxidative stress: a vicious cycle or a double-edged sword? *Antioxid. Redox Signal.* 9, 2277–2293. doi: 10.1089/ars.2007.1782
- Manta, B., Comini, M., Medeiros, A., Hugo, M., Trujillo, M., and Radi, R. (2013). Trypanothione: a unique bis-glutathionyl derivative in trypanosomatids. *Biochim. Biophys. Acta* 1830, 3199–3216. doi: 10.1016/j.bbagen.2013.01.013
- Marchini, F. K., de Godoy, L. M. F., Rampazzo, R. C. P., Pavoni, D. P., Probst, C. M., Gnad, F., et al. (2011). Profiling the *Trypanosoma cruzi* phosphoproteome. *PLoS ONE* 6:e25381. doi: 10.1371/journal.pone.0025381
- Martínez, A., Prolo, C., Estrada, D., Rios, N., Alvarez, M. N., Piñeyro, M. D., et al. (2019). Cytosolic Fe-superoxide dismutase safeguards *Trypanosoma cruzi* from macrophage-derived superoxide radical. *Proc. Natl. Acad. Sci. U.S.A.* 116, 8879–8888. doi: 10.1073/pnas.1821487116
- Martínez-Calvillo, S., Vizuet-de-Rueda, J. C., Florencio-Martínez, L. E., Manning-Cela, R. G., and Figueroa-Angulo, E. E. (2010). Gene expression in trypanosomatid parasites. *J. Biomed. Biotechnol.* 2010, 1–15. doi: 10.1155/2010/525241
- Maya, J. D., Bollo, S., Nuñez-Vergara, L. J., Squella, J. A., Repetto, Y., Morello, A., et al. (2003). *Trypanosoma cruzi*: effect and mode of action of nitroimidazole and nitrofurant derivatives. *Biochem. Pharmacol.* 65, 999–1006. doi: 10.1016/S0006-2952(02)01663-5
- Maya, J. D., Repetto, Y., Agosin, M., Ojeda, J. M., Tellez, R., Gaule, C., et al. (1997). Effects of nifurtimox and benznidazole upon glutathione and trypanothione content in epimastigote, trypomastigote and amastigote forms of *Trypanosoma cruzi*. *Mol. Biochem. Parasitol.* 86, 101–106. doi: 10.1016/S0166-6851(96)02837-X
- McCord, J. (2004). Iron, free radicals, and oxidative injury. *J. Nutr.* 134, 3171S–3172S. doi: 10.1093/jn/134.11.3171S
- Menna-Barreto, R. F. S. (2019). Cell death pathways in pathogenic trypanosomatids: lessons of (over)kill. *Cell Death Dis.* 10:93. doi: 10.1038/s41419-019-1370-2
- Mesias, A. C., Sasoni, N., Arias, D. G., Brandán, C. P., Orban, O. C. F., Kunick, C., et al. (2018). Trypanothione synthetase confers growth, survival advantage and resistance to anti-protozoal drugs in *Trypanosoma cruzi*. *Free Radic. Biol. Med.* 130:23–34. doi: 10.1016/j.freeradbiomed.2018.10.436
- Michels, P. A. M., Bringaud, F., Herman, M., and Hannaert, V. (2006). Metabolic functions of glycosomes in trypanosomatids. *Biochim. Biophys. Acta* 1763, 1463–1477. doi: 10.1016/j.bbamcr.2006.08.019
- Montero, D., Tachibana, C., Winther, J. R., and Appenzeller-Herzog, C. (2013). Intracellular glutathione pools are heterogeneously concentrated. *Redox Biol.* 1, 508–513. doi: 10.1016/j.redox.2013.10.005
- Moretti, N. S., Cestari, I., Anupama, A., Stuart, K., and Schenkman, S. (2018). Comparative proteomic analysis of lysine acetylation in *Trypanosomes*. *J. Proteome Res.* 17, 374–385. doi: 10.1021/acs.jproteome.7b00603
- Morillo, C. A., Marin-Neto, J. A., Avezum, A., Sosa-Estani, S., Rassi, A., Rosas, F., et al. (2015). Randomized trial of benznidazole for chronic Chagas' cardiomyopathy. *N. Engl. J. Med.* 373, 1295–1306. doi: 10.1056/NEJMoa1507574
- Moutiez, M., Aumercier, M., Teissier, E., Parmentier, B., Tartar, A., and Sergheraert, C. (1994). Reduction of a trisulfide derivative of glutathione by glutathione reductase. *Biochem. Biophys. Res. Commun.* 202, 1380–1386. doi: 10.1006/bbrc.1994.2083
- Mukherjee, S., Belbin, T. J., Spray, D. C., Iacobas, D. A., Weiss, L. M., Kitsis, R. N., et al. (2003). Microarray analysis of changes in gene expression in a murine model of chronic chagasic cardiomyopathy. *Parasitol. Res.* 91, 187–196. doi: 10.1007/s00436-003-0937-z
- Murta, S. M. F., Krieger, M. A., Montenegro, L. R., Campos, F. F. M., Probst, C. M., Ávila, A. R., et al. (2006). Deletion of copies of the gene encoding old yellow enzyme (TcOYE), a NAD(P)H flavin oxidoreductase, associates with *in vitro*-induced benznidazole resistance in *Trypanosoma cruzi*. *Mol. Biochem. Parasitol.* 146, 151–162. doi: 10.1016/j.molbiopara.2005.12.001
- Neumann, C. A., Krause, D. S., Carman, C. V., Das, S., Dubey, D. P., Abraham, J. L., et al. (2003). Essential role for the peroxiredoxin Prdx1 in erythrocyte antioxidant defence and tumour suppression. *Nature* 424, 561–565. doi: 10.1038/nature01819
- Nogueira, N. P., de Souza, C. F., Saraiva, F. M., Sultano, P. E., Dalmau, S. R., Bruno, R. E., et al. (2011). Heme-induced ROS in *Trypanosoma cruzi* activates CaMKII-like that triggers epimastigote proliferation. One helpful effect of ROS. *PLoS ONE* 6:e25935. doi: 10.1371/journal.pone.0025935
- Nogueira, N. P., Saraiva, F. M. S., Oliveira, M. P., Mendonça, A. P. M., Inacio, J. D. F., Almeida-Amaral, E. E., et al. (2017). Heme modulates *Trypanosoma cruzi* bioenergetics inducing mitochondrial ROS production. *Free Radic. Biol. Med.* 108, 183–191. doi: 10.1016/j.freeradbiomed.2017.03.027
- Nogueira, N. P., Saraiva, F. M. S., Sultano, P. E., Cunha, P. R. B. B., Laranja, G. A. T., Justo, G. A., et al. (2015). Proliferation and differentiation of *Trypanosoma cruzi* inside its vector have a new trigger: redox status. *PLoS ONE* 10:e0116712. doi: 10.1371/journal.pone.0116712

- Okazaki, S., Naganuma, A., and Kuge, S. (2005). Peroxiredoxin-mediated redox regulation of the nuclear localization of Yap 1, a transcription factor in budding yeast. *Antioxid. Redox Signal.* 7, 327–334. doi: 10.1089/ars.2005.7.327
- Olin-Sandoval, V., González-Chávez, Z., Berzunza-Cruz, M., Martínez, I., Jasso-Chávez, R., Becker, I., et al. (2012). Drug target validation of the trypanothione pathway enzymes through metabolic modelling. *FEBS J.* 279, 1811–1833. doi: 10.1111/j.1742-4658.2012.08557.x
- Onn, I., Milman-shtepel, N., and Shlomai, J. (2004). Redox potential regulates binding of universal minicircle sequence binding protein at the kinetoplast DNA replication origin. *Eukaryot. Cell* 3, 277–287. doi: 10.1128/EC.3.2.277-287.2004
- Oza, S. L., Tetaud, E., Ariyanayagam, M. R., Warnon, S. S., and Fairlamb, A. H. (2002). A single enzyme catalyses formation of trypanothione from glutathione and spermidine in *Trypanosoma cruzi*. *J. Biol. Chem.* 277, 35853–35861. doi: 10.1074/jbc.M204403200
- Paes, M. C., Cosentino-Gomes, D., de Souza, C. F., Nogueira, N. P., de, A., and Meyer-Fernandes, J. R. (2011). The role of heme and reactive oxygen species in proliferation and survival of *Trypanosoma cruzi*. *J. Parasitol. Res.* 2011:174614. doi: 10.1155/2011/174614
- Paiva, C. N., Feijó, D. F., Dutra, F. F., Carneiro, V. C., Freitas, G. B., Alves, L. S., et al. (2012). Oxidative stress fuels *Trypanosoma cruzi* infection in mice. *J. Clin. Invest.* 122, 2531–2542. doi: 10.1172/JCI58525
- Paiva, C. N., Medei, E., and Bozza, M. T. (2018). ROS and *Trypanosoma cruzi*: Fuel to infection, poison to the heart. *PLoS Pathog.* 14, 1–19. doi: 10.1371/journal.ppat.1006928
- Parodi-Talice, A., Monteiro-Goes, V., Arrambide, N., Avila, A. R., Duran, R., Correa, A., et al. (2007). Proteomic analysis of metacyclic trypomastigotes undergoing *Trypanosoma cruzi* metacyclogenesis. *J. Mass Spectrom.* 42, 1422–1432. doi: 10.1002/jms.1267
- Patel, S., Hussain, S., Harris, R., Sardiwal, S., Kelly, J. M., Wilkinson, S. R., et al. (2010). Structural insights into the catalytic mechanism of *Trypanosoma cruzi* GPXI (glutathione peroxidase-like enzyme I). *Biochem. J.* 425, 513–522. doi: 10.1042/BJ20091167
- Patterson, S., and Wyllie, S. (2014). Nitro drugs for the treatment of trypanosomatid diseases: past, present, and future prospects. *Trends Parasitol.* 30, 289–298. doi: 10.1016/j.pt.2014.04.003
- Paveto, C., Gu, M. C., Esteve, I., Martino, V., Coussio, J., and Flawia, M. M. (2004). Anti-*Trypanosoma cruzi* activity of green tea (*Camellia sinensis*) catechins. *Antimicrob. Agents Chemother.* 48, 69–74. doi: 10.1128/AAC.48.1.69-74.2004
- Peloso, E. F., Dias, L., Queiroz, R. M. L., Leme, A. F. P. P., Pereira, C. N., Carnielli, C. M., et al. (2016). *Trypanosoma cruzi* mitochondrial trypanothione peroxidase is located throughout the cell and its pull down provides one step towards the understanding of its mechanism of action. *Biochim. Biophys. Acta* 1864, 1–10. doi: 10.1016/j.bbapap.2015.10.005
- Pereira, M., Soares, C., Canuto, G. A. B., Tavares, M. F. M., Colli, W., and Alves, M. J. M. (2015). Down regulation of NO signaling in *Trypanosoma cruzi* upon parasite-extracellular matrix interaction: changes in protein modification by nitrosylation and nitration. *PLoS Negl. Trop. Dis.* 9:e0003683. doi: 10.1371/journal.pntd.0003683
- Pérez-Fuentes, R., Guégan, J. F., Barnabé, C., López-Colombo, A., Salgado-Rosas, H., Torres-Rasgado, E., et al. (2003). Severity of chronic Chagas disease is associated with cytokine/antioxidant imbalance in chronically infected individuals. *Int. J. Parasitol.* 33, 293–299. doi: 10.1016/S0020-7519(02)00283-7
- Phan, I. Q. H., Davies, D. R., Moretti, N. S., Shanmugam, D., Cestari, I., Anupama, A., et al. (2015). Iron superoxide dismutases in eukaryotic pathogens: new insights from *Apicomplexa* and *Trypanosoma* structures. *Acta Crystallogr. Sect. F Struct. Biol. Commun.* 71, 615–621. doi: 10.1107/S2053230X15004185
- Philpott, C. C., Ryu, M. S., Frey, A., and Patel, S. (2017). Cytosolic iron chaperones: proteins delivering iron cofactors in the cytosol of mammalian cells. *J. Biol. Chem.* 292, 12764–12771. doi: 10.1074/jbc.R117.791962
- Phull, A. R. R., Nasir, B., Haq, I. U., and Kim, S. J. (2018). Oxidative stress, consequences and ROS mediated cellular signaling in rheumatoid arthritis. *Chem. Biol. Interact.* 281, 121–136. doi: 10.1016/j.cbi.2017.12.024
- Piacenza, L., Alvarez, M. N. M., Peluffo, G., and Radi, R. (2009a). Fighting the oxidative assault: the *Trypanosoma cruzi* journey to infection. *Curr. Opin. Microbiol.* 12, 415–421. doi: 10.1016/j.mib.2009.06.011
- Piacenza, L., Irigoien, F., Alvarez, M. N., Peluffo, G., Taylor, M. C., Kelly, J. M., et al. (2007). Mitochondrial superoxide radicals mediate programmed cell death in *Trypanosoma cruzi*: cytoprotective action of mitochondrial iron superoxide dismutase overexpression. *Biochem. J.* 403, 323–334. doi: 10.1042/BJ20061281
- Piacenza, L., Peluffo, G., Alvarez, M. N., Kelly, J. M., Wilkinson, S. R., and Radi, R. (2008). Peroxiredoxins play a major role in protecting *Trypanosoma cruzi* against macrophage- and endogenously-derived peroxynitrite. *Biochem. J.* 410, 359–368. doi: 10.1042/BJ20071138
- Piacenza, L., Zago, M. P., Peluffo, G., Alvarez, M. N., Basombrio, M. A., and Radi, R. (2009b). Enzymes of the antioxidant network as novel determiners of *Trypanosoma cruzi* virulence. *Int. J. Parasitol.* 39, 1455–1464. doi: 10.1016/j.ijpara.2009.05.010
- Picchi, G. F. A., Zulkievicz, V., Krieger, M. A., Zanchin, N. T., Goldenberg, S., and De Godoy, L. M. F. (2017). Post-translational modifications of *Trypanosoma cruzi* canonical and variant histones. *J. Proteome Res.* 16, 1167–1179. doi: 10.1021/acs.jproteome.6b00655
- Piñeyro, M. D., Arcari, T., Robello, C., Radi, R., and Trujillo, M. (2011a). Trypanothione peroxidases from *Trypanosoma cruzi*: high efficiency in the catalytic elimination of hydrogen peroxide and peroxynitrite. *Arch. Biochem. Biophys.* 507, 287–295. doi: 10.1016/j.abb.2010.12.014
- Piñeyro, M. D., Parodi-Talice, A., Portela, M., Arias, D. G., Guerrero, S. A., and Robello, C. (2011b). Molecular characterization and interactome analysis of *Trypanosoma cruzi* trypanothione peroxidase 1. *J. Proteomics* 74, 1683–1692. doi: 10.1016/j.jprot.2011.04.006
- Polishchuk, R., and Lutsenko, S. (2013). Golgi in copper homeostasis: a view from the membrane trafficking field. *Histochem. Cell Biol.* 140, 285–295. doi: 10.1007/s00418-013-1123-8
- Protter, D. S. W., and Parker, R. (2016). Principles and properties of stress granules. *Trends Cell Biol.* 26, 668–679. doi: 10.1016/j.tcb.2016.05.004
- Remacle, J., Raes, M., Toussaint, O., Renard, P., and Rao, G. (1995). Low levels of reactive oxygen species as modulators of cell function. *Mutat. Res.* 316, 103–122. doi: 10.1016/0921-8734(95)90004-7
- Richie, J. P., Skowronski, L., Abraham, P., and Leutinger, Y. (1996). Blood glutathione concentrations in a large-scale human study. *Clin. Chem.* 42, 64–70.
- Rigalli, J. P., Perdomo, V. G., Ciriaci, N., Francés, D. E. A., Ronco, M. T., Bataille, A. M., et al. (2016). The trypanocidal benzimidazole promotes adaptive response to oxidative injury: involvement of the nuclear factor-erythroid 2-related factor-2 (Nrf2) and multidrug resistance associated protein 2 (MRP2). *Toxicol. Appl. Pharmacol.* 304, 90–98. doi: 10.1016/j.taap.2016.05.007
- Rios, L. E., Vázquez-Chagoyán, J. C., Pacheco, A. O., Zago, M. P., and Garg, N. J. (2019). Immunity and vaccine development efforts against *Trypanosoma cruzi*. *Acta Trop.* 200:105168. doi: 10.1016/j.actatropica.2019.105168
- Rodrigues, D. C., Silva, R., Rondinelli, E., and Urményi, T. P. (2010). *Trypanosoma cruzi*: modulation of HSP70 mRNA stability by untranslated regions during heat shock. *Exp. Parasitol.* 126, 245–253. doi: 10.1016/j.exppara.2010.05.009
- Rodríguez-Morales, O., Monteón-Padilla, V., Carrillo-Sánchez, S. C., Rios-Castro, M., Martínez-Cruz, M., Carabarin-Lima, A., et al. (2015). Experimental vaccines against Chagas disease: a journey through history. *J. Immunol. Res.* 2015, 1–8. doi: 10.1155/2015/489758
- Romaniuk, M. A., Cervini, G., and Cassola, A. (2016). Regulation of RNA binding proteins in trypanosomatid protozoan parasites. *World J. Biol. Chem.* 7, 146–157. doi: 10.4331/wjbc.v7.i1.146
- Romaniuk, M. A., Frasca, A. C., and Cassola, A. (2018). Translational repression by an RNA-binding protein promotes differentiation to infective forms in *Trypanosoma cruzi*. *PLoS Pathog.* 14:e1007059. doi: 10.1371/journal.ppat.1007059
- Rouault, T. A. (2012). Biogenesis of iron-sulfur clusters in mammalian cells: new insights and relevance to human disease. *Dis. Model. Mech.* 5, 155–164. doi: 10.1242/dmm.009019
- Sánchez, M., Sabio, L., Gálvez, N., Capdevila, M., and Dominguez-Vera, J. M. (2017). Iron chemistry at the service of life. *IUBMB Life* 69, 382–388. doi: 10.1002/iub.1602
- Sano, R., and Reed, J. C. (2013). ER stress-induced cell death mechanisms. *Biochim. Biophys. Acta* 1833, 3460–3470. doi: 10.1016/j.bbamcr.2013.06.028
- Santello, F. H., Frare, E. O., dos Santos, C. D., Toldo, M. P. A., Kawasse, L. M., Zucoloto, S., et al. (2007). Melatonin treatment reduces the severity of experimental *Trypanosoma cruzi* infection. *J. Pineal Res.* 42, 359–363. doi: 10.1111/j.1600-079X.2007.00427.x
- Santos Souza, H. F., Real, D., Leonardi, D., Rocha, S. C., Alonso, V., Serra, E., et al. (2017). Development and *in vitro/in vivo* evaluation of a novel benzimidazole

- liquid dosage form using a quality-by-design approach. *Trop. Med. Int. Health* 22, 1514–1522. doi: 10.1111/tmi.12980
- Scalise, M. L., Arrúa, E. C., Rial, M. S., Esteva, M. I., Salomon, C. J., and Fichera, L. E. (2016). Promising efficacy of benzimidazole nanoparticles in acute *Trypanosoma cruzi* murine model: *in-vitro* and *in-vivo* Studies. *Am. J. Trop. Med. Hyg.* 95, 388–393. doi: 10.4269/ajtmh.15-0889
- Schmunis, G. A. (2007). Epidemiology of Chagas disease in non-endemic countries: the role of international migration. *Mem. Inst. Oswaldo Cruz* 102, 75–85. doi: 10.1590/S0074-02762007005000093
- Sela, D., Yaffe, N., and Shlomai, J. (2008). Enzymatic mechanism controls redox-mediated protein-DNA interactions at the replication origin of kinetoplast DNA minicircles. *J. Biol. Chem.* 283, 32034–32044. doi: 10.1074/jbc.M804417200
- Shackelford, R. E., Kaufmann, W. K., and Paules, R. S. (2000). Oxidative stress and cell cycle checkpoint function. *Free Radic. Biol. Med.* 28, 1387–1404. doi: 10.1016/S0891-5849(00)00224-0
- Shah-Simpson, S., Lentini, G., Dumoulin, P. C., and Burleigh, B. A. (2017). Modulation of host central carbon metabolism and *in situ* glucose uptake by intracellular *Trypanosoma cruzi* amastigotes. *PLoS Pathog.* 13:e1006747. doi: 10.1371/journal.ppat.1006747
- Sharapov, M. G., and Novoselov, V. I. (2019). Catalytic and signaling role of peroxiredoxins in carcinogenesis. *Biochemistry* 84, 79–100. doi: 10.1134/S0006297919020019
- Shoham, S., and Youdim, M. B. H. (2004). Nutritional iron deprivation attenuates kainate-induced neurotoxicity in rats: implications for involvement of iron in neurodegeneration. *Ann. N. Y. Acad. Sci.* 1012, 94–114. doi: 10.1196/annals.1306.008
- Silber, A. M., Tonelli, R. R., Lopes, C. G., Cunha-e-silva, N., Torrecilhas, A. C. T., Schumacher, R. I., et al. (2009). Glucose uptake in the mammalian stages of *Trypanosoma cruzi*. *Mol. Biochem. Parasitol.* 168, 102–108. doi: 10.1016/j.molbiopara.2009.07.006
- Silva, T. M., Peloso, E. F., Vitor, S. C., Ribeiro, L. H. G., and Gadelha, F. R. (2011). O₂ consumption rates along the growth curve: new insights into *Trypanosoma cruzi* mitochondrial respiratory chain. *J. Bioenerg. Biomembr.* 43, 409–417. doi: 10.1007/s10863-011-9369-0
- Singh, R., Purkait, B., Abhishek, K., Saini, S., Das, S., Verma, S., et al. (2016). Universal minicircle sequence binding protein of *Leishmania donovani* regulates pathogenicity by controlling expression of cytochrome - b. *Cell Biosci.* 6:13. doi: 10.1186/s13578-016-0072-z
- Skouta, R., Dixon, S. J., Wang, J., Dunn, D. E., Orman, M., Shimada, K., et al. (2014). Ferrostatins inhibit oxidative lipid damage and cell death in diverse disease models. *J. Am. Chem. Soc.* 136, 4551–4556. doi: 10.1021/ja411006a
- Smircich, P., Eastman, G., Bispo, S., Duhagon, M. A., Guerra-Slompo, E. P., Garat, B., et al. (2015). Ribosome profiling reveals translation control as a key mechanism generating differential gene expression in *Trypanosoma cruzi*. *BMC Genomics* 16:443. doi: 10.1186/s12864-015-1563-8
- Somyajit, K., Gupta, R., Sedlackova, H., Neelsen, K. J., Ochs, F., Rask, M. B., et al. (2017). Redox-sensitive alteration of replisome architecture safeguards genome integrity. *Science* 358, 797–802. doi: 10.1126/science.aao3172
- Souza, C. F., Carneiro, A. B., Silveira, A. B., Laranja, G. A. T., Silva-Neto, M. A. C., Costa, S. C. G., et al. (2009). Heme-induced *Trypanosoma cruzi* proliferation is mediated by CaM kinase II. *Biochem. Biophys. Res. Commun.* 390, 541–546. doi: 10.1016/j.bbrc.2009.09.135
- Sullivan, J. L. (2004). Is stored iron safe? *J. Lab. Clin. Med.* 144, 280–284. doi: 10.1016/j.lab.2004.10.006
- Talevi, A., Carrillo, C., and Comini, M. A. (2018). The thiol-polyamine metabolism of *Trypanosoma cruzi*: molecular targets and drug repurposing strategies. *Curr. Med. Chem.* 25, 6614–6635. doi: 10.2174/0929867325666180926151059
- Tanowitz, H. B., Weiss, L. M., and Montgomery, S. P. (2011). Chagas disease has now gone global. *PLoS Negl. Trop. Dis.* 5:e1136. doi: 10.1371/journal.pntd.0001136
- Teixeira, A. R. L., Gomes, C., Lozzi, S. P., Hecht, M. M., Rosa, A. D. C., Monteiro, P. S., et al. (2009). Environment, interactions between *Trypanosoma cruzi* and its host, and health. *Cad. Saude Publ.* 25(Suppl. 1), S32–S44. doi: 10.1590/S0102-311X2009001300004
- Teixeira, S. M. R., and DaRocha, W. D. (2003). Control of gene expression and genetic manipulation in the *Trypanosomatidae*. *Genet. Mol. Res.* 31, 148–158. Available online at: <http://www.funpecrp.com.br/gmr/year2003/vol1-2/pdf/sim0008.pdf>
- Tonelli, R. R., da Silva Augusto, L., Castilho, B. A., and Schenkman, S. (2011). Protein synthesis attenuation by phosphorylation of eIF2 α is required for the differentiation of *Trypanosoma cruzi* into infective forms. *PLoS ONE* 6:e27904. doi: 10.1371/journal.pone.0027904
- Torres-Silva, C. F., Repolés, B. M., Ornelas, H. O., Macedo, A. M., Franco, G. R., Junho Pena, S. D., et al. (2018). Assessment of genetic mutation frequency induced by oxidative stress in *Trypanosoma cruzi*. *Genet. Mol. Biol.* 41, 466–474. doi: 10.1590/1678-4685-gmb-2017-0281
- Trochine, A., Creek, D. J., Faral-Tello, P., Barrett, M. P., and Robello, C. (2014). Benzimidazole biotransformation and multiple targets in *Trypanosoma cruzi* revealed by metabolomics. *PLoS Negl. Trop. Dis.* 8:e2844. doi: 10.1371/journal.pntd.0002844
- Tseng, A. H. H., Wu, L. H., Shieh, S. S., and Wang, D. L. (2014). SIRT3 interactions with FOXO3 acetylation, phosphorylation and ubiquitinylation mediate endothelial cell responses to hypoxia. *Biochem. J.* 464, 157–168. doi: 10.1042/BJ20140213
- Tzfati, Y., Abeliovich, H., Kapeller, I., and Shlomai, J. (1992). A single-stranded DNA-binding protein from *Crithidia fasciculata* recognizes the nucleotide sequence at the origin of replication of kinetoplast DNA minicircles. *Proc. Natl. Acad. Sci. U.S.A.* 89, 6891–6895. doi: 10.1073/pnas.89.15.6891
- Ursic-Bedoya, R. J., and Lowenberger, C. A. (2007). *Rhodnius prolixus*: identification of immune-related genes up-regulated in response to pathogens and parasites using suppressive subtractive hybridization. *Dev. Comp. Immunol.* 31, 109–120. doi: 10.1016/j.dci.2006.05.008
- Valko, M., Jomova, K., Rhodes, C. J., Kuča, K., and Musilek, K. (2016). Redox- and non-redox-metal-induced formation of free radicals and their role in human disease. *Arch. Toxicol.* 90, 1–37. doi: 10.1007/s00204-015-1579-5
- Van der Paal, J., Neyts, E. C., Verlact, C. C. W., and Bogaerts, A. (2016). Effect of lipid peroxidation on membrane permeability of cancer and normal cells subjected to oxidative stress. *Chem. Sci.* 7, 489–498. doi: 10.1039/C5SC02311D
- Vanrell, M. C., Losinno, A. D., Cueto, J. A., Balcazar, D., Fraccaroli, L. V., Carrillo, C., et al. (2017). The regulation of autophagy differentially affects *Trypanosoma cruzi* metacyclogenesis. *PLoS Negl. Trop. Dis.* 11:e0006049. doi: 10.1371/journal.pntd.0006049
- Veal, E. A., Findlay, V. J., Day, A. M., Bozonet, S. M., Evans, J. M., Quinn, J., et al. (2004). A 2-Cys peroxiredoxin regulates peroxide-induced oxidation and activation of a stress-activated MAP kinase. *Mol. Cell* 15, 129–139. doi: 10.1016/j.molcel.2004.06.021
- Vyatkin, G., Bhatia, V., Gerstner, A., Papaconstantinou, J., and Garg, N. (2004). Impaired mitochondrial respiratory chain and bioenergetics during chagasic cardiomyopathy development. *Biochim. Biophys. Acta* 1689, 162–173. doi: 10.1016/j.bbadis.2004.03.005
- Walker, D. M., Oghumu, S., Gupta, G., McGwire, B. S., Drew, M. E., and Satoskar, A. R. (2013). Mechanisms of cellular invasion by intracellular parasites. *Cell. Mol. Life Sci.* 71, 1245–1263. doi: 10.1007/s00018-013-1491-1
- Wan, X., Gupta, S., Zago, M. P., Davidson, M. M., Dousset, P., Amoroso, A., et al. (2012). Defects of mtDNA replication impaired mitochondrial biogenesis during *Trypanosoma cruzi* infection in human cardiomyocytes and chagasic patients: the role of Nrf1/2 and antioxidant response. *J. Am. Heart Assoc.* 1:e003855. doi: 10.1161/JAHA.112.003855
- Wan, X., Wen, J. J., Koo, S. J., Liang, L. Y., and Garg, N. J. (2016). SIRT1-PGC1 α -NF κ B pathway of oxidative and inflammatory stress during *Trypanosoma cruzi* infection: benefits of SIRT1-targeted therapy in improving heart function in Chagas disease. *PLoS Pathog.* 12:e1005954. doi: 10.1371/journal.ppat.1005954
- Wang, X., and Hai, C. (2016). Novel insights into redox system and the mechanism of redox regulation. *Mol. Biol. Rep.* 43, 607–628. doi: 10.1007/s11033-016-4022-y
- Weinlich, R., Oberst, A., Beere, H. M., and Green, D. R. (2017). Necroptosis in development, inflammation and disease. *Nat. Rev. Mol. Cell Biol.* 18, 127–136. doi: 10.1038/nrm.2016.149
- Wen, J., Yachelini, P. C., Sembaj, A., Manzur, R. E., and Garg, N. J. (2006). Increased oxidative stress is correlated with mitochondrial dysfunction in chagasic patients. *Free Radic. Biol. Med.* 41, 270–276. doi: 10.1016/j.freeradbiomed.2006.04.009
- Wen, J. J., Dhimann, M., Whorton, E. B., and Garg, N. J. (2008). Tissue-specific oxidative imbalance and mitochondrial dysfunction during

- Trypanosoma cruzi* infection in mice. *Microbes Infect.* 10, 1201–1209. doi: 10.1016/j.micinf.2008.06.013
- Wen, J. J., and Garg, N. (2004). Oxidative modification of mitochondrial respiratory complexes in response to the stress of *Trypanosoma cruzi* infection. *Free Radic. Biol. Med.* 37, 2072–2081. doi: 10.1016/j.freeradbiomed.2004.09.011
- Wen, J. J., Porter, C., and Garg, N. J. (2017). Inhibition of NFE2L2-antioxidant response element pathway by mitochondrial reactive oxygen species contributes to development of cardiomyopathy and left ventricular dysfunction in Chagas disease. *Antioxid. Redox Signal.* 27, 550–566. doi: 10.1089/ars.2016.6831
- Whitten, M., Sun, F., Tew, I., Schaub, G., Soukou, C., Nappi, A., et al. (2007). Differential modulation of *Rhodnius prolixus* nitric oxide activities following challenge with *Trypanosoma rangeli*, *T. cruzi* and bacterial cell wall components. *Insect Biochem. Mol. Biol.* 37, 440–452. doi: 10.1016/j.ibmb.2007.02.001
- Whitten, M. M., Mello, C. B., Gomes, S. A., Nigam, Y., Azambuja, P., Garcia, E. S., et al. (2001). Role of superoxide and reactive nitrogen intermediates in *Rhodnius prolixus* (Reduviidae)/*Trypanosoma rangeli* interactions. *Exp. Parasitol.* 98, 44–57. doi: 10.1006/expr.2001.4615
- Wilkinson, S., Obado, S., Mauricio, I., and Kelly, J. (2002a). *Trypanosoma cruzi* expresses a plant-like ascorbate-dependent hemoperoxidase localized to the endoplasmic reticulum. *Proc. Natl. Acad. Sci. U.S.A.* 99, 13453–13458. doi: 10.1073/pnas.202422899
- Wilkinson, S. R., Bot, C., Kelly, J. M., and Hall, B. S. (2011). Trypanocidal activity of nitroaromatic prodrugs: current treatments and future perspectives. *Curr. Top. Med. Chem.* 11, 2072–2084. doi: 10.2174/156802611796575894
- Wilkinson, S. R., and Kelly, J. M. (2003). The role of glutathione peroxidases in trypanosomatids. *Biol. Chem.* 384, 517–525. doi: 10.1515/BC.2003.060
- Wilkinson, S. R., Meyer, D. J., and Kelly, J. M. (2000). Biochemical characterization of a trypanosome enzyme with glutathione-dependent peroxidase activity. *Biochem. J.* 352(Pt 3), 755–761. doi: 10.1042/0264-6021:3520755
- Wilkinson, S. R., Meyer, D. J., Taylor, M. C., Bromley, E. V., Miles, M. A., and Kelly, J. M. (2002b). The *Trypanosoma cruzi* enzyme TcGPXI is a glycosomal peroxidase and can be linked to trypanothione reduction by glutathione or tryparedoxin. *J. Biol. Chem.* 277, 17062–17071. doi: 10.1074/jbc.M111126200
- Wilkinson, S. R., Prathalingam, S. R., Taylor, M. C., Horn, D., and Kelly, J. M. (2005). Vitamin C biosynthesis in trypanosomes: a role for the glycosome. *Proc. Natl. Acad. Sci. U.S.A.* 102, 11645–11650. doi: 10.1073/pnas.0504251102
- Wilkinson, S. R., Taylor, M. C., Horn, D., Kelly, J. M., and Cheeseman, I. (2008). A mechanism for cross-resistance to nifurtimox and benznidazole in trypanosomes. *Proc. Natl. Acad. Sci. U.S.A.* 105, 5022–5027. doi: 10.1073/pnas.0711014105
- Wilkinson, S. R., Taylor, M. C., Touitha, S., Mauricio, I. L., Meyer, D. J., and Kelly, J. M. (2002c). TcGPXII, a glutathione-dependent *Trypanosoma cruzi* peroxidase with substrate specificity restricted to fatty acid and phospholipid hydroperoxides, is localized to the endoplasmic reticulum. *Biochem. J.* 364, 787–794. doi: 10.1042/bj20020038
- Winter, W. E., Bazydlo, L. A. L., and Harris, N. S. (2014). The molecular biology of human iron metabolism. *Lab. Med.* 45, 92–102. doi: 10.1309/LMF28S2GIMXNWHMM
- Wippel, H. H., Malgarin, J. S., Martins, S., de, T., Vidal, N. M., Marcon, B. H., et al. (2018). The nuclear RNA-binding protein RBSR1 interactome in *Trypanosoma cruzi*. *J. Eukaryot. Microbiol.* 66, 244–253. doi: 10.1111/jeu.12666
- Wong, H. S., Dighe, P. A., Mezera, V., Monternier, P. A., and Brand, M. D. (2017). Production of superoxide and hydrogen peroxide from specific mitochondrial sites under different bioenergetic conditions. *J. Biol. Chem.* 292, 16804–16809. doi: 10.1074/jbc.R117.789271
- Xie, Z., and Klionsky, D. J. (2007). Autophagosome formation: core machinery and adaptations. *Nat. Cell Biol.* 9, 1102–1109. doi: 10.1038/ncb1007-1102
- Yoshiji, H., Nakae, D., Mizumoto, Y., Horiguchi, K., Tamura, K., Denda, A., et al. (1992). Inhibitory effect of dietary iron deficiency on inductions of putative preneoplastic lesions as well as 8-hydroxydeoxyguanosine in dna and lipid peroxidation in the livers of rats caused by exposure to a choline-deficient l-amino acid defined diet. *Carcinogenesis* 13, 1227–1233. doi: 10.1093/carcin/13.7.1227
- Zago, M. P., Hosakote, Y. M., Koo, S., Dhiman, M., Piñeyro, M. D., Parodi-Talice, A., et al. (2016). TcI isolates of *Trypanosoma cruzi* exploit the antioxidant network for enhanced intracellular survival in macrophages and virulence in mice. *Infect. Immun.* 84, 1842–1856. doi: 10.1128/IAI.00193-16
- Zhao, Y. G., and Zhang, H. (2018). Autophagosome maturation: an epic journey from the ER to lysosomes. *J. Cell Biol.* 18, 757–770. doi: 10.1083/jcb.201810099

Conflict of Interest: The authors declare that the research was conducted in the absence of any commercial or financial relationships that could be construed as a potential conflict of interest.

Copyright © 2019 Mesías, Garg and Zago. This is an open-access article distributed under the terms of the Creative Commons Attribution License (CC BY). The use, distribution or reproduction in other forums is permitted, provided the original author(s) and the copyright owner(s) are credited and that the original publication in this journal is cited, in accordance with accepted academic practice. No use, distribution or reproduction is permitted which does not comply with these terms.



An Evolutionary View of *Trypanosoma Cruzi* Telomeres

Jose Luis Ramirez*

Fundación Instituto de Estudios Avanzados and United Nations University UNU-BIOLAC, Caracas, Venezuela

OPEN ACCESS

Edited by:

Martin Craig Taylor,
University of London, United Kingdom

Reviewed by:

Bibo Li,
Cleveland State University,
United States

Richard McCulloch,
University of Glasgow,
United Kingdom

*Correspondence:

Jose Luis Ramirez
ramjoseluis@gmail.com

Specialty section:

This article was submitted to
Parasite and Host,
a section of the journal
Frontiers in Cellular and Infection
Microbiology

Received: 26 September 2019

Accepted: 06 December 2019

Published: 10 January 2020

Citation:

Ramirez JL (2020) An Evolutionary
View of *Trypanosoma Cruzi*
Telomeres.
Front. Cell. Infect. Microbiol. 9:439.
doi: 10.3389/fcimb.2019.00439

Like in most eukaryotes, the linear chromosomes of *Trypanosoma cruzi* end in a nucleoprotein structure called the telomere, which is preceded by regions of variable length called subtelomeres. Together telomeres and subtelomeres are dynamic sites where DNA sequence rearrangements can occur without compromising essential interstitial genes or chromosomal synteny. Good examples of subtelomeres involvement are the expansion of human olfactory receptors genes, variant surface antigens in *Trypanosoma brucei*, and *Saccharomyces cerevisiae* mating types. *T. cruzi* telomeres are made of long stretches of the hexameric repeat 5'-TTAGGG-OH-3', and its subtelomeres are enriched in genes and pseudogenes from the large gene families RHS, TS and DGF1, DEAD/H-RNA helicase and N-acetyltransferase, intermingled with sequences of retrotransposons elements. In particular, members of the Trans-sialidase type II family appear to have played a role in shaping the current *T. cruzi* telomere structure. Although the structure and function of *T. cruzi* telomeric and subtelomeric regions have been documented, recent experiments are providing new insights into *T. cruzi*'s telomere-subtelomere dynamics. In this review, I discuss the co-evolution of telomere, subtelomeres and the TS gene family, and the role that these regions may have played in shaping *T. cruzi*'s genome.

Keywords: *Trypanosoma cruzi* (*T. cruzi*), telomeres, evolutionary dynamics, genome, sialidases

INTRODUCTION

Trypanosoma cruzi causes Chagas disease a debilitating and often lethal malaise affecting millions of people in Latin American countries. *T. cruzi* populations are very variable and this variability is due in part to a clonal population structure, genome plasticity and abundance of repeated sequences. Nearly 50% of the total genome is made of repeated sequences, some of which code for protein families such as the Transsialidases (TS), mucins (MUC), mucins associated proteins (MASP), Disperse gene family 1 (DGF-1), Retrotransposon Hot Spot proteins, and retrotransposons elements (El-Sayed et al., 2005).

The Trans-sialidase family is divided into eight groups (Freitas et al., 2011), and the family name derives from enzymes included in the first group that can transfer host sialic acid onto the parasite's surface MUC. The rest of the TS groups have no enzymatic activity but code for surface glycoproteins involved in infectivity, adhesion, and evasion from the host immune response. MUC are not only receptors for sialic acid (Di Noia et al., 1995) but together with MASP proteins (Bartholomeu et al., 2009) provide a developmentally regulated shield that protects the parasite in hostile environments. DGF-1 are integrin-like proteins (Gonzalez et al., 2009; Kawashita et al., 2009; Lander et al., 2010) that are developmentally regulated, but whose role has not been deciphered. The Retrotransposon Hot Spot (RHS) family codes in *T. brucei* for nuclear and perinuclear proteins

and their sequences are targets for the insertion of RIME/ingi non-LTR retrotransposons (Bringaude et al., 2002). In *T. cruzi* RHS genes are frequently interrupted by the non-LTR retrotransposon LTC1 (Bringaude et al., 2006).

Early experiments in Manning's lab (Peterson et al., 1989; Ruef et al., 1994) revealed that two members of the Transialidase family type II (TSII) located in the vicinity of the telomere were highly expressed, whereas another member, in a more internal chromosomal location, showed a lower expression level (Peterson et al., 1989). After this original report, Freitas-Junior et al. (1999) and Chiurillo et al. (1999) confirmed the presence of TSII gene members in the subtelomeres of several *T. cruzi* strains. The cloning of *T. cruzi*'s telomeric and subtelomeric regions using a vector-adaptor complementing the last nine nucleotides of the telomere (Chiurillo et al., 1999, 2002; Kim et al., 2005), allowed us to define the sequence of the telomeric repeat, and have a detailed view of a large segment of the subtelomere.

Subtelomeres are often described as regions of genomic instability (Baird, 2018), and this observation is supported by the abundance of retrotransposon fragments and pseudogenes in *T. cruzi* telomeric clones, but they also represent a buffer region to minimize chromosome damage when telomere attrition occurs. However, despite this unstable environment, complete gene copies of DGF-1, TS, and RHDEAD/H-RNA helicase and N-acetyltransferase in *T. cruzi* subtelomeres are expressed, indicating that a positive selection is preserving the integrity of these genes at these locations (Moraes Barros et al., 2012). At the end of subtelomeres, there is a 189 base pairs sequence with homology for the 3' and 5'UTRs sequences of a gp85 gene (TSII) that we dubbed the 189 bp junction (Kim et al., 2005). A recapitulation of the possible events associated with the creation of this junction was proposed by Kim et al. (2005), Chiurillo et al. (2017) in which tandem repeats of TSII genes suffered breakages, excisions and rejoining to generate the junction. After this junction, the chromosomes are capped by runs of hexameric repeats of variable length ending in a single strand terminus 5'-TTAGGG-OH-3'.

THE EVOLUTION OF *T. cruzi* TELOMERES AND THE ROLE OF MEMBERS OF THE TSII GENE FAMILY IN SHAPING ITS GENOME

The intimate association between telomeres and TSII (gp85) sequences raises many questions about the creation of *T. cruzi* telomeres, such as how and when TS II family members were incorporated into the 189 bp junction? Were they part of transposon elements that eventually evolved into a primitive telomere? Did they come along with the telomeric repeats?

When we examine the structure of eukaryotic telomeres we observe a tremendous diversity in telomeric repeats and sequences associated with telomeres, the extreme case of Diptera where transposons assumed the role of telomeres. Telomeres arose during eukaryogenesis as a need to protect the ends of linear chromosomes from exonucleases degradation, prevent chromosome rearrangements, and facilitate the replication of the DNA lagging strand. This process may have started with the

endosymbiosis of an ancestral phagotrophic host cell (Cavalier-Smith, 2002) and an α -proteobacterium carrying Type II introns. Type II introns are Eubacterial mobile retroelements with ribozyme and reverse transcriptase activities. Eventually, Type II introns were transferred into the host cell genome and gave rise to the spliceosome, the non-LTR transposons and telomerase (Garavis et al., 2013; Podlevsky and Chen, 2016). According to this hypothesis, these non-LTR transposons were inserted at several genome locations, including the chromosome ends, originating the prototelomeres.

On the other hand, although still debatable, based on the sequence homogeneity of the transialidases within the animal kingdom, and their sequence homology with their very variable bacterial counterparts (Roggentin et al., 1993) proposed that sialidases originated in ancestors of the Echinodermata and Deuterostomate animals, and later these genes were horizontally transferred to bacteria via viruses. However, Schwerdtfeger and Melzig (2010) argued that the irregular appearance of sialidases in invertebrates does not support a common evolution of this gene family. In agreement with this view, in the *Trypanosomatidae* family, a taxon that includes pathogenic flagellates, we also observe this kind of patchy inheritance, since of all genera within this family the TS genes are only present in the genus *Trypanosoma*.

It is assumed that the first trypanosome to acquire sialidase genes was *T. brucei* or a common ancestor of both *T. brucei* and *T. cruzi*. The separation *Trypanosoma brucei* from *Trypanosoma cruzi* occurred approximately 100 millions of years during the Gondwanaland breakage (Briones et al., 1995; Stevens et al., 1999), and since then, the TS family suffered an expansion exclusively in the *T. cruzi* clade (Chiurillo et al., 2016a). During this long separation, the two species developed different survival strategies within their vectors and hosts. *T. brucei* uses the telomeric-subtelomeric compartment as a specialized expression site for variable antigenic determinants. On the contrary, *T. cruzi* acts like a stealth invader jamming the vertebrate host immune system through a simultaneous expression of multiple surface antigens (Millar et al., 1999), and among these, members of the TS family play an important role.

How the expansion of TSII genes occurred in *T. cruzi* is unknown, but likely, several events of gene mutation, duplication, recombination, transposition, and genetic drift generated the current picture of the TS family. Vestiges of these events are the salad of sequences derived from retrotransposon elements and Retrotransposons Hot Spot (RHS) genes scattered through the genome, and particularly in *T. cruzi* subtelomeres (Figure 1). The abundance of these elements at the subtelomere suggests the active participation of these regions in shaping the parasite genome (Kim et al., 2005). Regarding the telomeric repeat 5'-TTAGGG-OH 3', it is found in Plantae, Chromoalveolata, Excavata (where Trypanosomatids are included) and Rhizaria supergroups, a reason why some authors (Dressen et al., 2007; Fulneckova et al., 2013) have suggested that it was the repeat of the ancestral Eukaryotic telomeres. Thus, a safe assumption is that the TS sequences in the subtelomeric transition (189 bp junction) appeared after the hexameric repeats were already fixed, and perhaps the fixation of the 189 bp

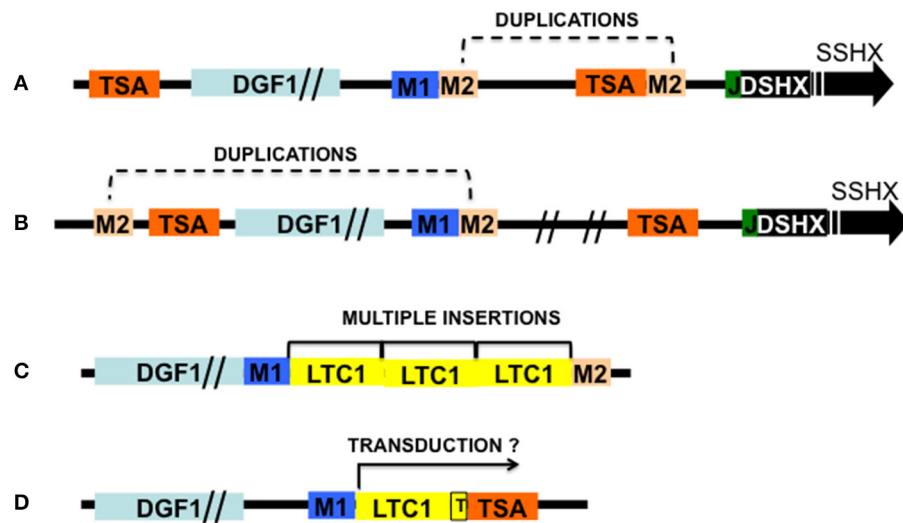


FIGURE 1 | Schematic representation of *T. cruzi* telomeric recombinants and two recombinants containing retrotransposons associated sequences. Modules M1 and M2 are LTC1 retrotransposon flanking sequences: M1, RS13TC+RS1Tc (upstream); M2, Seq3Tc + SIRE associated sequences SZ (downstream); TSA, transialidase genes (or pseudogenes); L1Tc, LTC1 non-LTR retrotransposon (genes and pseudogenes); DGF1, Disperse gene family 1 genes (or pseudogenes); J, 189 bp junction; DSHX, double strand hexameric sequences; SSHX, single strand hexameric sequences. **(A)** Telomeric BAC6 recombinant containing *T. cruzi* subtelomere and telomere showing duplication of M2. **(B)** Telomeric cosmid C6 showing M2 duplications. **(C)** Recombinant pBAC62 showing multiple LTC1 retrotransposons inserted between M1 and M2. **(D)** Recombinant pBAC52 showing a TSA gene located downstream of 213 bp of a truncated LTC1 (T) flanked upstream by the insertion sequence GTATCTTTG and a poly A track. Probably the TSA gene was transduced by the retrotransposon. Sizes are approximated; the flanking sequences are part of the Retrotransposon Hot Spot proteins. Adapted from Kim et al. (2005), Olivares et al. (2013).

junction has to do with its adaptation to the telomeric function, thus this sequence appears to be an integral part of *T. cruzi* telomere. Chiurillo et al. (2017) have proposed that the 189 bp junction may act as a seed to stabilize and/or create new telomeres via telomerase, but it is also possible that it was adopted as a recognition site for other proteins that contribute to the telomeric function.

GENE FAMILIES AND SUBTELOMERES

In *T. cruzi* apart from the TS family other gene families suffered big expansions, namely RHS, DFG-1, MASP, and MUC and these genes tend to form clusters at multiple locations in the genome, in some cases covering whole chromosomes (El-Sayed et al., 2005; Weatherly et al., 2009; Berna et al., 2018; Callejas-Hernández et al., 2018). Except for MUC and MASP families, these expanded families are often found at chromosomal terminal locations (El-Sayed et al., 2005; Weatherly et al., 2009; Moraes Barros et al., 2012; Callejas-Hernández et al., 2018). Therefore it is not surprising to detect members of these families when *T. cruzi* telomeres and subtelomeres are cloned (Chiurillo et al., 1999; Freitas-Junior et al., 1999). Thus, the *T. cruzi* genome is organized in blocks of syntenic non-repeated gene sequences at more interstitial locations, and non-syntenic blocks consisting of repeated genes that are intermingled with retrotransposons and other highly repeated elements, some of which are located at subtelomeres (El-Sayed et al., 2005). The presence of many repeated genes may propitiate recombination

events that, although not desirable for housekeeping genes, favor the generation of variability for genes coding for surface proteins.

The uniqueness of terminal chromosomal locations (subtelomeres) as a ground for the generation of new capabilities has been well documented among other organisms in yeast (Haber, 1998), *Plasmodium* (Scherf et al., 2008), *T. brucei* (Horn, 2004), and the expansion of human odor receptors (Mefford et al., 2001). Based on these observations and in the composition of *T. cruzi* telomeres and subtelomeres, we proposed that subtelomeres were places where the variability of some of these multigene families was generated, and in later events, the gene variants were mobilized to different locations in the genome (Kim et al., 2005).

HYPOTHETICAL MECHANISMS TO GENERATE GENE VARIABILITY

What are the mechanisms that may generate gene variability in *T. cruzi*, and how has the mobilization of gene variants occurred? Is the variability generated by gene conversion or unequal crossing over? Are these processes still occurring in *T. cruzi* populations?

Our first attempt to address these questions was through *in silico* simulation studies using as inputs real gene sequences generated by the *T. cruzi* genome project (Azuaje et al., 2007). The simulations evaluated the generation of variability by introducing different mutagenic pressures in housekeeping genes, and members of gene families with presence at subtelomeres. The premise was that mutation rates would be a trade-off between the generation of variability to expand

adaptive capabilities, and the need to keep important core functions. This study concluded that housekeeping genes were more robust against the introduction of random point mutations than genes coding for surface proteins and that the most effective mechanism to introduce variability was gene conversion. The energetic burden of keeping a large number of pseudogenes is an indication that they play an important role in the parasite, an observation that prompted us to include pseudogenes of RHS, TS, and DGF-1 in our simulations. The results confirmed the potential of pseudogenes to contribute to the generation of variability. This finding contradicts the idea that pseudogenes are merely relics of gene deterioration (Rogers et al., 2011) or pseudogenization.

An important piece of information came from experiments using *T. cruzi* artificial chromosomes (pTAC) carrying the 189 bp junction, hexameric repeats, and drug selection markers (Curto et al., 2014). When *T. cruzi* epimastigotes were transformed with these pTCAs, they were able to replicate with surprising stability for 150 generations in the presence of the selection drug, or 60 generations without it. In other words, the pTACs showed non-detectable sequence exchange with the host chromosomes and replicated and segregated without the presence of centromeres, or perhaps the telomere was fulfilling this role. In a more recent experiment (Chiurillo et al., 2016b), addressed the possibility of chromosomal sequence exchanges by introducing a cutting site for the rare meganuclease I-SceI within the RHS gene of one pTACs (pTAC-D6CISceI*) harboring larger portions of *T. cruzi* subtelomeres. After transforming this pTAC into *T. cruzi* cells expressing the meganuclease I-SceI, and confirming that double-strand breaks (DSBs) were produced, the probing pTAC was examined to check whether the DSBs were repaired. Out of seven clones studied, six showed repairs, as evidenced by the disappearance of the I-SceI site, and the reversion to the original pTAC (pTAC-D6C*). The most likely explanation is that the repair events used as template the host subtelomere homologous to the pTAC. The seventh clone was repaired losing the I-SceI site, but the sequences around the repair site shared homology with the subtelomere of another chromosome (ectopic recombination). From these experiments several conclusions can be derived: first chromosomal exchanges at the subtelomere can be promoted by the introduction DSBs; second the repair mechanism for these DSBs is homologous recombination (HR), or some version of it (Dressen et al., 2007); third, events involving exchanges with non-homologous chromosomes (ectopic recombination) can occur, with the possibility of generating gene variants. These experiments don't rule out that similar exchanges can occur at more interstitial locations. The absence of detectable recombination in earlier pTAC experiments was likely due to a lack of sufficient homology with any given chromosome subtelomere, and/or that DSBs are strictly necessary to induce recombination.

Contrary to most eukaryotes in *T. brucei* and *T. cruzi* the most important repair mechanism for DSBs repair is HR, with minor participation of microhomology repair (MHR). To detect MHR-DSB repair, it was necessary to abolish HR (Glover et al., 2008).

In *T. cruzi* out of the potential genes that participate in HR, RAD51 plays a central role in facilitating homologous

strand invasion (Gomes Passos Silva et al., 2018). An interesting activity discovered after massive gamma radiation of *T. cruzi* cells was tyrosyl-DNA phosphodiesterase I (Tdr-I), an enzyme that plays an important role in Topoisomerase I mediate DNA DBS repair (Das et al., 2010). No genes for NHEJ have been found in *T. cruzi* (Gomes Passos Silva et al., 2018). MHR seems to occur in chromosomal rearrangements when single DSB is introduced by Cas9 endonuclease (Lander et al., 2015; Soares Medeiros et al., 2017).

An efficient HR repair mechanism in *T. cruzi* may explain the rapid karyotype and cell growth recovery after massive irradiation with 500 Gy of gamma radiation (Garcia et al., 2016), and the difficulty in generating mutations (indels) in CRISPR experiments involving a single DSB vs. gene replacement (Lander et al., 2015; Soares Medeiros et al., 2017). But also, the prevalence of a very stringent HR repair mechanism in genomes with a large number of repeated sequences, like *T. cruzi*, hampers (but does not eliminate) chromosomal-internal recombination events that can be detrimental to the organism.

Thus, we believe that an important source for the generation of variability in some *T. cruzi* surface proteins is subtelomeric recombination promoted by DSBs followed by a dispersion of these variants either by transpositions or ectopic recombination events. Further duplications events and genetic drift produced the current clusters that we see at several locations of the *T. cruzi*'s genome.

Along this line, experiments with meganuclease I-Sce-I in *T. brucei* (Dressen et al., 2007) revealed that the introduction of a DSB in telomeric VSG gene promoted antigenic switching via gene conversion. The break is resolved by a replication mechanism induced by this break (Break Induced Replication, BIR). Similar detailed studies to determine how DSBs repair occurs in *T. cruzi* are missing due in part to the lack of an RNAi machinery and/or inducible promoters coupled to CRISPR-Cas9 vectors.

As mentioned before, despite this stringent HR mechanism interstitial chromosome rearrangement leading to karyotype changes can occur via ectopic recombination within multigene families through duplicated sites flanking these sequences (Figures 1A,B).

HOW DSBs CAN BE INTRODUCED IN *T. cruzi* SUBTELOMERES?

In *T. cruzi* retrotransposon elements occupy nearly 5% of its genome and among these elements, the L1Tc non-LTR retrotransposon has the necessary machinery for its mobilization (Macías et al., 2018). L1Tc genome codes for an AP endonuclease activity (NL1Tc) capable of introducing breaks for the insertion of the retrotransposon, but also plays a role in repairing DSBs produced by daunorubicin (Olivares et al., 2013). Other retrotransposon elements like SLAKS and CZAR code for site-specific endonucleases (Macías et al., 2018). So, some DSBs may be introduced in the subtelomeres by retrotransposon nucleases, and HR repairs the break using as templates homologous chromatids, or on occasion non-homologous

chromatids (ectopic recombination). In *T. cruzi* there are active L1Tc transposons and no RNAi machinery to counteract their activities. Several observations about the organization of multigene families reveal close associations with retrotransposon sequences i.e., most DGF-1 and TSII copies are flanked by RHS (Olivares et al., 2000; Kim et al., 2005) or L1Tc retrotransposon sequences, the duplications of RHS and L1Tc genes at both sides of these genes suggest the occurrence of ectopic recombination events (Figure 1; Olivares et al., 2000). Although L1Tc appears to be randomly distributed in *T. cruzi*'s genome, 50% of its copies are associated with RHS genes flanked by the putative insertion site 5'-TGCAGACAT-OH-3' (Olivares et al., 2000; Figures 1B,C). Also, they are found inserted downstream the sequence GA (x)₂AXGA (x)₅txTATG↑A(x)₁₁↑ where arrows mark the single strand cleavage sites (El-Sayed et al., 2005; Bringaud et al., 2006). How frequent DBSs leading to genetic recombination and gene variability occurs is difficult to assess, since as shown in the experiments with meganuclease I-Sce-I (Chiurillo et al., 2016b), DBSs are mainly repaired by HR using as template homolog chromosomes.

The MASP superfamily is associated with the site-specific retrotransposon TcTREZO (Souza et al., 2007). These elements are frequently found flanking MASP genes, thus providing potential sites for HR. Since TcTREZO is species-specific, it must have appeared after the separation of *T. cruzi* and *T. brucei*, and it may have played an important role in the expansion of the MASP family. MASPs proteins present highly conserved N and C terminal sequences, and a variable middle region, also besides, their gene's 5' and 3' UTRs are highly conserved (Bartholomeu et al., 2009). So sequence evolution in this gene family is quite different from the rest of the repeated families. Interestingly other retrotransposons and members of the gp85, DFG-1, and RHS gene families frequently interrupt MASP clusters.

Duplication and mobilization of genes can also occur via piggybacking the retrotransposon reverse transcriptase machinery by the transduction of genes neighboring the retrotransposons insertion site (Figure 1D). The termination signal for transposon transcriptases is usually weak, thus transcription can run through neighboring segments which can be duplicated and mobilized elsewhere (Xing et al., 2006). So far no experiments have been conducted to address this type of event in *T. cruzi*, although the size of the DNA segments that non-LTR retrotransposons can transduce is usually small (1 or 3 Kbp), making it an, unlike mechanism to mobilize large genes like DGF-1 (>10 Kbp).

In *T. brucei*, in the case of non-recombinational gene conversion for antigenic switching, alternatives for the

generation of subtelomeres DSBs have been proposed, such as accelerated transcription, conflicts between replication and transcription machineries (da Silva et al., 2018), and TERRA (Telomeric Repeat-containing RNA) transcription leading to the formation of R-loops (Nanavaty et al., 2017; Saha et al., 2019). Since antigenic variation is a vital phenomenon for the survival of *T. brucei* populations, it is not surprising that redundant mechanisms exist to make sure that antigenic switching occurs. In the case of *T. cruzi*, not such extensive studies have been done, and it is possible that R-loops formation or transcription-replication conflicts may also contribute to the generation of subtelomere DBSs. In this review, I favored the role of retrotransposons in the generation of DBSs, given the ubiquity of these elements in the *T. cruzi* genome, their close association with important surface antigens families, and the absence of RNAi machinery.

CONCLUSIONS

Once *T. cruzi* telomeres were fixed, members of the TS II family positioned at the subtelomeres co-evolved to be part of the transition to the telomeric repeat. Although the reason for the fixation of this junction is still unknown, it suggests a potential telomeric function for this region. The variability of some surface proteins and their localization at the subtelomeres together with retrotransposon elements suggests that these regions are grounds for the generation genetic variability. We propose that DBSs introduced in the subtelomeres by retrotransposon nucleases are repaired by homologous recombination, and when the repair includes non-homologous chromatids there is a possibility to generate gene variants. These variants are mobilized elsewhere either by transposition or ectopic recombination. Gene families increased their numbers by gene duplication to achieve higher expression levels. MUC and MASP superfamilies likely evolved in later events not related to the subtelomeres.

AUTHOR CONTRIBUTIONS

The author confirms being the sole contributor of this work and has approved it for publication.

ACKNOWLEDGMENTS

The publication cost was partially covered by the Programme UNU-BIOLAC. Thanks to Don Humphreys and Sharon Sumpter for English revision.

REFERENCES

- Azuaje, F. J., Ramirez, J. L., and Franco Da Silveira, J. (2007). *In silico*, biologically-inspired modeling of genomic variation generation in surface proteins of *Trypanosoma cruzi*. *Kinetoplastid Biol. Dis.* 6, 1–12. doi: 10.1186/1475-9292-6-6
- Baird, D. M. (2018). Telomeres and genomic evolution *Phil. Trans. R. Soc. B* 373:20160437. doi: 10.1098/rstb.2016.0437
- Bartholomeu, D. C., Cerqueira, G. C., Leao, A. C. A., daRocha, W. D., Pais, F. S., Macedo, C., et al. (2009). Genomic organization and expression profile of the mucin-associated surface protein (masp) family of the human pathogen *Trypanosoma cruzi*. *Nucleic Acids Res.* 37, 3407–3417. doi: 10.1093/nar/gkp172
- Berna, L., Rodriguez, M., Chiribao, M. L., Parodi-Talice, A., Pita, S., Rijo, G., et al. (2018). Expanding an expanded genome: long-read sequencing of *Trypanosoma cruzi*. *Microb. Genom.* 4:e00017. doi: 10.1099/mgen.0.000177

- Bringaud, F., Bartholomeu, D. C., Blandin, G., Delcher, A., Baltz, T., El-Sayed, N. M., et al. (2006). The *Trypanosoma cruzi* L1Tc and NARTc non-LTR retrotransposons show relative site-specificity for insertion. *Mol. Biol. Evol.* 23, 411–420. doi: 10.1093/molbev/msj046
- Bringaud, F., Biteau, N., Melville, S. E., Hez, S., and El-Sayed, N. M. (2002). A new, expressed multigene family containing a hot spot for insertion of retroelements are associated with polymorphic subtelomeric regions of *Trypanosoma brucei* Euk. *Cell* 1, 137–151. doi: 10.1128/EC.1.1.137-151.2002
- Briones, M. R., Egima, C. M., Eichinger, D., and Schenkman, S. (1995). Trans-sialidase genes expressed in mammalian forms of *Trypanosoma cruzi* evolved from ancestor genes expressed in insect forms of the parasite. *J. Mol. Evol.* 41, 120–131. doi: 10.1007/BF00170663
- Callejas-Hernández, F., Rastrojo, A., Poveda, C., Gironès, N., and Fresno, M. (2018). Genomic assemblies of newly sequenced *Trypanosoma cruzi* strains reveal new genomic expansion and greater complexity. *Sci. Rep.* 8:14631. doi: 10.1038/s41598-018-32877-2
- Cavalier-Smith, T. (2002). The phagotrophic origin of eukaryotes and phylogenetic classification of Protozoa. *Int. J. Syst. Evol. Microbiol.* 52, 297–354. doi: 10.1099/00207713-52-2-297
- Chiurillo, M. A., Antonio, C. R., Mendes Marini, M., Torres de Souza, R., and Franco Da Silveira, J. (2017). Chromosomes ends and the telomere biology in *Trypanosomatids*. *Front. Parasitol.* 1, 104–133. doi: 10.2174/9781681084053117010006
- Chiurillo, M. A., Cano, I., Franco Da Silveira, J., and Ramirez, J. L. (1999). Organization of telomeric and sub-telomeric regions of chromosomes from the protozoan parasite *Trypanosoma cruzi*. *Mol. Biochem. Parasitol.* 100, 173–183. doi: 10.1016/S0166-6851(99)00047-X
- Chiurillo, M. A., Cortez, D. R., Lima, F. M., Cortez, C., Ramírez, J. L., Martins, A. G., et al. (2016a). The diversity and expansion of the trans-sialidase gene family is a common feature in *Trypanosoma cruzi* clade members. *Infect. Genet. Evol.* 37, 266–274. doi: 10.1016/j.meegid.2015.11.024
- Chiurillo, M. A., Moraes Barros, R. R., Souza, R. T., Marini, M. M., Antonio, C. R., Cortez, D. R., et al. (2016b). Subtelomeric I-SceI-mediated double-strand breaks are repaired by homologous recombination in *Trypanosoma cruzi*. *Front. Microbiol.* 7:2041. doi: 10.3389/fmicb.2016.02041
- Chiurillo, M. A., Santos, M. R. M., Franco Da Silveira, J., and Ramirez, J. L. (2002). An improved general approach for cloning and characterizing telomeres: the protozoan parasite *Trypanosoma cruzi* as a model organism. *Gene* 294, 197–204. doi: 10.1016/S0378-1119(02)00768-0
- Curto, M. L., de Lorenzi, H. A., Moraes Barros, R. R., Souza, R., Levin, M. J., Da Silveira, J. F., et al. (2014). Cloning and expression of transgenes using linear vectors in *Trypanosoma cruzi*. *Int. J. Parasitol.* 44, 447–456. doi: 10.1016/j.ijpara.2014.03.009
- da Silva, M. S., Hovel-Miner, G. A., Briggs, E. M., Elias, M. C., and McCulloch, R. (2018). Evaluation of mechanisms that may generate DNA lesions triggering antigenic variation in African trypanosomes. *PLoS Pathog.* 14:e1007321. doi: 10.1371/journal.ppat.1007321
- Das, B. B., Dexheimer, T. S., Maddali, K., and Pommier, Y. (2010). Role of tyrosyl-DNA phosphodiesterase (TDP1) in mitochondria. *PNAS* 107, 19790–19795. doi: 10.1073/pnas.1009814107
- Di Noia, J. M., Sanchez, D. O., and Frasch, A. C. (1995). The protozoan *Trypanosoma cruzi* has a family of genes resembling the mucin genes of mammalian cells. *J. Biol. Chem.* 270, 24146–24149. doi: 10.1074/jbc.270.41.24146
- Dressen, O., Li, B., and Cross, G. A. M. (2007). Telomere structure and function in trypanosomes: a proposal. *Nat. Rev. Microbiol.* 5, 70–75. doi: 10.1038/nrmicro1577
- El-Sayed, N. M., Myler, P. J., Bartholomeu, D. C., Nilsson, D., Aggarwal, G., Tran, A.-N., et al. (2005). The genome sequence of *Trypanosoma cruzi*, the etiological agent of Chagas' disease. *Science* 309, 410–415. doi: 10.1126/science.1112631
- Freitas, L. M., Lopes dos Santos, S., Rodrigues-Luiz, G. F., Mendes, T. A. O., Rodrigues, T. S., Gazzinelli, R. T., et al. (2011). Genomic analyses, gene expression and antigenic profile of the trans-sialidase superfamily of *Trypanosoma cruzi* reveal an undetected level of complexity. *PLoS ONE* 6:e25914. doi: 10.1371/journal.pone.0025914
- Freitas-Junior, L., Marques Porto, R., Pirrit, L. A., Schenkman, S., and Scherf, A. (1999). The identification of the telomeres in *Trypanosoma cruzi* reveals highly heterogeneous lengths in different parasite strains. *Nucleic Acids Res.* 27, 2451–2456. doi: 10.1093/nar/27.12.2451
- Fulneckova, J., Ševčíková, T., Falkus, J., Lukešová, A., Lukeš, M., Vlček, C. et al. (2013). A broad phylogenetic survey unveils the diversity and evolution of telomeres in eukaryotes. *Gen. Biol. Evol.* 5, 468–483. doi: 10.1093/gbe/evt019
- Garavis, M., Gonzalez, C., and Villasante, A. (2013). On the origin of the eukaryotic chromosome: the role of noncanonical DNA structures in telomere evolution. *Genome Biol. Evol.* 5, 1142–1150. doi: 10.1093/gbe/evt079
- Garcia, J. B. F., Vieira da Rocha, P., Costa-Silva, H. M., Alves, C.eres, C. L., and Machado, C. R., Cruz, A.K. (2016). *Leishmania major* and *Trypanosoma cruzi* present distinct DNA damage responses. *Mol. Biochem. Parasitol.* 207, 23–32. doi: 10.1016/j.molbiopara.2016.05.004
- Glover, L., McCulloch, R., and Horn, D. (2008). Sequence homology and microhomology dominate chromosomal double-strand break repair in African trypanosomes. *Nucleic Acids Res.* 36, 2608–2618. doi: 10.1093/nar/gkn104
- Gomes Passos Silva, D., da Silva Santos, S., Nardelli, S. C., Mendes, I. C., Guimarães Freire, N. C., Marcal Repolês, B., et al. (2018). The *in vivo* and *in vitro* roles of *Trypanosoma cruzi* Rad51 in the repair of DNA double-strand breaks and oxidative lesions. *PLOS Neg. Trop. Dis.* 12:e0006875. doi: 10.1371/journal.pntd.0006875
- Gonzalez, A. M., Azuaje, F. J., Ramirez, J. L., Da Silveira, J. F., and Dorronsoro, J. R. (2009). Machine learning techniques for automated classification of adhesin-like proteins in *Trypanosoma cruzi*. *IEEE/ACM Trans. Comp. Biol. Bioinf.* 6, 695–702. doi: 10.1109/TCBB.2008.125
- Haber, J. E. (1998). Mating-Type Gene Switching in *Saccharomyces cerevisiae*. *Annu. Rev. Genet.* 32, 561–599. doi: 10.1146/annurev.genet.32.1.561
- Horn, D. (2004). The molecular control of antigenic variation in *Trypanosoma brucei*. *Curr. Mol. Med.* 4, 563–574. doi: 10.2174/1566524043360078
- Kawashita, S. Y., Da Silva, C. V., Mortara, R. A., Burleigh, B., and Briones, M. R. S. (2009). Homology, paralogy, and function of dgf-1, a highly disperse *Trypanosoma cruzi* specific gene family and its implications for information entropy of its encoded proteins. *Mol. Biochem. Parasitol.* 165, 19–31. doi: 10.1016/j.molbiopara.2008.12.010
- Kim, D., Chiurillo, M. A., El-Sayed, N. M., Jones, K., Santos, M. M. R., Porcile, P. E., et al. (2005). Telomere and subtelomere of *Trypanosoma cruzi* chromosomes are enriched in (pseudo) genes of retrotransposon hot spot and trans-sialidase-like gene families: the origins of *T. cruzi* telomeres. *Gene* 346, 153–161. doi: 10.1016/j.gene.2004.10.014
- Lander, N., Bernal, C., Diez, N., Afñez, N., Docampo, R., and Ramirez, J. L. (2010). Localization and developmental regulation of a disperse gene family 1 protein in *Trypanosoma cruzi*. *Infect. Immun.* 78, 231–241. doi: 10.1128/IAI.00780-09
- Lander, N., Li, Z.-H., Niyogi, S., and Docampo, R. (2015). CRISPR/Cas9-induced disruption of paraflagellar rod protein 1 and 2 genes in *Trypanosoma cruzi* reveals their role in flagellar attachment. *MBio* 6: e01015. doi: 10.1128/mBio.01012-15
- Macías, F., Afonso-Lehmann, R., López, M. C., Gómez, I., and Thomas, M. C. (2018). Biology of *Trypanosoma cruzi* retrotransposons: from an enzymatic to a structural point of view. *Curr. Genom.* 19, 110–118. doi: 10.2174/1389202918666170815150738
- Mefford, H. C., Linardopoulou, E., Coil, D., van den Engh, G., and Trask, B. J. (2001). Comparative sequencing of a multicopy subtelomeric region containing olfactory receptor genes reveals multiple interactions between non-homologous chromosomes. *Hum. Mol. Genet.* 10, 2363–2372. doi: 10.1093/hmg/10.21.2363
- Miller, A. E., Wleklinski-Lee, M., and Kahn, S. J. (1999). The surface Protein superfamily of *Trypanosoma cruzi* stimulates a solarized Th1 response that Becomes anergic. *J. Immunol.* 162, 6092–6099.
- Moraes Barros, R. R., Marini, M. M., Antônio, C. R., Cortez, D. R., Miyake, A. M., and Lima, F. M., et al. (2012). Anatomy and evolution of telomeric and subtelomeric regions in the human protozoan parasite *Trypanosoma cruzi*. *BMC Genom.* 13:229. doi: 10.1186/1471-2164-13-229
- Nanavaty, V., Sandhu, R., Jehi, S. G., Pandya, U. M., and Li, B. (2017). *Trypanosoma brucei* RAP1 maintains telomere and subtelomere integrity by suppressing TERRA and telomeric RNA: DNA hybrids. *Nucleic Acids Res.* 45, 5785–5796. doi: 10.1093/nar/gkx184
- Olivares, M., Lopez, M. C., Garcia-Perez, J. L., Briones, P., Pulgar, M., and Thomas, M. C. (2013). The endonuclease NLI^{Tc} encoded by the LINE L1^{Tc}

- from *Trypanosoma cruzi* protects parasites from daunorubicin DNA damage. *Biochim. Biophys. Acta* 1626, 25–32. doi: 10.1016/S0167-4781(03)00022-8
- Olivares, M., Thomas, M. C., Lopez-Barajas, A., Requena, J. M., Garcia-Perez, J. L., and Angel, S. (2000). Genome clustering of the *Trypanosoma cruzi* nonlong terminal L1Tc retrotransposon with defined intersperse repeated DNA elements. *Electrophoresis* 21, 2973–2982. doi: 10.1002/1522-2683(20000801)21:14<2973::AID-ELPS2973>3.0.CO;2-4
- Peterson, D. S., Fouts, D. L., and Manning, J. E. (1989). The 85-kd surface antigen gene of the *Trypanosoma cruzi* is telomeric and a member of a multigene family. *EMBO J.* 8, 3911–3916. doi: 10.1002/j.1460-2075.1989.tb08571.x
- Podlevsky, J. D., and Chen, J.-L. (2016). Evolutionary perspectives of telomerase RNA structure and function. *RNA Biol.* 13, 720–732. doi: 10.1080/15476286.2016.1205768
- Rogers, M. B., Hilley, J. D., Dickens, N. J., Wilkes, J., Bates, P. A., Depledge, D. P., et al. (2011). Chromosome and gene copy number variation allow structural change between species and strains of *Leishmania major*. *Gen. Res.* 21, 2129–2142. doi: 10.1101/gr.122945.111
- Roggentin, P., Schauer, R., Hoyer, L. L., and Vimr, E. R. (1993). The sialidase superfamily and its spread by horizontal gene transfer. *Mol. Microbiol.* 9, 915–921. doi: 10.1111/j.1365-2958.1993.tb01221.x
- Ruef, B. J., Dawson, B. D., Tewari, D., Fouts, D. L., and Manning, J. E. (1994). Expression and evolution of members of the *Trypanosoma cruzi* trypomastigote surface antigen multigene family. *Mol. Biochem. Parasitol.* 63, 109–120. doi: 10.1016/0166-6851(94)90013-2
- Saha, A., Nanavaty, V. P., and Li, B. (2019). Telomere and subtelomere R-loops and antigenic variation in trypanosomes. *J. Mol. Biol.* doi: 10.1016/j.jmb.2019.10.025. [Epub ahead of print].
- Scherf, A., Lopez-Rubio, J. J., and Riviere, L. (2008). Antigenic variation in *Plasmodium falciparum*. *Annu. Rev. Microbiol.* 62, 445–470. doi: 10.1146/annurev.micro.61.080706.093134
- Schwerdtfeger, S. M., and Melzig, M. F. (2010). Sialidases in biological systems *Pharmazie* 65, 551–561. doi: 10.1002/chin.201047267
- Soares Medeiros, L. C., South, L., Peng, D., Bustamante, J. M., and Wang, W., Bunkofsky, et al. (2017). Rapid, selection-free, high-efficiency genome editing in protozoan parasites using CRISPR-Cas9 ribonucleoproteins. *MBio* 8, e01788–17. doi: 10.1128/mBio.01788-17
- Souza, R. T., Santos, M. R. M., Lima, F. M., El-Sayed, N. M., Myler, P. J., Ruiz, J. C., et al. (2007). New *Trypanosoma cruzi* repeated element that shows site specificity for insertion eukaryot. *Cell* 6, 1228–1238. doi: 10.1128/EC.00036-07
- Stevens, J. R., Noyes, H. A., Dover, G. A., and Gibson, W. C. (1999). The ancient and divergent origins of the human pathogenic trypanosomes, *Trypanosoma brucei* and *T. cruzi*. *Parasitology* 118, 107–116. doi: 10.1017/S0031182098003473
- Weatherly, D. B., Boehlke, C., and Tarleton, R. L. (2009). Chromosome level assembly of the hybrid *Trypanosoma cruzi* genome. *BMC Genomics* 10:255. doi: 10.1186/1471-2164-10-255
- Xing, J., Wan, G., Belancio, V. P., Cordaux, R., Deininger, P. L., and Batzer, M. A. (2006). Emergence of primate genes by retrotransposon mediated sequence transduction *PNAS* 103, 17608–17613. doi: 10.1073/pnas.0603224103

Conflict of Interest: The author declares that the research was conducted in the absence of any commercial or financial relationships that could be construed as a potential conflict of interest.

Copyright © 2020 Ramirez. This is an open-access article distributed under the terms of the Creative Commons Attribution License (CC BY). The use, distribution or reproduction in other forums is permitted, provided the original author(s) and the copyright owner(s) are credited and that the original publication in this journal is cited, in accordance with accepted academic practice. No use, distribution or reproduction is permitted which does not comply with these terms.



A Novel Calcium-Activated Potassium Channel Controls Membrane Potential and Intracellular pH in *Trypanosoma cruzi*

Patricia Barrera^{1†}, Christopher Skorka^{2†}, Michael Boktor², Noopur Dave² and Veronica Jimenez^{2*}

¹ Department of Biological Science, College of Natural Sciences and Mathematics, California State University Fullerton, Fullerton, CA, United States, ² Departamento de Biología, Facultad de Ciencias Exactas y Naturales, Instituto de Histología y Embriología IHEM-CONICET, Facultad de Medicina, Universidad Nacional de Cuyo, Mendoza, Argentina

OPEN ACCESS

Edited by:

Nobuko Yoshida,
Federal University of São Paulo, Brazil

Reviewed by:

Ariel Mariano Silber,
University of São Paulo, Brazil
David M. Engman,
Cedars-Sinai Medical Center,
United States

*Correspondence:

Veronica Jimenez
vjimenezortiz@fullerton.edu

[†]These authors have contributed
equally to this work

Specialty section:

This article was submitted to
Parasite and Host,
a section of the journal
Frontiers in Cellular and Infection
Microbiology

Received: 19 November 2019

Accepted: 16 December 2019

Published: 15 January 2020

Citation:

Barrera P, Skorka C, Boktor M,
Dave N and Jimenez V (2020) A Novel
Calcium-Activated Potassium Channel
Controls Membrane Potential and
Intracellular pH in *Trypanosoma cruzi*.
Front. Cell. Infect. Microbiol. 9:464.
doi: 10.3389/fcimb.2019.00464

Trypanosoma cruzi develops in environments where nutrient availability, osmolarity, ionic concentrations, and pH undergo significant changes. The ability to adapt and respond to such conditions determines the survival and successful transmission of *T. cruzi*. Ion channels play fundamental roles in controlling physiological parameters that ensure cell homeostasis by rapidly triggering compensatory mechanisms. Combining molecular, cellular and electrophysiological approaches we have identified and characterized the expression and function of a novel calcium-activated potassium channel (TcCAKC). This channel resides in the plasma membrane of all 3 life stages of *T. cruzi* and shares structural features with other potassium channels. We expressed TcCAKC in *Xenopus laevis* oocytes and established its biophysical properties by two-electrode voltage clamp. Oocytes expressing TcCAKC showed a significant increase in inward currents after addition of calcium ionophore ionomycin or thapsigargin. These responses were abolished by EGTA suggesting that TcCAKC activation is dependent of extracellular calcium. This activation causes an increase in current and a negative shift in reversal potential that is blocked by barium. As predicted, a single point mutation in the selectivity filter (Y313A) completely abolished the activity of the channels, confirming its potassium selective nature. We have generated knockout parasites deleting one or both alleles of TcCAKC. These parasite strains showed impaired growth, decreased production of trypomastigotes and slower intracellular replication, pointing to an important role of TcCAKC in regulating infectivity. To understand the cellular mechanisms underlying these phenotypic defects, we used fluorescent probes to evaluate intracellular membrane potential, pH, and intracellular calcium. Epimastigotes lacking the channel had significantly lower cytosolic calcium, hyperpolarization, changes in intracellular pH, and increased rate of proton extrusion. These results are in agreement with previous reports indicating that, in trypanosomatids, membrane potential and intracellular pH maintenance are linked. Our work shows TcCAKC is a novel potassium channel that contributes to homeostatic regulation of important physiological processes in *T. cruzi* and provides new avenues to explore the potential of ion channels as targets for drug development against protozoan parasites.

Keywords: potassium channel, intracellular calcium, membrane potential, electrophysiology, *Trypanosoma cruzi*

INTRODUCTION

Ion homeostasis is central to all life forms. Cellular composition must to be regulated in a dynamic manner in order to preserve a relatively constant intracellular environment, even under the most extreme external changes (Pasantes-Morales, 2016). *Trypanosoma cruzi*, the causing agent of Chagas disease, develops in environments with different physiological conditions, including variations in ionic concentrations, pH, and osmolality (Jimenez, 2014). In the hindgut of the insect vector, epimastigotes are exposed to large changes in ionic gradients, including potassium (K^+), calcium (Ca^{2+}) and protons (Kollien et al., 2001). As metacyclic trypomastigotes invade host cells and become intracellular, they also experience significant changes in ionic gradients. Due to the dynamic nature of the environments *T. cruzi* faces throughout its life cycle, it must be able to successfully respond to these environmental changes to ensure survival and propagation between vector and host (Rassi and Marin-Neto, 2010). Ion channels play a role in controlling a wide array of important physiological processes including membrane potential regulation, pH, cell volume, cell proliferation, and death (Lang et al., 2007; Bae et al., 2011; Pasantes-Morales, 2016). They are also validated targets for treatment of highly prevalent diseases such as cardiovascular pathologies (Gill et al., 1992; Turley et al., 2016) and are currently being re-evaluated as potential drug targets against parasitic infections (Meier et al., 2018). In protozoans, ion channel characterization lags behind the general progress of the field, mostly due to technical limitations for direct electrophysiological recordings in motile cells, but in recent years we have gained insight into the role of calcium channels in trypanosomes (Chiurillo et al., 2017; Huang and Docampo, 2018; Potapenko et al., 2019; Rodriguez-Duran et al., 2019).

K^+ channels are a diverse group of well-characterized ion channels expressed in many different organisms, from bacteria to eukaryotes (MacKinnon, 2003). One important class of K^+ channels are the calcium-activated potassium channels (CAKC). CAKCs regulate membrane potential (Gui et al., 2012; Alix et al., 2014; Rohmann et al., 2015; Yang, 2016), cell volume regulation and renal K^+ excretion (Latorre et al., 2017; Sforza et al., 2018) among other cellular functions.

CAKCs are formed by α -subunits with six to seven transmembrane domains, which tetramerize to create the pore-forming region of the channel (Lee and Cui, 2010). This class of channels can be divided into three subclasses by their sequence homology and biophysical properties (Prole and Marrion, 2012). The large conductance (BK) subclass of channels are characterized by ion conductance around 300 pS, voltage sensitivity and activation by Ca^{2+} binding to the RCK “calcium bowl” domain of the protein (Horriggan and Aldrich, 2002; Hite et al., 2017). The second subclass is the small conductance (SK) channels, which are characterized by a conductance between 10 and 25 pS, and activation through calcium-calmodulin binding domains (Bond et al., 1999). The final subclass is the intermediate conductance (IK) channels, which activate like SK channels, but their conductance varies between that of BKs and SKs (Kaczmarek et al., 2017; Sforza et al., 2018). *In silico* analysis of

Trypanosoma genomes reveals the presence of putative CAKCs (Prole and Marrion, 2012), but homology analysis failed to identify other type of K^+ channels or accessory subunits usually required for channel trafficking and function. Steinmann et al. showed the role of a heteromeric potassium channel in *T. brucei* membrane potential maintenance (Steinmann et al., 2015) and the presence of a K^+ channel with atypical features, found in the acidocalcisomes of *T. brucei* (Steinmann et al., 2017). We have previously characterized a non-selective cation channel and its participation in cell volume regulation in *T. cruzi* (Jimenez and Docampo, 2012). Additionally, membrane vesicles isolated from epimastigotes and reconstituted in liposomes showed the presence of, at least, two K^+ permeable pathways (Jimenez et al., 2011), but the precise nature of the channels responsible for these currents remained elusive. Here, we describe the identification, molecular characterization and physiological role of a novel calcium-activated potassium channel (TcCAKC) in *T. cruzi*. This channel shares structural and functional features with other CAKCs, regulates key physiological parameters such as membrane potential, and is essential for parasite infectivity.

MATERIALS AND METHODS

Sequence Analysis and Structure Prediction

Putative sequences for CAKC channels were identified in Trypanopdb.org (Aslett et al., 2009). Predicted protein sequences for TcCAKC CL Brener Esmeraldo-like (TcCLB.506529.150) and Non-Esmeraldo-like haplotypes (TcCLB.510885.60) were compared with the putative sequences for *Trypanosoma brucei* (Tb927.1.4450) and *Leishmania major* (LmjF.20.0090) homologs. Multisequence alignments and sequence similarity analysis were performed in Geneious Prime with Clustal Omega BLOSUM62 (www.geneious.com). Topology predictions were done comparing the transmembrane domain predictions of TopPred, TMPred, and TMHMM 2.0 (https://www.expasy.org/tools/). Putative calmodulin binding domains were identified using EML (http://elm.eu.org/search.html) and Calmodulin Target Database (http://calcium.uhnres.utoronto.ca/ctdb/ctdb/sequence.html).

Localization

A fragment of 387 bp of TcCAKC was amplified with primers 5' ATGAAGGGGGGAGACAATA 3' and 5' TTAGGGGTGTT TCCGCACAA 3' and cloned into pET28(a) with restriction sites BamHI and NotI. The plasmid was transformed in *E. coli* pLys-S for expression of a His-tagged fragment of TcCAKC. After purification with Ni-Agarose, the recombinant protein was injected in rabbits to obtain polyclonal antibodies against the channel (Cocalico). The affinity purified final bleeds were used for immunofluorescence assays in the parasites. Briefly, epimastigotes, bloodstream trypomastigotes and amastigotes were fixed for 30 min in 4% paraformaldehyde. Fixed cells were attached to poly-L-lysine-treated glass coverslips for 10 min. Samples were permeabilized with 0.3% Triton X-100 for 3 min, washed in 1x PBS three times and incubated in 50 mM NH_4Cl

for 30 min at room temperature. After blocking overnight at 4°C in 3% bovine serum albumin (BSA) solution, the cells were incubated with antibodies against TcCAKC (1:100), FcBP (1:1,000), Calmodulin (SIGMA) (1:250) or SSP1 (1:100) as indicated. Anti-SSP1 (# NR-50891) was obtained from BEI Resources, NIAID, NIH. The secondary antibodies were conjugated with Alexa-fluor 488 or 594 (1:3,000) (Thermo Fischer Scientific, Inc., Waltham, MA). Coverslips were mounted with Fluoromount-G® (SouthernBiotech, Birmingham, AL) containing DAPI (5 µg/mL). Immunofluorescence samples were imaged in an Olympus® IX83 inverted microscope system and processed with CellSense Olympus software.

Cloning and Expression of TcCAKC in Yeast

The complete ORF of TcCAKC was amplified with forward primer 5' CGGGATCCACCAATGGAGGGGGGAGACAATAC 3' and reverse primer 5' GGAATTCCTGTTGCTTTTGCC ATCCG 3' and cloned into pYES2 vector with restriction sites BamHI and EcoRI (underlined). The gene was verified by primer walking sequencing and transfected into *Saccharomyces cerevisiae* PLY232 (wild-type) and PLY246 (trk1Δ trk2Δ and tok1Δ null mutants) strains kindly provided by Dr. Per O. Ljungdahl (Ludwig Institute for Cancer Research, Sweden) (Bertl et al., 2003). Wild type cells were maintained at 30°C in standard YPD medium and the mutants were supplemented with 50 mM KCl pH 5.8. Transformed cells were selected in synthetic minimal defined medium without uracil, pH 5.8 [SC ura(-) medium] supplemented with 100 mM KCl to maintain the mutant under viable conditions. Positive clones were confirmed by PCR and expression of TcCAKC was induced switching the carbon source from 2% raffinose to 2% galactose. Complementation studies were done seeding serial dilutions of the complemented mutants in SC ura(-)-galactose agar plates without KCl added, keeping them at 30°C for 3–5 days. Wild-type strains transformed with TcCAKC or with the empty vector were used as a control.

Site Directed Mutagenesis and Expression in Oocytes

Site directed mutagenesis of the selectivity filter was done using GeneArt Site Directed Mutagenesis kit (Invitrogen) following the manufacturer protocol. Primers were designed to replace residue 313 (Y) for alanine (Y313A) (forward primer 5' ACGATTTCAACGGTTGGCGCGGGAGATATTATTCC 3' and reverse primer 5' CACCACTGCTAAAGTTGCCAACCGCGCC CTCTATA 3') using the ORF of TcCAKC cloned into TOPO-Blunt II as template and mutations were verified by sequencing. For expression in *Xenopus laevis* oocytes, TOPO-Blunt II vector containing the ORFs for TcCAKC or TcCAKC Y313A was purified and linearized with AseI. Coding RNA (cRNA) was obtained by *in vitro* transcription with mMessage mMachine T7 kit following the manufacturer's protocol (Ambion). The cRNA length and polyadenylation was verified by non-denaturing gel analysis. Injection of 20 ng (20–40 nL) of the cRNA into chemically defolliculated oocytes (EcoCyte Bioscience) was done using the Nano-Inject II system as

previously reported (Jimenez and Docampo, 2015). Oocytes were maintained in Barth's solution (88 mM NaCl, 1 mM KCl, 0.33 mM Ca(NO₃)₂, 0.41 mM CaCl₂, 0.82 mM MgSO₄, 2.4 mM NaHCO₃, 5 mM HEPES, 0.1 mg/mL penicillin/streptomycin) at 18°C with daily changes of the solution. Recordings were done at 72 h post injection. Oocytes injected with RNase free DEPC water were used as controls.

Electrophysiological Recordings

TcCAKC activity was evaluated by two-electrode voltage clamp on oocytes expressing TcCAKC or TcCAKC-Y313A using an Oocyte clamp system OC725 (Warner Instruments). Acquisition of data was done at 10 kHz, with Digidata 1550, and analyzed in pClamp 10. Intracellular electrodes were pulled to resistance of 1–4 MOhms and filled with 3 M KCl solution. Before recording, oocytes were placed in ND-96 recording solution (in mM: NaCl 96, KCl 2, CaCl₂ 1.8, MgCl₂, Na pyruvate 2.5 mM, HEPES 5 mM pH 7.4). The steady-state current of oocytes were recorded in response to voltage steps between –80 and 40 mV, with a holding potential of –60 mV. All recordings were performed in ND-96 recording solution or ND-96 calcium-free solution containing 1 µM calcium-activated chloride channel blocker 4,4'-Diisothiocyanato-2,2'-stilbenedisulfonic acid (DIDS) to reduce background current during recording. Treatment with 1 µM calcium ionophore ionomycin was applied to bath solution during recording to induce activation of K⁺ currents. Pre-incubation of oocytes with 1 µM thapsigargin, a smooth endoplasmic reticulum calcium pump blocker for 30 min was done to test the effects of increased cytosolic free calcium released from intracellular stores. The average current for any voltage pulse was measured using pClamp10 and plotted against the applied voltage pulse. A Student's *t*-test was run between the experimental condition and the control oocytes to compare the average current at each voltage pulse. Differences in reversal potential toward theoretical equilibria of particular ions can be indicative of the ions permeating across the membrane. To measure the effect of TcCAKC expression on membrane permeability, injected oocytes were held under voltage ramps from –80 to 40 mV and reversal potential differences were calculated by subtracting pre-ionomycin treatment reversal potential from post-ionomycin reversal potential ($V_{rev} = V_I - V_F$). Statistics were performed by running a one factor ANOVA with a *post-hoc* Bonferroni correction to compare experimental traces of TcCAKC, and TcCAKC Y313A with control injected oocytes.

Generation of TcCAKC Knockouts and Phenotypic Analysis

Homologous Recombination

TcCAKC knockouts were obtained by sequential allelic replacement by homologous recombination. Recombination cassettes were obtained by PCR of neomycin or hygromycin resistance genes flanked by 500 bp of TcCAKC 5' and 3' UTRs. The fragments were amplified with allele specific primers and cloned into TOPO-Blunt II vector. Constructs verified by sequencing were purified, linearized, and transfected into CL strain epimastigotes using AMAXA nucleofactor system protocol

U-033. Selection was carried out with 250 µg/ml of G418 and 100 µg/ml of hygromycin. Once selection was complete, parasite populations were subcloned by serial dilution and screened by PCR to verify the correct insertion of the replacement cassettes using primers annealing upstream and downstream of TcCAKC UTRs.

Level of expression of TcCAKC in single-allele replacement (sKO) and double-allele replacement parasites (dKO) was evaluated by qPCR. Epimastigotes were collected during mid-log phase of growth, washed once with 1x PBS pH 7.4 and homogenized in TRI Reagent®. Total mRNA was extracted following the manufacturer protocol (Sigma-Aldrich, St. Louis, MO) followed by chloroform/ ethanol precipitation cDNA was obtained using SuperScript® III First-Strand Synthesis System (ThermoFisher Scientific, Inc., Waltham, MA) and oligo-dT₍₂₀₎ primers. cDNA was analyzed by qPCR with Power SYBR Green PCR Master Mix (Applied Biosystems) and primers forward 5' GAACGTGGTTCGGGTCAATCT 3' and reverse 5' GAGGCGACGTGTGTGAGAAT 3'. All qPCR results were normalized against GAPDH and tubulin as housekeeping gene and indicated as $\Delta\Delta Cq$ Mean \pm SD of at least 3 independent experiments in triplicate.

Phenotypic Analysis of Mutants

CL strain epimastigotes were cultured in LIT media supplemented with 10% inactivated Fetal bovine serum (FBS) at 28°C. Knockout parasites were maintained with 250 µg/mL G418 (sKO) plus 100 µg/mL hygromycin (dKO) (Bone and Steinert, 1956). To evaluate the growth of the parasites, cells were diluted to a concentration of 1×10^6 /mL in LIT media supplemented with FBS and antibiotics and counted every 24 h for 5 days in a Z2 Cell Counter (Beckman Instruments). Cell counts were taken in triplicate from three independent experiments. Statistics were ran using one factor ANOVA with *post-hoc* Bonferroni test to compare mutant and wild-type (WT) cells. To evaluate the infective capacity of the mutants, differentiation to metacyclic trypomastigote forms was induced under chemically defined conditions using triatomine artificial urine (TAU) medium as described (Contreras et al., 1985). Epimastigotes at 4 days of growth were collected by centrifugation at $1,600 \times g$ for 10 min, washed once in phosphate buffered saline solution (PBS) pH 7.4, resuspended in TAU media and incubated 2 h at 28°C. The supernatant was collected and resuspended in TAU with amino acids (TAU3AAG), incubated for up to 7 days at 28°C, collected by centrifugation resuspended in 5 mL of Dulbecco's Modified Eagles Media (DMEM) supplemented with 20% fresh FBS to eliminate residual epimastigotes.

In vitro Infection Assays

HEK-293 cells were plated onto coverlips in 12 well plates (1,000 cells/well) and incubated in supplemented HG-DMEM overnight at 37°C with 5% CO₂. Infections were performed at a multiplicity of infection (MOI) of 25:1 with either WT, sKO or dKO mutant trypomastigotes. After 6 h, the cells were washed 3 times with Hank's media and fresh DMEM was added. Coverslips were fixed in 4% paraformaldehyde-PBS at 6, 24, and

48 h, stained with DAPI (5 µg/ml) and mounted in Fluoromont media for quantification of intracellular parasites. All infection quantifications were done in 4 coverslips per experiment, in 3 or more independent experiments. At least 100 host cells were quantified per coverslip. The number of host cells vs. parasites was compared by Student *t*-test.

Fluorometric Measurements

All fluorometric measurements were done in WT, sKO, and dKO TcCAKC epimastigotes collected at 4 days of growth. Cells were pelleted at 1,600 g for 10 min at room temperature, washed three times with Buffer-A with Glucose (BAG: in mM NaCl 116, KCl 5.4, MgSO₄ 0.8, glucose 5, HEPES 50 pH 7.3) and resuspended at a density of 1×10^9 cells/mL in the appropriate buffer for the measurement. Recordings were done on a Hitachi F7000 spectrofluorometer. For all the experiments, ionic replacement was done by substituting Na⁺, K⁺ or both by N-Methyl-D-glucamine (NMDG) in the corresponding standard buffer.

Membrane Potential

Aliquots of 1×10^8 cells were diluted in Standard buffer (in mM: NaCl 135, KCl 5, CaCl₂ 1, MgSO₄ 1, glucose 5, HEPES 10 pH 7.4) plus 1 µM DisBac₂(3). Fluorescence was recorded at 1 Hz with excitation at 530 nm and emission at 560 nm. Calibration was performed by adding 1 µM of gramicidin to WT epimastigotes in NMDG Buffer (composition) and increasing concentrations of K⁺ gluconate (0.1, 1, 2, 5, 10, 25, 50, 100 mM). Calibration potentials were calculated using the theoretical Nernst potential equation [$V_{eq} = \frac{RT}{zF} \ln(\frac{[K^+]_{out}}{[K^+]_{in}})$], where $[K^+]_{in}$ was assumed to be 120 mM (Van Der Heyden and Docampo, 2002). A linear line of best fit was generated and the equation for this line was used for interpolation of experimental data. Experimental measurements were done as described above. Resting membrane potential was averaged over the first 100 s of baseline recording. All recordings were done in Standard buffer unless otherwise indicated.

Intracellular pH

Epimastigotes were loaded with 6 µM BCECF-AM at 30°C for 30 min in standard buffer, washed twice and resuspended at a concentration of 1×10^9 cells/mL in Standard buffer. Fluorescence was measured with excitation wavelengths of 490/440 nm and emission of 530 nm. Recordings were done in Standard Buffer unless otherwise indicated. Calibration was done in high K⁺ Standard Buffer (135 mM KCl, 1 mM MgSO₄, 1 mM CaCl₂, 5 mM glucose and 10 mM HEPES-Tris, pH 7.4), with 1 µM nigericin at various pHs (6, 6.5, 7.0, 7.4, 7.6, 8.0). Once stabilized, the fluorescent reading for any pH was averaged over 100 s and plotted against pH. The linear fit was then used to interpolate the experimental data.

Proton Extrusion

Measurements of proton extrusion were done in the presence of 0.38 µM BCECF Free acid mixed with 1×10^8 epimastigotes in low buffer standard solution (in mM: NaCl 135, KCl 5, CaCl₂ 1, MgSO₄ 1, glucose 5, HEPES 0.1 pH 7.4) (Benchimol et al., 1998). The recordings were done at excitation wavelengths of 490/440 nm and emission of 530 nm. Calibration was performed

as indicated above. Differences in proton extrusion were measured by looking at differences in the slope over the first 50 s of recording (Initial rate of extrusion) or in the last 200 s of recording (Final). All experiments were done in low buffered standard buffer unless otherwise indicated.

Intracellular Calcium

Epimastigotes were loaded with 5 μ M Fura2-AM (Molecular Probes) in BAG for 30 min at 30°C, washed twice and resuspended in BAG at a concentration of 5×10^8 cells/ml. Aliquots of 5×10^7 cells were taken for each measurement with excitation at 340/380 nm and emission at 525 nm. Recordings were performed in BAG unless otherwise indicated. Calibration was done by permeabilizing cells in BAG + 1 mM EGTA and then adding increasing concentrations of CaCl_2 . The concentration of free calcium available was calculated using MaxChelator software (<https://somapp.ucdmc.ucdavis.edu/pharmacology/bers/maxchelator/CaEGTA-TS.htm>) and the K_d was calculated according to the manufacturer protocol. Experimental recordings were allowed to stabilize at baseline before addition of 1.8 mM CaCl_2 and averaged for 100 s after stabilization. For all the experiments, ionic replacement was done by substituting Na^+ , K^+ or both by N-Methyl-D-glucamine (NMDG) in the corresponding standard buffer.

RESULTS

TcCAKC Shares Structural Features With Other Calcium-Activated Potassium Channels

The genome of *T. cruzi* CL strain contains two sequences that share homology with calcium-activated potassium channels. CL Brener Esmeraldo-like (TcCLB.506529.150) and Non-Esmeraldo-like haplotypes (TcCLB.510885.60) are 94% identical at the protein level and show 45% identity with *T. brucei* TbK1 (Tb927.1.4450) (Steinmann et al., 2015) and 37% identity with *L. major* homolog LmjF20.0090 (Figure S1). BlastP analysis of Trypanosoma sequences only shows significant homology with sequences encoding for calcium-activated potassium channels (CAKCs), although the overall identity is below 20%. Based on this, we named the channel TcCAKC and further analysis revealed conserved features found in other CAKCs. The channel has 6 transmembrane domains, a conserved selectivity filter (TVGYG) in the loop between TM5 and TM6 and multiple putative calmodulin binding sites (Figure S2), previously described as the mechanism that mediates the calcium dependency of intermediate conductance channels (Sforza et al., 2018). Unlike CAKCs of large conductance, TcCAKC does not possess calcium binding sites, suggesting that its activation is rather mediated by Ca^{2+} -Calmodulin binding, as it has been shown for IK and SK channels.

Localization in the Parasites

Immunolocalization analysis with specific antibodies against TcCAKC show a distinct punctate localization in the periphery of trypomastigotes, epimastigotes, and amastigotes (Figure 1A).

Co-localization with SSP-1 (Figure 1B), a membrane marker for trypomastigotes, confirms that TcCAKC is expressed at the surface of the parasites. As expected based on the topology and sequence analysis, the channel colocalizes with calmodulin (Figure 2B, bottom panel) and flagellar calcium-binding protein (FCaBP-Figure 2B), an important calcium sensor in the flagellum of trypanosomatids (Buchanan et al., 2005).

Functional Studies

Yeast Complementation

To demonstrate the function of TcCAKC as a potassium channel we expressed the protein in *S. cerevisiae* PLY246 (*trk1* Δ *trk2* Δ and *tok1* Δ null mutant). In this strain, the principal K^+ permeation pathways have been eliminated and the cells require the supplementation of the media with high amounts of this ion to sustain their growth (Bertl et al., 2003). After 2 h of induction TcCAKC was expressed in the yeast vacuole and at later points (24 h) in the plasma membrane (Figure S3A). Importantly, the channel expression was able to revert the growth phenotype of this mutant providing evidence that it is, in fact, a K^+ permeable channel (Figure S3B).

Electrophysiological Characterization

Two-electrode voltage clamp recordings of *X. laevis* oocytes expressing TcCAKC showed a stable resting membrane potential of -22.8 ± 7 mV ($n = 24$), similar to the membrane potential of control oocytes injected with DEPC water (-26.8 ± 6 mV, $n = 24$), indicating that the expression of the channel did not significantly affect the health of the oocytes. When cells were subjected to a voltage step protocol from -80 to 40 mV with a holding potential of -60 mV, oocytes expressing TcCAKC (Figure 2A black line) did not show significant differences in their currents compared with control cells (Figure 2A blue line). Addition of ionomycin (IO) did not induce a significant increase in the currents of the control cells, but it elicited a strong current in the TcCAKC expressing cells (Figure 2A red line). Similar activation was observed after incubating the oocytes with thapsigargin to release Ca^{2+} from the endoplasmic reticulum (Figure 2B red line). When extracellular Ca^{2+} was chelated by addition of EGTA to the medium, the effect of ionomycin was abolished (Figure 2C), indicating that the activation can be triggered by Ca^{2+} from intracellular stores or by influx from the extracellular media. These results confirm that TcCAKC is able to form functional channels by itself and its activity requires increase in cytosolic Ca^{2+} . It is important to point out that all recordings were performed in the presence of 1 μ M DIDS to block endogenous currents resulting from the activation of calcium-dependent chloride channels, abundant in *X. laevis* oocytes (Weber W., 1999). TcCAKC activity induced by thapsigargin (Figure 3A red line) was blocked by 1 mM BaCl_2 (Figure 3A black line) while 4-aminopyridine had no significant effect (Figure 3A blue line). To confirm the selective nature of the channel, we mutated the tyrosine at position 313 for alanine (Y313A) and performed similar experiments as described above. This mutation, located in the middle of the conserved selectivity filter (TVGYG), is predicted to render an inactive channel (Heginbotham et al., 1994; Noskov and Roux,

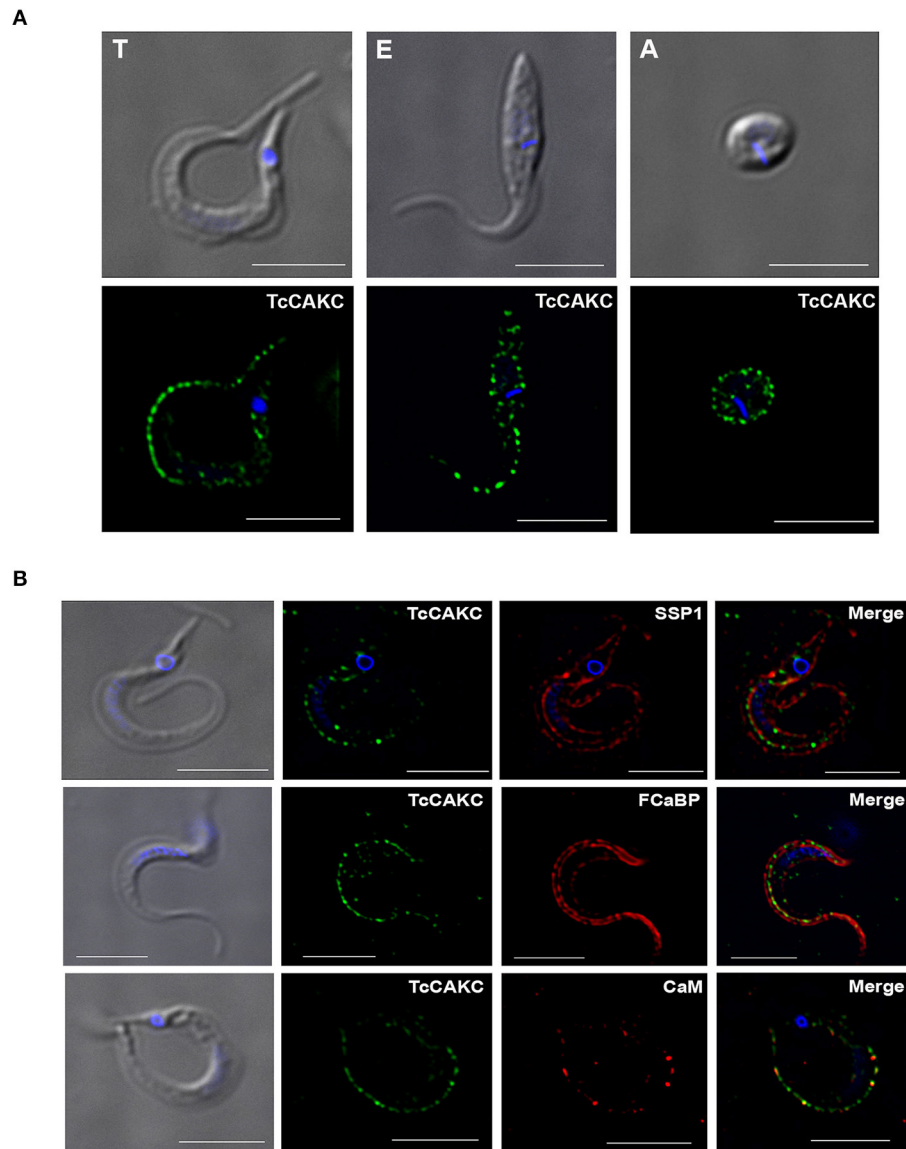


FIGURE 1 | TcCAKC localization. **(A)** Immunofluorescence analysis of *T. cruzi* trypomastigotes (T), epimastigotes (E), and amastigotes (A) with polyclonal antibodies against the channel (green). **(B)** Trypomastigotes immunofluorescence showing TcCAKC (green) colocalization with membrane marker SSP-1 (red), and calcium binding proteins FCaBP and calmodulin. Nuclei and kinetoplasts were DAPI stained. Bar size: 10 μ m.

2006). Indeed, oocytes expressing TcCAKC-Y313A showed no current activation upon treatment with ionomycin (**Figure 3B** green line).

Reversal potential is the voltage at which there is no net current across the membrane and is indicative of the type of ions permeating through a membrane (Hille, 1978). Voltage ramps between -80 and 40 mV were used to test if TcCAKC activation leads to differences in oocyte permeability to K^+ . TcCAKC expressing oocytes treated with ionomycin had a shift in reversal potential of -19.6 mV (**Figure 3C** red), while control and TcCAKC-Y313A expressing oocytes had almost no shifts in reversal potential [**Figure 3C** control -2.14 mV

(black) and TcCAKC-Y313A 0.43 mV (green)]. The shift in reversal potential for the TcCAKC oocytes is in the direction of the theoretical Nernst Potential for K^+ (-80.5 mV, assuming $[K^+]_{\text{intra}}$ of the oocyte is 120 mM, based on previous literature; Weber W. M., 1999), indicates an increase in membrane permeability to K^+ , further confirming TcCAKC as a K^+ conducting channel.

Overall, the functional complementation of K^+ deficient yeast and the biophysical characterization of TcCAKC expressed in *X. laevis* oocytes provide solid evidence that this is a calcium-activated potassium channel that can form functional pores without co-expression of additional subunits.

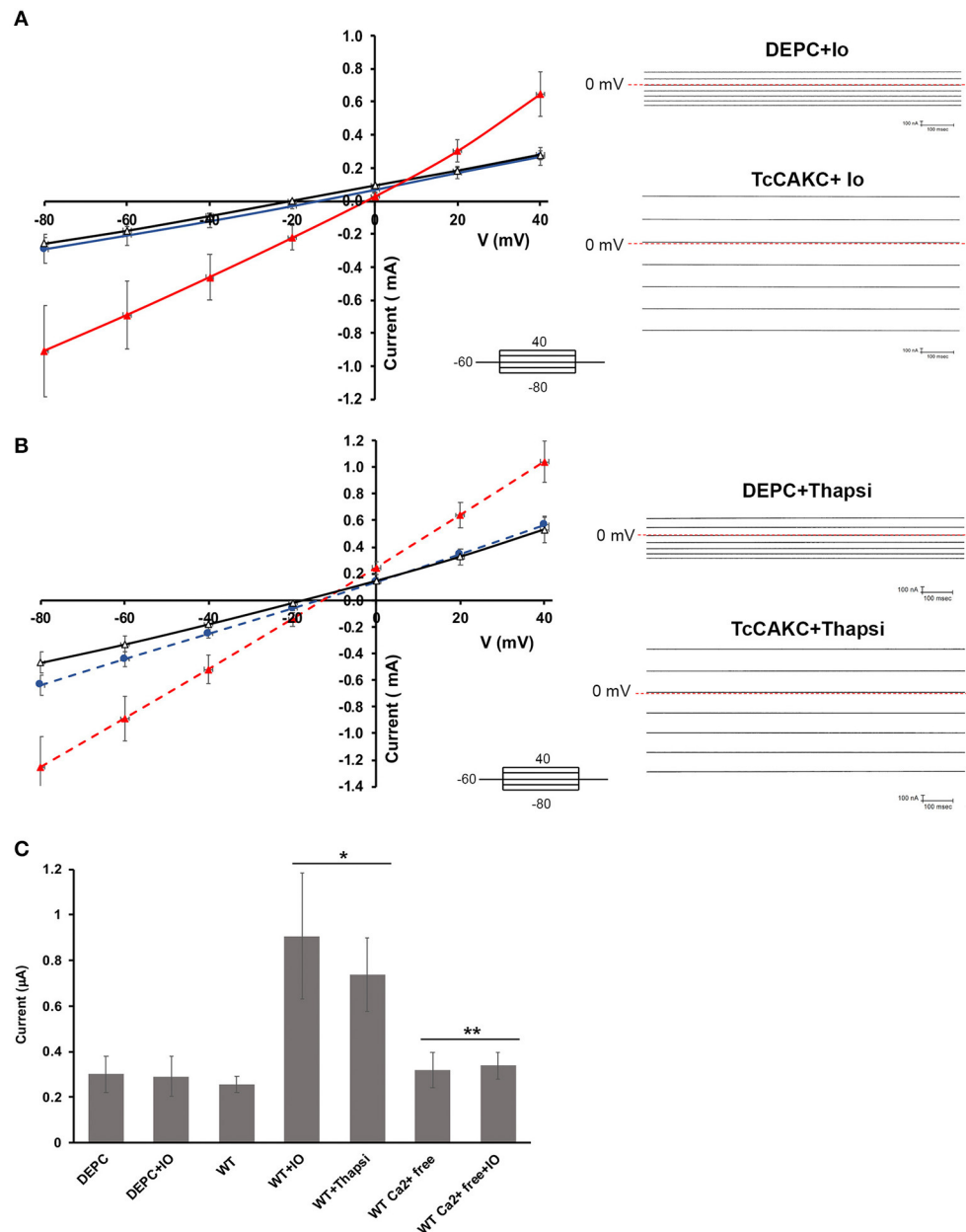


FIGURE 2 | Electrophysiological characterization of TcCAKC. **(A)** Current-voltage relationship of oocytes expressing TcCAKC in the absence (black) or presence (red) of 1 μ M ionomycin. Control currents are obtained from oocytes injected with DEPC water and treated with 1 μ M ionomycin (blue line). Representative traces are shown in the right panel. Values are Mean \pm SD of $n = 18$ oocytes. **(B)** Current-voltage relationship of oocytes expressing TcCAKC (red) or control (blue) preincubated with thapsigargin ($n = 15$). TcCAKC currents in absence of thapsigargin are indicated in black. Representative traces are shown in the right panel. All recordings are in ND-96 buffer with a holding potential of -60 and 20 mV step protocol between -80 and 40 mV. **(C)** Maximum currents at -80 mV (in absolute values) for oocytes under the indicated conditions. Calcium free conditions were achieved by addition of 1 mM EGTA in ND 96 buffer without added CaCl_2 . Values are Mean \pm SD of $n = 15$ oocytes. * $p < 0.01$ respect to the WT, ** $p < 0.01$ respect to the corresponding condition without EGTA.

TcCAKC-KO Impairs Growth and Infectivity in the Parasites

To evaluate the role of TcCAKC in *T. cruzi*, we sequentially replaced both alleles of the gene by homologous recombination with antibiotic resistance cassettes flanked by 500 bp of the 5' and 3'UTR of the gene specific for each haplotype (Figure 4A).

The introduction of the first replacement cassette (neomycin) eliminated the Esmeraldo-like allele (in chromosome 6s), while the non-Esmeraldo like allele (6p) was replaced by a hygromycin resistance gene (Figure 4A). The level of expression was verified by qPCR (Figure 4B), and as expected, ablation of one allele (sKO) decreased the transcript levels by $\sim 50\%$ while elimination

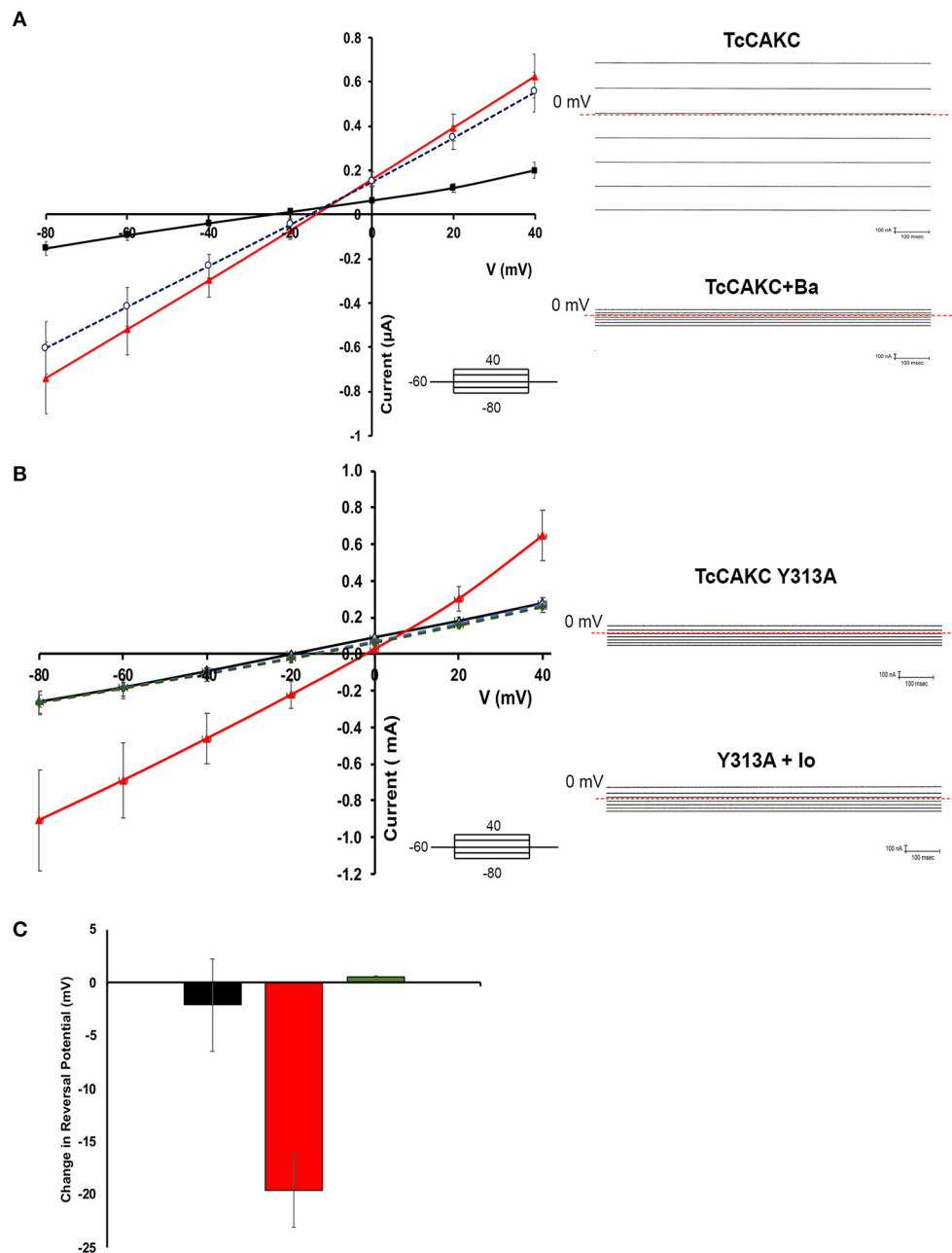


FIGURE 3 | Blockage characteristics of TcCAKC. **(A)** Current-voltage relationship showing the effect of potassium channel blockers on thapsigargin-elicited TcCAKC currents (red line). One millimolar of extracellular BaCl₂ significantly reduced the current (black line) while up to 300 μM 4-AP had no significant effect. Values are Mean ± SD of *n* = 10 oocytes from 3 independent days or recording. Representative traces are shown in the right panel. **(B)** Current-voltage relationship of oocytes expressing WT TcCAKC in absence (black line) or presence (red line) of ionomycin or TcCAKC-Y313A mutant (dotted green and blue lines). Values are Mean ± SD of *n* = 15 oocytes from 3 independent experiments. Representative traces are shown in the right panel. **(C)** Quantification of the reversal potential calculated from the currents obtained under ramp protocols in control oocytes (black), cells expressing TcCAKC (red) or TcCAKC-Y313A (green). Values are Mean ± SD of *n* = 35 oocytes from 7 independent experiments.

of both (dKO) decreased the mRNA levels more than 95%. As a consequence of *TcCAKC* ablation, the growth of sKO and dKO epimastigotes is severely impaired (**Figure 4C**) but despite a very low rate of replication, the phenotype is not lethal, suggesting that K⁺ homeostasis is one of many determinants of parasites

fitness. Importantly, dKO parasites have a significant decrease in infectivity, with low production of intracellular amastigotes (**Figures 4D,E**). These infections are non-productive, as the amastigotes fail to differentiate to trypomastigotes and escape the cells. We were not able to recover tissue-derived trypomastigotes

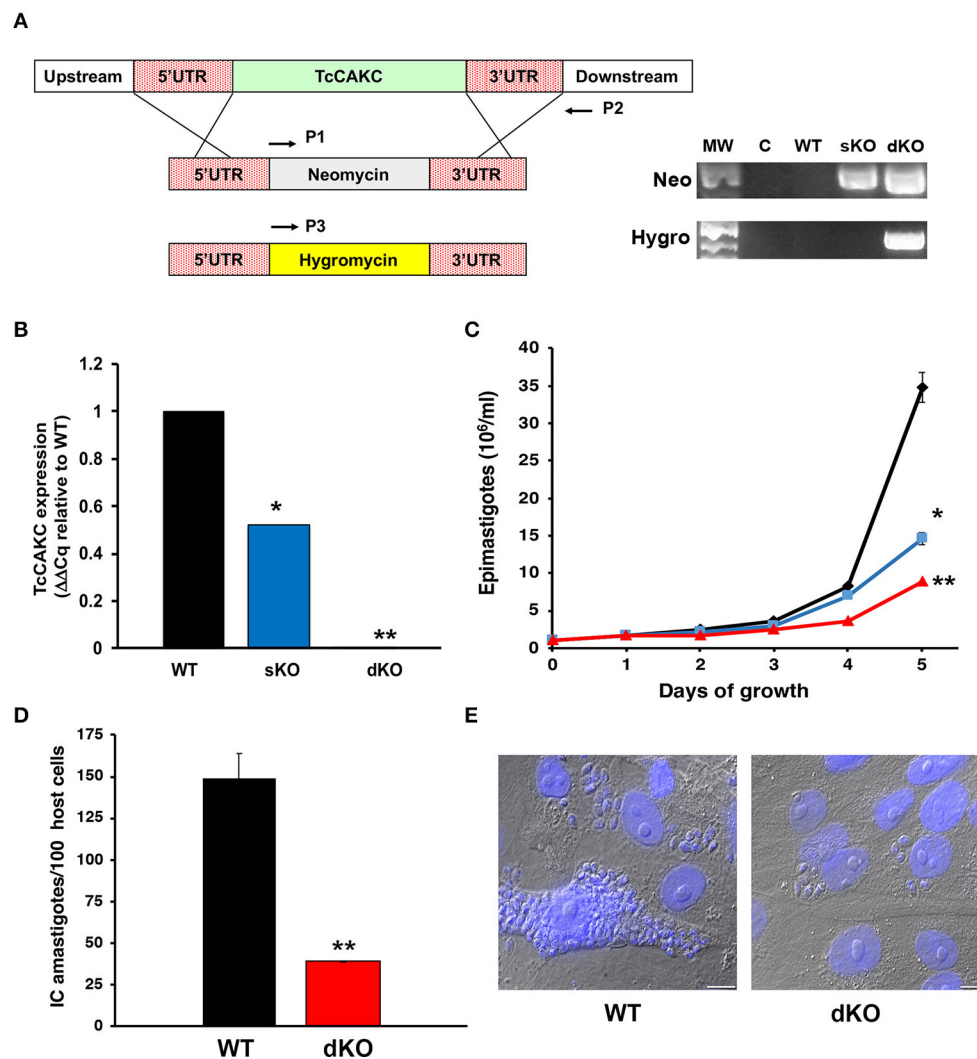


FIGURE 4 | Effect of TcCAKC knockout in *T. cruzi* fitness. **(A)** Schematic representation of the allelic replacement strategy for TcCAKC and genomic DNA screening showing the correct insertion of the drug resistance cassettes, screened with primers P1–P2 (neomycin) and P1–P3 (hygromycin). **(B)** qPCR analysis of TcCAKC expression levels in epimastigotes wild type (WT), one (sKO) or both (dKO) TcCAKC alleles replaced. Values are expressed as $\Delta\Delta Cq$ and normalized using GAPDH and tubulin as housekeeping genes. Mean \pm SD of 3 independent experiments. $***p < 0.01$ respect to WT. **(C)** Growth curve of epimastigotes WT (black), sKO (blue) and dKO (red). Mean \pm SD of 3 independent experiments. $***p < 0.05$ respect to WT at day 5 of growth. **(D)** Quantification of intracellular amastigotes comparing WT and dKO parasites at 48 h post-infection. At least 100 host cells were counted in 4 coverslips per experiment, 3 independent experiments. Mean \pm SD of 3 independent experiments, $**p < 0.01$. **(E)** Representative images of infections quantified in **(D)**. The cells were fixed and DAPI stained for quantification.

from the supernatant of the cultures and all infection assays were done with metacyclic trypomastigotes differentiated *in vitro*. This is not surprising given the fact that intracellular amastigotes develop in a high potassium environment, where TcCAKC seems to be playing an essential role in parasite homeostasis.

TcCAKC Regulates Key Physiological Parameters

Membrane Potential

Since other CAKCs have major influences on membrane potential modulation in eukaryotic cells, it was of interest to elucidate its role in *T. cruzi*. To test this, fluorometric

measurements of resting membrane potential and membrane potential responses were performed to compare differences between WT and mutant epimastigotes. In standard buffer, dKO mutants had a hyperpolarized resting membrane potential (-154.7 ± 5.66 mV, $N = 5$) when compared to either the WT parasites (-104.1 ± 5.19 mV, $N = 5$) and sKO parasites (-97.03 ± 9.63 mV, $N = 5$) (Table 1, Figure 5A). This result suggests that TcCAKC plays a role in membrane potential maintenance in *T. cruzi* by allowing the influx of K^+ to the cells. These results are in agreement with previous research, showing that K^+ causes depolarization on epimastigotes and suggesting the presence of a K^+ conducting pathway (Van Der Heyden and Docampo, 2002) responsible for this effect.

TABLE 1 | Resting membrane potential.

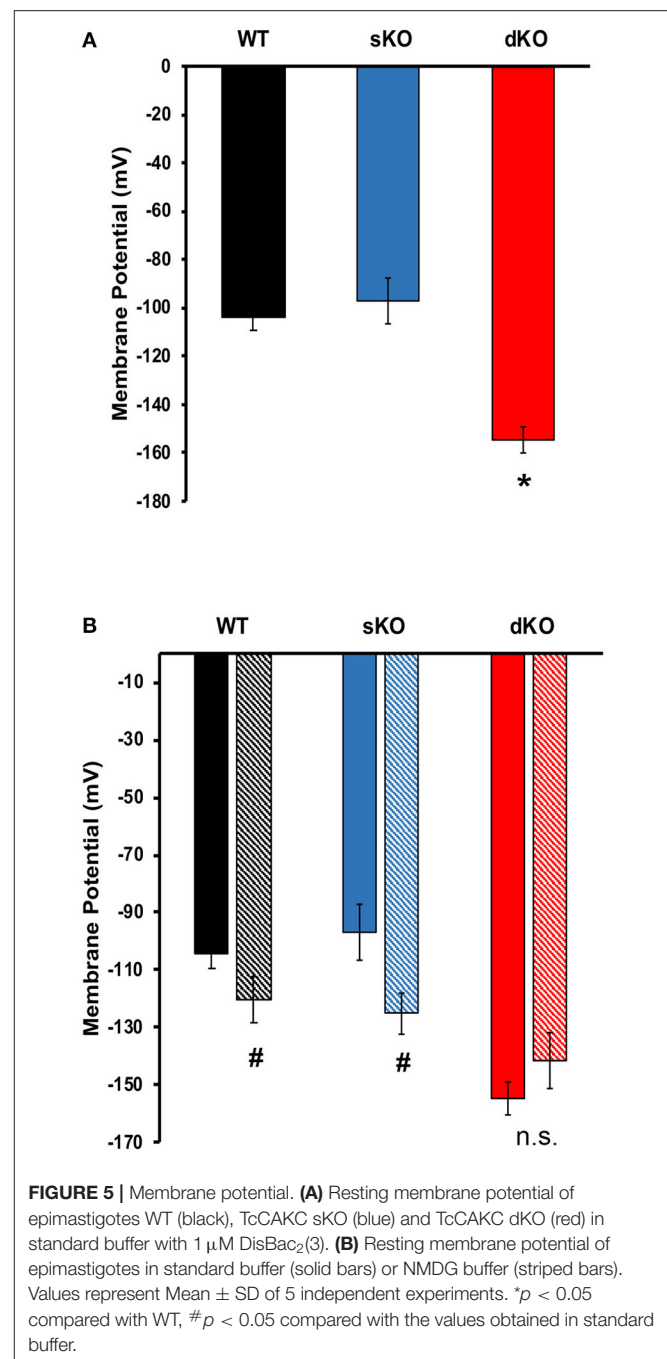
	WT (mV)	sKO (mV)	dKO (mV)
Standard	-104.05±5.19	-97.03±9.63	-154.70±5.65*
Na ⁺ free	-101.96±2.70	-102.13±2.67	-154.24±4.88*
K ⁺ free	-109.20±2.47	-111.30±3.28	-149.65±3.79*
NMDG	-120.40±7.95 [#]	-125.00±7.21 [#]	-141.40±9.81*

Resting membrane potential of epimastigotes in various ionic environments. Epimastigotes were recorded in 1 μ M DisBac₂(3). Data is average resting membrane potential from first 100 s of recording. Data presented as Mean \pm SD. * p < 0.05 when compared to WT in same conditions. [#] p < 0.05 when compared to same cell type in standard buffer using a Two-Way ANOVA with post-hoc Bonferroni correction. N = 5 for all conditions.

The WT and knockout mutants were recorded to ion depleted buffers to test if the extracellular ionic composition has an effect on membrane potential in the parasite. Na⁺ free, and K⁺ free buffers (Table 1) did not have significant effects on the resting membrane potential of any of the cell lines. Replacement of Na⁺ and K⁺ with non-permeating cation N-methyl-D-glucamine (NMDG), produced significant depolarization in WT (-120.40 \pm 7.95 mV) and sKO (-125.00 \pm 7.45 mV) parasites but did not further hyperpolarize the dKO epimastigotes (Figure 5B). These results support previously reported evidence that *T. cruzi* membrane potential is not maintained by Na⁺/K⁺ balance, but is instead primarily dependent on protons (Van Der Heyden and Docampo, 2000). Our results also indicate that, although Na⁺ and K⁺ are not the main driver of membrane potential, the presence of at least one of these ions is required for proper membrane potential homeostasis, presumably to fuel exchangers that contribute to the proton-motive force. To maintain the electrochemical gradients, TcCAKC could be one of the K⁺ influx pathways and its ablation in the dKO parasites pushes the membrane potential to more hyperpolarized values.

pH and Proton Extrusion

Since TcCAKC KO had an important effect on membrane potential maintenance, and previous studies have described protons as the primary regulator of membrane potential in *T. cruzi* (Van Der Heyden and Docampo, 2000), it was vital to interrogate the role TcCAKC had on intracellular pH (pH_i) regulation. The pH_i of WT (7.36 \pm 0.131) and sKO (7.45 \pm 0.082) epimastigotes was similar to previously reported values (Van Der Heyden and Docampo, 2000) but dKO parasites had a drastic intracellular alkalinization (8.01 \pm 0.124) (Figure 6A solid bars, Table 2). No ionic replacement (Na⁺, K⁺, or NMDG) caused a significant change in the cytosolic pH of the WT parasites, but replacement of both Na⁺ and K⁺ with NMDG caused acidification in sKO and dKO epimastigotes suggesting a less robust homeostatic potential when TcCAKC expression is decreased (Figure 6A, striped bars and Table 2). These results confirm previous findings in *T. cruzi* showing an interdependency of pH and membrane potential, linked via proton regulation (Van Der Heyden and Docampo, 2002; Vieira et al., 2005). As TcCAKC dKO cells present a hyperpolarized membrane potential, this is also transduced in a relative proton deficit and the observed cytosolic alkalinization.



To further explore the link between TcCAKC-mediated K⁺ influx and pH regulation we performed pH_i measurements in standard buffer in the presence of 1 mM BaCl₂, a blocker that showed a strong effect in the TcCAKC currents in oocytes (Figure 3A). This divalent cation induced a significant acidification in the WT parasites (Figure 6B) but only a marginal effect in the dKO, indicating that the K⁺ influx through the channel is necessary for pH compensatory mechanisms, perhaps by K⁺/H⁺ and Na⁺/H⁺ exchangers. To test this hypothesis, we measured the rate of proton extrusion in epimastigotes and

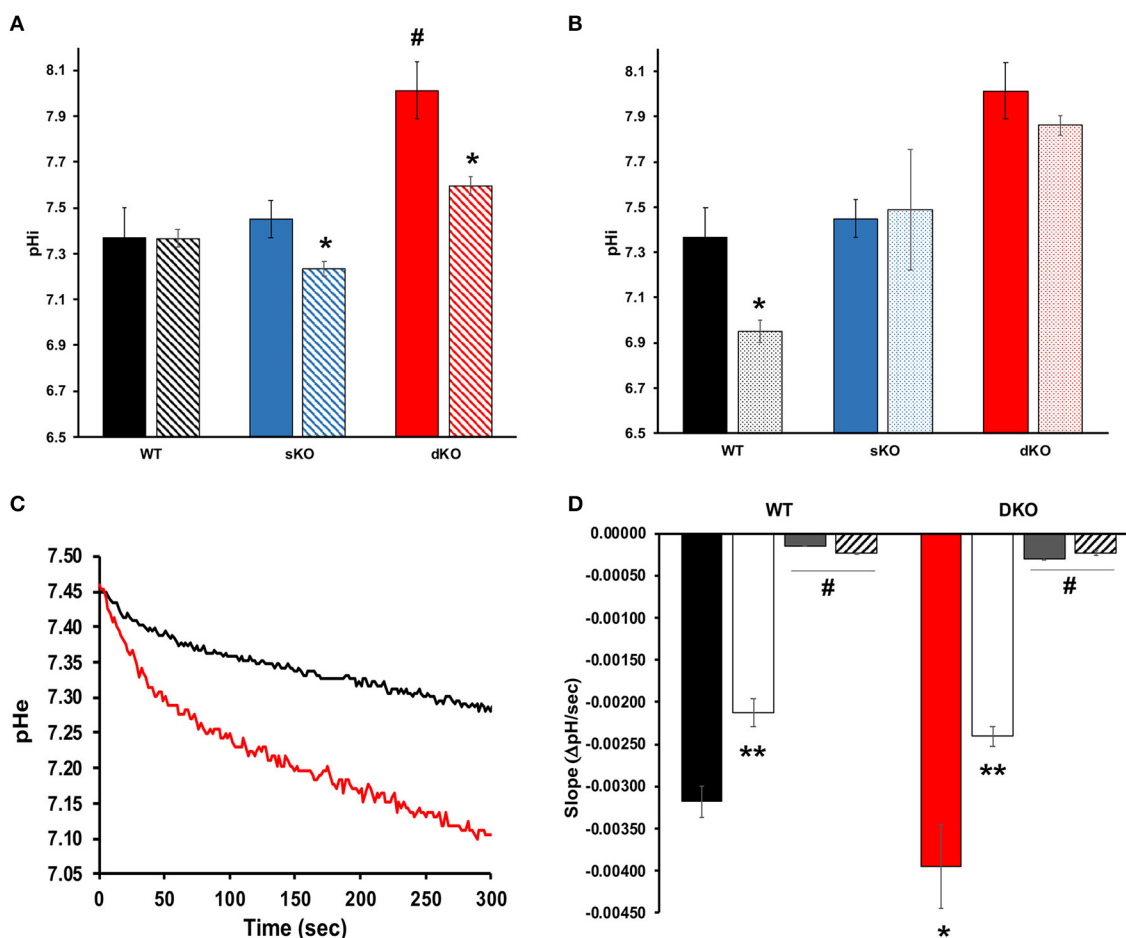


FIGURE 6 | Intracellular pH and proton extrusion. **(A)** Intracellular pH measurements of epimastigotes in standard (solid bars) or NMDG buffer (striped bars). Values represent Mean \pm SD of 4 independent experiments. # indicates $p < 0.05$ compared with WT, * $p < 0.05$ compared with the values obtained in standard buffer. **(B)** Effect of BaCl₂ on pH regulation. Values of intracellular pH were compared in standard buffer with (dotted bars) or without (solid bars) 1 mM BaCl₂. * $p < 0.05$ from 4 independent experiments. **(C)** Representative traces showing proton extrusion in epimastigotes WT (black trace) or TcCAK dKO (red trace) measured with BCECF free acid. **(D)** Slope analysis for the first 50 s of proton extrusion under standard low buffering solution conditions (WT: black bar, dKO: red bar), K⁺-free (white bars), Na⁺ free (gray bars) or NMDG buffer (striped bars). Values are Mean \pm SD of 4 independent experiments. * $p < 0.05$ compared with WT in standard buffer, ** $p < 0.05$ for each strain in K⁺ free compared with the values obtained in standard buffer, # $p < 0.05$ of Na⁺ free or NMDG buffer compared with standard conditions.

TABLE 2 | Intracellular pH of epimastigotes.

	WT	sKO	dKO
Standard	7.36 \pm 0.131	7.45 \pm 0.082	8.01 \pm 0.124*
Na ⁺ free	7.19 \pm 0.241	7.44 \pm 0.110	8.02 \pm 0.037*
K ⁺ free	7.58 \pm 0.097	7.43 \pm 0.044	7.87 \pm 0.184
NMDG	7.37 \pm 0.072	7.23 \pm 0.031*	7.59 \pm 0.04*

Intracellular pH (pH_{intra}) of epimastigotes in various ionic environments. Measurements made in epimastigotes loaded with BCECF-AM. Data is average pH from first 50 s of recording before any treatment given. Data presented as M \pm SD. * $p < 0.05$ when compared to the WT strain in the same condition. Two Factor ANOVA with post-hoc Bonferroni correction. N = 4 for all conditions.

found a significantly higher rate of proton extrusion in dKO parasites (**Figure 6C** red line) compared with WT (**Figure 6C** black line). Rate of extrusion measured in extracellular buffer

lacking K⁺ was reduced by 34% both in WT and dKO parasites (**Figure 6D** white bars) and was almost completely eliminated in absence of Na⁺ (**Figure 6D** gray bars) or when both ions were replaced by NMDG (**Figure 6D** striped bars). This provides strong evidence of the presence of active ion exchangers in *T. cruzi*.

Intracellular Calcium Levels

Calcium plays a central role in *T. cruzi*, regulating cell infectivity (Moreno et al., 1994; Caradonna and Burleigh, 2011) and signaling (Burleigh and Woolsey, 2002; Docampo and Huang, 2014). Intracellular calcium balance depends on strict membrane potential regulation as the main plasma membrane permeation pathways are voltage-gated calcium channel (Verheugen et al., 1995; Christel and Lee, 2012; Harraz and Altier, 2014). Thus, we investigated whether TcCAK

TABLE 3 | Baseline $[Ca^{2+}]_{intra}$ in epimastigotes.

	WT	sKO	dKO
BAG	105 ± 6.69	98.5 ± 9.05	55.4 ± 8.84*
Na ⁺ Free	35.2 ± 19.7 [#]	54.3 ± 4.92 [#]	44.9 ± 10.1
K ⁺ Free	35.8 ± 7.39 [#]	55.1 ± 5.35 [#]	71.7 ± 11.34
NMDG	14.7 ± 2.67 [#]	58.5 ± 11.4 [#]	25.4 ± 9.13

Intracellular Ca^{2+} concentrations ($[Ca^{2+}]_{intra}$ in nM) of epimastigotes in various ionic environments. Fura-2AM loaded epimastigotes were used to measure $[Ca^{2+}]_{intra}$. Baseline data is average $[Ca^{2+}]_{intra}$ for first 50 s of recording. Data presented as $M \pm SD$. * $p < 0.05$ when compared to the WT strain in the same condition. [#] $p < 0.05$ when compared to standard conditions in the same strain. Multiple conditions were analyzed by ANOVA with post-hoc Bonferroni correction. $N = 5$ for all experiments.

function affects calcium homeostasis in the parasites. Fluo2-AM loaded dKO epimastigotes in BAG had a lower steady state intracellular calcium (55.4 ± 8.84 nM) compared with WT (105 ± 6.69 nM) and sKO (98.5 ± 9.05 nM) as it is shown in **Figures 7A,B**. Upon addition of 1.8 mM extracellular calcium, WT and sKO show a robust increase in cytosolic calcium (**Figure 7A** black and blue lines, respectively), while dKO have a modest increase (**Figure 7A** red line), reaching levels similar to WT under baseline conditions (first 50 s). Given the significant difference in intracellular calcium observed in the TcCAKC dKOs, we compared calcium concentrations under ionic replacement conditions by normalizing the values respect to the initial fluorescence ratio for each cell line. WT epimastigotes show a reduced cytosolic calcium increase when under Na⁺ free, K⁺ free or NMDG conditions (**Figure 7C** and **Table 3**) indicating that, at least 60% of the increase is dependent of monovalent cations. This effect can be attributed to direct activity of channel and exchangers or indirectly through decrease of the open probability of voltage-gated calcium channels, as we have observed that in absence of monovalent cations epimastigotes are hyperpolarized (**Figure 5B**). As expected, the cytosolic calcium levels stayed lower in dKOs under all ionic conditions (**Figures 7D,E** and **Table 3**).

In summary, ablation of TcCAKC has a profound effect on cellular homeostasis, with epimastigotes showing a significant hyperpolarization, increase in intracellular pH and rate of proton extrusion, and decrease in cytosolic Ca^{2+} concentrations. These results, together with the observed reduction in growth rate and the inability to produce sustained infection in mammalian cells supports the role of TcCAKC as key regulator of *T. cruzi* physiological fitness.

DISCUSSION

Ion channels properties and their roles in a diverse range of cellular functions have been extensively studied in mammalian cells and bacteria. Surprisingly, much less information is available regarding ion channel function in other organisms and especially in protozoan parasites. Ion channels show highly conserved functional domains but the overall sequence identity is low, making difficult their finding by bioinformatics methods. At the

same time, their divergence from channels present in mammalian hosts provide a unique opportunity for the development of selective new drugs.

This work provides molecular and functional evidences of the expression of a calcium-activated potassium channel required for parasite growth and infectivity. TcCAKC shares general structural features with other CAKCs: a 6 transmembrane domain topology, with a highly conserved selectivity filter (TVGYG) in the loop between TM5 and TM6 and a long C terminal domain. Unlike CAKCs of large conductance (BK), TcCAKC does not have Ca^{2+} binding sites known as “calcium bowls” Instead, putative calmodulin binding domains were predicted at the C- and N terminal ends of the protein. This is characteristic of CAKCs of intermediate and low conductance, which activation depends on calcium-calmodulin binding (Kaczmarek et al., 2017; Sforza et al., 2018). TcCAKC was expressed in all three main life stages of the parasites and colocalized with calcium-binding proteins FCBP and calmodulin, providing further support of its activation via calcium-calmodulin complexes.

TbK1, the *T. brucei* homolog previously described does not possess a conserved selectivity filter and requires dimerization with TbK2 to produce significant currents when expressed in *X. laevis* oocytes (Steinmann et al., 2015). In contrast, TcCAKC expression and analysis by two-electrode voltage clamp produced robust and reproducible currents that require activation by calcium, indicating that TcCAKC encodes an α -pore forming subunit able to traffic and assemble into functional channels. No accessory β -subunits of K⁺ channels have been identified in *T. cruzi*, but recent reports have shown that KHARON, a protein complex unique to trypanosomatids, is required for correct targeting of calcium in *T. brucei* (Sanchez et al., 2016) and glucose transporters in Leishmania (Tran et al., 2013), highlighting a non-canonical pathway for membrane protein trafficking in these parasites.

The electrophysiological characterization of TcCAKC confirms its calcium-dependency and our results show that either intra or extracellular pools can be used as a source for activation of the channel. Interestingly, barium significantly decreases the current elicited by TcCAKC, while other typical K⁺ channel blockers such as 4-AP and TEA had no significant effect. Barium has been described as a potent modulator with activation and blockage effects depending on cell and channel types (Inomoto and Tokimasa, 1998; Zhou et al., 2012; Wrighton et al., 2015; Kourghi et al., 2017), but its lack of selectivity precludes its use as a potential therapeutic drug. Recently, it has been shown that combination of antibiotics with zinc restore the susceptibility of antibiotic resistant Gram (-) bacteria (Magallon et al., 2019). This approach is worth of consideration, as the combination of anti-parasitic drugs of low efficacy with barium or other less toxic metals could increase the susceptibility of the parasites and provide new avenues for drug development.

In the parasites, TcCAKC knockout has a dramatic effect on the growth of epimastigotes and impairs infectivity, with a reduction of the number of intracellular amastigotes and lack of production of tissue-derived trypomastigotes. It is well-documented the role that K⁺ channels play in regulating cell proliferation in tumoral (Liu et al., 2017; Steudel et al., 2017) and

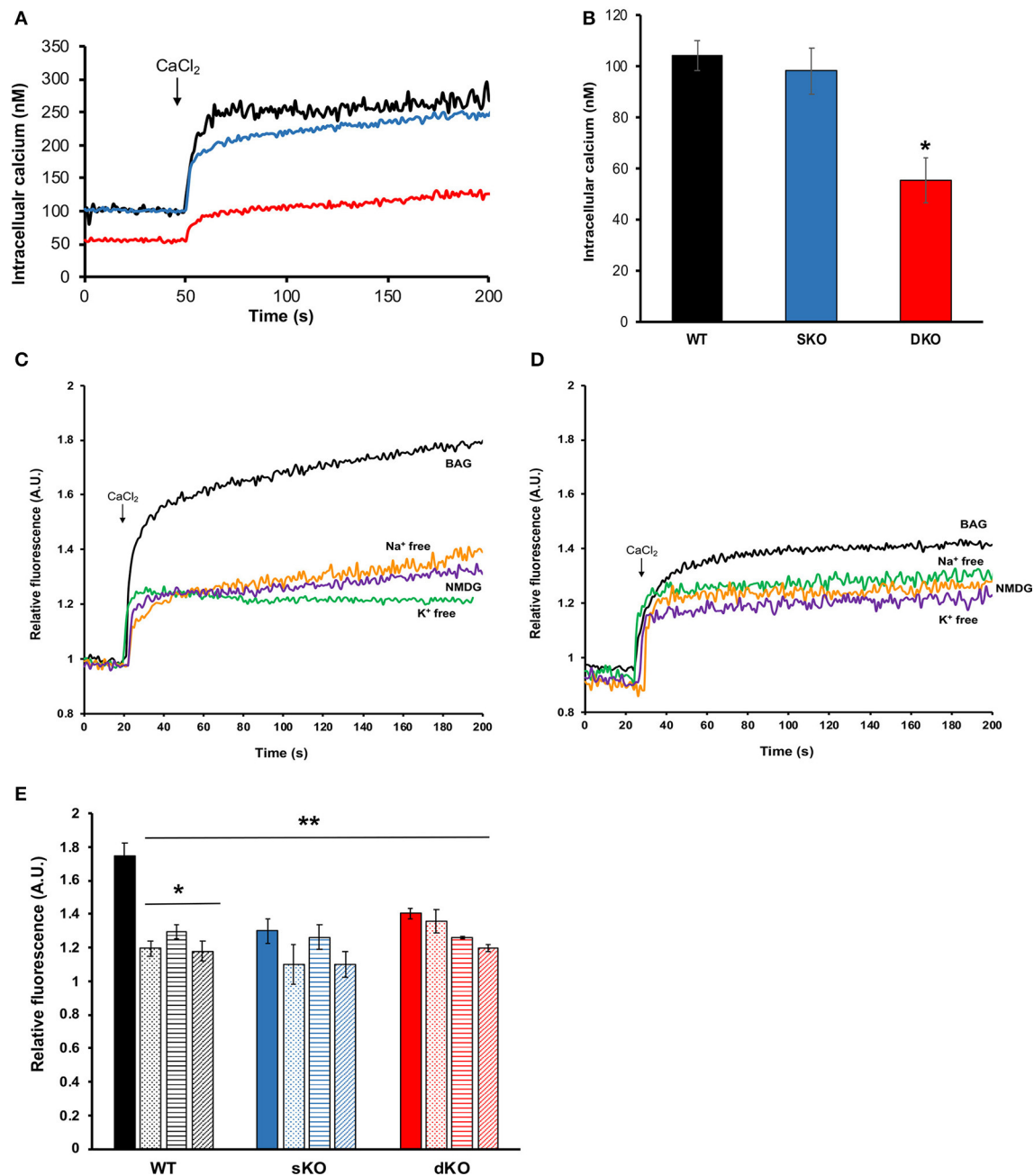


FIGURE 7 | Intracellular calcium measurements. **(A)** Representative traces of Fura-2 AM loaded epimastigotes showing intracellular calcium concentrations for WT (black trace), sKO (blue trace) or dKO (red trace) in BAG. At 50 s of recording, 1.8 mM CaCl_2 was added to the extracellular buffer. **(B)** Quantification of baseline intracellular calcium in BAG prior to extracellular calcium addition. Values are Mean \pm SD of 5 independent experiments. * $p < 0.05$ compared with WT. **(C,D)** Representative traces of intracellular calcium measurements (in relative fluorescence units for comparison purposes) of WT **(C)** and TcCAKs dKO **(D)**, in the indicated buffer conditions. **(E)** Intracellular calcium changes (in relative units) upon CaCl_2 addition in WT (black), sKO (blue), and dKO (red) epimastigotes in BAG (solid bars), Na^+ free (dotted bars), K^+ free (horizontal stripe bars) or NMDG buffer (striped bars). Values are Mean \pm SD of 5 independent experiments. * $p < 0.05$ compared with BAG, ** $p < 0.05$ of each condition and strain compared with WT in BAG. Statistical analysis for multiple conditions was done by two-way ANOVA with *post-hoc* Bonferroni correction.

non-tumoral cells (He et al., 2011; Urrego et al., 2014). CAKCs control the progression of the cell cycle by mechanisms associated with K^+ permeation and by signaling pathways activated independently of the channel pore activity (reviewed in Urrego

et al., 2014). Coordinated oscillation of K^+ channels expression and activity are linked to the expression of cyclins. Moreover, hyperpolarization of cells causes arrest in G1/S checkpoint and decreases cell proliferation (Wonderlin et al., 1995; Márián et al.,

2000; Ouadid-Ahidouch et al., 2004). Activation of K^+ potassium channels also maintains an electrochemical gradient that favors Ca^{2+} influx into the cells, regulating proliferation through signaling (Lee et al., 1993; Lin et al., 1993; Lallet-Daher et al., 2009). As we evaluated the phenotype of TcCAKC dKO cells, we found a significant decrease in the resting membrane potential toward hyperpolarized potentials and a reduction in cytosolic Ca^{2+} concentration. It is plausible to think that TcCAKC is playing similar roles in *T. cruzi* as the ones described in other cell types where CAKCs regulate cell replication rates. Our results demonstrate that, while the channel participates in resting membrane potential maintenance, K^+ is not the primary driver of the electrical gradient across membranes as cells are able to maintain their membrane potential in absence of this ion. This agrees with previous evidences showing the role of H^+ and Na^+ ATPases in *T. cruzi* membrane potential regulation (Van Der Heyden and Docampo, 2002). Van der Heyden et al. also demonstrated that increase in extracellular K^+ causes depolarization (Van Der Heyden and Docampo, 2002). Since the theoretical V_{eq} for K^+ in the recording conditions was -85 mV, K^+ would flow inward to the cell through conductive pathways, so the loss of TcCAKC would cause hyperpolarization due to less positive charge build-up in the cytosol. Membrane potential and intracellular pH homeostasis are linked with one another in *T. cruzi* due to the regulation of membrane potential by H^+ ATPases

located in the membrane (Van Der Heyden and Docampo, 2000). TcCAKC deletion caused significant alkalization compared to that of WT or sKO parasites, which correlates with the hyperpolarization of dKO cells. A similar link between these two parameters has been shown in *Arabidopsis* (Gambale and Uozumi, 2006). Ba^{2+} treatment only caused acidification in WT but not in sKO or dKOs parasites, also suggesting that pH regulation is partially K^+ dependent. Membrane potential and changes in intracellular pH were accompanied by an increase in the rate of proton extrusion in the dKO compared with WT parasites. The rate of proton extrusion was moderately decreased in absence of K^+ , but practically abolished in absence of Na^+ arguing about the presence of Na^+/H^+ and K^+/H^+ exchangers. Biochemical evidences support the presence of these transporters in *T. cruzi* (Van Der Heyden and Docampo, 2002; Gil et al., 2003), and at least 1 gene encoding for a putative Na^+/H^+ antiporter (TcCLB.510511.9) is present in the *T. cruzi* genome, but no expression or functional evidences have been reported.

The evidences found in the literature together with the results reported here are drawing a clearer picture of how *T. cruzi* regulates ionic homeostasis (Figure 8). The resting membrane potential is maintained primarily by H^+ ATPases and only partially supported by K^+ (Van Der Heyden and Docampo, 2002). The activity of these ATPases is possible due to proton gradients maintained by metabolic activity and exchangers such as Na^+/H^+ and K^+/H^+ antiporters. Yet, the intracellular environment is abundant in K^+ that can be mobilized via non-selective cation channels (Jimenez and Docampo, 2012), TcCAKC and most probably other K^+ channels (Jimenez et al., 2011). With a resting membrane potential close to -100 mV, TcCAKC could be mediating K^+ influx that buffers the hyperpolarization effect caused by H^+ efflux and activates voltage gated Ca^{2+} channels. In the absence of TcCAKC the reduction in inward currents will cause a shift in membrane potential to more negative values, alkalization of the cytosol and decrease in calcium levels. As consequence of inadequate ionic homeostasis and changes in membrane potential, the replication rate and infectivity of the parasites is severely impaired. This working model provides us with a roadmap to keep interrogating canonical and non-canonical functions of ion channels in trypanosomatids and to explore new avenues for drug development targeting these unique proteins.

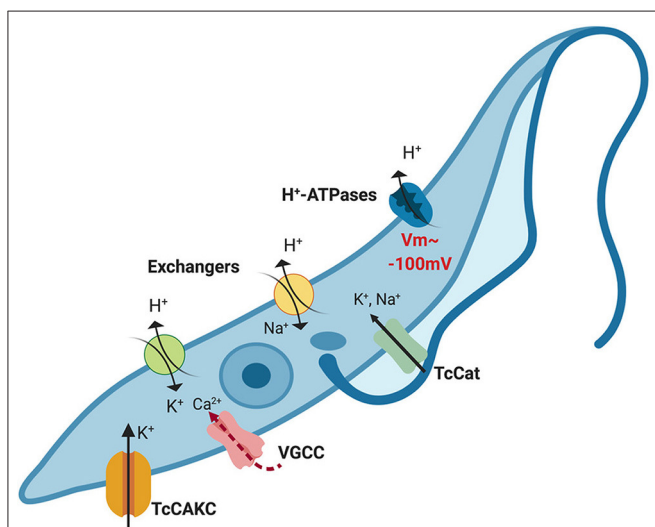


FIGURE 8 | Proposed model of ionic homeostasis in *T. cruzi*. H^+ ATPases maintain the gradient of protons that drive the resting membrane potential, which is about -100 mV in epimastigotes. Additionally, Na^+/H^+ and K^+/H^+ exchangers contribute to H^+ extrusion mobilizing other monovalent ions. Intracellular potassium concentration is balanced through the combined action of channels and exchangers. Given the negative membrane potential beyond the theoretical equilibrium potential for K^+ (~ -80 mV), activation of TcCAKC can mediate K^+ efflux until the membrane potential reaches values higher than the equilibrium potential, when the electrochemical gradient will drive K^+ out of the cells. Depolarization of the membrane could then activate voltage-gated calcium channels (VGCC), responsible for oscillations of the intracellular Ca^{2+} concentration. For simplicity purposes, in this model we have omitted PMCA and SERCA-like pumps that participate in intracellular calcium homeostasis.

DATA AVAILABILITY STATEMENT

The datasets generated for this study are available on request to the corresponding author.

AUTHOR CONTRIBUTIONS

PB and ND were responsible for the design and execution of the mutant and knockout cell lines. CS and MB performed growth assays, electrophysiological recordings, and fluorometric measurements. VJ designed and directed the study, analyzed data, provided funding, and wrote the manuscript.

FUNDING

Funding for this work was provided by NIH-NIAID grant R00AI101167 to VJ.

ACKNOWLEDGMENTS

We would like to thank Dr. Roberto Docampo for his guidance and support in the initial steps of this work, Dr. Per O.

Ljungdahl for generously providing yeast strains, Dr. David Engman for FCBP antibodies and Dr. Douglas Pace for fruitful scientific discussions.

SUPPLEMENTARY MATERIAL

The Supplementary Material for this article can be found online at: <https://www.frontiersin.org/article/10.3389/fcimb.2019.00464/full#supplementary-material>

REFERENCES

- Alix, P., Venkatesan, K., Scuvée-Moreau, J., Massotte, L., Nguyen Trung, M. L., Cornil, C. A., et al. (2014). Mechanism of the medium-duration afterhyperpolarization in rat serotonergic neurons. *Eur. J. Neurosci.* 39, 186–196. doi: 10.1111/ejn.12408
- Aslett, M., Aurrecochea, C., Berriman, M., Brestelli, J., Brunk, B. P., Carrington, M., et al. (2009). TriTrypDB: a functional genomic resource for the *Trypanosomatidae*. *Nucleic Acids Res.* 38(Suppl. 1), D457–D462. doi: 10.1093/nar/gkp851
- Bae, C., Sachs, F., and Gottlieb, P. A. (2011). The mechanosensitive ion channel *Piezol* is inhibited by the peptide GsMTx4. *Biochemistry* 50, 6295–6300. doi: 10.1021/bi200770q
- Benchimol, M., De Souza, W., Vanderheyden, N., Zhong, L., Lu HG., Moreno, S. N., et al. (1998). Functional expression of a vacuolar-type H⁺-ATPase in the plasma membrane and intracellular vacuoles of *Trypanosoma cruzi*. *Biochem. J.* 332 (Pt 3), 695–702. doi: 10.1042/bj3320695
- Bertl, A., Ramos, J., Ludwig, J., Lichtenberg-Fraté, H., Reid, J., Bihler, H., et al. (2003). Characterization of potassium transport in wild-type and isogenic yeast strains carrying all combinations of *trk1*, *trk2* and *tok1* null mutations. *Mol. Microbiol.* 47, 767–780. doi: 10.1046/j.1365-2958.2003.03335.x
- Bond, C. T., Maylie, J., and Adelman, J. P. (1999). Small-conductance calcium-activated potassium channels. *Ann. N. Y. Acad. Sci.* 868, 370–378. doi: 10.1111/j.1749-6632.1999.tb11298.x
- Bone, G. J., and Steinert, M. (1956). Induced change from culture form to blood-stream form in *Trypanosoma mega*. *Nature* 178:362. doi: 10.1038/178362a0
- Buchanan, K. T., Ames, J. B., Asfaw, S. H., Wingard, J. N., Olson, C. L., Campana, P. T., et al. (2005). A flagellum-specific calcium sensor. *J. Biol. Chem.* 280, 40104–40111. doi: 10.1074/jbc.M505777200
- Burleigh, B. A., and Woolsey, A. M. (2002). Cell signalling and *Trypanosoma cruzi* invasion. *Cell Microbiol.* 4, 701–711. doi: 10.1046/j.1462-5822.2002.00226.x
- Caradonna, K. L., and Burleigh, B. A. (2011). Mechanisms of host cell invasion by *Trypanosoma cruzi*. *Adv. Parasitol.* 76, 33–61. doi: 10.1016/B978-0-12-385895-5.00002-5
- Chiurillo, M. A., Lander, N., Bertolini, M. S., Storey, M., Vercesi, A. E., and Docampo, R. (2017). Different roles of mitochondrial calcium uniporter complex subunits in growth and infectivity of *Trypanosoma cruzi*. *MBio* 8, e00574-17. doi: 10.1128/mBio.00574-17
- Christel, C., and Lee, A. (2012). Ca²⁺-dependent modulation of voltage-gated Ca²⁺ channels. *Biochim. Biophys. Acta* 1820, 1243–1252. doi: 10.1016/j.bbagen.2011.12.012
- Contreras, V. T., Salles, J. M., Thomas, N., Morel, C. M., and Goldenberg, S. (1985). *In vitro* differentiation of *Trypanosoma cruzi* under chemically defined conditions. *Mol. Biochem. Parasitol.* 16, 315–327. doi: 10.1016/0166-6851(85)90073-8
- Docampo, R., and Huang, G. (2014). Calcium signaling in trypanosomatid parasites. *Cell Calcium* 57, 194–202. doi: 10.1016/j.ccca.2014.10.015
- Gambale, F., and Uozumi, N. (2006). Properties of shaker-type potassium channels in higher plants. *J. Membr. Biol.* 210, 1–19. doi: 10.1007/s00232-006-0856-x
- Gil, J. R., Soler, A., Azzouz, S., and Osuna, A. (2003). Ion regulation in the different life stages of *Trypanosoma cruzi*. *Parasitol. Res.* 90, 268–272. doi: 10.1007/s00436-003-0847-0
- Gill, J., Heel, R. C., and Fitton, A. (1992). Amiodarone. An overview of its pharmacological properties, and review of its therapeutic use in cardiac arrhythmias. *Drugs* 43, 69–110. doi: 10.2165/00003495-199243010-00007
- Gui, L., LaGrange, L. P., Larson, R. A., Gu, M., Zhu, J., and Chen, Q. H. (2012). Role of small conductance calcium-activated potassium channels expressed in PVN in regulating sympathetic nerve activity and arterial blood pressure in rats. *Am. J. Physiol. Regul. Integr. Comp. Physiol.* 303, R301–R310. doi: 10.1152/ajpregu.00114.2012
- Harraz, O. F., and Altier, C. (2014). STIM1-mediated bidirectional regulation of Ca(2+) entry through voltage-gated calcium channels (VGCC) and calcium-release activated channels (CRAC). *Front. Cell. Neurosci.* 8:43. doi: 10.3389/fncel.2014.00043
- He, M. L., Liu, W. J., Sun, H. Y., Wu, W., Liu, J., Tse, H. F., et al. (2011). Effects of ion channels on proliferation in cultured human cardiac fibroblasts. *J. Mol. Cell. Cardiol.* 51, 198–206. doi: 10.1016/j.yjmcc.2011.05.008
- Heginbotham, L., Lu, Z., Abramson, T., and MacKinnon, R. (1994). Mutations in the K⁺ channel signature sequence. *Biophys. J.* 66, 1061–1067. doi: 10.1016/S0006-3495(94)80887-2
- Hille, B. (1978). Ionic channels in excitable membranes. Current problems and biophysical approaches. *Biophys. J.* 22, 283–294. doi: 10.1016/S0006-3495(78)85489-7
- Hite, R. K., Tao, X., and MacKinnon, R. (2017). Structural basis for gating the high-conductance Ca(2+)-activated K(+) channel. *Nature* 541, 52–57. doi: 10.1038/nature20775
- Horrigan, F. T., and Aldrich, R. W. (2002). Coupling between voltage sensor activation, Ca²⁺ binding and channel opening in large conductance (BK) potassium channels. *J. Gen. Physiol.* 120, 267–305. doi: 10.1085/jgp.20028605
- Huang, G., and Docampo, R. (2018). The mitochondrial Ca(2+) uniporter complex (MCUC) of *Trypanosoma brucei* is a hetero-oligomer that contains novel subunits essential for Ca(2+) uptake. *MBio* 9, e01700-18. doi: 10.1128/mBio.01700-18
- Inomoto, C., and Tokimasa, T. (1998). Effects of barium on delayed rectifier potassium current in bullfrog sympathetic neurons pretreated with wortmannin. *Tokai J. Exp. Clin. Med.* 23, 213–219.
- Jimenez, V. (2014). Dealing with environmental challenges: mechanisms of adaptation in *Trypanosoma cruzi*. *Res. Microbiol.* 165, 155–165. doi: 10.1016/j.resmic.2014.01.006
- Jimenez, V., and Docampo, R. (2012). Molecular and electrophysiological characterization of a novel cation channel of *Trypanosoma cruzi*. *PLoS Pathog.* 8:e1002750. doi: 10.1371/journal.ppat.1002750
- Jimenez, V., and Docampo, R. (2015). TcPho91 is a contractile vacuole phosphate sodium symporter that regulates phosphate and polyphosphate metabolism in *Trypanosoma cruzi*. *Mol. Microbiol.* 97, 911–925. doi: 10.1111/mmi.13075
- Jimenez, V., Henriquez, M., Galanti, N., and Riquelme, G. (2011). Electrophysiological characterization of potassium conductive pathways in *Trypanosoma cruzi*. *J. Cell. Biochem.* 112, 1093–1102. doi: 10.1002/jcb.23023
- Kaczmarek, L. K., Aldrich, W. R., George Chandy, K., Stephan Grissmer, Wei, D. A., and Heike Wulff. (2017). International union of basic

- and clinical pharmacology. C. Nomenclature and properties of calcium-activated and sodium-activated potassium channels. *Pharmacol. Rev.* 69, 1–11. doi: 10.1124/pr.116.012864
- Kollien, A. H., Grospietsch, T., Kleffmann, T., Zerbst-Boroffka, I., and Schaub, G. A., et al. (2001). Ionic composition of the rectal contents and excreta of the reduviid bug *Triatoma infestans*. *J. Insect Physiol.* 47, 739–747. doi: 10.1016/S0022-1910(00)00170-0
- Kourghi, M., Nourmohammadi, S., Pei, J. V., Qiu, J., McGaughey, S., Tyerman, S. D., et al. (2017). Divalent cations regulate the ion conductance properties of diverse classes of aquaporins. *Int. J. Mol. Sci.* 18:E2323. doi: 10.3390/ijms18112323
- Lallet-Daher, H., Roudbaraki, M., Bavencoffe, A., Mariot, P., Gackière, F., Bidaux, G., et al. (2009). Intermediate-conductance Ca^{2+} -activated K^{+} channels (IKCa1) regulate human prostate cancer cell proliferation through a close control of calcium entry. *Oncogene* 28, 1792–1806. doi: 10.1038/onc.2009.25
- Lang, F., Föller, M., Lang, K., Lang, P., Ritter, M., Vereninov, A., et al. (2007). Cell volume regulatory ion channels in cell proliferation and cell death. *Methods Enzymol.* 428, 209–225. doi: 10.1016/S0076-6879(07)28011-5
- Latorre, R., Castillo, K., Carrasquel-Ursulaez, W., Sepulveda, R. V., Gonzalez-Nilo, F., Gonzalez, C., et al. (2017). Molecular determinants of BK channel functional diversity and functioning. *Physiol. Rev.* 97, 39–87. doi: 10.1152/physrev.00001.2016
- Lee, U. S., and Cui, J. (2010). BK channel activation: structural and functional insights. *Trends Neurosci.* 33, 415–423. doi: 10.1016/j.tins.2010.06.004
- Lee, Y. S., Sayeed, M. M., and Wurster, R. D. (1993). Inhibition of cell growth by K^{+} channel modulators is due to interference with agonist-induced Ca^{2+} release. *Cell Signal.* 5, 803–809. doi: 10.1016/0898-6568(93)90041-J
- Lin, C. S., Boltz, R. C., Blake, J. T., Nguyen, M., Talento, A., Fischer, P. A., et al. (1993). Voltage-gated potassium channels regulate calcium-dependent pathways involved in human T lymphocyte activation. *J. Exp. Med.* 177, 637–645. doi: 10.1084/jem.177.3.637
- Liu, L., Zhan, P., Nie, D., Fan, L., Lin, H., Gao, L., et al. (2017). Intermediate-Conductance- Ca^{2+} -activated K^{+} channel IKCa1 is upregulated and promotes cell proliferation in cervical cancer. *Med. Sci. Monit. Basic Res.* 23, 45–57. doi: 10.12659/MSMBR.901462
- MacKinnon, R. (2003). Potassium channels. *FEBS Lett.* 555, 62–65. doi: 10.1016/S0014-5793(03)01104-9
- Magallon, J., Chiem, K., Tran, T., Ramirez, M. S., Jimenez, V., Tolmasky, M. E., et al. (2019). Restoration of susceptibility to amikacin by 8-hydroxyquinoline analogs complexed to zinc. *PLoS ONE* 14:e0217602. doi: 10.1371/journal.pone.0217602
- Márian, T., Balkay, L., Krasznai, Z., and Trón, L. (2000). Membrane permeability changes induce hyperpolarization in transformed lymphoid cells under high-density culture conditions. *Cytometry* 41, 186–92. doi: 10.1002/1097-0320(20001101)41:3<186::aid-cyto5>3.0.co;2-j
- Meier, A., Erler, H., and Beitz, E. (2018). Targeting channels and transporters in protozoan parasite infections. *Front. Chem.* 6:88. doi: 10.3389/fchem.2018.00088
- Moreno, S. N., Silva, J., Vercesi, A. E., and Docampo, R. (1994). Cytosolic-free calcium elevation in *Trypanosoma cruzi* is required for cell invasion. *J. Exp. Med.* 180, 1535–1540. doi: 10.1084/jem.180.4.1535
- Noskov, S. Y., and Roux, B. (2006). Ion selectivity in potassium channels. *Biophys. Chem.* 124, 279–291. doi: 10.1016/j.bpc.2006.05.033
- Ouadid-Ahidouch, H., Roudbaraki, M., Delcourt, P., Ahidouch, A., Joury, N., and Prevarskaya, N. (2004). Functional and molecular identification of intermediate-conductance Ca^{2+} -activated K^{+} channels in breast cancer cells: association with cell cycle progression. *Am. J. Physiol. Cell Physiol.* 287, C125–C134. doi: 10.1152/ajpcell.00488.2003
- Pasantes-Morales, H. (2016). Channels and volume changes in the life and death of the cell. *Mol. Pharmacol.* 90, 358–370. doi: 10.1124/mol.116.104158
- Potapenko, E., Negrão, N. W., Huang, G., and Docampo, R. (2019). The acidocalcisome inositol-1,4,5-trisphosphate receptor of *Trypanosoma brucei* is stimulated by luminal polyphosphate hydrolysis products. *J. Biol. Chem.* 294, 10628–10637. doi: 10.1074/jbc.RA119.007906
- Prole, D. L., and Marrion, N. V. (2012). Identification of putative potassium channel homologues in pathogenic protozoa. *PLoS ONE* 7:e32264. doi: 10.1371/journal.pone.0032264
- Rassi, A., and Marin-Neto, J. A. (2010). Chagas disease. *Lancet* 375, 1388–1402. doi: 10.1016/S0140-6736(10)60061-X
- Rodriguez-Duran, J., Pinto-Martinez, A., Castillo, C., and Benaim, G. (2019). Identification and electrophysiological properties of a sphingosine-dependent plasma membrane Ca^{2+} channel in *Trypanosoma cruzi*. *FEBS J.* 286, 3909–3925. doi: 10.1111/febs.14947
- Rohmann, K. N., Wersinger, E., Braude, J. P., Pyott, S. J., and Fuchs, P. A. (2015). Activation of BK and SK channels by efferent synapses on outer hair cells in high-frequency regions of the rodent cochlea. *J. Neurosci.* 35, 1821–1830. doi: 10.1523/JNEUROSCI.2790-14.2015
- Sanchez, M. A., Tran, K. D., Valli, J., Hobbs, S., Johnson, E., Gluenz, E., et al. (2016). KHARON is an essential cytoskeletal protein involved in the trafficking of flagellar membrane proteins and cell division in African trypanosomes. *J. Biol. Chem.* 291, 19760–19773. doi: 10.1074/jbc.M116.739235
- Sforza, L., Megaro, A., Pessia, M., Franciolini, F., and Catacuzzeno, L. (2018). Structure, gating and basic functions of the Ca^{2+} -activated K^{+} channel of intermediate conductance. *Curr. Neuropharmacol.* 16, 608–617. doi: 10.2174/1570159X15666170830122402
- Steinmann, M. E., González-Salgado, A., Bütikofer, P., Mäser, P., and Sigel, E. (2015). A heteromeric potassium channel involved in the modulation of the plasma membrane potential is essential for the survival of African trypanosomes. *FASEB J.* 29, 3228–3237. doi: 10.1096/fj.15-271353
- Steinmann, M. E., Schmidt, R. S., Bütikofer, P., Mäser, P., and Sigel, E. (2017). TbIRK is a signature sequence free potassium channel from *Trypanosoma brucei* locating to acidocalcisomes. *Sci. Rep.* 7:656. doi: 10.1038/s41598-017-00752-1
- Steudel, F. A., Mohr, J. C., Stegen, B., Nguyen, Y. H., Barnert, A., Steinle, M., et al. (2017). SK4 channels modulate Ca^{2+} signalling and cell cycle progression in murine breast cancer. *Mol. Oncol.* 11, 1172–1188. doi: 10.1002/1878-0261.12087
- Tran, K. D., Rodriguez-Contreras, D., Vieira, D. P., Yates, P. A., David, L., Beatty, W., et al. (2013). KHARON1 mediates flagellar targeting of a glucose transporter in *Leishmania mexicana* and is critical for viability of infectious intracellular amastigotes. *J. Biol. Chem.* 288, 22721–22733. doi: 10.1074/jbc.M113.483461
- Turley, S. L., Francis, K. E., Lowe, D. K., and Cahoon, W. D. (2016). Emerging role of ivabradine for rate control in atrial fibrillation. *Ther. Adv. Cardiovasc. Dis.* 10, 348–352. doi: 10.1177/1753944716669658
- Urrego, D., Tomczak, A. P., Zahed, F., Stühmer, W., and Pardo, L. A. (2014). Potassium channels in cell cycle and cell proliferation. *Philos. Trans. R. Soc. Lond. B Biol. Sci.* 369:20130094. doi: 10.1098/rstb.2013.0094
- Van Der Heyden, N., and Docampo, R. (2000). Intracellular pH in mammalian stages of *Trypanosoma cruzi* is K^{+} -dependent and regulated by H^{+} -ATPases. *Mol. Biochem. Parasitol.* 105, 237–251. doi: 10.1016/S0166-6851(99)00184-X
- Van Der Heyden, N., and Docampo, R. (2002). Proton and sodium pumps regulate the plasma membrane potential of different stages of *Trypanosoma cruzi*. *Mol. Biochem. Parasitol.* 120, 127–139. doi: 10.1016/S0166-6851(01)00444-3
- Verheugen, J. A., Vijverberg, H. P., Oortgiesen, M., and Cahalan, M. D. (1995). Voltage-gated and Ca^{2+} -activated K^{+} channels in intact human T lymphocytes. Noninvasive measurements of membrane currents, membrane potential, and intracellular calcium. *J. Gen. Physiol.* 105, 765–794. doi: 10.1085/jgp.105.6.765
- Vieira, M., Rohloff, P., Luo, S., Narcisca, L., Silva, E. C., Docampo, R., et al. (2005). Role for a P-type H^{+} -ATPase in the acidification of the endocytic pathway of *Trypanosoma cruzi*. *Biochem. J.* 392(Pt 3), 467–474. doi: 10.1042/BJ200-51319
- Weber, W. (1999). Ion currents of *Xenopus laevis* oocytes: state of the art. *Biochim. Biophys. Acta* 1421, 213–233. doi: 10.1016/S0005-2736(99)00135-2
- Weber, W. M. (1999). Endogenous ion channels in oocytes of *Xenopus laevis*: recent developments. *J. Membr. Biol.* 170, 1–12. doi: 10.1007/s002329900532
- Wonderlin, W. F., Woodfork, K. A., and Strobl, J. S. (1995). Changes in membrane potential during the progression of MCF-7 human mammary tumor cells through the cell cycle. *J. Cell. Physiol.* 165, 177–185. doi: 10.1002/jcp.1041650121

- Wrighton, D. C., Muench, S. P., and Lippiat, J. D. (2015). Mechanism of inhibition of mouse Slo3 (KCa 5.1) potassium channels by quinine, quinidine and barium. *Br. J. Pharmacol.* 172, 4355–4363. doi: 10.1111/bph.13214
- Yang, K. (2016). Regulation of excitability in tonic firing substantia gelatinosa neurons of the spinal cord by small-conductance Ca(2+)-activated K(+) channels. *Neuropharmacology* 105, 15–24. doi: 10.1016/j.neuropharm.2016.01.001
- Zhou, Y., Zeng, X. H., and Lingle, C. J. (2012). Barium ions selectively activate BK channels via the Ca2+-bowI site. *Proc. Natl. Acad. Sci. U.S.A.* 109, 11413–11418. doi: 10.1073/pnas.1204444109

Conflict of Interest: The authors declare that the research was conducted in the absence of any commercial or financial relationships that could be construed as a potential conflict of interest.

Copyright © 2020 Barrera, Skorka, Boktor, Dave and Jimenez. This is an open-access article distributed under the terms of the Creative Commons Attribution License (CC BY). The use, distribution or reproduction in other forums is permitted, provided the original author(s) and the copyright owner(s) are credited and that the original publication in this journal is cited, in accordance with accepted academic practice. No use, distribution or reproduction is permitted which does not comply with these terms.



Identification and Localization of the First Known Proteins of the *Trypanosoma cruzi* Cytostome Cytopharynx Endocytic Complex

Nathan Michael Chasen¹, Isabelle Coppens² and Ronald Drew Etheridge^{1*}

¹ Department of Cellular Biology, Center for Tropical and Emerging Global Diseases (CTEGD), University of Georgia, Athens, GA, United States, ² Bloomberg School of Public Health, Johns Hopkins University, Baltimore, MD, United States

OPEN ACCESS

Edited by:

Nobuko Yoshida,
Federal University of São Paulo, Brazil

Reviewed by:

Carlos A. Buscaglia,
National Council for Scientific and
Technical Research
(CONICET), Argentina
Wanderley De Souza,
Federal University of Rio de
Janeiro, Brazil

*Correspondence:

Ronald Drew Etheridge
ronald.etheridge@uga.edu

Specialty section:

This article was submitted to
Parasite and Host,
a section of the journal
Frontiers in Cellular and Infection
Microbiology

Received: 14 October 2019

Accepted: 10 December 2019

Published: 17 January 2020

Citation:

Chasen NM, Coppens I and
Etheridge RD (2020) Identification and
Localization of the First Known
Proteins of the *Trypanosoma cruzi*
Cytostome Cytopharynx Endocytic
Complex.
Front. Cell. Infect. Microbiol. 9:445.
doi: 10.3389/fcimb.2019.00445

The etiological agent of Chagas disease, *Trypanosoma cruzi*, is an obligate intracellular parasite that infects an estimated 7 million people in the Americas, with an at-risk population of 70 million. Despite its recognition as the highest impact parasitic infection of the Americas, Chagas disease continues to receive insufficient attention and resources in order to be effectively combatted. Unlike the other parasitic trypanosomatids that infect humans (*Trypanosoma brucei* and *Leishmania* spp.), *T. cruzi* retains an ancestral mode of phagotrophic feeding via an endocytic organelle known as the cytotome-cytopharynx complex (SPC). How this tubular invagination of the plasma membrane functions to bring in nutrients is poorly understood at a mechanistic level, partially due to a lack of knowledge of the protein machinery specifically targeted to this structure. Using a combination of CRISPR/Cas9 mediated endogenous tagging, fluorescently labeled overexpression constructs and endocytic assays, we have identified the first known SPC targeted protein (CP1). The CP1 labeled structure co-localizes with endocytosed protein and undergoes disassembly in infectious forms and reconstitution in replicative forms. Additionally, through the use of immunoprecipitation and mass spectrometry techniques, we have identified two additional CP1-associated proteins (CP2 and CP3) that also target to this endocytic organelle. Our localization studies using fluorescently tagged proteins and surface lectin staining have also allowed us, for the first time, to specifically define the location of the intriguing pre-oral ridge (POR) surface prominence at the SPC entrance through the use of super-resolution light microscopy. This work is a first glimpse into the proteome of the SPC and provides the tools for further characterization of this enigmatic endocytic organelle. A better understanding of how this deadly pathogen acquires nutrients from its host will potentially direct us toward new therapeutic targets to combat infection.

Keywords: cytotome, cytopharynx, *Trypanosoma cruzi*, kinetoplastid, endocytic, endocytosis, pre-oral ridge, SPC

INTRODUCTION

The causal agent of Chagas disease, *Trypanosoma cruzi*, is an obligate intracellular parasite of the kinetoplastid family that infects upwards of 7 million people in the Americas with ~30% developing life-threatening clinical disease (WHO, 2015; Perez-Molina and Molina, 2018). Like many trypanosomatids that cause disease in humans, *T. cruzi* is characterized by having a dixenous (two-host) life cycle that alternates between the hematophagous triatomine insect vector and its endothermic vertebrate reservoir that includes humans. Although the acute stage of infection is generally controlled by a highly effective immune response, total clearance does not occur, resulting in a life-long and often debilitating chronic infection (Groom et al., 2017). We currently lack the basic tools to effectively combat this pathogen, as methods of diagnosis are unreliable and drug treatments (Nifurtimox and Benznidazole) are both highly toxic and unable to eliminate the infection entirely (Camandaroba et al., 2003; Mejia et al., 2012; Molina-Garza et al., 2014; Maguire, 2015; Kansime et al., 2018). As with any attempt to control an infectious disease, a better understanding of *T. cruzi*'s basic biology is necessary for the effective identification of the areas where these parasites are most susceptible to therapeutic intervention (Alvarez et al., 2016).

One of the most poorly understood aspects of *T. cruzi* biology centers around the question of how this parasite exploits host resources in order to proliferate. Some important clues, however, have come from phylogenetic analyses tracing the evolution of kinetoplastids and their transition from bacterivorous predators to obligatory parasites. Although the most heavily studied kinetoplastids are the disease causing parasites of humans and domesticated animals (*Trypanosoma* spp. and *Leishmania* spp.), these organisms originally evolved from environmentally ubiquitous free-living, flagellated protozoans of the Excavata supergroup (phylum Euglenozoa) (Simpson et al., 2002; Lukes et al., 2014). These early branching eukaryotes comprise a diverse family of flagellates characterized primarily by the presence of an “excavated” feeding groove used to funnel food into the mouth of the cell, a plasma membrane pore known as the cytostome. This pore is continuous with a single tubular invagination (cytopharynx) adjacent to the flagellar pocket that extends to the posterior end of the cell. Extracellular material captured via this feeding apparatus [referred to collectively here as the cytostome-cytopharynx complex (SPC)] is subsequently endocytosed and targeted for lysosomal degradation (Eger and Soares, 2012). The extant free-living relatives of trypanosomatids, broadly classified as bodonids (e.g., *Bodo saltans*), can be found in virtually any marine or freshwater habitat where they primarily filter feed using the SPC endocytic pathway to phagocytose their bacterial prey. It has therefore been assumed that SPC mediated phagotrophy of prokaryotes was, most likely, the ancestral mode of nutrient acquisition in the first kinetoplastids (Stevens, 2014; Flegontova et al., 2018). With the recent identification of the earliest branching monoxenous trypanosomatid, *Paratrypanosoma confusum*, as the “missing link” between *B. saltans* and the dixenous trypanosomatids (Simpson et al., 2002; Stevens, 2008), it has become clear

that obligatory parasitism first began as an association with the arthropod lineage (propagated via fecal/oral transmission) and that the dixenous parasitism we see in the pathogenic trypanosomatids likely arose independently on several occasions. It is notable that the dixenous stercorearian trypanosomes (which includes *T. cruzi*) still rely on fecal transmission from the insect to their vertebrate host. This initial transition of free-living kinetoplastids into arthropod parasites coincided with an acute reduction in the size of their genome (~50% gene loss), which included the loss of many metabolic pathways (Oppenheimer et al., 2016). This streamlining was also accompanied by the abandonment of their second flagellum (Deschamps et al., 2011; Harmer et al., 2018). Despite all these changes however, the SPC structure of monoxenous trypanosomatids has remained intact, suggesting a continued role in nutrient uptake suited for life in the insect gut. Curiously, in the second major transition of the pathogenic trypanosomatids to a dixenous lifestyle, *T. cruzi* alone retained the SPC whereas the salivarian lineages (*Trypanosoma brucei* and *Leishmania* spp.) abandoned this endocytic structure entirely (Porto-Carreiro et al., 2000; Field and Carrington, 2009).

Although we do not know definitively why *T. cruzi* has retained the SPC, there is clearly an interesting correlation between the distinct replicative niches inhabited by a parasite and its mode of nutrient uptake. *T. brucei*, for example, divides extracellularly in the bloodstream of mammals where the host provides simple amino acids and sugars at high levels that can be readily transported across its plasma membrane to facilitate growth (Mazet et al., 2013; Creek et al., 2015; Mathieu et al., 2017; Marchese et al., 2018). Apparently, only host iron sequestering proteins, such as transferrin, still need to be brought into the parasite cell directly via receptor-mediated endocytosis at the flagellar pocket (Coppens et al., 1987; Schell et al., 1991; Mach et al., 2013). *Leishmania* spp. on the other hand, do replicate within host cells, but rather than live freely in the cytoplasm, they reside within lysosome-like vacuoles of specialized phagocytic cells. As a result, *Leishmania* spp. occupy a low pH environment replete with proteases that actively digest host macromolecules into a milieu of simple nutrients (Alexander, 1975; Antoine et al., 1990; Russell et al., 1992). *T. cruzi* is therefore the only trypanosomatid that lives directly in the host cytoplasm and is one of the few protozoan parasites that inhabit the cytosol of nucleated cells, making this replicative niche a surprisingly rare choice (de Souza et al., 2010; Barrias et al., 2013). One possible reason for this rarity comes from recent work demonstrating that the cytosolic environment of host cells is far less conducive to pathogen growth than previously thought (Goetz et al., 2001). The cytosol, despite having abundant macromolecules, is deficient in freely available amino acids, when compared to the mammalian bloodstream or host cell lysosomes (O’Riordan and Portnoy, 2002; Abu Kwaik and Bumann, 2013). *T. cruzi* may have retained the SPC, in part, as a mechanism for amastigotes to harvest host cytoplasmic macromolecules as the fuel required for rapid parasite growth. Direct digestion of these materials via the SPC complex would provide *T. cruzi* with metabolites that are otherwise scarce in the host cytoplasm. This seemingly “non-specific” method of nutrient uptake could also explain how *T. cruzi* is able to grow and propagate in such a wide variety

of hosts and cell types (Browne et al., 2017). Alternatively, the loss of the SPC in *T. brucei* or *Leishmania* sp. may be due to the fact that these organisms undergo critical developmental changes in the mid and foregut of their arthropod vectors whereas *T. cruzi* alone develops into its infectious stage in the hindgut as part of its stercorarian transmission lifestyle (reviewed in Goncalves et al., 2018). The SPC may therefore serve a critical role for trypanosomatids needing to successfully navigate the insect hindgut. It appears as though the fecal/oral transmission route for the monoxenous trypanosomatids like *P. confusum* is the ancestral form of transmission still retained by *T. cruzi* albeit as part of its vertebrate transmission strategy (Flegontov et al., 2013).

Our current understanding of the complex organization and dynamics of the SPC in *T. cruzi* is derived primarily from a combination of extensive electron microscopy studies including scanning, transmission and tomography based 3D reconstructions (Steinert and Novikoff, 1960; Milder and Deane, 1969; Preston, 1969; Martinez-Palomo et al., 1976; De Souza et al., 1978a,b; Souto-Padron and de Souza, 1983; Okuda et al., 1999; Vatarunakamura et al., 2005; Correa et al., 2007; Souza, 2009; Alcantara et al., 2014). First, the membrane tubule itself is embedded between two distinct sets of microtubule root fibers; one set of triplet microtubules initiating at the cytostome entrance and a second quartet of microtubules beginning at the centrosome near the base of the flagellar pocket, abutting the plasma membrane to form an intriguing surface prominence known as the pre-oral ridge (POR) before descending again into the cytosol and serving as a guide for the construction of the cell spanning SPC structure (Alcantara et al., 2014). In addition to its structural complexity, the SPC is also highly dynamic, as it disassembles in the infectious/non-dividing forms (metacyclics and trypomastigotes) and reconstitutes itself in the replicative stages (epimastigotes and amastigotes) (Vidal et al., 2016). It is also thought to break down during cytokinesis (Alcantara et al., 2017). Although the cytostome membrane pore and tubular invagination are lost during disassembly, the underlying microtubule structures appear more stable, potentially allowing for the rapid regeneration of this organelle (Alcantara et al., 2014). The ultimate result of these changes is that endocytosis ceases in the metacyclic and trypomastigote forms, only to become measurable again after stage conversion and cell division resumes (Vidal et al., 2016). Why the SPC disassembles in these non-replicative stages of *T. cruzi* has never been determined, but it may function as a defense against bringing in host antimicrobial proteins or more simply because the infectious forms are no longer replicating and have no need to consume additional complex metabolites. Despite the detailed structural analysis of the SPC, there is still a great deal that remains unknown about this primordial feeding apparatus including the identity of proteins responsible for its construction, function and capture of endocytosed cargo.

We report here the identification of the first known proteins specifically targeted to the enigmatic cytostome-cytopharynx complex in *T. cruzi*. Our initially identified SPC targeted protein (CP1), was endogenously Ty-epitope tagged and shown to localize with several fluorescently labeled cargo proteins, consistent with its targeting to the endocytic organelle. As

expected, the CP1 localization to the SPC was dynamically regulated and disassembled in the infectious trypomastigote and reestablished in the replicative stages. Overexpressed CP1-mNeon-Ty underwent normal trafficking and thus facilitated visualization of the SPC for the first time in live parasites. When characterizing the localization of CP1, we observed that co-staining of the parasite surface with the mannose binding lectin Concanavalin A (ConA) allowed us to determine, using super-resolution light microscopy alone, the region of the SPC entrance and pre-oral ridge, which we suspect plays an instrumental role in the binding efficiency of nutrient endocytosis. Finally, our immunoprecipitation (IP) of CP1, followed by mass spectrometry (MS) analysis led to the identification of two additional SPC associated proteins (CP2 and CP3), which also label the protein endocytic pathway, thus validating their interaction with CP1. This work reveals a first glimpse into the proteome of the SPC and provides the necessary tools for further characterization of this unusual endocytic organelle.

MATERIALS AND METHODS

Parasite Cultures

Epimastigotes of *T. cruzi* Y strain were cultured in LDNT/LIT medium (Kirchhoff et al., 1984) supplemented with 15% FBS. Aliquots of FBS (VWR, USDA certified) were freshly heat inactivated at 76°C for 40 min (to help improve epimastigote viability at low numbers) prior to addition to the media (this heat inactivated FBS will precipitate if frozen). To obtain amastigotes, 1 mL of maximum density epimastigotes were differentiated to metacyclic trypomastigotes via prolonged starvation in depleted LIT media (for at least 3 days). The resulting parasites were then incubated overnight with fresh FBS (with intact complement) to kill any remaining epimastigotes. The surviving metacyclic trypomastigotes were added to flasks containing human foreskin fibroblasts (HFF) grown in High Glucose Dulbecco's Modified Eagle's Medium (DMEM-HG) (Hyclone) supplemented with L-glutamine and 10% heat-inactivated (56°C) Cosmic Calf serum (CCS) (Hyclone). After 24–48 h media was replaced with medium containing only 1% (CCS) for further culturing.

Generation of Cloning Constructs and Transfection

C-terminal tagging of CP1 was performed as described by Lander et al. (2016), the Ty epitope sequence, fused to a downstream hygromycin selection cassette, were first amplified with 40bp homology arms for insertion upstream of the CP1 stop codon (P1 and P2). This product was co-transfected with the SpCas9 vector generated by Lander et al. modified to contain a gRNA protospacer (P6) targeted to a site between the two chosen 40 bp homology regions. Mutants were selected with both Hygromycin (250 µg/mL) (Fisher Scientific) and G418 (400 µg/mL) (Corning). For overexpression of mNeon-Ty tagged proteins, we utilized the pTREX vector (Martinez-Calvillo et al., 1997) modified with a *T. cruzi* optimized and “fixed” Neomycin resistance cassette (IDT Geneblock) (see **Figure 3A**) that allowed us to stringently select with 2,000 µg/mL G418. We also modified the vector to contain a *T. cruzi* optimized mNeon-Ty sequence (Shaner et al., 2013) (IDT Geneblock). Final vector products

were generated and assembled using standard Gibson assembly parameters (Gibson et al., 2009) and primers (CP1: P7,P8 CP2: P9,P10 CP3: P11,P12) using the NEB HiFi Assembly kit. P6 and P7 primers were utilized to amplify the vector for Gibson assembly. Parasites were transfected as described by Lander et al. (2015) using a BTX ECM830 (Harvard Apparatus). Primers used for cloning are identified in **Supplementary Table 1**.

Western Blot Analysis and Immunofluorescence Assays

For Western blot lysates, 1×10^7 epimastigotes were spun down at $1,200 \times g$ then washed 1x in PBS. Pellets were then resuspended in 1x SDS PAGE sample buffer (LICOR) containing β -mercaptoethanol. Half of the sample (5×10^6 epimastigote equivalent) was loaded into each well and Western blotting was performed via the general established protocol. Western blotting antibody dilutions: 1:500 for α -CP1 mouse and 1:1,500 for α -Ty mouse (mAb BB2) (Gay et al., 2016) LICOR 800 α -mouse was used as secondary antibody at 1:20,000 and images were taken in a BioRad Chemidoc. Total protein loading controls were imaged from stain-free TGX gels prior to membrane transfer. Immunofluorescence assays (IFA) were performed as previously described (Chasen et al., 2017) with modifications for epimastigotes. Epimastigote were washed in nutrient free pH 7.2 Triatomine Artificial Urine media (nfTAU) (Chiurillo et al., 2017) prior to fixation in nfTAU containing 3.5% paraformaldehyde (Electron Microscopy Sciences). Cold fixation solution was added to parasites and allowed to fix and equilibrate to room temperature for 20–30 min. Fixed parasites were allowed to adhere in nfTAU to poly-L-lysine coated coverslips for 30 min prior to proceeding with the IFA protocol. IFA antibody dilutions: 1:500 for α -CP1 mouse and 1:1,100 for α -Ty mouse monoclonal. α -mouse Alexafluor-488 and Alexafluor-568 antibodies were used as secondary antibodies. Coverslips were mounted to slides using Prolong Antifade mounting media (Invitrogen).

Endocytosis Assays

For fluorescent epimastigote endocytosis assays, 1×10^7 epimastigotes were chilled on ice and then spun down in a 4°C centrifuge at 1,200 g. Parasites were then resuspended in 500 μl of chilled complete TAU (pH 7.2) containing 25 $\mu\text{g}/\text{mL}$ BSA-Rhodamine (Rockland Immunochemicals), 25 $\mu\text{g}/\text{mL}$ Transferrin-488 (Molecular Probes), and 10 $\mu\text{g}/\text{mL}$ α -Rabbit Alexafluor-568 IgG (Thermo Fisher) and then incubated at 28°C for 25 min. Parasites were then spun down at 4°C and the supernatant removed prior to resuspension of the pellet in 1.5 mL of 4°C nfTAU containing 4% paraformaldehyde (Electron Microscopy Sciences). Fixation was allowed to progress at room temperature for 30 min before spinning down for slide mounting and fluorescence imaging as described above.

For intracellular amastigote endocytosis assays, coverslips with HFF monolayers were treated with CellTrace CFSE as described in the commercial protocol (Invitrogen). After labeling, cells were washed three times and followed by

a 3 h recovery in 10% FBS containing DMEM-HG. CP1-Ty trypanomastigotes were then added to the culture and 48 hrs later amastigotes were lysed out of the cells using a 16-gauge needle. Amastigotes were fixed and attached to coverslips as described above for epimastigotes. Otherwise, IFAs were performed as described above using α -Ty primary antibody (mAb BB2) and Alexafluor-568 secondary (Thermo Fisher). For cytochalasin B experiments, epimastigotes were pre-treated for 10 min at 28°C with cytochalasin B (300 μM , Enzo Lifesciences) prior to performing the endocytosis assay. Cytochalasin B concentration was maintained during entirety of the assay.

Concanavalin a Labeling of mNeon Overexpression Mutants

Prior to fixation, 1×10^7 epimastigotes of the mNeon overexpression lines were chilled, spun at 1,200 g, and washed 1x ice-cold nfTAU (pH 7.2). They were then incubated on ice in TAU (pH 7.2) containing 10 $\mu\text{g}/\text{mL}$ Rhodamine Conjugated Concanavalin A (ConA) (Vector Laboratories). After spinning down in a pre-chilled 4°C centrifuge, the supernatant was removed, and the pellet was immediately resuspended in 1.5 mL of cold fixative (4% paraformaldehyde in nfTAU pH 7.2) and allowed to equilibrate to room temperature for 30 min, fixed parasites were resuspended in nfTAU prior to adhering to coverslips as described above.

Fluorescent Microscopy

IFA and routine fluorescence images were taken using the Zeiss Elyra S1 Structured Illumination Microscope in the Center for Tropical and Emerging Diseases microscopy core.

Immunoelectron Microscopy

CP1-Ty epimastigotes were washed twice with PBS before fixation in 4% paraformaldehyde (Electron Microscopy Sciences, PA) in 0.25 M HEPES (pH 7.4) for 1 h at room temperature and then in 8% paraformaldehyde in the same buffer overnight at 4°C . Parasites were pelleted in 10% fish skin gelatin, and the gelatin-embedded pellets were infiltrated overnight with 2.3 M sucrose at 4°C and frozen in liquid nitrogen. Ultrathin cryosections were incubated in PBS and 1% fish skin gelatin containing mouse α -Ty antibody at a 1/100 dilution and then exposed to the secondary antibody that was revealed with 10-nm protein A-gold conjugates. Sections were observed and images were recorded with a Philips CM120 electron microscope (Eindhoven, the Netherlands) under 80 kV.

Analysis of Sequence, Alignment, Tree Generation, and Structure Prediction

Alignments were generated using T-Coffee (Madeira et al., 2019) and figures were generated using Jalview 2 software (Waterhouse et al., 2009). Tree was generated in Geneious Prime using the Jukes-Cantor and neighbor-joining parameters with the *B. saltans* CP2 related sequence as an outgroup. Consensus tree was generated using a random seed and 100 bootstrapped replicates with a support threshold of 90%.

Structure predictions were generated using the I-TASSER server (Yang and Zhang, 2015).

Purification of Recombinant Antigen and Mouse Polyclonal Antibody Generation

The chosen antigenic region of CP1 (CP1Ag) was identified using the IEDB suite of antigenicity prediction software (<http://tools.immuneepitope.org/bcell/>) (Chou and Fasman, 1978; Emini et al., 1985; Karplus and Schulz, 1985; Parker et al., 1986; Kolaskar and Tongaonkar, 1990; Bogitsh et al., 1995; Larsen et al., 2006; Jespersen et al., 2017). The DNA sequence for CP1Ag was amplified from *T. cruzi* genomic DNA and cloned into the pET-32 LIC/EK vector (Novagen), which adds an N-terminal thioredoxin and histidine tag to the expressed protein. Recombinant CP1Ag was expressed and initially purified via a nickel-affinity column (HisPur Thermo Fisher) as previously described (Chasen et al., 2017). This initial purified fraction was digested using biotinylated thrombin to cleave the N-terminal thioredoxin-tag and histidine tag. After thrombin removal, the antigen was again passed through the nickel column and the purified tag-less antigen was gently eluted using 10 mM imidazole, leaving the tag attached to the column.

Antibodies in mice were generated as previously described (Chasen et al., 2019). Swiss Webster mice (Charles River) were inoculated intraperitoneally with 100 µg of Cp1Ag mixed with complete Freund's adjuvant, followed by two boosts with 50 µg of CP1-Ag, with each boost being mixed with incomplete Freund's adjuvant. The final serum was collected by cardiac puncture after CO₂ euthanasia. The animal protocol used was approved by the UGA Institutional Animal Care and Use Committee (IACUC).

CO-IMMUNOPRECIPITATION AND MASS-SPECTROMETRY

For each immunoprecipitation, a 50 mL culture of epimastigotes was grown to mid-log phase ($1\text{--}2 \times 10^7$ epimastigotes/mL) and a co-immunoprecipitation using the Ty peptide for elution was performed as described by Huet et al. (2018). For identification of excised bands, matrix assisted laser desorption ionization (MALDI) was performed using a Bruker Autoflex (TOF) mass spectrometer. Shotgun mass spectrometry of eluates was performed on an Orbitrap Elite system with ESI ion source and an interchangeable nanospray source.

EPIMASTIGOTE GROWTH ASSAYS

2.5×10^6 epimastigotes of each strain were resuspended in LIT containing 15% heat inactivated FBS. Counting was performed every 24 h using a Coulter Counter (Beckman Coulter). Growth assays were performed in triplicate and fold-change significance was determined via unpaired *t*-tests using the Prism Software Suite.

RESULTS

Identification of the First Cytostomal Protein (CP1) Specifically Targeted to the Cytostome-Cytopharynx Endocytic Organelle

As part of an ongoing epitope tagging and localization screen being conducted in the Y-strain of *T. cruzi*, we utilized a CRISPR/Cas9 mediated endogenous tagging strategy as described by Lander et al. whereby the Cas9 nuclease, in combination with a gRNA targeting the 3' end of the hypothetical protein (TriTrypDB: TcCLB.506789.150, NCBI Accession: XP_819915.1) (**Figure 1A**) was transfected into parasites. This was followed by dual selection of both a repair template containing the introduction of a C-terminal Ty-epitope (Hygromycin) and the gRNA/Cas9 expression vector (G418) (**Figure 1B**). A diagnostic PCR to assess the loci specific modifications to the genomic DNA demonstrated a product of the predicted size for the epitope tagged locus only in the tagged strain with no products being observed for the parental locus, confirming the successful tagging of both genomic loci (**Figure 1C**). The annotated open reading frame (ORF) of this gene, which we have renamed CP1, encodes for an 841 amino acid (aa) protein, with a predicted isoelectric point of 5.57 and a predicted molecular weight of 93.0 kDa. Although annotated as a hypothetical protein, CP1 does contain a predicted structural maintenance of chromosome (SMC) domain (TIGR02168, 455–670 aa) (**Figure 1A**) most likely due to the presence of a potential coiled coil structure. This protein lacks any orthologs outside the closely related *Trypanosoma theileri*, *Trypomastix rangeli*, and *Trypanosoma grayii*. A western blot of CP1-Ty epimastigote lysate showed CP1-Ty to migrate at a size of ~80 kDa (**Figure 1I**), which is below the predicted molecular weight of 93 kDa, potentially indicating N-terminal processing or post-translation modification of CP1-Ty. In images from immunofluorescence assays (IFA) taken using super-resolution structured illumination microscopy (SR-SIM), we noted the localization of CP1-Ty to a distinct linear structure that was present in both of the replicating stages, the epimastigote and amastigote (**Figures 1D,F**), but was absent in the non-replicating trypomastigote stage (**Figure 1E**). This structure, and its stage-specific nature, were reminiscent of the endocytic organelle of *T. cruzi*, referred to here as the cytotome/cytopharynx complex (SPC) (summarized in **Figure 1G**). Cryogenic immuno-electron microscopy (CryoIEM) analysis of CP1-Ty also showed its localization to convoluted, multibranched tubular structures in proximity to the flagellar pocket (FP) and kinetoplast (K) (**Figure 1H**).

CP1 Labels the Protein Endocytic Pathway of the Cytostome-Cytopharynx Complex

As previous work in the field supported the role of the SPC as the primary route of protein endocytosis in *T. cruzi* epimastigotes, we performed endocytosis assays to confirm that the CP1 labeled structure was targeting to this endocytic organelle. We fed epimastigotes fluorescent Transferrin (**Figure 2A**), goat Immunoglobulin (IgG) (**Figure 2B**), and Bovine Serum Albumin

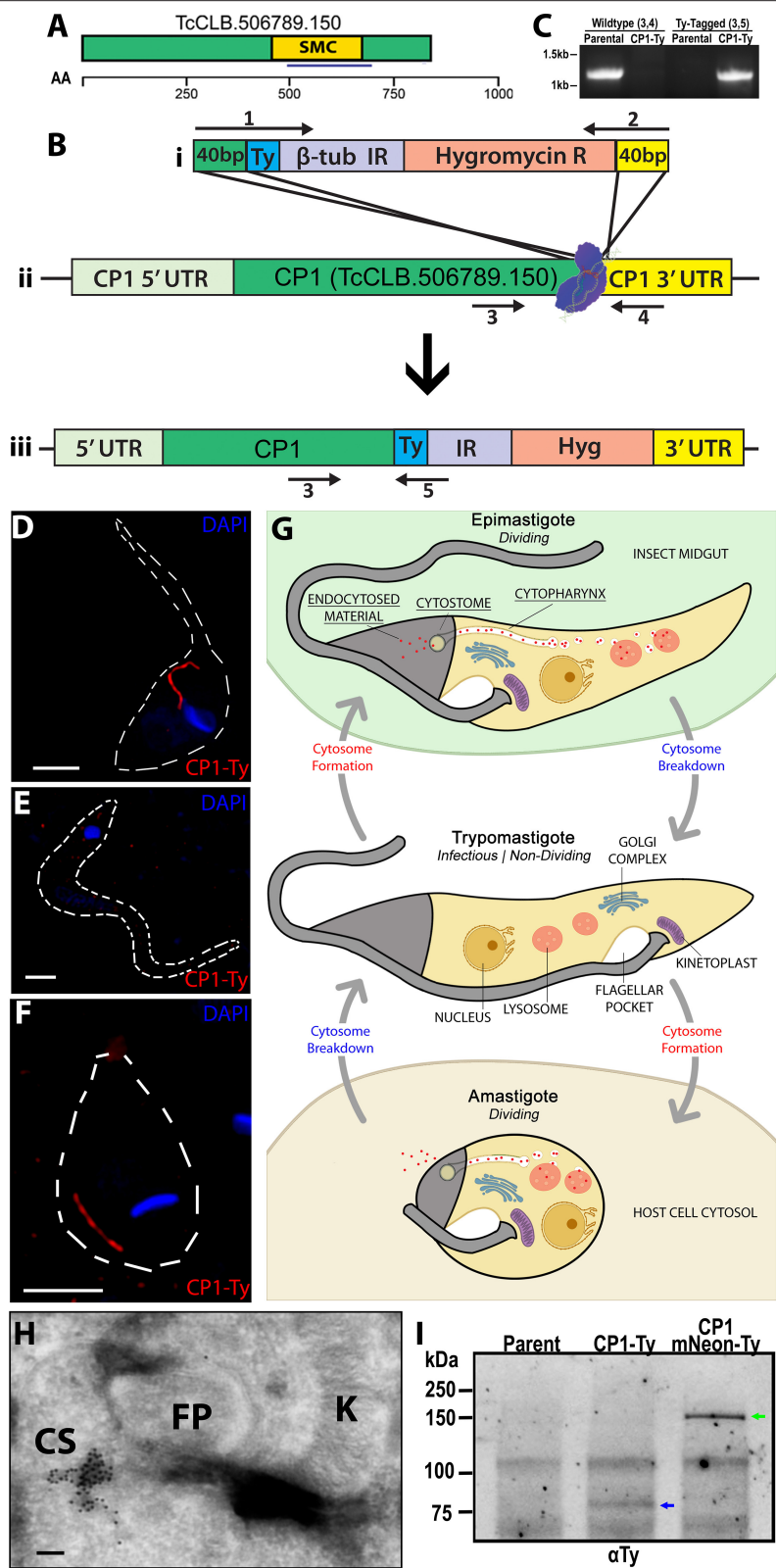
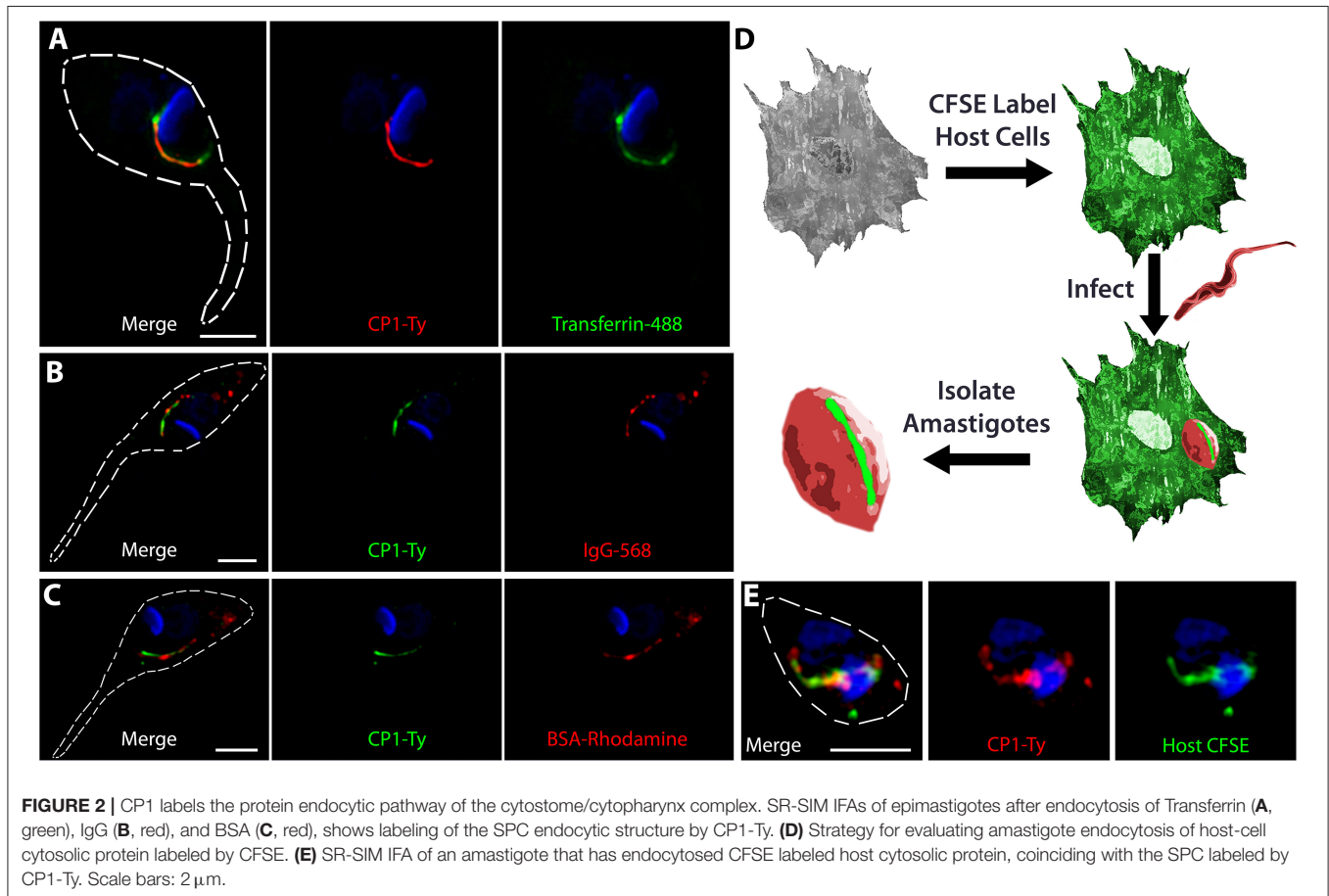


FIGURE 1 | Endogenous Tagging of a cytotome-cytopharynx complex Protein. **(A)** Schematic of CP1 with annotated structural maintenance of chromosome domain (SMC) and chosen antigenic region for later antibody generation (blue underline) (see **Supplementary Figure 5**). An amino acid scale is below the schematic. *(Continued)*

FIGURE 1 | (B) Cartoon showing CRISPR Cas9 C-terminal tagging strategy used to tag CP1. A guide RNA with a protospacer targeted to the CP1 3' UTR near the ORF directs spCas9 to form a double stranded break (**Bii**). A Ty-tagging repair template containing 40 bp homology, for both the 3' end of the CP1 ORF and the 3' side of the cut-site (**Bii**), was co-transfected to endogenously tag the CP1 locus (**Biii**). (**C**) PCR of genomic DNA from CP1-Ty mutants confirms the C-terminal tagging of both endogenous CP1 loci. (**D–F**) SR-SIM IFA showing the linear structure labeled by CP1-Ty in an epimastigote (**D**) and amastigote (**F**). In (**E**), a trypomastigote lacking the CP1-Ty labeled structure is shown. (**G**) Cartoon showing the structure and breakdown of the SPC in the different *T. cruzi* life cycle stages. (**H**) Cryogenic immunoelectron microscopy of an epimastigote showing immuno-gold labeling of CP1-Ty at the cytostome (CS). Gold particles are 10 nm. (**I**) α Ty immunoblot of lysates from Parental, CP1-Ty, and CP1-mNeon-Ty overexpression mutants shows a faint band of CP1-Ty (blue arrow) and a strong band of overexpressed CP1-mNeon-Ty (green arrow) Scale bars: IFA 2 μ m, EM 100 nm.

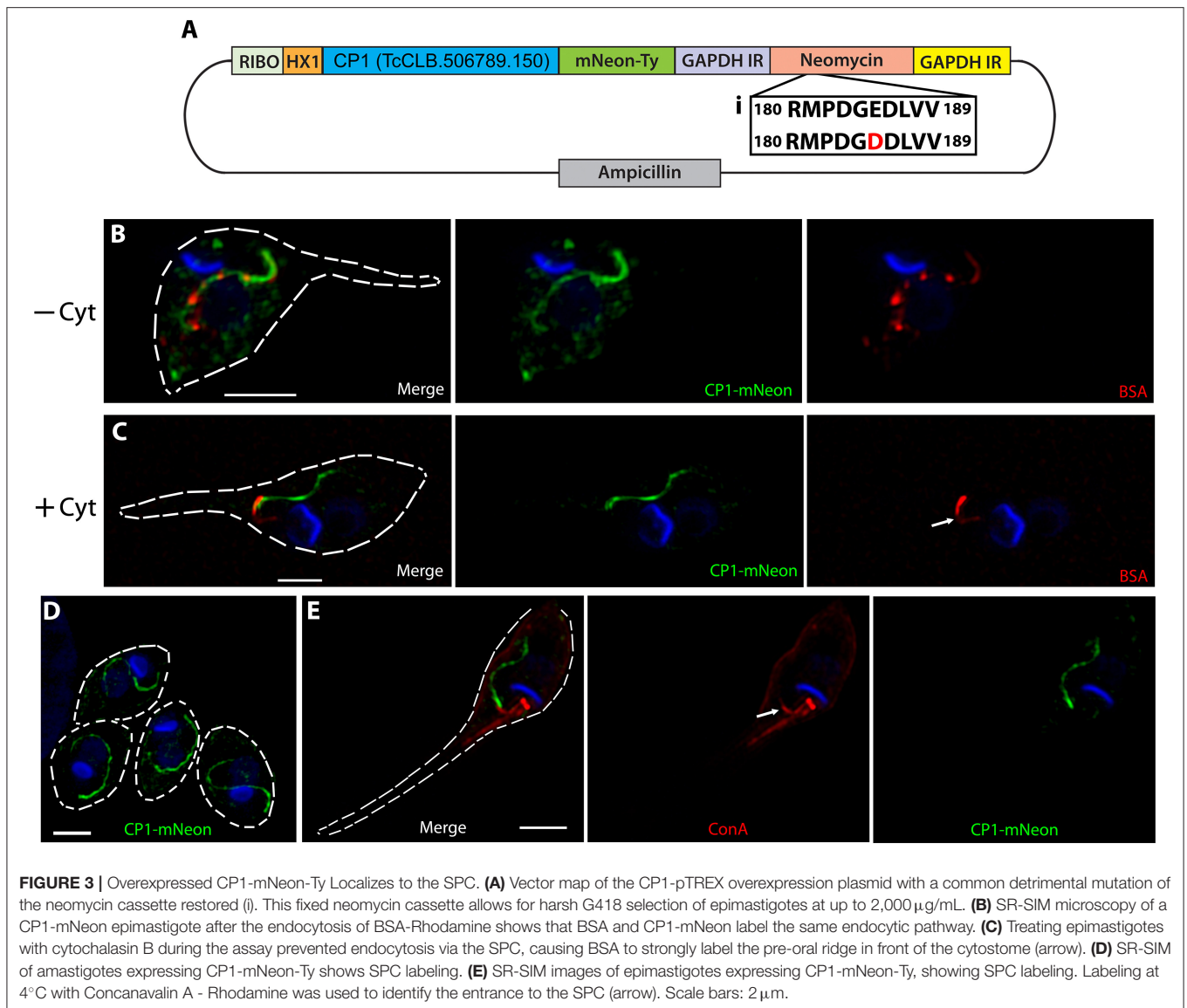


(BSA) (**Figure 2C**) to label the endocytic pathway and observed, through co-staining, that CP1-Ty labeled the endocytic pathway of the SPC for all three proteins. The SPC is remarkable in its apparent lack of specificity for cargo as it appears capable of endocytosing any protein we provide. It is notable that we only observed endocytosis via the SPC and failed to detect protein uptake through the flagellar pocket. This is in stark contrast to *T. brucei* which endocytoses exclusively through its flagellar pocket and to previously published reports of *T. cruzi* (de Figueiredo and Soares, 2000; Kalb et al., 2014). In order to evaluate endocytosis in intracellular amastigotes, we stained host cells first with the free-amine labeling fluorescent dye CFSE followed by infection with trypomastigotes from the CP1-Ty tagged line. After conversion to replicative amastigotes and growth for 48 h, amastigotes were released mechanically, fixed and stained with α -Ty antibodies (summarized in **Figure 2D**).

We observed that endocytosed CFSE labeled host-cell protein colocalized with the CP1-Ty labeled structure in amastigotes, further confirming that this structure was the endocytic organelle (**Figure 2E**). These images also showed, for the first time, that amastigotes endocytose human host-cell cytosolic protein via the SPC.

Fluorescently Tagged and Overexpressed CP1 Traffics to the Cytostome-Cytopharynx Complex

When cloning the CP1-mNeon-Ty overexpression constructs (**Figure 3A**) we sequenced the drug marker of the pTREX vector and observed a G \rightarrow T point mutation in the conserved catalytic region of the neomycin phosphate transferase II protein (NPTII). This mutation results in a substitution of an aspartic acid for



the glutamic acid at position 182 and is known to dramatically reduce the resistance conferred by NPTII (Yenofsky et al., 1990). It had been suggested in this prior report that this less active form of the neomycin drug resistance marker may have been inadvertently propagated throughout numerous constructs in multiple research communities. We hypothesized that this mutation may be the cause for the lack of G418 resistance conferred to epimastigotes (200–400 $\mu\text{g/mL}$) (Torres-Silva et al., 2018), which results in slow killing of wild type parasites lacking the cassette as well as potentially forcing the massive duplication and ultimately exaggerated overexpression by this vector in the resulting stable transfectants. To decrease the time of selection after transfection, we replaced the NPTII coding region with a *T. cruzi* codon-optimized version lacking the E182D substitution and increased drug selection pressure (Figure 3A, inset). This “fixed” version of NPTII allowed selection of our CP1-mNeon-Ty overexpressing epimastigotes with higher

drug selection conditions up to 2,000 $\mu\text{g/mL}$ of G418. Western blot analysis of lysate from this mutant population showed a strong band around the predicted molecular weight of 132 kDa (Figure 1I). SR-SIM microscopy revealed that the fusion protein of CP1-mNeon-Ty trafficked normally in epimastigotes as it colocalized with endocytosed BSA-Rhodamine along the length of the endocytic pathway (Figure 3B). When these mutants were pre-treated with Cytochalasin B, we observed that endocytosis was prevented (Figure 3C) as has previously been described (Bogitsh et al., 1995). As observed in this endocytosis blocking experiment (+Cyt), BSA clearly binds strongly to a region adjacent to the SPC entrance, also known as the pre-oral ridge (POR), which lies between the entrance of the flagellar pocket and the cytostome. The binding of a number of proteins at the POR prior to being endocytosed has been observed previously in primarily EM experiments (Vidal et al., 2016). It was also observed in our localization experiments,

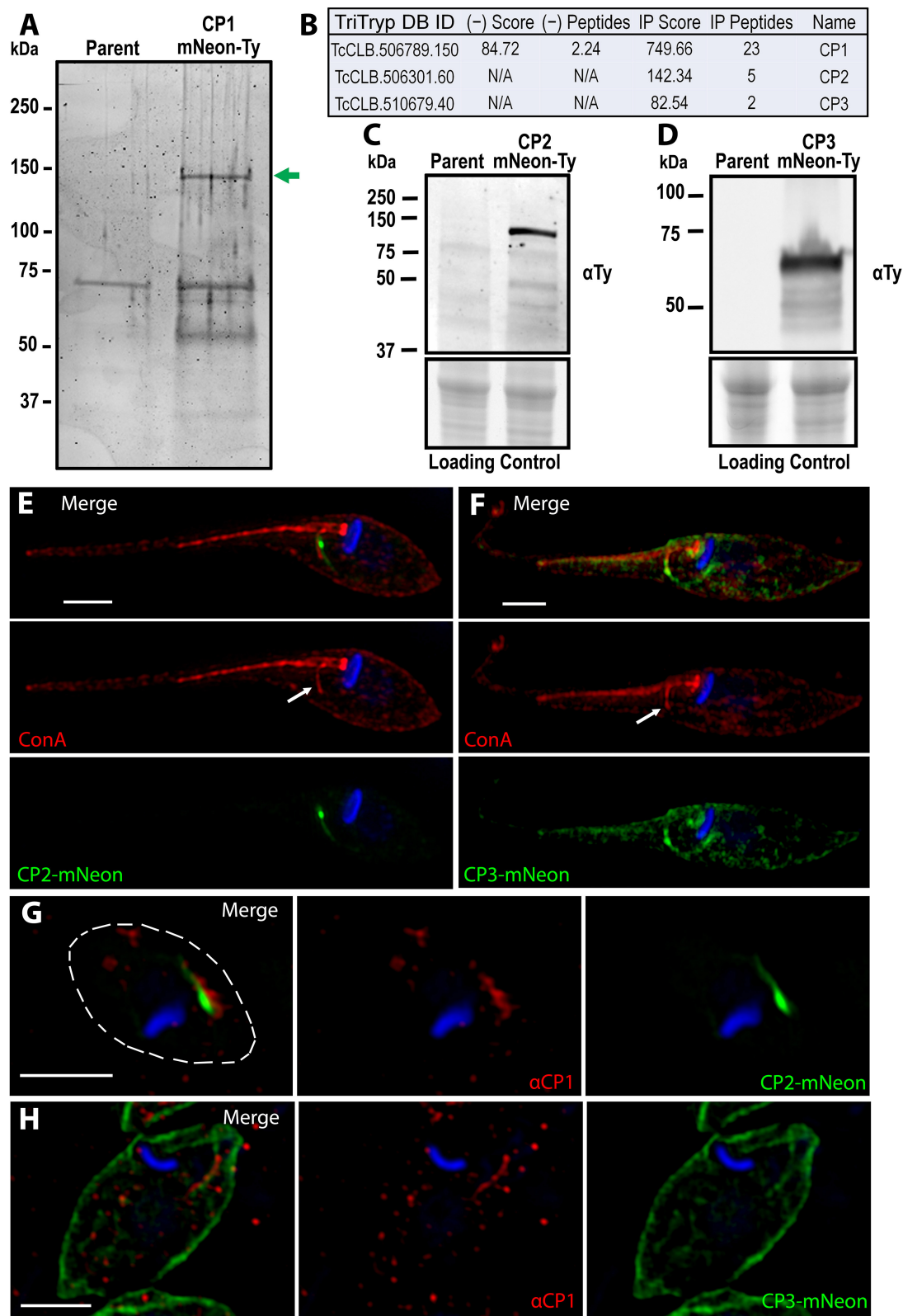


FIGURE 4 | Identification of the CP1 associated proteins CP2 and CP3. **(A)** SDS page gel of CP1-mNeon-Ty CoIP eluate stained for total protein. Several bands are present in the CoIP that are absent from the control IP using parental lysate. Band excision and MALDI mass-spectroscopy (MS) analysis confirmed that the upper
(Continued)

FIGURE 4 | band (green arrow) is CP1-mNeon-Ty. **(B)** Notable hits from Orbitrap shotgun MS of the CP1 CoIP eluate revealed two hypothetical protein (CP2, CP3) in addition to CP1. α Ty immunoblots of lysates from CP2-mNeon-Ty **(C)** and CP3-mNeon-Ty **(D)** overexpressing epimastigotes show that the tagged protein are expressed. **(E,F)** SR-SIM of CP2-mNeon-Ty and CP3-mNeon-Ty overexpressing mutants showing SPC labeling. 4°C labeling of with Concanavalin A -Rhodamine labels the SPC pre-oral ridge (white arrows). CP2-mNeon-Ty **(G)** and CP3-mNeon-Ty **(H)** in amastigotes also localize to the SPC, labeled by α CP1. Scale bars: 2 μ m.

that in the absence of a permeabilization step, the endocytosed cargo displayed a markedly packet-like appearance (**Figure 3B**, see BSA-Rhodamine) as opposed to the continuous linear presentation of cargo observed when cells are permeabilized (see **Figure 2A**). When amastigotes expressing CP1-mNeon-Ty were imaged within host cells, the same tubular pattern reminiscent of the SPC was again observed (**Figure 3D**). By combining the CP1-mNeon-Ty expressing parasites with Concanavalin A (ConA) staining at 4°C, followed by fixation, we observed a unique labeling of two linear structures emerging from the flagellar pocket with one following the parasite body along the flagellar attachment zone and the other stopping abruptly at the POR and SPC entrance. This staining pattern seemed to confirm for the first time using light microscopy, what had been seen in prior reports using EM techniques, that the POR contains a concentration of mannose containing glycans (**Figure 3E** arrow) (Martinez-Palomo et al., 1976). The CP1-mNeon-Ty overexpressing parasites also allowed us to validate previous findings that parasites undergoing division (**Supplementary Figure 1A**) and infectious trypomastigotes (**Supplementary Figure 1B**) lack defined SPC structures (Alcantara et al., 2017).

Identification of Two Additional Cytostome-Cytopharynx Proteins Associated With CP1

Taking advantage of our identification of CP1, we performed an immunoprecipitation to identify other SPC proteins for the continued characterization of this organelle and its structural components. We generated soluble lysate under native preserving conditions from our CP1-mNeon-Ty overexpressing parasite line and performed a pulldown using α -Ty antibody conjugated to paramagnetic beads with protein complexes being eluted through the use of excess Ty peptide. Eluates were run on an SDS-PAGE gel and proteins were visualized using BioRad Oriole Total Protein Stain. Individual band analysis combined with MALDI based-mass spectrometry demonstrated that the uppermost band was CP1-mNeon-Ty, confirming a successful pulldown (**Figure 4A**). Whole complex liquid chromatography-tandem mass spectrometry (LC-MS/MS) analysis revealed two additional proteins of interest that were both absent from the control and with a notable lack of orthologs in the SPC-less *T. brucei* and *Leishmania* spp. (**Figure 4B**).

The first target to be characterized, CP2 (TcCLB.506301.60 NCBI Accession: XP_807919.1), is a hypothetical protein that, like CP1 is found only in the closely related *Trypanosoma* species, as well as within the earliest branching trypanosomatid *P. confusum*, which retains the SPC (Skalicky et al., 2017). This protein is 720 aa long with a predicted molecular weight of 80 kDa and isoelectric point of 5.02. CP2, like CP1, also

contains a predicted SMC domain (TIGR02168, 35-307 aa) (**Supplementary Figure 2A**). The C-terminal region of CP2 is also highly conserved amongst all predicted orthologs (675–720 aa) (**Supplementary Figure 2B**). This region has an I-TASSER predicted structure (Yang and Zhang, 2015) similar to that of a coiled-coil domain (**Supplementary Figure 2C**) which suggests the region may play a role in protein-protein interactions or oligomerization (Truebestein and Leonard, 2016). Notably, a 14-residue region of this domain (700–713 aa) (**Supplementary Figure 2B**, underline) is perfectly conserved amongst the predicted CP2 orthologs, even in the more distantly related *Paratrypanosoma confusum* (**Supplementary Figures 2E, 3**). This suggests that the region plays a significant role in the protein's function or targeting, as it is under significant selective pressure to resist even minor modifications. To test the potential role of this 45 aa conserved region of CP2 in SPC targeting, it was fused to the C-terminus of mNeon (mNeon-CP2ct) and transiently overexpressed in epimastigotes. We observed, via fluorescence microscopy, an SPC-like structure resulting in transfected parasites, suggesting a role for this region in targeting CP2 to the cytostome (**Supplementary Figure 2D**). The second protein of interest, CP3 (TcCLB.510679.40, NCBI Accession: XP_807127.1) exists as multiple copies in several *T. cruzi* strains (i.e. Sylvio, Dm28C, TCC) but was found to exist only as a single copy in the CL Brener strain. Orthologs of CP3 were present only in the closely related species to *T. cruzi*, as was observed with CP1. CP3 is predicted to be 455 aa in length with a molecular weight of 52 kDa and isoelectric point of 8.96. Unlike in CP1 and CP2, no identifiable domains were found within this protein sequence.

We generated mutants overexpressing CP2-mNeon-Ty and CP3-mNeon-Ty and immunoblots revealed bands of ~110 kDa (**Figure 4C**) and 60 kDa (**Figure 4D**) respectively. The CP2 band matches the predicted molecular weight for CP2-mNeon-Ty (108 kDa), but the CP3 band is smaller than the 80 kDa predicted molecular weight, suggestive of post-translational processing that may affect its migration (**Figure 4E**). In CP2-mNeon-Ty expressing epimastigotes, this protein presents a strong signal near the SPC entrance as well as along the tubule itself (**Figure 4E**). CP3-mNeon-Ty also localized to the SPC in epimastigotes, but additionally localized diffusely to disparate areas of the cell which may be due to overexpression (**Figure 4F**). The dispersed labeling of CP3 suggests a potential minor affinity for cytoskeletal microtubules when overexpressed (Angelopoulos, 1970) however because the most intense labeling is along the SPC it suggests that CP3 may be labeling one or both of the microtubule root fibers associated with the endocytic structure that can also be seen in **Supplementary Figure 4** (Kalb et al., 2014; Alcantara et al., 2017). To demonstrate the co-localization of CP2 and CP3 fusions to the SPC in amastigotes, we generated a polyclonal mouse antibody against

a 240 amino acid antigenic region of CP1 recombinantly expressed in *E. coli* (**Supplementary Figure 5A**) (α -CP1). This region was identified through the combined use of the 7 IEDB antibody epitope prediction analysis methods (see Materials and Methods section). This region was further confirmed to not contain epitopes that had significant sequence similarity to other proteins in human cells or *T. cruzi*. This antigen (CP1Ag) was purified and isolated from the N-terminal tag prior to mouse inoculation (**Supplementary Figure 5B**). Immunoblots with α -CP1 recognized CP1-mNeon-Ty in lysates (**Supplementary Figure 5C**). The antibody was also capable of labeling endogenous levels of CP1 in IFAs of wildtype epimastigotes (**Supplementary Figure 5D**). Labeling of the SPC structure with α -CP1 demonstrated a clear overlap with both CP2 and CP3-mNeon-Ty in intracellular amastigotes (**Figures 4G,H**). We observed a mild but significant difference in the growth rates of CP3-mNeon-Ty overexpressing epimastigotes relative to the parental line (**Supplementary Figure 6**).

DISCUSSION

Here we report the identification and initial characterization of the first three known molecular components of the cytostome/cytopharynx complex (SPC) in *T. cruzi*. Given that the SPC is responsible for the endocytosis of extracellular material during the replicative epimastigote and amastigote stages, it is hypothesized to be a critical organelle for obtaining the necessary nutrients to support the high energetic demands of parasite replication. Our initial identification of CP1 was made possible by the recent development of efficient genomic modification tools (e.g., CRISPR/Cas9) in this parasite that we have employed in an ongoing protein localization screen. Our examination of endogenously tagged CP1-Ty showed its targeting to a linear structure seen only in the replicating forms and absent from the infectious stages, in line with previous examinations of the parasite endocytic structure (Vidal et al., 2016). In fluorescence-based protein feeding assays, CP1 co-localized with a variety of endocytosed cargo, confirming it to be a bona fide SPC resident protein. These studies highlighted the broad specificity of the SPC by showing that it was capable of shuttling BSA, IgG, Transferrin, and CFSE labeled host protein through this endocytic pathway. Surprisingly, we failed to observe any endocytosis of cargo, including albumin (BSA), via the flagellar pocket in our assays suggesting that the SPC may be the exclusive endocytic route for whole protein uptake in this parasite (Soares and de Souza, 1991; de Figueiredo and Soares, 2000; Kalb et al., 2014).

The overexpression of a CP1-mNeon-Ty fusion demonstrated that neither targeting nor viability was compromised as a result of the large fluorescent tag. This fusion product facilitated the first analysis of the SPC under native conditions and showed that the near-linear stream of endocytosed cargo seen in our initial feeding assays may be, in part, an artifact of sample permeabilization as parasites free from this processing step contained a regular array of repeating vesicle-like structures along the CP1 labeled SPC organelle. This also suggested the presence of two distinct functional subregions in the structure

labeled by CP1: a short funnel-shaped cavity at the entrance followed by an array of regularly spaced budded vesicles being trafficked to the lysosomes for digestion. Additionally, while images showing pre-oral ridge (POR) labeling by Concanavalin A has been shown in electron microscopy images (Martinez-Palomo et al., 1976; De Souza et al., 1978b), this is the first demonstration of its use to label the POR in fluorescence light microscopy and this method can now be used to dissect this surface region's unique properties in future studies. In this and prior work, the POR often presents as a "sticky" patch on the cell surface where endocytosed cargo, even in the presence of endocytic blocking agents (e.g., CytB), binds specifically. Intriguingly, this POR region may function in a manner analogous to many free-living bacterivorous protozoa that coat the area around their cytostome entrance with lectins in order to enhance the capture of bacterial prey (Roberts et al., 2006; Wootton et al., 2007; Martel, 2009). It is tempting to speculate that, in addition to the organelle itself, *T. cruzi* may have retained surface receptor-like molecules to capture protein cargo and thus increase the efficiency of endocytosis like its predatory ancestors. Transmission EM analyses have also shown that the POR ridge surface membrane composition is distinctly lacking in transmembrane proteins yet is extremely glycan rich in comparison to the rest of the parasite membrane and appears to originate from the flagellar pocket itself (Martinez-Palomo et al., 1976). The river-like appearance of the POR membrane connecting the cytostome to the flagellar pocket suggests a potential mechanism to preserve overall membrane homeostasis whereby the membrane being "pulled" into the SPC originates from vesicle fusion events within the flagellar pocket itself (Souto-Padron and de Souza, 1983). A continued dissection of the role of the POR membrane and its associated surface proteins may shed light on how the process of SPC mediated endocytosis functions and is regulated.

In this work we also report the initial characterization of SPC targeted proteins derived from IP and MS analyses. Associated with CP1, we identified two additional hypothetical proteins named CP2 and CP3 that target to the SPC as shown through co-localization with our in-house derived α -CP1 antibody. While the hypothetical nature of CP1, CP2, and CP3, make it more challenging to predict the role they play in endocytosis, future studies will involve the generation of either deletion or conditional knockdown mutants to elucidate their function. We suspect that CP2 may be the most important of the proteins for SPC function, due to the presence of an ortholog in its more distant relative, *P. confusum*. CP2 also presents a highly conserved C-terminal region of 14 perfectly conserved amino acids. This region may serve as either a trafficking signal or an important interacting domain that does not tolerate amino acid changes despite potentially hundreds of millions of years of divergent evolution. (Marks et al., 1995; Nishimura and Balch, 1997; van Hennik et al., 2003; Bedoukian et al., 2008; De Marcos Lousa et al., 2012; Starodubova et al., 2017). The C-terminal region's predicted similarity to a coiled-coil domain also lends credence to it serving a role in protein-protein interactions (Truebestein and Leonard, 2016).

Continued mutagenesis and fusion protein studies with this domain will help uncover the functional significance of this conserved region.

It is reasonable to expect that the SPC is composed of a variety of additional proteins that contribute to both its form and function and we believe that future in-depth characterizations of these proteins will increase our understanding of the *T. cruzi* endocytic machinery and its role in the parasite life cycle and pathogenesis. With this being the first report of proteins specifically targeted to the SPC structure in this or any organism, we now have the necessary tools to initiate an examination of the mechanistic underpinnings of this unique protozoan organelle.

DATA AVAILABILITY STATEMENT

All datasets generated for this study are included in the article/**Supplementary Material**.

AUTHOR CONTRIBUTIONS

NC and RE designed and performed the experiments, analyzed the data, and generated the figures. IC performed immuno-electron microscopy experiments and analysis. RE and NC wrote the manuscript with author input.

FUNDING

All sources of funding for this research are derived from the National Institutes of Health (NIH). This work was supported by an R21 exploratory grant (1R21AI146447) which supports an examination of the unique endocytic organelle of *Trypanosoma cruzi* as well as a post-doctoral T32 training fellowship (T32AI060546). Funding for publication fees are a part of the R21 exploratory grant budget.

ACKNOWLEDGMENTS

We thank Rick L. Tarleton for key biological materials and financial support; Roberto Docampo and Noelia Lander for reagents and advice in molecular manipulations of *T. cruzi*; Menna G. Etheridge for the production of *T. cruzi* life cycle graphics; Muthugapatti Kandasamy at the University of Georgia Biomedical Microscopy Core and Julie Nelson at the CTEGD Cytometry Shared Resource Lab for technical assistance. We would like to acknowledge the University of Georgia Proteomics and Mass Spectrometry (PAMS) facility.

REFERENCES

Abu Kwaik, Y., and Bumann, D. (2013). Microbial quest for food *in vivo*: 'nutritional virulence' as an emerging

SUPPLEMENTARY MATERIAL

The Supplementary Material for this article can be found online at: <https://www.frontiersin.org/articles/10.3389/fcimb.2019.00445/full#supplementary-material>

Supplementary Figure 1 | SPC labeling is absent during cytokinesis and the trypomastigote stage. **(A)** Amastigote labeling of the SPC by CP1-mNeon (ii) is absent in amastigotes undergoing cytokinesis (i), determined by the presence of a cleavage furrow (red arrow) and two nuclei (asterisk). **(B)** The SPC labeling by CP1-mNeon seen in amastigotes (ii), is absent in a trypomastigote (i). Scale bars: 2 μ m.

Supplementary Figure 2 | The highly conserved C-terminal region of CP2 is sufficient to traffic mNeon to the cytostome/cytopharynx complex. **(A)** Cartoon showing CP2 and its predicted SMC domain over an amino acid scale line. The red line annotates the highly conserved C-terminal region (675–720 aa). **(B)** Alignment of the highly conserved C-terminal region. The black line identifies a notable 14 amino acid region that maintains 100% identity among all orthologs, even in the more distantly related *P. confusum*. **(C)** The ITASSER predicted structure of the conserved C-terminal region is similar to that of a coil-coil protein interaction domain. The confidence score (range –5.0 lowest to +1.0 highest) of the predicted structure is high at –0.7. **(D)** Fluorescence image of an epimastigote overexpressing mNeon fused to the 45 aa CP2 C-terminal region (see **B**) shows SPC labeling (arrow). **(E)** A bootstrapped Jukes-Cantor neighbor-joining tree analysis of CP2 orthologs using the alignment from **Supplementary Figure 3**. The weakly related potential ortholog from *B. saltans*, which is missing the C-terminal region entirely was used as the outgroup. Branches are labeled with their bootstrap value.

Supplementary Figure 3 | Alignment of CP2 orthologs for tree analysis. T-coffee alignment of the CP2 orthologs from *T. cruzi* CL Brener (NCBI: XP_807919.1), *T. cruzi* Dm28c (Genbank: ESS69597.1), *T. cruzi* Sylvio (Genbank: EKG03371.1), *T. cruzi* Marinkellei (Genbank: EKF31948.1), *T. rangelli* (Genbank: ESL08911.1), *T. theileri* (NCBI: XP_028885643.1), *P. confusum* (TriTrypDB: PCON_0003310), *B. saltans* (Genbank: CUG86305.1).

Supplementary Figure 4 | CP3-mNeon labels structures reminiscent of the microtubule root fibers. Fluorescent image of the CP3-mNeon shows labeling of the microtubule root fibers associated with the paraflagellar region (arrow) and SPC. Scale bar: 2 μ m.

Supplementary Figure 5 | In-house generated α CP1 antibody labels the SPC. **(A)** Amino acid sequence of the chosen CP1 antigenic region (blue) with the N-terminal tag from the Pet32 LIC/EK vector (red). The black underlined region is the portion of the N-terminal tag that remains with the antigen after thrombin cleavage. **(B)** Purification of CP1 antigen for antibody generation. CP1 antigen (blue arrow) in the primary elution from Ni^{2+} column is thrombin digested, which cleaves off the N-terminal tag containing the 6x histidines (red arrow). The digested eluate is then passed through a Ni^{2+} column again, followed by a gentle elution with 10 mM imidazole. Pure, 6xHis tag-free CP1 antigen (green arrow) was eluted by this step and this purified antigen was then used for mouse inoculation. **(C)** Immunoblot of Parental and CP1-mNeon-Ty overexpressing mutant lysates showing the labeling of CP1-mNeon-Ty by polyclonal mouse α CP1 antibody. **(D)** SR-SIM IFA of Y strain epimastigotes showing α CP1 labeling of the SPC. Scale bars: 2 μ m.

Supplementary Figure 6 | Epimastigotes overexpressing CP3-mNeon exhibit a growth defect. **(A)** Growth assays of Parental (Y Strain), CP1-mNeon, CP2-mNeon, and CP3-mNeon epimastigotes. **(B)** Fold change in parasites during 48 h of exponential growth (24–72 h) shows a significant reduction in growth of the CP3-mNeon overexpressing mutants. * $p < 0.05$.

Supplementary Table 1 | Primers utilized in this work.

paradigm. *Cell Microbiol.* 15, 882–890. doi: 10.1111/cmi.12138

Alcantara, C. L., Vidal, J. C., de Souza, W., and Cunha-e-Silva, N. L. (2014). The three-dimensional structure of the cytostome-cytopharynx complex of

- Trypanosoma cruzi* epimastigotes. *J. Cell Sci.* 127, 2227–2237. doi: 10.1242/jcs.135491
- Alcantara, C. L., Vidal, J. C., de Souza, W., and Cunha-e-Silva, N. L. (2017). The cytotome-cytopharynx complex of *Trypanosoma cruzi* epimastigotes disassembles during cell division. *J. Cell Sci.* 130, 164–176. doi: 10.1242/jcs.187419
- Alexander, J. (1975). Effect of the antiphagocytic agent cytochalasin B on macrophage invasion by *Leishmania mexicana* promastigotes and *Trypanosoma cruzi* epimastigotes. *J. Protozool.* 22, 237–240. doi: 10.1111/j.1550-7408.1975.tb05858.x
- Alvarez, M. G., Bertocchi, G. L., Cooley, G., Albareda, M. C., Viotti, R., Perez-Mazliah, D. E., et al. (2016). Treatment success in *Trypanosoma cruzi* infection is predicted by early changes in serially monitored parasite-specific T and B cell responses. *PLoS Negl. Trop. Dis.* 10:e0004657. doi: 10.1371/journal.pntd.0004657
- Angelopoulos, E. (1970). Pellicular microtubules in the family Trypanosomatidae. *J. Protozool.* 17, 39–51. doi: 10.1111/j.1550-7408.1970.tb05157.x
- Antoine, J. C., Prina, E., Jouanne, C., and Bongrand, P. (1990). Parasitophorous vacuoles of *Leishmania amazonensis*-infected macrophages maintain an acidic pH. *Infect. Immun.* 58, 779–787.
- Barrias, E. S., de Carvalho, T. M., and De Souza, W. (2013). *Trypanosoma cruzi*: entry into mammalian host cells and parasitophorous vacuole formation. *Front. Immunol.* 4:186. doi: 10.3389/fimmu.2013.00186
- Bedoukian, M. A., Whitesell, J. D., Peterson, E. J., Clay, C. M., and Partin, K. M. (2008). The stargazin C terminus encodes an intrinsic and transferable membrane sorting signal. *J. Biol. Chem.* 283, 1597–1600. doi: 10.1074/jbc.M708141200
- Bogitsh, B. J., Ribeiro-Rodrigues, R., and Carter, C. E. (1995). *In vitro* effects of mannan and cytochalasin B on the uptake of horseradish peroxidase and [14C]sucrose by *Trypanosoma cruzi* epimastigotes. *J. Parasitol.* 81, 144–148. doi: 10.2307/3283912
- Browne, A. J., Guerra, C. A., Alves, R. V., da Costa, V. M., Wilson, A. L., Pigott, D. M., et al. (2017). The contemporary distribution of *Trypanosoma cruzi* infection in humans, alternative hosts and vectors. *Sci. Data* 4:170050. doi: 10.1038/sdata.2017.50
- Camandaroba, E. L., Reis, E. A., Goncalves, M. S., Reis, M. G., and Andrade, S. G. (2003). *Trypanosoma cruzi*: susceptibility to chemotherapy with benznidazole of clones isolated from the highly resistant Colombian strain. *Rev. Soc. Bras. Med. Trop.* 36, 201–209. doi: 10.1590/S0037-86822003000200002
- Chasen, N. M., Asady, B., Lemgruber, L., Vommaro, R. C., Kissinger, J. C., Coppens, I., et al. (2017). A glycosylphosphatidylinositol-anchored carbonic anhydrase-related protein of *Toxoplasma gondii* is important for rhoptry biogenesis and virulence. *mSphere* 2, e00027-17. doi: 10.1128/mSphere.00027-17
- Chasen, N. M., Stasic, A. J., Asady, B., Coppens, I., and Moreno, S. N. J. (2019). The vacuolar zinc transporter tgznt protects *Toxoplasma gondii* from zinc toxicity. *mSphere* 4:e00086-19. doi: 10.1128/mSphere.00086-19
- Chiurillo, M. A., Lander, N., Bertolini, M. S., Storey, M., Vercesi, A. E., and Docampo, R. (2017). Different roles of mitochondrial calcium uniporter complex subunits in growth and infectivity of *Trypanosoma cruzi*. *MBio* 8:e00574-17. doi: 10.1128/mBio.00574-17
- Chou, P. Y., and Fasman, G. D. (1978). Prediction of the secondary structure of proteins from their amino acid sequence. *Adv. Enzymol. Relat. Areas Mol. Biol.* 47, 45–148. doi: 10.1002/9780470122921.ch2
- Coppens, I., Oppendoes, F. R., Courtoy, P. J., and Baudhuin, P. (1987). Receptor-mediated endocytosis in the bloodstream form of *Trypanosoma brucei*. *J. Protozool.* 34, 465–473. doi: 10.1111/j.1550-7408.1987.tb03216.x
- Correa, J. R., Atella, G. C., Vargas, C., and Soares, M. J. (2007). Transferrin uptake may occur through detergent-resistant membrane domains at the cytopharynx of *Trypanosoma cruzi* epimastigote forms. *Mem. Inst. Oswaldo Cruz* 102, 871–876. doi: 10.1590/S0074-02762007005000117
- Creek, D. J., Mazet, M., Achcar, F., Anderson, J., Kim, D. H., Kamour, R., et al. (2015). Probing the metabolic network in bloodstream-form *Trypanosoma brucei* using untargeted metabolomics with stable isotope labelled glucose. *PLoS Pathog.* 11:e1004689. doi: 10.1371/journal.ppat.1004689
- de Figueiredo, R. C., and Soares, M. J. (2000). Low temperature blocks fluid-phase pinocytosis and receptor-mediated endocytosis in *Trypanosoma cruzi* epimastigotes. *Parasitol. Res.* 86, 413–418. doi: 10.1007/s004360050686
- De Marcos Lousa, C., Gershlick, D. C., and Denecke, J. (2012). Mechanisms and concepts paving the way towards a complete transport cycle of plant vacuolar sorting receptors. *Plant Cell* 24, 1714–1732. doi: 10.1105/tpc.112.095679
- de Souza, W., de Carvalho, T. M., and Barrias, E. S. (2010). Review on *Trypanosoma cruzi*: host cell interaction. *Int. J. Cell Biol.* 2010:295394. doi: 10.1155/2010/295394
- De Souza, W., de Carvalho, T. U., Benchimol, M., and Chiari, E. (1978a). *Trypanosoma cruzi*: ultrastructural, cytochemical and freeze-fracture studies of protein uptake. *Exp. Parasitol.* 45, 101–115. doi: 10.1016/0014-4894(78)90050-4
- De Souza, W., Martinez-Palomo, A., and Gonzalez-Robles, A. (1978b). The cell surface of *Trypanosoma cruzi*: cytochemistry and freeze-fracture. *J. Cell Sci.* 33, 85–299.
- Deschamps, P., Lara, E., Marande, W., Lopez-Garcia, P., Ekelund, F., and Moreira, D. (2011). Phylogenomic analysis of kinetoplastids supports that trypanosomatids arose from within bodonids. *Mol. Biol. Evol.* 28, 53–58. doi: 10.1093/molbev/msq289
- Eger, I., and Soares, M. J. (2012). Endocytosis in *Trypanosoma cruzi* (Euglenozoa: Kinetoplastea) epimastigotes: visualization of ingested transferrin-gold nanoparticle complexes by confocal laser microscopy. *J. Microbiol. Methods* 91, 101–105. doi: 10.1016/j.mimet.2012.07.013
- Emini, E. A., Hughes, J. V., Perlow, D. S., and Boger, J. (1985). Induction of hepatitis A virus-neutralizing antibody by a virus-specific synthetic peptide. *J. Virol.* 55, 836–839.
- Field, M. C., and Carrington, M. (2009). The trypanosome flagellar pocket. *Nat. Rev. Microbiol.* 7, 775–786. doi: 10.1038/nrmicro2221
- Flegontov, P., Votycka, J., Skalicky, T., Logacheva, M. D., Penin, A. A., Tanifuji, G., et al. (2013). Paratrypanosoma is a novel early-branching trypanosomatid. *Curr. Biol.* 23, 1787–1793. doi: 10.1016/j.cub.2013.07.045
- Flegontova, O., Flegontov, P., Malviya, S., Poulain, J., de Vargas, C., Bowler, C., et al. (2018). Neobodonids are dominant kinetoplastids in the global ocean. *Environ. Microbiol.* 20, 878–889. doi: 10.1111/1462-2920.14034
- Gay, G., Braun, L., M., Brenier-Pinchart, P., Vollaie, J., Josserand, V., R., Bertini, L., et al. (2016). *Toxoplasma gondii* TgIST co-opts host chromatin repressors dampening STAT1-dependent gene regulation and IFN- γ -mediated host defenses. *J. Exp. Med.* 213, 1779–1798. doi: 10.1084/jem.20160340
- Gibson, D. G., Young, L., Chuang, R. Y., Venter, J. C., Hutchison, C. A. 3rd., and Smith, H. O. (2009). Enzymatic assembly of DNA molecules up to several hundred kilobases. *Nat. Methods* 6, 343–345. doi: 10.1038/nmeth.1318
- Goetz, M., Bubert, A., Wang, G., Chico-Calero, I., J., Vazquez-Boland, A., Beck, M., et al. (2001). Microinjection and growth of bacteria in the cytosol of mammalian host cells. *Proc. Natl. Acad. Sci. U.S.A.* 98, 12221–12226. doi: 10.1073/pnas.211106398
- Goncalves, C. S., Avila, A. R., de Souza, W. M., Motta, C. M., and Cavalcanti, D. P. (2018). Revisiting the *Trypanosoma cruzi* metacyclogenesis: morphological and ultrastructural analyses during cell differentiation. *Parasit. Vec.* 11:83. doi: 10.1186/s13071-018-2664-4
- Groom, Z. C., Protopapas, A. D., and Zochios, V. (2017). Tropical diseases of the myocardium: a review. *Int. J. Gen. Med.* 10, 101–111. doi: 10.2147/IJGM.S130828
- Harmer, J., Yurchenko, V., Nenarokova, A., Lukes, J., and Ginger, M. L. (2018). Farming, slaving and enslavement: histories of endosymbioses during kinetoplastid evolution. *Parasitology* 145, 1311–1323. doi: 10.1017/S0031182018000781
- Huet, D., Rajendran, E., van Dooren, G. G., and Lourido, S. (2018). Identification of cryptic subunits from an apicomplexan ATP synthase. *Elife* 7:e38097. doi: 10.7554/eLife.38097
- Jespersen, M. C., Peters, B., Nielsen, M., and Marcattili, P. (2017). BepiPred-2.0: improving sequence-based B-cell epitope prediction using conformational epitopes. *Nucleic Acids Res.* 45, W24–W29. doi: 10.1093/nar/gkx346
- Kalb, L. C., Frederico, Y. C., Batista, C. M., Eger, I., Fragoso, S. P., and Soares, M. J. (2014). Clathrin expression in *Trypanosoma cruzi*. *BMC Cell Biol.* 15:23. doi: 10.1186/1471-2121-15-23

- Kansiime, F., Adibaku, S., Wamboga, C., Idi, F., Kato, C. D., Yamuah, L., et al. (2018). A multicentre, randomised, non-inferiority clinical trial comparing a nifurtimox-eflornithine combination to standard eflornithine monotherapy for late stage *Trypanosoma brucei* gambiense human African trypanosomiasis in Uganda. *Parasit. Vec.* 11:105. doi: 10.1186/s13071-018-2634-x
- Karplus, P., and Schulz, G. (1985). Prediction of chain flexibility in proteins. *Naturwissenschaften* 72, 212–213. doi: 10.1007/BF01195768
- Kirchhoff, L. V., Hieny, S., Shiver, G. M., Snary, D., and Sher, A. (1984). Cryptic epitope explains the failure of a monoclonal antibody to bind to certain isolates of *Trypanosoma cruzi*. *J. Immunol.* 133, 2731–2735.
- Kolaskar, A. S., and Tongaonkar, P. C. (1990). A semi-empirical method for prediction of antigenic determinants on protein antigens. *FEBS Lett.* 276, 172–174. doi: 10.1016/0014-5793(90)80535-Q
- Lander, N., Chiurillo, M. A., Storey, M., Vercesi, A. E., and Docampo, R. (2016). CRISPR/Cas9-mediated endogenous C-terminal tagging of *Trypanosoma cruzi* genes reveals the acidocalcisome localization of the inositol 1,4,5-trisphosphate receptor. *J. Biol. Chem.* 291, 25505–25515. doi: 10.1074/jbc.M116.749655
- Lander, N., Li, Z. H., Niyogi, S., and Docampo, R. (2015). CRISPR/Cas9-induced disruption of paraflagellar rod protein 1 and 2 genes in *Trypanosoma cruzi* reveals their role in flagellar attachment. *MBio* 6:e01012. doi: 10.1128/mBio.01012-15
- Larsen, J. E., Lund, O., and Nielsen, M. (2006). Improved method for predicting linear B-cell epitopes. *Immunome Res.* 2:2. doi: 10.1186/1745-7580-2-2
- Lukes, J., Skalicky, T., Tyc, J., Votycka, J., and Yurchenko, V. (2014). Evolution of parasitism in kinetoplastid flagellates. *Mol. Biochem. Parasitol.* 195, 115–122. doi: 10.1016/j.molbiopara.2014.05.007
- Mach, J., Tachezy, J., and Sutak, R. (2013). Efficient iron uptake via a reductive mechanism in procyclic *Trypanosoma brucei*. *J. Parasitol.* 99, 363–364. doi: 10.1645/GE-3237.1
- Madeira, F., Park, Y. M., Lee, J., Buso, N., Gur, T., Madhusoodanan, N., et al. (2019). The EMBL-EBI search and sequence analysis tools APIs in 2019. *Nucleic Acids Res.* 47, W636–W641. doi: 10.1093/nar/gkz268
- Maguire, J. H. (2015). Treatment of chagas' disease—time is running out. *N. Engl. J. Med.* 373, 1369–1370. doi: 10.1056/NEJMe1510170
- Marchese, L., Nascimento, J. F., Damasceno, F. S., Bringaud, F., Michels, P. A. M., and Silber, A. M. (2018). The uptake and metabolism of amino acids, and their unique role in the biology of pathogenic trypanosomatids. *Pathogens* 7:E36. doi: 10.3390/pathogens7020036
- Marks, M. S., Roche, P. A., van Donselaar, E., Woodruff, L., Peters, P. J., and Bonifacio, J. S. (1995). A lysosomal targeting signal in the cytoplasmic tail of the beta chain directs HLA-DM to MHC class II compartments. *J. Cell Biol.* 131, 351–369. doi: 10.1083/jcb.131.2.351
- Martel, C. M. (2009). Conceptual bases for prey biorecognition and feeding selectivity in the microplanktonic marine phagotroph *Oxyrrhis marina*. *Microb. Ecol.* 57, 589–597. doi: 10.1007/s00248-008-9421-8
- Martinez-Calvillo, S., Lopez, I., and Hernandez, R. (1997). pRIBOTEX expression vector: a pTEX derivative for a rapid selection for *Trypanosoma cruzi* transfectants. *Gene* 199, 71–76. doi: 10.1016/S0378-1119(97)00348-X
- Martinez-Palomo, A., DeSouza, W., and Gonzalez-Robles, A. (1976). Topographical differences in the distribution of surface coat components and intramembrane particles. A cytochemical and freeze-fracture study in culture forms of *Trypanosoma cruzi*. *J. Cell Biol.* 69, 507–513. doi: 10.1083/jcb.69.2.507
- Mathieu, C., Macedo, J. P., Hurlimann, D., Wirdnam, C., Haindrich, A. C., Suter Grottemeyer, M., et al. (2017). Arginine and lysine transporters are essential for *Trypanosoma brucei*. *PLoS ONE* 12:e0168775. doi: 10.1371/journal.pone.0168775
- Mazet, M., Morand, P., Biran, M., Bouyssou, G., Courtois, P., Daulouede, S., et al. (2013). Revisiting the central metabolism of the bloodstream forms of *Trypanosoma brucei*: production of acetate in the mitochondrion is essential for parasite viability. *PLoS Negl. Trop. Dis.* 7:e2587. doi: 10.1371/journal.pntd.0002587
- Mejia, A. M., Hall, B. S., Taylor, M. C., Gomez-Palacio, A., Wilkinson, S. R., Triana-Chavez, O., et al. (2012). Benzimidazole-resistance in *Trypanosoma cruzi* is a readily acquired trait that can arise independently in a single population. *J. Infect. Dis.* 206, 220–228. doi: 10.1093/infdis/jis331
- Milder, R., and Deane, M. P. (1969). The cytostome of *Trypanosoma cruzi* and *T. conorhini*. *J. Protozool.* 16, 730–737. doi: 10.1111/j.1550-7408.1969.tb02335.x
- Molina-Garza, Z. J., Bazaldua-Rodriguez, A. F., Quintanilla-Licea, R., and Galaviz-Silva, L. (2014). Anti-*Trypanosoma cruzi* activity of 10 medicinal plants used in northeast Mexico. *Acta Trop.* 136, 14–18. doi: 10.1016/j.actatropica.2014.04.006
- Nishimura, N., and Balch, W. E. (1997). A di-acidic signal required for selective export from the endoplasmic reticulum. *Science* 277, 556–558. doi: 10.1126/science.277.5325.556
- Okuda, K., Esteve, M., Segura, E. L., and Bijovsky, A. T. (1999). The cytostome of *Trypanosoma cruzi* epimastigotes is associated with the flagellar complex. *Exp. Parasitol.* 92, 223–231. doi: 10.1006/expr.1999.4419
- Oppendoes, F. R., Butenko, A., Flegontov, P., Yurchenko, V., and Lukes, J. (2016). Comparative metabolism of free-living bodo saltans and parasitic trypanosomatids. *J. Eukaryot. Microbiol.* 63, 657–678. doi: 10.1111/jeu.12315
- O'Riordan, M., and Portnoy, D. A. (2002). The host cytosol: front-line or home front? *Trends Microbiol.* 10, 361–364. doi: 10.1016/S0966-842X(02)02401-0
- Parker, J. M., Guo, D., and Hodges, R. S. (1986). New hydrophilicity scale derived from high-performance liquid chromatography peptide retention data: correlation of predicted surface residues with antigenicity and X-ray-derived accessible sites. *Biochemistry* 25, 5425–5432. doi: 10.1021/bi00367a013
- Perez-Molina, J. A., and Molina, I. (2018). Chagas disease. *Lancet* 391, 82–94. doi: 10.1016/S0140-6736(17)31612-4
- Porto-Carreiro, I., Attias, M., Miranda, K., De Souza, W., and Cunha-e-Silva, N. (2000). *Trypanosoma cruzi* epimastigote endocytic pathway: cargo enters the cytostome and passes through an early endosomal network before storage in reservosomes. *Eur. J. Cell Biol.* 79, 858–869. doi: 10.1078/0171-9335-00112
- Preston, T. M. (1969). The form and function of the cytostome-cytopharynx of the culture forms of the elasmobranch haemoflagellate *Trypanosoma raiaae* Laveran & Mesnil. *J. Protozool.* 16, 320–333. doi: 10.1111/j.1550-7408.1969.tb02278.x
- Roberts, E. C., Zubkov, M. V., Martin-Cereceda, M., Novarino, G., and Wootton, E. C. (2006). Cell surface lectin-binding glycoconjugates on marine planktonic protists. *FEMS Microbiol. Lett.* 265, 202–207. doi: 10.1111/j.1574-6968.2006.00484.x
- Russell, D. G., Xu, S., and Chakraborty, P. (1992). Intracellular trafficking and the parasitophorous vacuole of *Leishmania mexicana*-infected macrophages. *J. Cell Sci.* 103, 1193–111210.
- Schell, D., Evers, R., Preis, D., Ziegelbauer, K., Kiefer, H., Lottspeich, F., et al. (1991). A transferrin-binding protein of *Trypanosoma brucei* is encoded by one of the genes in the variant surface glycoprotein gene expression site. *EMBO J.* 10, 1061–1066. doi: 10.1002/j.1460-2075.1991.tb08045.x
- Shaner, N. C., Lambert, G. G., Chammas, A., Ni, Y., Cranfill, P. J., Baird, M. A., et al. (2013). A bright monomeric green fluorescent protein derived from *Branchiostoma lanceolatum*. *Nat. Methods* 10, 407–409. doi: 10.1038/nmeth.2413
- Simpson, A. G., Lukes, J., and Roger, A. J. (2002). The evolutionary history of kinetoplasts and their kinetoplasts. *Mol. Biol. Evol.* 19, 2071–2083. doi: 10.1093/oxfordjournals.molbev.a004032
- Skalicky, T., Dobakova, E., Wheeler, R. J., Tesarova, M., Flegontov, P., Jirsova, D., et al. (2017). Extensive flagellar remodeling during the complex life cycle of Paratrypanosoma, an early-branching trypanosomatid. *Proc. Natl. Acad. Sci. U.S.A.* 114, 11757–11762. doi: 10.1073/pnas.1712311114
- Soares, M. J., and de Souza, W. (1991). Endocytosis of gold-labeled proteins and LDL by *Trypanosoma cruzi*. *Parasitol. Res.* 77, 461–468. doi: 10.1007/BF00928410
- Souto-Padron, T., and de Souza, W. (1983). Freeze-fracture localization of filipin-cholesterol complexes in the plasma membrane of *Trypanosoma cruzi*. *J. Parasitol.* 69, 129–137. doi: 10.2307/3281287
- Souza, W. (2009). Structural organization of *Trypanosoma cruzi*. *Mem. Inst. Oswaldo Cruz* 104(Suppl. 1), 89–100. doi: 10.1590/S0074-02762009000900014
- Starodubova, E. S., Kuzmenko, Y. V., Latanova, A. A., Preobrazhenskaya, O. V., and Karpov, V. L. (2017). [C-terminal lysosome targeting domain of CD63 modifies cellular localization of rabies virus glycoprotein]. *Mol. Biol.* 51, 460–463. doi: 10.1134/S0026893317020020
- Steinert, M., and Novikoff, A. B. (1960). The existence of a cytostome and the occurrence of pinocytosis in the *Trypanosome*, *Trypanosoma Mega*. *J. Biophys. Biochem. Cytol.* 8, 563–569. doi: 10.1083/jcb.8.2.563

- Stevens, J. R. (2008). Kinetoplastid phylogenetics, with special reference to the evolution of parasitic trypanosomes. *Parasite* 15, 226–232. doi: 10.1051/parasite/2008153226
- Stevens, J. R. (2014). Free-living bodonids and derived parasitic trypanosomatids: but what lies in between? *Trends Parasitol.* 30, 113–114. doi: 10.1016/j.pt.2014.01.002
- Torres-Silva, C. F., Repoles, B. M., Ornelas, H. O., Macedo, A. M., Franco, G. R., Junho Pena, S. D., et al. (2018). Assessment of genetic mutation frequency induced by oxidative stress in *Trypanosoma cruzi*. *Genet. Mol. Biol.* 41, 466–474. doi: 10.1590/1678-4685-gmb-2017-0281
- Truebestein, L., and Leonard, T. A. (2016). Coiled-coils: the long and short of it. *Bioessays* 38, 903–916. doi: 10.1002/bies.201600062
- van Hennik, P. B., ten Klooster, J. P., Halstead, J. R., Voermans, C., Anthony, E. C., Divecha, N., et al. (2003). The C-terminal domain of Rac1 contains two motifs that control targeting and signaling specificity. *J. Biol. Chem.* 278, 39166–39175. doi: 10.1074/jbc.M307001200
- Vatarunakamura, C., Ueda-Nakamura, T., and de Souza, W. (2005). Visualization of the cytostome in *Trypanosoma cruzi* by high resolution field emission scanning electron microscopy using secondary and backscattered electron imaging. *FEMS Microbiol. Lett.* 242, 227–230. doi: 10.1016/j.femsle.2004.11.008
- Vidal, J. C., Alcantara, C. L., de Souza, W., and Cunha-e-Silva, N. L. (2016). Loss of the cytostome-cytopharynx and endocytic ability are late events in *Trypanosoma cruzi* metacyclogenesis. *J. Struct. Biol.* 196, 319–328. doi: 10.1016/j.jsb.2016.07.018
- Waterhouse, A. M., Procter, J. B., Martin, D. M., Clamp, M., and Barton, G. J. (2009). Jalview version 2—a multiple sequence alignment editor and analysis workbench. *Bioinformatics* 25, 1189–1191. doi: 10.1093/bioinformatics/btp033
- WHO (2015). Chagas disease in Latin America: an epidemiological update based on 2010 estimates. *Wkly. Epidemiol. Rec.* 90, 33–43.
- Wootton, E. C., Zubkov, M. V., Jones, D. H., Jones, R. H., Martel, C. M., Thornton, C. A., et al. (2007). Biochemical prey recognition by planktonic protozoa. *Environ. Microbiol.* 9, 216–222. doi: 10.1111/j.1462-2920.2006.01130.x
- Yang, J., and Zhang, Y. (2015). I-TASSER server: new development for protein structure and function predictions. *Nucleic Acids Res.* 43:W174–W181. doi: 10.1093/nar/gkv342
- Yenofsky, R. L., Fine, M., and Pellow, J. W. (1990). A mutant neomycin phosphotransferase II gene reduces the resistance of transformants to antibiotic selection pressure. *Proc. Natl. Acad. Sci. U. S. A.* 87:3435–3439. doi: 10.1073/pnas.87.9.3435

Conflict of Interest: The authors declare that the research was conducted in the absence of any commercial or financial relationships that could be construed as a potential conflict of interest.

Copyright © 2020 Chasen, Coppens and Etheridge. This is an open-access article distributed under the terms of the Creative Commons Attribution License (CC BY). The use, distribution or reproduction in other forums is permitted, provided the original author(s) and the copyright owner(s) are credited and that the original publication in this journal is cited, in accordance with accepted academic practice. No use, distribution or reproduction is permitted which does not comply with these terms.



The Influence of Recombinational Processes to Induce Dormancy in *Trypanosoma cruzi*

Bruno Carvalho Resende¹, Anny Carolline Silva Oliveira², Anna Carolina Paganini Guañabens², Bruno Marçal Repolês¹, Verônica Santana¹, Priscila Mazzochi Hiraiwa³, Sérgio Danilo Junho Pena¹, Glória Regina Franco¹, Andrea Mara Macedo¹, Erich Birelli Tahara¹, Stênio Perdigão Fragoso³, Luciana Oliveira Andrade² and Carlos Renato Machado^{1*}

¹ Laboratory of Biochemistry Genetics, Department of Biochemistry and Immunology, ICB, Universidade Federal de Minas Gerais, Belo Horizonte, Brazil, ² Laboratory of Cellular and Molecular Biology, Department of Morphology, ICB, Universidade Federal de Minas Gerais, Belo Horizonte, Brazil, ³ Laboratory of Functional Genomics, Instituto Carlos Chagas, Oswaldo Cruz Foundation (FIOCRUZ), Curitiba, Brazil

OPEN ACCESS

Edited by:

Noelia Lander,
University of Georgia, United States

Reviewed by:

Gonzalo Cabrera,
University of Chile, Chile
Ulrike Kemmerling,
University of Chile, Chile

*Correspondence:

Carlos Renato Machado
crmachad@icb.ufmg.br

Specialty section:

This article was submitted to
Parasite and Host,
a section of the journal
Frontiers in Cellular and Infection
Microbiology

Received: 11 November 2019

Accepted: 08 January 2020

Published: 28 January 2020

Citation:

Resende BC, Oliveira ACS, Guañabens ACP, Repolês BM, Santana V, Hiraiwa PM, Pena SDJ, Franco GR, Macedo AM, Tahara EB, Fragoso SP, Andrade LO and Machado CR (2020) The Influence of Recombinational Processes to Induce Dormancy in *Trypanosoma cruzi*. *Front. Cell. Infect. Microbiol.* 10:5. doi: 10.3389/fcimb.2020.00005

The protozoan *Trypanosoma cruzi* is the causative agent of Chagas disease, a neglected tropical disease that affects around 8 million people worldwide. Chagas disease can be divided into two stages: an acute stage with high parasitemia followed by a low parasitemia chronic stage. Recently, the importance of dormancy concerning drug resistance in *T. cruzi* amastigotes has been shown. Here, we quantify the percentage of dormant parasites from different *T. cruzi* DTUs during their replicative epimastigote and amastigote stages. For this study, cells of *T. cruzi* CL Brener (DTU TcVI); Bug (DTU TcV); Y (DTU TcII); and Dm28c (DTU TcI) were used. In order to determine the proliferation rate and percentage of dormancy in epimastigotes, fluorescent-labeled cells were collected every 24 h for flow cytometer analysis, and cells showing maximum fluorescence after 144 h of growth were considered dormant. For the quantification of dormant amastigotes, fluorescent-labeled trypomastigotes were used for infection of LLC-MK2 cells. The number of amastigotes per infected LLC-MK2 cell was determined, and those parasites that presented fluorescent staining after 96 h of infection were considered dormant. A higher number of dormant cells was observed in hybrid strains when compared to non-hybrid strains for both epimastigote and amastigote forms. In order to investigate, the involvement of homologous recombination in the determination of dormancy in *T. cruzi*, we treated CL Brener cells with gamma radiation, which generates DNA lesions repaired by this process. Interestingly, the dormancy percentage was increased in gamma-irradiated cells. Since, we have previously shown that naturally-occurring hybrid *T. cruzi* strains present higher transcription of RAD51—a key gene in recombination process—we also measured the percentage of dormant cells from *T. cruzi* clone CL Brener harboring single knockout for RAD51. Our results showed a significative reduction of dormant cells in this *T. cruzi* CL Brener RAD51 mutant, evidencing a role of homologous recombination in the process of dormancy in this parasite. Altogether, our data suggest the existence of an adaptive difference between *T. cruzi* strains to generate dormant cells, and that homologous recombination may be important for dormancy in this parasite.

Keywords: recombination, *Trypanosoma cruzi*, dormancy, DNA metabolism, infection

INTRODUCTION

The hemoflagellate *Trypanosoma cruzi* is an intracellular, protozoan parasite, and the etiological agent of Chagas disease, an infectious malady that currently affects ~8 million people worldwide. Mostly present at tropical and subtropical regions of the globe, Chagas disease is considered the most important parasitic infection in Latin America (WHO, 2019). It presents an acute phase with a relatively short duration, during which some signals and symptoms can be identified in infected individuals, such as an injury at the site of Triatominae vector bite—the chagoma or Romaña sign—and fever. Following the acute phase, the disease progresses to a chronic phase, during which is observed low parasitemia and a variable clinical course characterized by digestive, neurological, and cardiac complications (Rassi and Marin-Neto, 2010). Clinical diversity among patients has been shown to be a consequence of both host and parasite genetic variability (Vago et al., 2000). *T. cruzi* has been defined as a clonal species, but hybrid populations have also been found in nature, suggesting that events of genetic exchange may be pivotal to the genetic variability found in this parasite (Tomasini and Diosque, 2015).

Recently, *T. cruzi* strains were divided into six discrete typing units (DTUs)—TcI to TcVI—and each DTU discriminates genetically similar *T. cruzi* groups (Zingales et al., 2009). TcI occurs across North, Central, and South America—especially in Colombia and Venezuela—and is represented by strains with high replication rates and high parasitemia, leading to high mortality around 20–30 days post-infection (Zingales et al., 2012; Zingales, 2018). TcII presents higher replication and infection rates when compared to TcI, with a parasitemia peak around 12–20 days post-infection, when it promotes high mortality levels (Zingales et al., 2012; Oliveira et al., 2017). TcIII leads to low parasitemia, with its peak around 15–20 days post-infection, and is not related with chronic cases, being rarely documented in human infection (Zingales et al., 2012; Ragone et al., 2015). TcIV shows low virulence, with significant lower levels of parasitemia in comparison to TcII, but presents high prevalence in humans. Interestingly, TcV and TcVI are comprised of naturally-occurring hybrid strains resulting from genetic exchange events between TcII and TcIII. TcV and TcVI are less infective and display lower replication rates, but are largely related with severe chronic and congenital human disease. They occur mostly in South America within domestic transmission cycles (Zingales et al., 2012; Brenière et al., 2016; Oliveira et al., 2017).

In its heteroxenic cycle, *T. cruzi* metacyclic trypomastigotes—which are released together with triatomine feces—are capable of infecting different cell types from the mammalian host. Host cell infection occurs through the interaction between parasite surface and molecules from the host cell (Andrade and Andrews, 2005; Fernandes and Andrews, 2012). The internalized trypomastigotes differentiate into amastigotes, and begin replication in cytoplasm of the host cell, until they differentiate back into trypomastigotes. Extracellular-released trypomastigotes may infect neighboring cells, or even reach the bloodstream, and spread through the whole organism infecting other tissues (De Souza, 1999).

Recently, Sánchez-Valdéz et al. (2018) described the occurrence of cellular dormancy in *T. cruzi* during *in vivo* and *in vitro* experimental infection. Dormancy is a state involved in resistance to non-optimal environmental conditions of life in which cells become arrested. Dormancy has been described in various organisms: in fungi, it has been shown to avoid spore germination in harmful conditions (Wyatt et al., 2013); in bacteria, dormancy is well-known to occur in order to preserve the ability of colonizing the host even after the exposure to antibiotics (Harms et al., 2016). Cancerous cells can also undergo a dormant state upon exposure to chemotherapeutic agents aimed to eliminate replicative, active cells (Naumov et al., 2001). In protozoa, dormancy has been characterized in *Plasmodium* sp., the causative agent of malaria. In *Plasmodium*, the dormant form is recognized as a specific stage, called hypnozoite, and is associated with the recurrence of the disease and drug resistance (Markus, 2012). For *T. cruzi*, it was demonstrated that replicative-arrested amastigotes failed to incorporate nucleotide analog 5-ethynyl-2'-deoxyuridine (EdU), but were able to perform differentiation into trypomastigotes. Interestingly, those dormant parasites were resistant to doses of benznidazole 50-fold higher than the regular IC₅₀ dose. Dormant cells recovered growth after 30 days post-infection (Sánchez-Valdéz et al., 2018).

Our group has shown through different works that homologous recombination is essential in *T. cruzi* once it allows this parasite to repair DNA double strand breaks (DSBs), as well as it is also implicated in genetic exchange between *T. cruzi* cells (Alves et al., 2018). We have also shown that this parasite survives up to 500 Gy of gamma radiation—which induces DSBs—repairing DNA lesions within 48 h, and recovering cell growth 96 h after irradiation (Regis-da-Silva et al., 2006). Noteworthy, TcRad51, a protein involved in homologous recombination, has demonstrated to play a major role in recombinational process in *T. cruzi*. RAD51 is involved in the process of double strand DNA invasion through homology, forming a D-loop which will be processed by other proteins involved in this pathway (Holloman, 2011). *T. cruzi* overexpressing TcRAD51 is capable of resolving DSBs in both epimastigotes and amastigotes. On the other hand, TcRAD51-deficient epimastigotes and amastigotes are unable to properly repair DSBs (Gomes Passos Silva et al., 2018). Homologous recombination and TcRad51 also play a relevant role in genetic exchange processes since the overexpression of TcRAD51 is capable of stabilizing hybrid *T. cruzi* cells. In fact, naturally-hybrid *T. cruzi*'s populations show higher expression of TcRAD51 when compared to the non-hybrid ones (Alves et al., 2018).

In the present work, we used CellTrace™ CFSE Cell Proliferation Kit to assess *T. cruzi* asynchronous replication, focusing on dormant, replicatively-arrested cells in epimastigotes and amastigotes from different *T. cruzi* groups, as well as in parasites exposed to gamma radiation or deficient in TcRAD51. We verified that naturally-occurring hybrid cells—which express more TcRAD51—present a higher percentage of dormant epimastigotes and amastigotes when compared to non-hybrid ones. In epimastigotes, gamma radiation was able to

increase dormancy, while CL Brener TcRAD51 single knockout cells (CL Brener^{RAD51+/-}) presented decreased dormancy when compared to wild-type cells (CL Brener^{WT}). Altogether, our data suggest that homologous recombination may play a key role in dormancy signaling.

MATERIALS AND METHODS

Cell Types and Cellular Culture

T. cruzi epimastigotes were maintained at 28°C in liver infusion tryptose (LIT) medium supplemented with 10% inactivated fetal bovine serum (Gibco), 200 units/mL penicillin, and 200 µg/L streptomycin sulfate. *T. cruzi* clones CL Brener and Y were provided by Dr. Egler Chiari (Universidade Federal de Minas Gerais); clone Bug was provided by Dr. Bianca Zingales (Universidade de São Paulo); and clone Dm28c was provided by Dr. Stenio Fragoso (Fiocruz—Paraná). CL Brener^{RAD51+/-} were generated by Gomes Passos Silva et al. (2018). Rhesus monkey kidney cells (LLC-MK2; Hull et al., 1962) monolayers were maintained in 10% Dulbecco's Modified Eagle's Medium (10% DMEM; Sigma Aldrich), containing 10% FBS, 200 units/mL penicillin, and 200 µg/L streptomycin sulfate. Metacyclic trypomastigotes obtained from axenic cultures of *T. cruzi* at stationary phase were used to initiate parasite intracellular life cycle in LLC-MK2 cells. Infection was performed in 2% DMEM (2% FBS, 200 units/mL penicillin, and 200 µg/L streptomycin sulfate). LLC-MK2 culture was washed on a daily basis with PBS buffer containing Ca²⁺ and Mg²⁺ (PBS^{+/+}) to remove epimastigotes from the medium. Released tissue-culture trypomastigotes (TCTs) were purified as described previously (Andrews et al., 1987), and used to maintain parasite intracellular life cycle and to perform all experiments involving these cells.

CFSE Labeling and Sorting

Populations of *T. cruzi* epimastigotes were labeled with CellTrace CFSE (ThermoFisher) following the manufacturer instructions. Briefly, 2×10^7 epimastigotes/mL were incubated for 20 min at 28°C with 10 mM CFSE in PBS buffer, protected from light. The excess of CFSE was quenched with 5 volumes of LIT medium for 5 min. After that, cells were centrifuged at $3,000 \times g$ for 10 min and resuspended in fresh LIT medium at the concentration of 1×10^7 cells/mL. Aliquots from CFSE-stained epimastigote cultures were collected during 144 h, counted in a cytometry chamber and analyzed by flow cytometry to assess fluorescence intensity and replication profile. For some experiments, parasites were irradiated with a dose of 1,541 Gy/h for 19 min and 28 s using a cobalt (⁶⁰Co) irradiator located at Laboratório de Irradiação Gama (CDTN/CNEN, UFMG), prior to CFSE labeling and culture growth. FACScan or FACSCalibur flow cytometers were used for data collection (Benckton-Dickson) and 10,000 events for each condition were analyzed using the software FlowJo VX. FACSaria (Benckton-Dickson) sorter was used to create an enriched population of epimastigotes that had not replicated since the beginning of the analyses (24 h) until the stationary phase (144 h).

Mammalian Cell Infection and Immunostaining

For cell infections 4×10^4 LLC-MK2 cells were suspended in 10% DMEM and added onto 13 mm round glass coverslips inserted into each well of a 24-well plate. Plated cells were then incubated at 37°C with 5% CO₂ for 24 h before infection with purified trypomastigotes from Dm28c, Y, CL Brener^{WT}, CL Brener^{RAD51+/-}, or Bug strains previously labeled with CellTrace CFSE. For trypomastigote CFSE labeling, parasites were incubated for 20 min at 37°C with 10 mM CFSE in PBS buffer. The excess of CFSE was quenched with 2% DMEM for 5 min. After that, cells were centrifuged at $3,000 \times g$ for 10 min and resuspended with 5 volumes of 2% DMEM. Infection was performed (protected from light) at a multiplicity of infection (MOI) of 50 for 1 h in 2% DMEM. Afterwards, cells were washed five times with PBS^{+/+} and re-incubated in 2% DMEM for additional 24, 48, 7, and 96 h, until overnight fixation with 4% PFA at 4°C, temperature which samples were stored until processed for immunofluorescence.

After fixation, coverslips with attached cells were washed three times with PBS^{+/+} in order to remove cell fixative, incubated for 20 min with PBS containing 2% BSA (PBS/BSA) and processed for an inside/outside immunofluorescence invasion assay as previously described (Andrews et al., 1987). Briefly, extracellular parasites were immunostained with rabbit anti-*T. cruzi* polyclonal antibodies (Andrade and Andrews, 2004) in a 1:500 dilution in PBS/BSA for 1 h at room temperature, washed and labeled with Alexa Fluor-546 conjugated anti-rabbit IgG antibody (Thermo Fischer Scientific) in a proportion of 1:500 in PBS/BSA for 45 min. After that, DNA from host cells and parasites was stained for 1 min with 0.1 µM DAPI (4',6-Diamidino-2-Phenylindole, Dihydrochloride—Sigma) in PBS, mounted, and examined on a Zeiss Axio Vert.A1 microscope equipped with an AXIOCAM ICM1 camera controlled by the ZEN Image Software (Zeiss).

RNA Extraction and cDNA Synthesis

T. cruzi total RNA was extracted from 1×10^8 cells using TRIzol (Invitrogen) according to the manufacturer recommendations. After RNA extraction, contaminant DNA was removed from samples through the use of TURBO DNA-Free Kit (Ambion, ThermoFisher). In order to verify possible persistence of contaminant DNA, each sample was submitted to a PCR carried out using the primers listed in Table 1. Treatment with TURBO DNA-free Kit was repeated until PCR was negative. A total of 1 µg of clean RNA were used for cDNA synthesis reaction using the High Capacity cDNA Reverse Transcription Kit (Life

TABLE 1 | Primers used on Real-time PCR quantification.

Primer	Sequence
RTTcRad51Fw	5'-GGC TGT CAA GGG TAT CAG TG-3'
RTTcRad51Rev	5'-AAC CAC TGC GGA TGT AA GC-3'
RTGAPDH2Fw	5'-CGGTGGACGGTGTGTCCGGT-3'
RTGAPDH2Rev	5'-CCGTCAGCTTGCCCTGGGTG-3'

Technologies). As negative control, a reaction with no reverse transcriptase was carried out.

Quantitative Real-Time PCR

Reactions were performed using SYBR Green PCR Master Mix (Applied Biosystems). For each reaction, 10 ng cDNA, 300 nM primers, 5 μ L SYBR Green Master Mix 2X, and DNase/RNase-free water—for a total volume of 10 μ L of reaction—were used. Reactions were performed in a 384-well plate in technical and biological triplicates. Glyceraldehyde 3-phosphate dehydrogenase gene (GAPDH) was used as a loading control. All primers used in the quantification experiments are listed in **Table 1**. The relative amount of TcRAD51 transcripts were calculated by the $2^{-\Delta\Delta C_t}$ method.

Statistical Analysis

Statistical analyses were performed using GraphPad Prism 5 version 5.01 (San Diego, USA). Data were analyzed through one-way ANOVA with Bonferroni Comparison Test as post-test. $p < 0.05$ was reported as significant.

RESULTS

Epimastigote Dormancy Is Strain-Dependent in *T. cruzi*

In order to evaluate if epimastigote dormancy is related to the genetic background in *T. cruzi*, we tested cells from four different DTUs: Dm28c (TcI), Y (TcII), CL Brener (TcVI), and Bug (TcV). For such, we labeled epimastigotes from all aforementioned strains with CellTrace™ CFSE Cell Proliferation Kit (Item 2.2), and followed its fluorescence decay during 144 h of culture through flow cytometry. Cellular duplication should reduce CFSE fluorescence intensity by 0.55-fold after each cycle, indicating that cells whose CFSE fluorescence intensity remains at high levels over time can be considered as dormant. Fluorescence intensity at the very beginning of cellular culture (0 h) was not considered for analysis in order to avoid biased interpretations due to an inevitable loss of CFSE right after cellular labeling. After 144 h of monitoring, we observed that naturally-occurring hybrid strains CL Brener and Bug showed a lower growth rate when compared to non-hybrid strains Dm28c and Y (**Figure 1A**). Interestingly, we also verified that all strains studied present arrested parasites in all time points analyzed. However, we also observed that CL Brener and Bug display an increased percentage of arrested parasites compared to Dm28c and Y during the 144 h of culture (**Figures 1B,C**). In fact, CL Brener and Bug consistently presented a higher percentage of dormant cells since 24 h of culture through the end of the experiment (**Figure 1B**). Altogether, these results indicate that *T. cruzi* epimastigotes from naturally-occurring hybrid strains exhibit an increased ability to enter in dormancy.

Dormant Epimastigotes Can Resume Cellular Duplication in Fresh Conditions

In order to verify, if arrested *T. cruzi* cells can resume their cellular duplication and, if so, what is the pattern of

growth wherever it occurs, we used the cell sorter FACSARIA (Beckton-Dickson) to obtain a population enriched in dormant epimastigotes from Bug strain—as it presented the highest percentage of dormant cells from all strains studied (**Figure 1**). For such, Bug epimastigotes exhibiting a sustained CFSE fluorescence intensity at 144 h (half the median at 24 h point) culture were sorted by FACSARIA in fresh LIT, allowing an enrichment of 1,550% (62% of dormant cells after sorting vs. 4% of dormant cells before sorting) (**Figure 2A**). CFSE fluorescence intensity decay of this population was then followed over time. We verified that in all time points analyzed (24 and 48 h), CFSE intensity progressively decreased, indicating cellular duplication (**Figures 2A,B**). Interestingly, we also noticed that the percentage of dormant epimastigotes 48 h post-sorting and growth was similar to that one observed for Bug epimastigote cultures at 144 h of growth pre-sorting—around 4% (**Figure 2B**).

Amastigote Dormancy Is Also Strain-Dependent in *T. cruzi*

Since duplication rates and the percentage of dormant cells in *T. cruzi* epimastigotes were dependent on the genetic background (**Figure 1**), we hypothesized that this dependency could be also observed for amastigotes. We then performed infection of LLC-MK2 cells using trypomastigotes from Dm28c, Y, CL Brener, and Bug strains, and followed their intracellular transformation into amastigotes and replication of the latter for a period of 96 h of infection. The percentage of infected LLC-MK2 cells and the percentage of CFSE-positive amastigotes were evaluated. The latter was evaluated by determining the number of CFSE-labeled from the total amastigotes found in 100 LLC-MK2 infected cells. Amastigotes presenting high CFSE fluorescence intensity 96 h post-infection were considered arrested. We observed that the invasion rate of LLC-MK2 cells by CL Brener and Bug—naturally-occurring hybrids—was lower in relation to the invasion rate observed for Dm28c and Y—non-hybrid strains (**Figure 3A**). Interestingly, the highest number of total Dm28c and CL Brener amastigotes (i.e., CFSE-positive and negative amastigotes) per cell was observed 72 h post-infection, with a reduction in this number 96 h post-infection (**Figure 3B**). This decline is likely related to the fact that for these strains about 4% of the cells (3.3% in CL Brener strain, and 4.3% in Dm28c strain) were infected with only one parasite 96 h post-infection.

Ninety-six hours post-infection, most amastigotes present in LLC-MK2 cells were CFSE-negative due to fluorescence decay promoted by cellular replication. Therefore, at this time point, CFSE-positive amastigotes represent those parasites which underwent few duplication events, and thus can be classified as dormant cells. Interestingly, we verified that the percentage of dormant amastigotes from CL Brener and Bug was higher in relation to Dm28c and Y (**Figure 3C**), in similar fashion to the results obtained with epimastigotes (**Figure 1**). Finally, it is noteworthy that CFSE-positive trypomastigotes were found inside LLC-MK2 cells at 96 h post infection (**Figure 3D**), strongly suggesting that they had derived from dormant amastigotes.

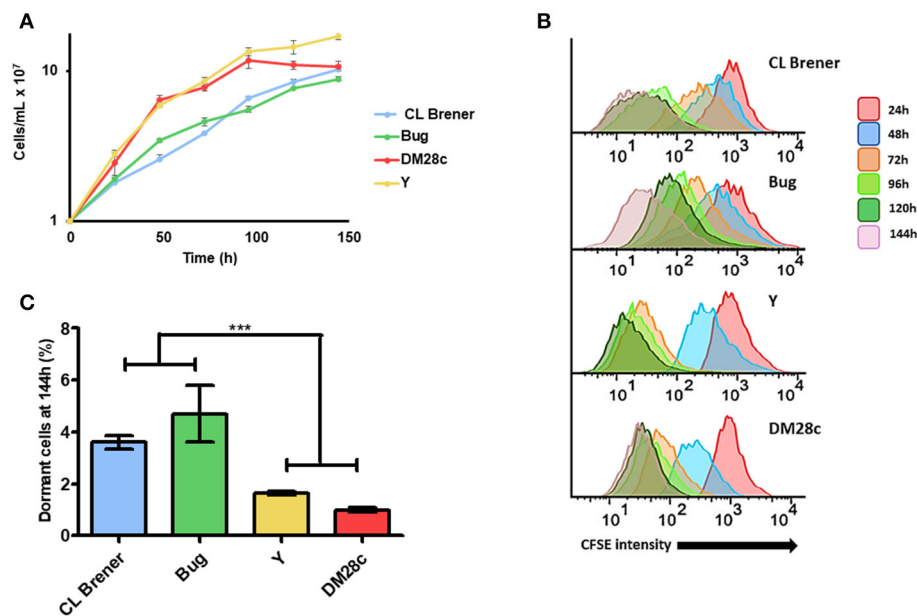


FIGURE 1 | Dormancy in epimastigote forms of *T. cruzi* wild type strains. **(A)** Cellular growth curves from four different strains (CL Brener, Bug, DM28c, and Y). At 0 h, 1×10^7 cells were treated with CFSE and samples were counted every 24 h for 144 h. **(B)** Flow cytometry histograms of epimastigote cultures from each strain from 24 to 144 h. CFSE intensity was assessed every 24 h until 144 h, and arrested cells were considered those ones which exhibited similar CFSE intensity at 144 h when compared to the level of half median of 24 h. **(C)** Average of percentage of dormant cells in CL Brener, Bug, Y, and DM28c strains at 144 h was detected in flow cytometry histograms. Representative results of three experiments. Asterisks indicate statistically significant differences among groups (P -value < 0.05).

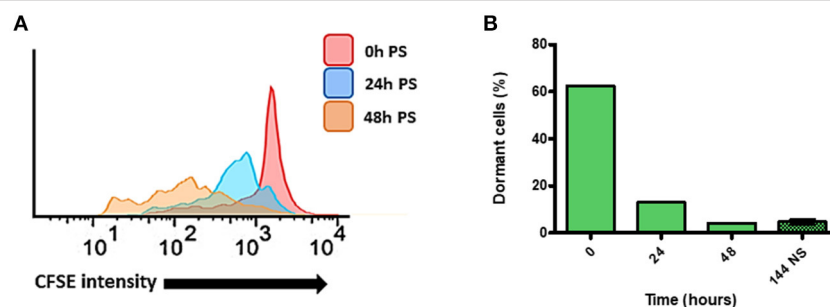


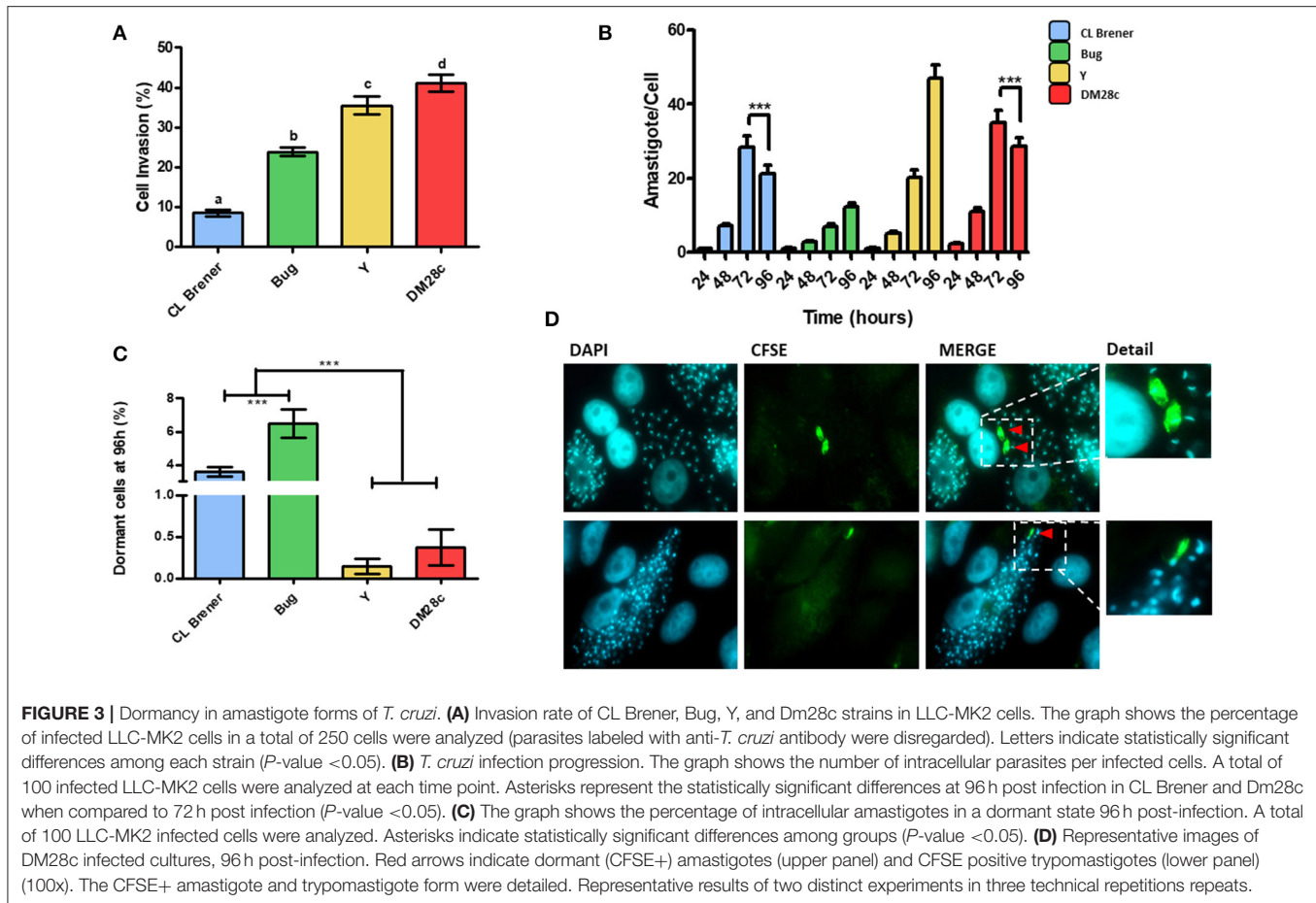
FIGURE 2 | Quantification of dormant replication cells after sorting of dormant epimastigote cells. **(A)** Flow cytometry histograms of dormant epimastigotes of Bug strain after sorting. Cells sorted (0 h post-sorting; PS) were resuspended in fresh medium, and CFSE intensity was followed every 24 h until 48 h PS. Cells that exhibited similar CFSE intensity at each point when compared to the level of half median of 0 h PS were considered arrested cells. **(B)** The percentage of arrested cells after sorting as detected in flow cytometry histograms in each time point. The percentage of dormant cell before sorting at 144 h is presented for comparison.

Dormant Amastigotes Can Be Converted Into Infecting Trypomastigotes

The high prevalence of LLC-MK2 cells harboring one amastigote 96 h post-infection (Figure 3) led us to ask if those cells were newly-infected or if the single hosted-amastigote had not been capable of forming an amastigote nest. We then sought to investigate the replication dynamics of trypomastigote-derived amastigotes in LLC-MK2. We found that, 24 h post infection, 50% of Dm28c-infected LLC-MK2 cells presented more than one amastigote, while infection carried out with Y, CL Brener, and Bug led to 100% of LLC-MK2 infected cells harboring a single amastigote (Figure 4A); this suggests that, in the very

beginning of the infection, Dm28c replicates at a higher rate when compared to the other strains studied. Another observation is that the percentage of LLC-MK2 cells carrying a single amastigote decreases over time (Figure 4A).

Since the Dm28c strain exhibited a higher replication rate, we further evaluated whether arrested Dm28c amastigotes could be detected earlier in relation to arrested amastigotes from Y, CL Brener, and Bug strains. For such, we assumed that the earlier the CFSE-labeled amastigotes become arrested, the lower should be their number in relation to CFSE-negative amastigotes at later time points—e.g., 96 h post infection. We then determined the median of parasites per infected LLC-MK2



cell 96 h post-infection for each strain, and further divided the LLC-MK2 cells into two groups: one in which the number of infecting amastigotes was higher than the median (group #1), and another one in which the number of infecting amastigotes was lower than the median (group #2). For the Dm28c strain, CFSE-positive amastigotes were mostly found in LLC-MK2 cells from group #1, and for Y and Bug strains, CFSE-positive amastigotes were mostly found in LLC-MK2 cells from group #2. The CL Brener strain exhibited the same percentage of CFSE-positive amastigotes in both groups #1 and #2 (Figure 4B).

One general observation is that the number of LLC-MK2 cells infected with one amastigote decreases over time; however, infection with Dm28c and CL Brener strains leads to an increase in the number of LLC-MK2 cells infected with just one parasite at later times of infection (Figure 4A). For Dm28c, the percentage of LLC-MK2 cells with one amastigote rises from 0.6% (72 h post-infection) to 4.3% (96 h post-infection), and for CL Brener it increases from 3% (48 h post-infection) to 6% (72 h post-infection) (Figure 4A). These observations suggest that there is a phenomenon of reinfection taking place at these time intervals. We further evaluated the percentage of LLC-MK2 cells infected with a single amastigote, in this case CFSE-positive or CFSE-negative, at 96 h post-infection. We verified that the percentage of CFSE-positive CL Brener amastigotes in cells infected with just one parasite was 15% at 96 h post-infection (Figure 4C).

This number means a large increase in CFSE positive cells, since within 72 h CFSE positive parasites represent only 2% of all parasites present. For Dm28c, these parasites represented 1% (of all parasites present) and 40% (in cells infected with only one parasite), for 72 and 96 h post-infection, respectively (Figures 4C,D). These results suggest that arrested parasites are more prone to reinfection than non-arrested ones.

Homologous Recombination Induces Dormancy in *T. cruzi* Epimastigotes

Gamma radiation generates DSBs in DNA, which are repaired by homologous recombination in *T. cruzi*. We have previously shown that epimastigotes exposed to 500 Gy of gamma radiation enter in a cell cycle arrest for 4 days, by the end of which are able to resume their cellular growth (Gomes Passos Silva et al., 2018). In order to analyze in detail how gamma radiation affects epimastigotes of *T. cruzi* from CL Brener strain, we irradiated cells with 500 Gy of gamma rays and labeled them immediately with CFSE. As expected, cellular growth recovery was observed at 96 h post-radiation, with a consequent decay in CFSE fluorescence intensity (Figures 5A,B). However, we also verified that the percentage of arrested epimastigotes at 144 h of culture was significantly higher for gamma ray-treated epimastigotes when compared to non-treated ones at same time points (Figures 5B,C). These data suggest that DNA repair

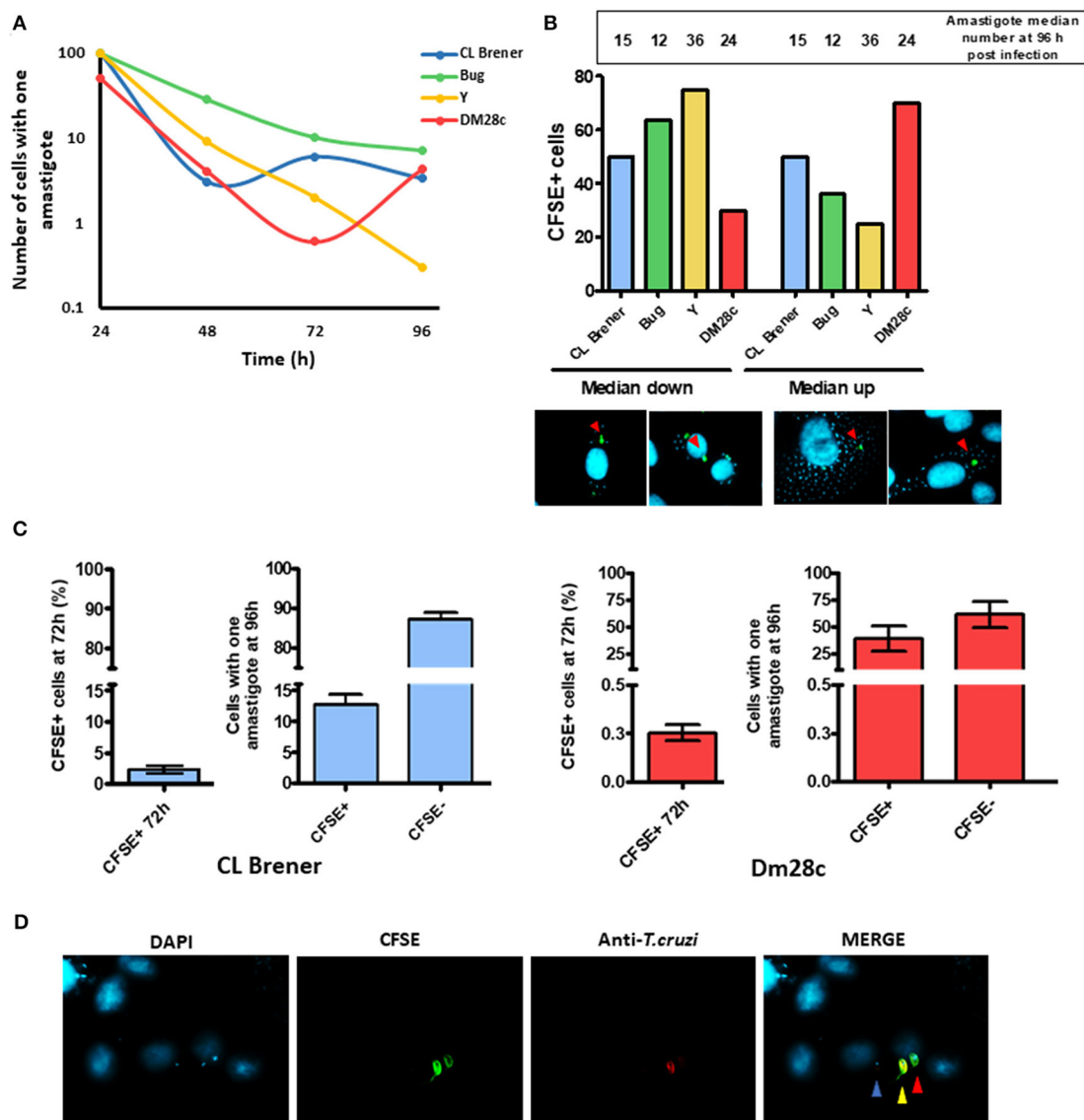


FIGURE 4 | Dormant reinfection characterization. **(A)** The graph shows the percentage of cells infected with a single amastigote along the infection. A total of 100 infected LLC-MK2 cells were analyzed at each time point and the infected cells with just one amastigote were counted. **(B)** The graph shows the percentage of cells containing CFSE-positive parasites according two groups of cells: one in which the number of intracellular parasites was higher than the median, and another one in which the number was lower than the median at 96 h post-infection. Values indicated in the bar are the median for each strain at 96 h post-infection. Below the graph, a representative figure depicting what was considered as cells with CFSE-positive parasites in a median down group or in median up group is shown. **(C)** The graph shows the percentage of cells infected with a single parasite from CL Brener or Dm28c strains at 96 h that is either CFSE-positive or -negative. A hundred single-infected cells were analyzed per assay. For the sake of comparison, besides each graphic the percentage of total CFSE positive CL Brener or Dm28c parasites at 72 h post-infection is shown. **(D)** Representative image of a cell infected with a single parasite (Dm28c strain), CFSE+ (red arrow) or CFSE- parasite (blue arrow) at 96 h post-infection. An external trypomastigote form is also shown (yellow arrow).

through homologous recombination elicited by DSBs induces arrested cells in *T. cruzi* epimastigotes.

RAD51 mRNA Levels Are Directly Correlated With Dormancy in *T. cruzi*

We have described previously that distinct responses to DSBs, through homologous recombination, observed in different *T. cruzi* DTUs are related to their variable TcRAD51 transcription levels (Alves et al., 2018). Then, in order to verify if there is a

direct relation between TcRAD51 mRNA levels and the rate of arrested cells in the strains studied here—Dm28c, Y, CL Brener, and Bug—we performed a qRT-PCR assay to determine the TcRAD51 transcription levels. We then verified that the relative TcRAD51 transcription levels of Dm28c, Y and Bug strains vary (0.64 ± 0.10 , 0.45 ± 0.08 , and 1.43 ± 0.62 , respectively) when compared to the CL Brener strain (Figure 6). In fact, those variations show that non-hybrid strains—i.e., Dm28c and Y—display decreased TcRAD51 mRNA levels in relation to the

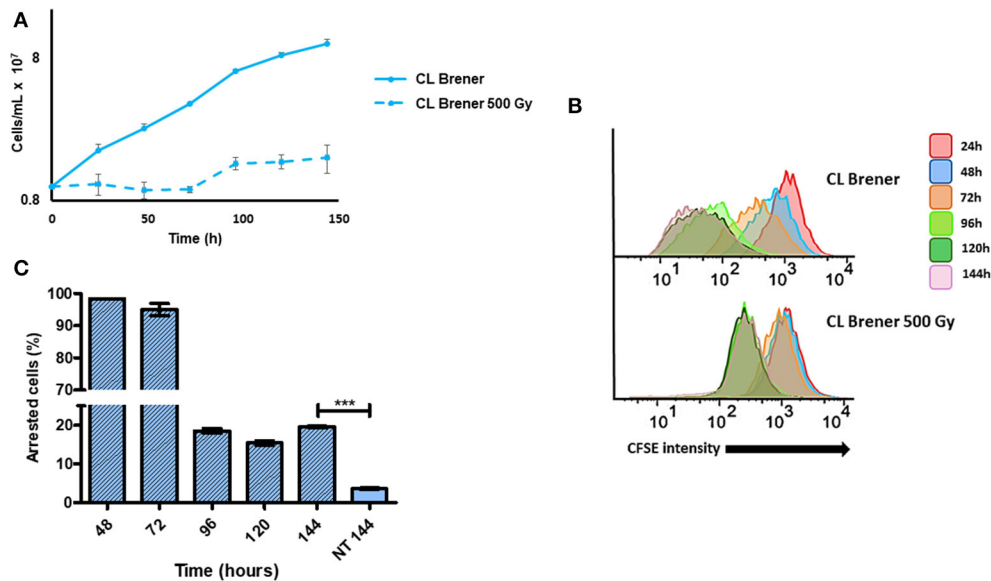


FIGURE 5 | Dormancy in epimastigotes from CL Brener strain after gamma radiation exposure. **(A)** A 144 h-growth curve of wild-type *T. cruzi* CL Brener strain exposed or not to 500 Gy of gamma irradiation. **(B)** Flow cytometry histograms of CFSE fluorescence intensity decay over time from epimastigotes exposed or not to 500 Gy. Cells that have similar CFSE fluorescence intensity compared to the level of half median of 24 h time point were considered as arrested. **(C)** The graph shows the percentage of arrested parasites determined by flow cytometry showing half of CFSE median intensity observed at 24 h of growth. The percentage of dormant parasites at 144 h- from a culture without exposure to gamma radiation (NT 144 h) is shown for the sake of comparison. Representative results of three distinct experiments are shown. Asterisks indicate statistically significant differences among groups (P -value <0.05).

CL Brener strain—a naturally-occurring hybrid. In line with this rationale, another naturally-occurring hybrid strain—Bug—exhibit increased TcRAD51 transcription when compared to the non-hybrid strains studied, being surprisingly higher when also compared to the CL Brener TcRAD51 mRNA levels.

CL Brener^{RAD51+/-} Epimastigotes Exhibit Decreased Dormancy

Since increased TcRAD51 transcription levels are directly related to higher dormancy in *T. cruzi* (Figure 6), we hypothesized that the CL Brener^{RAD51+/-} mutant, which harbors only one copy of TcRAD51 (Gomes Passos Silva et al., 2018), would exhibit a decreased percentage of arrested parasites when compared to CL Brener^{WT}. In fact, epimastigote cultures of CL Brener^{RAD51+/-} showed a decreased percentage of cells presenting high CFSE fluorescence intensity, indicating a high duplication rate and a reduced percentage of dormant cells when compared to CL Brener^{WT} parasites (Figures 7B,C). Interestingly, the reduction in the number of arrested parasites for CL Brener^{RAD51+/-} did not alter their rate of growth (Figure 7B), despite the fact that CFSE fluorescence intensity decay is different between CL Brener^{WT} cells and CL Brener^{RAD51+/-} mutants (Figure 7B).

CL Brener^{RAD51+/-} Mutants Exhibit Changes in Infectivity, Replication, and Morphology

In order to further investigate the impact of single deletion of TcRAD51 in *T. cruzi* on infectivity and replication, we carried out infection of LLC-MK2 cells using CL Brener^{RAD51+/-} and CL Brener^{WT} trypomastigotes. We observed that CL

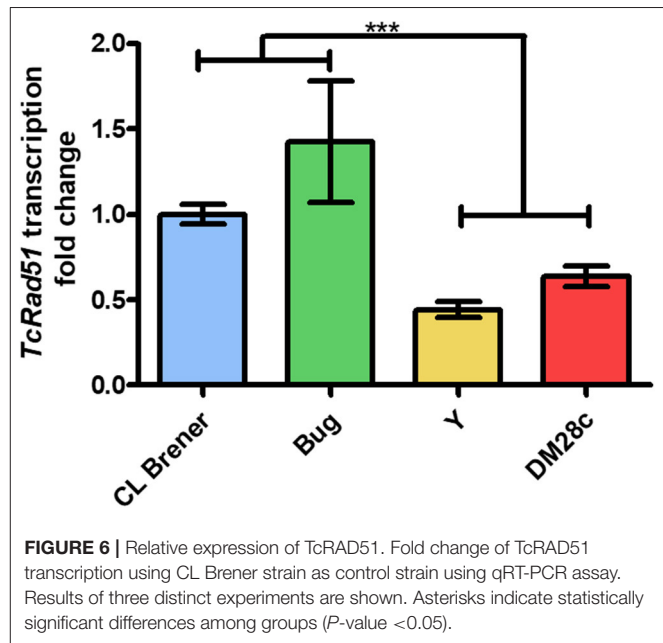


FIGURE 6 | Relative expression of TcRAD51. Fold change of TcRAD51 transcription using CL Brener strain as control strain using qRT-PCR assay. Results of three distinct experiments are shown. Asterisks indicate statistically significant differences among groups (P -value <0.05).

Brener^{RAD51+/-} mutants were less efficient to invade the cells than their WT counterparts (Figure 8A). As previously reported by Alves et al. (2018), CL Brener^{RAD51+/-} cells also showed a decreased replication rate in LLC-MK2 cells (Figure 8B). Nonetheless, the percentage of CFSE-positive parasites 96 h post-infection was also lower in CL Brener^{RAD51+/-} than in CL Brener^{WT} (Figure 8C).

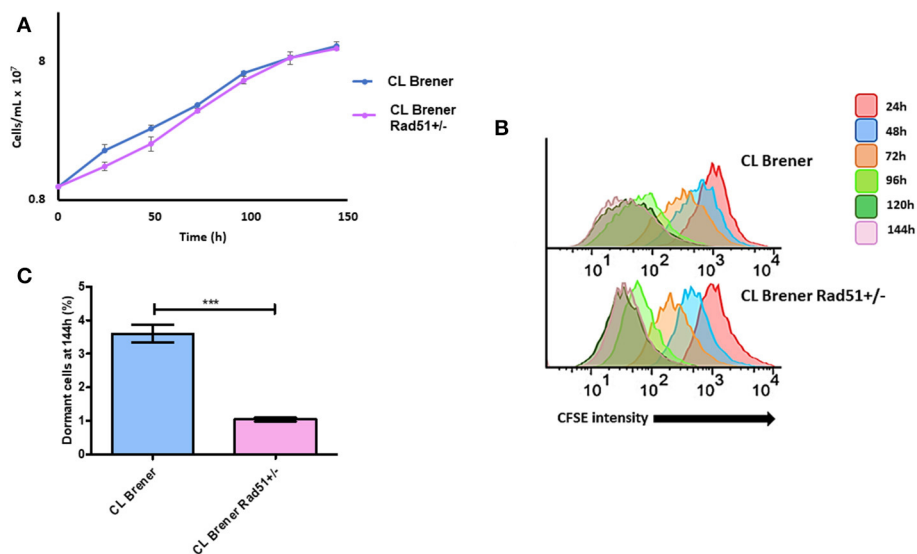


FIGURE 7 | Dormancy in epimastigote forms of *T. cruzi* CL Brener *Rad51*^{+/-}. **(A)** Cellular growth curve of CL Brener wild-type strain and *Rad51*^{+/-} mutant. At 0 h, 1×10^7 cells were treated with CFSE, and samples were analyzed each 24 h for 144 h. **(B)** Flow cytometry histograms of epimastigote cultures from each strain. CFSE fluorescence intensity was followed every 24 h until 144 h. Cells that exhibited similar CFSE fluorescence intensity at 144 h when compared to the level of half median of 24 h were considered as dormant. **(C)** Average of dormant cells percentages in CL Brener and *Rad51*^{+/-} mutants at 144 h was detected in flow cytometry histograms. Representative results of three experiments are shown. Asterisks indicate statistically significant differences among groups (*P*-value < 0.05).

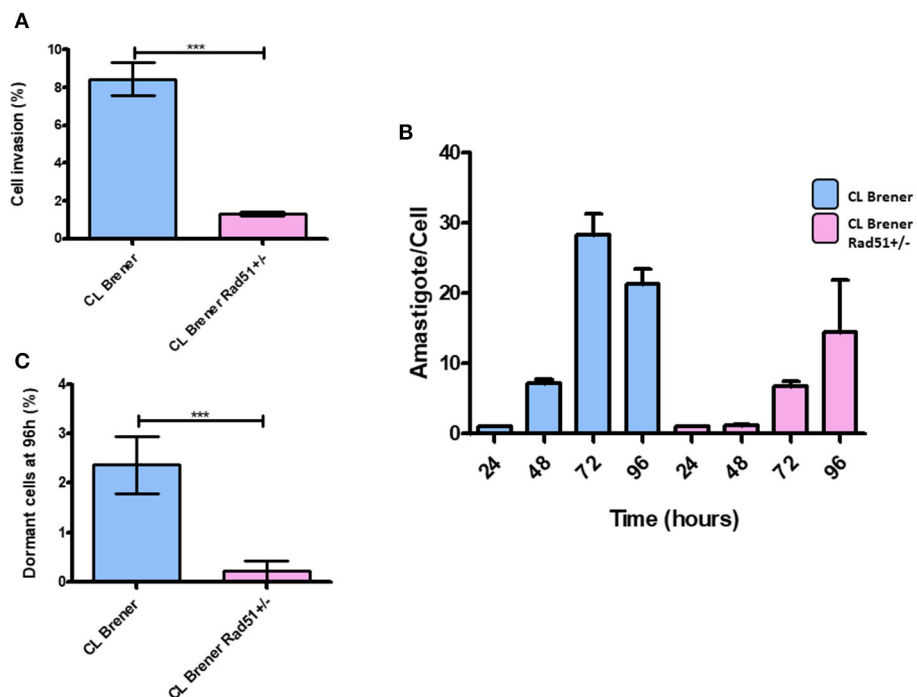


FIGURE 8 | Dormancy in amastigote forms of *T. cruzi* CL Brener *Rad51*^{+/-}. **(A)** The graph shows the percentage of infected cells in LLC-MK2 cultures infected by *T. cruzi* CL Brener *Rad51*^{+/-} mutants and WT cells. The number of 250 LLC-MK2 cells were analyzed (parasites labeled with anti-*T. cruzi* antibody were disregarded). Asterisk indicate statistically significant differences between strains (*P*-value < 0.05). **(B)** The graph shows the rate of intracellular parasitic replication in LLC-MK2 cultures exposed to *T. cruzi* CL Brener *Rad51*^{+/-} mutants and WT cells during 96 h of parasite exposure. A total of 100 infected LLC-MK2 cells were analyzed at each time point. **(C)** Percentage of intracellular parasites from *T. cruzi* CL Brener *Rad51*^{+/-} mutants and WT cells showing high CFSE labeling 96 h post-infection. One hundred infected LLC-MK2 cells were analyzed, and the percentage of CFSE-positive ones in relation to the total number of intracellular parasites was determined.

DISCUSSION

In 2018, Sánchez-Valdéz et al. first showed that *T. cruzi* has the ability to enter into a dormant state as they observed that some amastigotes interrupted their cellular replication during an *in vitro* infection using Vero cells (Sánchez-Valdéz et al., 2018). In this work, we sought to further investigate whether *T. cruzi* dormancy also occurs in epimastigotes, as well as if dormancy is a strain-dependent process in this parasite. In order to monitor *T. cruzi* replication, we used CFSE, a compound that covalently binds to lysine residues from the cellular protein content, without disrupting cellular growth (Lyons et al., 2013). Additionally, the high stability of this compound grants labeling analysis for several months, allowing the tracking of human cellular division for eight or more generations (Luzyanina et al., 2013). These characteristics make CFSE labeling a valuable tool of cell cycle dynamics using fluorescence microscopy and cytometry (Tuominen-Gustafsson et al., 2006). In fact, other techniques commonly used to monitor cell cycle, such as bromodeoxyuridine and tritiated thymidine incorporation, present limited applications—the former technique, for instance, is only feasible in situations in which cells undergo a limited number of replication events; the latter, precludes the analysis of single cell proliferation (Lyons et al., 2013).

During each cycle of cellular duplication, CFSE fluorescence intensity decreases to the half of its initial median, allowing the detection of newly-generated cells (Lyons and Parish, 1994). In addition, our group observed that arrested-cells (obtained by the exposure to 500 Gy of gamma radiation) show a slight reduction in CFSE fluorescence intensity after 24 h of culture growth, although this intensity decrease is not related to a replicational event (data not shown). This small decay in CFSE labeling may be due to the instability of covalent bonds established between lysine residues and CFSE, as previously reported in lymphocytes (Parish et al., 2009). For this reason, we considered the time point of 24 h of culture growth as the maximum value of CFSE fluorescence intensity for all analyses. Thus, since replication is expected to promote a 0.55-fold drop in total CFSE fluorescence intensity by each replication cycle, *T. cruzi* cells which maintained CFSE fluorescence intensity above the median of CFSE fluorescence intensity observed at 24 h of cellular growth were considered as dormant cells.

Based on the aforementioned conditions, we showed that 24 h of culture growth is enough to observe cellular replication in all strains tested. Additionally, there is a percentage of epimastigotes that do not duplicate during 144 h of culture growth, indicating cell arrest, which characterizes a dormancy state in this stage of *T. cruzi*'s life cycle. Also, we observed that non-hybrid strains—i.e., Dm28c and Y—exhibit higher replication rate than naturally-occurring hybrid strains—CL Brener and Bug. In fact, Dm28c and Y reached the stationary phase of growth earlier than CL Brener and Bug. These results correlate well with the percentage of cells that did not undergo replication after 144 h of cellular culture. While naturally-occurring hybrid strains showed accumulation of arrested cells through the 144 h time interval, characterizing an asynchronous replication pattern, non-hybrid strains went opposite ways, with a higher and more synchronized

duplication rate. Indeed, the decay of CFSE fluorescence intensity over time supports this conclusion as CL Brener and Bug showed a wider distribution of CFSE labeling when compared to Dm28c and Y, certainly due to their asynchronous replication cell cycle.

In order to further investigate whether arrested *T. cruzi* parasites still kept the ability to replicate, we set out an isolation protocol using FACSaria to generate a culture enriched in dormant epimastigotes. We were able to obtain a culture of Bug epimastigotes enriched in 1,550%, and observed that the majority (96%) of arrested epimastigotes can resume cellular replication once in fresh LIT medium, while 4% from total epimastigotes remained arrested. Dumoulin and Burleigh (2018), through the use of CFSE to monitor amastigote replication, showed the existence of a replicative plasticity of *T. cruzi* under nutritional depletion. It is possible that, under those conditions, *T. cruzi* arrested cells were still able to replicate, but the environmental conditions—i.e., culture reaching the stationary phase and lack of nutrients in the culture medium—may have prevented cellular replication. In fact, the addition of fresh culture medium could be a signal for the replication recovery we observed in our conditions.

As cited above, even in enriched cultures of dormant Bug epimastigotes, we still found a percentage of parasites (4%) that did not undergo replication after being resuspended in fresh LIT. Interestingly, this percentage corresponds to the percentage of dormant epimastigotes present in the original Bug epimastigote culture before sorting. These results may indicate that induction of dormancy in a defined percentage of cells may be an intended process, which acts in parallel with replication recovery promoted by fresh LIT. In this context, in which extracellular molecular signaling appears to play a role in the cellular fate of a given organism, we hypothesize that a mechanism that can resemble quorum-sensing may be determining this phenotype in *T. cruzi*. In fact, quorum-sensing has been observed in other trypanosomatids such as *Trypanosoma brucei* (Mony and Matthews, 2015). In this parasite, a molecule called stumpy induction factor (SIF) is capable of retarding parasite growth, in a density-dependent way, when it is cultured *in vitro*. A percentage from total parasite population, however, does not respond to the molecule, allowing asynchronous growth. SIF is already shown to modulate the expression of proteins involved in homologous recombination in *T. brucei* (Mony and Matthews, 2015). Besides that, arrested/dormant cells are observed for a number of other organisms: fungal dormant spores seem to avoid germination in harmful conditions through a very well-regulated way (Wyatt et al., 2013); in bacteria, the generation of dormant cells is stimulated in a way that perseveration of host colonization can be conducted in the case of a catastrophic event like antibiotic exposure (Harms et al., 2016); in protozoa, the arrested/dormant state has already been characterized as a specific form of *Plasmodium* sp. called hypnozoite—hypnozoites have been associated with the recurrence of malaria, as well as with drug resistance during treatment of this disease (Markus, 2012). In addition, cancerous cells also present a dormant state, which helps escaping chemotherapy, aimed to kill replicatively-active cells (Naumov et al., 2001).

We then went on to further investigate whether dormancy could be also observed in *T. cruzi* amastigotes. For such, we infected LLC-MK2 cells with CFSE pre-labeled trypomastigotes, and followed CFSE fluorescence intensity over time. CFSE-positive amastigotes found after 96 h of infection were considered arrested. First, it was possible to observe that hybrid strains—CL Brener and Bug—were less infective than non-hybrid strains—DM28c and Y—corroborating previous data from Zingales et al. (1997). Second, CL Brener and Bug strains exhibited the highest percentages of arrested amastigotes, showing a negative correlation between dormancy and infectivity in *T. cruzi*.

Considering the intracellular replication of *T. cruzi*, non-hybrid strains DM28c and Y presented an increased rate of replication cycle when compared to naturally-occurring hybrid CL Brener and Bug ones, which is in line with their virulence in mice (Medeiros et al., 2010) and in LLC-MK2 cells (Zingales et al., 1997). In fact, *T. cruzi*'s virulence also correlates with the percentage of arrested cells found in those strains. Dm28c and Y present high replication rates, low dormancy and increased virulence, while CL Brener and Bug exhibit low replication rates, high dormancy and decreased virulence. In addition, Dm28c and CL Brener also displayed a reduction in the average number of amastigotes present in LLC-MK2 cells from 72 to 96 h post-infection (Figure 3B). It is likely that these reduction in the average number of intracellular parasites per infected cell is due to parasite reinfection events, since for these cultures, although the proportion of cells containing a single amastigote drops 48 h post-infection it rises again at 96 h post-infection. On the other hand, the percentage of LLC-MK2 cells infected by a single *T. cruzi* amastigote from Y and Bug strains does not rise at 96 h post-infection. We further verified that the aforementioned reinfection process is performed efficiently by CFSE-positive parasites, since a significant proportion of these reinfection events occurred by CFSE positive parasites, more than 15% for CL Brener and 40% for DM28c strain. When we consider that the percentage of CFSE-positive cells 72 h post-infection was around 0.5 and 2% for Dm28c and CL Brener, respectively, we can assume that arrested amastigotes not only present the ability to differentiate into new trypomastigotes (Sánchez-Valdéz et al., 2018), but also exhibit increased infectivity in relation to non-arrested parasites. One possible reason by which they would be more infective relies on the possibility that the earlier one *T. cruzi* becomes arrested, the lesser changes would be observed in its surface proteins in relation to the parental amastigote. Therefore, *T. cruzi* cells presenting high infection ability would be selected to perpetrate further waves of reinfection in the host. This scenario could be a valuable strategy for *T. cruzi* to establish the chronic phase of Chagas disease, since these arrested parasites would partially halt host-cell colonization, reducing the number of trypomastigotes released to the extracellular milieu, thus decreasing parasite detection by the host immune system. This hypothesis would be in accordance with the clinically-observed patterns of Chagas disease progression and strain-dependent chronicity, in which naturally-hybrid strains show higher rates of chronification (Oliveira et al., 2017). On the other hand, *T. cruzi* strains that present less percentage of arrested cells would

be less prone to establish a chronic infection. In fact, there is no reinfection process performed by CFSE-positive parasites when LLC-MK2 cells are infected by the Y strain (data not shown). Interestingly, data from experimental infection in mice show that animals exhibit high parasitemia within few days of infection with the Y strain, which usually leads to death, with few cases of chronicity (Zingales et al., 2012). On the contrary, infection with *T. cruzi* from CL Brener strain usually leads to chronification during experimental infection in mice (Medeiros et al., 2010).

Sánchez-Valdéz et al. (2018) hypothesized that homologous recombination is the cause for dormancy in *T. cruzi*. It is well-known that the recombination pivot is TcRad51, a protein responsible for the repair of DSBs—either induced by high levels of gamma radiation, or caused by other genotoxic agents that lead to transcriptional and replicational fork arrest (Regis-da-Silva et al., 2006; Gomes Passos Silva et al., 2018). We then observed the effect of gamma radiation in inducing arrest in *T. cruzi* epimastigotes. Gamma rays, as previously described (Regis-da-Silva et al., 2006; Alves et al., 2018; Gomes Passos Silva et al., 2018), prevented parasite replication for 72 h, with growth recovery being observed after 96 h (Figure 5A). Despite replication recovery, at 144 h of culture, the percentage of dormant cells was still higher in irradiated cultures when compared to non-irradiated ones, corroborating the role of homologous recombination in inducing arrested cells. In fact, transcriptional levels of TcRAD51 from the strains used in this study led us to establish a correlation between the rate of arrested parasites and the relative level of TcRAD51 mRNA. As previously shown by Alves et al. (2018), naturally-occurring hybrid strains displayed increased transcription rates of TcRAD51 when compared to non-hybrid ones, showing that the higher the transcription of TcRAD51, the higher the number of arrested cells. Altogether, these observations reinforce the role of homologous recombination process in the induction dormancy in *T. cruzi*.

In order to check, the importance of homologous recombination in *T. cruzi* dormancy, we next investigated the percentage of dormant amastigotes and infectivity of a *T. cruzi* mutant from strain CL Brener which lacks one of the two copies of TcRAD51 (CL Brener^{RAD51+/-}), which was previously characterized by our group (Gomes Passos Silva et al., 2018). CL Brener^{RAD51+/-} epimastigotes showed a reduction in the number of arrested cells without growth impair (Figures 7A,B). These observations corroborated the direct relationship between homologous recombination and dormancy in *T. cruzi*.

Interestingly, CL Brener^{RAD51+/-} trypomastigotes also exhibited reduced infectivity. Previous data from our group showed that, in Dm28c strain, the complete depletion of TOPO3α gene—which encodes Topo3α, an enzyme responsible for the resolution of recombination products (Capranico et al., 2017)—was similarly able to reduce parasite infection rate (unpublished data).

Altogether, our data show that the ability to enter in an arrested state is a strain-dependent phenomenon in *T. cruzi*, and that homologous recombination may play a role in this process. Additional studies are needed to better characterize the biology of the arrested cells—both epimastigotes and amastigotes—in this

organism and the function of recombination in the induction of dormancy.

DATA AVAILABILITY STATEMENT

The raw data supporting the conclusions of this article will be made available by the authors, without undue reservation, to any qualified researcher.

AUTHOR CONTRIBUTIONS

BCR conceptualized the study, carried out the formal analysis and investigation, and wrote the original draft of the article. CM conceptualized the study, carried out the formal analysis, and wrote the article. AO, AG, VS, and PH carried out the investigation and formal analysis. BMR carried out the investigation and formal analysis, and wrote the article. SP acquired funding and resources. GF and AM carried out the formal analysis, and acquired funding and resources. ET carried

out the formal analysis, acquired funding and resources, and wrote the article. SF carried out the formal analysis, wrote the methodology, and conceptualized the study. LA and CM conceptualized the study, carried out the formal analysis and investigation, wrote the article, acquired funding and resources, and wrote the methodology.

FUNDING

FAPEMIG (APQ-01419-14), CAPES, and CNPq provided financial support for this work.

ACKNOWLEDGMENTS

We are grateful to Lorraine Diniz de Carvalho Silva for technical support. Authors also thank the Program for Technological Development of Tools for Health-PDTIS-FIOCRUZ subunit RPT08L—Flow Cytometry, Carlos Chagas Institute, FIOCRUZ-PR for the use of its facilities.

REFERENCES

- Alves, C. L., Repolès, B. M., da Silva, M. S., Mendes, I. C., Marin, P. A., Aguiar, P. H. N., et al. (2018). The recombinase Rad51 plays a key role in events of genetic exchange in *Trypanosoma cruzi*. *Sci. Rep.* 8, 1–12. doi: 10.1038/s41598-018-31541-z
- Andrade, L. O., and Andrews, N. W. (2004). Lysosomal fusion is essential for the retention of *Trypanosoma cruzi* inside host cells. *J. Exp. Med.* 200, 1135–1143. doi: 10.1084/jem.20041408
- Andrade, L. O., and Andrews, N. W. (2005). Opinion: the *Trypanosoma cruzi* - host-cell interplay: location, invasion, retention. *Nat. Rev. Microbiol.* 3, 819–823. doi: 10.1038/nrmicro1249
- Andrews, N. W., Hong, K. S., Robbins, E. S., and Nussenzweig, V. (1987). Stage-specific surface antigens expressed during the morphogenesis of vertebrate forms of *Trypanosoma cruzi*. *Exp. Parasitol.* 64, 474–484. doi: 10.1016/0014-4894(87)90062-2
- Brenière, S. F., Waleckx, E., and Barnabé, C. (2016). Over six thousand *Trypanosoma cruzi* strains classified into discrete typing units (DTUs): attempt at an inventory. *PLoS Negl. Trop. Dis.* 10, 1–19. doi: 10.1371/journal.pntd.0004792
- Capranico, G., Marinello, J., and Chillemi, G. (2017). Type I DNA topoisomerases. *J. Med. Chem.* 60, 2169–2192. doi: 10.1021/acs.jmedchem.6b00966
- De Souza, W. (1999). A short review on the morphology of *Trypanosoma cruzi*: from 1909 to 1999. *Mem. Inst. Oswaldo Cruz* 94, 17–36. doi: 10.1590/S0074-02761999000700003
- Dumoulin, P. C., and Burleigh, B. A. (2018). Stress-induced proliferation and cell cycle plasticity of intracellular *Trypanosoma cruzi* amastigotes. *Mbio* 9, e00673–e00618. doi: 10.1128/mBio.00673-18
- Fernandes, M. C., and Andrews, N. W. (2012). Host cell invasion by *Trypanosoma cruzi*: a unique strategy that promotes persistence. *FEMS Microbiol. Rev.* 36, 734–747. doi: 10.1111/j.1574-6976.2012.00333.x
- Gomes Passos Silva, D., da Silva Santos, S., Nardelli, S. C., Mendes, I. C., Freire, A. C. G., Repolès, B. M., et al. (2018). The *in vivo* and *in vitro* roles of *Trypanosoma cruzi* Rad51 in the repair of DNA double strand breaks and oxidative lesions. *PLoS Negl. Trop. Dis.* 12:e0006875. doi: 10.1371/journal.pntd.0006875
- Harms, A., Maisonneuve, E., and Gerdes, K. (2016). Mechanisms of bacterial persistence during stress and antibiotic exposure. *Science* 354:aaf4268. doi: 10.1126/science.aaf4268
- Holloman, W. K. (2011). Unraveling the mechanism of BRCA2 in homologous recombination. *Nat. Struct. Mol. Biol.* 18, 748–754. doi: 10.1038/nsmb.2096
- Hull, R. N., Cherry, W. R., and Tritch, O. J. (1962). Growth characteristics of monkey kidney cell strains LLC-Mk1, LLC-Mk2, and LLC-MK2(NCTC-3196) and their utility in virus research. *J. Exp. Med.* 115, 903–918. doi: 10.1084/jem.115.5.903
- Luzyanina, T., Cupovic, J., Ludewig, B., and Bocharov, G. (2013). Mathematical models for CFSE labelled lymphocyte dynamics: asymmetry and time-lag in division. *J. Math. Biol.* 69, 1547–1583. doi: 10.1007/s00285-013-0741-z
- Lyons, A. B., Blake, S. J., and Doherty, K. V. (2013). Flow cytometric analysis of cell division by dilution of CFSE related dyes. *Curr. Protoc. Cytom.* Chapter 9:Unit 9.11. doi: 10.1002/0471142956.cy0911s64
- Lyons, A. B., and Parish, C. R. (1994). Determination of lymphocyte division by flow cytometry. *J. Immunol. Methods* 171, 131–137. doi: 10.1016/0022-1759(94)90236-4
- Markus, M. B. (2012). Dormancy in mammalian malaria. *Trends Parasitol.* 28, 39–45. doi: 10.1016/j.pt.2011.10.005
- Medeiros, M., Araújo-Jorge, T. C., Batista, W. S., Da Silva, T. M. O. A., and De Souza, A. P. (2010). *Trypanosoma cruzi* infection: do distinct populations cause intestinal motility alteration? *Parasitol. Res.* 107, 239–242. doi: 10.1007/s00436-010-1871-5
- Mony, B. M., and Matthews, K. R. (2015). Assembling the components of the quorum sensing pathway in African trypanosomes. *Mol. Microbiol.* 96, 220–232. doi: 10.1111/mmi.12949
- Naumov, G. N., MacDonald, I. C., Chambers, A. F., and Groom, A. C. (2001). Solitary cancer cells as a possible source of tumour dormancy? *Semin. Cancer Biol.* 11, 271–276. doi: 10.1006/scbi.2001.0382
- Oliveira, T. D., dos Santos, B. N., Galdino, T. S., Hasslocher-Moreno, A. M., Bastos, O. M. P., and Sousa, M. A. (2017). *Trypanosoma cruzi* i genotype among isolates from patients with chronic chagas disease followed at the evandro chagas national institute of infectious diseases (FIOCRUZ, Brazil). *Rev. Soc. Bras. Med. Trop.* 50, 35–43. doi: 10.1590/0037-8682-0406-2016
- Parish, C. R., Glidden, M. H., Quah, B. J. C., and Warren, H. S. (2009). Use of the intracellular fluorescent dye CFSE to monitor lymphocyte migration and proliferation. *Curr. Protoc. Immunol.* Chapter 4: Unit 4.9. doi: 10.1002/0471142735.im0409s84
- Ragone, P. G., Brandán, C. P., Rumi, M. M., Tomasini, N., Lauthier, J. J., Cimino, R. O., et al. (2015). Experimental evidence of biological interactions among different isolates of *Trypanosoma cruzi* from the Chaco Region. *PLoS ONE* 10:e0119866. doi: 10.1371/journal.pone.0119866
- Rassi, A. Jr., and Marin-Neto, A. (2010). Seminar Chagas disease. *Lancet* 375, 1388–1402. doi: 10.1016/S0140-6736(10)60061-X
- Regis-da-Silva, C. G., Freitas, J. M., Passos-Silva, D. G., Furtado, C., Augusto-Pinto, L., Pereira, M. T., et al. (2006). Characterization of the *Trypanosoma cruzi* Rad51 gene and its role in recombination events associated with the parasite resistance to ionizing radiation. *Mol. Biochem. Parasitol.* 149, 191–200. doi: 10.1016/j.molbiopara.2006.05.012
- Sánchez-Valdéz, F. J., Padilla, A., Wang, W., Orr, D., and Tarleton, R. L. (2018). Spontaneous dormancy protects *Trypanosoma cruzi* during extended drug exposure. *Elife* 7, 1–20. doi: 10.7554/eLife.34039

- Tomasini, N., and Diosque, P. (2015). Evolution of *Trypanosoma cruzi*: clarifying hybridisations, mitochondrial introgressions and phylogenetic relationships between major lineages. *Mem. Inst. Oswaldo Cruz* 110, 403–413. doi: 10.1590/0074-02760140401
- Tuominen-Gustafsson, H., Penttinen, M., Hytönen, J., and Viljanen, M. K. (2006). Use of CFSE staining of borreliae in studies on the interaction between borreliae and human neutrophils. *BMC Microbiol.* 6:92. doi: 10.1186/1471-2180-6-92
- Vago, A. R., Andrade, L. O., Leite, A. A., d'Ávila Reis, D., Macedo, A. M., Adad, S. J., et al. (2000). Genetic characterization of *Trypanosoma cruzi* directly from tissues of patients with chronic chagas disease: differential distribution of genetic types into diverse organs. *Am. J. Pathol.* 156, 1805–1809. doi: 10.1016/S0002-9440(10)65052-3
- WHO. (2019). *Chagas Disease (American Trypanosomiasis)*. WHO. Available online at: <https://www.who.int/chagas/en/> (accessed September 25, 2019).
- Wyatt, T. T., Wösten, H. A. B., and Dijksterhuis, J. (2013). *Fungal Spores for Dispersion in Space and Time, 1st Edn*. Utrecht: Elsevier Inc. doi: 10.1016/B978-0-12-407672-3.00002-2
- Zingales, B. (2018). *Trypanosoma cruzi* genetic diversity: something new for something known about Chagas disease manifestations, serodiagnosis and drug sensitivity. *Acta Trop.* 184, 38–52. doi: 10.1016/j.actatropica.2017.09.017
- Zingales, B., Andrade, S. G., Briones, M. R. S., Campbell, D. A., Chiari, E., Fernandes, O., et al. (2009). A new consensus for *Trypanosoma cruzi* intraspecific nomenclature: second revision meeting recommends TcI to TcVI. *Mem. Inst. Oswaldo Cruz* 104, 1051–1054. doi: 10.1590/S0074-02762009000700021
- Zingales, B., Miles, M. A., Campbell, D. A., Tibayrenc, M., Macedo, A. M., Teixeira, M. M. G., et al. (2012). The revised *Trypanosoma cruzi* subspecific nomenclature: rationale, epidemiological relevance and research applications. *Infect. Genet. Evol.* 12, 240–253. doi: 10.1016/j.meegid.2011.12.009
- Zingales, B., Pereira, M. E. S., Almeida, K. A., Umezawa, E. S., Nehme, N. S., Oliveira, R. P., et al. (1997). Biological parameters and molecular markers of clone CL brener - the reference organism of the *Trypanosoma cruzi* genome project. *Mem. Inst. Oswaldo Cruz* 92, 811–814. doi: 10.1590/S0074-02761997000600016

Conflict of Interest: The authors declare that the research was conducted in the absence of any commercial or financial relationships that could be construed as a potential conflict of interest.

Copyright © 2020 Resende, Oliveira, Gualiabens, Repolês, Santana, Hiraiwa, Pena, Franco, Macedo, Tahara, Fragoso, Andrade and Machado. This is an open-access article distributed under the terms of the Creative Commons Attribution License (CC BY). The use, distribution or reproduction in other forums is permitted, provided the original author(s) and the copyright owner(s) are credited and that the original publication in this journal is cited, in accordance with accepted academic practice. No use, distribution or reproduction is permitted which does not comply with these terms.



Structure, Properties, and Function of Glycosomes in *Trypanosoma cruzi*

Wilfredo Quiñones¹, Héctor Acosta¹, Camila Silva Gonçalves², Maria Cristina M. Motta², Melisa Gualdrón-López³ and Paul A. M. Michels^{4*}

¹ Laboratorio de Enzimología de Parásitos, Facultad de Ciencias, Universidad de Los Andes, Mérida, Venezuela, ² Laboratório de Ultraestrutura Celular Hertha Meyer, Centro de Ciências da Saúde, Instituto de Biofísica Carlos Chagas Filho, Universidade Federal Do Rio de Janeiro, Rio de Janeiro, Brazil, ³ Instituto Salud Global, Hospital Clinic-Universitat de Barcelona, and Institute for Health Sciences Trias i Pujol, Barcelona, Spain, ⁴ Centre for Immunity, Infection and Evolution and Centre for Translational and Chemical Biology, The University of Edinburgh, Edinburgh, United Kingdom

OPEN ACCESS

Edited by:

Noelia Lander,
University of Georgia, United States

Reviewed by:

Wolfgang Schliebs,
Ruhr-Universität Bochum, Germany
Julio A. Urbina,
Instituto Venezolano de
Investigaciones Científicas
(IVIC), Venezuela

*Correspondence:

Paul A. M. Michels
paul.michels@ed.ac.uk

Specialty section:

This article was submitted to
Parasite and Host,
a section of the journal
Frontiers in Cellular and Infection
Microbiology

Received: 12 October 2019

Accepted: 15 January 2020

Published: 31 January 2020

Citation:

Quiñones W, Acosta H,
Gonçalves CS, Motta MCM,
Gualdrón-López M and Michels PAM
(2020) Structure, Properties, and
Function of Glycosomes in
Trypanosoma cruzi.
Front. Cell. Infect. Microbiol. 10:25.
doi: 10.3389/fcimb.2020.00025

Glycosomes are peroxisome-related organelles that have been identified in kinetoplastids and diplomonads. The hallmark of glycosomes is their harboring of the majority of the glycolytic enzymes. Our biochemical studies and proteome analysis of *Trypanosoma cruzi* glycosomes have located, in addition to enzymes of the glycolytic pathway, enzymes of several other metabolic processes in the organelles. These analyses revealed many aspects in common with glycosomes from other trypanosomatids as well as features that seem specific for *T. cruzi*. Their enzyme content indicates that *T. cruzi* glycosomes are multifunctional organelles, involved in both several catabolic processes such as glycolysis and anabolic ones. Specifically discussed in this minireview are the cross-talk between glycosomal metabolism and metabolic processes occurring in other cell compartments, and the importance of metabolite translocation systems in the glycosomal membrane to enable the coordination between the spatially separated processes. Possible mechanisms for metabolite translocation across the membrane are suggested by proteins identified in the organelle's membrane—homologs of the ABC and MCF transporter families—and the presence of channels as inferred previously from the detection of channel-forming proteins in glycosomal membrane preparations from the related parasite *T. brucei*. Together, these data provide insight in the way in which different parts of *T. cruzi* metabolism, although uniquely distributed over different compartments, are integrated and regulated. Moreover, this information reveals opportunities for the development of drugs against Chagas disease caused by these parasites and for which currently no adequate treatment is available.

Keywords: trypanosomes, glycosomes, peroxisomes, glycolysis, metabolic networks, metabolite transport, biogenesis, drug discovery

INTRODUCTION

Like other kinetoplastids, *Trypanosoma cruzi* contains peroxisome-related organelles called glycosomes (Figures 1A–D). Peroxisomes constitute a family of organelles that are present in all superphyla of eukaryotes. Despite their diversity in protein content and size, these organelles are homologous and share important features of their biogenesis and morphology and some functions (1). Glycosomes are authentic members of this family, but characterized by containing enzymes of

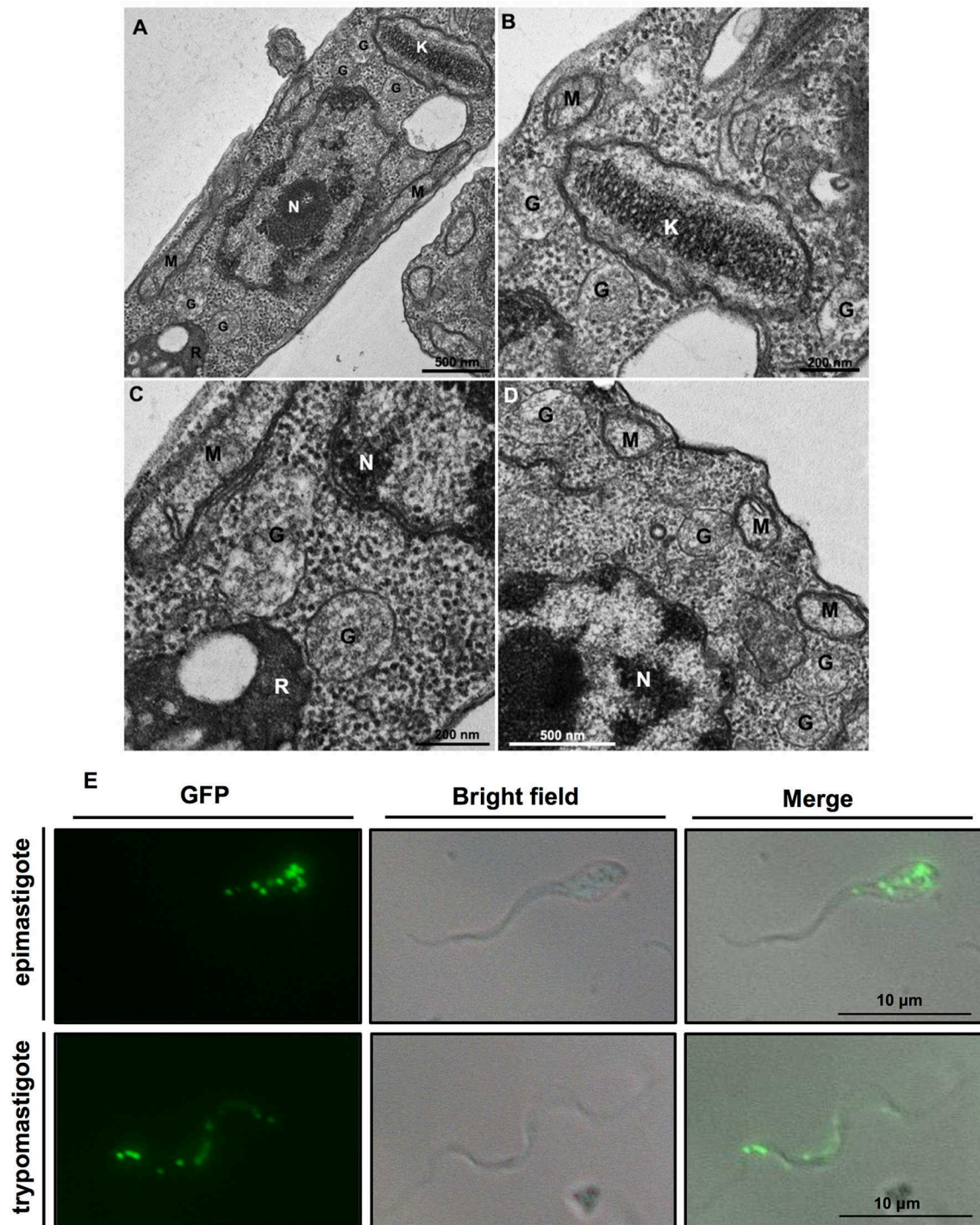


FIGURE 1 | (A–D) Ultrastructure of *Trypanosoma cruzi* epimastigote form showing glycosomes (G) and their proximity to other cell structures, especially the kinetoplast (K) and mitochondrial branches (M). Glycosomes are also seen close to reservosomes (R); N, nucleus. **(B,C)** Are insets that show areas of **(A)** with higher magnification. Cells were processed to transmission electron microscopy as follows. Protists were fixed for 1 h in 2.5% type II glutaraldehyde (Sigma, Missouri, USA) diluted in 0.1 M cacodylate buffer (pH 7.2). Then, they were washed twice in cacodylate buffer and post-fixed (1% osmium tetroxide, 0.8% potassium ferrocyanide, 5 mM calcium chloride diluted in 0.1 M cacodylate buffer) for 1 h. After fixation, samples were washed in cacodylate buffer, dehydrated in a graded series of acetone solutions (50%, 70%, 90%, and two exchanges of 100% acetone) for 10 min each step, and embedded in Polybed resin. Ultrathin sections were stained with 5% uranyl acetate for 45 min and lead citrate for 5 min before observation in a Jeol 1200ex operating at 80 kV. **(E)** *T. cruzi* contains multiple glycosomes distributed throughout the cell body as demonstrated by fluorescent puncta in transgenic epimastigotes and metacyclic trypomastigotes expressing green fluorescent protein (GFP) containing a C-terminal PTS1 (-SKL) to target it to glycosomes.

the glycolytic and gluconeogenic pathways. In some cases, such as *Trypanosoma brucei* living in the mammalian bloodstream, glycolytic enzymes may even comprise over 90% of the glycosomal protein content. Probably, the common ancestor of the Kinetoplastea and Diplonemida sequestered these enzymes in their peroxisomes (Gualdrón-López et al., 2012a; Gabaldón et al., 2016; Morales et al., 2016).

Trypanosomatids possess multiple small glycosomes. Approximately 60–65 of these organelles with an average diameter of 0.27 μm have been reported for bloodstream-form *T. brucei*, distributed throughout the cell body, often in clusters, with the number increasing to ~ 120 during parasite growth up to cell division (Oppendoes et al., 1984; Tetley and Vickerman, 1991; Hughes et al., 2017), whereas 50 glycosomes have been found in different life-cycle stages of *T. cruzi* (Soares and de Souza, 1988; Soares et al., 1989) (**Figure 1E**). Importantly, many of the glycosomal enzymes, as well as their sequestering inside the organelles have been shown to be essential for the viability of different trypanosomatids, rendering the organelles promising targets for new drugs to be developed (Galland and Michels, 2010; Barros-Alvarez et al., 2014; Dawidowski et al., 2017). In this minireview, we will highlight some recent findings about glycosomes, particularly from *T. cruzi*. More detailed information about glycosomes can be found elsewhere (Gualdrón-López et al., 2012a; Barros-Alvarez et al., 2014; Allmann and Bringaud, 2017).

PROTEOME OF *T. CRUZI* GLYCOSOMES

The proteome of *T. cruzi* glycosomes has recently been determined for the organelles isolated from cultured epimastigotes (Acosta et al., 2019). Many enzymes previously identified in glycosomes of *T. brucei* (Vertommen et al., 2008; Güther et al., 2014) and *Leishmania* spp. (Jardim et al., 2018) were also detected in the *T. cruzi* organelles: enzymes involved in glycolysis and gluconeogenesis with their auxiliary branches from phosphoenolpyruvate (PEP) comprising pyruvate phosphate dikinase (PPDK) and enzymes of the succinate production/utilization pathway, the pentose-phosphate pathway (PPP), biosynthesis of sugar-nucleotides, purines, and pyrimidines, sterols and ether-lipids and β -oxidation of fatty acids as well as enzymes involved in detoxification of oxygen radicals (**Figure 2**). Interestingly, also detected were enzymes for two possible novel routes for the reoxidation of the glycolytically produced NADH. The first route might involve a D-isomer specific 2-hydroxyacid dehydrogenase (HADH); this enzyme might catalyze the reduction of the pyruvate to lactate, whereas the enzymes for the second route are a putative aldehyde dehydrogenase (ALDH) that could reduce and decarboxylate pyruvate to acetaldehyde and an oxidoreductase (alcohol dehydrogenase, ADH) for the NADH-dependent reduction of acetaldehyde to ethanol (see also Figure 1 in Acosta et al., 2019). However, functional studies to prove these routes remain to be performed. Further identified, and characterized by our group were several enzymes previously reported to be present in *T. cruzi* but absent from *T. brucei*, such as a

glucokinase (GlcK), galactokinase (GALK) and a unique form of phosphoglycerate kinase (PAS-PGK) with at its N-terminus a PAS domain, known to possess signaling and regulatory functions (Cáceres et al., 2007; Rojas-Pirela et al., 2018; Acosta et al., 2019).

Sterol synthesis is an essential metabolic process for *T. cruzi* and *Leishmania* spp. These trypanosomatids produce a special class of these lipids, including ergosterol and other C-24 methylated sterols, which are required for growth and viability of the parasites, but are absent from mammalian host cells (Soares and de Souza, 1991; Urbina, 1997). Previously, it has been shown that various enzymes of sterol synthesis in *T. brucei* and *L. major* are present in multiple intracellular compartments, including glycosomes (Carrero-Lérida et al., 2009). Various enzymes of the pathway were also detected in our proteomic analysis of *T. cruzi* glycosomes (**Figure 2**) (Acosta et al., 2019). Because of the unique aspects of the process in these parasites, several of its enzymes are being considered as a drug target (reviewed in de Souza and Fernandes-Rodrigues, 2009; Buckner and Urbina, 2012).

INTEGRATION OF GLYCOSOMES IN OVERALL *T. CRUZI* METABOLISM

Although glycosomes contain an extensive metabolic network, for most pathways only parts are present in the organelles (**Figure 2**). For glycolysis and gluconeogenesis the majority of the enzymes are compartmentalized, whereas for other pathways, such as the pentose-phosphate metabolism, purine salvage and biosynthesis of pyrimidines and ether lipids only some enzymes were detected in the organelles (Acosta et al., 2019). Moreover, enzymes showed often a dual distribution over glycosomes and cytosol, either due to partial compartmentalization (e.g., Concepción et al., 1999) or represented by distinct isoenzymes (e.g., Barros-Alvarez et al., 2014). This spatial organization of pathways implies that glycosomal metabolism is firmly embedded in the trypanosomatid's overall metabolism and that many metabolites that serve as substrates or products of glycosomal metabolism have to cross the membrane to connect them to the cytosolic parts of the pathways or for their further metabolism in other pathways located in different cellular compartments such as cytosol or mitochondrion. A well-studied example is the last part of the glycolytic pathway where either 1,3-bisphosphoglycerate or 3-phosphoglycerate exits glycosomes to the cytosol where it is converted via PEP to pyruvate by pyruvate kinase (PYK) that is then in part metabolized by pyruvate dehydrogenase and the tricarboxylic acid cycle in the mitochondrion. Alternatively, PEP enters the glycosomes for the production of succinate or pyruvate by the auxiliary branches of the glycolytic pathway mentioned above (Acosta et al., 2004). In addition, the succinate producing branch has a cytosolic shunt involving fumarate hydratase. The distribution of fluxes through these different pathways and the concomitant translocation of metabolites across the glycosomal membrane seem to be controlled by the requirement

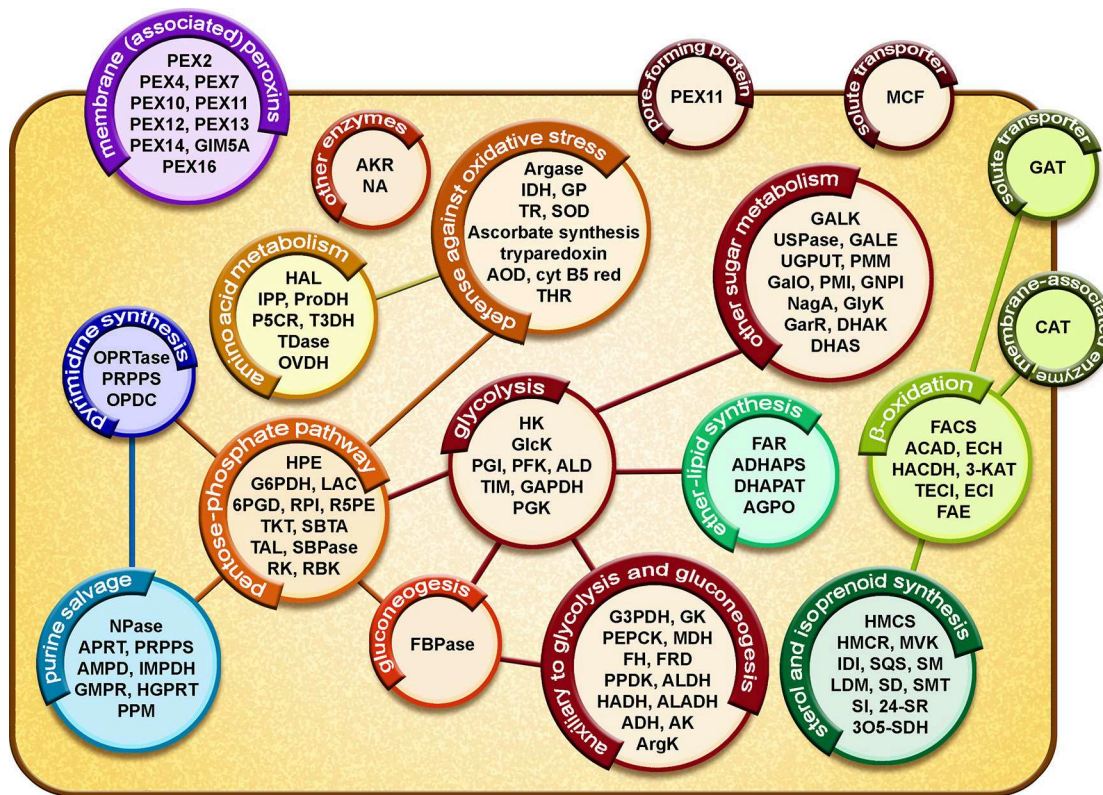


FIGURE 2 | Diagrammatic representation of the glycosomal proteome of *T. cruzi* epimastigotes. Proteins involved in metabolic pathways, solute transport and glycosome biogenesis are represented in circles. Lines represent connections between different processes by exchange of metabolites. **Glycolysis:** HXK, hexokinase; GlcK, glucokinase; PGI, phosphoglucose isomerase; PFK, phosphofructokinase; ALD, aldolase; TIM, triosephosphate isomerase; GAPDH, glyceraldehyde-3-phosphate dehydrogenase; PGK, phosphoglycerate kinase. **Auxiliary to glycolysis and gluconeogenesis:** G3PDH, glycerol-3-phosphate dehydrogenase; GK, glycerol kinase; PEPCK, phosphoenolpyruvate carboxy kinase; MDH, malate dehydrogenase; FH, fumarate hydratase; FRD, NADH-fumarate reductase; PPDH, pyruvate phosphate dikinase; ALDH, aldehyde dehydrogenase; HADH, D-isomer specific 2-hydroxyacid dehydrogenase-protein; ALADH, alanine dehydrogenase; ADH, alcohol dehydrogenase; AK, adenylate kinase; ArgK, arginine kinase. **Other sugar metabolism:** GALK, galactokinase; USPase, UDP-sugar pyrophosphorylase; GALE, UDP-galactose 4-epimerase; UGPUT, UTP-glucose-1-phosphate uridylyltransferase; PMM, phosphomannomutase-like protein; GalO, L-galactonolactone oxidase; PMI, phosphomannose isomerase; GNPI, glucosamine-6-phosphate isomerase; NagA, N-acetylglucosamine-6-phosphate deacetylase-like protein; GlyK, glycerate kinase; GarR, 2-hydroxy-3-oxopropionate reductase; DHAK, dihydroxyacetone kinase; DHAS, dihydroxyacetone synthase. **Pentose-phosphate pathway:** HPE, D-hexose-6-phosphate-1-epimerase; G6PDH, glucose-6-phosphate dehydrogenase; LAC, lactonase; 6PGD, 6-phosphogluconate dehydrogenase; RPI, ribulose-5-phosphate isomerase; R5PE, ribulose-5-phosphate epimerase; TKT, transketolase; SBTA, sedoheptulose-1,7-phosphate transaldolase; TAL, transaldolase; SBPase, sedoheptulose-1,7-bisphosphatase; RK, ribulokinase; RBK, ribokinase. **Gluconeogenesis:** FBPase, fructose-1,6-bisphosphatase. **Ether-lipid synthesis:** FAR, fatty-acyl-CoA reductase; ADHAPS, alkyl-DHAP synthase; DHAPAT, DHAP acyltransferase; AGPO, 1-alkyl G3P(NADP⁺)-oxidoreductase. **β -oxidation:** FACS, fatty-acyl CoA synthetase; ACAD, acyl-CoA dehydrogenase; ECH, enoyl-CoA hydratase; HADH, 3-hydroxyacyl-CoA dehydrogenase; 3-KAT, 3-ketoacyl-CoA thiolase; TECI, 3,2-trans-enoyl-CoA isomerase; ECI, enoyl-CoA isomerase; FAE, fatty acid elongase. **Sterol and isoprenoid synthesis:** HMCS, 3-hydroxy-3-methylglutaryl CoA synthase; HMCR, 3-hydroxy-3-methylglutaryl CoA reductase; MVK, mevalonate kinase; IDI, isopentenyl-diphosphate delta-isomerase; SQS, squalene synthase; SM, squalene monooxygenase; LDM, lanosterol 14- α -demethylase; SD, NAD(P)-dependent steroid dehydrogenase protein; SMT, sterol 24-C-methyltransferase; SI, C-8 sterol isomerase; 24-SR, sterol C-24 reductase; 3O5-SDH, 3-oxo-5- α -steroid 4-dehydrogenase. **Purine salvage:** NPase, nucleoside phosphorylase; APRT, adenine phosphoribosyltransferase; PRPPS, phosphoribosyl pyrophosphate synthetase; AMPD, AMP deaminase; IMPDH, inosine-5'-monophosphate dehydrogenase; GMPPR, guanosine monophosphate reductase; HGPRT, hypoxanthine-guanine phosphoribosyltransferase; PPM, phosphopentomutase. **Pyrimidine synthesis:** OPRTase, orotate phosphoribosyltransferase; PRPPS, phosphoribosylpyrophosphate synthetase; OPDC, orotidine-5-phosphate decarboxylase. **Amino acid metabolism:** HAL, histidine ammonia-lyase; IPP, imidazolonepropionase; ProDH, proline dehydrogenase; P5CR, pyrroline-5-carboxylate reductase; T3DH, L-threonine-3-dehydrogenase; TDase, threonine dehydratase-like, OVDH, 2-oxoisovalerate dehydrogenase alpha subunit. **Defense against oxidative stress:** Argase, arginase; IDH, isocitrate dehydrogenase; GP, glutathione peroxidase-like protein; TR, trypanothione reductase; SOD, iron superoxide dismutase; AOD, acetylornithine deacetylase-like; Cyt B5 red, Cytochrome-B5 reductase; THR, thiol-dependent reductase 1. **Other enzymes:** AKR, aldo-keto reductase; NA, nicotinamidase. **Membrane (associated) proteins:** PEX, peroxin; GIM5A, glycosomal integral membrane protein 5. **Pore-forming protein:** PEX11. **Solute transporters:** MCF, mitochondrial carrier family protein; GAT, ABC transporter. **Membrane-associated enzyme:** CAT, carnitine/choline O-acyltransferase. For a detailed assessment of the results and a presentation of glycosomal metabolic pathways (see Acosta et al., 2019).

for maintaining an intraglycosomal balance between both ATP production and consumption and NAD⁺/NADH reduction and oxidation (Acosta et al., 2004).

This integration of glycosomal pathways in the trypanosome's overall metabolism has implications for the mechanisms by which metabolites cross the glycosomal membrane and may

provide clues about the function of the organelles and the selective force that led to its evolution. These aspects will be discussed in the next sections.

SOLUTE TRANSLOCATION ACROSS THE GLYCOSOMAL MEMBRANE

Studies of metabolite translocation across the glycosomal membrane have been predominantly performed for *T. brucei*. These studies revealed a similar situation as for peroxisomes of different organisms: the existence of two groups of transporters, half-size ABC transporters and proteins of the Mitochondrial Carrier Family (MCF), as well as pore-forming proteins (reviewed in Gualdrón-López et al., 2013). Based on the situation in peroxisomes and some preliminary experiments with *T. brucei* glycosomes (Visser et al., 2007; Igoillo-Esteve et al., 2011; Antonenkov and Hiltunen, 2012; Gualdrón-López et al., 2012b), it was proposed that the ABC and MCF transporters are involved in the import of large molecules like fatty-acids and cofactors (ATP, NAD⁺, etc.) into glycosomes, while smaller molecules, with an estimated Mr of approximately 400 Da, such as glycolytic intermediates and inorganic ions pass through pores (Gualdrón-López et al., 2013). It has recently been shown in yeast that peroxin PEX11, previously identified as a factor involved in division and proliferation of peroxisomes from mammals, yeasts and plants, acts also as a protein in the formation of pores conducting solutes with Mr below 300–400 Da (Mindthoff et al., 2016). Trypanosomatid glycosomal membranes do contain PEX11 homologs. An additional pore-forming protein, Pxmp2, has been detected in mouse peroxisomes and functionally characterized. Electrophysiological experiments suggested that additional pore-forming proteins are also likely present in glycosomes but remain to be identified (Gualdrón-López et al., 2012b).

Proteomic analysis has revealed in *T. brucei* glycosomes other hypothetical membrane proteins which may be involved in translocation of other, notably large solutes, for example sugar-nucleotides, however this remains to be determined (Güther et al., 2014). The proteome of *T. cruzi* glycosomes showed a very similar repertoire of membrane-associated (candidate) transporters as in *T. brucei* (Acosta et al., 2019). Intriguingly, in glycosomes of both *T. brucei* and *T. cruzi* a putative carnitine O-acyltransferase (CAT) was found (Güther et al., 2014; Acosta et al., 2019). However, no acyl-carnitine translocase was detected that would suggest import of acyl-carnitines as alternative to that of acyl-CoAs via the ABC transporter GAT1 (Igoillo-Esteve et al., 2011) for providing acyl-CoAs for β -oxidation and ether-lipid biosynthesis. This situation seems reminiscent to mammalian and yeast peroxisomes for which it has been suggested that its CAT serves to produce acyl-carnitines from acyl-CoA derivatives that have been shortened by β -oxidation within the organelles. Carnitine esters are smaller than the corresponding CoA derivatives and may exit through the channels to the cytosol where they are converted back to free carnitine and acetyl(acyl)-CoAs by cytosolic and mitochondrial CATs (Antonenkov and Hiltunen, 2012). For a more detailed discussion about solute

translocation across glycosomal membranes and transporters, see references (Gualdrón-López et al., 2013; Acosta et al., 2019).

The energization of metabolite transport through peroxisomal and glycosomal membranes has been a matter of debate for several years. It was clearly established that fatty-acid transport is mediated by ABC transporters driven by ATP hydrolysis at the cytosolic face of the organellar membrane (Wanders and Tager, 1998; Visser et al., 2007; Igoillo-Esteve et al., 2011). In contrast, data about the possible involvement of H⁺ or ion gradients to drive translocation of other solutes were contradictory (reviewed in Wanders and Tager, 1998; Antonenkov and Hiltunen, 2006). Several previous studies, using either radioactively labeled probes, often weak acids or bases, or fluorescent compounds containing a peroxisomal-targeting sequence (PTS), or by ³¹P-NMR, claimed the existence of a pH gradient across the membrane of these organelles. However, in some cases an intraorganellar matrix with alkaline pH compared to the cytosol was reported, while in other cases it was considered acidic. Furthermore, H⁺ or ion pumps or transporters for small solutes have so far never unambiguously been identified in any peroxisomal membrane (Antonenkov and Hiltunen, 2006, 2012; Visser et al., 2007). Recently, a fluorescein-tagged peptide containing a PTS has also been used in studies with procyclic *T. brucei* (Lin et al., 2013, 2017). The authors reported a slightly acidic intraglycosomal pH that was regulated independently from the cytosolic pH in cells subjected to variable nutrient availability. Based on inhibition studies, V-ATPases and Na⁺/H⁺ exchangers were invoked. However, no specific H⁺ or ion pumps have been identified thus far in glycosomes either, except one report of a V-ATPase in the proteome of bloodstream forms but not procyclic *T. brucei* (Colasante et al., 2006). Careful interpretation of proteome data about peroxisomes/glycosomes is required because it should be realized that these organelles, despite their high buoyant density, are notoriously difficult to isolate in intact form and free of contaminants from other organelles, because of their apparent high fragility (Antonenkov and Hiltunen, 2006) and, as has become apparent in recent years, their physical interactions with other organelles such as ER and mitochondria (Fransen et al., 2017; Kim, 2017; Shai et al., 2018). To obtain a high-confidence proteome of these organelles requires specific methods such as their enrichment by epitope tagging as done by Güther et al. (2014). Moreover, as has been argued (e.g., Antonenkov and Hiltunen, 2006, 2012), it is not clear how the presence of non-selective (with regard to anions vs. cations) transmembrane channels allowing permeation of solutes and ions with Mr < ~400 Da could be compatible with the active creation of pH gradients and membrane potentials across peroxisomal/glycosomal membranes. Additionally, the notion of a specific intraglycosomal pH is not obvious. Most peroxisomes are small spherical organelles; for bloodstream-form *T. brucei* an average diameter of 0.27 μ m has been reported (Oppendoes et al., 1984; Tetley and Vickerman, 1991), with those in other trypanosomatids having comparable dimensions. This corresponds with a volume of 0.0108 μ m³, implying that, at pH 7, on average, a glycosome would contain only 0.65 free H⁺ (i.e., using the definition of pH and Avogadro's number: $10^{-7} \times 6.022 \times 10^{23} \times 0.0108 \times 10^{-15}$ free H⁺/glycosome). The

addition of a single free H^+ would result in an intraglycosomal pH drop of ~ 0.4 . It is important to realize that such calculations provide averaged values: averaged in time and space, over the total number of glycosomes in a trypanosome. Establishment of a pH is a dynamic process, involving metabolic reactions and the continuous protonation/deprotonation of many groups (of proteins, metabolites, phospholipids, etc.). One may thus wonder if the apparent response of the probes is affected by specific properties of the organelles, such as the high density of proteins with relatively high pI values—both considerably higher than in cytosol, the relatively high membrane/matrix ratio and/or the presence of inorganic polyphosphate (Negreiros et al., 2018). Because of the existence of non-selective, relatively large pores in the membrane, it seems realistic to consider that the cytosol and the matrix of the glycosomes form a continuum with regard to H^+ and inorganic ions. Nonetheless, the higher density of proteins in the glycosomal matrix compared to the cytosol, the relatively high pI values of glycosomal enzymes and the presence of pores may be responsible for the creation of a Donnan equilibrium of H^+ , inorganic ions and small solutes (metabolites) across the membrane, i.e., slightly different concentrations on both sides, responsible for a (small) membrane potential and/or pH gradient. Furthermore, as argued by Antonenkov and Hiltunen (2006), the inconsistency in results obtained in different experiments for the intraperoxisomal pH may indicate it is a dynamic parameter depending on the physiological conditions in the cell. This is in line with the notion that some pH gradient across the peroxisomal membrane may be the created—transiently or constantly—by the Donnan equilibrium. Membrane-potential or pH-sensitive probes may thus respond to such differences (Gualdrón-López et al., 2012b; discussed in Antonenkov and Hiltunen, 2012).

BIOGENESIS OF GLYCOSOMES

Glycosome biogenesis has been studied in detail in *T. brucei* and to a lesser extent in *Leishmania* spp. (reviewed in Galland and Michels, 2010; Gualdrón-López et al., 2013; Haanstra et al., 2016; Bauer and Morris, 2017). However, few studies have been devoted to this process in *T. cruzi*. The biogenesis occurs in a similar way as that of peroxisomes in other eukaryotes, involving mostly homologous proteins called peroxins or PEX proteins. Peroxins are involved in different stages of peroxisome formation, such as the posttranslational insertion of membrane proteins and import of matrix proteins. The organelles can be formed by two mechanisms: (i) budding from special parts of the endoplasmic reticulum (ER) after insertion of some (or all) peroxisomal membrane proteins (PMPs), followed by fusion with pre-existing peroxisomes and maturation involving matrix protein import, or (ii) PMPs and matrix proteins are directly sorted to existing peroxisomes. Lipids for growing and proliferating peroxisomes are provided by the vesicular transport from the ER, but may also be delivered via not yet well-studied non-vesicular routes involving contact sites between the organelles and the ER (Jansen and Van der Klei, 2019). The import of peroxisomal and glycosomal matrix proteins

can occur by translocation of fully folded proteins and even multimeric complexes (Yang et al., 2018). This process starts in the cytosol by recognition of a peroxisomal-targeting signal (PTS), in most cases either a sequence motif at the C-terminus (PTS1) or one near the N-terminus (PTS2), in newly synthesized proteins by either of two cytosolic receptors of the peroxin family. The receptor-ligand complexes dock subsequently at the peroxisomal membrane where a series of interactions between different peroxins take place, culminating in the formation of a large transient pore through which the receptor-matrix protein complexes are imported into the organelles. The receptors are cycled back to the cytosol by an ubiquitin- and ATP-dependent mechanism to perform more rounds of import (Galland and Michels, 2010; Meinecke et al., 2010; Gualdrón-López et al., 2013).

A considerable number of *T. brucei* homologs of mammalian and yeast peroxins involved in PMP insertion and matrix protein import have been identified and characterized, and shown to be involved in glycosome biogenesis (Kalel et al., 2015, 2019; Banerjee et al., 2019; and reviewed in Galland and Michels, 2010; Gualdrón-López et al., 2013). Orthologous genes have been detected in the genome of *T. cruzi* and several of the proteins in its glycosomal proteome (Acosta et al., 2019).

POLYPHOSPHATES IN GLYCOSOMES

Docampo and coworkers have shown that trypanosomes synthesize and store inorganic polyphosphate (polyP) in their acidocalcisomes. Recently, they also reported the presence of important amounts of long-chain polyP in the nucleolus and glycosomes of *T. brucei* and *T. cruzi*, where it interacts with proteins. In glycosomes it displays affinity to several enzymes of carbon metabolism (Negreiros et al., 2018). The reason for the presence of polyP in glycosomes remains to be established. Maybe it acts as a negatively charged scaffold in the creation of an assembly of the intraglycosomal enzymes which have generally a high pI and are present at high density (Misset et al., 1986). This notion is supported by the observation that glycosomal proteins remain largely packed in a complex when the membrane of purified glycosomes is dissolved by Triton-X-100 or permeabilized by digitonin; the complex is only disrupted at elevated ionic strength (Misset and Opperdoes, 1984; Misset et al., 1986). Alternatively or additionally, polyP may play a regulatory role in the enzyme activities, like PPi that has been shown to inhibit the activities of several glycosomal enzymes, such as *T. cruzi*, *L. mexicana* and one of the *T. brucei* hexokinases (HKs) (Cáceres et al., 2003; Pabón et al., 2007; Chambers et al., 2008) and *T. cruzi* PEP carboxykinase (Acosta et al., 2004), but this has not yet been tested for polyP. In addition, PPi plays a role as substrate or product in several reactions within glycosomes (Acosta et al., 2019). Interestingly, when a yeast exopolyphosphatase was expressed in *T. brucei* glycosomes, the intraglycosomal polyP levels decreased, while the glycolytic flux was also affected and the parasites became more susceptible to oxidative stress (Negreiros et al., 2018). Furthermore, the *T. brucei* genome contains genes

encoding five proteins belonging to the Nudix superfamily, comprising enzymes that hydrolyse a wide range of organic pyrophosphates. Two of them, TbNH2 and TbNH4 possess polyP exopolyphosphatase and endopolyphosphatase activities, respectively. While TbNH4 localizes to the cytosol and nucleus, TbNH2 was detected in the glycosomes (Colasante et al., 2006; Güther et al., 2014; Cordeiro et al., 2019). TbNH2 has the tripeptide –SSI at its C-terminus, a possible PTS1 (Colasante et al., 2006), suggesting that the protein plays a role in polyP homeostasis in the organelles. However, no Nudix hydrolase was found in the glycosomal proteome of *T. cruzi* epimastigotes (Acosta et al., 2019). The *T. cruzi* genome encodes a TbNH2 ortholog (60% identical, 80% similar), but with a somewhat different C-terminal sequence (–SAL or –DSI, dependent on the strain) that may not be able to sort the protein to the organelles. Therefore, further research is required to establish if Nudix proteins are involved in glycosomal polyP hydrolysis. Whether polyP serves as glycosomal storage of PPi that is known to regulate the activity of several glycosomal enzymes seems questionable if PPi may easily pass through the pores in the membrane.

GLYCOSOMAL REPROGRAMMING DURING DIFFERENTIATION OF TRYPANOSOMES

T. cruzi, like other dioxenous trypanosomatid parasites, undergoes an elaborate life cycle involving extracellular replicative epimastigotes in the triatomine digestive tube, non-replicative extracellular metacyclic and bloodstream trypomastigotes in the insect and mammalian host, respectively, and replicative amastigotes intracellularly in the cytosol of the mammalian cells. The different developmental stages differ importantly in morphology, but also in metabolism to adapt to the large nutritional conditions encountered in the different niches (Maugeri et al., 2011; Barisón et al., 2017; Avila et al., 2018; Marchese et al., 2018; Mattos et al., 2019). Since glycosomes harbor many enzymes of intermediary metabolism as well as enzymes of other metabolic processes which are differentially expressed, glycosomal metabolism has to undergo reprogramming.

Indeed, levels and activities of glycosomal enzymes differ importantly between bloodstream-form and procyclic *T. brucei* (Hart et al., 1984). As for *T. cruzi*, a comparison of the proteome of glycosomes from epimastigotes harvested from the exponential and stationary growth phase, which, respectively, rely primarily on glucose and amino acids as carbon and energy source (Barros-Alvarez et al., 2014; Barisón et al., 2017), showed only small qualitative differences in the repertoire of both intraglycosomal enzymes and proteins in the glycosomal membrane (Acosta et al., 2019). It remains to be determined to what extent quantitative and/or qualitative differences occur in the glycosomal proteome during *in vivo* differentiation between the different life-cycle stages. Another recent study, in which *T. cruzi* trypomastigotes were analyzed before and after *in vitro* interaction with extracellular matrix

(ECM), provides further information to the question to what extent quantitative and/or qualitative differences occur in the glycosomal proteome during *in vivo* differentiation between life-cycle stages (Mattos et al., 2019). Interactions with ECM components are essential prior to the invasion of mammalian host cells by *T. cruzi*. The authors reported important changes in the cellular phosphoproteome of the trypomastigotes, notably concerning proteins of carbon metabolism. A decrease of phosphorylation was observed for the glycosomal enzymes hexokinase (HK), phosphofructokinase (PFK) and PPDK, the cytosolic PYK, 6-phosphofructo-2-kinase/fructose-2-bisphosphatase (PFK2/FBPase2) and alanine transferase (ALT), and PGK that is present in both compartments, whereas phosphorylation of glycosomal fumarate reductase (FRD) was increased. These changes correlated with a decrease of activities of HK and PYK, as well as changes in the concentration of various intermediates of carbon metabolism. Together, the data indicate that phosphorylation of these enzymes, both glycosomal and cytosolic, plays an important role to control their activity and that the interaction of trypomastigotes with ECM components serves as trigger for the cells to prepare for intracellular life as amastigotes, by decreasing the glycolytic activity through dephosphorylation of the enzymes. Previously, differential phosphorylation of proteins, including glycosomal enzymes, has also been demonstrated when bloodstream-form and procyclic *T. brucei* were compared (Urbaniak et al., 2013).

The mechanism by which the life-cycle stage dependent glycosome reprogramming occurs has not yet been studied in *T. cruzi*, but has been addressed in *T. brucei* and *Leishmania* spp. (Hart et al., 1984; Mottram and Coombs, 1985; Colasante et al., 2006; Herman et al., 2008; Vertommen et al., 2008; Brennand et al., 2011; Cull et al., 2014). Data indicate that this reprogramming involves mainly degradation of organelles containing the redundant enzyme repertoire by pexophagy—i.e., the autophagy process characteristic for peroxisome degradation—while new organelles are formed with an enzyme content that is appropriate for the conditions to be encountered by the new developmental form. Glycosomal proteins are encoded by genes in the nucleus and regulation of the glycosomal enzyme content is thought to occur via mechanisms controlling both expression of genes in general and that of genes for metabolic enzymes in particular in trypanosomes, i.e., mainly post-transcriptionally (Kafková et al., 2018; Clayton, 2019). Furthermore, it is feasible that the relative abundance of different proteins in the organelles is also dependent on differential rates of their import, since the sequence motif variants of PTS exhibit different import efficiencies (Sommer et al., 1992).

It has been proposed that compartmentalization of glycolysis and other core metabolic processes in glycosomes has evolved as a mechanism by which kinetoplastid organisms can adapt, by the turnover of the organelles through pexophagy and synthesis of new ones, their metabolism efficiently to large and sudden environmental changes as they encounter during their life cycle, possibly facilitating the emergence of a parasitic life style in many of these organisms (Herman et al., 2008; Brennand et al., 2011; Gualdrón-López et al., 2012a; Gabaldón et al., 2016).

Furthermore, in *T. brucei*, glycosomes have been shown to play a role in the parasite's differentiation. The organelles contain the serine/threonine phosphatase PIP39 with a PTS1 (–SRL) at its C-terminus. This protein is part of a protein phosphatase cascade that regulates the differentiation of the non-replicating short-stumpy bloodstream forms to the proliferating procyclic forms in the tsetse fly (Szöör et al., 2010). In the short-stumpy forms in the bloodstream, PIP39 is kept inactivated and dephosphorylated in the cytosol, by interaction with tyrosine phosphatase PTP1 at a periplagellar pocket location, closely associated with a flagellar pocket ER contact site, coincident with the location of a regulator of stumpy-form transcripts, REG9.1 (Szöör et al., 2019). When the parasites are taken up in the fly, the lowered temperature at ~20°C triggers an elevated expression of PAD proteins—members of the Major Facilitator Superfamily, most related to carboxylate transporters in other organisms—in the trypanosome's plasma membrane, allowing the uptake of citrate/cis-aconitate. This leads to disruption of the PTP1-PIP39 complex, PIP39 becoming phosphorylated and active, and relocated to glycosomes, whereas PTP1 becomes dispersed to a non-glycosomal, possibly cytosolic location. Szöör et al. (2019) proposed that the location of the “stumpy regulatory nexus” (STuRN) containing the PTP1-PIP39 complex and REG9.1 is similar to that of the pre-peroxisomal vesicles budding from the ER. After disruption of the complex, PIP39 is sequestered into glycosomes newly formed at this site. STuRN will so coordinate life-cycle differentiation with reprogramming of the glycosomal metabolic machinery.

T. cruzi contains a TbPIP39 homolog (59% identical, 77% similar, and also containing the PTS1 –SRL) that was detected in the proteome of epimastigote glycosomes (Acosta et al., 2019), as well as a TbPTP1 homolog (61% identical, 75% similar) (Szöör et al., 2006). It will be interesting to determine if PIP39 and PTP1 play a similar role, upon being triggered by a species-specific signal, in life-cycle differentiation of *T. cruzi* as they do in *T. brucei*.

CONCLUSIONS

Glycosomes are authentic members of the peroxisome-organelle family, but have as distinguishable feature the sequestering of enzymes of glycolysis and other core processes of carbon metabolism. Although glycolysis is important, and in some trypanosomatid life-cycle stages essential for ATP production, there are several reasons why these organelles should not be considered as the cells “ATP factories” or as “energy-transducing organelles” comparable to mitochondria. First, ATP production and hydrolysis by all processes together—catabolic and anabolic ones—within the organelles seem to be kept in balance, net ATP production occurs outside the organelles. Contrary to mitochondria, there is no evidence for ATP delivery, in exchange for ADP, from the matrix to the cytosol. Also intraglycosomal NAD⁺ reduction and NADH oxidation are in balance; excess reducing power is transferred to the cytosol by a shuttle and from there to the mitochondrion. In contrast, mitochondrial shuttles serve to transfer electrons from cytosolic NADH to the organellar

NAD⁺, mainly for subsequent oxidative phosphorylation. Translocation of adenine nucleotides and nicotinic adenine nucleotides by transporters across the glycosomal membrane has not yet been demonstrated, but possibly occurs to provide cofactors, after their synthesis in the cytosol, to proliferating organelles, rather than to serve for balancing the stoichiometry of intraglycosomal metabolic processes. Second, there is no evidence that peroxisomal membranes are involved in energy transduction, like the inner-mitochondrial membrane derived from the cytoplasmic membrane of the ancestral endosymbiotic bacterium. Peroxisomal membranes originate mainly from the ER and incorporate proteins that form pores allowing the passage of molecules up to ~400 Da, but not the larger ATP, NAD(H) and other cofactors. It is therefore unlikely that they form a permeability barrier for H⁺ and inorganic ions. Import and efflux of metabolites occurs probably by diffusion through the pores and is dependent on their gradients, rather than transmembrane H⁺ or ion gradients, and on the control of the fluxes by the enzymes within and outside the organelles. Moreover, the notion of a separate matrix pH for small organelles as glycosomes is doubtful. Glycosomal function(s) should therefore rather be sought in other aspects such as assembly of enzymes in functional, efficient complexes and/or the coordinated turnover of major units of metabolic machinery by autophagy and biogenesis of the organelles during life-cycle differentiation (Herman et al., 2008; Brennand et al., 2011; Gualdrón-López et al., 2012a; Gabaldón et al., 2016).

An as yet unsolved question is how long-chain polyP is sequestered within glycosomes. There are no indications for its synthesis in these organelles. It is probably “piggyback” imported in association with the positively charged matrix proteins through the transient pores formed by peroxins which have the ability to transport proteins, even when folded, in multimeric form or with bound, large artificial ligands (Häusler et al., 1996; Meinecke et al., 2010; Yang et al., 2018).

Although the origin of peroxisomes and glycosomes is unrelated to that of mitochondria, it is important to realize that recent research has established contact sites, vesicular traffic, coordinated proliferation, and sharing of physiological functions between peroxisomes and mitochondria (Fransen et al., 2017; Kim, 2017; Shai et al., 2018). This aspect requires further study and has not yet been addressed for the organelles in trypanosomatids.

Finally, although glycosomes are evolutionarily related to peroxisomes, and share some functions, there are also considerable differences in enzyme content and aspects of their biogenesis. The large evolutionary distance between human and trypanosomes has resulted in large differences in the proteins involved. These differences, together with the essentiality of glycosomes and several of its metabolic processes make a variety of the trypanosomatid enzymes and peroxins promising drug targets. Indeed, selective, potent inhibitors of some glycosomal proteins have been developed that interfere with metabolic processes like sterol biosynthesis and glycosome biogenesis or function and kill the parasites

(Buckner and Urbina, 2012; Barros-Alvarez et al., 2014; Dawidowski et al., 2017).

AUTHOR CONTRIBUTIONS

The experiments to create **Figures 1A–D** were performed by CG and MM, those for **Figure 1E** by MG-L, HA, and WQ made **Figure 2**. Each of the authors contributed to the design and preparation of the manuscript, and approved it for publication.

REFERENCES

- Acosta, H., Burchmore, R., Naula, C., Gualdrón-López, M., Quintero-Troconis, E., Cáceres, A. J., et al. (2019). Proteomic analysis of glycosomes from *Trypanosoma cruzi* epimastigotes. *Mol. Biochem. Parasitol.* 229, 62–74. doi: 10.1016/j.molbiopara.2019.02.008
- Acosta, H., Dubourdieu, M., Quiñones, W., Cáceres, A., Bringaud, F., and Concepción, J. L. (2004). Pyruvate phosphate dikinase and pyrophosphate metabolism in the glycosome of *Trypanosoma cruzi* epimastigotes. *Comp. Biochem. Physiol. B Biochem. Mol. Biol.* 138, 347–356. doi: 10.1016/j.cbpc.2004.04.017
- Allmann, S., and Bringaud, F. (2017). Glycosomes: a comprehensive view of their metabolic roles in *T. brucei*. *Int. J. Biochem. Cell Biol.* 85, 85–90. doi: 10.1016/j.biocel.2017.01.015
- Antonov, V. D., and Hiltunen, J. K. (2006). Peroxisomal membrane permeability and solute transfer. *Biochim. Biophys. Acta* 1763, 1697–1706. doi: 10.1016/j.bbamcr.2006.08.044
- Antonov, V. D., and Hiltunen, J. K. (2012). Transfer of metabolites across the peroxisomal membrane. *Biochim. Biophys. Acta* 1822, 1374–1386. doi: 10.1016/j.bbadi.2011.12.011
- Avila, C. C., Mule, S. N., Rosa-Fernandes, L., Viner, R., Barisón, M. J., Costa-Martins, A. G., et al. (2018). Proteome-wide analysis of *Trypanosoma cruzi* exponential and stationary growth phases reveals a subcellular compartment-specific regulation. *Genes* 9:E413. doi: 10.3390/genes9080413
- Banerjee, H., Knoblauch, B., and Rachubinski, R. A. (2019). The early-acting glycosome biogenic protein Pex3 is essential for trypanosome viability. *Life Sci. Alliance* 2:e201900421. doi: 10.26508/lsa.201900421
- Barisón, M. J., Rapado, L. N., Merino, E. F., Furusho, P. R., Mantilla, B. S., Marchese, L., et al. (2017). Metabolomic profiling reveals a finely tuned, starvation-induced metabolic switch in *Trypanosoma cruzi* epimastigotes. *J. Biol. Chem.* 292, 8964–8977. doi: 10.1074/jbc.M117.778522
- Barros-Alvarez, X., Cáceres, A. J., Michels, P. A., Concepción, J. L., and Quiñones, W. (2014). The phosphoglycerate kinase isoenzymes have distinct roles in the regulation of carbohydrate metabolism in *Trypanosoma cruzi*. *Exp. Parasitol.* 143, 39–47. doi: 10.1016/j.exppara.2014.05.010
- Barros-Alvarez, X., Gualdrón-López, M., Acosta, H., Cáceres, A. J., Graminha, M. A., Michels, P. A., et al. (2014). Glycosomal targets for anti-trypanosomatid drug discovery. *Curr. Med. Chem.* 21, 1679–1706. doi: 10.2174/09298673113209990139
- Bauer, S., and Morris, M. T. (2017). Glycosome biogenesis in trypanosomes and the *de novo* dilemma. *PLoS Negl. Trop. Dis.* 11:e0005333. doi: 10.1371/journal.pntd.0005333
- Brennan, A., Gualdrón-López, M., Coppens, I., Rigden, D. J., Ginger, M. L., and Michels, P. A. (2011). Autophagy in parasitic protists: unique features and drug targets. *Mol. Biochem. Parasitol.* 177, 83–99. doi: 10.1016/j.molbiopara.2011.02.003
- Buckner, F. S., and Urbina, J. A. (2012). Recent developments in sterol 14-demethylase inhibitors for chagas disease. *Int. J. Parasitol. Drugs Drug Resist.* 2, 236–242. doi: 10.1016/j.ijpdr.2011.12.002
- Cáceres, A. J., Portillo, R., Acosta, H., Rosales, D., Quiñones, W., Avilán, L., et al. (2003). Molecular and biochemical characterization of hexokinase from *Trypanosoma cruzi*. *Mol. Biochem. Parasitol.* 126, 251–262. doi: 10.1016/S0166-6851(02)00294-3

FUNDING

The research by WQ and HA was financially supported by Fondo Nacional de Ciencia, Tecnología Innovación (FONACIT) in Project MC-2007001425, that of MM by FAPERJ and CNPq. MG-L is a postdoctoral fellow supported by the Plan Estratégico de Investigación e Innovación en Salud (PERIS, SLT002/16/00179) of the Generalitat de Catalunya, Spain.

- Cáceres, A. J., Quiñones, W., Gualdrón, M., Cordeiro, A., Avilán, L., Michels, P. A., et al. (2007). Molecular and biochemical characterization of novel glucokinases from *Trypanosoma cruzi* and *Leishmania* spp. *Mol. Biochem. Parasitol.* 156, 235–245. doi: 10.1016/j.molbiopara.2007.08.007
- Carrero-Lérida, J., Pérez-Moreno, G., Castillo-Acosta, V. M., Ruiz-Pérez, L. M., and González-Pacanowska, D. (2009). Intracellular location of the early steps of the isoprenoid biosynthetic pathway in the trypanosomatids *Leishmania major* and *Trypanosoma brucei*. *Int. J. Parasitol.* 39, 307–314. doi: 10.1016/j.ijpara.2008.08.012
- Chambers, J. W., Kearns, M. T., Morris, M. T., and Morris, J. C. (2008). Assembly of heterohexameric trypanosome hexokinases reveals that hexokinase 2 is a regulable enzyme. *J. Biol. Chem.* 283, 14963–14970. doi: 10.1074/jbc.M802124200
- Clayton, C. (2019). Regulation of gene expression in trypanosomatids: living with polycistronic transcription. *Open Biol.* 9:190072. doi: 10.1098/rsob.190072
- Colasante, C., Ellis, M., Ruppert, T., and Voncken, F. (2006). Comparative proteomics of glycosomes from bloodstream form and procyclic culture form *Trypanosoma brucei brucei*. *Proteomics* 6, 3275–3293. doi: 10.1002/pmic.200500668
- Concepción, J. L., Chataing, B., and Dubourdieu, M. (1999). Purification and properties of phosphoglucose isomerases of *Trypanosoma cruzi*. *Comp. Biochem. Physiol. B Biochem. Mol. Biol.* 122, 211–222. doi: 10.1016/S0305-0491(99)00002-4
- Cordeiro, C. D., Ahmed, M. A., Windle, B., and Docampo, R. (2019). NUDIX hydrolases with inorganic polyphosphate exo- and endopolyphosphatase activities in the glycosome, cytosol and nucleus of *Trypanosoma brucei*. *Biosci. Rep.* 39:BSR20190894. doi: 10.1042/BSR20190894
- Cull, B., Prado Godinho, J. L., Fernandes Rodrigues, J. C., Frank, B., Schurigt, U., Williams, R. A., et al. (2014). Glycosome turnover in *Leishmania major* is mediated by autophagy. *Autophagy* 10, 2143–2157. doi: 10.4161/auto.36438
- Dawidowski, M., Emmanouilidis, L., Kalel, V. C., Tripsianes, K., Schorpp, K., Hadian, K., et al. (2017). Inhibitors of PEX14 disrupt protein import into glycosomes and kill *Trypanosoma* parasites. *Science* 355, 1416–1420. doi: 10.1126/science.aal1807
- de Souza, W., and Fernandes-Rodrigues, J. C. (2009). Sterol biosynthesis pathway as target for anti-trypanosomatid drugs. *Interdiscip. Perspect. Infect. Dis.* 2009:642502. doi: 10.1155/2009/642502
- Fransen, M., Lismont, C., and Walton, P. (2017). The peroxisome-mitochondria connection: how and why? *Int. J. Mol. Sci.* 18:1126. doi: 10.3390/ijms18061126
- Gabalón, T., Ginger, M. L., and Michels, P. A. (2016). Peroxisomes in parasitic protists. *Mol. Biochem. Parasitol.* 209, 35–45. doi: 10.1016/j.molbiopara.2016.02.005
- Galland, N., and Michels, P. A. (2010). Comparison of the peroxisomal matrix protein import system of different organisms. exploration of possibilities for developing inhibitors of the import system of trypanosomatids for anti-parasite chemotherapy. *Eur. J. Cell Biol.* 89, 621–637. doi: 10.1016/j.ejcb.2010.04.001
- Gualdrón-López, M., Brennan, A., Avilán, L., and Michels, P. A. (2013). Translocation of solutes and proteins across the glycosomal membrane of trypanosomes; possibilities and limitations for targeting with trypanocidal drugs. *Parasitology* 140, 1–20. doi: 10.1017/S0031182012001278
- Gualdrón-López, M., Brennan, A., Hannaert, V., Quiñones, W., Cáceres, A. J., Bringaud, F., et al. (2012a). When, how and why glycolysis became compartmentalised in the Kinetoplast: a new look at an ancient organelle. *Int. J. Parasitol.* 42, 1–20. doi: 10.1016/j.ijpara.2011.10.007

- Gualdrón-López, M., Vapola, M. H., Miinalainen, I. J., Hiltunen, J. K., Michels, P. A., and Antonenkov, V. D. (2012b). Channel-forming activities in the glycosomal fraction from the bloodstream form of *Trypanosoma brucei*. *PLoS ONE* 7:e34530. doi: 10.1371/journal.pone.0034530
- Güther, M. L., Urbaniak, M. D., Tavendale, A., Prescott, A., and Ferguson, M. A. (2014). High-confidence glycosome proteome for procyclic form *Trypanosoma brucei* by epitope-tag organelle enrichment and SILAC proteomics. *J. Proteome Res.* 13, 2796–2806. doi: 10.1021/pr401209w
- Haanstra, J. R., González-Marciano, E. B., Gualdrón-López, M., and Michels, P. A. (2016). Biogenesis, maintenance and dynamics of glycosomes in trypanosomatid parasites. *Biochim. Biophys. Acta* 1863, 1038–1048. doi: 10.1016/j.bbamcr.2015.09.015
- Hart, D. T., Misset, O., Edwards, S. W., and Opperdoes, F. R. (1984). A comparison of the glycosomes (microbodies) isolated from *Trypanosoma brucei* bloodstream form and cultured procyclic trypomastigotes. *Mol. Biochem. Parasitol.* 12, 25–35. doi: 10.1016/0166-6851(84)90041-0
- Häusler, T., Stierhof, Y. D., Wirtz, E., and Clayton, C. (1996). Import of a DHFR hybrid protein into glycosomes *in vivo* is not inhibited by the folate-analogue aminopterin. *J. Cell Biol.* 132, 311–324. doi: 10.1083/jcb.132.3.311
- Herman, M., Pérez-Morga, D., Schtickzelle, N., and Michels, P. A. (2008). Turnover of glycosomes during life-cycle differentiation of *Trypanosoma brucei*. *Autophagy* 4, 294–308. doi: 10.4161/auto.5443
- Hughes, L., Borrett, S., Towers, K., Starborg, T., and Vaughan, S. (2017). Patterns of organelle ontogeny through a cell cycle revealed by whole-cell reconstructions using 3D electron microscopy. *J. Cell Sci.* 130, 637–647. doi: 10.1242/jcs.198887
- Igoillo-Esteve, M., Mazet, M., Deumer, G., Wallemacq, P., and Michels, P. A. (2011). Glycosomal ABC transporters of *Trypanosoma brucei*: characterisation of their expression, topology and substrate specificity. *Int. J. Parasitol.* 41, 429–438. doi: 10.1016/j.ijpara.2010.11.002
- Jansen, R. L. M., and Van der Klei, I. J. (2019). The peroxisome biogenesis factors Pex3 and Pex19: multitasking proteins with disputed functions. *FEBS Lett.* 593, 457–474. doi: 10.1002/1873-3468.13340
- Jardim, A., Hardie, D. B., Boitz, J., and Borchers, C. H. (2018). Proteomic profiling of *Leishmania donovani* promastigote subcellular organelles. *J. Proteome Res.* 17, 1194–1215. doi: 10.1021/acs.jproteome.7b00817
- Kafková, L., Tu, C., Pazzo, K. L., Smith, K. P., Debler, E. W., Paul, K. S., et al. (2018). *Trypanosoma brucei* PRMT1 is a nucleic acid binding protein with a role in energy metabolism and the starvation stress response. *MBio* 9:e02430-18. doi: 10.1128/mBio.02430-18
- Kalel, V. C., Li, M., Gaussmann, S., Delhommel, F., Schäfer, A. B., Tippler, B., et al. (2019). Evolutionary divergent PEX3 is essential for glycosome biogenesis and survival of trypanosomatid parasites. *Biochim. Biophys. Acta Mol. Cell Res.* 1866:118520. doi: 10.1016/j.bbamcr.2019.07.015
- Kalel, V. C., Schliebs, W., and Erdmann, R. (2015). Identification and functional characterization of *Trypanosoma brucei* peroxin 16. *Biochim. Biophys. Acta* 1853, 2326–2337. doi: 10.1016/j.bbamcr.2015.05.024
- Kim, P. (2017). Peroxisome biogenesis: a union between two organelles. *Curr. Biol.* 27, R271–R274. doi: 10.1016/j.cub.2017.02.052
- Lin, S., Morris, M. T., Ackroyd, P. C., Morris, J. C., and Christensen, K. A. (2013). Peptide-targeted delivery of a pH sensor for quantitative measurements of intraglycosomal pH in live *Trypanosoma brucei*. *Biochemistry* 52, 3629–3637. doi: 10.1021/bi400029m
- Lin, S., Voyton, C., Morris, M. T., Ackroyd, P. C., Morris, J. C., and Christensen, K. A. (2017). pH regulation in glycosomes of procyclic form *Trypanosoma brucei*. *J. Biol. Chem.* 292, 7795–7805. doi: 10.1074/jbc.M117.784173
- Marchese, L., Nascimento, J. F., Damasceno, F. S., Bringaud, F., Michels, P. A. M., and Silber, A. M. (2018). The uptake and metabolism of amino acids and their unique role in the biology of pathogenic trypanosomatids. *Pathogens* 7:E36. doi: 10.3390/pathogens7020036
- Mattos, E. C., Canuto, G., Manchola, N. C., Magalhães, R. D. M., Crozier, T. W. M., Lamont, D. J., et al. (2019). Reprogramming of *Trypanosoma cruzi* metabolism triggered by parasite interaction with the host cell extracellular matrix. *PLoS Negl. Trop. Dis.* 13:e0007103. doi: 10.1371/journal.pntd.0007103
- Maugeri, D. A., Cannata, J. J., and Cazzulo, J. J. (2011). Glucose metabolism in *Trypanosoma cruzi*. *Essays Biochem.* 51, 15–30. doi: 10.1042/bse0510015
- Meinecke, M., Cizmowski, C., Schliebs, W., Krüger, V., Beck, S., Wagner, R., et al. (2010). The peroxisomal importomer constitutes a large and highly dynamic pore. *Nat. Cell Biol.* 12, 273–277. doi: 10.1038/ncb2027
- Mindthoff, S., Grunau, S., Steinfort, L. L., Girzalsky, W., Hiltunen, J. K., Erdmann, R., et al. (2016). Peroxisomal Pex11 is a pore-forming protein homologous to TRPM channels. *Biochim. Biophys. Acta* 1863, 271–283. doi: 10.1016/j.bbamcr.2015.11.013
- Misset, O., Bos, O. J., and Opperdoes, F. R. (1986). Glycolytic enzymes of *Trypanosoma brucei*. simultaneous purification, intraglycosomal concentrations and physical properties. *Eur. J. Biochem.* 157, 441–453. doi: 10.1111/j.1432-1033.1986.tb09687.x
- Misset, O., and Opperdoes, F. R. (1984). Simultaneous purification of hexokinase, class-I fructose-bisphosphate aldolase, triosephosphate isomerase and phosphoglycerate kinase from *Trypanosoma brucei*. *Eur. J. Biochem.* 144, 475–483. doi: 10.1111/j.1432-1033.1984.tb08490.x
- Morales, J., Hashimoto, M., Williams, T. A., Hirawake-Mogi, H., Makiuchi, T., Tsubouchi, A., et al. (2016). Differential remodelling of peroxisome function underpins the environmental and metabolic adaptability of diplomonads and kinetoplastids. *Proc. Biol. Sci.* 283:20160520. doi: 10.1098/rspb.2016.0520
- Mottram, J. C., and Coombs, G. H. (1985). *Leishmania mexicana*: subcellular distribution of enzymes in amastigotes and promastigotes. *Exp. Parasitol.* 59, 265–274. doi: 10.1016/0014-4894(85)90081-5
- Negreiros, R. S., Lander, N., Huang, G., Cordeiro, C. D., Smith, S. A., Morrissey, J. H., et al. (2018). Inorganic polyphosphate interacts with nucleolar and glycosomal proteins in trypanosomatids. *Mol. Microbiol.* 110, 973–994. doi: 10.1111/mmi.14131
- Opperdoes, F. R., Baudhuin, P., Coppens, I., De Roe, C., Edwards, S. W., Weijers, P. J., et al. (1984). Purification, morphometric analysis, and characterization of the glycosomes (microbodies) of the protozoan hemoflagellate *Trypanosoma brucei*. *J. Cell Biol.* 98, 1178–1184. doi: 10.1083/jcb.98.4.1178
- Pabón, M. A., Cáceres, A. J., Gualdrón, M., Quiñones, W., Avilán, L., and Concepción, J. L. (2007). Purification and characterization of hexokinase from *Leishmania mexicana*. *Parasitol. Res.* 100, 803–810. doi: 10.1007/s00436-006-0351-4
- Rojas-Pirela, M., Rigden, D. J., Michels, P. A., Cáceres, A. J., Concepción, J. L., and Quiñones, W. (2018). Structure and function of Per-ARNT-Sim domains and their possible role in the life-cycle biology of *Trypanosoma cruzi*. *Mol. Biochem. Parasitol.* 219, 52–66. doi: 10.1016/j.molbiopara.2017.11.002
- Shai, N., Yifrach, E., Van Roermund, C. W. T., Cohen, N., Bibi, C., IJlst, L., et al. (2018). Systematic mapping of contact sites reveals tethers and a function for the peroxisome-mitochondria contact. *Nat. Commun.* 9:1761. doi: 10.1038/s41467-018-03957-8
- Soares, M. J., and de Souza, W. (1991). Endocytosis of gold-labeled proteins and LDL by *Trypanosoma cruzi*. *Parasitol. Res.* 77, 461–468. doi: 10.1007/BF00928410
- Soares, M. J., and de Souza, W. (1988). Cytoplasmic organelles of trypanosomatids: a cytochemical and stereological study. *J. Submicrosc. Cytol. Pathol.* 20, 349–361.
- Soares, M. J., Souto-Pradón, T., Bonaldo, M. C., Goldenberg, S., and de Souza, W. (1989). A stereological study of the differentiation process in *Trypanosoma cruzi*. *Parasitol. Res.* 75, 522–527. doi: 10.1007/BF00931160
- Sommer, J. M., Cheng, Q. L., Keller, G. A., and Wang, C. C. (1992). *In vivo* import of firefly luciferase into the glycosomes of *Trypanosoma brucei* and mutational analysis of the C-terminal targeting signal. *Mol. Biol. Cell* 3, 749–759. doi: 10.1091/mbc.3.7.749
- Szőör, B., Ruberto, I., Burchmore, R., and Matthews, K. R. (2010). A novel phosphatase cascade regulates differentiation in *Trypanosoma brucei* via a glycosomal signalling pathway. *Genes Dev.* 24, 1306–1316. doi: 10.1101/gad.570310
- Szőör, B., Simon, D. V., Rojas, F., Young, J., Robinson, D. R., Krüger, T., et al. (2019). Positional dynamics and glycosomal recruitment of developmental regulators during trypanosome differentiation. *MBio* 10:e00875-19. doi: 10.1128/mBio.00875-19
- Szőör, B., Wilson, J., McElhinney, H., Taberner, L., and Matthews, K. R. (2006). Protein tyrosine phosphatase TbPTP1: a molecular switch controlling life cycle differentiation in trypanosomes. *J. Cell Biol.* 175, 293–303. doi: 10.1083/jcb.200605090
- Tetley, L., and Vickerman, K. (1991). The glycosomes of trypanosomes: number and distribution as revealed by electron spectroscopic imaging and 3-D reconstruction. *J. Microsc.* 162, 83–90. doi: 10.1111/j.1365-2818.1991.tb03118.x

- Urbaniak, M. D., Martin, D. M., and Ferguson, M. A. (2013). Global quantitative SILAC phosphoproteomics reveals differential phosphorylation is widespread between the procyclic and bloodstream form lifecycle stages of *Trypanosoma brucei*. *J. Proteome Res.* 12, 2233–2244. doi: 10.1021/pr400086y
- Urbina, J. A. (1997). Lipid biosynthesis pathways as chemotherapeutic targets in kinetoplastid parasites. *Parasitology* 114 (Suppl. 1), S91–S99. doi: 10.1017/S0031182097001194
- Vertommen, D., Van Roy, J., Szikora, J. P., Rider, M. H., Michels, P. A., and Oppendoes, F. R. (2008). Differential expression of glycosomal and mitochondrial proteins in the two major life-cycle stages of *Trypanosoma brucei*. *Mol. Biochem. Parasitol.* 158, 189–201. doi: 10.1016/j.molbiopara.2007.12.008
- Visser, W. F., Van Roermund, C. W., IJlst, L., Waterham, H. R., and Wanders, R. J. (2007). Metabolite transport across the peroxisomal membrane. *Biochem. J.* 401, 365–375. doi: 10.1042/BJ20061352
- Wanders, R. J., and Tager, J. M. (1998). Lipid metabolism in peroxisomes in relation to human disease. *Mol. Aspects Med.* 19, 69–154. doi: 10.1016/S0098-2997(98)00003-X
- Yang, J., Pieuchot, L., and Jedd, G. (2018). Artificial import substrates reveal an omnivorous peroxisomal importomer. *Traffic* 19, 786–797. doi: 10.1111/tra.12607

Conflict of Interest: The authors declare that the research was conducted in the absence of any commercial or financial relationships that could be construed as a potential conflict of interest.

Copyright © 2020 Quiñones, Acosta, Gonçalves, Motta, Gualdrón-López and Michels. This is an open-access article distributed under the terms of the Creative Commons Attribution License (CC BY). The use, distribution or reproduction in other forums is permitted, provided the original author(s) and the copyright owner(s) are credited and that the original publication in this journal is cited, in accordance with accepted academic practice. No use, distribution or reproduction is permitted which does not comply with these terms.



Landmarks of the Knowledge and *Trypanosoma cruzi* Biology in the Wild Environment

Ana Maria Jansen*, Samanta Cristina das Chagas Xavier and André Luiz R. Roque

Oswaldo Cruz Institute, Oswaldo Cruz Foundation, Rio de Janeiro, Brazil

OPEN ACCESS

Edited by:

Nobuko Yoshida,
Federal University of São Paulo, Brazil

Reviewed by:

Celio Geraldo Freire-de-Lima,
Federal University of Rio de Janeiro, Brazil
Aldo Solari Illescas,
University of Chile, Chile

*Correspondence:

Ana Maria Jansen
anamariajansen2@gmail.com

Specialty section:

This article was submitted to
Parasite and Host,
a section of the journal
Frontiers in Cellular and Infection
Microbiology

Received: 07 November 2019

Accepted: 10 January 2020

Published: 06 February 2020

Citation:

Jansen AM, Xavier SCC and Roque ALR (2020) Landmarks of the Knowledge and *Trypanosoma cruzi* Biology in the Wild Environment. *Front. Cell. Infect. Microbiol.* 10:10. doi: 10.3389/fcimb.2020.00010

Trypanosomatids are ancient parasitic eukaryotes that still maintain prokaryotic characteristics. *Trypanosoma cruzi*, a primarily wild mammal parasite, infected humans already long before European colonization of the Americas. *T. cruzi* heterogeneity remains an unsolved question, and until now, it has still not been possible to associate *T. cruzi* genotypes with any biological or epidemiological feature. One of the first biochemical attempts to cluster the *T. cruzi* subpopulations recognized three main subpopulations (zymodemes) that have been associated with the transmission cycles in the wild (Z1; Z3) and in the domestic environment (Z2). The description of wild mammal species harboring Z2 two decades later challenged this assemblage attempt. Currently, the genotypes of *T. cruzi* are assembled in seven discrete typing units (DTUs). The biology of *T. cruzi* still shows novelties such as the description of epimastigotes multiplying and differentiating to metacyclic trypomastigotes in the lumen of the scent glands of *Didelphis* spp. and the capacity of the true meiosis in parallel to clonal reproduction. The study of the transmission cycle among wild animals has broken paradigms and raised new questions: (i) the interaction of the *T. cruzi* DTUs with each of its mammalian host species displays peculiarities; (ii) the impact of mixed genotypes and species on the transmissibility of one or another species or on pathogenesis is still unknown; (iii) independent *T. cruzi* transmission cycles may occur in the same forest fragment; (iv) the capacity to act as a reservoir depends on the peculiarities of the host species and the parasite genotype; and (v) faunistic composition is a defining trait of the *T. cruzi* transmission cycle profile. The development of models of environmental variables that determine the spatial distribution of the elements that make up *T. cruzi* transmission by spatial analysis, followed by map algebra and networking, are the next steps toward interpreting and dealing with the new profile of Chagas disease with its many peculiarities. There is no way to solve this neglected disease once and for all if not through a multidisciplinary look that takes into account all kinds of human and animal activities in parallel to environmental variations.

Keywords: trypanosomatids, *Trypanosoma cruzi*, wild mammals, transmission cycle, reservoirs, spatial analysis

INTRODUCTION

In addition to being a successful parasite, *T. cruzi* presents a very interesting story. It was first observed by Carlos Chagas in 1909 in the digestive tract of a triatomine (*Panstrongylus megistus*) examined after his attention was drawn to insects that sucked people's blood (Chagas, 1909). Since he was in Lassance, a poor little town in the interior of Minas Gerais State, and did not have

laboratory facilities, Chagas asked his mentor and director, Oswaldo Cruz, to put infected triatomines in contact with marmosets (*Callithrix penicillata*). Three weeks later, Oswaldo Cruz observed trypomastigote forms in the blood of these animals. In contrast to what was thought by Chagas and Cruz (that the parasites were transmitted by the insects' bites), the marmosets probably became infected by the ingestion of the infected bugs, resulting in the first demonstration of the oral infection of wild mammals (Coura, 2009). Oswaldo Cruz urged Carlos Chagas to perform experimental infections in other animals soon done on mice, guinea pigs, rabbits, dogs and monkeys. In 1909, Carlos Chagas returned to Lassance, where he began to examine animals and humans. First, he identified trypomastigote forms in the blood of a cat; then, also in 1909, he detected the same trypomastigote forms in the blood of a child (Chagas, 1909). In 1912, Carlos Chagas described the presence of trypomastigotes in the blood of an armadillo and in a specimen of *Panstrongylus geniculatus* collected in the armadillo's burrow (Chagas, 1912). Chagas described the acute form of human disease in 1916 (Coura et al., 2014). Thus, a new species of *Trypanosoma*, its vector and mammalian hosts, and the human disease due to this trypanosome species were described by the same scientist, an exceptional fact in medicine. Despite having observed *T. cruzi* in one armadillo, Carlos Chagas did not link the wild and domestic cycles; moreover, the distance and lack of connectivity between the wild and domestic environments becomes very clear in the description of the armadillo as a "depository of *T. cruzi* in the external world" (Chagas, 1912). In the same manuscript, for the first time, Chagas also suggested, based on the epidemiological data available, that *Triatoma infestans* was also implicated in *T. cruzi* transmission to humans. Later, this triatomine species was recognized as the most important domiciliated vector in several countries of South America.

Trypanosoma cruzi belongs to the family Trypanosomatidae, an ancient diverging eukaryotic monophyletic group of parasites that includes monoxenic and heteroxenic species. Trypanosomes still share many molecular characteristics with both prokaryotes and eukaryotes. Very recently, the meiotic machinery of higher eukaryotes has been described in *T. cruzi*. This mechanism was very early described in *T. b. brucei* (Gibson and Bailey, 1994; Gibson et al., 2008; Peacock et al., 2014), in *Leishmania* parasites (Akopyants et al., 2009), and in *T. congolense* (Van den Broeck et al., 2018), but not in *T. b. gambiense*, which was confirmed to be completely clonal (Schwabl et al., 2019).

Trypanosomatids are considered important because some of their representatives are etiological agents of important diseases for humans and animals of economic interest. This anthropocentric view drained the main study efforts for these species, providing poor attention to some other species that were associated with insects and, in a pejorative manner, called as "lower trypanosomatids." With the awareness of the deep interdependence of environmental, human, animal and plant health, in addition to the emergence of molecular tools with higher analytical power, researchers have widened the interest of other taxa of trypanosomes and their hosts. This broader look also resulted in the awareness that the limits of parasite

host specificity may be quite blurred. Thus, since 1980, cases of monoxenic trypanosomatids infecting humans in mixed infections with *Leishmania* spp. have been reported. These findings increased in number until the description of a fatal human case of a visceral leishmaniasis-like disease associated with a parasite related to *Crithidia* spp. (Maruyama et al., 2019). Wild free-ranging mammals infected solely by *Crithidia mellificae* have already been described (Rangel et al., 2019). These findings, in addition to the consciousness of the multifactorial character of the parasitism phenomenon and its consequences, have broken numerous paradigms. Among them, parasites are necessarily pathogenic agents, the concept of which is a reservoir and the evolution of the parasitism phenomenon, among others. A broader view of what is parasitism is important in the study of *Trypanosoma* spp., a ubiquitous taxon that displays complex life histories.

The importance of the consideration and study of the spatial characteristics in which the encounter between these actors, parasite and host, occurs, is becoming increasingly clear. In this sense, cartographic tools have been contributing to such an extent that they can no longer be dispensed. Filling in the gaps in the knowledge of these ancient eukaryotic organisms will surely improve our understanding of the complexity of the evolutionary process of living beings in general.

In this article, we will focus on *Trypanosoma cruzi*, not only as the etiological agent of Chagas disease but also as one of the most successful parasite species. We will mention here some key points from the longtime study and debate on the subject that has lasted for over a century (Figure 1). We will also present a current state of the art of the transmission cycle of *T. cruzi* in the wild as well as questions that are still controversial and unanswered.

TRYPANOSOMA CRUZI: A PRIMARILY WILD MAMMAL PARASITE

T. cruzi infection was first described as an indoor transmitted trypanosomiasis involving humans living in poor housing and nocturnal domiciliated hematophagous bugs (*Conorhinus megistus*, now named *Panstrongylus megistus*) that lived in mudhouse walls (Chagas, 1909). In the following decades, some studies conducted especially in Brazil, Colombia, Venezuela and Costa Rica searched for *T. cruzi* in wild mammals, aiming to understand their role in the epidemiology of human disease. However, it was only during the seminal studies conducted by Mauro Pereira Barretto (from 1962 to 1981) in Brazil that this protozoan parasite started to be considered a primarily wild enzootic organism, maintained by wild mammals and triatomines (Barretto, 1967a). Nevertheless, the same author described trypanosomiasis due to *T. cruzi* as an amphixenosis that fitted very well in Pavlovsky's nidality postulate (Pavlovsky, 1967). Influenced by the studies of MP Barretto, the scientific community started to consider that the disruption of the ecological equilibrium in a wild environment could result in outbreaks of human disease. The main aspects observed by Barretto in that time (and now observed in the recent Chagas disease outbreaks) were (i) forest fragmentation, reducing areas

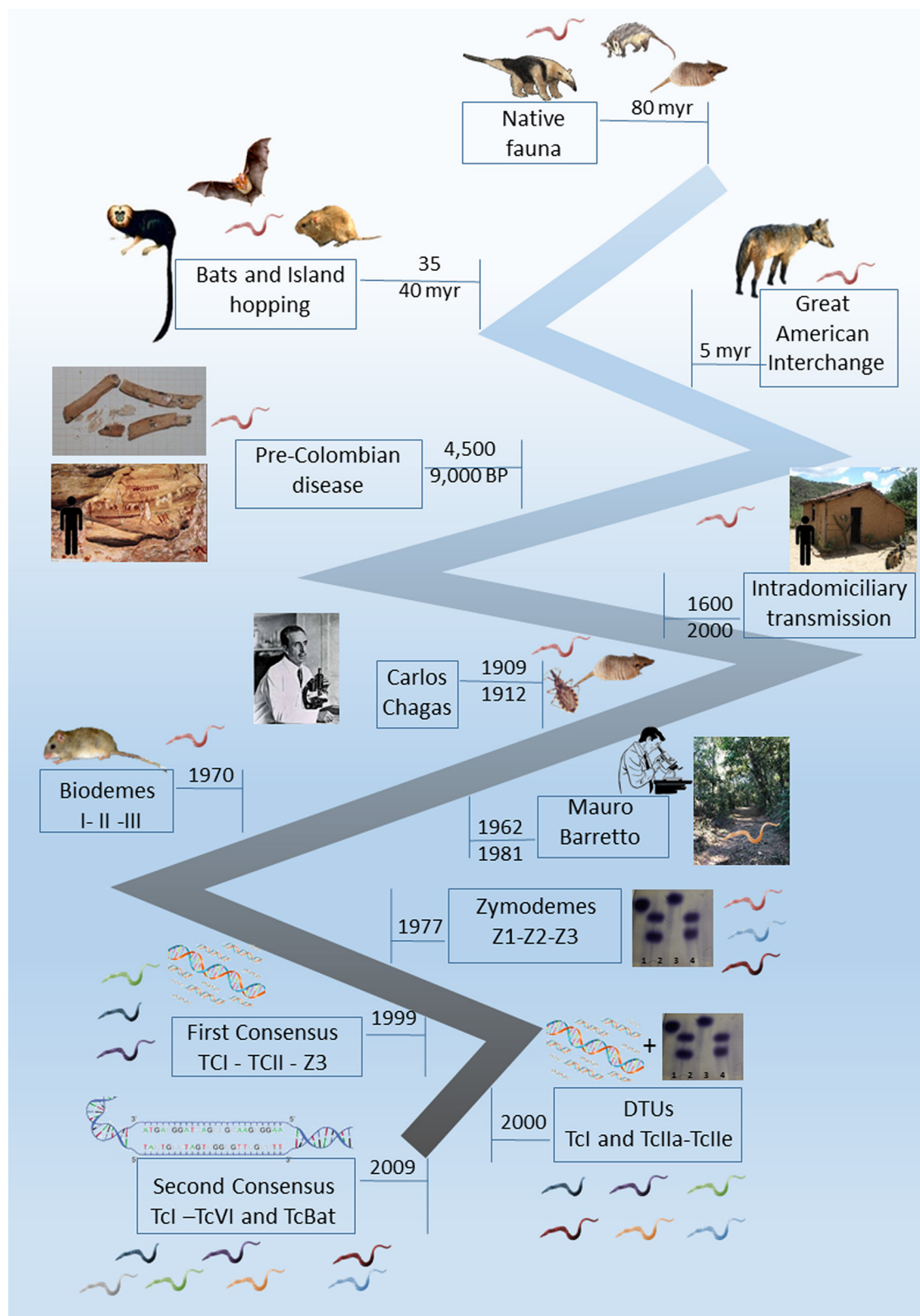


FIGURE 1 | Timeline landmarks of the knowledge of *Trypanosoma cruzi* biology.

for mammals and vectors; (ii) the displacement of host and vectors to new areas; (iii) proximity to human dwellings and their annexes; (iv) and the contact between infected vectors and humans (or human's prepared food or beverage) (Barretto, 1967b; Roque et al., 2008; Xavier et al., 2012). When Barretto finished his studies, he described more than one hundred mammal species naturally infected by *T. cruzi*, and the oral route was proposed to be the most efficient transmission via the wild. At that moment, this trypanosomiasis due to *T. cruzi* was no longer seen as a "human parasitosis" (Barretto and Ribeiro, 1979).

A very important landmark in the construction of the knowledge of this parasitosis was the discovery that humans became infected by *T. cruzi* probably since their arrival in the Americas and not just after South America's European colonization. *T. cruzi* infection was demonstrated in mummies from Chinchorro populations dated on 9,000 years BP (Aufderheide et al., 2004). Cardiac lesions compatible with the clinical outcome of chronic Chagas disease patients were also observed in mummies from the Chilean Atacama Desert (Rothhammer et al., 1985). In Brazil, the most ancient mummies found infected by this parasite are dated from 7,000 to 4,500 years BP and were derived from Central Brazil (Lima et al., 2008). In the Brazilian Northeast Region, ancient humans responsible for the rock paintings in one of the regions that display the most ancient registers of human presence (Serra da Capivara, in the Brazilian Northeast Region) were most likely exposed to infected *Triatoma brasiliensis* during the long time required to perform their paintings (Araújo et al., 2003). Accordingly, the domestication of *Cavia* sp. in the Andean Valley and the presence of wild mammals attracted to stocked grains adjacent to human dwellings were important factors for the establishment of the domiciliary populations of *T. infestans* (and consequently, the intradomiciliary transmission scenario described by Chagas) (Dias and Coura, 1997).

T. CRUZI GENOTYPES AND ITS ECOLOGY: A PHENOMENON NOT YET FULLY UNDERSTOOD

The heterogeneity of *T. cruzi* had already been observed by Carlos Chagas, who detected slim and wide blood trypomastigotes and, most likely influenced by his experience with malaria, attributed the different forms to male and female merozoites (Chagas, 1909). Later, several authors described different patterns of cell growth and differentiation in axenic cultures, demonstrating that the heterogeneity observed was not only morphological but could result in distinct success in replicating and differentiating into infective forms.

The first attempt to cluster the observed heterogeneity among *T. cruzi* subpopulations was proposed by Sonia Andrade in the 1970s and was based on the different infection patterns observed in Swiss mice experimentally infected with different *T. cruzi* strains. Three Biodemes were proposed: Biodeme I for strains that resulted in high virulence and mortality in 10–12 dpi; Biodeme II in the cases of mild virulence and mortality after only 20–25 dpi; and Biodeme III, which resulted in a slow increase

in parasitemia and no mortality in infected mice (Andrade et al., 1970; Andrade and Magalhães, 1997). This proposition, however, was time-consuming, dependent on laboratory animal availability, and isolates certainly underwent selection pressure due to the experimental infection. Brener (1977) suggested the classification of two polar types based on morphology and tissue tropism, describing an aggressive pole represented by the Y strain and a benign pole exemplified by the CL strain. The biological, immunological, drug resistance and clinical differences that were being unveiled were so impressive that it was even proposed to consider that *T. cruzi* was in fact a species complex and not a single species and that the taxon should be referred to as the "*cruzi* complex" (Coura et al., 1966).

The characterization of *T. cruzi* subpopulations by a biochemical tool was successfully proposed by Michael Miles and coauthors in 1977 based on enzyme electrophoresis (Miles et al., 1977). This proposition was certainly one of the most important landmarks in the study of *T. cruzi* biology, and the three main zymodeme groups proposed (Z1, Z2, and Z3) were the basis for the first nomenclature consensus proposed in 1999 (Anonymous, 1999). Another important zymodeme described in the Southern Cone of South America was the so-called Z2 Bolivian or Zymodeme 39 (named TcV in the current *T. cruzi* nomenclature), which is a hybrid parasite that is the result of a natural product of meiosis recombination between the parentals TcII and TcIII. This *T. cruzi* genotype was described by its heterozygous profile of the isoenzyme glucose phosphate isomerase, which gave important information long ago (Apt et al., 1987; Brenière et al., 1989). The majority of the molecular studies on *T. cruzi* that started to be conducted approximately a decade later confirmed the differentiation into the two main (and parental) groups, *T. cruzi* TcI (Z1) and TcII (Z2) (Clark and Pung, 1994; Tibayrenc, 1995; Souto et al., 1996).

Since their description, the different zymodemes were associated with different transmission cycles: Z1 and Z3 were associated with the transmission cycles in the wild and Z2 in the domestic environment. The domestic cycle of *T. cruzi* transmission was proposed to be somewhat independent from the sylvatic one, although sometimes overlapping (Miles et al., 1980; Apt et al., 1987; Zingales et al., 1998). This proposition was supported, in part, by two important features: (i) *T. cruzi* TcI (Z1) is the most ubiquitous subpopulation and, because of that, is the most frequently detected subpopulation in the wild (Fernandes et al., 1999; Noireau et al., 2009; Jansen et al., 2015); and (ii) *T. cruzi* TcII (Z2) was the subpopulation that was consistently isolated from human cases in the formerly endemic areas of Central Brazil, especially maintained by *T. infestans* in indoor transmission. This subpopulation was therefore associated with the domestic cycle of *T. cruzi* transmission and with the severe clinical conditions that occurred in 30% of the infected people (Chapman et al., 1984; Fernandes et al., 1999). It was more than two decades later, through the description of a well-established transmission cycle involving free-ranging golden lion tamarins (GLTs; *Leontopithecus rosalia*) and *T. cruzi* Z2 subpopulations (later confirmed as DTU TcII), that this association was challenged (Lisboa et al., 2000, 2006). Moreover, the infection by *T. cruzi* TcII in GLTs was followed up for more than a decade

and was demonstrated to be the most stable and expressive transmission cycle of this DTU in the wild (Lisboa et al., 2015). Since these initial findings, *T. cruzi* DTU TcII has been described in several other wild mammal species throughout Latin America, including rodents, marsupials, bats and carnivores (Jansen et al., 2015). To date, it has not been possible to unequivocally associate *T. cruzi* genotypes with any biological response variable, including the biome and environment (as first proposed) or host species (as proposed secondly).

The advances of the molecular techniques for *T. cruzi* characterization since the late 1980s, and the most diverse targets proposed, showed that *T. cruzi* heterogeneity was much higher than the biochemical studies could reveal and made it possible to study the parasite at a much higher level of detail. Soon after the first nomenclature consensus was published, six discrete phylogenetic lineages (later named discrete typing units—DTUs) were proposed (Brisse et al., 2000). The former Z1 and Z2 comprised one DTU each, Z3 was divided into 2 distinct DTUs, and the hybrid isolates were grouped into two other DTUs. This division was based on the second (and currently valid) nomenclature consensus that divided the *T. cruzi* subpopulations into 6 DTUs, named TcI to TcVI (Zingales et al., 2009). A putative seventh DTU, Tcbat, was described as a DTU associated with bats, although human infections by this DTU were already reported (Marcili et al., 2009; Guhl et al., 2014; Ramírez et al., 2014).

It is not surprising that TcI was initially associated with the sylvatic cycles because TcI is the most widespread DTU, being detected in all areas of *T. cruzi* transmission (Jansen et al., 2015). This DTU was first associated with opossums; however, while individuals from the *Didelphis* genus were most commonly infected by TcI (Fernandes et al., 1999; Jansen et al., 2015; Roman et al., 2018b), individuals from the *Philander* genus were found to be infected by both TcI and TcII at similar rates (Fernandes et al., 1999; Pinho et al., 2000; Jansen et al., 2015). *T. cruzi* TcII infection may be detected in concomitant infection with TcI in *Didelphis* individuals (Jansen et al., 2018). The proposed association among TcI, *Didelphis* sp. and the arboreal stratum (Yeo et al., 2005) did not consider that *Didelphis* spp. are scansorial and not arboreal mammals, i.e., *Didelphis* sp. may also use the terrestrial and arboreal strata. This DTU, along with DTUs III and IV, is involved in human cases in the Amazonian basin, currently the region that reported more than 90% of new cases in Brazil and severe acute phases (Monteiro W. M. et al., 2010; Monteiro et al., 2012).

The DTU TcII included *T. cruzi* subpopulations derived from patients from formerly endemic areas, where clinical symptoms of chronic Chagas disease were common and severe, and because of that, this DTU was associated with a domestic cycle of parasite transmission. Reports on TcII-infected wild mammals are less numerous in comparison to those on TcI, but TcII also presents a noteworthy host range and is widely distributed in nature (Jansen et al., 2015). TcII is the second most frequently found genotype infecting wild mammals in Brazil, including mammals of the Amazon basin region (Lima et al., 2014).

Undoubtedly a turning point, an important milestone in the discussion of genetic diversity in *T. cruzi* was the recent description of panmixia in some *T. cruzi* subpopulations (Schwabl et al., 2019). The description of this phenomenon

in some isolates of Ecuador sheds light on a decades-long debate related to the largely clonal character of the taxon. More intriguing is the description of clonal groups that may occur in sympatry with clonal groups that the authors propose to have experienced in past hybridization events. These fascinating findings largely explain the extreme diversity of *T. cruzi* and its extreme adaptability to species and tissues of its numerous vertebrate and invertebrate hosts. Additionally, the studies of Schwabl and coauthors postpone further the possibility of understanding the ecological significance of the genetic diversity of *T. cruzi* (Schwabl et al., 2019).

NOVELTIES ON *T. CRUZI* BIOLOGY SHOWN BY OPOSSUMS

Another milestone in the history of the study of *T. cruzi* biology came in 1984 with the discovery of extracellular forms of *T. cruzi* (epimastigote and trypomastigote) in *Didelphis aurita* opossum smelling glands (Deane et al., 1984a). This finding showed that opossums can act as reservoirs and vectors of *T. cruzi*.

Opossums, like many other mammals, have a pair of anal glands. These glands have a wrap that is partly made up of a striated muscle layer and a small portion of pearly looking connective tissue. When threatened or stressed, these animals expel the extremely bad smelling content of these glands as a defense mechanism. Within the scent glands, the flagellates are preferentially disposed around the glandular epithelium, an area rich in hyaluronic acid. That is, the scent glands do not constitute a reservoir within the reservoir. Interestingly, when injected directly into the scent glands, *Leptomonas* sp. and *Chirithidia* sp. are able to establish stable infections, surviving, multiplying and even eliciting a humoral immune response. Taken together, these findings led Deane and coauthors to propose scent glands as the steppingstone for the adaptation of *T. cruzi* to this mammalian host that they considered the more ancient host of *T. cruzi* (Deane et al., 1984a).

Maria Deane and her colleagues conducted a pioneering long-term study on the interaction of *T. cruzi* with the opossum *D. aurita*. These studies included experimentally infected animals born in captivity and naturally infected animals. *Didelphis* opossums are likely to be ancient *T. cruzi* hosts, and that likelihood was the authors' motivation for the studies. These studies showed that *D. aurita* displayed a very distinct infection pattern when infected by the Y strain (TcII) in comparison to the infections caused by the F strain (TcI): opossums were shown to rapidly eliminate the former from the peripheral circulation while maintaining blood-detectable parasitemias when infected by the latter. In other words, it became clear that opossums differ in their infectious potential for TcI and TcII. Moreover, these studies have shown that from an early age, approximately 50 days but still in the marsupial pouch, *D. aurita* is able to control *T. cruzi* infection (Jansen et al., 1994). This does not apply to newborns because didelphids are born still at the embryonic stage and therefore very immature. Newborn didelphids do not reject grafts, do not have individualized back paws, and their eyes and ears are sealed; therefore, they are entirely dependent on

the incubation conditions of the marsupium for their survival. Deane's findings shed light on an important aspect of *T. cruzi* biology—the peculiar character of the interaction of *T. cruzi* with its mammalian hosts. Accordingly, it was observed that *D. aurita* maintains high parasitemias by DTU TcI but not by DTU TcII in contrast to another didelphid marsupial species, *Philander opossum*, that responds with high parasitemias when inoculated with DTU TcII (Legey et al., 1999). Further studies on wild mammals have shown the complexity of *T. cruzi* transmission cycles in the natural environment. It has been seen that different *T. cruzi* DTUs can infect the same mammal and be transmitted by the same triatomine specimen. Studies of experimental *T. cruzi* infection in opossum initiated by Maria Deane were a paradigm break because they showed that strain Y, considered “aggressive,” was far from deserving of this adjective in opossum infections. High intraperitoneal Y strain inocula are in fact extremely virulent and pathogenic to mice (Andrade et al., 1970; Andrade and Magalhães, 1997). The findings of Maria Deane reinforced that virulence and pathogenicity are not exclusive attributes of the parasite and that virulence does not necessarily result in pathogenicity. Indeed, opossums maintain long-lasting high parasitemias by F (TcI strain) that are detectable by blood cultures for a long time without significant damage (Jansen et al., 1991). Additionally, golden lion tamarins (GLTs) are able to maintain natural infections by *T. cruzi* TcII without clinical biochemical or cardiological impairment (Monteiro R. V. et al., 2010; Lisboa et al., 2015).

An interesting aspect of the interaction of *T. cruzi* with opossums is the absence of congenital or neonatal transmission in *D. aurita*. The hypothesis that the absence of a placenta and the long period of breastfeeding of didelphids could result in transmission to neonates was not confirmed. Furthermore, the newly weaned puppies showed some protection against experimental infection, probably due to the antibodies passed during the long period of breastfeeding. The reproductive investment of opossums is postpartum: after a short gestational period of 13 days, neonates maintain themselves attached to the nipples. It is only at 45 days after birth that the newborns begin to try other foodstuffs, but they still return to the marsupial pouch. The total independence of the young happens approximately 100 days after birth (Jansen et al., 1994). These studies were only possible after the standardization of a serological test to diagnose *T. cruzi* infection in opossums. In nature, most infected animals do not have parasitemia detectable by fresh blood smear examination or blood culture; therefore, serological tests are important. However, this is an important bottleneck—there are simply no commercial serological tests on the market. We adapted an indirect immunofluorescence reaction by including a rabbit elicited intermediate anti-opossum IgG antibody, revealing the reaction with a commercial anti-rabbit IgG fluorescein antibody (Jansen et al., 1985). Recently, one of us (SCX) started to purify and label with fluorescein an anti-opossum IgG.

T. cruzi infection in wild mammals displays an aggregated distribution, occurs in the six biomes of Brazil (a country of continental dimensions) and involves all mammalian orders. It is worth mentioning that parasitemias are not high. Rarely

are positive fresh blood tests reported, and positive blood cultures that also demonstrate infective potential were observed in 8% of 6,587 wild mammals examined (Jansen et al., 2018). Procyonidae (*Nasua nasua*), Primates (*Leontopithecus rosalia* and *Sapajus libidinosus*), and Marsupialia (especially *Philander* spp. and *Didelphis* spp.) more frequently demonstrate positive hemocultures, i.e., infectious potential, than other taxa (Jansen et al., 2018).

The transmission of *T. cruzi* may occur between all animals of a given forest stratum or be limited to one stratum only, as observed by Fernandes et al. (1999). This implies important consequences, the first being the importance of the accuracy of the sample calculation of both species and the number of animals to be examined. Failure to take into account that, even within the same forest fragment, independent transmission cycles may be taking place will certainly result in important biases that may compromise environmental management decision-making or the determination of epidemiological risk factors for public health. To determine which animal species play the role of the reservoir, we need to examine a representative number of representative species. For example, in the southeastern Atlantic rainforest (Rio de Janeiro), golden lion tamarins are the reservoirs of *T. cruzi* and not *D. aurita*, a species that is classically defined as a *T. cruzi* reservoir (Lisboa et al., 2015).

Considering the peculiarities in the interaction of *T. cruzi* with the mammalian host species and that *T. cruzi* is able to infect hundreds of mammalian species, one can compare the enzootic scenario of transmission in the wild to the ever-changing figures of a kaleidoscope resulting from the countless arrangements of its colored components. As the faunal composition of each locality defines the enzootic scenario, assessing the risk of human infection necessarily includes considering, beyond the triatomine fauna, the mammalian hosts and reservoirs.

ARE LABORATORY *T. CRUZI* STRAINS REPRESENTATIVE OF THE NATURAL POPULATIONS?

T. cruzi is a highly diverse taxon expressed by differences in infectious competences, generation time and life strategies, as exemplified by the existence of cloned subpopulations and sexually reproducing subpopulations within the taxon (Berry et al., 2019). These characteristics make the study of this parasite very difficult because it raises the question of the representativeness of laboratory samples and raises the question of the reproducibility in the laboratory of what happens in nature. Two difficult obstacles to overcome show that there are no representative laboratory samples: the subsampling and the selective pressures inherent to laboratory maintenance methods exerted on natural populations of *T. cruzi*.

Subsampling seems very probable considering that *T. cruzi* infects hundreds of host species that are transmitted in complex life cycles, from the southern United States to southern Argentina. Representative samples of both animal species as well as of regions and even biomes are unlikely to have been collected. Clonal heterogeneity in *T. cruzi* was long ago demonstrated by

biological, biochemical, immunochemical, parasitological, and histopathological parameters by several authors (Lanar et al., 1981; Dvorak, 1984; Tibayrenc et al., 1986). More recently, molecular analysis methods showed that there is high diversity even within DTUs (Roman et al., 2018a,b).

The already classic reference strains, such as the Y, Colombiana, Esmereldo, CL, and other strains, are highly passaged strains, kept for many years in laboratories, and are therefore subjected to the selective pressures inherent to these methods and hardly represent the diversity of *T. cruzi*. The selection of *T. cruzi* strains according to the experimental protocol was observed decades ago in experimentally infected mice (Deane et al., 1984b). The observed 10-fold difference in the rate of growth of epimastigotes (Dvorak, 1984) shows that many biological clones are lost by “*in vivo*” or “*in vitro*” passages. Clonal selection certainly also occurs in the natural environment and is directed by the host species (mammal or triatomine) infection route and other factors. Considering that each species (and even individual) interacts differently with the different subpopulations of *T. cruzi*, it is possible to conclude that the possibilities of combinations are endless.

Given that the true diversity of *T. cruzi* is very likely underestimated, attempts to associate parasite genotypes with host species or environment-related variables should be proposed with caution. Finally, when faced with such a complex model, it is prudent not to dogmatize and to always be open to reviewing concepts.

HUMAN INFECTION AND DISEASE AFTER *T. INFESTANS* CONTROL

Although Barretto has drawn attention to the correlation between environmental disruption and the onset of human disease, this knowledge has not been incorporated into the routine of preventive actions. Nor could it be incorporated because the transmission of *T. cruzi* to humans was basically intradomiciliar by *T. infestans*, an exotic species in Brazil that interestingly never adapted to the wild environment of any Brazilian biome. Therefore, the successful campaign to eliminate indoor *T. cruzi* transmission by *T. infestans* was based on single measures that could be taken in all areas of transmission, including the spraying of houses and attachments, educational campaigns and *T. infestans* collections. Thus, it was possible to use the same vector combat methodology throughout.

Despite the focus of the present study not being human disease or infection, the control of intradomicile *T. cruzi* transmission by *T. infestans* in Brazil is an issue worth mentioning. This was indeed a very important landmark. In fact, the Chagas Disease Control Program established in Brazil in 1975 achieved, in this continental-sized country, a highly successful campaign, starting from millions of infected people to zero in 25 years (Schofield and Maudlin, 2001). In terms of public health, this was an enormous milestone. Even though it was not technically complicated, it was necessary to train and supervise a large number of men who had to undergo hard work in some cases in very severe climatic conditions, working under standard protocols across

the vast area, all without today's communication facilities. An additional difficulty was the local peculiarities of several regions of the country. It was proposed that the control of *T. infestans* in the Northeast would be easier to fight because of the short time of existence of this triatomine in the region and a putative lower adaptation level to the conditions of that biome (Ramos and Carvalho, 2001). Will there be intrahome transmission of *T. cruzi* again? It is hard to know. In addition to the improvements that have occurred in several housings, it was proposed that habitat change and adaptation to a new environment constitute a long evolutionary process in triatomines (Schofield et al., 1999).

Currently, Chagas disease is of concern again but with an entirely new, challenging and very complex epidemiological profile. Trypanosomiasis by *T. cruzi* is a neglected disease despite being a reemerging parasitosis and is no longer restricted to the new world. This spillover to nonendemic areas, including other continents out of the Americas, is mainly due to uncontrolled migratory movements, blood transfusion and organ transplantation (Franco-Paredes et al., 2009). Additionally, the enzootic nature of Chagas disease has been extending its limits, as has been observed in the southern United States, where an increase in the number of infected dogs as well as an increase in the areas of occurrence have been described (Curtis-Robles et al., 2017). Dogs are the last barrier between the wild cycle of transmission and the human environment. A recent review on the subject estimated that there are 300,000 *T. cruzi*-infected humans in the United States (Andrade et al., 2014). This number is likely underestimated.

OUTBREAKS AND ACUTE CASES OF CHAGAS DISEASE

In Latin America, outbreaks and cases of oral Chagas disease have been increasing worryingly, especially because, in general, they result in severe clinical manifestations contrary to what is known of this infection in animals. Opossums fed on infected triatomine or mice serologically convert much later than when infected subcutaneously and do not have patent parasitemia like humans. What makes the early diagnosis of Chagas disease fundamental is the increased chance of cure of the infected individuals who has early access to treatment and the increased chance of those infected and precociously treated individuals remaining asymptomatic and not progressing to the severe forms of disease.

What makes early detection of *T. cruzi* infection so difficult is, in addition to the lack of local prepared staff, the lack of pathognomonic signs and the diversity of epidemiological scenarios in which oral cases and outbreaks occur. In fact, although *T. cruzi* infection is always associated with the consumption of food contaminated by infected triatomines, there are numerous variables that are still unknown. Thus, the outbreak of Chagas disease that occurred in 2005 in southern Brazil, in Santa Catarina, related to the consumption of contaminated sugarcane juice, raised several tantalizing hypotheses that were being discarded as the real cause was brought to light as, for example, sugarcane plantations would favor the multiplication

of triatomines. It was found that the contamination occurred at the sugarcane mill located near a window in which infected triatomines fell into from a neighboring palm tree probably attracted by light (Roque et al., 2008; Steindel et al., 2008). The origin of the contaminated food that resulted in the outbreak reported in Redenção/CE in the northern part of Brazil was never clarified because the wild transmission cycle of *T. cruzi* was observed in different parts of the municipality (Roque et al., 2008). Despite the presence of *T. cruzi*-infected wild mammals in the surroundings (as is the common scenario throughout the country), both municipalities displayed good sanitary conditions and the predominance of an urban profile. Humans in those areas did not expose themselves or their food to triatomine bugs. There was never a case or outbreak in these localities again.

A contrasting transmission scenario was observed in the Amazon region, where contaminated açai fruit (*Euterpe oleracea*) juice was associated with the great majority of current cases in Brazil (Santos et al., 2018). In these outbreaks, the precariousness of local sanitary and educational conditions associated with the presence of infected bugs, eventually infesting the panniers used to transport the fruits, resulted in human cases, always in the more dry and hot period of the year, coinciding with both the açai harvest and the increased flying activities of the bugs (Xavier et al., 2014). Several cases were reported in the riverside population, usually as a familial outbreak. The difficulties in access to health professionals, the lack of information about the transmission and symptoms and, mainly, the complete absence of sanitary care likely resulted in the underestimation of such outbreaks.

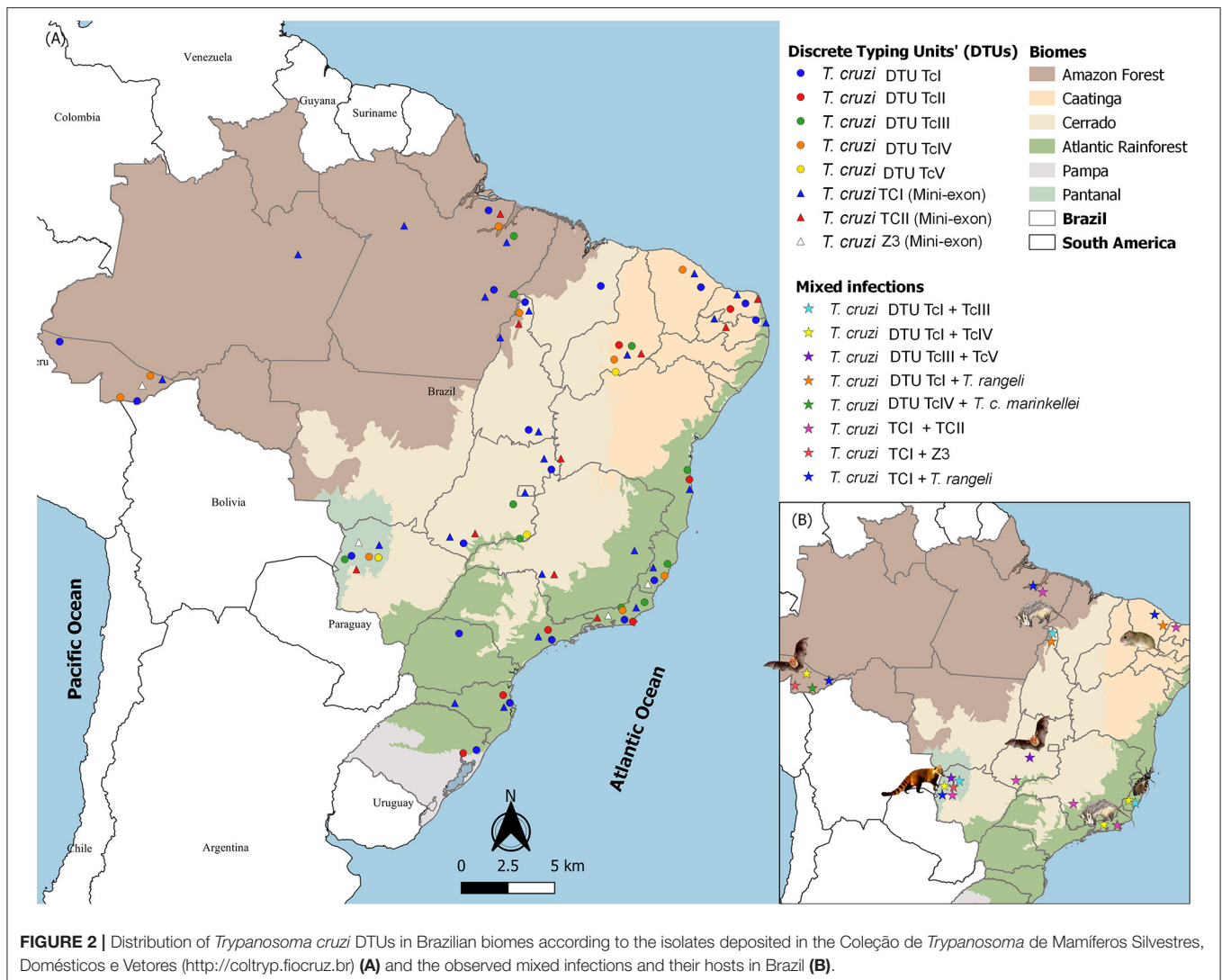
A common conceptual error is that triatomine bugs are found colonizing açai palm trees. In fact, the distribution of bugs in Amazonian palm trees is neither homogeneous nor random but is much more intense in palm trees with higher accumulation of organic material (Abad-Franch et al., 2010). This is the opposite characteristic of the açai palm trees. The attracting factor for bugs starts after the açai fruit collection and is associated with the harvest, transport and characteristics of the fruit itself. After harvest, a natural fermentation process of the fruit produces carbonic gas, heat and humidity that can attract insects, especially in the sunset, when hundreds of açai panniers are maintained on the riverbanks near artificial light while the boats arrive to transport the fruits to be negotiated. These are the conditions in which the fruits are sold in Belém, one of the largest municipalities of the Brazilian Amazon region and the one that reports a higher number of new cases of ACD annually. Infected triatomines transported with açai fruits and derived from nearby islands are responsible for the contamination of juices that are sold in the urban areas of Belém, in an epidemiological feature named “*Distantiae Transmission*” (Xavier et al., 2014). This feature may also occur when one beverage is produced (and contaminated) in one area but is consumed and responsible for infecting people in other areas. This situation occurred in the largest Chagas disease oral outbreak ever reported in a school in the urban area of Caracas, Venezuela. Guava juice produced in a rural area was contaminated with feces of infected *Panstrongylus geniculatus* and served in the school, resulting in more than one hundred cases of Chagas disease (Alarcón de Noya et al., 2010).

In addition to beverages, *T. cruzi* may be transmitted through different comestibles, even by solid food. In 2009, one familiar Chagas disease outbreak was reported in Tocantins State, Brazil, associated with the consumption of babaçu palm heart. In this case, the instrument used to cut vegetation probably came in contact with an infected bug (probably cutting its body), and this same instrument was used to cut the palm heart before distributing it to the families. Additionally, in the same state, an outbreak in Ananás municipality in 2012 received attention due to the high number of infected people (12 cases). This latter case was associated with the consumption of bacaba fruit (*Oenocarpus bacaba*) juice, produced in a similar manner as açai, but with cultural differences associated with its consumption that can directly impact the number of infected people. In this sense, açai fruit juice is consumed daily in some Amazon areas, usually immediately after its preparation and only by the family due to its low income. Contaminated açai juices result in familial Chagas disease outbreaks, usually involving 4 or 5 people. On the other hand, bacaba juice is sporadically consumed and, due to its high output (up to 10 liters), it is usually consumed with friends and for more than 1 day. Contaminated juices, in this feature, can result in an increase in the number of infected people, as was the case of the outbreak reported in Ananás. The most recent outbreak in Brazil occurred in September 2019, resulting in the infection of 16 individuals, and was associated with the consumption of the fruit of the patawa tree (*Oenocarpus bataua*), a palm tree that reaches 25 m height. This highly appreciated palm tree is found in the Amazon basin, and its fruits are used for several purposes, including juice preparation. Altogether, these cases demonstrate that, more than a specific food, human outbreak cases are the result of poor sanitary education and poor practices of food manipulation.

Oral infection may occur directly by contact with infected triatomine feces, independent of comestibles, as was observed by fatal case of a 2-year-old boy from Guarapari, in the Brazilian Southeast Region. The infection was associated with *Triatoma vitticeps*, a triatomine considered to be a secondary vector due to its delay of defecation after a blood meal but that demonstrated to be quite efficient in concomitantly hosting several *T. cruzi* DTUs and *T. dionisii*. The boy was infected by handling this *T. vitticeps* specimen (Dario et al., 2016).

One of the largest Brazilian outbreaks of Chagas disease occurred in Ibimirim, in the Brazilian Northeast Region, and was tentatively associated with food. Moreover, the real source of infection that resulted in 30 treated individuals was not yet identified 6 months later. Certainly, it was not due to the most commonly described beverages in other outbreaks (sugarcane, açai, or bacaba). These distinct epidemiological scenarios throughout Brazil show the necessity of distinct control measures.

The definitive control of Chagas disease is possible and, more than that, is urgent. It should not be possible that this parasitosis is still a scourge more than one hundred years after its discovery and so much accumulated knowledge. However, control will be possible only under an integrated multidisciplinary focus and not by the traditional control measures. Spraying in this new epidemiological scenario is the worst control method.



The development of an understanding of all cultural, social and economic realities of the outbreak areas and, obviously, all epidemiological features, including fauna composition hosts and vectors, will be the only way to define and adopt the correct measures that must include economic, health and educational improvement.

T. CRUZI AND ITS SUCCESSFUL TRANSMISSION STRATEGY IN NATURE

Pioneers in epidemiology postulated that all infected organisms are equally capable of infecting other organisms; that is, they have similar infectious competence. Further studies did not confirm this postulate but proposed the 20/80 rule; that is, a few individuals (humans or animals) are responsible for controlling transmission (Woolhouse et al., 1997). Obviously, the emergence of a superspreader is also regulated by other variables, such as immunosuppression and concomitant infections. This

phenomenon has already been described in numerous parasitic diseases, including *Leishmania infantum* (Duthie et al., 2018).

Trypanosoma cruzi is a mammalian hematozoan that depends on an insect vector for its passage to another mammalian host. The chances of infecting a hematophagous insect are increased, among others, if the parasitic population in peripheral blood is high. Interestingly, parasites in fresh blood smears or other blood tests of infected mammals are extremely rare in Brazil, independent of the *T. cruzi* DTU. Positive blood cultures or positive xenodiagnoses are parasitological enrichment methods that indicate high parasitemia and, therefore, the infectious potential of the animal. Working with hemocultures under field conditions is safer than working with xenodiagnoses, which includes a longer restraining time of the animal and is not free of accidents that result in the evasion of insects. The examination of 6,587 free-ranging wild mammals showed that 8% of all tested animals displayed positive blood cultures. **Figure 2A** shows the distribution of *T. cruzi* DTUs in Brazil, a country of continental dimensions and a large variety of environments and biocenoses.

Note that TcI and TcII are the most frequently encountered DTUs in all biomes, followed by TcIII and TcIV. TcV is the most rarely found DTU. Four aspects deserve to be highlighted: (i) the transmission strategies of the less frequent DTUs; (ii) the fact that these DTUs are detected at extremely distant points; (iii) the lack of association of DTUs with biomes; and (iv) the high diversity of DTUs in a relatively small area of the southeastern Atlantic Forest. Increasing studies of habitats and areas will probably add information that may change this map. All of these questions show that the biological history of *T. cruzi* is far from complete. Numerous chapters are still to be written about the biological history of *T. cruzi* that will likely include even more spectacular landmarks than those highlighted here.

Still considering the positive hemocultures, opossums, mainly *Philander* spp. and *Didelphis* spp., the coati *Nasua nasua*, the capuchin monkey *Sapajus libidinosus* and the golden lion tamarin *Leontopithecus rosalia*, were the mammals that demonstrated higher rates of positivity, demonstrating infectious potential (Jansen et al., 2018). This does not seem to be a superspreader maintenance strategy. The possible survival strategy of *T. cruzi* in the wild seems to depend on the sum of the high parasitemia periods of the assemblage of individuals and animal species that make up a particular community. Apparently, most mammalian species have high parasitemia periods for short times, i.e., infectious potential for a limited time. Only some species have a long period of high parasitemia detectable by blood culture, which means a long period of infectious potential, as mentioned above. Most likely, infected animals with negative blood culture had already passed their early stages of infection and infectious potential. To validate this hypothesis, it would be necessary to have representative samples of *T. cruzi* and mammalian species.

Another question refers to the permanence of the less frequent *T. cruzi* genotypes in nature. The two possible hypotheses are (i) that at some point in the infection, these genotypes had a high circulating blood population; or (ii) other unknown transmission mechanisms warrant transmission in low parasitemias, as is the case in Brazil of the DTUs TcV and TcVI that are rarely found in nature. A plausible explanation can be drawn from a Santa Catarina outbreak in 2005. At that location, the wild mammal fauna was restricted to marsupials of the genus *Didelphis* whose blood cultures indicated in TcI in contrast to the human cases that were all by TcII. One specimen of *Triatoma tibiamaculata* had a mixed TcI and TcII infection (Roque et al., 2008). The mystery was only resolved by PCR of *Didelphis* serum, which showed the presence of TcII in the opossum (Lima et al., 2014). As has been described, *Didelphis* rapidly controls TcII infections at subpatent levels (Jansen et al., 1991).

A clear demonstration of how biased associations can be established is provided by Guarapari's case of the child who became orally infected by *T. cruzi* by his hand that had manipulated an infected triatomine (Dario et al., 2016). This child presented infection in the cardiac tissue by DTUs TcI, TcII, TcIII, TcIV, and *T. dionisii*. Reports of mixed human infections with such diversity of *T. cruzi* taxonomic units are very rare, especially by *T. dionisii*, which is a bat-associated trypanosome species. This is most likely due to the rarity

of histopathological examinations followed by the molecular characterization of tissues of individuals in the acute phase, i.e., very recently infected. This individual would likely not maintain such diversity indefinitely. Infections by some DTUs could be self-solving. At least *T. dionisii*, the bat-associated species, would probably have been eliminated or at least remained as a cryptic infection. Additionally, even total blood PCR is not necessarily representative of the richness of trypanomatid genotypes and species that infect a particular individual, not to mention the selective pressures exerted on the parasites by the immune response. The parasitological history of an individual is totally ignored when it is examined at later stages of infection. This results in at least two biases: (i) clinical manifestations are attributed only to that species or genotype that eventually is detected, and the possible effects of an initial multiple infection are totally ignored; and (ii) associations between the host and parasite (species or genotypes) are established based only on one single finding that is very probably not necessarily representative.

There are still many open questions on this topic, one of which specifically refers to the transmission of these genotypes and species that are so rarely found in nature. Are they becoming extinct, or are they beginning a process of expansion?

MIXED INFECTIONS

Mixed infections by species or by subpopulations of the same species are common phenomena in nature. They are difficult to follow because wildlife capture and recapture studies require very expensive infrastructure as well as specific diagnostic kits. However, although recognized as a potential selective filter, 16% of molecular characterization on the cultures derived from wild mammal's blood or infected triatomine feces revealed mixed infections, with TcI and TcII being the most frequent combination (Jansen et al., 2015). Mixed infections by distinct *T. cruzi* DTUs or *Trypanosoma* species were observed in all Brazilian biomes, but the host most frequently associated in these mixed infections varies: bats in the Amazon Forest and Cerrado, opossums also in the Amazon Forest and Atlantic Rainforest, coatis in Pantanal, caviomorph rodents from the *Thrichomys* genus in Caatinga and triatomines, mainly *Triatoma vitticeps*, in the Atlantic Rainforest (Figure 2B).

Theoretical models predict an increase in virulence based on the competitive advantage of the most virulent subpopulations (Cressler et al., 2016). This would be the case with competition for nutrients. However, there are other variables that may alter this fate, such as the host immune response or the parasite's realized niche. Mixed infection is a topic that has been receiving increasing attention due to the possible impacts on the host. Concerning genotypes of *T. cruzi*, Magalhães and coauthors evaluated the impact of *T. cruzi* DTUs TcIV and TcV on human monocytes (Magalhães et al., 2019). The authors observed that unlike single infections, coinfections resulted in increased expression of IL10 and TNF, which led the authors to conclude that mixed infection has the potential to favor parasite control. Other authors suggest that, in contrast, mixed infections tend to increase pathogenicity. Under natural conditions, the presence

of *T. dionisii* and *T. cruzi* TcI, TcII, TcIII, and TcIV has been observed in the cardiac tissue of a child who died of acute orally acquired Chagas disease (Dario et al., 2016). It was not possible in this case to make any prediction on the course of this infection, but the acute course of the disease (3 weeks) followed by death makes one think that in this case, perhaps the effect of the mixed infection would have had the opposite effect (Dario et al., 2016). In fact, the evaluation of the resultant coinfection of distinct *T. cruzi* genotypes is a difficult task due to the numerous variables involved: age, nodule size, the sequence of infections in relation to DTUs, the presence of other parasites, and immunological status, among many others.

By means of a barcoding and next-generation sequencing approach, two cases of coinfections of TcI with TcVI and TcIV were described in non-human primates from Louisiana in the southern USA (Herrera et al., 2019). The same methodological approach was used to test human *T. cruzi* infection, showing that Chagasic patients in Yucatan (Mexico) displayed infections by diverse *T. cruzi* DTUs. The authors detected the presence of TcI, TcII, TcV, and TcVI in single and mixed infections. In fact, 47% of individuals presented infections due to multiple *T. cruzi* DTUs (Villanueva-Lizama et al., 2019).

Still concerning free-ranging wild mammals, small rodents were also able to harbor multiple *T. cruzi* DTUs, as demonstrated by metabarcoding, in addition to conventional PCR and Sanger sequencing (Pronovost et al., 2018). Bats and marsupials have been proposed as bioaccumulators of *Trypanosoma* spp. since they may display infections by several trypanosome species from different clades: *T. cruzi*, *T. dionisii*, *T. lainsoni*, and *T. genarii* (Rodrigues et al., 2019).

The use of blood clots for the extraction of *Trypanosoma* spp. DNA and nested PCR using generalist primers followed by Sanger sequencing demonstrated to be a reliable parasitological method that is more accessible than next-generation sequencing, which is still costly, especially for developing countries. Using this protocol, it was possible to access an expressive *Trypanosoma* diversity and to identify trypanosomes not cultivable in axenic medium and/or mixed infections of animals with low parasitemia (Rodrigues et al., 2019).

A PROMISING INTERACTIVE TOOL TO UNRAVEL *T. CRUZI* BIOLOGY

Studying biological phenomena without considering the scenario in which they occur results in the loss of precious and potentially enlightening information. The determination of the spatial distribution of the elements that compose the epidemiological chain of a parasitic disease is of pivotal importance for the determination of trends and risk evaluation. Moreover, it is worth mentioning that the attempts to control a given multihost parasite that displays a huge intraspecific heterogeneity and a complex transmission cycle as expressed by different epidemiological and enzootiological scenarios employing one single measure will be insufficient. The sustainability of successful control of Chagas in multiple current epidemiological scenarios requires multidisciplinary studies. All of the host species select

subpopulations of *T. cruzi* in a unique way and present different infection patterns that depend on numerous macro (landscape) and micro (individual peculiarities) variables.

The study of landscape by the classic methodology of mapping by means of discrete typing units and sharp boundaries does not consider transition areas. Nevertheless, environmental and biological phenomena are typically continuous and exhibit a gradual transition from one to another. The fuzzy logic developed by Zadeh in the 1960s is able to solve the strongly non-linear nature of uncertainty and subjectivity inherent in biological data. Furthermore, the spatial analysis by the fuzzy inference method is a cartographic approach that makes it possible to model the spatial distribution of continuous biological phenomena, representing these distribution levels. Modeling by fuzzy logic allows the incorporation of multidisciplinary expert knowledge into the evaluation process. Despite posing as a paradigm break in comparison to the valuation methodologies based on classic logic, fuzzy theory facilitates dialog between the professionals of exact sciences, responsible for computational implementation, and experts from different biological areas because it allows the use of linguistic variables and simplistic logical rules. Such logic has been vastly used in biological modeling due to its peculiar features, especially the capacity to model complex and non-linear problems in a simple way.

Fuzzy logic is a novel approach for Chagas disease risk prediction. This model already demonstrated the possibility of identifying areas with different degrees of risk, thus allowing a continuous and integrated representation of the variables involved in *T. cruzi* transmission in nature. The output data obtained can be used to support decision-making in epidemiological surveillance of Chagas disease and are certainly an example that can be applied to several other parasite infections in distinct areas (Xavier et al., 2016). Fuzzy models are highly promising for evaluating *T. cruzi* (and potentially all other parasite species as well as transmission risk areas). The term “map algebra” was established by Dana Tomlin in the early 1980s (Tomlin, 1990) with the development of the “Map Analysis Package GIS.” Map algebra provides tools to perform spatial analysis operations and is based on matrix algebra, which refers to the algebraic manipulation of matrices (as maps in raster data structures). Spatial analysis by the interpolation method, followed by map algebra, is able to model the spatial distribution of biological phenomena and their distribution and eventual association with other parameters or variables, enhancing the decision power of responsible authorities. Acute Chagas disease outbreaks are increasing in the Amazon basin as a result of oral transmission. This scenario requires a new approach to identify hotspot transmission areas and implement control measures. A geospatial approach using interpolation and map algebra methods to evaluate mammalian fauna was demonstrated to be a reliable strategy to detect hotspot transmission areas in the wild. The construction of maps with mammalian fauna variables, including the infection rates by *T. cruzi*, in dogs and in small wild mammal species, demonstrated that a high prevalence of *T. cruzi* infection in dogs and small wild mammals was associated with a lower richness in mammals. Consequently, it was shown that monitoring *T. cruzi* infection in dogs may be a valuable tool for

detecting a lower richness of small wild mammals in the fauna and elucidating the transmission cycle of *T. cruzi* in the wild. The results obtained by visual examination of the maps were validated by statistical analysis (Xavier et al., 2012).

CONCLUDING REMARKS

Here, we briefly described some features that have been landmarks in the course of knowledge building on *Trypanosoma cruzi*. Because it is such a complex parasite, *T. cruzi*, to date, still displays contradictory or even obscure biology. While the main attributes of *T. cruzi* (infectivity and disease in humans, wild and domestic hosts, transmission to humans by domicile adapted triatomines) were revealed in a few years by Carlos Chagas, the *T. cruzi* diversity, pathogenesis, peculiar features of the interaction of *T. cruzi* with its numerous hosts and its multiplication and dispersion strategies still constitute a puzzle. Undoubtedly, the huge technological advance and the consequent stronger analytical power allowed the resolution of many of these issues. However, the current epidemiological profile of Chagas disease, due to the oral route, constitutes a challenge and a scourge, especially for people with less access to adequate sanitary conditions and medical care. One of the possible obstacles to controlling this parasitosis does not depend solely on technology but relies on the conceptual framework of researchers and technicians that is often rigid, poorly resilient and open to the new, disregarding the hyperbolic doubt of René Descartes' (1637) concept about the importance of the need to continually inquire the truth of what is presented as true. This kind of attitude is paralyzing, just as paralyzing as the lack of self-confidence and the hesitation to publish their findings. Science also includes intuition beyond assumptions built on solid foundations. This is exemplified by the pioneering study of an oral outbreak in Nova Teutônia, Santa Catarina State, Southern Brazil. It was a boarding school where several young people became ill and Chagas disease was diagnosed. At the time, all searches for triatomines resulted in vain. The outbreak remained unexplained. One of the authors, Nery-Guimarães, hypothesized that perhaps the ingestion of food that had been contaminated by the urine of *T. cruzi*-infected opossums could be the cause (Nery-Guimarães et al., 1968). It was not far from the truth. In 1984, almost 20 years later, Deane and coauthors described the extracellular cycle of *T. cruzi* in the opossum scent glands of *D. aurita* (Deane et al., 1984a). So also did Carlos Chagas: he made the discoveries that made him famous while in charge of studying malaria in the region where a railway was built. As soon as he was informed by a construction engineer of the blood-sucking insects, he did not hesitate to collect and examine them. He also examined domestic and wild animals as well as humans. Accordingly, he closed the main contours of this new zoonosis.

Technological advancement has resulted in new insights into the parasitism phenomenon and consequently in the reformulation of concepts. An example is the definition of what constitutes a reservoir. Carlos Chagas defined the armadillo as a "depository," probably disregarding, as expected at that time,

that a host receives and exerts selective pressures on the parasites. The very concepts of reservoir and of what is a parasite have been changing since the days of Carlos Chagas. In this sense, the most didactic and clear definition of what is a reservoir does not refer to the number of species or the ability to cause or not to damage but defines reservoir as one animal species or a set of animal species responsible for maintaining the parasite in the wild. This set of animals will be different for each location and time scale (Jansen et al., 2015; adapted from Ashford, 1997).

Parasitic specificity has also been revisited as a consequence of technological innovation, and the awareness of the importance of including wild animals and their parasites in parasitology studies has increased. Trypanosomatids are no exception: reports of the occurrence of trypanosomatids in unfamiliar hosts are increasing, undermining paradigms of host species and *Trypanosoma* spp. associations. A clear understanding of host-parasite interaction and the mechanisms involved in this adaptation process are important from the academic point of view but also for public health, because in times of profound climate change, emerging diseases result precisely from parasitic spillover to unfamiliar hosts. The acquisition and loss of host species are common events in the parasitism phenomenon and can happen independent of a long-term coevolutionary process. Actually, ecological host fitting is a process of spillover that depends on the preexisting attributes of the parasite (Araujo et al., 2015) and is probably an important driving force for the diversification of generalist parasites such as *T. cruzi*.

The answers to most of the still open questions of *T. cruzi* biology may be found in its ancient hosts, i.e., the wild mammals in nature.

AUTHOR CONTRIBUTIONS

AJ and AR wrote the manuscript. SX performed figures. All authors conceived, designed the manuscript, read, and approved the final manuscript.

FUNDING

This study was funded by the Instituto Oswaldo Cruz (IOC/Fiocruz), Fundação Carlos Chagas Filho de Amparo a Pesquisa do Rio de Janeiro (FAPERJ), and Conselho Nacional de Desenvolvimento Científico e Tecnológico (CNPq). The funders had no role in study design, data collection and analysis, decision to publish, or preparation of the manuscript.

ACKNOWLEDGMENTS

The authors thank to Dr. Vera Bongertz for many helpful comments on the manuscript. Data from *T. cruzi* isolates derived from Coleção de *Trypanosoma* de Mamíferos Silvestres, Domésticos e Vetores-Instituto Oswaldo Cruz Foundation (COLTRYP/IOC-FIOCRUZ). We offer thanks to the Program of Technological Development and Inputs for Health/Instituto Oswaldo Cruz Foundation (PDTIS/FIOCRUZ) sequencing platform for sequencing our samples.

REFERENCES

- Abad-Franch, F., Ferraz, G., Campos, C., Palomeque, F. S., Grijalva, M. J., Aguilar, H. M., et al. (2010). Modeling disease vector occurrence when detection is imperfect: infestation of Amazonian palm trees by triatomine bugs at three spatial scales. *PLoS Negl. Trop. Dis.* 4:e620. doi: 10.1371/journal.pntd.0000620
- Akopyants, N. S., Kimblin, N., Secundino, N., Patrick, R., Peters, N., Lawyer, P., et al. (2009). Demonstration of genetic exchange during cyclical development of *Leishmania* in the sand fly vector. *Science* 324, 265–268. doi: 10.1126/science.1169464
- Alarcón de Noya, B., Díaz-Bello, Z., Colmenares, C., Ruiz-Guevara, R., Mauriello, L., Zavala-Jaspe, R., et al. (2010). Large urban outbreak of orally acquired acute Chagas disease at a school in Caracas, Venezuela. *J. Infect. Dis.* 201, 1308–1315. doi: 10.1086/651608
- Andrade, D. V., Gollob, K. J., and Dutra, W. O. (2014). Acute Chagas disease: new global challenges for an old neglected disease. *PLoS Negl. Trop. Dis.* 8:e3010. doi: 10.1371/journal.pntd.0003010
- Andrade, S. G., Carvalho, M. L., and Figueira, R. M. (1970). Caracterização morfológica e histopatológica de diferentes cepas do *Trypanosoma cruzi*. *Gaz Méd Bahia* 70, 245–250.
- Andrade, S. G., and Magalhães, J. B. (1997). Biodemas e zymodemas of *Trypanosoma cruzi* strains: correlation with clinical data and experimental pathology. *Rev. Soc. Bras. Med. Trop.* 30, 27–35. doi: 10.1590/S0037-86821997000100006
- Anonymous (1999). Recommendations from a satellite meeting. *Mem. Inst. Oswaldo Cruz* 94, 429–432. doi: 10.1590/S0074-02761999000700085
- Apt, W., Aguilera, X., Arribada, A., Gomez, L., Miles, M. A., and Widmer, G. (1987). Epidemiology of Chagas' disease in northern Chile: isozyme profiles of *Trypanosoma cruzi* from domestic and sylvatic transmission cycles and their association with cardiopathy. *Am. J. Trop. Med. Hyg.* 37, 302–307. doi: 10.4269/ajtmh.1987.37.302
- Araújo, A., Jansen, A. M., Bouchet, F., Reinhard, K., and Ferreira, L. F. (2003). Parasitism, the diversity of life, and paleoparasitology. *Mem. Inst. Oswaldo Cruz* 98 (Suppl. 1), 5–11. doi: 10.1590/S0074-02762003000900003
- Araujo, S. B., Braga, M. P., Brooks, D. R., Agosta, S. J., Hoberg, E. P., von Hartenthal, F. W., et al. (2015). Understanding host-switching by ecological fitting. *PLoS ONE* 10:e0139225. doi: 10.1371/journal.pone.0139225
- Ashford, R. W. (1997). What it takes to be a reservoir host. *Bel. J. Zool* 127, 85–90.
- Aufderheide, A. C., Salo, W., Madden, M., Streitz, J., Buikstra, J., Guhl, F., et al. (2004). A 9,000-year record of Chagas' disease. *Proc. Natl. Acad. Sci. U.S.A.* 101, 2034–2039. doi: 10.1073/pnas.0307312101
- Barretto, M. P. (1967a). Estudos sobre reservatórios e vetores silvestres do *Trypanosoma cruzi*. XVII. Contribuição para o estudo dos focos naturais da tripanossomose americana com especial referência à região nordeste do estado de São Paulo, Brasil. *Rev. Soc. Bras. Med. Trop.* 1, 23–36. doi: 10.1590/S0037-86821967000200002
- Barretto, M. P. (1967b). Estudos sobre reservatórios e vetores silvestres do *Trypanosoma cruzi*. XXII. Modificações dos focos naturais da tripanossomose americana e suas consequências. *Rev. Soc. Bras. Med. Trop.* 1, 167–173. doi: 10.1590/S0037-86821967000400002
- Barretto, M. P., and Ribeiro, R. D. (1979). Reservatórios silvestres do *Trypanosoma* (*Schizotrypanum*) *cruzi* Chagas, 1909. *Rev. Inst. Adolfo Lutz* 39, 25–36.
- Berry, A. S. F., Salazar-Sánchez, R., Castillo-Neyra, R., Borrini-Mayori K., Chipana-Ramos, C., Vargas-Maquera, M., et al. (2019). Sexual reproduction in a natural *Trypanosoma cruzi* population. *PLoS Negl. Trop. Dis.* 13:e0007392. doi: 10.1371/journal.pntd.0007392
- Brener, Z. (1977). Symposium on new approaches in research on American trypanosomiasis. *Bol. Oficina Sanit. Panam.* 83, 106–118.
- Brenière, S. F., Carrasco, R., Revollo, S., Aparicio, G., Desjeux, P., and Tibayrenc, M. (1989). Chagas' disease in Bolivia: clinical and epidemiological features and zymodeme variability of *Trypanosoma cruzi* strains isolated from patients. *Am. J. Trop. Med. Hyg.* 41, 521–529. doi: 10.4269/ajtmh.1989.41.521
- Brise, S., Dujardin, J. C., and Tibayrenc, M. (2000). Identification of six *Trypanosoma cruzi* lineages by sequence-characterised amplified region markers. *Mol. Biochem. Parasitol.* 111, 95–105. doi: 10.1016/S0166-6851(00)00302-9
- Chagas, C. (1909). Nova tripanosomiase humana: estudos sobre a morfologia e o ciclo evolutivo do *Schizotrypanum* n. gen., n. sp., agente etiológico de nova entidade mórbida do homem. *Mem. Inst. Oswaldo Cruz* 1, 159–218. doi: 10.1590/S0074-02761909000200008
- Chagas, C. (1912). Sobre um trypanosomo do tatú *Tatusia novemcincta*, transmitido pela *Triatoma geniculata* Latr. (1811): Possibilidade de ser o tatu um depositário do *Trypanosoma cruzi* no mundo exterior (Nota Prévia). *Brazil-Médico* 26, 305–306.
- Chapman, M. D., Baggaley, R. C., Godfrey-Fausset, P. F., Malpas, T. J., White, G., Canese, J., et al. (1984). *Trypanosoma cruzi* from the Paraguayan Chaco: isoenzyme profiles of strains isolated at Makthlawaiya. *J. Protozool.* 31, 482–486. doi: 10.1111/j.1550-7408.1984.tb02999.x
- Clark, C. G., and Pung, O. J. (1994). Host specificity of ribosomal DNA variation in sylvatic *Trypanosoma cruzi* from North America. *Mol. Biochem. Parasitol.* 66, 175–179. doi: 10.1016/0166-6851(94)90052-3
- Coura, J. R. (2009). “Relevância do trabalho pioneiro de Carlos Chagas que descreve a descoberta da nova tripanossomiase humana,” in *Clássicos em Doença de Chagas*, eds J. R. Carneiro, N. Azevedo, T. Araújo-Jorge, J. Lannes-Vieira, M. N. C. Soeiro, and L. Klein (Rio de Janeiro: Editora Fiocruz), 128–130.
- Coura, J. R., Albajar, P. A. V., and Junqueira, A. C. V. (2014). Ecoepidemiology, short history and control of Chagas disease in the endemic countries and the new challenge for non-endemic countries. *Mem. Inst. Oswaldo Cruz* 109, 856–862. doi: 10.1590/0074-0276140236
- Coura, J. R., Ferreira, L. F., Rubens, J., Pereira, N. C., and da Silva, J. R. (1966). Trypanosome of *cruzi*-like complex in a sylvan reservoir in Guanabara State. Study of its pathogenicity. *Rev. Inst. Med. Trop. São Paulo* 8, 125–133.
- Cressler, C. E., McLeod, D. V., Rozins, C., van den Hoogen, J., and Day, T. (2016). The adaptive evolution of virulence: a review of theoretical predictions and empirical tests. *Parasitology* 143, 915–930. doi: 10.1017/S003118201500092X
- Curtis-Robles, R., Snowden, K. F., Dominguez, B., Dinges, L., Rodgers, S., Mays, G., et al. (2017). Epidemiology and molecular typing of *Trypanosoma cruzi* in naturally-infected hound dogs and associated Triatomine vectors in Texas, USA. *PLoS Negl. Trop. Dis.* 11:e0005298. doi: 10.1371/journal.pntd.0005298
- Dario, M. A., Rodrigues, M. S., Barros, J. H., Xavier, S. C., D'Andrea, P. S., Roque, A. L., et al. (2016). Ecological scenario and *Trypanosoma cruzi* DTU characterization of a fatal acute Chagas disease case transmitted orally (Espírito Santo state, Brazil). *Parasit. Vectors* 9:477. doi: 10.1186/s13071-016-1754-4
- Deane, M. P., Lenzi, H. L., and Jansen, A. (1984a). *Trypanosoma cruzi*: vertebrate and invertebrate cycles in the same mammal host, the opossum *Didelphis marsupialis*. *Mem. Inst. Oswaldo Cruz* 79, 513–515. doi: 10.1590/S0074-02761984000400021
- Deane, M. P., Sousa, M. A., Pereira, N. M., Gonçalves, A. M., Momen, H., and Morel, C. M. (1984b). *Trypanosoma cruzi*: inoculation schedules and re-isolation methods select individual strains from doubly infected mice, as demonstrated by schizodeme and zymodeme analyses. *J. Protozool.* 31, 276–280. doi: 10.1111/j.1550-7408.1984.tb02960.x
- Dias, J. C. P., and Coura, J. R. (1997). “Epidemiologia,” in *Clínica e Terapêutica da Doença de Chagas. Uma Abordagem Prática para o Clínico Geral*, eds J. C. P. Dias and J. R. Coura (Rio de Janeiro: Editora Fiocruz), 33–66.
- Duthie, M. S., Lison, A., and Courtenay, O. (2018). Advances toward diagnostic tools for managing zoonotic visceral leishmaniasis. *Trends Parasitol.* 34, 881–890. doi: 10.1016/j.pt.2018.07.012
- Dvorak, J. A. (1984). The natural heterogeneity of *Trypanosoma cruzi*: biological and medical implications. *J. Cell. Biochem.* 24, 357–371. doi: 10.1002/jcb.240240406
- Fernandes, O., Mangia, R. H., Lisboa, C. V., Pinho, A. P., Morel, C. M., Zingales, B., et al. (1999). The complexity of the sylvatic cycle of *Trypanosoma cruzi* in Rio de Janeiro state (Brazil) revealed by the non-transcribed spacer of the mini-exon gene. *Parasitology* 118 (Pt. 2), 161–166. doi: 10.1017/S0031182098003709
- Franco-Paredes, C., Bottazzi, M. E., and Hotez, P. J. (2009). The unfinished public health agenda of Chagas disease in the era of globalization. *PLoS Negl. Trop. Dis.* 3:e470. doi: 10.1371/journal.pntd.0000470
- Gibson, W., and Bailey, M. (1994). Genetic exchange in *Trypanosoma brucei*: evidence for meiosis from analysis of a cross between drug-resistant transformants. *Mol. Biochem. Parasitol.* 64, 241–252. doi: 10.1016/0166-6851(94)00017-4
- Gibson, W., Peacock, L., Ferris, V., Williams, K., and Bailey, M. (2008). The use of yellow fluorescent hybrids to indicate mating in *Trypanosoma brucei*. *Parasit. Vectors* 1:4. doi: 10.1186/1756-3305-1-4

- Guhl, F., Auderheide, A., and Ramirez, J. D. (2014). From ancient to contemporary molecular eco-epidemiology of Chagas disease in the Americas. *Int. J. Parasitol.* 44, 605–612. doi: 10.1016/j.ijpara.2014.02.005
- Herrera, C., Majeau, A., Didier, P., Falkenstein, K. P., and Dumonteil, E. (2019). *Trypanosoma cruzi* diversity in naturally infected nonhuman primates in Louisiana assessed by deep sequencing of the mini-exon gene. *Trans. R. Soc. Trop. Med. Hyg.* 113, 281–286. doi: 10.1093/trstmh/try119
- Jansen, A. M., Leon, L., Machado, G. M., da Silva, M. H., Souza-Leão, S. M., and Deane, M. P. (1991). *Trypanosoma cruzi* in the opossum *Didelphis marsupialis*: parasitological and serological follow-up of the acute infection. *Exp. Parasitol.* 73, 249–259. doi: 10.1016/0014-4894(91)90096-F
- Jansen, A. M., Madeira, F. B., and Deane, M. P. (1994). *Trypanosoma cruzi* infection in the opossum *Didelphis marsupialis*: absence of neonatal transmission and protection by maternal antibodies in experimental infections. *Mem. Inst. Oswaldo Cruz* 89, 41–45. doi: 10.1590/S0074-02761994000100008
- Jansen, A. M., Moriearty, P. L., Castro, B. G., and Deane, M. P. (1985). *Trypanosoma cruzi* in the opossum *Didelphis marsupialis*: an indirect fluorescent antibody test for the diagnosis and follow-up of natural and experimental infections. *Trans. R. Soc. Trop. Med. Hyg.* 79, 474–477. doi: 10.1016/0035-9203(85)90069-0
- Jansen, A. M., Xavier, S. C., and Roque, A. L. R. (2015). The multiple and complex and changeable scenarios of the *Trypanosoma cruzi* transmission cycle in the sylvatic environment. *Acta Trop.* 151, 1–15. doi: 10.1016/j.actatropica.2015.07.018
- Jansen, A. M., Xavier, S. C. D. C., and Roque, A. L. R. (2018). *Trypanosoma cruzi* transmission in the wild and its most important reservoir hosts in Brazil. *Parasit. Vectors* 11:502. doi: 10.1186/s13071-018-3067-2
- Lanar, D. E., Levy, L. S., and Manning, J. E. (1981). Complexity and content of the DNA and RNA in *Trypanosoma cruzi*. *Mol. Biochem. Parasitol.* 3, 327–341. doi: 10.1016/0166-6851(81)90006-2
- Legey, A. P., Pinho, A. P., Chagas Xavier, S. C., Leon, L. L., and Jansen, A. M. (1999). Humoral immune response kinetics in *Philander opossum* and *Didelphis marsupialis* infected and immunized by *Trypanosoma cruzi* employing an immunofluorescence antibody test. *Mem. Inst. Oswaldo Cruz* 94, 371–376. doi: 10.1590/S0074-02761999000300016
- Lima, V. S., Iniguez, A. M., Otsuki, K., Fernando Ferreira, L., Araújo, A., Vicente, A. C., et al. (2008). Chagas disease in ancient hunter-gatherer population, Brazil. *Emerging Infect. Dis.* 14, 1001–1002. doi: 10.3201/eid1406.070707
- Lima, V. S., Xavier, S. C. C., Maldonado, I. F., Roque, A. L. R., Vicente, A. C., and Jansen, A. M. (2014). Expanding the knowledge of the geographic distribution of *Trypanosoma cruzi* TcII and TcV/TcVI genotypes in the Brazilian Amazon. *PLoS ONE* 9:e116137. doi: 10.1371/journal.pone.0116137
- Lisboa, C. V., Dietz, J., Baker, A. J., Russel, N. N., and Jansen, A. M. (2000). *Trypanosoma cruzi* infection in *Leontopithecus rosalia* at the Reserva Biológica de Poco das Antas, Rio de Janeiro, Brazil. *Mem. Inst. Oswaldo Cruz* 95, 445–452. doi: 10.1590/S0074-0276200000400002
- Lisboa, C. V., Mangia, R. H., Luz, S. L., Kluczkowski, A. Jr, Ferreira, L. F., Ribeiro, C. T., et al. (2006). Stable infection of primates with *Trypanosoma cruzi* I and II. *Parasitology* 133(Pt. 5), 603–611. doi: 10.1017/S0031182006000722
- Lisboa, C. V., Monteiro, R. V., Martins, A. F., Xavier, S. C., Lima Vdos, S., and Jansen, A. M. (2015). Infection with *Trypanosoma cruzi* TcII and TcI in free-ranging population of lion tamarins (*Leontopithecus* spp.): an 11-year follow-up. *Mem. Inst. Oswaldo Cruz* 110, 394–402. doi: 10.1590/0074-02760140400
- Magalhães, L. M. D., Passos, L. S. A., Chiari, E., Galvão, L. M. C., Koh, C. C., Rodrigues-Alves, M. L., et al. (2019). Co-infection with distinct *Trypanosoma cruzi* strains induces an activated immune response in human monocytes. *Parasite Immunol.* 41:e12668. doi: 10.1111/pim.12668
- Marcili, A., Lima, L., Cavazzana, M., Junqueira, A. C., Veludo, H. H., Maia Da Silva, F., et al. (2009). A new genotype of *Trypanosoma cruzi* associated with bats evidenced by phylogenetic analyses using SSU rDNA, cytochrome b and Histone H2B genes and genotyping based on ITS1 rDNA. *Parasitology* 136, 641–655. doi: 10.1017/S0031182009005861
- Maruyama, S. R., de Santana, A. K. M., Takamiya, N. T., Takahashi, T. Y., Rogerio, L. A., Oliveira, C. A. B., et al. (2019). Non-Leishmania parasite in fatal visceral leishmaniasis-like disease, Brazil. *Emerg. Infect. Dis.* 25, 2088–2092. doi: 10.3201/eid2511.181548
- Miles, M. A., Lanham, S. M., de Souza, A. A., and Póvoa, M. (1980). Further enzymic characters of *Trypanosoma cruzi* and their evaluation for strain identification. *Trans. R. Soc. Trop. Med. Hyg.* 74, 221–237. doi: 10.1016/0035-9203(80)90251-5
- Miles, M. A., Toye, P. J., Oswald, S. C., and Godfrey, D. G. (1977). The identification by isoenzyme patterns of two distinct strain-groups of *Trypanosoma cruzi*, circulating independently in a rural area of Brazil. *Trans. R. Soc. Trop. Med. Hyg.* 71, 217–225. doi: 10.1016/0035-9203(77)90012-8
- Monteiro, R. V., Dietz, J. M., and Jansen, A. M. (2010). The impact of concomitant infections by *Trypanosoma cruzi* and intestinal helminths on the health of wild golden and golden-headed lion tamarins. *Res. Vet. Sci.* 89, 27–35. doi: 10.1016/j.rvsc.2010.01.001
- Monteiro, W. M., Magalhães, L. K., de Sá, A. R., Gomes, M. L., Toledo, M. J., Borges, L., et al. (2012). *Trypanosoma cruzi* IV causing outbreaks of acute Chagas disease and infections by different haplotypes in the Western Brazilian Amazonia. *PLoS ONE* 7:e41284. doi: 10.1371/journal.pone.0041284
- Monteiro, W. M., Magalhães, L. K., Santana Filho, F. S., Borborema, M., Silveira, H., and Barbosa, M. D. (2010). *Trypanosoma cruzi* TcIII/Z3 genotype as agent of an outbreak of Chagas disease in the Brazilian Western Amazonia. *Trop. Med. Int. Health* 15, 1049–1051. doi: 10.1111/j.1365-3156.2010.02577.x
- Nery-Guimarães, F., Silva, N., Clausell, D. T., Mello, A. L., Rapone, T., Snell, T., et al. (1968). Um surto epidêmico de doença de Chagas de provável transmissão digestiva, ocorrido em Teutônia (Estrela, Rio Grande do Sul). *Hospital* 73, 1767–1804.
- Noireau, F., Diosque, P., and Jansen, A. M. (2009). *Trypanosoma cruzi*: adaptation to its vectors and its hosts. *Vet. Res.* 40, 26. doi: 10.1051/vetres/2009009
- Pavlovsky, E. N. (1967) *Natural Nidality of Transmissible Diseases in Relation to Landscape Epidemiology of Zooanthroposes*. Moscow: Peace Publishers.
- Peacock, L., Bailey, M., Carrington, M., and Gibson, W. (2014). Meiosis and haploid gametes in the pathogen *Trypanosoma brucei*. *Curr. Biol.* 24, 181–186. doi: 10.1016/j.cub.2013.11.044
- Pinho, A. P., Cupolillo, E., Mangia, R. H., Fernandes, O., and Jansen, A. M. (2000). *Trypanosoma cruzi* in the sylvatic environment: distinct transmission cycles involving two sympatric marsupials. *Trans. R. Soc. Trop. Med. Hyg.* 94, 509–514. doi: 10.1016/S0035-9203(00)90069-5
- Pronovost, H., Peterson, A. C., Chavez, B. G., Blum, M. J., Dumonteil, E., and Herrera, C. P. (2018). Deep sequencing reveals multiclonality and new discrete typing units of *Trypanosoma cruzi* in rodents from the southern United States. *J. Microbiol. Immunol. Infect.* doi: 10.1016/j.jmii.2018.12.004. [Epub ahead of print].
- Ramírez, J. D., Hernández, C., Montilla, M., Zambrano, P., Flórez, A. C., Parra, E., et al. (2014). First report of human *Trypanosoma cruzi* infection attributed to TcBat genotype. *Zoonoses Public Health* 61, 477–479. doi: 10.1111/zph.12094
- Ramos, A. N. Jr., and Carvalho, D. M. (2001). Epidemiologia da Endemia Chagásica no Município de João Costa, Sudeste do Piauí, Brasil. *Cad Saude Coletiva UFRJ* 9, 82–83. Available online at: <http://www.cadernos.iesc.ufrj.br/cadernos/index.php/features-sp-417739839/2003-2/2001/no1-jan-jun>
- Rangel, D. A., Lisboa, C. V., Novaes, R. L. M., Silva, B. A., Souza, R. F., Jansen, A. M., et al. (2019). Isolation and characterization of trypanosomatids, including *Crithidia mellificae*, in bats from the Atlantic Forest of Rio de Janeiro, Brazil. *PLoS Negl. Trop. Dis.* 13:e0007527. doi: 10.1371/journal.pntd.0007527
- Rodrigues, M. S., Lima, L., Xavier, S. C. D. C., Herrera, H. M., Rocha, F. L., Roque, A. L. R., et al. (2019). Uncovering *Trypanosoma* spp. diversity of wild mammals by the use of DNA from blood clots. *Int. J. Parasitol. Parasites. Wildl.* 8, 171–181. doi: 10.1016/j.ijppaw.2019.02.004
- Roman, F., das Chagas Xavier, S., Messenger, L. A., Pavan, M. G., Miles, M. A., Jansen, A. M., et al. (2018a). Dissecting the phyloepidemiology of *Trypanosoma cruzi* I (TcI) in Brazil by the use of high resolution genetic markers. *PLoS Negl. Trop. Dis.* 21:e0006466. doi: 10.1371/journal.pntd.0006466
- Roman, F., Iniguez, A. M., Yeo, M., and Jansen, A. M. (2018b). Multilocus sequence typing: genetic diversity in *Trypanosoma cruzi* I (TcI) isolates from Brazilian didelphids. *Parasit. Vectors* 11:107. doi: 10.1186/s13071-018-2696-9
- Roque, A. L. R., Xavier, S. C., da Rocha, M. G., Duarte, A. C., D'Andrea, P. S., and Jansen, A. M. (2008). *Trypanosoma cruzi* transmission cycle among wild and domestic mammals in three areas of orally transmitted Chagas disease outbreaks. *Am. J. Trop. Med. Hyg.* 79, 742–749. doi: 10.4269/ajtmh.2008.79.742
- Rothhammer, F., Allison, M. J., Núñez, L., Standen, V., and Arriaza, B. (1985). Chagas' disease in pre-Columbian South America. *Am. J. Phys. Anthropol.* 68, 495–498. doi: 10.1002/ajpa.1330680405

- Santos, V. R. C. D., Meis, J., Savino, W., Andrade, J. A. A., Vieira, J. R. D. S., Coura, J. R., et al. (2018). Acute Chagas disease in the state of Pará, Amazon Region: is it increasing? *Mem. Inst. Oswaldo Cruz* 113:e170298. doi: 10.1590/0074-02760170298
- Schofield, C. J., Diotaiuti, L., and Dujardin, J. P. (1999). The process of domestication in Triatominae. *Mem. Inst. Oswaldo Cruz* 94(Suppl. 1), 375–378. doi: 10.1590/S0074-02761999000700073
- Schofield, C. J., and Maudlin, I. (2001). Trypanosomiasis control. *Int. J. Parasitol.* 31, 614–9. doi: 10.1016/S0020-7519(01)00162-X
- Schwabl, P., Imamura, H., Van den Broeck, F., Costales, J. A., Maiguashca-Sánchez, J., Miles, M. A., et al. (2019). Meiotic sex in Chagas disease parasite *Trypanosoma cruzi*. *Nat. Commun.* 10:3972. doi: 10.1038/s41467-019-11771-z
- Souto, R. P., Fernandes, O., Macedo, A. M., Campbell, D. A., and Zingales, B. (1996). DNA markers define two major phylogenetic lineages of *Trypanosoma cruzi*. *Mol. Biochem. Parasitol.* 83, 141–152. doi: 10.1016/S0166-6851(96)02755-7
- Steindel, M., Kramer Pacheco, L., Scholl, D., Soares, M., de Moraes, M. H., Eger, I., et al. (2008). Characterization of *Trypanosoma cruzi* isolated from humans, vectors, and animal reservoirs following an outbreak of acute human Chagas disease in Santa Catarina State, Brazil. *Diagn. Microbiol. Infect. Dis.* 60, 25–32. doi: 10.1016/j.diagmicrobio.2007.07.016
- Tibayrenc, M. (1995). Population genetics of parasitic protozoa and other microorganisms. *Adv. Parasitol.* 36, 47–115. doi: 10.1016/S0065-308X(08)60490-X
- Tibayrenc, M., Ward, P., Moya, A., and Ayala, F. J. (1986). Natural populations of *Trypanosoma cruzi*, the agent of Chagas disease, have a complex multiclonal structure. *Proc. Natl. Acad. Sci. U.S.A.* 83, 115–119. doi: 10.1073/pnas.83.1.115
- Tomlin, D. (1990). *Geographic Information System and Cartographic Modeling*. New York, NY: Prentice Hall.
- Van den Broeck, F., Tavernier, L. J. M., Vermeiren, L., Dujardin, J. C., and Van Den Abbeele, J. (2018). Mitonuclear genomics challenges the theory of clonality in *Trypanosoma congolense*: Reply to Tibayrenc and Ayala. *Mol. Ecol.* 27, 3425–3431. doi: 10.1111/mec.14809
- Villanueva-Lizama, L., Teh-Poot, C., Majeau, A., Herrera, C., and Dumonteil, E. (2019). Molecular genotyping of *Trypanosoma cruzi* by next-generation sequencing of the mini-exon gene reveals infections with multiple parasite discrete typing units in chagasic patients from Yucatan, Mexico. *J. Infect. Dis.* 219, 1980–1988. doi: 10.1093/infdis/jiz047
- Woolhouse, M. E., Dye, C., Etard, J. F., Smith, T., Charlwood, J. D., Garnett, G. P., et al. (1997). Heterogeneities in the transmission of infectious agents: implications for the design of control programs. *Proc. Natl. Acad. Sci. U.S.A.* 94, 338–342. doi: 10.1073/pnas.94.1.338
- Xavier, S. C., Roque, A. L., Bilac, D., de Araújo, V. A., da Costa Neto, S. F., Lorosa, E. S., et al. (2014). Distantiae transmission of *Trypanosoma cruzi*: a new epidemiological feature of acute Chagas disease in Brazil. *PLoS Negl. Trop. Dis.* 8:e2878. doi: 10.1371/journal.pntd.0002878
- Xavier, S. C., Roque, A. L., Lima V dos, S., Monteiro, K. J., Otaviano, J. C., Ferreira da Silva, L. F., et al. (2012). Lower richness of small wild mammal species and Chagas disease risk. *PLoS Negl. Trop. Dis.* 6:e1647. doi: 10.1371/journal.pntd.0001647
- Xavier, S. C., Teixeira, M. G., Roque, A. L. R., Jansen, A. M., and Ferreira-da-Silva, L. F. C. (2016). “Applying Fuzzy Model to map vulnerability areas of *Trypanosoma cruzi* transmission,” in *Models and Methods for Supporting Decision-Making in Human Health and Environment Protection, 1st Edn*, eds C. N. Bouza, F. L. Mello, and M. J. Negreiros (New York, NY: Nova Science Publishers), 85–101.
- Yeo, M., Acosta, N., Llewellyn, M., Sánchez, H., Adamson, S., Miles, G. A., et al. (2005). Origins of Chagas disease: *Didelphis* species are natural hosts of *Trypanosoma cruzi* I and armadillos hosts of *Trypanosoma cruzi* II, including hybrids. *Int. J. Parasitol.* 35, 225–233. doi: 10.1016/j.ijpara.2004.10.024
- Zingales, B., Andrade, S. G., Briones, M. R., Campbell, D. A., Chiari, E., Fernandes, O., et al. (2009). A new consensus for *Trypanosoma cruzi* intraspecific nomenclature: second revision meeting recommends TcI to TcVI. *Mem. Inst. Oswaldo Cruz* 104, 1051–1054. doi: 10.1590/S0074-02762009000700021
- Zingales, B., Souto, R. P., Mangia, R. H., Lisboa, C. V., Campbell, D. A., Coura, J. R., et al. (1998). Molecular epidemiology of American trypanosomiasis in Brazil based on dimorphisms of rRNA and mini-exon gene sequences. *Int. J. Parasitol.* 28, 105–112. doi: 10.1016/S0020-7519(97)00178-1

Conflict of Interest: The authors declare that the research was conducted in the absence of any commercial or financial relationships that could be construed as a potential conflict of interest.

Copyright © 2020 Jansen, Xavier and Roque. This is an open-access article distributed under the terms of the Creative Commons Attribution License (CC BY). The use, distribution or reproduction in other forums is permitted, provided the original author(s) and the copyright owner(s) are credited and that the original publication in this journal is cited, in accordance with accepted academic practice. No use, distribution or reproduction is permitted which does not comply with these terms.



Disruption of Intracellular Calcium Homeostasis as a Therapeutic Target Against *Trypanosoma cruzi*

Gustavo Benaim^{1,2*}, Alberto E. Paniz-Mondolfi^{1,3}, Emilia Mia Sordillo^{3,4} and Nathalia Martinez-Sotillo¹

¹ Instituto de Estudios Avanzados, Caracas, Venezuela, ² Facultad de Ciencias, Instituto de Biología Experimental, Universidad Central de Venezuela, Caracas, Venezuela, ³ Department of Pathology, Molecular, and Cell-Based Medicine, Icahn School of Medicine at Mount Sinai, New York, NY, United States, ⁴ Institute for Health Sciences, Mount Sinai St. Luke's & Mount Sinai West, New York, NY, United States

OPEN ACCESS

Edited by:

Nobuko Yoshida,
Federal University of São Paulo, Brazil

Reviewed by:

Veronica Jimenez,
California State University, Fullerton,
United States

Rubem Figueiredo Sadok
Menna-Barreto,
Oswaldo Cruz Foundation
(Fiocruz), Brazil

*Correspondence:

Gustavo Benaim
gbenaim@gmail.com

Specialty section:

This article was submitted to
Parasite and Host,
a section of the journal
Frontiers in Cellular and Infection
Microbiology

Received: 11 November 2019

Accepted: 24 January 2020

Published: 14 February 2020

Citation:

Benaim G, Paniz-Mondolfi AE,
Sordillo EM and Martinez-Sotillo N
(2020) Disruption of Intracellular
Calcium Homeostasis as a
Therapeutic Target Against
Trypanosoma cruzi.
Front. Cell. Infect. Microbiol. 10:46.
doi: 10.3389/fcimb.2020.00046

There is no effective cure for Chagas disease, which is caused by infection with the arthropod-borne parasite, *Trypanosoma cruzi*. In the search for new drugs to treat Chagas disease, potential therapeutic targets have been identified by exploiting the differences between the mechanisms involved in intracellular Ca^{2+} homeostasis, both in humans and in trypanosomatids. In the trypanosomatid, intracellular Ca^{2+} regulation requires the concerted action of three intracellular organelles, the endoplasmic reticulum, the single unique mitochondrion, and the acidocalcisomes. The single unique mitochondrion and the acidocalcisomes also play central roles in parasite bioenergetics. At the parasite plasma membrane, a Ca^{2+} -ATPase (PMCA) with significant differences from its human counterpart is responsible for Ca^{2+} extrusion; a distinctive sphingosine-activated Ca^{2+} channel controls Ca^{2+} entrance to the parasite interior. Several potential anti-trypanosomatid drugs have been demonstrated to modulate one or more of these mechanisms for Ca^{2+} regulation. The antiarrhythmic agent amiodarone and its derivatives have been shown to exert trypanocidal effects through the disruption of parasite Ca^{2+} homeostasis. Similarly, the amiodarone-derivative dronedarone disrupts Ca^{2+} homeostasis in *T. cruzi* epimastigotes, collapsing the mitochondrial membrane potential ($\Delta\Psi_m$), and inducing a large increase in the intracellular Ca^{2+} concentration ($[\text{Ca}^{2+}]_i$) from this organelle and from the acidocalcisomes in the parasite cytoplasm. The same general mechanism has been demonstrated for SQ109, a new anti-tuberculosis drug with potent trypanocidal effect. Miltefosine similarly induces a large increase in the $[\text{Ca}^{2+}]_i$ acting on the sphingosine-activated Ca^{2+} channel, the mitochondrion and acidocalcisomes. These examples, in conjunction with other evidence we review herein, strongly support targeting Ca^{2+} homeostasis as a strategy against Chagas disease.

Keywords: trypanosomatids, calcium, new drugs candidates, signaling, therapeutic target

INTRODUCTION

At present, there are no approved, highly effective therapies against *Trypanosoma cruzi*. The strategic rationale for current investigative efforts has been directed by consideration of the biological differences between the parasite and the host (mammalian) cells. The basic premise of this approach recognizes that Ca^{2+} is an essential signaling messenger in all eukaryotic cells

studied so far, including trypanosomatids, and that fluctuation of the intracellular Ca^{2+} concentration ($[\text{Ca}^{2+}]_i$) is finely regulated, by diverse mechanisms at the plasma membrane level and by intracellular organelles. It has been extensively demonstrated that the various mechanisms responsible for regulation of $[\text{Ca}^{2+}]_i$ in trypanosomatids differ in many important features, from those in the host counterpart. Disruption of intracellular Ca^{2+} homeostasis by any means is lethal for all mammalian cells, since this is a driver to apoptotic processes or to necrosis (Nicotera et al., 1992), and appears also to be the case in trypanosomatids (Benaim and Garcia, 2011), including *T. cruzi*.

This review will focus on the similarities and differences between the general homeostatic systems responsible for the regulation of the $[\text{Ca}^{2+}]_i$ present in *T. cruzi* and in humans, that promote the ability of anti-trypanosomatid drugs acting on Ca^{2+} homeostasis to selectively cause parasitic death while minimally affecting the human host.

THE REQUIREMENT FOR INTRACELLULAR Ca^{2+} REGULATION IN PRIMORDIAL CELLS AND ITS ROLE AS AN ESSENTIAL SIGNAL IN TRYPANOSOMATIDS

Calcium is the fifth most abundant element on the Earth's crust, and the third most abundant metal (Carafoli and Krebs, 2016). Consequently, from the beginning of life on Earth, cells have had to deal with the presence of high concentrations of calcium, with the added problem that most calcium salts possess low solubility. Similarly, intracellular calcium complicates the choice of phosphate compounds as energy currency and phosphate-based bioenergetics, due to the poor solubility of calcium phosphate salts. This has implications not only for adenosine triphosphate (ATP) as an energy currency, but also for pyrophosphate (PP_i), an important alternative energy coin in *T. cruzi*, as we will discuss below. For this reason, early in evolution cells were forced to develop sophisticated mechanisms to maintain a very low concentration of Ca^{2+} in the cytoplasm (usually below 100 nanomolar). Accordingly, Ca^{2+} has largely been compartmentalized in intracellular organelles, in which its concentration is very similar to the millimolar range encountered outside the cell, i.e., 4 orders of magnitude higher than in the cytoplasm. The extreme difference between the concentration of Ca^{2+} in the cytoplasm and in the exterior *milieu*, is even more remarkable when considered in the context of ionic distributions predicted for other cations by the Nernst equation. The difference between the intracellular and the extracellular concentrations calculated is far larger for Ca^{2+} than for any other ion normally present inside the cells (e.g., Na^+ , K^+ , Mg^{2+} , H^+). Maintaining the difference is associated with a high energy cost. However, throughout evolution, cells have taken advantage of this large Ca^{2+} electrochemical gradient to use it as an essential signaling messenger. The role of Ca^{2+} in cell signaling has been widely recognized in all eukaryotic cells so far studied including *T. cruzi* (Benaim and Garcia, 2011; Docampo and Huang, 2015; Schoijet et al.,

2019). In the next section we will summarize different cell functions regulated either directly or indirectly by Ca^{2+} ions in this parasite.

DIFFERENT PROCESSES REGULATED BY Ca^{2+} IN TRYPANOSOMATIDS

The function of Ca^{2+} as a signaling messenger in trypanosomatids is well-documented (Table 1). For example, in *T. cruzi* and *T. brucei*, Ca^{2+} binding proteins are important for the adhesion of the flagellum to the cell body and for flagellar activity (Maldonado et al., 1997; Docampo and Huang, 2015). In *Crithidia oncopelti*, Ca^{2+} plays a similar role in controlling flagellar activity, the direction of its flagellar wave propagation, and therefore its displacement (Holwill and McGregor, 1976). Specifically, the direction of the wave in the axoneme of *C. oncopelti* has been shown to be dependent on the $[\text{Ca}^{2+}]_i$ (Surgue et al., 1988). A role for calmodulin in determining the wave direction in *C. oncopelti* has also been proposed (Surgue et al., 1988).

Ca^{2+} also plays an important role in the infectivity of several trypanosomatids, by increasing their capacity to invade host-cells. A transient $[\text{Ca}^{2+}]_i$ increase has been observed in trypomastigotes of *T. cruzi* (Yakubu et al., 1994) or amastigotes of *L. amazonensis* during their interaction with the host cell (Docampo and Huang, 2015), and in *L. donovani* during infection of macrophages (Misra et al., 1991). Furthermore, in the case of *T. cruzi*, bloodstream trypomastigotes invade the cells through a set of Ca^{2+} -mediated interactions that trigger a signaling cascade in both the host cell and the parasite (Cortez et al., 2003; Walker et al., 2014). Ca^{2+} signaling through receptors for IP_3 , TcIP_3R , and TbIP_3R (see below) has been shown to modulate proliferation in *T. cruzi* (Docampo and Huang, 2015) and *T. brucei* (Huang et al., 2013), both *in vivo* and *in vitro*, as well as the cellular differentiation of these parasites.

The relationship between invasion by *T. cruzi* trypomastigotes and increased $[\text{Ca}^{2+}]_i$ in the parasite was first demonstrated during *in vitro* infection of L6E9 myoblasts monolayers (Moreno et al., 1994). After association with the myoblasts, parasite $[\text{Ca}^{2+}]_i$ increased from 20–30 to 340 nM; this increase was not observed in parasites that were not associated with myoblasts. Pretreatment of the parasites with Ca^{2+} chelators resulted in up to a 63% decreased in their ability to invade the myoblasts. A similar decrease was observed after addition of the chelating agent ethylene glycol tetraacetic acid (EGTA) to the host cell cultures, reducing the infective capacity of *T. cruzi* to 72 % (Moreno et al., 1994).

The increase in $[\text{Ca}^{2+}]_i$ in the host cell has been attributed to the expression of two glycoprotein membrane receptors expressed at the surface of the metacyclic trypomastigotes, gp82 and, to a lesser extent, the gp35/50 mucin-like protein. These parasites receptors mediate host Ca^{2+} signaling as a result of the contact between *T. cruzi* and the mammalian host cell (Burleigh and Andrews, 1998). Transient changes in $[\text{Ca}^{2+}]_i$ also appear to be necessary for the fusion of the host cell lysosome to the plasma membrane during the invasion of *T. cruzi* (Burleigh and

TABLE 1 | Some Calcium effects in different trypanosomatids.

	References
Microtubule assembly in <i>T. brucei</i>	Dolan et al., 1986; Robinson et al., 1991
Flagellar movements in <i>C. oncopelti</i>	Holwill and McGregor, 1976; Surgue et al., 1988
Flagellar movements in <i>T. cruzi</i> and <i>T. brucei</i>	Maldonado et al., 1997; Docampo and Huang, 2015
Cellular differentiation in <i>H. samuelpessoai</i>	Thomas et al., 1981
Cellular differentiation in <i>T. cruzi</i> and <i>T. brucei</i>	Lammel et al., 1996; Cortez et al., 2003; Walker et al., 2014; Docampo and Huang, 2015;
Cellular differentiation in <i>L. donovani</i>	Morrow et al., 1981
Invasion of the host cell in <i>T. cruzi</i> and other trypanosomatids	Misra et al., 1991; Moreno et al., 1994; Yakubu et al., 1994; Lu et al., 1997; Ruiz et al., 1998; Huang et al., 2013
Macrophage interaction in <i>Leishmania</i> spp.	Moreira et al., 1996; Cunningham, 2002; Dey et al., 2006; Naderer et al., 2011; Walker et al., 2014
Growth and proliferation in <i>L. donovani</i> and <i>T. brucei</i>	Selvapandiyar et al., 2001, 2007; Docampo and Huang, 2015
Nitric oxide transduction pathway in <i>T. cruzi</i>	Paveto et al., 1995
Osmoregulation in <i>T. cruzi</i>	Rohloff et al., 2003
Variant surface glycoprotein (VSG) release in <i>T. brucei</i>	Voorheis et al., 1982
Plasma membrane Ca^{2+} -ATPase (PMCA) in different trypanosomatids	Benaim and Romero, 1990; Benaim et al., 1991, 1993a,b, 1995, 2013; Perez-Gordones et al., 2017; Ramírez-Iglesias et al., 2018
Calmodulin (CaM) in different trypanosomatids	Ruben et al., 1983; Benaim et al., 1987, 1995, 1998; Chung and Swindel, 1990; Benaim and Villalobo, 2002; Salas et al., 2005; Garcia-Marchan et al., 2009; Perez-Gordones et al., 2017
CaM stimulation of cAMP-phosphodiesterase in <i>T. cruzi</i>	Téllez-iñón et al., 1985
Ca^{2+} -CaM Dependent protein kinase in <i>T. cruzi</i>	Ogueta et al., 1994, 1996, 1998
Calcium-stimulated adenylyl cyclase	D'Angelo et al., 2002
Flagellar Ca^{2+} binding protein	Engman et al., 1989

Andrews, 1998). Furthermore, activation of the parasite tyrosine kinase proteins (PTK), which is also Ca^{2+} -dependent, is involved in the internalization of *T. cruzi* in the host cell; while inhibition of parasite PTK activity decreases phosphorylation of the 175-kDa protein (p175) halting the ability of the parasites to enter the cells (Yoshida et al., 2000).

In *Leishmania* sp. a prolonged increase in the parasite $[\text{Ca}^{2+}]_i$, after invasion of mammalian cells, can trigger events that lead to parasite death by apoptosis (Moreira et al., 1996; Naderer et al., 2011). The uptake of Ca^{2+} by the parasite's organelles is essential for its thermotolerance between 34 and 37°C, the temperature within the host cell. In addition, it has been suggested that the entry and regulation of Ca^{2+} and calcineurin signaling are necessary for the early and long-term adaptive responses of the parasite to environmental stressors found in the mammalian host (Naderer et al., 2011).

There is also evidence that Ca^{2+} signaling influences the differentiation of *T. cruzi* epimastigotes into metacyclic trypomastigotes through changes in cytosolic Ca^{2+} observed during this process (Lammel et al., 1996; Docampo and Huang, 2015). Ca^{2+} signaling participates in cell differentiation in *Herpetomona samuelpessoai* in a similar fashion (Thomas et al., 1981). Likewise, changes in the cytosolic Ca^{2+} levels are observed during the differentiation of the procyclic stages of *T. brucei* in the bloodstream (Walker et al., 2014).

In *L. donovani*, Ca^{2+} signaling has been shown to participate in the differentiation of the amastigote stage to promastigote (Morrow et al., 1981). Also in *L. donovani*, its cysteine Ca^{2+} -dependent protease caldonopain, a relative of calpain, has been shown to have a key role in catabolism, endogenous protein

processing, cell invasion, and other biological actions (Dey et al., 2006). Moreover, these proteases are involved in the host-parasite interaction. The proteolytic activity of cytosolic caldonopain has been shown to be elevated in the presence of Ca^{2+} at the time of infection, and has been demonstrated to be involved in the metabolic turnover of intracellular proteins. Caldonopain activity may be essential for parasite survival during infection, to maintain intracellular Ca^{2+} homeostasis, and may play an important role in the signal transduction pathway (Dey et al., 2006).

One way in which promastigotes of *L. donovani* have been found to evade host defenses is by inhibiting fusion between the host cell phagosome and the endosome. The promastigotes alter their lipophosphoglycans molecules (LPG) by reducing the fusogenic properties of the membrane (Cunningham, 2002). In general, LPG, which is highly expressed on the surface of metacyclic promastigotes, interferes with the insertion of the membrane attack complex, and promastigote specific kinases deactivate the classical complement pathway (Walker et al., 2014). Once the parasite has passed into its amastigote phase, chelation of Ca^{2+} by LPG acts to protect the parasite within the phagolysosome. Ca^{2+} can bind to LPG repeating units near phosphate groups without altering glycan structure and the altered Ca^{2+} mobilization can lead to disturbed signal transduction, which in turn can drive defective PKC activation, thus increasing survival (Cunningham, 2002).

Cell growth and proliferation also appear to correlate with the parasite $[\text{Ca}^{2+}]_i$. In *L. donovani*, the centrins, which are Ca^{2+} -binding proteins, directly influence the rate of parasite growth, which is exponential when parasite $[\text{Ca}^{2+}]_i$ is high, and

stationary when the level is low. Of note, parasite knockout mutants lacking centrin show selective growth arrest of axenic amastigotes but not promastigotes (Selvapandiyan et al., 2001). In *T. brucei* centrins are involved in the segregation of organelles, coordination of nuclear and cellular division, and flagellar motility (Selvapandiyan et al., 2007; Docampo and Huang, 2015). On the other hand, *T. brucei* possesses an inositol 1,4,5-trisphosphate receptor (TbIP₃R) in its acidocalcisomes involved in the Ca²⁺ signaling pathways. It has been shown that the presence of this receptor is necessary for the growth and establishment of infection of these organisms (Huang et al., 2013).

In *T. brucei*, the presence of Ca²⁺ is required for firm attachment of the microtubule-associated protein (MAP) p41 to the cytoskeleton, as well as for successful assembly of dimers and microtubular assembly. Even though p41 is normally found bound to cytoskeleton and preassembled microtubules of trypanosome tubulins, it remains tightly bound when calcium ions are present (Robinson et al., 1991). It has been known that Ca²⁺ initiates selective and complete depolymerization of the microtubules of *Trypanosoma brucei*, which supports the fact that this cation actively participates in the microtubular assembly (Dolan et al., 1986).

In addition, Ca²⁺ signaling also participates in osmoregulation in *T. cruzi* (Docampo and Huang, 2015), and in the transduction routes of nitric oxide in *T. cruzi* (Paveto et al., 1995). Ca²⁺ also plays an important role in the variant surface glycoproteins (VSG) release in *T. brucei* (Voorheis et al., 1982).

INTRACELLULAR Ca²⁺ REGULATION IN HUMAN CELLS AND CRITICAL DIFFERENCES WITH RESPECT TO *TRYPANOSOMA CRUZI*

Trypanosoma cruzi parasites must confront extreme changes in the extracellular Ca²⁺ concentration during different life cycle stages. In epimastigotes and trypomastigotes inside the insect host, the extracellular Ca²⁺ concentration is in the millimolar range, but for the amastigotes inside cardiac muscle cells this concentration falls well-below the submicromolar range. In eukaryotic cells, in general, intracellular Ca²⁺ regulation is a *conditio sine qua non* for the function of this cation as a signaling molecule, being achieved by the concerted participation of several mechanisms located in intracellular organelles and at the plasma membrane.

Among the organelles in mammals, the endoplasmic reticulum and the mitochondria have central roles in reestablishing submicromolar Ca²⁺ levels in the cytoplasm, after any transient increases. In *T. cruzi*, there is, in addition, another very important system, the acidocalcisomes. Acidocalcisomes are acidic vacuoles loaded with Ca²⁺, polyphosphates and other ions, that are essential for viability in trypanosomatids, but which are only present in specialized cells (e.g., platelets, mast cells, basophils) in humans (Patel and Docampo, 2010; Huang et al., 2014). Accordingly, the acidocalcisomes are considered as

a potential target for the action of drugs against these parasites (see below) (**Figure 1**). Mitochondria are able to accumulate Ca²⁺ in large quantities, through a so-called mitochondrial Ca²⁺ uniporter (MCU) that utilizes the electrochemical H⁺ gradient across the internal mitochondrial membrane (De Stefani et al., 2011) to dissipate energy as Ca²⁺ is accumulated (**Figure 1**). This MCU is widely conserved throughout evolution, being present in all mitochondria so far described, including the trypanosomatid single unique mitochondrion (Docampo and Vercesi, 1989; Benaim et al., 1990). The low affinity of the MCU for Ca²⁺ is such that for a long time it was not included as a true Ca²⁺ regulator. Instead, it was presumed to function as an import mechanism to fulfill the demands for Ca²⁺ of at least three different mitochondrial dehydrogenases. However, by utilizing the mitochondrial-targeted aequorin, a protein that emits light when bind to Ca²⁺, it was clearly demonstrated that the mitochondria indeed participate in Ca²⁺ signaling, not only in mammals (Rizzuto et al., 1992; Pozzan et al., 2003) but also in trypanosomatids (Xiong et al., 1997; Ramakrishnan and Docampo, 2018), since this organelle was able to flash when a particular signal increased the parasite [Ca²⁺]_i. The explanation for these observations is that some mitochondria can physically approach Ca²⁺ channels in particular *loci* inside the cell, below the plasma membrane and near certain organelles where the locally-released Ca² can reach concentrations compatible with the low affinity of the MCU (Benaim et al., 1990). This fact has allowed the triumphal return of the mitochondria to the signaling scenario. More recently, two subunits of the *Trypanosoma cruzi* MCU complex containing canonical EF hand domains (MICU1 and MICU2), have been studied by the use of the CRISPR/Cas9 system, demonstrating that albeit their overexpression does not significantly affect mitochondrial Ca²⁺ uptake, their ablation has a large effect on the cation uptake by the mitochondria supporting their role in the stabilization of the MCU complex (Bertolini et al., 2019). In the case of *T. brucei*, the MCU complex was found to possess two additional subunits not found in mammals named TbMCUc and TbMCUd, which are essential for mitochondrial Ca²⁺ uptake (Huang and Docampo, 2018). These two units have been identified and characterized in *T. cruzi* (TcMCUc and TcMCUd). By the use of the CRISPR/Cas9 system it has been shown that overexpression of these genes drives an increase of mitochondrial Ca²⁺ uptake. Conversely, knockout of any of these genes leads to a loss of Ca²⁺ uptake, although the mitochondrial membrane potential is maintained (Chiurillo et al., 2019). Since TcMCUc and TcMCUd are not present in mammals and are of significant importance in several functions in *T. cruzi*, mainly related to its bioenergetics, they represent an attractive alternative drug target against these parasites (Chiurillo et al., 2019).

The advanced application of the CRISPR/Cas9 system to investigation of *T. cruzi* biology (Lander and Chiurillo, 2019) has enormously facilitated the finding and characterization of many proteins in these parasites. The recent identification in *T. cruzi* of a mitochondrial pyruvate dehydrogenase phosphatase (TcPDP) that is sensitive to physiological Ca²⁺ concentration and is able to stimulate the activity of a mitochondrial pyruvate dehydrogenase, stimulating energy metabolism through the

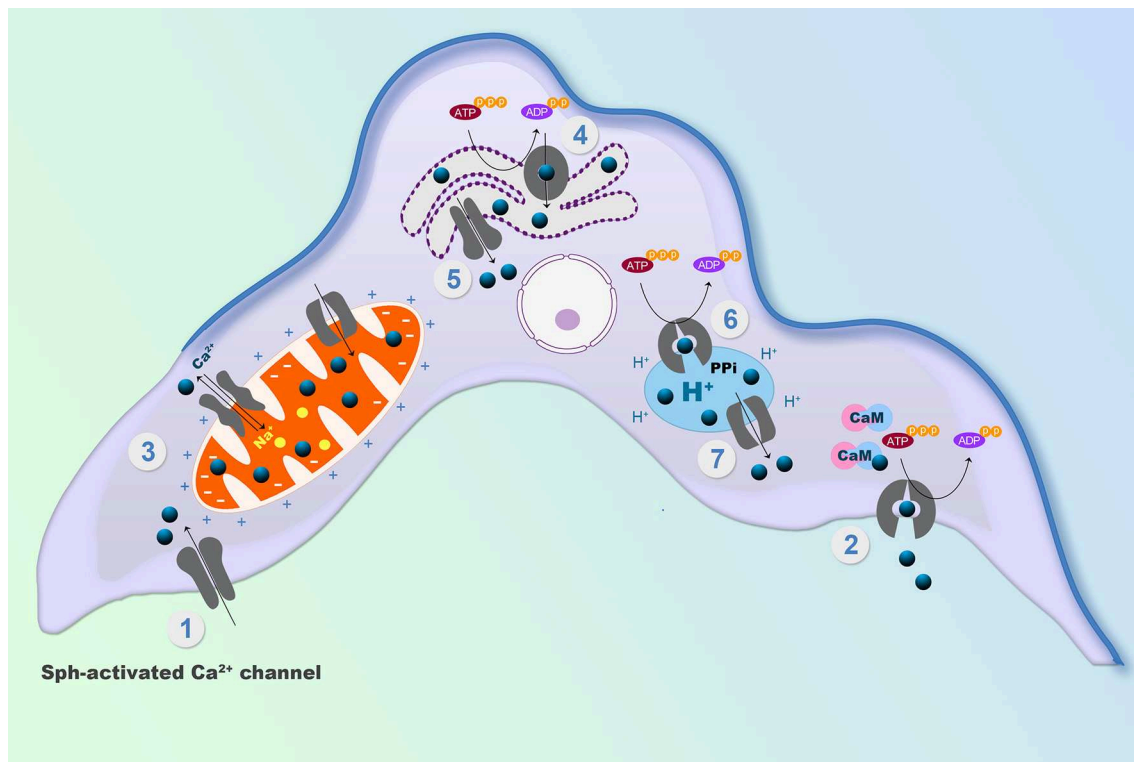


FIGURE 1 | Schematic representation of the mechanisms involved in the intracellular Ca^{2+} regulation in *Trypanosoma cruzi*. (1) Sphingosine-activated Ca^{2+} channel, responsible for Ca^{2+} entry. (2) Calmodulin-regulated plasma membrane Ca^{2+} Pump, responsible for Ca^{2+} extrusion. (3) Mitochondrial Ca^{2+} Uniporter (MCU) and a $\text{Na}^+/\text{Ca}^{2+}$ exchanger at the unique parasit mitochondrion. (4) SERCA type Ca^{2+} Pump at the endoplasmic reticulum and (5) a Ca^{2+} channel for Ca^{2+} release. (6) A PMCA type Ca^{2+} -ATPase, responsible for Ca^{2+} accumulation in acidocalcisomes and (7) an IP_3 Receptor for Ca^{2+} release from the acidocalcisomes to the cytoplasm (See text for detailed explanations).

Krebs cycle activation, has provided further insight into the role of Ca^{2+} in *T. cruzi* bioenergetics (Lander et al., 2018). The activity of this enzyme was demonstrated to be required for *T. cruzi* growth, differentiation, and infectivity (Lander et al., 2018).

The endoplasmic reticulum possesses a Ca^{2+} pump, the sarco(endo)plasmic reticulum Ca^{2+} -ATPase (SERCA) that accumulates large amounts of Ca^{2+} by transporting the cation at the expense of ATP hydrolysis, and has high Ca^{2+} affinity (Benaim and Garcia, 2011), enabling a high Ca^{2+} concentration inside this organelle, similar to the extracellular milieu (i.e., around 2 mM) (Figure 1).

The activity of the SERCA in mammalian cells is inhibited by thapsigargin and cyclopiazonic acid, and also by the sphingolipid sphingosine (Benaim et al., 2016). In *T. cruzi*, a Ca^{2+} -ATPase (TcSCA) that localizes at the endoplasmic reticulum (ER), has been partially characterized (Furuya et al., 2001), and shown to possess several sequence motifs found in SERCA. Although TcSCA can be inhibited by cyclopiazonic acid, thapsigargin fails to inhibit the enzyme (Furuya et al., 2001); the effect of sphingosine has not been studied so far. In mammals, there are at least two Ca^{2+} channels in the ER, the IP_3 Receptor (IP_3R) and the Ryanodine receptor (RyR, more predominant in excitable cells), that allow the Ca^{2+} release to the cytoplasm when they are opened by a particular signal. The activity

of IP_3R is modulated by IP_3 , the product of the hydrolysis of PIP_2 by several isoforms of PLC (Furuichi et al., 1989). By contrast, addition of IP_3 fails to cause Ca^{2+} release in *T. cruzi*, although the machinery for the synthesis of IP_3 has been well documented in trypanosomatids (Docampo and Pignataro, 1991). Interestingly, in trypanosomatids, the IP_3 receptor appears to be present in acidocalcisomes (see below). These organelles possess several different transporters, pumps and exchangers, for the accumulation of Ca^{2+} and other cations, such as a Vacuolar type H^+ -ATPase, a Ca^{2+} -ATPase similar to that found at the plasma membrane (PMCA), as well as other distinct Ca^{2+} transport mechanisms (Huang et al., 2014). Notably, acidocalcisomes possesses a proton pumping pyrophosphatase (H^+ -PPase) that allows the accumulation of H^+ , and hence the acidification of this organelles. The name of the organelle is derived from this capability, together with its capacity for Ca^{2+} accumulation (Docampo and Huang, 2015). Acidocalcisomes possess large amounts of orthophosphate (P_i), polyphosphates and particularly pyrophosphate (PP_i), which is particularly important for *T. cruzi*, and other trypanosomatids and apicomplexan parasites (e.g., *Plasmodium spp.*).

In contrast to their human hosts, which are dependent on hydrolysis of ATP, these parasites can use PP_i , which has essentially the same free energy of hydrolysis of ATP,

as an alternative energy currency (Docampo and Huang, 2015). Of course, this difference has been exploited in the development of a possible pharmaceutical target against Chagas disease, by the use of bisphosphonates, a group of molecules that are able to selectively inhibit pyrophosphatases (Montalvetti et al., 2001). Interestingly, H^+ -PPases have also been found at the plasma membrane and in the Golgi apparatus (Martínez et al., 2002), where the pyrophosphate analogs aminomethylenediphosphonate and imidodiphosphate block the acidification of plasma membrane vesicles in *T. cruzi*. This evidence demonstrates, as expected, that H^+ -PPases are not localized solely to acidocalcisomes, but are present in other *loci* that may utilize PPi as an energy source.

Substantial recent experimental evidence in *T. cruzi* supports localization of the IP_3R in the acidocalcisome and not at the ER. Furthermore, experiments with CRISPR/Cas9 and other techniques (Lander et al., 2016) have demonstrated that the parasite IP_3R is fully functional when IP_3 is present. This receptor (Tc IP_3R) has been cloned, expressed, and associated with proliferation, differentiation virulence, and infectivity (Hashimoto et al., 2013), by the K. Mikoshiba Group, who first discover the IP_3R (Furuichi et al., 1989). In that work immunofluorescent labeling was used to demonstrate the localization of this receptor to the ER, as for mammalian cells. However, it appears that observation may have been the result of over-expression, since the use of the CRISPR/Cas9 system for C-terminal tagging of genes in *T. cruzi* (Lander et al., 2016) allows the confirmation of acidocalcisomes as the organelles where IP_3R was indeed present. The localization of this receptor in acidocalcisomes and the contractile vacuole complex, together with the differences in sequences, emphasizes an essential distinction between *T. cruzi* and its human counterpart that could be a useful consideration for a rational therapeutic development.

Because IP_3R -mediated Ca^{2+} signaling is key to a plethora of cellular events in *T. cruzi* such as transformation and replication in its various developmental stages the potential use of receptor antagonists requiring this Ca^{2+} signaling cascade as well as Tc IP_3R inhibitors could emerge as potential therapeutic targets that could be of benefit from a clinical standpoint. Comparisons amongst human and *T. cruzi* IP_3R s primary structure may assist in identifying other likely inhibitory compounds by high-throughput or virtual screening of chemical libraries (Hashimoto et al., 2013).

The endoplasmic reticulum, the mitochondrion and acidocalcisomes act in concert whenever an elevation of the $[Ca^{2+}]_i$ has occurred, necessitating their participation to return the concentration to the cytoplasmic basal level. However, the capacity of these organelles is limited by their volume as compartments. Thus, the mechanisms of Ca^{2+} regulation located at the plasma membrane are responsible for the long-term regulation of the $[Ca^{2+}]_i$, since they, in principle, are able to extrude Ca^{2+} against a virtually infinite space (Figure 2). At the plasma membrane of human cells there are only two mechanisms described for Ca^{2+} extrusion, a Na^+/Ca^{2+} exchanger present mainly in excitable cells, and a plasma membrane Ca^{2+} -ATPase (PMCA), which has been identified in all eukaryotic cells so far

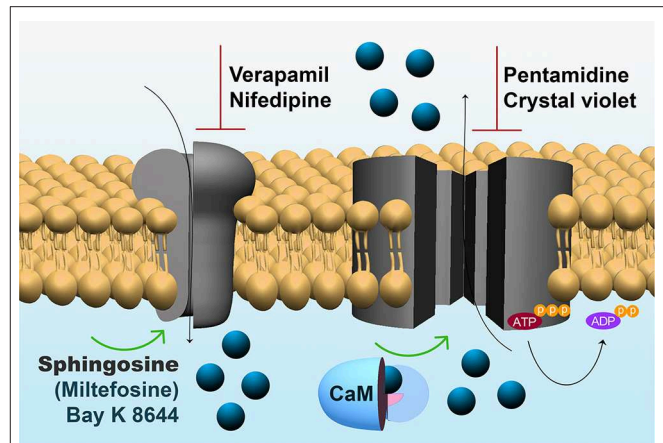


FIGURE 2 | Expanded model of Ca^{2+} regulating mechanisms within the parasites plasma membrane. **Left:** The sphingosine-stimulated Ca^{2+} channel, where the activation by Bay K 8466 and miltefosine and the inhibition by nifedipine and verapamil are depicted. **Right:** The CaM-stimulated PMCA, where the inhibition by pentamidine and crystal violet are shown (See text for explanations).

described, including *T. cruzi* (Benaim et al., 1991). Attempts to identify a Na^+/Ca^{2+} exchanger in trypanosomatids have been unsuccessful (Benaim et al., 1993a; Docampo and Huang, 2015), supporting the ubiquitousness of the PMCA. This Ca^{2+} pump has a very high affinity for Ca^{2+} , and is stimulated by calmodulin (CaM), the also ubiquitous Ca^{2+} -binding protein, present in all eukaryotic cells (Benaim and Villalobo, 2002). CaM increases the affinity of the enzyme for Ca^{2+} and ATP, also raises its V_{max} by a very well-known mechanism in humans (Benaim et al., 1984). This Ca^{2+} -sensing protein binds to an auto-inhibitory CaM-binding domain removing it from the active site, thus increasing its affinity for their substrates, Ca^{2+} and ATP (Benaim et al., 1984). In *T. cruzi* the PMCA also has been identified (Benaim et al., 1991), isolated by mean of a CaM-affinity column and partially characterized (Benaim et al., 1995), but appears to diverge from its human counterpart at the CaM-binding domain (Figure 2). Albeit the CaM-binding domain in *T. cruzi* PMCA (TcCa1) has not been characterized fully, recent studies on *Trypanosoma equiperdum* (a *T. brucei*-related hemoflagellate parasite that causes infection in cattle), have demonstrated that the CaM-binding domain of the PMCA of *T. equiperdum* possesses a non-canonical sequence (Perez-Gordones et al., 2017; Ramírez-Iglesias et al., 2018). This Ca^{2+} -ATPase contains a 28 amino acid-region in the C-terminal tail that has been proposed to assume an α -helix conformation within a 1–18 (Trp-1, Phe-18) CaM binding motif (Perez-Gordones et al., 2017). Another difference is that unlike CaM in human cells, which interacts with the CaM-binding domain solely with the C-terminal half (78–148 aa) of the PMCA protein (Guerini et al., 1984), *T. equiperdum* CaM appears to wrap the CaM-binding domain of the parasite PMCA (Perez-Gordones et al., 2017; Ramírez-Iglesias et al., 2018). The sequence of the CaM-binding domain of *T. equiperdum* is very similar to that present in the

in the *T. cruzi* PMCA, suggesting that with all likelihood, the characterization performed on the enzyme from *T. equiperdum*, can be extrapolated to the *T. cruzi* PMCA. In fact, the CaM-Binding domain from *T. cruzi* PMCA, albeit bearing a 1–17 CaM binding motif instead of the 1–18 motif present in *T. equiperdum* (since there is a gap by the lack of one amino acid), can still form an α -helix predicted to be able to bind CaM (G. Benaim, unpublished observations).

The differences between human and *T. cruzi* CaM deserve special consideration, given that this ubiquitous Ca^{2+} binding protein has been highly-conserved in eukaryotes, with trypanosomatids being a remarkable exception. Although vertebrate and trypanosomatid CaMs all have 148 amino acids, and the structure of CaM is identical in all vertebrates, there are 16 amino acid substitutions between *T. cruzi* CaM when compared to vertebrate CaM (~89 % homology) (Garcia-Marchan et al., 2009). Trypanosomes contain three genes tandemly repeated for CaM, and this protein is highly expressed in these parasites (Chung and Swindel, 1990). We have calculated, based on an estimated volume of the *T. cruzi* epimastigote, and based on the assumption that the quantity of CaM obtained in the purification procedure is fully conservative (i.e., All the CaM from the batch was isolated), that the CaM concentration in trypanosomatids is about $2\ \mu\text{M}$ (Benaim, G. Unpublished observations). This concentration is similar to that found in the mammalian tissues (i.e., brain and testis) in which the highest concentrations of this Ca^{2+} -binding protein are found, emphasizing the critical importance of this protein in *T. cruzi*.

Vertebrate CaM is characterized by a Ca^{2+} -shift when run on SDS-PAGE in the presence or absence of the calcium chelator EGTA (i.e., with or without Ca^{2+}). This trademark of CaM is probably due to the increase in the α -helix content and the concomitantly increase in the hydrophobic character of the protein, or the acquisition of a more globular shape, even in the presence of SDS (Garcia-Marchan et al., 2009). Similarly, a Ca^{2+} -shift also has been observed in *T. cruzi* CaM. However, albeit possessing the same molecular mass as the vertebrate CaM, *T. cruzi* CaM migrates more to the anode (lower apparent molecular mass), likely due to its more hydrophobic character. This is concordant with circular dichroism studies, which have confirmed that in the presence of Ca^{2+} the α -helix content of *T. cruzi* CaM is increased in comparison to mammal CaM (Garcia-Marchan et al., 2009).

At present, the full significance of these differences in the molecular structure of this important protein is not known. As mentioned, CaM is able to stimulate the *T. cruzi* PMCA; the affinity of the human PMCA for CaM is slightly lower than for *T. cruzi* CaM. In addition, the CaM-anatagonists trifluoperazine and calmidazolium, have been shown to have less inhibitory activity when the PMCA is stimulated by the *T. cruzi* CaM when compared to rat CaM (Garcia-Marchan et al., 2009). These findings raise the possibility that there is a still-undiscovered CaM target in this parasite that could reflect the prominent differences in structure encountered between the *T. cruzi* and vertebrate proteins.

On the other hand, it has been demonstrated that CaM phosphorylation may vary based on its target enzyme (Benaim

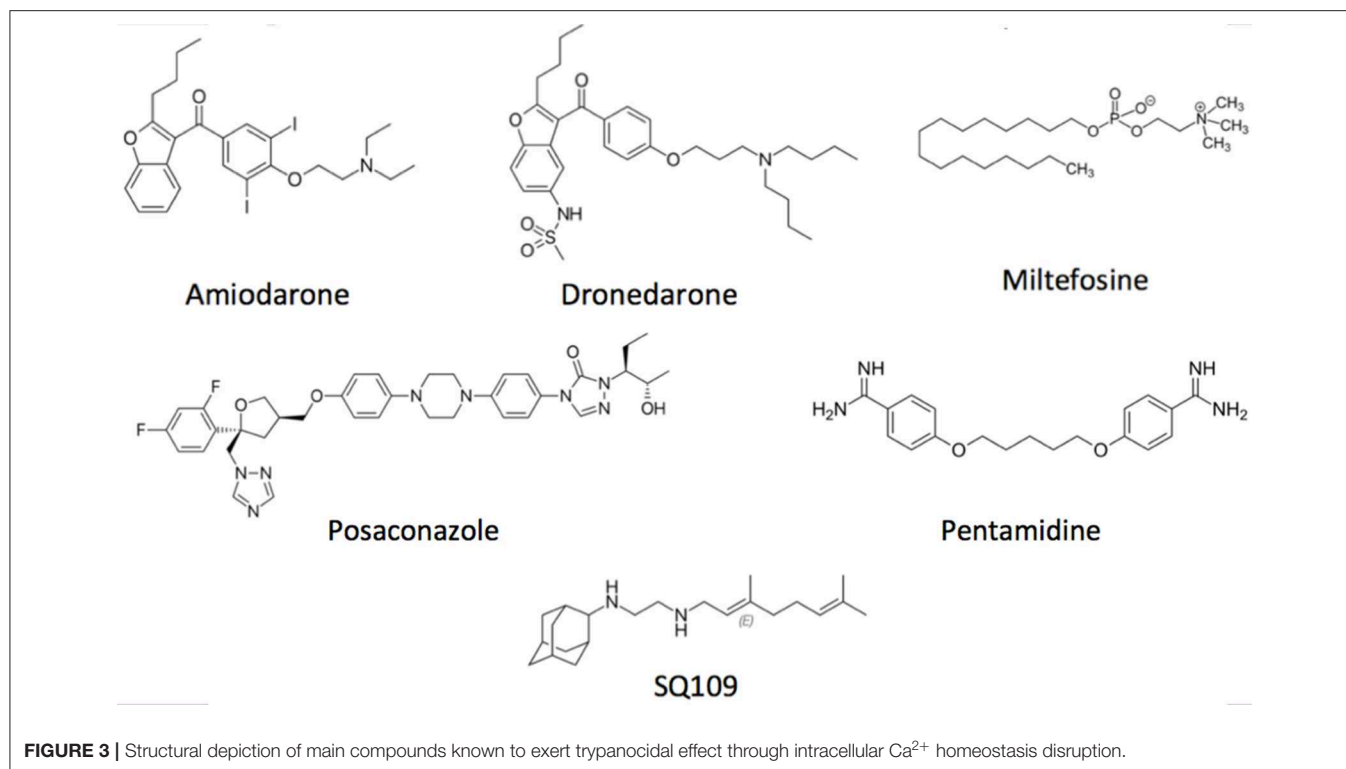
and Villalobo, 2002; Salas et al., 2005). The composition of phosphorylatable aminoacids in *T. cruzi* CaM differs significantly from its vertebrate counterpart. For example, vertebrate CaM bears four serine and 12 threonine residues, whereas *T. cruzi* CaM contains nine serine and nine threonine residues; thus, varying the pattern of phosphorylation of this protein when phosphorylated by the epidermal growth factor receptor (EGFR) in its known preference for Tyr motifs.

Given that *T. cruzi* CaM possesses only one tyrosine (Tyr-138) residue lacking the Tyr-99 motif, the main target of the EGFR, low-level phosphorylation occurs, as opposed to phosphorylation on serines and or threonines, which are significantly larger *T. cruzi* CaM when compared to that of vertebrates (Benaim et al., 1998). How this finding may affect CaM activity and its possible functional repercussion on the parasites physiology is a point that deserves further investigative attention.

The mechanism responsible for Ca^{2+} entry in *T. cruzi* has been discovered just recently (Figure 1). A sphingosine-stimulated plasma membrane Ca^{2+} -channel similar to that described in *L. mexicana* (Benaim et al., 2013) has been reported (Rodriguez-Duran et al., 2019), and characterized electrophysiologically by Patch Clamp techniques (Figure 2). This Ca^{2+} channel shares some characteristics with the human L-Type Voltage gated Ca^{2+} channel (VGCC), including inhibition by the VGCC blocker nifedipine, a dihydropyridine, and activation by Bay K8644, but differs from the L-type VGCC in its activation by sphingosine. Although there seems to be homology with the human orthologue VGCC, the *T. cruzi* channel differs in that it appears not to be voltage-dependent. Another remarkable difference from its human orthologue is its stimulation by miltefosine, a unique oral drug approved against visceral leishmaniasis, and also of potential use against Chagas disease (see below).

TARGETING INTRACELLULAR Ca^{2+} HOMEOSTASIS AS A STRATEGY AGAINST CHAGAS DISEASE

Concerning the main goal of this review, there are several drugs that produce their trypanocidal effect through disruption of parasite Ca^{2+} homeostasis. Amiodarone (Figure 3), a commonly used antiarrhythmic, has been shown to exert a potent effect directly on *T. cruzi*, by inducing a large increase in the $[\text{Ca}^{2+}]_i$ (Benaim et al., 2006). This effect was shown to be mediated by the release of the cation from intracellular compartments, since the effect was independent of the presence of calcium in the extracellular milieu. It was demonstrated that amiodarone acts directly on the mitochondrion, collapsing the electrochemical membrane potential of the parasite without affecting the host cell. This in turn induces rapid Ca^{2+} release to the cytoplasm (Benaim et al., 2006). Amiodarone also affects the acidocalcisomes, by inducing alkalinization, concomitantly with Ca^{2+} release. In concert, these effects induce the large intracellular Ca^{2+} elevation observed when *T. cruzi* is exposed to amiodarone. Similar results have been observed when dronedarone (Figure 3), another benzofuran derivative, was added instead of amiodarone to *T. cruzi* (Benaim et al., 2012).



Dronedarone, which was synthesized to overcome the adverse effects of amiodarone due to the presence of iodine in its structure and its extremely hydrophobic character, also appears to be even more effective than amiodarone *in vitro* against *T. cruzi*. The effect of dronedarone on the *T. cruzi* mitochondrion and acidocalcisomes was more rapid than that of its predecessor amiodarone, and also resulted in a lower IC_{50} ($0.75 \mu\text{M}$) than did amiodarone (IC_{50} $2.7 \mu\text{M}$) when determined on amastigotes inside mammalian host cells, the clinically relevant phase of the parasite (Benaim and Paniz-Mondolfi, 2012; Benaim et al., 2012). Interestingly, both antiarrhythmic were also very effective against *Leishmania mexicana*, a common causative agent of cutaneous leishmaniasis in the New World, demonstrating a very low IC_{50} on amastigotes inside macrophages (Serrano-Martín et al., 2009a,b; Benaim et al., 2014).

Importantly, amiodarone, when used in combination with miltefosine, induced parasitological cure of mice infected with *L. mexicana* (Serrano-Martín et al., 2009b). In cardiomyocytes, amiodarone directly acts on the recovery of F-actin fibrillar organization, connexin43 distribution, and the recovery of spontaneous contractility in *T. cruzi*-infected cardiac myocytes, simultaneously with the eradication of the infection (Adesse et al., 2011), further explaining and supporting the benefits of this drug *in vivo*. Amiodarone has been used successfully in a few cases for compassionate treatment of severe Chagas Disease in humans (Paniz-Mondolfi et al., 2009). Recently, evidence for the effectiveness of amiodarone *in vivo*, has been reported in a study trial including 105 infected privately-owned and military working dogs at Lackland Air Force Base in

Texas (USA) (Madigan et al., 2019) in which a combination treatment of amiodarone and itraconazole –an ergosterol synthesis inhibitor– was used. In this trial survivability of treated canines increased to 95.3%, compared to 53% of untreated controls. Concomitantly, treated dogs experienced 98.2% clinical improvement, compared to 27% of controls (Madigan et al., 2019). Notably, amiodarone has already proved beneficial for suppression of complicated ventricular arrhythmias in chagasic patients. In fact, amiodarone's proven efficacy when combined with benznidazole was demonstrated in the BENEFIT trial (Morillo et al., 2015), albeit apparently overlooked.

Reported amiodarone cardiotoxicity is not related to Ca^{2+} homeostasis but rather to blockade of potassium channels, which may lead to significant bradycardia and marked prolongation of the QT interval, and ultimately to the induction of polymorphic ventricular arrhythmias (Colunga-Biancatelli et al., 2019). Nevertheless, such events are very rare and usually multifactorial, with amiodarone still exhibiting the lowest pro-arrhythmic action when compared to other antiarrhythmic agents. Allelic variants of the coding region of congenital long QT syndrome have been reported in up to 15% of patients with amiodarone induced QT prolongation, thus suggesting the role of a distinct predisposing genetic background (Hoffmann et al., 2012). Of note, amiodarone has been shown to contribute to full cardiomyocyte structural and functional recovery after treatment (Adesse et al., 2011). The restoration of connexin43 expression and distribution, and of spontaneous contractility in cardiomyocytes (Adesse et al., 2011) translates clinically into reduction of arrhythmogenic events. Altogether, these findings

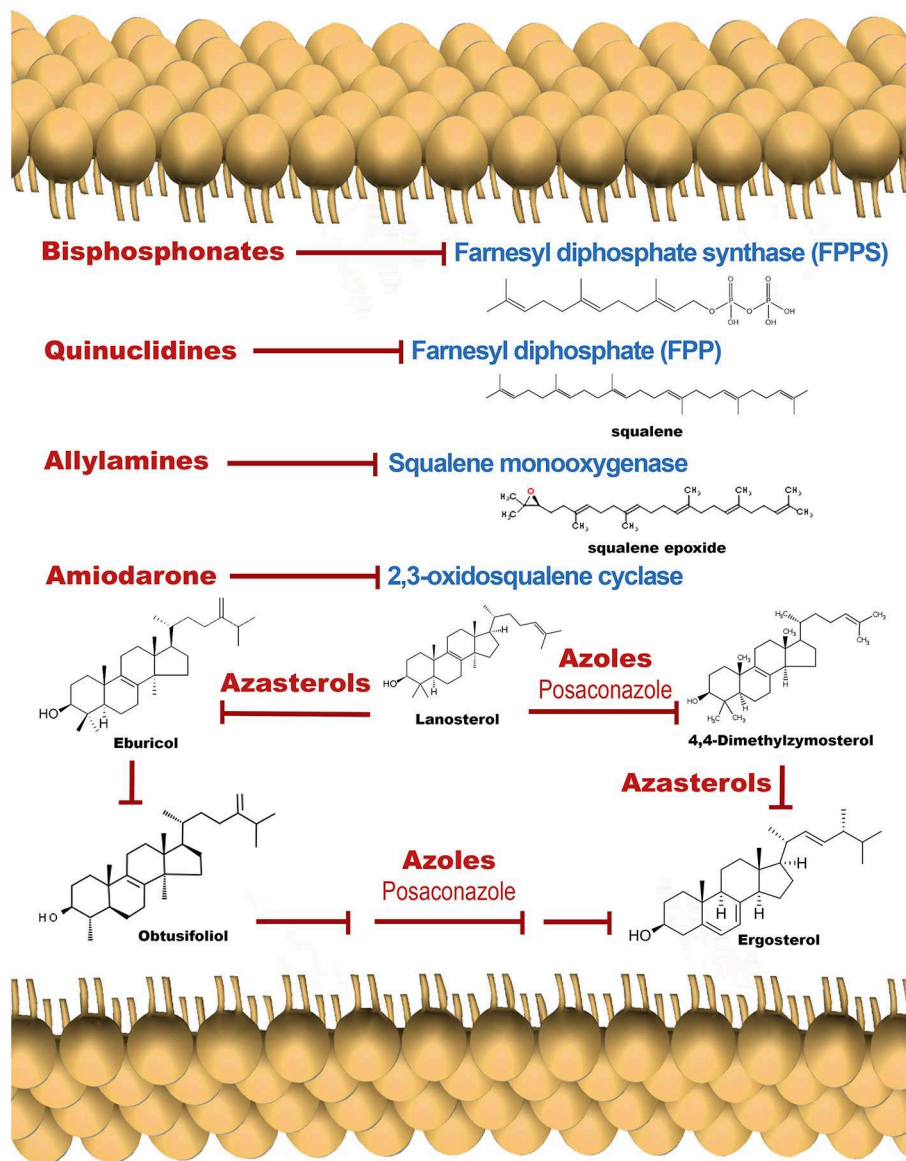


FIGURE 4 | Schematic representation of the ergosterol synthesis pathway, showing target points for the main inhibitors.

support further clinical evaluation of amiodarone as a potential treatment for Chagas disease.

More recently, a new benzofurane derivative with a construction design based on amiodarone's structure (Amioder) has been shown to display a potent effect on epimastigotes and cell-infected amastigotes from *T. cruzi* (Pinto-Martinez et al., 2018a). As expected, the mechanism of action, was similar to that of amiodarone, causing increased the $[Ca^{2+}]_i$, collapsing the electrochemical membrane potential of the mitochondrion, and alkalinizing the acidocalcisomes of the parasite. The same overall effect was also recently found by Amioder on *L. donovani* (Martinez-Sotillo et al., 2019).

Posaconazole (**Figure 3**), an inhibitor of ergosterol synthesis (**Figure 4**) acting on the enzyme C14- α -demethylase, and

already approved as antimycotic, has also shown to exert a dramatic effect on *T. cruzi*, and has proven effective in humans treated under compassionate use. In one case, a woman with systemic erythematosus lupus who developed acute Chagas disease during immunosuppressive treatment (methylprednisolone, prednisone, and cyclophosphamide), was successfully treated with posaconazole (Pinazo et al., 2010). On the other hand, experimentally, posaconazole has shown to dramatically increase the basal intracellular Ca^{2+} levels in epimastigotes from *T. cruzi*, provided that the parasites have been allowed to be depleted of endogenous ergosterol, by incubation for 96 h in the presence of 12.5 nM of the drug (Benaim et al., 2006). Therefore, posaconazole can also be included as a potential emerging antichagasic drug that acts

by perturbation of the intracellular Ca^{2+} homeostasis. However, despite displaying significant antitrypanosomal activity, results from the CHAGASAZOL trial indicated that the use of posaconazole resulted in a larger percentage of treatment failures than benznidazole (Molina et al., 2014). Benznidazole monotherapy was also shown to be superior to posaconazole in the STOP-CHAGAS trial (Morillo et al., 2017). Nevertheless, results of these trials should be examined carefully in the context of dosage, duration of treatment, and the nature of infecting parasite strain, since it has been demonstrated that these factors can influence treatment outcome. Dose adjustment and the use of novel delayed-release formulations with increased and sustained bioavailability will largely and positively influence treatment efficacy in future and ongoing trials (Urbina, 2017). By contrast, treatment with high dose posaconazole (400 mg BID) has proved successful for treatment of cutaneous leishmaniasis caused by *L. infantum* in a human patient (Paniz-Mondolfi et al., 2011).

Interestingly, pentamidine (**Figure 3**), an aromatic diamidine compound introduced in 1940s is also frequently used for treating Sleeping Sickness caused by *T. brucei*, as well as leishmaniasis. Use of pentamidine has been also suggested for Chagas disease, since it blocks the transport of putrescine, a precursor of trypanothione in trypanostomids (Díaz et al., 2014). Among the multiple functions attributed to this drug in these parasites, pentamidine is able to selectively inhibit the plasma membrane Ca^{2+} -ATPase (PMCA) activity and its associated Ca^{2+} transport in *T. brucei* (Benaim et al., 1993b), without affecting its human homologue enzyme. Instead, this drug behaves as a poor CaM antagonist (Benaim et al., 1993b).

Very similar results have been obtained by the use of crystal violet. This compound, a triphenylmethane dye has been described as effective against *T. cruzi* trypomastigotes in blood. Therefore, it has been used in some endemic areas in attempts to eliminate blood transmission of Chagas disease. Although it has been postulated to act through several mechanisms of action, crystal violet disrupts the Ca^{2+} homeostasis in *T. cruzi* epimastigotes and trypomastigotes, first by acting directly on the PMCA activity and its related Ca^{2+} transport, secondly dissipating the mitochondrial membrane potential with the concomitant release of Ca^{2+} , and finally releasing Ca^{2+} from the endoplasmic reticulum (Docampo et al., 1993).

In addition, different treatments with distinct drugs are potentiated in the presence of Ca^{2+} . For example, the effect of melarsoprol and also the combination of salicylhydroxamic acid with glycerol on African trypanosomiasis is significantly augmented when Ca^{2+} is present (Clarkson and Amole, 1982). Similarly, Ergosterone-coupled Triazol molecules trigger mitochondrial dysfunction, oxidative stress, and acidocalcisomal Ca^{2+} release in *Leishmania mexicana* (Figarella et al., 2015).

The anti-tuberculosis drug SQ109 (**Figure 3**), recently postulated as a promising candidate against resistant tuberculosis, and which is already in phase IIb-III clinical trials, acts on the lipid transporter MmpLs (Mycobacterial membrane proteins Large), which play crucial roles in transporting lipids, polymers and immunomodulators and which also extrude therapeutic drugs from the bacteria (Zhang et al., 2019). SQ109 has been recently investigated for activity against *T. cruzi*, where it was found to inhibit squalene synthase, responsible for a

crucial step in ergosterol synthesis, and also to have a major effect causing parasite death through Ca^{2+} homeostasis, causing the collapse of the mitochondrial electrochemical potential, and impairing the function of acidocalcisomes (Veiga-Santos et al., 2015). Similar results were obtained in *L. mexicana* (García-García et al., 2016) and *L. donovani* (Gil et al., 2020), but interestingly demonstrating a more profound effect on amastigote-infected macrophages, the clinically relevant phase of the parasite life cycle, with IC_{50} found to be at the nanomolar range ($\text{IC}_{50} \sim 7 \text{ nM}$).

An exception to the rule is Amphotericin B (AmB) a systemic antifungal once thought to exert its anti-parasitic effect through disruption of Ca^{2+} homeostasis. However, experimental evidence has demonstrated that although AmB is an efficient Ca^{2+} ionophore, the rapid permeabilization effect induced by AmB in *Leishmania* parasites is not dependent on an increase in $[\text{Ca}^{2+}]_i$, and is, at the same time, paradoxically enhanced by absence of external calcium (Cohen et al., 1990). Further, it has been demonstrated that, at low concentrations, AmB was able to form cation channels that collapsed the parasite membrane potential with no lytic effects; while, at high concentrations it provoked a salt influx via aqueous pores formation leading to osmotic changes inciting cell lysis (Ramos et al., 1996) and death of the parasite. In *T. cruzi*, AmB has shown to have a direct effect against all three developmental stages of the parasite, exhibiting a higher efficacy against the amastigote stage followed by the trypomastigote and epimastigote forms (De-Castro et al., 1993). This is important since it highlights the distinct susceptibility of vertebrate bound stages to this drug. To date, there is scarce information about the use of this polyene antifungal against *T. cruzi* in humans. However, its use in refractory cutaneous leishmania infections has been successfully documented (Morrison et al., 2010). There is insufficient evidence with which to make confident recommendations on the superiority in performance of conventional AmB deoxycholate over lipid-associated AmB compounds for treatment of trypanosomatid infections. However, liposomal AmB therapeutic failure has been reported for *Leishmania (L.) amazonensis* in humans (Morrison et al., 2010), and lack of efficacy has been demonstrated in murine models of acute and chronic *T. cruzi* infection (Clemons et al., 2017).

Another relevant drug against Chagas disease is the alkyllysophospholipid miltefosine (**Figure 3**), the only approved oral formulation against visceral leishmaniasis, the lethal form of the leishmania disease spectrum (Croft and Coombs, 2003), which has also shown promising anti-Trypanosomal activity (Luna et al., 2009; Saraiva et al., 2009; Rodriguez-Duran et al., 2019). Known mechanisms of action of miltefosine include inhibition of the synthesis of phosphatidylcholine, mitochondrial injury, and inhibition of the parasite cytochrome c oxidase (Pinto-Martinez et al., 2018b). In *T. cruzi*, this drug inhibits the biosynthesis of phosphatidylcholine 10–20 times more potently when compared to mammalian cells (Urbina, 2017). More recently, the spectrum of its mechanism of action has broadened, reporting a direct action on the disruption of the parasites Ca^{2+} homeostasis (Pinto-Martinez et al., 2018b; Rodriguez-Duran et al., 2019).

In *T. cruzi*, miltefosine is capable of opening a recently described sphingosine-activated plasma membrane Ca^{2+}

TABLE 2 | Targets of different drugs acting through disruption of Calcium homeostasis in different trypanosomatids.

Drugs	Targets	References
Amiodarone	Mitochondria, Acidocalcisomes, Ergosterol synthesis	Benaim et al., 2006; Serrano-Martín et al., 2009a,b; Benaim and Paniz-Mondolfi, 2012
Dronedarone	Mitochondria, Acidocalcisomes, Ergosterol synthesis	Benaim and Paniz-Mondolfi, 2012; Benaim et al., 2012, 2014
SQ109	Mitochondria, Acidocalcisomes, Ergosterol synthesis	Veiga-Santos et al., 2015; García-García et al., 2016; Gil et al., 2020
Amioder (Benzofuran derivative)	Mitochondria, Acidocalcisomes,	Pinto-Martínez et al., 2018a; Martínez-Sotillo et al., 2019
Miltefosine	Sph-activated Plasma membrane Ca^{2+} -Channel, Mitochondria, Acidocalcisomes	Pinto-Martínez et al., 2018b; Rodríguez-Duran et al., 2019
Posaconazole	Elevation of intracellular Ca^{2+}	Benaim et al., 2006

channel (Rodríguez-Duran et al., 2019) which allows the opening of Ca^{2+} currents in a similar fashion to the physiological activator of the channel sphingosine. Concomitantly, miltefosine has also been demonstrated to collapse the mitochondrial electrochemical membrane potential ($\Delta\psi$), and to induce a rapid alkalization of the parasites acidocalcisomes through direct action (Pinto-Martínez et al., 2018b). The synchronous action of miltefosine on Ca^{2+} permeability in the plasma membrane and membranes of intracellular organelles without affecting the human counterpart is to the best of our knowledge, a unique feature to this drug with vast potential beneficial effects for its use in humans.

Calcium channel blockers (CCB) have also shown promising therapeutic applications in trypanosomatid infections (Reimão et al., 2016). Many reports have demonstrated the action of Ca^{2+} channel antagonists from the L-type voltage-gated calcium channels VGCC as inhibitors of growth in different trypanosomatids (Tempone et al., 2009; De Rycker et al., 2016; Reimão et al., 2016; Kashif et al., 2017). Even though the substrate spectrum for action of calcium channel blockers in kinetoplastid parasites is predictably broad, it is very likely that these drugs directly act by activation of the aforementioned sphingosine-activated plasma membrane Ca^{2+} channel. If this were the case, aiming this channel as a potential anti-parasitic target would be an approach holding strong therapeutic implications. Further biophysical and biochemical characterization of this unique Ca^{2+} -transporting system is needed for deciphering yet unresolved mechanisms within the parasites.

To date, several non-dihydropyridine calcium channel blockers (CCBs) have proved effective for inhibiting *in vitro* growth of *L. infantum* promastigotes and *T. cruzi* epimastigotes (Reimão et al., 2016), as well as by acting indirectly on reversing resistance against stibogluconate by mechanisms that remain yet to be elucidated (Neal et al., 1989). Despite some concerns regarding the use of non-dihydropyridines CCBs in heart failure due to their effect on reduction of cardiac contractility and reduction of heart rate and cardiac conduction (Abernethy and Schwartz, 1999), its longstanding use in humans for the treatment of hypertension and the ever-increasing evidence of these compounds on affecting and reducing parasitemia *in vitro* make them a promising group for drug repurposing against kinetoplastid parasites.

An abbreviate list of the most important functional targets of the main drugs affecting intracellular Ca^{2+} homeostasis of these parasites is depicted in **Table 2**.

CONCLUDING REMARKS

The identification of new intracellular calcium-linked anti-parasitic targets is rapidly expanding the set of potential therapeutic options against trypanosomatid infections. Because target-based toxicity and side effects may arise due to cross reactivity with human homologues caution is advised when looking at structural differences between species while preferably choosing exquisitely selective anti-parasitic inhibitors. Many of these compounds are already a relevant part of the current clinical arsenal to treat Chagas disease and are likely to remain so for the foreseeable future; examples include the antiarrhythmic agent amiodarone and emerging benzofuran derivatives, as well as the calcium channel blockers. Others, such as the azole derivatives (e.g., posaconazole) and the new antituberculosis drug SQ109, are gaining relevance as they are repurposed as anti-parasitic drugs. An increasing body of experimental evidence supports the disruption of parasite Ca^{2+} homeostasis and intracellular Ca^{2+} storage compartments as strategic targets for treatment of trypanosomatids infections in humans.

AUTHOR CONTRIBUTIONS

GB conceive and wrote the review. AP-M, ES, and NM-S participate directly in the writing of the review.

FUNDING

This work was supported by Fondo Nacional de Ciencia, Tecnología e Investigación, Venezuela (FONACIT) (Grants 2017000274 and 2018000010), and the Consejo de Desarrollo Científico y Humanístico-Universidad Central de Venezuela (CDCH-UCV) Grant PG-03-8728-2013/2 to GB.

ACKNOWLEDGMENTS

The authors would like to thank Marilianna Marquez B.Sc. for assisting with the illustrations.

REFERENCES

- Abernethy, D. R., and Schwartz, J. B. (1999). Calcium-antagonist drugs. *N. Engl. J. Med.* 341, 1447–1157. doi: 10.1056/NEJM199911043411907
- Adesse, D., Meirelles Azzam, E., Meirelles, M. N., Urbina, J. A., and Garzoni, L. R. (2011). Amiodarone inhibits *Trypanosoma cruzi* infection and iromotes cardiac cell recovery with gap junction and cytoskeleton reassembly *in vitro*. *Antimicrob. Agents Chemother.* 55, 203–210. doi: 10.1128/AAC.01129-10
- Benaim, G., Bermudez, R., and Urbina, J. (1990). Ca^{2+} transport in isolated mitochondrial vesicles from *Leishmania braziliensis* promastigotes. *Mol. Biochem. Parasitol.* 39, 61–68. doi: 10.1016/0166-6851(90)90008-A
- Benaim, G., Casanova, P., Hernandez-Rodriguez, V., Mujica-Gonzalez, S., Parra-Gimenez, N., Plaza-Rojas, L., et al. (2014). Dronedarone, an amiodarone analog with an improved anti-*Leishmania mexicana* efficacy. *Antimicrob. Agents Chemother.* 58, 2295–2303. doi: 10.1128/AAC.01240-13
- Benaim, G., Cervino, V., Hermoso, T., Feliberti, P., and Laurentin, A. (1993a). Intracellular calcium homeostasis in *Leishmania mexicana*. Identification and characterization of a plasma membrane calmodulin-dependent Ca^{2+} -ATPase. *Biol. Res.* 26, 141–150.
- Benaim, G., Cervino, V., and Villalobo, A. (1998). Comparative phosphorylation of calmodulin from trypanosomatids and bovine brain by calmodulin-binding protein kinases. *Comp. Biochem. Physiol. Part C.* 120, 57–65. doi: 10.1016/S0742-8413(98)00006-1
- Benaim, G., and Garcia, C. R. S. (2011). Targeting calcium homeostasis as the therapy of Chagas' disease and leishmaniasis. *Trop. Biomed.* 28, 471–448.
- Benaim, G., García-Marchán, Y., Reyes, C., Uzcanga, G., and Figarella, K. (2013). Identification of a sphingosine-sensitive Ca^{2+} channel in the plasma membrane of *Leishmania mexicana*. *Biochem. Biophys. Res. Commun.* 430, 1091–1096. doi: 10.1016/j.bbrc.2012.12.033
- Benaim, G., Hernandez-Rodriguez, V., Mujica, S., Plaza-Rojas, L., Silva, M. L., Parra, N., et al. (2012). In vitro anti-*Trypanosoma cruzi* activity of dronedarone, a novel amiodarone derivative with an improved safety profile. *Antimicrob. Agents Chemother.* 56, 3720–3725. doi: 10.1128/AAC.00207-12
- Benaim, G., Lopez-Estraño, C., Docampo, R., and Moreno, S. N. J. (1993b). A calmodulin-stimulated Ca^{2+} pump in plasma membrane vesicles from *Trypanosoma brucei*. Selective inhibition by pentamidine. *Biochem. J.* 296, 759–763. doi: 10.1042/bj2960759
- Benaim, G., Losada, S., Gadelha, F. R., and Docampo, R. (1991). A calmodulin-activated (Ca^{2+} - Mg^{2+})-ATPase is involved in calcium transport by plasma membrane vesicles from *Trypanosoma cruzi*. *Biochem. J.* 280, 715–720. doi: 10.1042/bj2800715
- Benaim, G., Moreno, S. N. J., Hutchinson, G., Cervino, V., Hermoso, T., Romero, P. J., et al. (1995). Characterization of the plasma membrane calcium pump from *Trypanosoma cruzi*. *Biochem. J.* 306, 299–303. doi: 10.1042/bj3060299
- Benaim, G., and Paniz-Mondolfi, A. E. (2012). The emerging role of amiodarone and dronedarone in treatment of chronic chagasic cardiomyopathy. *Nat. Rev. Cardiol.* 9, 605–609. doi: 10.1038/nrcardio.2012.108
- Benaim, G., Pimentel, A. A., Feliberti, P., Mayora, A., Colman, L., Sojo, F., et al. (2016). Sphingosine inhibits the sarco(endo)plasmic reticulum Ca^{2+} -ATPase (SERCA) activity. *Biochem. Biophys. Res. Commun.* 473, 572–577. doi: 10.1016/j.bbrc.2016.03.123
- Benaim, G., and Romero, P. J. (1990). A calcium pump in plasma membrane vesicles from *Leishmania braziliensis*. *Biochim. Biophys. Acta* 1027, 79–84. doi: 10.1016/0005-2736(90)90051-O
- Benaim, G., Sanders, J. M., García-Marchan, Y., Colina, C., Lira, R., Caldera, A. R., et al. (2006). Amiodarone has intrinsic anti-*Trypanosoma cruzi* activity and acts synergistically with posaconazole. *J. Med. Chem.* 49, 892–899. doi: 10.1021/jm050691f
- Benaim, G., Szabo, V., and Cornivelli, L. (1987). Isolation and characterization of calmodulin from *Leishmania braziliensis* and *Leishmania mexicana*. *Acta Cientif. Venezol.* 38, 289–291.
- Benaim, G., and Villalobo, A. (2002). Phosphorylation of Calmodulin: functional implications. *Eur. J. Biochem.* 269, 3619–3631. doi: 10.1046/j.1432-1033.2002.03038.x
- Benaim, G., Zurini, M., and Carafoli, E. (1984). Different conformational states of purified Ca^{2+} -ATPase of the erythrocyte plasma membrane revealed by controlled trypsin proteolysis. *J. Biol. Chem.* 259, 8471–8477.
- Bertolini, M. S., Chiurillo, M. A., Lander, N., Vercesi, A. E., and Docampo, R. (2019). MICU1 and MICU2 play an essential role in mitochondrial Ca^{2+} uptake, growth, and infectivity of the human pathogen *Trypanosoma cruzi*. *MBio.* 10:e00348–19. doi: 10.1128/mBio.00348-19
- Burleigh, B. A., and Andrews, N. W. (1998). Signaling and host cell invasion by *Trypanosoma cruzi*. *Curr. Opin. Microbiol.* 1, 461–465. doi: 10.1016/S1369-5274(98)80066-0
- Carafoli, E., and Krebs, J. (2016). Why calcium? How Calcium Became the Best Communicator. *J. Biol. Chem.* 291, 20849–20857. doi: 10.1074/jbc.R116.735894
- Chiurillo, M. A., Lander, N., Bertolini, M. S., Vercesi, A. E., and Docampo, R. (2019). Functional analysis and importance for host cell infection of the Ca^{2+} -conducting subunits of the mitochondrial calcium uniporter of *Trypanosoma cruzi*. *Mol. Biol. Cell* 30, 1676–1690. doi: 10.1091/mbc.E19-03-0152
- Chung, S. H., and Swindel, J. (1990). Linkage of the calmodulin and ubiquitin loci in *Trypanosoma cruzi*. *Nuc. Acid Res.* 18, 4561–4569. doi: 10.1093/nar/18.15.4561
- Clarkson, A. B. Jr., and Amole, B. D. (1982). Role of calcium in trypanocidal drug action. *Science* 216, 1321–1323. doi: 10.1126/science.6805075
- Clemons, K. V., Sobel, R. A., Martinez, M., Correa-Oliveira, R., and Stevens, D. A. (2017). Lack of efficacy of liposomal amphotericin B against acute and chronic *Trypanosoma cruzi* infection in mice. *Am. J. Trop. Med. Hyg.* 97, 1141–1146. doi: 10.4269/ajtmh.16-0975
- Cohen, B. E., Benaim, G., Ruiz, M. C., and Michelangeli, F. (1990). Increased calcium permeability is not responsible for the rapid lethal effects of amphotericin B on *Leishmania* sp. *FEBS Lett.* 259, 286–288. doi: 10.1016/0014-5793(90)80028-H
- Colunga-Biancatelli, R. M. L., Congedo, V., Calvosa, L., Ciacchiarelli, M., Polidoro, M., and Iuliano, L. (2019). Adverse reactions of amiodarone. *J. Geriatr. Cardiol.* 16, 552–566. doi: 10.1155/2019/3418950
- Cortez, M., Neira, I., Ferreiram, D., Luquetti, A. O., Rassi, A., Atayde, V. D., et al. (2003). Infection by *Trypanosoma cruzi* metacyclic forms deficient in gp82 but expressing a related surface molecule, gp30. *Infect. Immun.* 71, 6184–6191. doi: 10.1128/IAI.71.11.6184-6191.2003
- Croft, S. L., and Coombs, G. H. (2003). Leishmaniasis—current chemotherapy and recent advances in the search for novel drugs. *Trends Parasitol.* 19, 502–508. doi: 10.1016/j.pt.2003.09.008
- Cunningham, A. C. (2002). Parasitic adaptive mechanisms in infection by *Leishmania*. *Exp. Mol. Pathol.* 72, 132–141. doi: 10.1006/exmp.2002.2418
- D'Angelo, M. A., Montagna, A. E., Sanguineti, S., Torres, H. N., and Flawiá, F. F. (2002). A novel calcium-stimulated adenyl cyclase from *Trypanosoma cruzi*, which interacts with the structural flagellar protein paraflagellar rod. *J. Biol. Chem.* 277, 35025–35034. doi: 10.1074/jbc.M204696200
- De Rycker, M., Thomas, J., Riley, J., Brough, S. J., Miles, T. J., and Gray, D. W. (2016). Identification of trypanocidal activity for known clinical compounds using a new *Trypanosoma cruzi* hit-discovery screening cascade. *PLoS Negl. Trop. Dis.* 10:e0004584. doi: 10.1371/journal.pntd.0004584
- De Stefani, R., Raffaello, A., Teardo, E., Szabo, I., and Rizzuto, R. (2011). A forty-kilodalton protein of the inner membrane is the mitochondrial calcium uniporter. *Nature* 476, 336–340. doi: 10.1038/nature10230
- De-Castro, S. L., Soeiro, M. N., Higashi, K. O., and Meirelles, M. N. (1993). Differential effect of amphotericin B on the three evolutive stages of *Trypanosoma cruzi* and on the host cell-parasite interaction. *Braz. J. Med. Biol. Res.* 26, 1219–1229.
- Dey, R., Bhattacharya, J., and Datta, S. C. (2006). Calcium-dependent proteolytic activity of a cysteine protease caldonopain is detected during *Leishmania* infection. *Mol. Cell. Biochem.* 281, 27–33. doi: 10.1007/s11010-006-0171-y
- Díaz, M. V., Miranda, M. R., Campos-Estrada, C., Reigada, C., Maya, J. D., Pereira, C. A., et al. (2014). Pentamidine exerts *in vitro* and *in vivo* anti *Trypanosoma cruzi* activity and inhibits the polyamine transport in *Trypanosoma cruzi*. *Acta Trop.* 134, 1–9. doi: 10.1016/j.actatropica.2014.02.012
- Docampo, R., Gadelha, F. R., Moreno, S. N. J., Benaim, G., Hoffmann, M. E., and Vercesi, A. E. (1993). Disruption of Ca^{2+} homeostasis in *Trypanosoma cruzi* by crystal violet. *J. Euk. Microbiol.* 40, 311–316. doi: 10.1111/j.1550-7408.1993.tb04921.x
- Docampo, R., and Huang, G. (2015). Calcium signaling in trypanosomatid parasites. *Cell Calcium* 57, 194–202. doi: 10.1016/j.ceca.2014.10.015

- Docampo, R., and Pignataro, O. P. (1991). The inositol phosphate/diacylglycerol signaling pathway in *Trypanosoma cruzi*. *Biochem. J.* 275, 407–411. doi: 10.1042/bj2750407
- Docampo, R., and Vercesi, A. E. (1989). Ca^{2+} transport by coupled *Trypanosoma cruzi* mitochondria *in situ*. *J. Biol. Chem.* 264, 108–111. doi: 10.1016/0003-9861(89)90202-6
- Dolan, M. T., Reid, C. G., and Voorheis, H. P. (1986). Calcium ions initiate the selective depolymerization of the pellicular microtubules in bloodstream forms of *Trypanosoma brucei*. *J. Cell. Sci.* 80, 123–140.
- Engman, D. M., Krause, K. H., Blumin, J. H., Kim, K. S., Kirchhoff, L. V., and Donelson, J. E. (1989). A novel flagellar Ca^{2+} -binding protein in trypanosomes. *J. Biol. Chem.* 264, 18627–18631.
- Figarella, K., Marsicobetre, S., Arocha, I., Colina, W., Hasegawa, M., Rodriguez, M., et al. (2015). Ergosterone-coupled Triazol molecules trigger mitochondrial dysfunction, oxidative stress, and acidocalcisomal Ca^{2+} release in *Leishmania mexicana* promastigotes. *Microb. Cell* 3, 14–28. doi: 10.15698/mic2016.01.471
- Furuichi, T., Yoshikawa, S., Miyawaki, A., Wada, K., Maeda, N., and Mikoshiba, K. (1989). Primary structure and functional expression of the inositol 1,4,5-trisphosphate-binding protein P400. *Nature* 342, 32–38. doi: 10.1038/342032a0
- Furuya, T., Okura, M., Ruiz, F. A., Scott, D. A., and Docampo, R. (2001). TcSCA complements yeast mutants defective in Ca^{2+} pumps and encodes a Ca^{2+} -ATPase that localizes to the endoplasmic reticulum of *Trypanosoma cruzi*. *J. Biol. Chem.* 276, 32437–32445. doi: 10.1074/jbc.M104000200
- García-García, V., Oldfield, E., and Benaim, G. (2016). Inhibition of *Leishmania mexicana* growth by the tuberculosis drug SQ109. *Antimicrob. Agents Chemother.* 60, 6386–6389. doi: 10.1128/AAC.00945-16
- García-Marchan, Y., Sojo, F., Rodriguez, E., Zerpa, N., Malave, C., Galindo-Castro, I., et al. (2009). *Trypanosoma cruzi* calmodulin: cloning, expression and characterization. *Exp. Parasitol.* 123, 326–333. doi: 10.1016/j.exppara.2009.08.010
- Gil, Z., Martinez-Sotillo, N., Pinto-Martinez, A., Mejias, F., Martinez, J. C., Galindo-Castro, I., et al. (2020). SQ109 inhibits proliferation of *Leishmania donovani* by the disruption of the parasite intracellular Ca^{2+} homeostasis collapsing the mitochondrial electrochemical potential ($\Delta\Psi_m$) and affecting acidocalcisomes. *Parasitol. Res.* 119, 649–657. doi: 10.1007/s00436-019-06560-y
- Guerini, D., Krebs, J., and Carafoli, E. (1984). Stimulation of the purified erythrocyte Ca^{2+} -ATPase by triptic fragments of calmodulin. *J. Biol. Chem.* 259, 15172–15177.
- Hashimoto, M., Enomoto, M., Morales, J., Kurebayashi, N., Sakurai, T., Hashimoto, T., et al. (2013). Inositol 1,4,5-trisphosphate receptor regulates replication, differentiation, infectivity and virulence of the parasitic protist *Trypanosoma cruzi*. *Mol. Microbiol.* 87, 1133–1150. doi: 10.1111/mmi.12155
- Hoffmann, C., Falzone, E., Augé, M., Dinanian, S., Mercier, F. J., et al. (2012). Long QT syndrome, amiodarone use, and the mechanism underlying lidocaine toxicity. *Anesth. Analg.* 115, 1253–1254. doi: 10.1213/ANE.0b013e31826b4789
- Holwill, M. E., and McGregor, J. L. (1976). Effects of calcium on flagellar movement in the trypanosome *Crithidia oncopelti*. *J. Exp. Biol.* 65, 229–242.
- Huang, G., Bartlett, P. J., Thomas, A. P., Moreno, S. N. J., and Docampo, R. (2013). Acidocalcisomes of *Trypanosoma brucei* have an inositol 1, 4, 5-trisphosphate receptor that is required for growth and infectivity. *Proc. Nat. Acad. Sci. U.S.A.* 110, 1887–1892. doi: 10.1073/pnas.1216955110
- Huang, G., and Docampo, R. (2018). The Mitochondrial Ca^{2+} uniporter complex (MCUC) of *Trypanosoma brucei* is a hetero-oligomer that contains novel subunits essential for Ca^{2+} uptake. *MBio* 2018:e01700–e01718. doi: 10.1128/mBio.01700-18
- Huang, G., Ulrich, P. N., Storey, M., Johnson, D., Tischer, J., Tovar, J. A., et al. (2014). Proteomic analysis of the acidocalcisome, an organelle conserved from bacteria to human cells. *PLOS Pathog.* 12:e1004555. doi: 10.1371/journal.ppat.1004555
- Kashif, M., Manna, P. P., Akhter, Y., Alaidarous, M., and Rub, A. (2017). Screening of novel inhibitors against *leishmania donovani* calcium ion channel to fight leishmaniasis. *Infect. Disord. Drug. Targets.* 17, 120–129. doi: 10.2174/1871526516666161230124513
- Lammel, E. M., Barbieri, M. A., Wilkowsky, S. E., Bertini, F., and Isola, E. L. (1996). *Trypanosoma cruzi*: involvement of intracellular calcium in multiplication and differentiation. *Exp. Parasitol.* 83, 240–249. doi: 10.1006/expr.1996.0070
- Lander, N., and Chiurillo, M. A. (2019). State-of-the-art CRISPR/Cas9 technology for genome editing in trypanosomatids. *J. Eukaryot. Microbiol.* 66, 981–991. doi: 10.1111/jeu.12747
- Lander, N., Chiurillo, M. A., Bertolini, M. S., Storey, M., Vercesi, A. E., and Docampo, R. (2018). Calcium-sensitive pyruvate dehydrogenase phosphatase is required for energy metabolism, growth, differentiation, and infectivity of *Trypanosoma cruzi*. *J. Biol. Chem.* 293, 17402–17417. doi: 10.1074/jbc.RA118.004498
- Lander, N., Chiurillo, M. A., Storey, M., Vercesi, A. E., and Docampo, R. (2016). CRISPR/Cas9-mediated endogenous C-terminal tagging of *Trypanosoma cruzi* genes reveals the acidocalcisome localization of the Inositol 1,4,5-trisphosphate receptor. *J. Biol. Chem.* 291, 25505–25515. doi: 10.1074/jbc.M116.749655
- Lu, H. G., Zhong, L., Chang, K. P., and Docampo, R. (1997). Intracellular Ca^{2+} pool content and signaling and expression of a calcium pump are linked to virulence in *Leishmania mexicana amazonensis* amastigotes. *J. Biol. Chem.* 272, 9464–9473. doi: 10.1074/jbc.272.14.9464
- Luna, K. P., Hernandez, I. P., Rueda, C. M., Zorro, M. M., Croft, S. L., and Escobar, P. (2009). *In vitro* susceptibility of *Trypanosoma cruzi* strains from Santander, Colombia, to hexadecylphosphocholine (miltefosine), nifurtimox and benznidazole. *Biomedica.* 29, 448–455.
- Madigan, R., Majoy, S., Ritter, K., Concepción, J. L., Márquez, M. E., Silva, S. C., et al. (2019). Successful treatment of canine Chagas disease using a combination of amiodarone and itraconazole. *J. Am. Vet. Med. Assoc.* 255, 317–329. doi: 10.2460/javma.255.3.317
- Maldonado, R. A., Linss, J., Thomaz, N., Olson, C. L., Engman, D. M., and Goldenberg, S. (1997). Homologues of the 24-kDa flagellar Ca^{2+} -binding protein gene of *Trypanosoma cruzi* are present in other members of the Trypanosomatidae family. *Exp. Parasitol.* 86, 200–205. doi: 10.1006/expr.1997.4159
- Martínez, R., Wang, Y., Benaim, G., Benchimol, M., de Souza, W., Scott, D. A., et al. (2002). A proton pumping pyrophosphatase in the Golgi apparatus and plasma membrane vesicles of *Trypanosoma cruzi*. *Mol. Biochem. Parasitol.* 120, 205–213. doi: 10.1016/S0166-6851(01)00456-X
- Martínez-Sotillo, N., Pinto-Martínez, A., Hejchman, E., and Benaim, G. (2019). Antiproliferative effect of a benzofuran derivative based on the structure of amiodarone on *Leishmania donovani* affecting mitochondria, acidocalcisomes and intracellular Ca^{2+} homeostasis. *Parasitol. Int.* 70, 112–117. doi: 10.1016/j.parint.2019.02.006
- Misra, S., Naskar, K., Sarkar, D., and Ghosh, D. K. (1991). Role of Ca^{2+} ion on *Leishmania*-macrophage attachment. *Mol. Cel. Biochem.* 102, 13–18. doi: 10.1007/bf00232154
- Molina, I., Gomez I Prat, J., Salvador, F., Treviño, B., Sulleiro, E., Serre, N., et al. Randomized trial of posaconazole and benznidazole for chronic Chagas' disease. (2014). *N. Engl. J. Med.* 370, 1899–1908. doi: 10.1056/NEJMoa1313122
- Montalvetti, A., Bailey, B. N., Martin, M. B., Severin, G. W., Oldfield, E., and Docampo, R. (2001). Bisphosphonates are potent inhibitors of *Trypanosoma cruzi* farnesyl pyrophosphate synthase. *J. Biol. Chem.* 276, 33930–33937. doi: 10.1074/jbc.M103950200
- Moreira, M. E. C., Del Portillo, H. A., Milder, R. V., Balanco, J. M. F., and Barcinski, M. A. (1996). Heat shock induction of apoptosis in promastigotes of the unicellular organism *Leishmania (Leishmania) amazonensis*. *J. Cell. Physiol.* 167, 305–313. doi: 10.1002/(SICI)1097-4652(199605)167:2<305::AID-JCP15>3.0.CO;2-6
- Moreno, S. N. J., Vercesi, A. E., and Docampo, R. (1994). Cytosolic-free calcium elevation in *Trypanosoma cruzi* is required for cell invasion. *J. Exp. Med.* 180, 1535–1540. doi: 10.1084/jem.180.4.1535
- Morillo, C. A., Marin-Neto, J. A., Avezum, A., Sosa-Estani, S., Rassi Jr., A., Rosa, F., et al. (2015). Randomized trial of benznidazole for chronic Chagas' disease. *N. Engl. J. Med.* 373, 1295–1306. doi: 10.1056/NEJMoa1507574
- Morillo, C. A., Waskin, H., Sosa-Estani, S., Del Carmen Bangher, M., Cuneo, C., Milesi, R., et al. (2017). Benznidazole and posaconazole in eliminating parasites in asymptomatic *T. cruzi* carriers: the STOP-CHAGAS trial. *J. Am. Coll. Cardiol.* 69, 939–947. doi: 10.1016/j.jacc.2016.12.023
- Morrison, B., Mendoza, I., Delgado, D., Reyes-Jaimes, O., Aranzazu, N., and Paniz-Mondolfi, A. E. (2010). Diffuse (anergic) cutaneous leishmaniasis responding to amphotericin B. *Clin. Exp. Dermatol.* 35:e116–e119. doi: 10.1111/j.1365-2230.2009.03737.x

- Morrow, C. D., Flory-Granger, B., and Krassner, S. M. (1981). Effect of the ionophores A23187 and X-537A (Lasalocid) and of the divalent cations Ca^{2+} , Mg^{2+} , Ba^{2+} and Mn^{2+} on transformation in *Leishmania donovani*. *Comp. Biochem. Physiol.* 69, 65–72. doi: 10.1016/0300-9629(81)90639-3
- Naderer, T., Dandash, O., and McConville, M. J. (2011). Calcineurin is required for *Leishmania major* stress response pathways and for virulence in the mammalian host. *Mol. Microbiol.* 80, 471–480. doi: 10.1111/j.1365-2958.2011.07584.x
- Neal, R. A., van Bueren, J., McCoy, N. G., and Iwobi, M. (1989). Reversal of drug resistance in *Trypanosoma cruzi* and *Leishmania donovani* by verapamil. *Trans. R. Soc. Trop. Med. Hyg.* 83, 197–198.
- Nicotera, P., Bellomo, G., and Orrenius, S. (1992). Calcium-mediated mechanisms in chemically induced cell death. *Annu. Rev. Pharmacol. Toxicol.* 32, 449–470. doi: 10.1146/annurev.pa.32.040192.002313
- Ogueta, S., Mac Intosh, G., and Téllez-Iñón, M. T. (1996). Regulation of Ca^{2+} /calmodulin-dependent protein kinase from *Trypanosoma cruzi*. *Mol. Biochem. Parasitol.* 78, 171–183. doi: 10.1016/S0166-6851(96)02622-9
- Ogueta, S. B., Macintosh, G. C., and Téllez Iñón, M. T. (1998). Stage-specific substrate phosphorylation by a Ca^{2+} /calmodulin-dependent protein kinase in *Trypanosoma cruzi*. *J. Euk. Microbiol.* 45, 392–396. doi: 10.1111/j.1550-7408.1998.tb05089.x
- Ogueta, S. B., Solari, A., and Téllez-Iñón, M. T. (1994). *Trypanosoma cruzi* epimastigote forms possess a Ca^{2+} -calmodulin dependent protein kinase. *FEBS Lett.* 337, 293–297. doi: 10.1016/0014-5793(94)80212-2
- Paniz-Mondolfi, A. E., Pérez-Álvarez, A. M., Lanza, G., Márquez, E., and Concepción, J. L. (2009). Amiodarone and itraconazole: a rational therapeutic approach for the treatment of chronic Chagas' disease. *Chemotherapy* 55, 228–233. doi: 10.1159/000219436
- Paniz-Mondolfi, A. E., Stavropoulos, C., Gelanew, T., Loucas, E., Perez Alvarez, A. M., Benaim, G., et al. (2011). Successful treatment of old world cutaneous leishmaniasis caused by *Leishmania infantum* with posaconazole. *Antimicrob. Agents Chemother.* 55, 1774–1776. doi: 10.1128/AAC.01498-10
- Patel, S., and Docampo, R. (2010). Acidic calcium stores open for business: expanding the potential for intracellular Ca^{2+} signaling. *Trends Cell. Biol.* 20, 277–286. doi: 10.1016/j.tcb.2010.02.003
- Paveto, C., Pereira, C., Espinosa, J., Montagna, A. E., Farber, M., Esteva, M., et al. (1995). The nitric oxide transduction pathway in *Trypanosoma cruzi*. *J. Biol. Chem.* 270, 16576–16579. doi: 10.1074/jbc.270.28.16576
- Perez-Gordones, M. C., Ramirez-Iglesias, J. R., Cervino, V., Uzcanga, G. L., Benaim, G., and Mendoza, M. (2017). Evidence of the presence of a calmodulin-sensitive plasma membrane Ca^{2+} -ATPase in *Trypanosoma equiperdum*. *Mol. Biochem. Parasitol.* 213, 1–11. doi: 10.1016/j.molbiopara.2017.02.001
- Pinazo, M. J., Espinosa, G., Gállego, M., López-Chejade, P. L., Urbina, J. A., and Gascón, J. (2010). Successful treatment with posaconazole of a patient with chronic Chagas disease and systemic lupus erythematosus. *Am. J. Trop. Med. Hyg.* 82, 583–587. doi: 10.4269/ajtmh.2010.09-0620
- Pinto-Martinez, A. K., Hernandez-Rodriguez, V., Rodriguez-Duran, J., Hejchman, E., and Benaim, G. (2018a). Anti-*Trypanosoma cruzi* action of a new benzofuran derivative based structure. *Exp. Parasitol.* 189, 8–15. doi: 10.1016/j.exppara.2018.04.010
- Pinto-Martinez, A. K., Rodriguez-Durán, J., Serrano-Martin, X., Hernandez-Rodriguez, V., and Benaim, G. (2018b). Mechanism of action of miltefosine on *Leishmania donovani* involves the impairment of acidocalcisome function and the activation of the sphingosine-dependent plasma membrane Ca^{2+} channel. *Antimicrob. Agents Chemother.* 62, 1–10. doi: 10.1128/AAC.01614-17
- Pozzan, T., Marco Mongillo, M., and Rudiger, R. (2003). Investigating signal transduction with genetically encoded fluorescent probes. *Eur. J. Biochem.* 270, 2343–2352. doi: 10.1046/j.1432-1033.2003.03615.x
- Ramakrishnan, S., and Docampo, R. (2018). Membrane proteins in trypanosomatids involved in Ca^{2+} homeostasis and signaling. *Genes* 9:304. doi: 10.3390/genes9060304
- Ramirez-Iglesias, J. R., Pérez-Gordones, M. C., del Castillo, J. R., Mijares, A., Benaim, G., and Mendoza, M. (2018). Identification and characterization of a calmodulin binding domain in the plasma membrane Ca^{2+} -ATPase from *Trypanosoma equiperdum*. *Mol. Biochem. Parasitol.* 222, 51–60. doi: 10.1016/j.molbiopara.2018.04.005
- Ramos, H., Valdivieso, E., Gamargo, M., Dagger, F., and Cohen, B. E. (1996). Amphotericin B kills unicellular leishmanias by forming aqueous pores permeable to small cations and anions. *J. Membr. Biol.* 152, 65–75. doi: 10.1007/s002329900086
- Reimão, J. Q., Mesquita, J. T., Ferreira, D. D., and Tempone, A. G. (2016). Investigation of calcium channel blockers as antiprotozoal agents and their interference in the metabolism of *Leishmania (L.) infantum*. *Evid.-Based Complement. Altern. Med. ECAM* 2016:1523691. doi: 10.1155/2016/1523691
- Rizzuto, R., Simpson, A. W., M., Brini, M., and Pozzan, T. (1992). Rapid changes of mitochondrial Ca^{2+} revealed by specifically targeted recombinant aequorin. *Nature* 358, 325–327. doi: 10.1038/358325a0
- Robinson, D., Beattie, P., Sherwin, T., and Gull, K. (1991). [25] Microtubules, tubulin, and microtubule-associated proteins of trypanosomes. *Meth. Enzymol.* 196, 285–299. doi: 10.1016/0076-6879(91)96027-O
- Rodriguez-Duran, J., Pinto-Martinez, A., Castillo, C., and Benaim, G. (2019). Identification and electrophysiological properties of a sphingosine-dependent plasma membrane Ca^{2+} channel in *Trypanosoma cruzi*. *FEBS J.* 286, 3909–3925. doi: 10.1111/febs.14947
- Rohloff, P., Rodrigues, C. O., and Docampo, R. (2003). Regulatory volume decrease in *Trypanosoma cruzi* involves amino acid efflux and changes in intracellular calcium. *Mol. Biochem. Parasitol.* 126, 219–230. doi: 10.1016/S0166-6851(02)00277-3
- Ruben, L., Eguagu, C., and Patton, C. (1983). African trypanosomes contain calmodulin which is distinct from host calmodulin. *Biochim. Biophys. Acta* 758, 104–113. doi: 10.1016/0304-4165(83)90290-8
- Ruiz, R. C., Favoreto, S., Dorta, M. L., Oshiro, M. E., Ferreira, A. T., Manque, P. M., et al. (1998). Infectivity of *Trypanosoma cruzi* strains is associated with differential expression of surface glycoproteins with differential Ca^{2+} signalling activity. *Biochem. J.* 330, 505–511. doi: 10.1042/bj3300505
- Salas, V., Sánchez-Tórriz, J., Cusido-Hita, D. M., García-Marchan, Y., Sojo, F., Benaim, G., et al. (2005). Characterisation of tyrosine-phosphorylation-defective calmodulin mutants. *Protein. Exp. Purif.* 41, 384–392. doi: 10.1016/j.pep.2005.01.004
- Saraiva, V. B., Wengert, M., Gomes-Quintana, E., Heise, N., and Caruso-Neves, C. (2009). Na^{+} -ATPase and protein kinase C are targets to 1-O-hexadecylphosphocholine (miltefosine) in *Trypanosoma cruzi*. *Arch. Biochem. Biophys.* 481, 65–71. doi: 10.1016/j.abb.2008.10.018
- Schoijet, A. C., Sternlieb, T., and Alonso, G. D. (2019). Signal transduction pathways as therapeutic target for Chagas disease. *Curr. Med. Chem.* 26, 1–17. doi: 10.2174/0929867326666190620093029
- Selvapandiyani, A., Duncan, R., Debrabant, A., Bertholet, S., Sreenivas, G., Negi, N. S., et al. (2001). Expression of a mutant form of *Leishmania donovani* centrin reduces the growth of the parasite. *J. Biol. Chem.* 276, 43253–43261. doi: 10.1074/jbc.M106806200
- Selvapandiyani, A., Kumar, P., Morris, J. C., Salisbury, J. L., Wang, C. C., and Nakhasi, H. L. (2007). Centrin1 is required for organelle segregation and cytokinesis in *Trypanosoma brucei*. *Mol. Biol. Cell* 18, 3290–3301. doi: 10.1091/mbc.e07-01-0022
- Serrano-Martín, X., García-Marchan, Y., Fernandez, A., Rodriguez, N., Rojas, H., Visbal, G., et al. (2009a). Amiodarone destabilizes the intracellular Ca^{2+} homeostasis and the biosynthesis of sterols in *Leishmania mexicana*. *Antimicrob. Agents Chemother.* 53, 1403–1410. doi: 10.1128/AAC.01215-08
- Serrano-Martín, X., Payares, G., DeLucca, M., Martinez, J. C., Mendoza-León, A., and Benaim, G. (2009b). Amiodarone and miltefosine act synergistically against *Leishmania mexicana* and can induce parasitological cure in a murine model of cutaneous leishmaniasis. *Antimicrob. Agents. Chemother.* 53, 5108–5113. doi: 10.1128/AAC.00505-09
- Surgue, P., Hirons, M. R., Adam, J. U., and Holwill, M. E. (1988). Flagellar wave reversal in the kinetoplastid flagellate *Crithidia oncopelti*. *Biol. Cell* 63, 127–131. doi: 10.1016/0248-4900(88)90051-2
- Téllez-Iñón, M. T., Ulloa, R. M., Torruella, M., and Torres, H. N. (1985). Calmodulin and Ca^{2+} -dependent cyclic AMP phosphodiesterase activity in *Trypanosoma cruzi*. *Mol. Biochem. Parasitol.* 17, 143–153. doi: 10.1016/0166-6851(85)90013-1
- Tempone, A. G., Taniwaki, N. N., and Reimão, J. Q. (2009). Antileishmanial activity and ultrastructural alterations of *Leishmania (L.) chagasi* treated

- with the calcium channel blocker nimodipine. *Parasitol Res.* 105, 499–505. doi: 10.1007/s00436-009-1427-8
- Thomas, E. M., de Souza, E. T., Esteves, M. J., Angluster, J., and de Souza, W. (1981). *Herpetomona ssamuelpessoi*: changes in cell shape and induction of differentiation by local anesthetic. *Exp. Parasitol.* 51, 366–372. doi: 10.1016/0014-4894(81)90123-5
- Urbina, J. A. (2017). Pharmacodynamics and follow-up period in the treatment of human *Trypanosoma cruzi* infection with Posaconazole. *J. Am. Coll. Cardiol.* 70, 299–300. doi: 10.1016/j.jacc.2017.03.611
- Veiga-Santos, P., Li, K., Lameira, L., de Carvalho, T. M., Huang, G., Galizzi, M., et al. (2015). SQ109: a new drug lead for Chagas disease. *Antimicrob. Agents Chemother.* 59, 1950–1961. doi: 10.1128/AAC.03972-14
- Voorheis, H. P., Bowles, D. J., and Smith, G. A. (1982). Characteristics of the release of the surface coat protein from bloodstream forms of *Trypanosoma brucei*. *J. Biol. Chem.* 257, 2300–2304.
- Walker, D. M., Oghumu, S., Gupta, G., McGwire, B. S., Drew, M. E., and Satoskar, A. R. (2014). Mechanisms of cellular invasion by intracellular parasites. *Cell. Mol. Life Sci.* 71, 1245–1263. doi: 10.1007/s00018-013-1491-1
- Xiong, Z. H., Ridgley, E. L., Enis, D., Olness, F., and Ruben, L. (1997). Selective transfer of calcium from an acidic compartment to the mitochondrion of *Trypanosoma brucei*. Measurements with targeted aequorins. *J. Biol. Chem.* 272, 31022–31028. doi: 10.1074/jbc.272.49.31022
- Yakubu, M. A., Majumder, S., and Kierszenbaum, F. (1994). Changes in *Trypanosoma cruzi* infectivity by treatments that affect calcium ion levels. *Mol. Biochem. Parasitol.* 66, 119–125. doi: 10.1016/0166-6851(94)90042-6
- Yoshida, N., Favoreto, S. Jr., Ferreira, A. T., and Manque, P. M. (2000). Signal transduction induced in *Trypanosoma cruzi* metacyclic trypomastigotes during the invasion of mammalian cells. *Brazilian J. Med. Biol. Res.* 33, 269–278. doi: 10.1590/S0100-879X2000000300003
- Zhang, B., Li, J., Yang, X., Wu, L., Zhang, J., Yang, Y., et al. (2019). Crystal structures of membrane transporter MmpL3, an anti-TB drug target. *Cell* 176, 636–648. doi: 10.1016/j.cell.2019.01.003

Conflict of Interest: The authors declare that the research was conducted in the absence of any commercial or financial relationships that could be construed as a potential conflict of interest.

Copyright © 2020 Benaim, Paniz-Mondolfi, Sordillo and Martinez-Sotillo. This is an open-access article distributed under the terms of the Creative Commons Attribution License (CC BY). The use, distribution or reproduction in other forums is permitted, provided the original author(s) and the copyright owner(s) are credited and that the original publication in this journal is cited, in accordance with accepted academic practice. No use, distribution or reproduction is permitted which does not comply with these terms.



RNA Binding Proteins and Gene Expression Regulation in *Trypanosoma cruzi*

Bruno A. A. Romagnoli, Fabiola B. Holetz, Lysangela R. Alves and Samuel Goldenberg*

Gene Expression Regulation Laboratory, Institute Carlos Chagas, Curitiba, Brazil

OPEN ACCESS

Edited by:

Noelia Lander,
University of Georgia, United States

Reviewed by:

Javier De Gaudenzi,
IIBIO-UNSAM-CONICET, Argentina
Zhuhong Li,
University of Georgia, United States

*Correspondence:

Samuel Goldenberg
samuel.goldenberg@fiocruz.br

Specialty section:

This article was submitted to
Parasite and Host,
a section of the journal
Frontiers in Cellular and Infection
Microbiology

Received: 24 October 2019

Accepted: 03 February 2020

Published: 20 February 2020

Citation:

Romagnoli BAA, Holetz FB, Alves LR
and Goldenberg S (2020) RNA
Binding Proteins and Gene Expression
Regulation in *Trypanosoma cruzi*.
Front. Cell. Infect. Microbiol. 10:56.
doi: 10.3389/fcimb.2020.00056

The regulation of gene expression in trypanosomatids occurs mainly at the post-transcriptional level. In the case of *Trypanosoma cruzi*, the characterization of messenger ribonucleoprotein (mRNP) particles has allowed the identification of several classes of RNA binding proteins (RBPs), as well as non-canonical RBPs, associated with mRNA molecules. The protein composition of the mRNPs as well as the localization and functionality of the mRNAs depend on their associated proteins. mRNPs can also be organized into larger complexes forming RNA granules, which function as stress granules or P-bodies depending on the associated proteins. The fate of mRNAs in the cell, and consequently the genes expressed, depends on the set of proteins associated with the messenger molecule. These proteins allow the coordinated expression of mRNAs encoding proteins that are related in function, resulting in the formation of post-transcriptional operons. However, the puzzle posed by the combinatorial association of sets of RBPs with mRNAs and how this relates to the expressed genes remain to be elucidated. One important tool in this endeavor is the use of the CRISPR/CAS system to delete genes encoding RBPs, allowing the evaluation of their effect on the formation of mRNP complexes and associated mRNAs in the different compartments of the translation machinery. Accordingly, we recently established this methodology for *T. cruzi* and deleted the genes encoding RBPs containing zinc finger domains. In this manuscript, we will discuss the data obtained and the potential of the CRISPR/CAS methodology to unveil the role of RBPs in *T. cruzi* gene expression regulation.

Keywords: *Trypanosoma cruzi*, gene expression regulation, RNA binding proteins, CRISPR/CAS, zinc finger protein, RNA granules

INTRODUCTION

Trypanosoma cruzi, as well as other trypanosomatids, displays several biological features that makes it unique in nature (De Souza, 1984; Rodrigues et al., 2014). One of the most striking features of organisms in the Kinetoplastida order is related to the transcription process, since mRNAs are transcribed as polycistronic units that are later processed to give rise to mature mRNAs (De Gaudenzi et al., 2011; Goldenberg and Avila, 2011). There are some special points concerning this process that should be highlighted. Although RNA polymerase II (RNA pol II) is involved in mRNA transcription, no canonical RNA polymerase II promoters have been identified in trypanosomatids (Clayton, 2016); the mRNAs within a given polycistron are not related in function or in temporal expression during the life cycle of the cells. Additionally, primary transcripts, with a few exceptions, are intronless. The mRNAs are processed by the mechanism of trans-splicing: a common 5'-leader

sequence of ~50 nucleotides (varying in size and sequence according to the species) is added to each mRNA within the polycistronic unit, concomitantly with the addition of a 3' poly-A tail (Palenchar and Bellofatto, 2006; Preußner et al., 2012). Some major questions have been raised concerning the points described above: How are the mRNAs selected for transport to the cytoplasm? How are stage-specific mRNAs selected for translation? To date, definitive answers to these questions are not available, but there are some clues regarding the key players in these processes, hence paving the way to unveiling the mechanisms involved in gene expression regulation in trypanosomes.

In the primitive RNA world, it is conceivable that RNAs existed as naked molecules. However, in all cells, RNAs are covered with proteins and exist as ribonucleoprotein complexes. The proteins associated with RNAs are named RNA-binding proteins (RBPs). There are different classes of RBPs based on the motifs that constitute the RNA binding domains (RBDs). The most common domains, such as the RNA recognition motif (RRM) and zinc finger (ZF) domain, will be discussed below. In addition to the canonical RBPs, there are several proteins involved in metabolism or the stress response that are also associated with RNA and are generally named unconventional RNA binding proteins. It is estimated that 3–10% of a given genome codes for RBPs, corroborating their important role in cell function (Glisovic et al., 2008).

RBPs participate in several biological processes, from RNA transcription to decay (Figure 1). In the course of transcription, RNA is wrapped up by RBPs that, in addition to protecting RNA from degradation, play a crucial role in RNA metabolism and fate in the cell. The processing of RNAs (splicing, alternative splicing or trans-splicing) depends on the correct recognition and exposure of RNA sequences to the splicing machinery (Lee and Rio, 2015). After processing, the mRNAs must be transported to the cytoplasm (Björk and Wieslander, 2017) and, once there, the mature mRNAs can be sequestered to the translation machinery for protein synthesis or stored in RNA granules, where they will be kept silent or targeted for degradation. RNA processing, transport within the cell and localization are mediated by RBPs that determine the fate of the mRNA according to their composition in a given mRNP complex (Gerstberger et al., 2014; Re et al., 2014).

The arrangement and assembly of RBPs in mRNP complexes is very dynamic (Müller-McNicoll and Neugebauer, 2013; Ross Buchan, 2014). Different sets of RBPs associate with the mRNA to provide its functionality. The combinatorial arrangement of proteins onto a given mRNP complex has yet to be elucidated and is undoubtedly a great challenge for researchers. It is possible that in addition to the genetic and the histone code, there exists an RBP code. Considering the number of known RBPs and moonlighting proteins with RBP functions, this code is complex and would ultimately determine the genes to be expressed.

The study and characterization of RBPs have greatly increased and improved recently with the development of modern tools that allow interactome studies (Castello et al., 2015; Smirnov et al., 2017). High-throughput techniques, such as mass spectrometry and NGS associated with immunoprecipitation

have allowed the isolation and characterization of RBP complexes. This has enabled confirmation of the existence of unconventional RBPs in addition to those that exhibit characteristic features.

mRNA DECAY AND TRANSLATION

Control of mRNA degradation and access to the translation machinery are very important post-transcriptional processes in *T. cruzi* gene expression regulation. mRNA decay and translation are closely related and can influence each other according to the specific binding proteins associated with the mRNA molecule.

In eukaryotes, the decay of most mRNAs is initiated by the removal of the poly(A) tail. The major mRNA decay pathway of many eukaryotes then proceeds by decapping (by the Dcp1/Dcp2 complex), followed by 5'-3' exonucleolytic degradation by the exoribonuclease Xrn1 (Parker and Song, 2004).

In trypanosomatids, the 5'-3' mRNA decay pathway is currently unknown, although deadenylation and mRNA cleavage processes have been extensively studied and appear to be conventional (Erben et al., 2013; Fadda et al., 2014). Removal of the mRNA cap has already been demonstrated *in vitro* (Milone, 2002), but these parasites seem to have developed a decapping mechanism that is different from the Dcp2/Dcp1-mediated decapping found in all other eukaryotes. In fact, the cap structure of trypanosomes is highly unusual: the m⁷GTP residue is followed by four methylated nucleotides forming the cap4 structure (Perry et al., 1987), justifying the need for a distinct decapping enzyme. Recently, Kramer and colleagues (Fritz et al., 2015) standardized a method for the isolation and purification of stress granules in *T. brucei*. From proteomic analyses of these granules, Kramer identified the TbALPH1 protein as the long-sought trypanosome decapping enzyme from trypanosomatids (Kramer, 2017). Depletion of TbALPH1 is lethal and results in a massive, global increase in mRNAs that are deadenylated but have not yet being degraded. This protein has all the characteristics of a decapping enzyme and is colocalized with the TbXRNA protein in the posterior pole granule. Although this posterior pole granule contains two enzymes that are involved directly in mRNAs decay, no mRNA decay intermediates have been found, raising the hypothesis that this granule maintains the separation of degradation enzymes from the pool of mRNAs in the cytoplasm, regulating mRNA decay in a global way. Such a tight, global regulation of mRNA decay is critical for life-cycle progression.

All trypanosomatid digenetic parasites possess non-proliferative life-cycle stages, which are essential for progression between insect and mammalian host. It is known that transcription and translation are downregulated in these stages (Elias et al., 2001; Tonelli et al., 2011), but the exact mechanisms that regulate these processes remain unknown.

Protein biosynthesis is considered a critical step and the ultimate goal for gene expression regulation in trypanosomatids. Recently, Smircich et al. (2015) assessed the extent of regulation of the transcriptome and the translome in both the non-infective (epimastigote) and infective (metacyclic

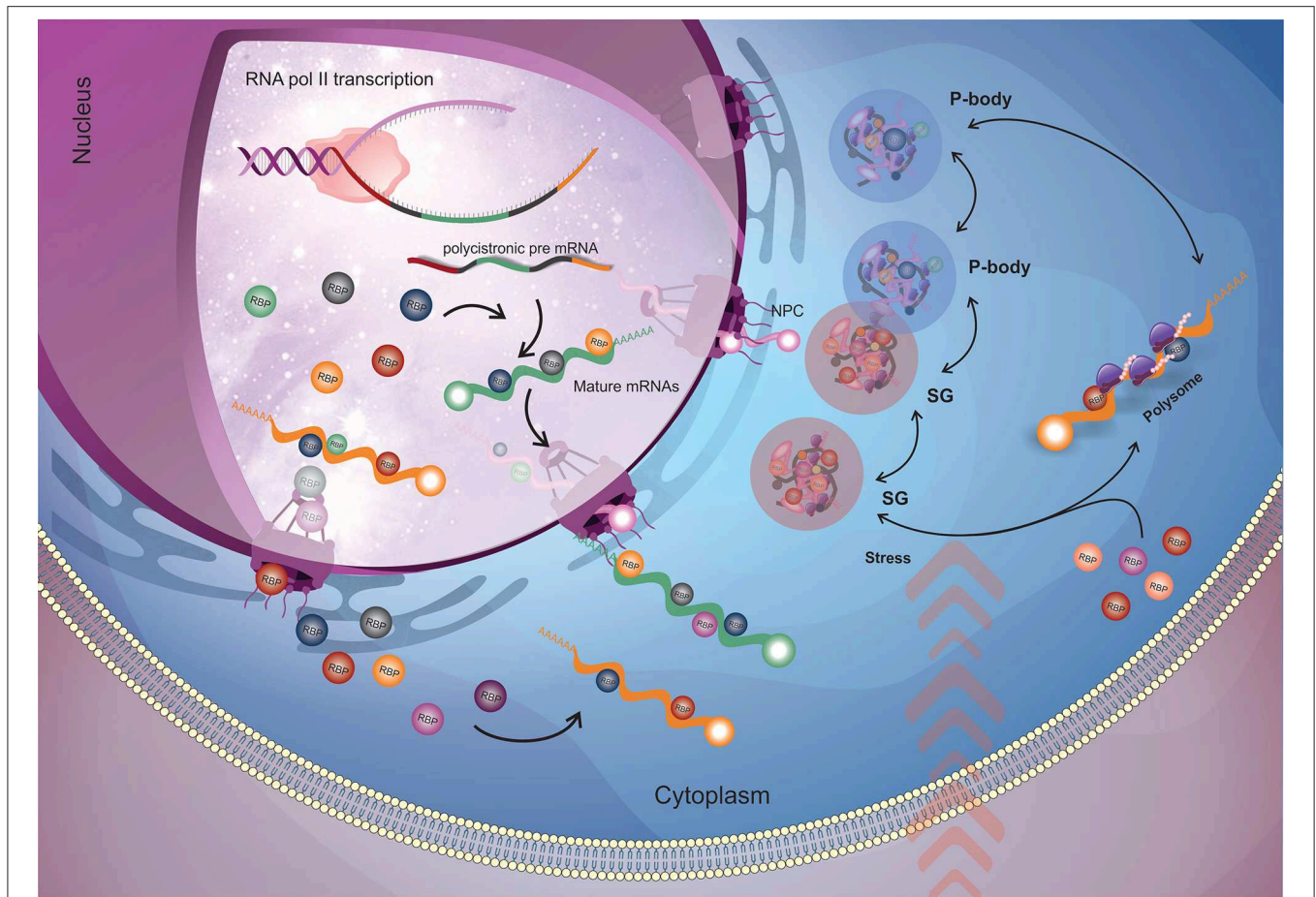


FIGURE 1 | General flow of RBPs action on the mRNA metabolism. Nuclear RBPs interact with their target mRNAs as soon as they start to be transcribed by RNA polymerase II (RNA pol II) and modulate mRNA maturation (trans-splicing and polyadenylation) and nuclear exportation processes. When the mRNAs arrive into the cytoplasm, cytoplasmic RBPs (along with the ones that came from nucleus) engage their targets and (in a combinatorial signaling) determine the mRNAs fate by directing them to the translational machinery or to RNP granules for storage or degradation. The dynamic destination and trade of mRNAs between those fates relies according to the cellular condition. When submitted to stress (e.g., nutrients availability, pH, temperature), stress granules appear, and in order to recover cell homeostasis, RBPs play a major role in rearranging RNA granules composition by dynamically changing the mRNAs that will address to translation machinery, storage in stress granules or degraded in P-bodies. RBP, RNA binding protein (round shapes); NPC, nuclear pore complex; SG, stress granules; P-body, processing bodies.

trypomastigote) forms of *T. cruzi* using RNA-Seq and ribosome profiling methods. The authors showed that a large subset of genes is modulated at the translation level between these two different developmental stages of *T. cruzi*, indicating a key role of translation control during differentiation into the infective form.

Translation initiation is a major contributing step to gene expression regulation and involves several translation initiation factors (eIFs). In eukaryotes, translation initiates with the binding of the tripartite mRNA-binding complex eIF4F (formed by the translation initiation factors eIF4E, eIF4A, and eIF4G) to the cap present at the 5' end of the mRNAs (Jagus et al., 2012), enabling the attachment of the 43S complex and the two ribosomal subunits to the initiation codon. eIF4E binds directly to the cap and represents a central control point in translational regulation (Jackson et al., 2010). eIF4G, a large scaffold protein, interacts with eIF4E, eIF4A, and PABP. eIF4A, a DEAD-box RNA helicase, unwinds the 5'

proximal region of mRNA. Trypanosomatids possess a large and unusual number of eIF4F translation initiation factor paralogs relative to mammals cells (Freire et al., 2017). There are six eIF4E (eIF4E1-6), five eIF4G (eIF4G1-5), and two eIF4A (eIF4A1-2) homologs. Moreover, trypanosomes have two PABPs (PABP1-2) and *Leishmania* has an additional PABP paralog (PABP3) (da Costa Lima et al., 2010).

The interactions between the different translation initiation factors that form the eIF4F complex have already been determined in *T. brucei* and *Leishmania*, and there are at least five distinct eIF4F (-like) complexes: eIF4E3:eIF4G4; eIF4E4:eIF4G3:PABP1; eIF4E5:eIF4G1; eIF4E5:eIF4G2; and eIF4E6:eIF4G2. It is currently accepted that eIF4E4:eIF4G3:PABP1 is the major translation initiation complex (Freire et al., 2017). However, the exact role of distinct eIF4F-like complexes has not yet been determined, although it is believed that they may be involved in the differential selection of

mRNAs. Despite extensive studies on these multiple homologs in *T. brucei* and *Leishmania*, little is known about these factors in *T. cruzi*, and no specific function for each homolog has been characterized. Nevertheless, we have performed a two-hybrid assay comprising screening for all eIF4Es, eIF4Gs, and PABPs from *T. cruzi*. We have identified and confirmed three new interactions: TceIF4E3:TcPABP1, TceIF4E3:TcPABP2, and TceIF4E5:TceIF4G5 (unpublished data). These results strongly suggest a distinct mechanism regarding the translational control of *T. cruzi*.

RNA GRANULES

In mammalian and yeast cells, mRNAs that are not being translated, or those destined for degradation, are compartmentalized into distinct cytoplasmic structures generally termed “RNA Granules” or “mRNP Granules” (messenger ribonucleoprotein granules). These granules can be classified in Processing bodies (P-bodies) and stress granules (SG), depending on the presence of specific proteins, and play key roles in the post-transcriptional regulation of gene expression. Stress granules are defined by the presence of translation initiation factors and are involved in the sorting and storage of mRNAs, whereas P-bodies are sites of storage and/or degradation of several transcripts formed by the presence of translation-repressor proteins and components of the mRNA degradation machinery (Sheth and Parker, 2003; Teixeira et al., 2005; Holetz et al., 2007; Anderson and Kedersha, 2008; Kedersha and Anderson, 2009). In addition, eukaryotic studies demonstrate that these structures can interact and exchange their components in a dynamic cycle with the exchange of mRNAs between translation, storage and degradation, indicating the decisive role of these structures in the control of gene expression at the posttranscriptional level (Decker and Parker, 2012).

Our previous work pioneered the identification of RNA granules with similarities to P-bodies in *T. cruzi* (Holetz et al., 2007, 2010). Since then, several studies have described the presence of different mRNP granules in *T. cruzi* and *T. brucei*. There are at least six types of mRNP granules in trypanosomatids, namely, P-body-like RNA granules, nutritional stress-induced RNA granules, heat shock-induced RNA granules, nuclear peripheral granules, posterior pole granule, and granules formed by tRNAs (Kramer, 2014). This vast repertoire of mRNP granules can be justified as an adaptation to the loss of transcriptional control. However, despite the importance of translational control and control of mRNA stability in the regulation of gene expression in trypanosomes, the connection between mRNP granules and life cycle regulation remains unknown in these parasites.

Proteins known to be involved in the formation of RNA granules in eukaryotes have been characterized in *T. cruzi*. TcDHH1 is present as a free protein or in polysome-independent complexes localized in *foci* that vary in number and size in response to nutritional stress and to cycloheximide/puromycin treatments, indicating that these structures are in equilibrium

with the translation machinery (Cassola et al., 2007; Holetz et al., 2007). Furthermore, TcDHH1 associates with developmentally regulated mRNAs. Accordingly, mRNAs associated with TcDHH1 in the epimastigote stage are those mainly expressed in the other forms of the *T. cruzi* life cycle (Holetz et al., 2010). Interestingly, Dallagiovanna et al. (2008) demonstrated the association of TcPUF6 with TcDHH1 in epimastigote forms but not in metacyclic trypomastigotes. Since TcPUF6 promotes the degradation of its target mRNAs in epimastigotes, it is likely that TcPUF6 regulates the degradation of its associated transcripts by its association with TcDHH1-containing complexes involved in mRNA degradation.

Recently, TcXRNA, the trypanosome Xrn1 homologous protein, was characterized in *T. cruzi* (Costa et al., 2018a). TcXRNA exhibits granular cytoplasmic cell localization, is constitutively expressed throughout the life cycle of *T. cruzi* and accumulates at the nuclear periphery when mRNA processing is inhibited. TcXRNA does not colocalize with TcDHH1 and TcCAF1 (a catalytic subunit of the Ccr4-Not deadenylase complex) granules in the cytoplasm. On the other hand, the colocalization of TcXRNA with distinct mRNP granules occurs mainly around the nucleus, which suggests the existence of an mRNA quality control checkpoint at the nuclear periphery, involving the activity of distinct proteins, such as TcXRNA, TcDHH1, and TcCAF1.

The precise function of mRNP granules as well as their relationship with translational control and life-cycle regulation remain poorly understood in *T. cruzi*. The data obtained so far indicate the existence of several types of granules formed as a result of different stimuli, whose assembly is dependent on mRNAs. Furthermore, although they can share several proteins, there are distinct structures that interact with each other dynamically. The mechanism that distinguishes mRNAs destined for storage or degradation in *T. cruzi* seems to depend on the combination of different protein components associated with the mRNAs, according to their expression levels during the life cycle, corroborating the complexity of the process of regulation of gene expression in this parasite.

RNA-BINDING PROTEINS IN *TRYPANOSOMA CRUZI*

RBPs With RRM Domains in *T. cruzi*

The RNA-recognition motif (RRM) is the most common and versatile domain found in RBPs as it can bind different molecules, such as single- and double-stranded RNA and DNA and interact with proteins. Due to its plasticity, RBPs that contain this domain are key players in RNA metabolism, acting from mRNA splicing to mRNA turnover (Cléry et al., 2008; Cléry and Frédéric, 2012). A summary of the RBPs studied in *T. cruzi* are described in **Table 1**.

In *T. cruzi*, most of the RBPs characterized to date present RRM domains and are involved in RNA metabolism by controlling the transcripts stability and turnover. One well-characterized RBP is TcUBP1, which presents a single RRM domain and form both stabilizing or destabilizing interactions

TABLE 1 | List of RBPs characterized in *T. cruzi*.

RBP name	RBP domain	Stage expression				Regulated throughout life cycle	Localization	References
		A	E	M	T			
TcAlba 30	ALBA	•	•	•	•	No	Cytoplasmatic	Pérez-Díaz et al., 2017
EF-1 α	Non canonical	•	•	•	•	Yes	Cytoplasmatic	Alves et al., 2015
TcPIWI-tryp	PIWI/OB-fold	•	•	•	•	No	Cytoplasmatic	Garcia Silva et al., 2010; Garcia-Silva et al., 2014
TcPUF1	PUF	–	•	–	–	Not reported	Cytoplasmatic	Caro et al., 2006
TcPUF6	PUF	•	•	•	•	No	Cytoplasmatic	Dallagiovanna et al., 2005, 2008
PABP1	RRM	•	•	•	•	No	Cytoplasmatic	Batista et al., 1994
TcDRBD2	RRM	•	•	•	•	No	Cytoplasmatic	Wippel et al., 2019
TcDRBD4/PTB2	RRM	Nr	•	Nr	Nr	Not reported	Cytoplasmatic /Nuclear	Jäger et al., 2007; De Gaudenzi et al., 2016
TcNrBD1	RRM	•	•	•	•	No	Cytoplasmatic	Oliveira et al., 2016
TcRBP3	RRM	–	•	–	–	Yes	Cytoplasmatic	De Gaudenzi et al., 2003
TcRBP4	RRM	–	•	–	–	Yes	Cytoplasmatic	De Gaudenzi et al., 2003
TcRBP5	RRM	•	•	•	•	Yes	Cytoplasmatic	De Gaudenzi et al., 2003
TcRBP6	RRM	•	•	•	•	Not reported	Cytoplasmatic	De Gaudenzi et al., 2003
TcRBP9	RRM	Nr	•	–	Nr	Yes	Cytoplasmatic	Wippel et al., 2018a
TcRBP19	RRM	•	–	–	–	Yes	Cytoplasmatic	Pérez-Díaz et al., 2007, 2012, 2013
TcRBP40	RRM	•	•	–	•	Yes	Cytoplasmatic *	Guerra-Slompo et al., 2012
TcRBP42	RRM	•	•	•	•	Not reported	Cytoplasmatic	Tyler Weisbarth et al., 2018
TcRBSR1	RRM	•	•	–	•	Yes	Cytoplasmatic /Nuclear	Wippel et al., 2018b
TcTRRM1/TcSR62	RRM/ZF(C2HC)	Nr	•	Nr	Nr	Not reported	Nuclear	Názer et al., 2011; Wippel et al., 2018b
TcUBP1	RRM	•	•	•	•	Yes	Cytoplasmatic	D'Orso and Frasch, 2002
TcUBP2	RRM	•	•	–	–	Yes	Cytoplasmatic	D'Orso and Frasch, 2002
TcZC3H29	ZF(C3H)	–	•	–	–	Yes	Cytoplasmatic	This work
TcZC3H31	ZF(C3H)	•	•	•	•	Yes	Cytoplasmatic	Alcantara et al., 2018
TcZC3H39	ZF(C3H)	•	•	•	•	No	Cytoplasmatic	Alves et al., 2014
TcZC3HTTP	ZF(C3H)	–	•	–	–	Yes	Cytoplasmatic	This work
TcZFP1	ZF(C3H)	•	•	•	•	Yes	Not reported	Mörking et al., 2004
TcZFP2	ZF(C3H)	•	•	•	•	Yes	Cytoplasmatic	Mörking et al., 2012
TcZFP8	ZF(C3H)	•	•	•	•	No	Nuclear	Ericsson et al., 2006

*TcRBP40 localizes in reservosomes in epimastigotes forms.

Nr, Not reported.

Other RBPs investigated in *T. cruzi* but without further characterization are TcPUF3, TcPUF5, TcPUF8 (Caro et al., 2006) and TcRBP10 (Wippel et al., 2018a).

depending on its partners in the mRNP complex (D'Orso and Frasch, 2002; Volpon et al., 2005; Li et al., 2012; Sabalette et al., 2019). The protein recognizes the AU-rich elements located at the 3'-untranslated region (UTR) of mucin *SMUGL* mRNAs (D'Orso and Frasch, 2002; Li et al., 2012). In addition, it has been recently shown that overexpression of TcUBP1 in epimastigotes increases by 10-fold the amount of transcripts coding for surface proteins and that they were being actively translated (Sabalette et al., 2019). The ectopic expression of TcUBP1 in trypomastigotes increased the infectivity rates, demonstrating the important role of this protein for the parasite virulence (Sabalette et al., 2019). TcUBP2 is another RRM-containing protein and is part of the TcUBP1 complex. It acts by binding to the poly(U) region of the *SMUGL* mucin mRNA that acts to control the expression of this transcript (D'Orso and Frasch, 2002).

TcDRBD4/PTB2 is an RBP presenting two RRM domains that play a role in the destabilization of the *ubp1* and *ubp2* mRNAs. It regulates splicing and prevents trans-splicing by binding in the regulatory elements present in the intercistronic region (ICR) of the *ubp1* and *ubp2* genes. These results indicate that TcDRBD4/PTB2 might act by covering the trans-splicing/polyadenylation signals (De Gaudenzi et al., 2016).

TcRBP19 presents a single RRM domain, whose ectopic overexpression impairs the parasite's life cycle and infection ability. This RBP led to a reduction in the number of infected cells (Pérez-Díaz et al., 2012). TcRBP19 presents a low level of expression in the epimastigote forms of the parasite. It was shown that this protein binds to the 3'-UTR region of its own transcript, decreasing its stability and suggesting its role as a destabilizing factor (Pérez-Díaz et al., 2013).

TcRBP40 also presents a single RRM domain. It binds to AG-rich regions in the 3'-UTR of target mRNAs coding for transmembrane proteins. In addition, the TcRBP40 protein is localized in reservosomes in the replicative epimastigote form; this organelle is associated with protein and lipid storage. In the mammalian-host forms of the parasite, amastigotes and trypomastigotes, it is diffused in the cytoplasm. This suggests a regulatory function for this protein due to its shift in cellular localization according to the developmental stage of the parasite (Guerra-Slompo et al., 2012).

TcRBP9 is a cytoplasmic protein that presents one RRM domain. The protein is associated with translational complexes, suggesting its involvement in translation regulation. RBP9 associates with other RBPs involved in RNA metabolism, such as ZC3H39, UBP1/2, NRBD1, and ALBA3/4. When parasites under stress were analyzed, irrespective of RBPs, the translation initiation factors eIF4E5, eIF4G5, eIF4G1, and eIF4G4 were also identified. In addition, the RBP9-mRNP complex regulates transcripts coding other RBPs, such as RBP5, RBP6, and RBP10 and proteins involved in metabolic processes. These results indicate that RBP9 is part of a cytoplasmic mRNP complex involved in mRNA metabolism and translation regulation (Wippel et al., 2018a).

TcNRBD1 is an RBP that contains two RRM domains and is expressed throughout the life cycle of *T. cruzi*. This protein is orthologous to the P34 and P37 proteins from *T. brucei*, although the role they play in these organisms is distinct. TcNRBD1 is localized at the perinuclear region and associates with either 80S ribosomes or polysomes, indicating its role in the translation process. This observation was corroborated by ribonomic analysis that showed several transcripts encoding ribosomal proteins associated with TcNRBD1. Proteomic analysis also indicated that TcNRBD1 associates with several ribosomal proteins from both the 40S and 60S subunits, reinforcing its role in the translation process (Oliveira et al., 2016).

TcRBSR1 is a predominantly nuclear RBP that contains one RRM domain and a serine-arginine (SR)-rich region; this protein seems to be developmentally regulated since no expression is detected in the infective metacyclic trypomastigote forms. Proteomic data showed that TcRBSR1 interacts with other RBPs, such as TcUBP1, TcUBP2, and TcTRRM1. An immunoprecipitation assay followed by RNA-seq indicated that RBSR1-mRNP binds to snoRNAs and snRNAs, leading to a hypothesis regarding its role in RNA processing in the nucleus (Wippel et al., 2018b).

TcRBP42 is a cytoplasmic RBP that presents one RRM domain and one NTF2-like domain. The NTF2 domain is associated with nuclear-cytoplasmic transport (Aibara et al., 2015). RBP42 is expressed in all developmental forms of *T. cruzi*, suggesting a role in gene expression regulation throughout the life cycle of the parasite. It was shown that overexpression of the protein did not lead to any alteration in the capacity of *T. cruzi* to differentiate into the metacyclic trypomastigote form or in cell infection capacity, as previously described for its ortholog in *T. brucei* (Tyler Weisbarth et al., 2018).

RBPs With the CCCH Zinc Finger Domain in *T. cruzi*

Zinc finger proteins (ZFP) were originally identified as DNA binding proteins with a molecular arrangement of two cysteine and two histidine residues that coordinate a zinc ion. However, it was later demonstrated that a class of zinc finger proteins characterized by the presence of the domain Cys-Cys-Cys-His (CCCH)- binds to RNA molecules (Hall, 2005).

In *T. cruzi*, the ZFP protein TcZFP1 presents a C(2)H(2) domain and specifically binds cytosine-rich repetitive sequences *in vitro* present in untranslated regions of many mRNAs in trypanosomatids (Mörking et al., 2004). TcZFP2 is also a C(2)H(2) ZFP that binds transcripts associated with parasite-host interactions. It was shown that the mRNAs bound to this protein are downregulated in the replicative forms, indicating that the TcZFP2 protein might act as a destabilizing factor (Mörking et al., 2012). In addition, TcZFP1 and TcZFP2 interact with each other via WW domain in TcZFP2A (Caro et al., 2005). TcZFP8 is a zinc finger protein that presents a nuclear localization that might act in RNA metabolism in *T. cruzi* nucleus (Ericsson et al., 2006).

The ZFP protein TcZC3H39 presents a CCCH domain and a U-box domain. The U-box domain is involved in substrate specificity for ubiquitination (Christensen and Klevit, 2009). TcZC3H39 is associated with the stress response in *T. cruzi*: it binds to highly expressed mRNAs that code for cytochrome c oxidase (COX) enzymes and ribosomal proteins, slowing their translation under stress conditions. Interestingly, TcZC3H39 associates with transcripts that are related in function, hence providing support to the RNA regulon theory (Alves et al., 2014).

TcZC3H31 is a cytoplasmic CCCH ZFP expressed in epimastigotes and metacyclic trypomastigotes. Deletion of *zc3h31* led to the impairment of epimastigote differentiation into the metacyclic trypomastigote form. In addition, when insects were infected with *zc3h31* KO cells, the parasites presented an altered morphology relative to wild-type cells, indicating a delay in differentiation. Moreover, in cells overexpressing TcZC3H31, the differentiation rate from epimastigotes into metacyclic trypomastigotes was more efficient than that in wild-type epimastigotes. These results indicate that this ZFP is an important cell cycle regulator in *T. cruzi* (Alcantara et al., 2018).

Other RBP Domains in *T. cruzi*

The PUF (Pumilio/Fem-3 mRNA binding factor) protein family of RBPs is very common in higher eukaryotes; these proteins recognize cis-elements in the 3'-UTR of the mRNAs, regulating their stability and function. In *T. cruzi*, there are eight putative PUF proteins annotated in the genome (Caro et al., 2006); the protein TcPUF6 was characterized in epimastigotes and demonstrated to be involved in the destabilization of specific mRNAs that are upregulated in the infective trypomastigote forms of the parasite (Dallagiovanna et al., 2008).

TcSR62 belongs to the family of serine/arginine (SR)-rich proteins; it is a cytoplasmic RBP implicated in the stress response in *T. cruzi* upon actinomycin D (ActD) treatment. TcSR62 relocates to the nucleolus when transcription is inhibited

in epimastigotes along with other RBPs, specifically PTB (polypyrimidine tract-binding protein) and PABP1 (poly A binding protein 1). Interestingly, the same pattern of nucleolar localization was observed with poly(A+) mRNAs after ActD treatment. Altogether, these results suggest that the nucleolus could play a role in accumulating and protecting mRNAs and associated RBPs when cells are subjected to a specific stress condition (Názer et al., 2011).

The canonical RNAi pathway is not functional in *T. cruzi*; however, a canonical Argonaute (AGO/PIWI), named TcPIWI-tryp, is present and expressed throughout the life cycle of the parasite (Garcia Silva et al., 2010). Sequencing of TcPIWI-tryp-associated RNAs showed enrichment for small RNAs, mainly derived from rRNAs and tRNAs. The composition of small RNAs in the *T. cruzi* TcPIWI/AGO protein is distinct from those identified in other eukaryotes, suggesting that in this parasite, the protein might present distinct biological functions (Garcia-Silva et al., 2014).

Members of the Alba (acetylation lowers binding affinity) protein family bind DNA and interact with distinct RNA molecules and form mRNP complexes. TcAlba30 is an Alba protein in *T. cruzi* that is expressed in all stages of the parasite life cycle. Ribonomic analysis showed that TcAlba30 can interact with β -amastin mRNA. When the protein was overexpressed, the levels of β -amastin decreased by 50%, indicating a role in the negative control of β -amastin expression (Pérez-Díaz et al., 2017).

There is much evidence showing that proteins without canonical RNA-binding domains (RBDs) can interact with RNA molecules; these are known as moonlighting proteins, and they have been extensively studied (Collingridge et al., 2010; Huberts et al., 2010; Lindner et al., 2013; Müller-McNicoll and Neugebauer, 2013; Gil-Bona et al., 2015). One example of an RNA binding protein lacking RBD in *T. cruzi* is elongation factor 1 α (EF-1 α), which plays a canonical role in translation. This protein responds to stress conditions by binding a specific subset of mRNAs. The associated mRNAs showed enrichment of gene sets involved in single-organism metabolic processes, amino acid metabolic processes, ATP and metal ion binding and glycolysis. EF-1 α co-sedimented with heavy complexes that were not associated with the translation machinery, reinforcing the “moonlighting” role of this protein during stress conditions (Alves et al., 2015).

KNOCKOUT OF RBP GENES

Despite all the advances regarding the function of RBPs in trypanosomes, the roles of many of these proteins in the parasite's gene regulatory network remain unknown. To address this issue, in addition to the already mentioned high-throughput techniques, other resourceful methodologies are being used to study RBPs. They consist essentially of genetic reverse approaches, such as overexpression and/or gene knockdown/knockout. Indeed, our current knowledge about the roles of individual RBPs came mostly from studies that modulated their endogenous levels by increasing and/or

decreasing/abolishing their expression and investigating the impact on the vital processes of the parasites, such as proliferation, differentiation, and infection, among others.

In *T. brucei*, studies involving RBP gene silencing (knockdown) by the interference RNA (RNAi) machinery provided a major contribution to the field and allowed the investigation of many RBP functions (Estévez, 2008; Archer et al., 2009; Ling et al., 2011; Subota et al., 2011; Das et al., 2012; Wurst et al., 2012; Droll et al., 2013; Levy et al., 2015). In *T. cruzi*, however, since the RNAi machinery is not functional, to understand the impact of the absence of a specific RBP, researchers had to attempt gene knockout by incorporating a DNA cassette containing a selective drug marker into a target gene by homologous recombination. However, due to the limitations of this methodology, only one group reported success in knocking out RBPs with this approach (Alcantara et al., 2018). Accordingly, this approach is not feasible in cases where the target gene is essential, which seems to be the case for many RBPs, as reported in *T. brucei* through gene silencing assays (Das et al., 2012; Wurst et al., 2012; Droll et al., 2013; Fernández-Moya et al., 2014; Jha et al., 2015; Levy et al., 2015).

Therefore, in order to further advance comprehension of this important set of regulatory proteins in *T. cruzi*, new and more efficient genetic editing technologies are required. Fortunately, the CRISPR/Cas9 DNA editing system has recently emerged as a resourceful and promising tool for reverse genetics approaches and has already been adapted for several organisms, including those that are considered challenging to manipulate genetically, as is the case with *T. cruzi* (Lander et al., 2015, 2016; Peng et al., 2015; Soares Medeiros et al., 2017; Costa et al., 2018b; Romagnoli et al., 2018). Recently, we proposed some modifications to previous CRISPR/Cas9 (Lander et al., 2015; Peng et al., 2015) methods for knockout generation in *T. cruzi* (Romagnoli et al., 2018). Our goal was to establish a protocol with maximum disruption efficiency and a way to investigate/confirm related phenotypes as quickly as possible, which is crucial considering that disruption of important regulatory elements is likely to be essential to the parasite. Briefly, our current strategy consists of generating a highly enriched and stable population expressing Cas9-GFP and then transfecting this population with desired *in vitro*-produced guide RNAs (gRNAs) to target RBP genes along with a repair single-stranded DNA template containing a unique restriction site and a sequence that encodes the stop codons in three different frames. Our initial strategy did not use a DNA donor for direct double-strand break repair (Romagnoli et al., 2018). However, based on other reports that highlighted an increase in gene disruption efficiency and specificity in the presence of a single-strand DNA donor (Lander et al., 2015; Zhang et al., 2017; Burle-Caldas et al., 2018), we incorporated the use of a DNA template into our strategy as well.

To date, a few reports with slightly different application strategies have used the CRISPR/Cas9 system to manage gene disruption in *T. cruzi*, but as yet, none have reported its use to knock out and study RBP genes. The knockout of RBP genes in *T. cruzi* should provide new clues about the role of RBPs in gene expression regulation of the parasite. We will show and

discuss below a CRISPR/Cas9 approach to perform the knockout of RBPs in *T. cruzi*, using as examples some of the RBPs that we are investigating.

In addition to the already mentioned TcZC3H39, we also present data from the knockout assays of two other RBPs, TcZC3H29 (TCDM_11529), and TcZC3H1TP (TCDM_03704). These two zinc finger proteins are unique to Kinetoplastida and contain C3H domains (Kramer et al., 2010). While TcZC3H29 has two C3H domains (C-X₇-C-X₅-CX₃-H and C-X₈-C-X₄-C-X₃-H), TcZC3H1TP has one C3H domain (C-X₈-C-X₅-C-X₃-H), and a DNAJ domain (Figure 2A). Proteins TcZC3H29 and TcZC3H1TP present cytoplasmatic localization with a granular pattern (Figure 2B), similar to that reported for TcZC3H39 (Alves et al., 2014). Our interest in these two particular RBPs was dictated by the fact that they are exclusively expressed in the non-infective epimastigote form (data not shown). Accordingly, they are downregulated in the course of differentiation into infective metacyclic trypomastigotes (Figure 2C). Interestingly, even ectopically overexpressed Flag-tagged TcZC3H29 and TcZC3H1TP were not detected in metacyclic trypomastigotes

(Figure 2D), thus indicating the existence of tight regulatory control acting at stage-specific expression levels and pointing their crucial role in *T. cruzi* development.

Initial attempts to use the CRISPR/Cas system involved knocking out *T. cruzi* GP72, and the cells presented the typical flagellum detachment phenotype (Lander et al., 2015; Romagnoli et al., 2018). Next, we attempted to knock out TcZC3H39, TcZC3H29, and TcZC3H1TP by performing electroporation with specific guide RNAs to target their respective genes (Supplementary Table 1). After transfection, major morphological changes were observed in the cultures (Figures 3A–C). For TcZC3H39 and TcZC3H29, cells presented a larger size, an extension of the posterior region and more than one flagellum per cell (Figures 3A–B, respectively). The cultures targeted with TcZC3H29 gene disruption presented additional flagella that were thinner and longer than those found in control parasites or when targeting TcZC3H39 or TcZC3H1TP (Figure 3 comparing B–D, A, and C, respectively). The targeting of TcZC3H1TP resulted in larger cells, but they did not have the body extension that was observed for the two other zinc

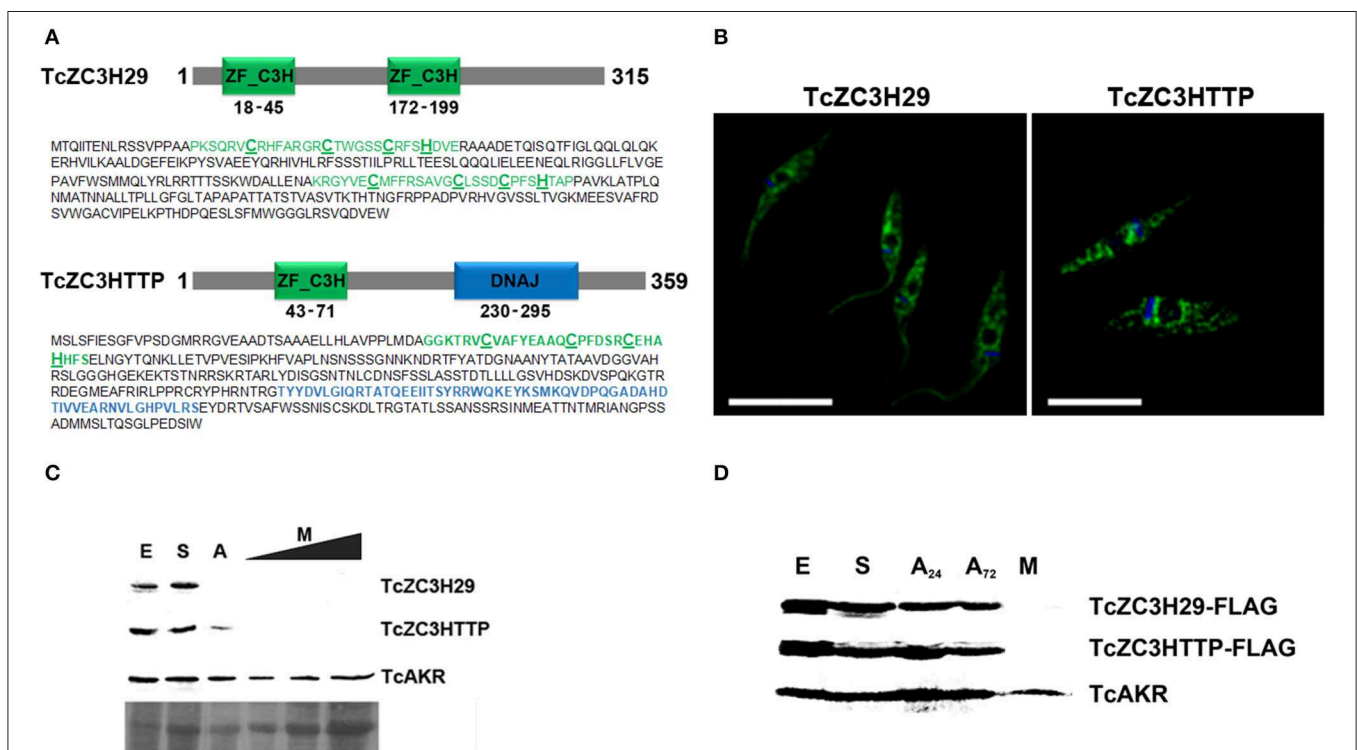
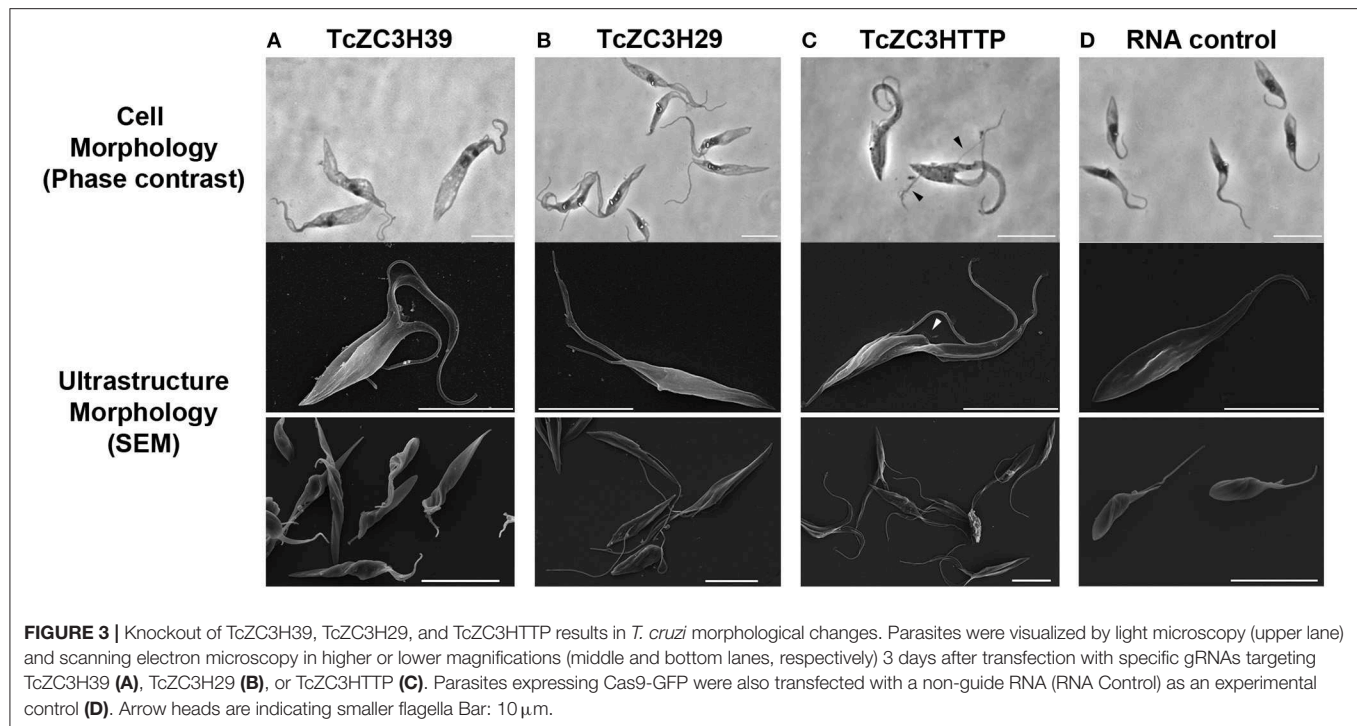


FIGURE 2 | The *T. cruzi* zinc finger proteins TcZC3H29 and TcZC3H1TP. **(A)** Graphic representation and amino acid sequences of the proteins. The zinc finger C3H domains are highlighted in green (with the cysteine and histidine residues underlined in bold) and the TcZC3H1TP DNAJ domain in blue. **(B)** Immunolocalization of TcZC3H29 and TcZC3H1TP. Epimastigotes were incubated with anti-TcZC3H29 (1:300) or anti-TcZC3H1TP (1:750), and an Alexa 488-conjugated goat anti-mouse antibody (1:600) was used for detection. The nucleus and kinetoplast are stained with DAPI. Bar = 10 μ m. **(C)** TcZC3H29 and TcZC3H1TP expression profiles during metacyclogenesis. Western blot of protein extracts obtained from 5×10^6 parasites in distinct differentiation stages. Epimastigotes (E), epimastigotes after 2 h of nutritional stress (S), nutritionally stressed epimastigotes in the adhesion stage (A) and metacyclic trypomastigotes (M). To further investigate the expression of TcZC3H29 and TcZC3H1TP in the infective form, increased amounts of metacyclic trypomastigotes extract (5×10^6 , 1×10^7 , and 1.5×10^7 parasites) were used. Detection was performed with antisera against TcZC3H29 (1:500) and TcZC3H1TP (1:1,000) and anti-TcAKR (1:1,000). TcAKR (Aldo-keto reductase, TCDM_00490) was used as a normalizer. A portion of the Ponceau-S stained blot is shown to demonstrate sample input. **(D)** 3xFLAG C-terminally tagged TcZC3H29 and TcZC3H1TP detection during metacyclogenesis. Protein extracts were prepared from 5×10^6 parasites at different metacyclogenesis stages and incubated with anti-FLAG antibodies (1:1,000). A₂₄—nutritionally stressed adhered epimastigotes after 24 h; A₇₂—nutritionally stressed adhered epimastigotes after 72 h.



finger RBP knockouts (Figure 3C). In addition, the cell division process of the transfected parasites seemed to be affected, as two fully formed flagella and duplication of the anterior region were frequently observed. Smaller flagella were also observed (Figure 3C). Surprisingly, parasites in final stages of cell division (just before cytokinesis, when cells are connected by their posterior end with one flagellum in each anterior end (Alcantara et al., 2017) were observed with another new flagellum already in each anterior end (Supplementary Figure 1), thus reinforcing the idea that these cells somehow lost at least part of their cell cycle coordination.

To further investigate the impact of targeting these zinc finger proteins on cell cycle, we analyzed the DNA content of transfected cells by flow cytometry from day 1 to 5 after gRNA transfection. In general, cell cycle kinetic analysis revealed an increase in the number of parasites at the G2/M phase when targeting TcZC3H39, TcZC3H29, or TcZC3HTTP (Figures 4A–C, respectively). The TcZC3H29 gene disruption attempt provoked a significant accumulation of parasites with double DNA content in the first 3 days of the analysis (Figure 4A), whereas TcZC3H39 and TcZC3HTTP presented this phenomenon throughout the entire kinetic analysis (Figures 4B–C). Interestingly, TcZC3HTTP targeting resulted in a significant number of parasites with DNA content slightly above the value considered to be double (Figure 4C). The meaning of this observation remains to be elucidated. Nevertheless, cell cycle analysis indicates that the attempt to knock out any of these zinc finger proteins impaired cell cycle progression, likely due to the inability of the cells to complete the division process, thus raising the possibility that TcZC3H39, TcZC3H29, and TcZC3HTTP are essential genes in *T. cruzi*.

Accordingly, all the attempts to clone (or even enrich) and culture the morphologically affected parasites have been unsuccessful (data not shown).

It is important to mention that TcZC3H39, TcZC3H29, and TcZC3HTTP gene disruption was performed at least three times using different designed gRNAs, and the observed effects were reproduced in all attempts with all guide RNAs (Supplementary Figure 2). In addition, the phenotypes observed for the zinc finger targets were not observed in the control Cas9-GFP expressing population, wild-type cells or even the Cas9-GFP population parasites transfected with a control RNA (Supplementary Figure 3). Additionally, these experiments were performed in parallel with the knockout of other known proteins, such as GP72 and α -tubulin, which presented previously described morphological phenotypes [data published elsewhere (Lander et al., 2015; Romagnoli et al., 2018)].

The changes observed in the TcZC3H39, TcZC3H29, and TcZC3HTTP knockout populations are specific and likely due to the absence of these proteins in *T. cruzi*. Western blot analysis to assess the expression of TcZC3H29 and TcZC3HTTP in the transfected populations showed the absence of the proteins only in the cultures electroporated with gRNAs targeting their encoding gene (Supplementary Figure 4). However, as yet we were not able to detect gene editing at the DNA level (data not shown).

This concern led us to adapt the experimental approach in order to improve the gene disruption identification capability. Hence, for TcZC3H39, TcZC3H29, and TcZC3HTTP knockouts, in addition to the respective designed guide RNAs to specifically target the genes, a DNA template was designed and included into the transfection process to direct specific gene repair.

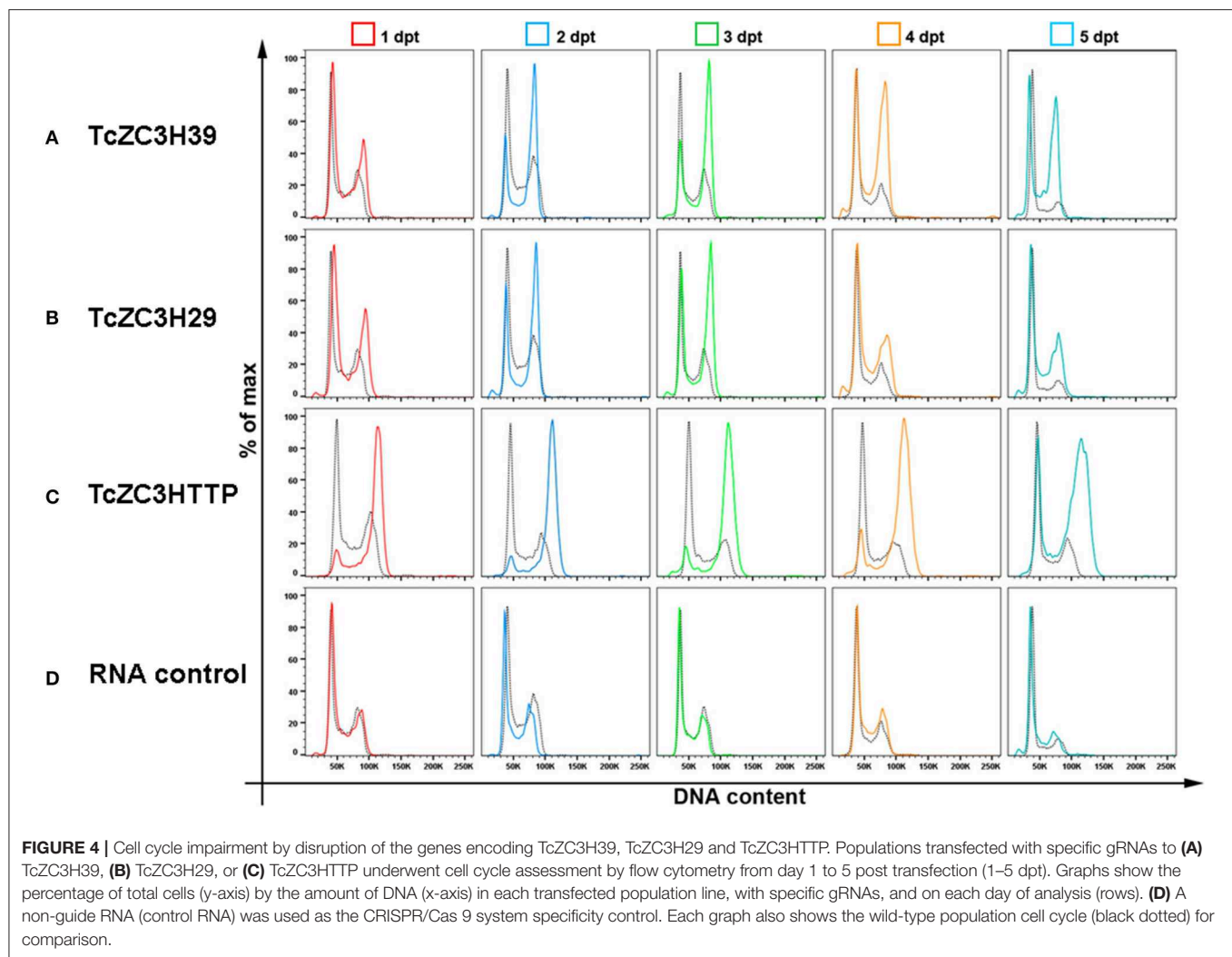


FIGURE 4 | Cell cycle impairment by disruption of the genes encoding TcZC3H39, TcZC3H29 and TcZC3HTTP. Populations transfected with specific gRNAs to (A) TcZC3H39, (B) TcZC3H29, or (C) TcZC3HTTP underwent cell cycle assessment by flow cytometry from day 1 to 5 post transfection (1–5 dpt). Graphs show the percentage of total cells (y-axis) by the amount of DNA (x-axis) in each transfected population line, with specific gRNAs, and on each day of analysis (rows). (D) A non-guide RNA (control RNA) was used as the CRISPR/Cas 9 system specificity control. Each graph also shows the wild-type population cell cycle (black dotted) for comparison.

This DNA template strategy was designed based on previous reports (Zhang and Matlashewski, 2015; Zhang et al., 2017; Burle-Caldas et al., 2018) and consists of a 77-nt single strand oligo DNA donor containing homology arms (30 nt at each end), a restriction site for *Bgl*II, and a sequence that encodes three stop codons in three different frames (Figure 5A). After transfecting the gRNAs along with their corresponding DNA donors (the TcZC3H39, TcZC3H29, and TcZC3HTTP genes), repair/disruption was confirmed by polymerase chain reaction directly from liquid culture (Alcantara et al., 2014). The amplified target gene products were digested with the *Bgl*II enzyme (Figure 5B). As shown, only the cultures co-transfected with the gRNAs and the related single-stranded DNA oligos successfully incorporated the *Bgl*II restriction site at the target gene although the DNA donor incorporation occurred with distinct efficiencies (Supplementary Figure 5). Furthermore, the amplified target genes were cloned into the pGEM-T Easy vector (Promega) and sequenced for correct repair visualization (Figure 5C). However, some of the PCR product remained undigested (Figure 5B, arrows), indicating that in the transfected

cultures there were parasites that did not have the target RBP gene disrupted/repared, or the editing may have occurred in one allele only. To test the hemi-knockout hypothesis, single-cell sorting was performed to individualize the transfected parasites. After growth, clones from all sorted cultures were tested again by PCR and *Bgl*II digestion. In all sorted populations, clones were observed that did not exhibit incorporation of the *Bgl*II restriction site (data not shown), thus pointing to the fact that gene disruption did not achieve 100% efficiency.

In order to further explore the hemi-knockout hypothesis, the clones that presented the *Bgl*II restriction site but also showed undigested product (meaning that they were not null mutants) were single cell cloned once more and further analyzed by PCR following a *Bgl*II digestion. All clones tested were partially digested with *Bgl*II (data not shown), indicating that they were in fact hemi-knockouts. Thus, at least two hemi-knockout clones for each ZFP target gene were submitted to a new transfection round with the corresponding gRNA and DNA donor previously used. This approach allowed to confirm the knockout of TcZC3HTTP gene by detecting the DNA donor insertion and complete PCR

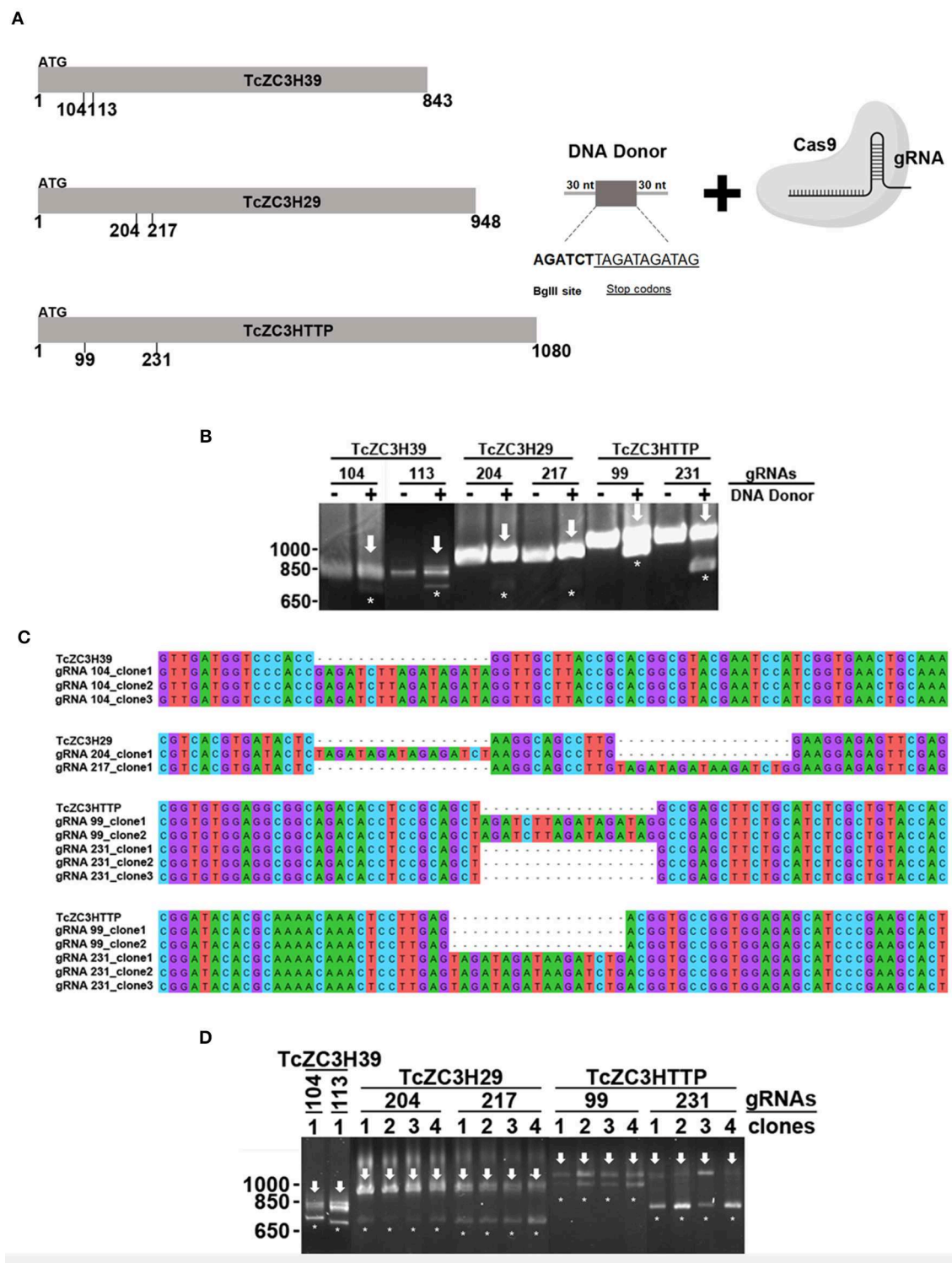


FIGURE 5 | Disruption of the genes encoding TcZC3H39, TcZC3H29, and TcZC3H2TP by CRISPR/Cas9 using a DNA donor strategy. **(A)** Scheme depicting the DNA donor strategy used for gene knockout. Zinc finger genes (represented on the left as TcZC3H39, TcZC3H29, and TcZC3H2TP) were targeted by Cas9 (through specific gRNA recognition) in different regions (the positions are indicated below each gene representation) along with a DNA template containing a 30-nt homology arm (at each end), a *Bgl*II restriction site (AGATCT) and a sequence that encodes stop codons in three different frames (TAGATAGATAG). **(B)** Genomic DNA from transfected populations with gRNAs targeting TcZC3H39, TcZC3H29, or TcZC3H2TP with (+) or without (–) the respective DNA donors was PCR amplified with

(Continued)

FIGURE 5 | specific primers for each zinc finger gene and digested with *Bgl*II for gene disruption visualization. Asterisks (*) highlight *Bgl*II restriction site incorporation by showing the digested products, whereas the remaining undigested amplicon is indicated by an arrow. **(C)** DNA sequencing of the *tczc3h39*, *tczc3h29*, and *tczc3http* genes showing correct insertion of the DNA donor. After transfection, zinc finger targeted genes were amplified from genomic DNA, cloned into the pGEM-T Easy vector (Promega) and transformed into the TOP10 chemically competent *Escherichia coli* strain. Then, plasmids were isolated from the positive clones (identified by PCR and *Bgl*II digestion) and sent for sequencing for gene disruption confirmation. **(D)** Confirmation of single cell sorted clones containing the *tczc3h39*, *tczc3h29*, or *tczc3http* disrupted genes. Genomic DNA from the single cell cloned (by flow cytometry) population was used for *tczc3h39*, *tczc3h29*, or *tczc3http* PCR amplification followed by *Bgl*II digestion. At least one clone is representatively shown for each gene according to the specific gRNA used to achieve gene knockout (indicated above).

product *Bgl*II digestion and also loss of TcZC3HHTTP protein expression by Western blot (**Figure 6**). We keep searching for null mutant clones to TcZC3H39 and TcZC3H29 coding genes as we will advance with the TcZC3HHTTP knockout parasites to the next step, that is to further investigate its related phenotype, specially regarding its impact in the context of *T. cruzi* gene expression regulation.

DISCUSSION

RBPs are considered essential factors in gene expression regulation, especially in trypanosomatids, where posttranscriptional processes are predominant. Indeed, advances in the understanding of RBP functions reinforce their actions as key players in coordinating mRNA metabolism and maintaining cell homeostasis. However, the contributions of several RBPs to the *T. cruzi* regulatory network remain to be determined. From all the RBPs studied in *T. cruzi* presented in this review, until now, only the function of TcZC3H31 has been investigated by a gene knockout approach (Alcantara et al., 2018). This lack of studies regarding RBP knockout in *T. cruzi* is mainly due to the challenge of genetically manipulating this parasite using classical knockout approaches, which are limited in the case of essential genes. In this context, the development and adaptation of the genetic editing tool, CRISPR/Cas9, has emerged as a great alternative to achieve RBP knockout in *T. cruzi*.

As a proof of concept, along with this review we present data from the knockout of three RBPs with C3H zinc finger domains in *T. cruzi* by using the CRISPR/Cas9 technique. TcZC3H39, TcZC3H29, and TcZC3HHTTP knockouts were achieved using two distinct approaches. One consisted of transfecting specific gRNAs for each target gene only into a Cas9-GFP-expressing population. The other approach involved co-transfecting a specific DNA donor template along with the related gRNA. By targeting the *tczc3h39*, *tczc3h29*, or *tczc3http* gene, we were able to see major morphological changes, cell cycle impairment (**Figures 3, 4**, respectively) and viability loss (data not shown). There were characteristic morphological alterations for each culture, and all modifications involved an increase in cell size and in the number and/or shape of the flagellum (**Figure 3**). Burle-Caldas and colleagues reported that disrupting GP72 without a DNA donor sequence to direct repair could lead to abnormal morphology depending on the gRNA used (Burle-Caldas et al., 2018). Although the changes observed in the knockout cultures for TcZC3H39, TcZC3H29, and TcZC3HHTTP were not seen in the controls (RNA control, gRNA-GFP, Cas9-GFP transfected with PBS), or even with the targeting of other non-RBP genes

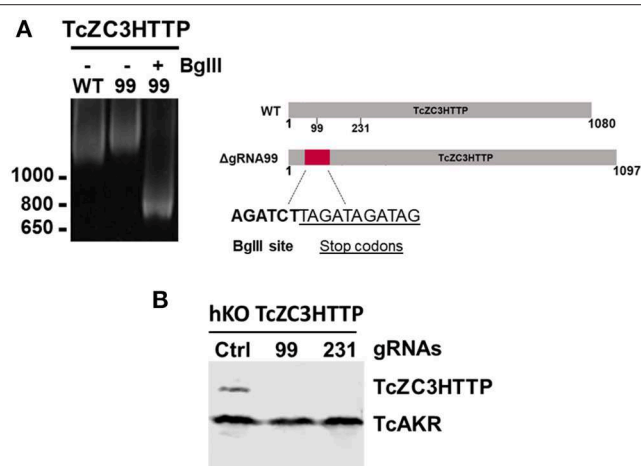


FIGURE 6 | TcZC3HHTTP knockout confirmation after transfection with specific gRNAs. **(A)** 5% polyacrylamide gel electrophoresis to confirm DNA donor incorporation in the TcZC3HHTTP gene. Genomic DNA from cloned population (by flow cytometry) was used for *tczc3http* PCR amplification followed by *Bgl*II digestion (left panel). Scheme depicting the expected increase in TcZ3HHTTP gene size and *Bgl*II site and stop codon sequence insertion. **(B)** Western blot assay to confirm TcZC3HHTTP gene disruption. TcZC3HHTTP Hemi-knockout cloned population were transfected once again with gRNAs targeting TcZC3HHTTP (gRNA 99 or gRNA 231) or a non-guide RNA control (Ctrl) and parasites were harvested and protein content extracted. Polyclonal antibodies against TcZC3HHTTP (1:1000) were used for protein detection. The amount of protein extract applied corresponded to 1×10^7 parasites and TcAKR protein was used as an input control. This experiment was performed twice.

[e.g., GP72, α -tubulin, β -tubulin (Romagnoli et al., 2018)], this raises a question about the specificity of the phenotypes observed for the zinc finger gene knockouts. However, it is worth mentioning that morphological changes similar to those we observed for TcZC3H39 and TcZC3H29 knockouts were also described when overexpressing TbZFP3 (Paterou et al., 2006) or when knocking down the RBPs ALBA3/4 (Subota et al., 2011), TbRRM1 (Levy et al., 2015), and TbZFP2 (Hendriks et al., 2001) in *T. brucei*. In 2001, Hendriks et al. identified a posterior end elongation phenotype in TbZFP2 knockdown parasites (caused by the polar extension of microtubules) that they termed a “nozzle” (Hendriks et al., 2001). Interestingly, TcZC3H39 and TcZC3H29 knockout parasites displayed a morphological phenotype resembling the “nozzle.” Moreover, the G2/M phase cell cycle arrest observed in the zinc finger RBP knockouts described herein (**Figure 4**) was also described in *T. brucei* when suppressing the genes encoding the RBPs TbPUF9 (Archer et al.,

2009), ALBA3/4 (Subota et al., 2011), TbZC3H11 (Droll et al., 2013), TbRRM1 (Levy et al., 2015), and TbZFP2 (Hendriks et al., 2001) by RNAi. These data corroborate the notion that the cell cycle alterations identified in the knockout populations for TcZC3H39, TcZC3H29, and TcZC3HTTP are specific and not the result of the non-specific activity of endonuclease Cas9. In addition to all the controls used in our experiment, the phenotypes reported in *T. brucei* came from RNAi studies and, therefore, did not involve DNA editing (double-strand breaks). When the expression levels of the aforementioned *T. brucei* RBPs were suppressed/abolished, there were effects on the cell cycle accompanied by major morphological changes, such as the nozzle phenotype. Hence, there is a strong correlation between cell cycle and cell morphology maintenance with RBPs. It remains to be elucidated whether this is a direct or indirect relation (through their RNA targets). Either way, this is the first evidence showing the nozzle phenotype and relating these morphological changes with cell cycle arrest due to the knockout of zinc finger proteins in *T. cruzi*.

To further support the idea that the observed phenotypes are specific to TcZC3H39, TcZC3H29, and TcZC3HTTP knockout, the co-transfection of DNA donor along with gRNAs allows detection of the precise insertion of the repair template into the target genes (Figure 5). However, although the previously described phenotypes (without DNA donor transfection) were reproduced, they were significantly less frequent relative to the approach using only gRNAs (Supplementary Figure 6). We found evidence that this was due to the selection of hemi-knockout populations (Figure 5D). How unintentional heterozygote parasites are generated by CRISPR/Cas9 remains to be explained, but it seems to occur preferably when cells are co-transfected with the DNA donor. Curiously, another group working with *T. cruzi* also observed this phenomenon (Soares Medeiros et al., 2017). In their report, Soares Medeiros et al. (2017) attempted to knock out the Galf and calreticulin (CRT) genes by CRISPR/Cas9 but only found clones presenting both WT and mutant alleles. Since those genes are single-copy genes and, for CRT, knockout by conventional approaches was unfruitful, authors associated the heterozygosity to genes that are potentially essential to the parasite (Soares Medeiros et al., 2017). According to this and based on all the evidence gathered from the phenotypes related to the disruption of TcZC3H39, TcZC3H29, and TcZC3HTTP, we believed that the generation of a hemi-knockout population reinforces the idea that these zinc finger genes may be essential for *T. cruzi*.

Performing a new round of transfection in those hemi-knockout populations allowed us to obtain null mutant clones for TcZC3HTTP, thus indicating that this protein is not essential in epimastigotes. However, since TcZC3HTTP is downregulated throughout metacyclogenesis, a lethal phenotype could be observed in this differentiation process. Therefore, it is very important to characterize these clones during this development stage.

The use of the CRISPR/Cas9 technique for RBP knockout will start to open a new era in gene expression regulation studies and advance the uncovering and mapping of regulatory gene networks in *T. cruzi*.

MATERIALS AND METHODS

T. cruzi Culture, gRNA and DNA Donor Preparation and Transfections

T. cruzi Dm28c epimastigotes were cultured at 28°C in liver infusion tryptose (LIT) medium supplemented with 10% heat-inactivated fetal bovine serum (FBS). The guide RNAs were obtained using the online Eukaryotic Pathogen CRISPR gRNA Design Tool (EuPaGDT) (Peng and Tarleton, 2015) and produced by *in vitro* transcription as previously described (Peng et al., 2015; Romagnoli et al., 2018). DNA donor sequences were designed to have a BglII restriction site (AGATCT) and a sequence encoding stop codons in three different frames (TAGATAGATAG), all flanked by 30-nt homology arms (according to their specific gRNA target sequence). gRNAs and donor sequences are in **Supplementary Table 1**. For transfection, 5×10^6 early-log phase Cas9-GFP expressing epimastigotes were harvested by centrifugation ($3,000 \times g$, 5 min), washed in PBS (pH 7.4) and resuspended in 100 µl of human T cell nucleofector solution at room temperature. For target gene disruption, 20 µg of a specific gRNA and 20 µg of respective donor DNA were added to the solution before electroporating the parasites with one electric pulse using the X-014 program in an Amaxa Nucleofector device. A DNA fragment of human 18S rRNA provided by the MEGAShortscript T7 kit (Thermo Fisher Scientific) was transcribed and used as a control (RNA control). After transfection, parasites were cultured in 25-cm² cell culture flasks containing 10 ml of LIT medium supplemented with 10% FBS.

Immunolocalization and Immunoblot Assays

For immunofluorescence assays, epimastigotes were harvested from culture, washed, fixed with 4% paraformaldehyde in PBS and added to poly-L-lysine-coated slides. Cells were then permeabilized with Triton X-100 in PBS (pH 8.0) for 5 min and blocked with bovine serum albumin (BSA, 1.5%). Parasites were incubated with anti-TcZC3H29 (1:300) or anti-TcZC3HTTP (1:750), and an Alexa 488-conjugated goat anti-mouse antibody (1:600) was used for detection. The nuclei and kinetoplast were stained with DAPI. Images were collected on Leica DMI6000 B (Leica-microsystems) equipment. Captured images were processed by deconvolution with LAS AF–Leica (Leica microsystems) software. Bar = 10 µm.

For western blot assays, wild-type and transfected epimastigotes (expressing TcZC3H29-3xFLAG or TcZC3HTTP-3xFLAG) were differentiated into metacyclic trypomastigotes as previously described (Contreras et al., 1985), and protein extract from different stages during differentiation was prepared. Protein extracts were separated by SDS-PAGE (13%) and transferred to a nitrocellulose membrane. After Ponceau S staining and blocking non-specific binding sites with 5% non-fat skim milk in PBST (PBS supplemented with 0.05% of Tween 20) for 1 h at 25°C, membranes were incubated with anti-TcZC3H29 (polyclonal, 1:500), anti-TcZC3HTTP (polyclonal, 1:1000), anti-TcAKR (polyclonal, 1:1000) or anti-FLAG antibodies (monoclonal, 1:1000) for 1 h at 25°C, washed three times with

PBST and incubated with goat anti-mouse IgG secondary antibodies conjugated to the fluorophore IRDye®680LT (LI-COR Biosciences). Fluorescence detection was performed with an Odyssey® scanner (LI-COR Biosciences).

Morphological Characterization

Panoptic staining and sample preparation and acquisition for scanning electron microscopy were performed as previously described (Romagnoli et al., 2018).

Flow Cytometry

DNA content determination was performed in a FACSCanto II machine (Becton-Dickinson). A total of 1×10^6 parasites were harvested ($3,000 \times g$, 5 min) and resuspended in 100 μ l of PBS and mixed with 100 μ l propidium iodide (PI) staining solution (3.4 mM Tris-HCl pH 7.4, 0.1% NP40, 10 μ g/ml RNase A, 10 mM NaCl, 30 μ g/ml propidium iodide). PI was excited by a blue laser (488 nm), and emitted light was collected by 585/42 bandpass. Single cells were gated based on pulse area (PE-A) vs. pulse width (PE-W) of the PE channel. Cellular aggregates and debris were excluded from cell cycle analysis. At least 10,000 events were recorded for each replicate, and data were analyzed using FlowJo V10.1r7 software. For single-cell sorting and cell enrichment, a BD FACSARIA II (Becton-Dickinson) machine was used.

DNA Amplification, Digestion, and Sequencing

DNA amplification was carried out by PCR with specific primers for TcZC3H39 (TCDM_00519), TcZC3H29 (TCDM_11529), and TcZC3HTTP (TCDM_03704) (Supplementary Table 1) directly from liquid culture as previously described (Alcantara et al., 2014). PCR conditions were as follows: 95°C for 2 min, followed by 40 cycles of 95°C for 15 s, 55°C for 15 s, and 72°C for 1 min and 15 s. Additionally, for pGEM-T easy (Promega) amplicon cloning, a final step of 72°C for 10 min

was included. PCR products were digested by BglII (New England Biolabs) at 37°C overnight. Amplified DNA and digestion products were visualized in a 3% agarose gel. For sequencing, plasmids containing the disrupted genes (previously confirmed by PCR and digestion) were purified with the QIAprep Spin Miniprep Kit (QIAGEN) and sequenced at WEMSeq Biotechnology (wemseq.com). Alignments were made using MEGA version 10.0.5.

DATA AVAILABILITY STATEMENT

The raw data supporting the conclusions of this article will be made available by the authors, without undue reservation, to any qualified researcher.

AUTHOR CONTRIBUTIONS

BR performed the experiments and wrote the manuscript. FH discussed the results and wrote the manuscript. LA collaborated on the discussion of the results and wrote the manuscript. SG collaborated on the discussion of the results and wrote the manuscript. All authors approve the submitted version.

ACKNOWLEDGMENTS

This work received financial support from Conselho Nacional de Desenvolvimento Científico e Tecnológico (CNPq, Brazil) and from Fundação Oswaldo Cruz (Fiocruz, Brazil). SG was a research fellow awardee from CNPq. We thank Wagner Nagib Birbeire for the schematic Figure 1.

SUPPLEMENTARY MATERIAL

The Supplementary Material for this article can be found online at: <https://www.frontiersin.org/articles/10.3389/fcimb.2020.00056/full#supplementary-material>

REFERENCES

- Aibara, S., Valkov, E., Lamers, M., and Stewart, M. (2015). Domain organization within the nuclear export factor Mex67:Mtr2 generates an extended mRNA binding surface. *Nucleic Acids Res.* 43, 1927–1936. doi: 10.1093/nar/gkv030
- Alcantara, C., de, L., Vidal, J. C., de Souza, W., and Cunha-e-Silva, N. L. (2017). The cytosome-cytopharynx complex of *Trypanosoma cruzi* epimastigotes disassembles during cell division. *J. Cell Sci.* 130, 164–176. doi: 10.1242/jcs.187419
- Alcantara, M. V., Frago, S. P., and Assine Picchi, G. F. (2014). Knockout confirmation for hurries: rapid genotype identification of trypanosoma cruzi transfectants by polymerase chain reaction directly from liquid culture. *Mem. Inst. Oswaldo Cruz* 109, 511–513. doi: 10.1590/0074-0276140010
- Alcantara, M. V., Kessler, R. L., Gonçalves, R. E. G., Marlière, N. P., Guarneri, A. A., Picchi, G. F. A., et al. (2018). Knockout of the CCCH zinc finger protein TcZC3H31 blocks *Trypanosoma cruzi* differentiation into the infective metacyclic form. *Mol. Biochem. Parasitol.* 221, 1–9. doi: 10.1016/j.molbiopara.2018.01.006
- Alves, L. R., Oliveira, C., and Goldenberg, S. (2015). Eukaryotic translation elongation factor-1 alpha is associated with a specific subset of mRNAs in *Trypanosoma cruzi*. *BMC Microbiol.* 15:104. doi: 10.1186/s12866-015-0436-2
- Alves, L. R., Oliveira, C., Mörking, P. A., Kessler, R. L., Martins, S. T., Romagnoli, B. A. A., et al. (2014). The mRNAs associated to a zinc finger protein from *Trypanosoma cruzi* shift during stress conditions. *RNA Biol.* 11, 921–933. doi: 10.4161/rna.29622
- Anderson, P., and Kedersha, N. (2008). Stress granules: the Tao of RNA triage. *Trends Biochem. Sci.* 33, 141–150. doi: 10.1016/j.tibs.2007.12.003
- Archer, S. K., Luu, V. D., De Queiroz, R. A., Brems, S., and Clayton, C. (2009). *Trypanosoma brucei* PUF9 regulates mRNAs for proteins involved in replicative processes over the cell cycle. *PLoS Pathog.* 5:e1000565. doi: 10.1371/journal.ppat.1000565
- Batista, J. A. N., Teixeira, S. M. R., Donelson, J. E., Kirchhoff, L. V., and de, S. Á. C. M. (1994). Characterization of a *Trypanosoma cruzi* poly(A)-binding protein and its genes. *Mol. Biochem. Parasitol.* 67, 301–312. doi: 10.1016/0166-6851(94)00133-2
- Björk, P., and Wieslander, L. (2017). Integration of mRNP formation and export. *Cell. Mol. Life Sci.* 74, 2875–2897. doi: 10.1007/s00018-017-2503-3
- Burle-Caldas, G. A., Soares-Simões, M., Lemos-Pechnicki, L., DaRocha, W. D., and Teixeira, S. M. R. (2018). Assessment of two CRISPR-Cas9 genome editing protocols for rapid generation of *Trypanosoma cruzi* gene knockout mutants. *Int. J. Parasitol.* 48, 591–596. doi: 10.1016/j.ijpara.2018.02.002
- Caro, F., Bercovich, N., Atorrasagasti, C., Levin, M. J., and Vázquez, M. P. (2005). Protein interactions within the TcZFP zinc finger family members of

- Trypanosoma cruzi*: implications for their functions. *Biochem. Biophys. Res. Commun.* 333, 1017–1025. doi: 10.1016/j.bbrc.2005.06.007
- Caro, F., Bercoich, N., Attorrasagasti, C., Levin, M. J., and Vázquez, M. P. (2006). *Trypanosoma cruzi*: analysis of the complete PUF RNA-binding protein family. *Exp. Parasitol.* 113, 112–124. doi: 10.1016/j.exppara.2005.12.015
- Cassola, A., De Gaudenzi, J. G., and Frasch, A. C. (2007). Recruitment of mRNAs to cytoplasmic ribonucleoprotein granules in trypanosomes. *Mol. Microbiol.* 65, 655–670. doi: 10.1111/j.1365-2958.2007.05833.x
- Castello, A., Horos, R., Strein, C., Fischer, B., Eichelbaum, K., Steinmetz, L. M., et al. (2015). Comprehensive identification of RNA-binding proteins by RNA interactome capture. *Methods Mol. Biol.* 1358, 131–139. doi: 10.1007/978-1-4939-3067-8_8
- Christensen, D. E., and Klevit, R. E. (2009). Dynamic interactions of proteins in complex networks: identifying the complete set of interacting E2s for functional investigation of E3-dependent protein ubiquitination. *FEBS J.* 276, 5381–5389. doi: 10.1111/j.1742-4658.2009.07249.x
- Clayton, C. E. (2016). Gene expression in kinetoplastids. *Curr. Opin. Microbiol.* 32, 46–51. doi: 10.1016/j.mib.2016.04.018
- Cléry, A., Blatter, M., and Allain, F. H. T. (2008). RNA recognition motifs: boring? Not quite. *Curr. Opin. Struct. Biol.* 18, 290–298. doi: 10.1016/j.sbi.2008.04.002
- Cléry, A., and Frédéric, H.-T. A. (2012). *From Structure to Function of RNA Binding Domains*. Austin, TX: Landes Bioscience, 137–158.
- Collingridge, P. W., Brown, R. W., and Ginger, M. L. (2010). Moonlighting enzymes in parasitic protozoa. *Parasitology* 137, 1467–1475. doi: 10.1017/S0031182010000259
- Contreras, V. T., Salles, J. M., Thomas, N., Morel, C. M., and Goldenberg, S. (1985). *In vitro* differentiation of *Trypanosoma cruzi* under chemically defined conditions. *Mol. Biochem. Parasitol.* 16, 315–327. doi: 10.1016/0166-6851(85)90073-8
- Costa, F. C., Francisco, A. F., Jayawardhana, S., Calderano, S. G., Lewis, M. D., Olmo, F., et al. (2018b). Expanding the toolbox for *Trypanosoma cruzi*: a parasite line incorporating a bioluminescence-fluorescence dual reporter and streamlined CRISPR/Cas9 functionality for rapid *in vivo* localisation and phenotyping. *PLoS Negl. Trop. Dis.* 12:e0006388. doi: 10.1371/journal.pntd.0006388
- Costa, J. F., Ferrarini, M. G., Nardelli, S. C., Goldenberg, S., Ávila, A. R., and Holetz, F. B. (2018a). *Trypanosoma cruzi* XRNA granules colocalise with distinct mRNP granules at the nuclear periphery. *Mem. Inst. Oswaldo Cruz.* 113:e170531. doi: 10.1590/0074-02760170531
- da Costa Lima, T. D., Moura, D. M. N., Reis, C. R. S., Vasconcelos, J. R. C., Ellis, L., Carrington, M., et al. (2010). Functional characterization of three leishmania poly(A) binding protein homologues with distinct binding properties to RNA and protein partners. *Eukaryot. Cell.* 9, 1484–1494. doi: 10.1128/EC.00148-10
- Dallagiovanna, B., Correa, A., Probst, C. M., Holetz, F., Smircich, P., de Aguiar, A. M., et al. (2008). Functional genomic characterization of mRNAs associated with TcPUF6, a pumilio-like protein from *Trypanosoma cruzi*. *J. Biol. Chem.* 283, 8266–8273. doi: 10.1074/jbc.M703097200
- Dallagiovanna, B., Pérez, L., Sotelo-Silveira, J., Smircich, P., Duhagon, M. A., and Garat, B. (2005). *Trypanosoma cruzi*: molecular characterization of TcPUF6, a Pumilio protein. *Exp. Parasitol.* 109, 260–264. doi: 10.1016/j.exppara.2005.01.003
- Das, A., Morales, R., Banday, M., Garcia, S., Hao, L., Cross, G. A., et al. (2012). The essential polysome-associated RNA-binding protein RBP42 targets mRNAs involved in *Trypanosoma brucei* energy metabolism. *RNA* 18, 1968–1983. doi: 10.1261/rna.033829.112
- De Gaudenzi, J. G., D'Orso, I., and Frasch, A. C. C. (2003). RNA recognition motif-type RNA-binding proteins in *Trypanosoma cruzi* form a family involved in the interaction with specific transcripts *in vivo*. *J. Biol. Chem.* 278, 18884–18894. doi: 10.1074/jbc.M301756200
- De Gaudenzi, J. G., Jäger, A. V., Izcoch, R., and Campo, V. A. (2016). Insights into the regulation of mRNA processing of polycistronic transcripts mediated by DRBD4/PTB2, a trypanosome homolog of the polypyrimidine tract-binding protein. *J. Eukaryot. Microbiol.* 63, 440–452. doi: 10.1111/jeu.12288
- De Gaudenzi, J. G., Noé, G., Campo, V. A., Frasch, A. C., and Cassola, A. (2011). Gene expression regulation in trypanosomatids. *Essays Biochem.* 51, 31–46. doi: 10.1042/bse0510031
- De Souza, W. (1984). Cell biology of *Trypanosoma cruzi*. *Int. Rev. Cytol.* 86, 197–283. doi: 10.1016/S0074-7696(08)60180-1
- Decker, C. J., and Parker, R. (2012). P-bodies and stress granules: possible roles in the control of translation and mRNA degradation. *Cold Spring Harb. Perspect. Biol.* 4:a012286. doi: 10.1101/cshperspect.a012286
- D'Orso, I., and Frasch, A. C. C. (2002). TcUBP-1, an mRNA destabilizing factor from trypanosomes, homodimerizes and interacts with novel AU-rich element- and poly(A)-binding proteins forming a ribonucleoprotein complex. *J. Biol. Chem.* 277, 50520–50528. doi: 10.1074/jbc.M209092200
- Droll, D., Minia, I., Fadda, A., Singh, A., Stewart, M., Queiroz, R., et al. (2013). Post-transcriptional regulation of the trypanosome heat shock response by a zinc finger protein. *PLoS Pathog.* 9:e1003286. doi: 10.1371/journal.ppat.1003286
- Elias, M. C. Q. B., Marques-Porto, R., Freymüller, E., and Schenkman, S. (2001). Transcription rate modulation through the *Trypanosoma cruzi* life cycle occurs in parallel with changes in nuclear organization. *Mol. Biochem. Parasitol.* 112, 79–90. doi: 10.1016/S0166-6851(00)00349-2
- Erben, E., Chakraborty, C., and Clayton, C. (2013). The CAF1-NOT complex of trypanosomes. *Front. Genet.* 4:299. doi: 10.3389/fgene.2013.00299
- Ericsson, A. O., Faria, L. O., Cruz, W. B., Martins, de Sá C., and Lima, B. D. (2006). TcZFP8, a novel member of the *Trypanosoma cruzi* CCHC zinc finger protein family with nuclear localization. *Genet. Mol. Res.* 5, 553–563.
- Estévez, A. M. (2008). The RNA-binding protein Tb DRBD3 regulates the stability of a specific subset of mRNAs in trypanosomes. *Nucleic Acids Res.* 36, 4573–4586. doi: 10.1093/nar/gkn406
- Fadda, A., Ryten, M., Droll, D., Rojas, F., Färber, V., Haanstra, J. R., et al. (2014). Transcriptome-wide analysis of trypanosome mRNA decay reveals complex degradation kinetics and suggests a role for co-transcriptional degradation in determining mRNA levels. *Mol. Microbiol.* 94, 307–326. doi: 10.1111/mmi.12764
- Fernández-Moya, S. M., Carrington, M., and Estévez, A. M. (2014). Depletion of the RNA-binding protein RBP33 results in increased expression of silenced RNA polymerase II transcripts in *Trypanosoma brucei*. *PLoS ONE* 9:e107608. doi: 10.1371/journal.pone.0107608
- Freire, E., Sturm, N., Campbell, D., and de Melo Neto, O. (2017). The role of cytoplasmic mRNA Cap-binding protein complexes in *Trypanosoma brucei* and other trypanosomatids. *Pathogens* 6:E55. doi: 10.3390/pathogens6040055
- Fritz, M., Vanselow, J., Sauer, N., Lamer, S., Goos, C., Siegel, T. N., et al. (2015). Novel insights into RNP granules by employing the trypanosome's microtubule skeleton as a molecular sieve. *Nucleic Acids Res.* 43, 8013–8032. doi: 10.1093/nar/gkv731
- García Silva, M. R., Tosar, J. P., Frugier, M., Pantano, S., Bonilla, B., Esteban, L., et al. (2010). Cloning, characterization and subcellular localization of a *Trypanosoma cruzi* argonaute protein defining a new subfamily distinctive of trypanosomatids. *Gene* 466, 26–35. doi: 10.1016/j.gene.2010.06.012
- García-Silva, M. R., Sanguinetti, J., Cabrera-Cabrera, F., Franzén, O., and Cayota, A. (2014). A particular set of small non-coding RNAs is bound to the distinctive argonaute protein of *Trypanosoma cruzi*: insights from RNA-interference deficient organisms. *Gene* 538, 379–384. doi: 10.1016/j.gene.2014.01.023
- Gerstberger, S., Hafner, M., and Tuschl, T. (2014). A census of human RNA-binding proteins. *Nat. Rev. Genet.* 15, 829–845. doi: 10.1038/nrg3813
- Gil-Bona, A., Llama-Palacios, A., Parra, C. M., Vivanco, F., Nombela, C., Monteoliva, L., et al. (2015). Proteomics unravels extracellular vesicles as carriers of classical cytoplasmic proteins in *Candida albicans*. *J. Proteome Res.* 14, 142–153. doi: 10.1021/pr5007944
- Glisovic, T., Bachorik, J. L., Yong, J., and Dreyfuss, G. (2008). RNA-binding proteins and post-transcriptional gene regulation. *FEBS Lett.* 582, 1977–1986. doi: 10.1016/j.febslet.2008.03.004
- Goldenberg, S., and Avila, A. R. (2011). Aspects of *Trypanosoma cruzi* stage differentiation. *Adv. Parasitol.* 75, 285–305. doi: 10.1016/B978-0-12-385863-4.00013-7
- Guerra-Slompo, E. P., Probst, C. M., Pavoni, D. P., Goldenberg, S., Krieger, M. A., and Dallagiovanna, B. (2012). Molecular characterization of the *Trypanosoma cruzi* specific RNA binding protein TcRBP40 and its associated mRNAs. *Biochem. Biophys. Res. Commun.* 420, 302–307. doi: 10.1016/j.bbrc.2012.02.154
- Hall, T. M. T. (2005). Multiple modes of RNA recognition by zinc finger proteins. *Curr. Opin. Struct. Biol.* 15, 367–373. doi: 10.1016/j.sbi.2005.04.004
- Hendriks, E. F., Robinson, D. R., Hinkins, M., and Matthews, K. R. (2001). A novel CCHC protein which modulates differentiation of *Trypanosoma brucei* to its procyclic form. *EMBO J.* 20, 6700–6711. doi: 10.1093/emboj/20.23.6700

- Holetz, F. B., Alves, L. R., Probst, C. M., Dallagiovanna, B., Marchini, F. K., Manque, P., et al. (2010). Protein and mRNA content of TcDHH1-containing mRNPs in *Trypanosoma cruzi*. *FEBS J.* 277, 3415–3426. doi: 10.1111/j.1742-4658.2010.07747.x
- Holetz, F. B., Correa, A., Avila, A. R., Nakamura, C. V., Krieger, M. A., and Goldenberg, S. (2007). Evidence of P-body-like structures in *Trypanosoma cruzi*. *Biochem. Biophys. Res. Commun.* 356, 1062–1067. doi: 10.1016/j.bbrc.2007.03.104
- Huberts, D. H., Venselaar, H., Vriend, G., Veenhuis, M., and van der Klei, I. J. (2010). The moonlighting function of pyruvate carboxylase resides in the non-catalytic end of the TIM barrel. *Biochim. Biophys. Acta* 1803, 1038–1042. doi: 10.1016/j.bbamcr.2010.03.018
- Jackson, R. J., Hellen, C. U. T., and Pestova, T. V. (2010). The mechanism of eukaryotic translation initiation and principles of its regulation. *Nat. Rev. Mol. Cell Biol.* 11, 113–127. doi: 10.1038/nrm2838
- Jäger, A. V., De Gaudenzi, J. G., Cassola, A., D'Orso, I., and Frasch, A. C. (2007). mRNA maturation by two-step trans-splicing/polyadenylation processing in trypanosomes. *Proc. Natl. Acad. Sci. U.S.A.* 104, 2035–2042. doi: 10.1073/pnas.0611125104
- Jagus, R., Bachvaroff, T. R., Joshi, B., and Place, A. R. (2012). Diversity of eukaryotic translational initiation factor eIF4E in protists. *Comp. Funct. Genomics* 2012:134839. doi: 10.1155/2012/134839
- Jha, B. A., Gazestani, V. H., Yip, C. W., and Salavati, R. (2015). The DRBD13 RNA binding protein is involved in the insect-stage differentiation process of *Trypanosoma brucei*. *FEBS Lett.* 589, 1966–1974. doi: 10.1016/j.febslet.2015.05.036
- Kedersha, N., and Anderson, P. (2009). Chapter 4 regulation of translation by stress granules and processing bodies. *Prog. Mol. Biol. Transl. Sci.* 90, 155–185. doi: 10.1016/S1877-1173(09)90004-7
- Kramer, S. (2014). RNA in development: how ribonucleoprotein granules regulate the life cycles of pathogenic protozoa. *Wiley Interdiscip. Rev. RNA* 5, 263–284. doi: 10.1002/wrna.1207
- Kramer, S. (2017). The ApaH-like phosphatase TbALPH1 is the major mRNA decapping enzyme of trypanosomes. *PLoS Pathog.* 13:e1006456. doi: 10.1371/journal.ppat.1006456
- Kramer, S., Kimblin, N. C., and Carrington, M. (2010). Genome-wide *in silico* screen for CCCH-type zinc finger proteins of *Trypanosoma brucei*, *Trypanosoma cruzi* and *Leishmania major*. *BMC Genomics* 11:283. doi: 10.1186/1471-2164-11-283
- Lander, N., Chirillo, M. A., Storey, M., Anibal, X., Vercesi, E., and Docampo, X. R. (2016). CRISPR/Cas9-mediated endogenous C-terminal tagging of the inositol 1,4,5-trisphosphate receptor. *J. Biol. Chem.* 291, 25505–25515. doi: 10.1074/jbc.M116.749655
- Lander, N., Li, Z.-H., Niyogi, S., and Docampo, R. (2015). CRISPR/Cas9-induced disruption of paraflagellar rod protein 1 and 2 genes in *Trypanosoma cruzi* reveals their role in flagellar attachment. *MBio* 6:e01012-15. doi: 10.1128/mBio.01012-15
- Lee, Y., and Rio, D. C. (2015). Mechanisms and regulation of alternative pre-mRNA splicing. *Annu. Rev. Biochem.* 84, 291–293. doi: 10.1146/annurev-biochem-060614-034316
- Levy, G. V., Bañuelos, C. P., Nittolo, A. G., Ortiz, G. E., Mendiondo, N., Moretti, G., et al. (2015). Depletion of the SR-related protein TbRRM1 leads to cell cycle arrest and apoptosis-like death in *Trypanosoma brucei*. *PLoS ONE* 10:e136070. doi: 10.1371/journal.pone.0136070
- Li, Z. H., De Gaudenzi, J. G., Alvarez, V. E., Mendiondo, N., Wang, H., Kissinger, J. C., et al. (2012). A 43-nucleotide U-rich element in 3'-untranslated region of large number of *Trypanosoma cruzi* transcripts is important for mRNA abundance in intracellular amastigotes. *J. Biol. Chem.* 287, 19058–19069. doi: 10.1074/jbc.M111.338699
- Lindner, S. E., Mikolajczak, S. A., Vaughan, A. M., Moon, W., Joyce, B. R., Sullivan, W. J., et al. (2013). Perturbations of plasmidium Puf2 expression and RNA-seq of Puf2-deficient sporozoites reveal a critical role in maintaining RNA homeostasis and parasite transmissibility. *Cell. Microbiol.* 15, 1266–1283. doi: 10.1111/cmi.12116
- Ling, A. S., Trotter, J. R., and Hendriks, E. F. (2011). A zinc finger protein, TbZC3H20, stabilizes two developmentally regulated mRNAs in trypanosomes. *J. Biol. Chem.* 286, 20152–20162. doi: 10.1074/jbc.M110.139261
- Milone, J. (2002). Identification of mRNA decapping activities and an ARE-regulated 3' to 5' exonuclease activity in trypanosome extracts. *Nucleic Acids Res.* 30, 4040–4050. doi: 10.1093/nar/gkf521
- Mörking, P. A., Dallagiovanna, B. M., Foti, L., Garat, B., Picchi, G. F., Umaki, A. C., et al. (2004). TcZFP1: a CCCH zinc finger protein of *Trypanosoma cruzi* that binds poly-C oligoribonucleotides *in vitro*. *Biochem. Biophys. Res. Commun.* 319, 169–177. doi: 10.1016/j.bbrc.2004.04.162
- Mörking, P. A., Rampazzo, R. C., Walrad, P., Probst, C. M., Soares, M. J., Gradia, D. F., et al. (2012). The zinc finger protein TcZFP2 binds target mRNAs enriched during *Trypanosoma cruzi* metacyclogenesis. *Mem. Inst. Oswaldo Cruz* 107, 790–799. doi: 10.1590/S0074-02762012000600014
- Müller-McNicoll, M., and Neugebauer, K. M. (2013). How cells get the message: dynamic assembly and function of mRNA-protein complexes. *Nat. Rev. Genet.* 14, 275–287. doi: 10.1038/nrg3434
- Názer, E., Verdún, R. E., and Sánchez, D. O. (2011). Nucleolar localization of RNA binding proteins induced by actinomycin D and heat shock in *Trypanosoma cruzi*. *PLoS ONE* 6:e19920. doi: 10.1371/journal.pone.0019920
- Oliveira, C., Carvalho, P. C., Alves, L. R., and Goldenberg, S. (2016). The role of the *Trypanosoma cruzi* TcNRBD1 protein in translation. *PLoS ONE* 11:e164650. doi: 10.1371/journal.pone.0164650
- Palenchar, J. B., and Bellofatto, V. (2006). Gene transcription in trypanosomes. *Mol. Biochem. Parasitol.* 146, 135–141. doi: 10.1016/j.molbiopara.2005.12.008
- Parker, R., and Song, H. (2004). The enzymes and control of eukaryotic mRNA turnover. *Nat. Struct. Mol. Biol.* 11, 121–127. doi: 10.1038/nsmb724
- Paterou, A., Walrad, P., Craddy, P., Fenn, K., and Matthews, K. (2006). Identification and stage-specific association with the translational apparatus of TbZFP3, a CCCH protein that promotes trypanosome life-cycle development. *J. Biol. Chem.* 281, 39002–39013. doi: 10.1074/jbc.M604280200
- Peng, D., Kurup, S. P., Yao, P. Y., Minning, T. A., and Tarleton, R. L. (2015). CRISPR-Cas9-mediated single-gene and gene family disruption in *Trypanosoma cruzi*. *MBio* 6:e02097-14. doi: 10.1128/mBio.02097-14
- Peng, D., and Tarleton, R. (2015). EuPaGDT: a web tool tailored to design CRISPR guide RNAs for eukaryotic pathogens. *Microb. Genomics* 1:e000033. doi: 10.1099/mgen.0.000033
- Pérez-Díaz, L., Correa, A., Moretão, M. P., Goldenberg, S., Dallagiovanna, B., and Garat, B. (2012). The overexpression of the trypanosomatid-exclusive TcRBP19 RNA-binding protein affects cellular infection by *Trypanosoma cruzi*. *Mem. Inst. Oswaldo Cruz* 107, 1076–1079. doi: 10.1590/S0074-02762012000800021
- Pérez-Díaz, L., Duhagon, M. A., Smircich, P., Sotelo-Silveira, J., Robello, C., Krieger, M. A., et al. (2007). *Trypanosoma cruzi*: molecular characterization of an RNA binding protein differentially expressed in the parasite life cycle. *Exp. Parasitol.* 117, 99–105. doi: 10.1016/j.exppara.2007.03.010
- Pérez-Díaz, L., Pastro, L., Smircich, P., Dallagiovanna, B., and Garat, B. (2013). Evidence for a negative feedback control mediated by the 3' untranslated region assuring the low expression level of the RNA binding protein TcRBP19 in *T. cruzi* epimastigotes. *Biochem. Biophys. Res. Commun.* 436, 295–299. doi: 10.1016/j.bbrc.2013.05.096
- Pérez-Díaz, L., Silva, T. C., and Teixeira, S. M. R. (2017). Involvement of an RNA binding protein containing Alba domain in the stage-specific regulation of beta-amastin expression in *Trypanosoma cruzi*. *Mol. Biochem. Parasitol.* 211, 1–8. doi: 10.1016/j.molbiopara.2016.12.005
- Perry, K. L., Watkins, K. P., and Agabian, N. (1987). Trypanosome mRNAs have unusual "cap 4" structures acquired by addition of a spliced leader. *Proc. Natl. Acad. Sci. U.S.A.* 84, 8190–8194. doi: 10.1073/pnas.84.23.8190
- Preußner, C., Jaé, N., and Bindereif, A. (2012). mRNA splicing in trypanosomes. *Int. J. Med. Microbiol.* 30, 221–224. doi: 10.1016/j.ijmm.2012.07.004
- Re, A., Joshi, T., Kulberkyte, E., Morris, Q., and Workman, C. T. (2014). RNA-protein interactions: an overview. *Methods Mol. Biol.* 1097, 491–521. doi: 10.1007/978-1-62703-709-9_23
- Rodrigues, J. C. F., Godinho, J. L. P., and de Souza, W. (2014). Biology of human pathogenic trypanosomatids: epidemiology, lifecycle and ultrastructure. *Subcell. Biochem.* 74, 1–42. doi: 10.1007/978-94-007-7305-9_1
- Romagnoli, B. A. A., Picchi, G. F. A., Hiraiwa, P. M., Borges, B. S., Alves, L. R., and Goldenberg, S. (2018). Improvements in the CRISPR/Cas9 system for high efficiency gene disruption in *Trypanosoma cruzi*. *Acta Trop.* 178, 190–195. doi: 10.1016/j.actatropica.2017.11.013
- Ross Buchan, J. (2014). MRNP granules assembly, function, and connections with disease. *RNA Biol.* 11, 1019–1030. doi: 10.4161/rna.29034

- Sabalette, K. B., Romaniuk, M. A., Noé, G., Cassola, A., Campo, V. A., and De Gaudenzi, J. G. (2019). The RNA-binding protein TcUBP1 up-regulates an RNA regulon for a cell surface-associated *Trypanosoma cruzi* glycoprotein and promotes parasite infectivity. *J. Biol. Chem.* 294:jbc.RA118.007123. doi: 10.1074/jbc.RA118.007123
- Sheth, U., and Parker, R. (2003). Decapping and decay of messenger RNA occur in cytoplasmic processing bodies. *Science* 300, 805–808. doi: 10.1126/science.1082320
- Smircich, P., Eastman, G., Bispo, S., Duhagon, M. A., Guerra-Slompo, E. P., Garat, B., et al. (2015). Ribosome profiling reveals translation control as a key mechanism generating differential gene expression in *Trypanosoma cruzi*. *BMC Genomics* 16:443. doi: 10.1186/s12864-015-1563-8
- Smirnov, A., Schneider, C., Hör, J., and Vogel, J. (2017). Discovery of new RNA classes and global RNA-binding proteins. *Curr. Opin. Microbiol.* 39, 152–160. doi: 10.1016/j.mib.2017.11.016
- Soares Medeiros, L. C., South, L., Peng, D., Bustamante, J. M., Wang, W., Bunkofsky, M., et al. (2017). Rapid, selection-free, high-efficiency genome editing in protozoan parasites using CRISPR-Cas9 ribonucleoproteins. *MBio* 8:e01788-17. doi: 10.1128/mBio.01788-17
- Subota, I., Rotureau, B., Blisnick, T., Ngwabyt, S., Durand-Dubief, M., Engstler, M., et al. (2011). ALBA proteins are stage regulated during trypanosome development in the tsetse fly and participate in differentiation. *Mol. Biol. Cell* 22, 4205–4219. doi: 10.1091/mbc.e11-06-0511
- Teixeira, D., Sheth, U., Valencia-Sanchez, M. A., Brengues, M., and Parker, R. (2005). Processing bodies require RNA for assembly and contain nontranslating mRNAs. *RNA* 11, 371–382. doi: 10.1261/rna.7258505
- Tonelli, R. R., da Silva Augusto, L., Castilho, B. A., and Schenkman, S. (2011). Protein synthesis attenuation by phosphorylation of eIF2 α is required for the differentiation of *Trypanosoma cruzi* into infective forms. *PLoS ONE* 6:e27904. doi: 10.1371/journal.pone.0027904
- Tyler Weisbarth, R., Das, A., Castellano, P., Fisher, M. A., Wu, H., and Bellofatto, V. (2018). The *Trypanosoma cruzi* RNA-binding protein RBP42 is expressed in the cytoplasm throughout the life cycle of the parasite. *Parasitol. Res.* 117, 1095–1104. doi: 10.1007/s00436-018-5787-9
- Volpon, L., D'Orso, I., Young, C. R., Frasch, A. C., and Gehring, K. (2005). NMR structural study of TcUBP1, a singleRRM domain protein from *Trypanosoma cruzi*: contribution of a beta hairpin to RNA binding. *Biochemistry* 44, 3708–3717. doi: 10.1021/bi047450e
- Wippel, H. H., Inoue, A. H., Vidal, N. M., Costa, J. F., da, Marcon, B. H., Romagnoli, B. A. A., et al. (2018a). Assessing the partners of the RBP9-mRNP complex in *Trypanosoma cruzi* using shotgun proteomics and RNA-seq. *RNA Biol.* 15, 1106–1118. doi: 10.1080/15476286.2018.1509660
- Wippel, H. H., Malgarin, J. S., Inoue, A. H., Leprevost, F. D. V., Carvalho, P. C., Goldenberg, S., et al. (2019). Unveiling the partners of the DRBD2-mRNP complex, an RBP in *Trypanosoma cruzi* and ortholog to the yeast SR-protein Gbp2. *BMC Microbiol.* 19:128. doi: 10.1186/s12866-019-1505-8
- Wippel, H. H., Malgarin, J. S., Martins, S., de, T., Vidal, N. M., Marcon, B. H., Miot, H. T., et al. (2018b). The nuclear RNA-binding protein RBSR1 interactome in *Trypanosoma cruzi*. *J. Eukaryot. Microbiol.* 66, 244–253. doi: 10.1111/jeu.12666
- Wurst, M., Seliger, B., Jha, B. A., Klein, C., Queiroz, R., and Clayton, C. (2012). Expression of the RNA recognition motif protein RBP10 promotes a bloodstream-form transcript pattern in *Trypanosoma brucei*: trypanosome RBP10 function. *Mol. Microbiol.* 83, 1048–1063. doi: 10.1111/j.1365-2958.2012.07988.x
- Zhang, W., Lypaczewski, P., and Matlashewski, G. (2017). Optimized CRISPR-Cas9 genome editing repair mechanisms. *Msp. Mol. Biol. Physiol.* 2:e00340-16. doi: 10.1128/mSphere.00340-16
- Zhang, W. W., and Matlashewski, G. (2015). CRISPR-Cas9-mediated genome editing in *Leishmania donovani*. *MBio* 6:e00861-15. doi: 10.1128/mBio.00861-15

Conflict of Interest: The authors declare that the research was conducted in the absence of any commercial or financial relationships that could be construed as a potential conflict of interest.

Copyright © 2020 Romagnoli, Holetz, Alves and Goldenberg. This is an open-access article distributed under the terms of the Creative Commons Attribution License (CC BY). The use, distribution or reproduction in other forums is permitted, provided the original author(s) and the copyright owner(s) are credited and that the original publication in this journal is cited, in accordance with accepted academic practice. No use, distribution or reproduction is permitted which does not comply with these terms.



The Influence of Environmental Cues on the Development of *Trypanosoma cruzi* in Triatominae Vector

Raíssa de Fátima Pimentel Melo¹, Alessandra Aparecida Guarneri² and Ariel Mariano Silber^{1*}

¹ Laboratório de Bioquímica de Tryps (LaBTryps), Departamento de Parasitologia, Instituto de Ciências Biomédicas, Universidade de São Paulo, São Paulo, Brazil, ² Vector Behaviour and Pathogen Interaction Group, Instituto René Rachou, Fundação Oswaldo Cruz, Belo Horizonte, Brazil

OPEN ACCESS

Edited by:

Noelia Lander,
University of Georgia, United States

Reviewed by:

Wanderley De Souza,
Federal University of Rio de
Janeiro, Brazil
Vicente de Paulo Martins,
University of Brasília, Brazil

*Correspondence:

Ariel Mariano Silber
asilber@usp.br

Specialty section:

This article was submitted to
Parasite and Host,
a section of the journal
Frontiers in Cellular and Infection
Microbiology

Received: 12 November 2019

Accepted: 15 January 2020

Published: 21 February 2020

Citation:

Melo RFP, Guarneri AA and Silber AM
(2020) The Influence of Environmental
Cues on the Development of
Trypanosoma cruzi in Triatominae
Vector.
Front. Cell. Infect. Microbiol. 10:27.
doi: 10.3389/fcimb.2020.00027

Trypanosoma cruzi, a hemoflagellate parasite, is the etiological agent of Chagas disease that affects about 6–7 million people worldwide, mostly in Latin America. The parasite life cycle is complex and alternates between an invertebrate host—Triatominae vector—and a mammalian host. The parasite adaptation to the several microenvironments through which it transits is critical to success in establishing infection. Moreover, environmental cues also play an important role on the parasite development, and it can modulate the infection. In the present study, we discussed how the temperature oscillations and the nutritional state of the invertebrate host can affect the parasite development, multiplication, and the differentiation process of epimastigote forms into metacyclic trypomastigotes, called metacyclogenesis. The impact of oxidative imbalance and osmotic stresses on the parasite–vector relationship are also discussed.

Keywords: *Trypanosoma cruzi*, Triatominae, temperature, nutritional state, oxidative imbalance, osmotic stress, host–parasite interaction

INTRODUCTION

Trypanosoma cruzi, a hemoflagellate parasite belonging to the order Kinetoplastida and the family Trypanosomatidae, is the etiological agent of Chagas disease, also known as American trypanosomiasis, and this potentially lethal disease is considered one of the most neglected human diseases by the WHO (World Health Organization, 2007). Chagas disease is a key human vector-borne zoonotic disease that is endemic in 21 Latin American countries and the southern region of the United States (Bern et al., 2011; World Health Organization, 2014). In addition, new cases have been reported in Europe (Perez-Molina et al., 2011), Canada (Schipper et al., 1980), New Zealand and Australia (Jackson et al., 2014), mainly due to population mobility between the Americas and the rest of the world (reviewed in Flores-Ferrer et al., 2018). In the United States, it is also noteworthy that autochthonous human infections have been reported and that a considerable number of seropositive blood donors have been identified (Buhaya et al., 2015). Chagas disease presents an acute phase, which is mostly asymptomatic, characterized by evident parasitemia, followed by a chronic phase, characterized by the absence of evident parasitemia and a robust humoral response. Although most chronically infected people are asymptomatic, 30–40% of patients develop cardiac diseases, digestive mega syndromes, or both (Rassi et al., 2010; De Oliveira et al., 2018). The chronicity of the pathogenesis of the disease has contributed to making it difficult to diagnose, compromising treatment. In addition, discontinuities in control initiatives launched in the 1990s have been responsible for a re-emergence of Chagas disease, which became a global economic and health issue (Flores-Ferrer et al., 2018).

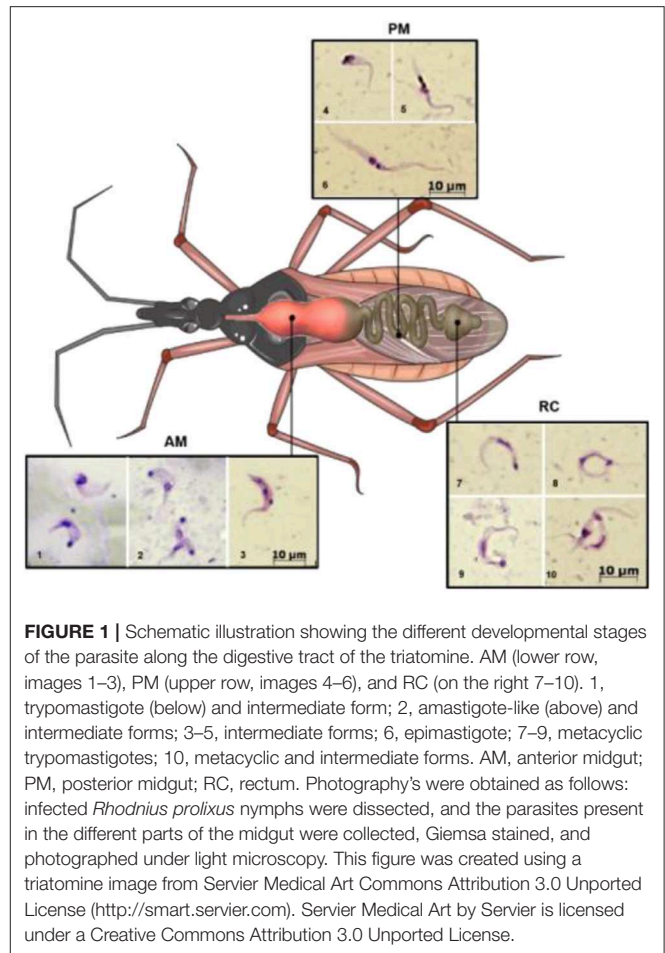
It is estimated that 6–7 million people worldwide are infected by *T. cruzi*, while another 65 million people, mainly in endemic areas, are at risk of acquiring the infection due to daily exposure to vector transmission (World Health Organization, 2014). In its natural cycle, the parasite is transmitted to mammals (including humans) by contaminated triatomine vectors (insects belonging to the order Hemiptera, family Reduviidae, and subfamily Triatominae). The triatomines constitute a subfamily of an otherwise predatory group of insects and comprise some 150 species. Epidemiologically, only ~20 species from the genera *Triatoma*, *Rhodnius*, and *Panstrongylus* are particularly relevant to *T. cruzi* transmission to humans, among which *Triatoma infestans*, *Triatoma dimidiata*, *Triatoma brasiliensis*, *Rhodnius prolixus*, and *Panstrongylus megistus* are considered the most important primary vectors (Gourbière et al., 2011; Guhl, 2017).

The complex life cycle of *T. cruzi* requires it to alternate between its invertebrate hosts (triatomines) and mammalian hosts. During its journey between the two kinds of hosts, the parasite encounters environments that result in physical, physicochemical biochemical, and immunological challenges. The adaptive response to such challenges results in the successful establishment of a long-lasting infection, which is critical for the transmission of the parasite to other hosts. Importantly, the responses to some of these challenges are not only related to parasite survival but can also trigger critical processes, such as differentiation to progress during the parasite life cycle; for example, stressors, such as an acidic pH or starvation may trigger the transition from one developmental stage (epimastigotes) to another (metacyclic trypomastigotes) (Jimenez, 2004). Environmental cues also play an important role in parasite development and can modulate the infection, which is supported by the existence of seasonal changes in a vector's infectivity (Asin and Catala, 1995).

In this review, we discuss how temperature oscillations and the nutritional status of the invertebrate host associated with different physicochemical properties and intrinsic factors in the microenvironment can affect parasite development and multiplication and the differentiation of epimastigote forms into metacyclic trypomastigotes (metacyclogenesis).

MORPHOLOGY AND LIFE CYCLE

During its life cycle, *T. cruzi* undergoes changes in its morphology as well as its biochemical and biological properties (such as infectivity and the ability to proliferate). In the intestinal tract of the kissing bug, three main stages are found (Chagas, 1909)—epimastigotes, trypomastigotes, and spheromastigotes—as well as many intermediate stages, which can be generically described as flagellates with either a drop-like shape (intermediate between spheromastigotes and epimastigotes or trypomastigotes) or a slender shape (intermediate between epimastigotes trypomastigotes) (Schaub, 1989), as represented in **Figure 1**. Epimastigotes are able to multiply and colonize the intestinal tract of the vector. Metacyclic trypomastigotes (non-replicative forms) develop in the rectum and are infectious in mammals (Kollien and Schaub, 1999). In the mammalian



host, intracellularly multiplying amastigotes are present, and as a result of successive binary fissions, they develop into non-replicative trypomastigotes (Tyler and Engman, 2001) via an intermediate transient epimastigote-like stage (also referred to in the literature as intracellular epimastigotes) (Almeida-de-Faria et al., 1999; Tyler and Engman, 2001).

During a bloodmeal, the infected triatomine insect sucks a significant amount of blood from the mammalian host, forcing the elimination of excrement from the insect's rectum and releasing metacyclic trypomastigotes. The parasites then contact the injured skin or mucosa and are internalized into this new host. As trypomastigote forms are not replicative, the establishment of the infection depends on the ability of the parasite to differentiate into a replicative stage, which only occurs inside mammalian host cells. For this reason, they must invade host cells and reach the cytosol, where they differentiate into amastigotes (De Souza et al., 2010). After several cycles of cell division, amastigotes differentiate into intracellular epimastigotes (Almeida-de-Faria et al., 1999) and then into trypomastigotes, which burst from infected cells into the extracellular environment. These parasites can infect neighboring cells or reach the bloodstream, where they can spread the infection to other tissues, or they can be ingested

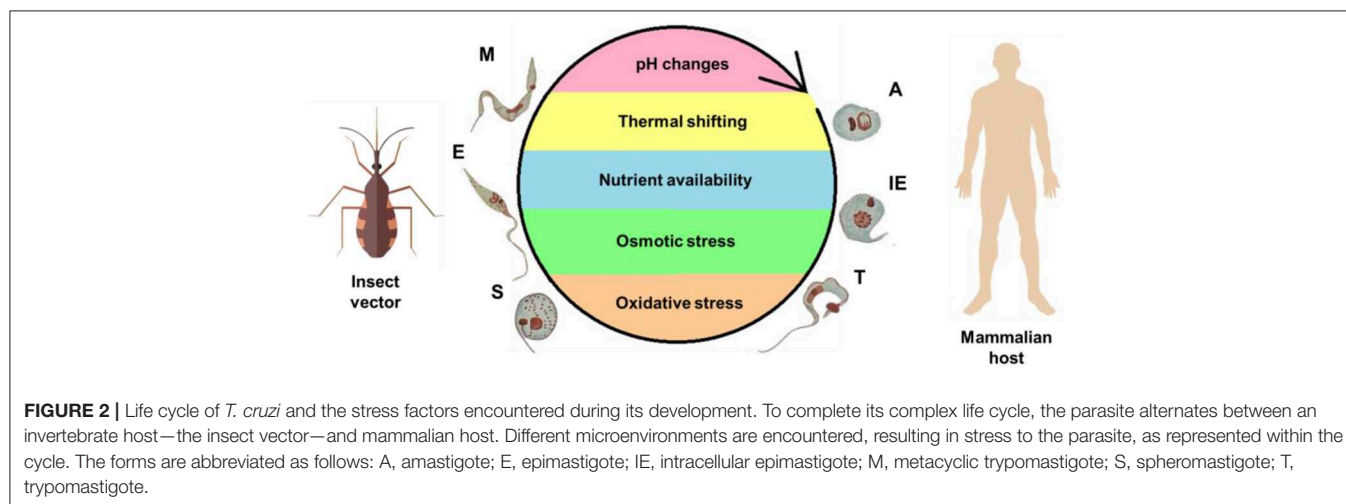
by a kissing bug during its bloodmeal, and the bug will then transmit the infection to other hosts (reviewed in Marchese et al., 2018). The classic description of the parasite's development in the digestive tract of the insect (Chagas, 1909; Dias, 1934), in which blood trypomastigotes differentiate into epimastigotes in the stomach and then multiply continuously in the intestine, reaching the rectum, where they differentiate into metacyclic trypomastigotes, was initially refuted by Brack. The author suggested that bloodstream trypomastigotes differentiate into rounded forms with free flagella referred to as spheromastigotes, which then multiply and differentiate into trypomastigotes or epimastigotes (Brack, 1968). In fact, Brener observed a large number of rounded or slightly pear-shaped parasites in stomach content samples ~72 and 96 h after infection. It has also been suggested that a different process of reproduction could occur in the anterior midgut (AM) with some degree of genetic exchange, characterized by the fusion of amastigote forms, followed by the apparent reorganization of DNA-containing organelles and subsequent detachment of new flagellates (Brener, 1972). The process in which the bloodstream trypomastigotes differentiate into epimastigotes is referred to as epimastigogenesis and apparently occurs in the posterior midgut (PM), where they initiate their replication. It is important to note that, although there is a paradigm concerning this issue, it has recently been shown that both trypomastigote stages of *T. cruzi* (cell-derived and metacyclic forms) are able to transform into epimastigotes. Interestingly, these “recently differentiated epimastigotes” exhibit relevant biological properties, such as resistance to complement-mediated lysis and both *in vitro* (cell culture) and *in vivo* (mouse) infectivity. This indicates dynamic behavior in which both metacyclogenesis and secondary epimastigogenesis can occur in the triatomine rectum (Kessler et al., 2017). Midgut colonization by *T. cruzi* was recently revisited by Ferreira and collaborators, and as reported by Dias (1934), epimastigogenesis was shown to be completed in the PM of *R. prolixus* (Ferreira et al., 2016) and not in the anterior midgut, as was assumed for quite some time. Furthermore, the AM seems to be an inhospitable environment for the parasite, since the trypomastigote population is severely reduced 24 h after invading this portion of the gut

(Dias et al., 2015; Ferreira et al., 2016; reviewed in Guarneri and Lorenzo, 2017). During this initial interval, it is assumed that the remaining parasites differentiate into intermediate or amastigote-like forms and quickly travel to the PM, where they will start to replicate (Guarneri and Lorenzo, 2017). At later stages in the rectum, some proportion of epimastigotes attach to the rectal cuticle as a prerequisite step to initiate metacyclogenesis (Garcia and Azambuja, 1991; Kollien and Schaub, 2000; Azambuja et al., 2005; Garcia et al., 2010). Briefly, the life cycle of *T. cruzi* (with the main stages) can be schematically illustrated as follows (Figure 2).

ENVIRONMENTAL CUES AND THEIR IMPACT ON PARASITE DEVELOPMENT IN THE INSECT HOST

The multiple environmental changes encountered by *T. cruzi* are a consequence of the different organisms (and multiple tissues therein) in which its life cycle takes place. This fact is probably closely related to the ability of *T. cruzi* to sense and adapt to these environments, maintain their cell homeostasis, and, ultimately, survive to extremely different physical, physicochemical, chemical, and nutritional conditions (Zuzarte-Luís and Mota, 2018). The main environmental variables that *T. cruzi* encounters during its life cycle are represented schematically (Figure 2) and include variations in temperature, fluctuations in the type and availability of nutrients, and changes in pH, osmolarity, ionic composition, and redox potential (Jimenez, 2004).

The influence of the insect vector gut microbiota on the parasite life cycle is an important issue. It is well-established that the composition of the intestinal microbiota can interfere with the effectiveness of the infection. Importantly, an inadequate balance between the bacterial and protozoan populations can compromise the establishment of the infection, since the two populations compete for resources in the intestine (De Oliveira et al., 2018). Previous studies by Azambuja and collaborators have shown that a few days after blood feeding, the number of bacteria



in the insect AM from *R. prolixus* increases considerably, leading to the lysis of erythrocytes and the *T. cruzi* Y strain (Azambuja et al., 2004, 2005). A recent posterior study demonstrated that the incubation of the *T. cruzi* Y strain with the bacterium *Serratia marcescens* led to parasite lysis. This effect was dependent on the ability of the bacterial strain to adhere to the protozoan surface via D-mannose-recognizing fimbriae. This seems to be a strain-dependent phenomenon, since different bacterial strains show different behaviors. The bacterium–protozoan attachment seems to result in a filamentous biofilm, which is critical for parasite–microbiota interactions in the gut of triatominae (Castro et al., 2007).

Keeping in mind the general context of this work, it is crucial to understand that environmental conditions have been recognized as being key to the dynamics of infectious diseases, affecting parasite transmission and virulence (Wolinska and King, 2009). In the case of *T. cruzi*, which colonizes different parts of the triatomine digestive tract, the environment varies in space and time, and many peculiarities of this variation can shape the outcome of insect infection. Changes in temperature can modulate the spread of the infection and exert profound and complex ecological feedback on its dynamics, for example, by changing the availability and quality of nutritional resources for the host (Cornet et al., 2014).

Temperature Variation

Similar to all terrestrial organisms, triatomines inhabit thermally heterogeneous environments, and this heterogeneity is a consequence of spatial (at large or small scales) and temporal variations (over years, months, seasonally, or during a single day). It is well-established that changes in temperature affect biological processes. The impact of such temperature changes on ectothermic animals, such as insects is greater because of their inability to control their body temperature (Rolandi and Schilman, 2018).

A recent study from Fellet et al. showed that the fecundity and fertility rates of *R. prolixus* are affected by the presence of *T. cruzi* depending on the temperature at which insects are maintained. The authors developed an experiment in which insects infected by *T. cruzi* in the second-instar nymph stage were maintained in a chamber at 25°C during nymphal development and after imaginal molting (this is a reference to differentiation to the adult phase, also referred to as the imaginal stage), or were maintained in a chamber at 30°C during nymphal development and transferred to 25°C after imaginal molting. In the first group, the capacity of the females to convert ingested blood into eggs (*e* value) was increased by the infection depending on the adult age, as was the hatching rate. For the second group, the analysis of the *e* values showed that the production of eggs was decreased in infected insects during the first reproductive cycle. However, the fertility of the eggs was decreased only in the third reproductive cycle (Fellet et al., 2014). In another study, *T. cruzi*-infected *R. prolixus* were maintained at four different temperatures (20, 24, 27, or 30°C), and a considerable delay in the time at which the insects triggered the molting process was observed across the temperatures. This extension of the intermolt period would be beneficial to the parasites, as they need time to

develop inside the insect before the next bloodmeal (in nymphs that feed to completion, the next bloodmeal only occurs after the molt). Parasite infection was also found to increase mortality rates at two intermediate temperatures, 24 and 27°C, but not at 21 or 30°C. It is important to note that, in this study, the insects were observed for 90 days, during which they did not receive additional bloodmeals. The lack of effects observed in the insects kept at 21°C was possibly related to a slowdown in insect metabolism imposed by the temperature, which maintained the nutritional resources at sufficient levels to allow the development of the parasite without affecting insect survival. At the other extreme, the highest temperature increased insect metabolism, leading to the rapid exhaustion of the energetic resources, which probably eliminated the parasites (Elliot et al., 2015).

In triatomine bugs, the prophenoloxidase (proPO) and phenoloxidase (PO) enzymatic cascade plays a role in the immune response related to defense against pathogens. In this regard, *Meccus pallidipennis*, a vector with high epidemiological importance in Mexico, was used to determine the activity of the proPO system against two *T. cruzi* strains in different intestinal regions and temperature conditions. In general, with increasing temperature (20–34°C), proPO activity decreased. In contrast, for the PO system, the highest activity values were observed at 30°C, and they were lower at 34°C. The more efficient proPO activity before a critical increase in temperature could be explained by the fact that this system works better at moderately higher temperatures but not when the temperature reaches a lethal limit. Increased temperatures negatively affect the triatomine life cycle. The presence of *T. cruzi* decreases insect survival, and this phenomenon is related to the strain and temperature. The insects are more affected by the Chilpancingo strain than by the Morelos strain, and these effects are even more perceivable at higher temperatures (34°C), suggesting a synergistic effect between temperature and the parasitic strain on insect survival (González-Rete et al., 2019).

In addition to changes in the physiology of triatomines, early studies have suggested that temperature has significant effects on the parasite–vector interaction, influencing the development of *T. cruzi* within the insect. According to Neves, who qualitatively characterized the parasite's life cycle in *T. infestans* at temperatures ranging from –5 to 37°C, complete parasite development occurs between 23 and 28°C (Neves, 1971). In addition to its direct influence, temperature may modulate parasite development by modifying some physiological processes of the vector, which is linked to variations in the *T. infestans* blood consumption (Catala et al., 1992) and could modify the environment in which the parasite multiplies and differentiates (Asin and Catala, 1995). However, it should be taken into account that these experiments refer to a description based on non-infected insect physiology.

The optimum temperature for the development of most triatomine species is 24–28°C (Jurberg and Galvão, 2006). Previous studies published by Wood demonstrated an increase in the parasite number and the presence of more active metacyclic and non-metacyclic forms when the excreted content of the insect vector was analyzed during warmer periods of the year compared to colder ones (Wood, 1938, 1941, 1943; Woon, 1942).

Subsequently, a study by the same author reported that lower environmental temperatures (22–23°C) decreased the release of metacyclic forms of *T. cruzi* from newly infected adult *T. protacta*, while higher environmental temperatures (28–34.5°C) increased their release. Under a higher temperature, metacyclic trypomastigotes appeared in vector feces on the 7th day after the infective blood meal, but they were not found under the lower temperature, at least until the 12th day. At this temperature, the fecal samples examined 36 days after the infective meal revealed few metacyclic forms (Wood, 1954). Finally, Phillips noted that in *R. prolixus*, metacyclic trypomastigotes can be found as early as the 2nd day after feeding on infected blood when the experimental temperature is 30°C, whereas they appear on the 7th day after the infective meal when the insects are maintained at 20°C (Phillips, 1960). Considering the different experimental conditions in which these studies were performed (regarding triatomine species, parasite strains, and the analyzed time period, among other factors), it is possible to conclude that the temperature dependence shows a similar pattern in all cases: lower temperatures delay the release of metacyclic trypomastigotes in feces, while at higher temperatures, infectious forms develop earlier.

Importantly, it is well-established that temperature affects the proliferation of epimastigotes. However, a small number of studies have provided evidence of how important this factor is for parasite proliferation in the triatomine host. Asin and Catalá conducted this evaluation by maintaining infected kissing bugs at 20 and 28°C. In this study, *T. infestans* had daily opportunities to consume blood, which is not the usual situation in nature. Although epimastigotes started to proliferate immediately at both temperatures, the epimastigote density increased slowly at 20°C compared to 28°C. Metacyclogenesis was also affected by the temperature change, since the presence of metacyclic forms within the insects' recta and feces was delayed at 20°C. Once differentiation into the infective stage was completed, the density of the metacyclic trypomastigotes in feces was similar at the two temperatures. As observed in the above-mentioned studies, this work also showed that a suboptimal temperature retards *T. cruzi* differentiation within the vector (Asin and Catalá, 1995).

Data regarding the proliferation of epimastigotes *in vitro* have been reported recently, indicating that epimastigotes grow optimally at a temperature of 28°C. The temperatures of 33 and 37°C were also evaluated, and it was observed that cells grew to a higher density at 33°C, while cell growth at 37°C was slightly greater than that observed at 28°C when CL strain clone 14 was used (Magdaleno et al., 2009), indicating that the optimal temperature may be strain dependent. In another study involving the CL strain, the epimastigote proliferation rate was found to increase together with the environmental temperature, with peak growth occurring at or above 30°C. Increased proliferation rates could have evolved as a “strategy” for increasing the parasite population, thus increasing the chances of transmission (due to a high population density in the intestine), even with the possible cost of killing the vector and interrupting transmission (Elliot et al., 2015).

Feeding Habits of Triatomines and Their Relationship With Oxidative Imbalance and Osmotic Stress

Since *T. cruzi* lives in the intestinal tract of a triatomine, the parasite may be affected by changes in the nutritional supply, i.e., by the ingestion of blood or starvation (Kollien and Schaub, 1999). In this context, some variables associated with the biology of the insect vector are important, such as the periodicity of feeding and the amount of blood that is taken in each bloodmeal. *In natura*, triatomine insects are able to go for months without feeding. In these cases, when they have the chance of taking a bloodmeal, they usually ingest a relatively large amount of blood; *R. prolixus* nymphs, for example, take approximately nine times their body weight in blood (Friend et al., 1965). A very interesting insight that may explain this behavior is found in a paper published by Sterkel et al., in which the authors compare the average weight of a mosquito and a human, noting a size difference of $\sim 4 \times 10^7$. The authors explain that “the defensive behavior of vertebrates provides a major protective effect against blood-sucking insects and makes feeding extremely dangerous for most hematophagous invertebrates. Consequently, the minimization of the number of visits to the vertebrate host is a common trend in the biology of most of these animals and is accomplished in large part by the ingestion of disproportionately large amounts of blood in a single meal” (Sterkel et al., 2017).

In triatomines, the body shape changes and the abdomen dilates considerably as soon as the insects begin their meal, since cuticle plasticization leads to the extension of the abdominal integument, allowing the accommodation of large amounts of blood in the anterior midgut (Bennet-Clark, 1962). Blood ingestion induces rapid changes in the rectum in particular. The large amount of blood ingested creates a number of challenges for the maintenance of homeostasis, impacting triatomine biology, increasing the weight of the insects, and affecting their movements. To cope with these challenges, shortly after the bloodmeal, triatomines reduce their weight by releasing excreta and large amounts of water. This is possible due to their extraordinarily efficient excretory system, which allows most of those compounds taken in with the blood that have little or no nutritional value (i.e., water and ions, including large quantities of Na^+ and Cl^-) to be expelled in a short time. Nutrient-rich blood cells are simultaneously concentrated (Maddrell, 1972). This phenomenon can be observed in *R. prolixus*, in which the secretory rate of the Malpighian tubules is increased by a factor of $\sim 1,000$ times after a bloodmeal (Maddrell, 1969). This rapid nutritional transition that occurs in the intestinal tract of the insect vector impacts the osmolarity of the surrounding environment and consequently results in osmotic stress to the parasite. One study demonstrated that after feeding, the first clear urine that was produced was generally almost isotonic with respect to the ingested blood and somewhat hypo-osmotic with respect to the hemolymph. Approximately 2.5 h later, the osmolarity of the urine increased slightly, and at 24 and 48 h after the bloodmeal, the osmolality of the urine had doubled, which represents a very hostile change for the parasite

(Wigglesworth, 1931; Kollien et al., 2001). This pattern may be related to the fact that, in the long term, the digestion of blood cells leads to an excess of ions, such as K^+ and Ca^{2+} as well as nitrogen-containing waste metabolites (uric acid and organic anions) resulting from the catabolism of bloodmeal proteins. In addition, the toxins present in the diet or produced via blood metabolism must be excreted (reviewed in O'Donnell, 2009).

The chemical composition of the large amount of vertebrate blood ingested by triatomine insects includes proteins, which account for almost 90% of the dry weight of vertebrate blood, among which hemoglobin is the most abundant (~150 mg/ml) (Sterkel et al., 2017). The contents of the blood are continuously digested via the action of proteases, releasing amino acids, small peptides, and heme. Potential hyperamino acid toxicity is prevented by protein digestion coupled to fast oxidative degradation pathways that convert amino acids into molecules that contribute to gut homeostasis. Heme is released mostly through the breakdown of hemoglobin. Similar to other trypanosomatids, *T. cruzi* is not able to synthesize heme because the complete biosynthesis pathway is absent. Taking into account the essentiality of heme, parasites are strictly dependent on its uptake from their hosts (Cupello et al., 2011; Merli et al., 2016), after which it is inserted into different heme proteins (reviewed in Merli et al., 2017). The high heme concentrations resulting from blood digestion have shaped some aspects of the gut cell biology of triatomines, such as the control of intracellular heme levels by microsomal heme oxygenase (HO). In *R. prolixus*, a unique heme-degradation pathway has been described. Heme is first modified by the addition of two cysteinyl glycine residues, and the porphyrin ring is then cleaved. Finally, the dipeptides are trimmed, resulting in the production of dicysteinyl-BV IX, CO, and iron (Paiva-Silva et al., 2006). A reduced but still significant amount of heme reaches the cytosol of midgut cells and the hemolymph, putting tissues at risk of oxidative damage because this can lead to the generation of reactive oxygen species (ROS) through the Fenton reaction. The Fenton reaction consists of the conversion of H_2O_2 into hydroxyl radicals, which are among the most potent known oxidants, using electrons donated by the Fe^{2+} atom present in the heme nucleus. These ROS can potentially damage biological molecules: they can inactivate proteins, disrupt the phospholipid bilayer of cell membranes, and damage DNA, which results in toxicity to the parasites (Schmitt et al., 1993). However, it is worth reinforcing that *T. cruzi* is strictly dependent on heme as a nutritional cofactor for its metabolism and as an integral component of a series of essential heme proteins (Lara et al., 2007). The need for a “dangerous” metabolite, such as heme that can accumulate in large quantities in the same niche inhabited by the parasite led us to think about possible fine-tuning strategies involved in the interaction between the parasite and its insect host. Parasites belonging to the genus *Plasmodium*, which are the etiological agents of malaria, are able to digest host-cell hemoglobin. They detoxify the excess free heme in the parasite's food vacuole by polymerizing it into a harmless dark-brown crystalline structure referred to as malaria pigment or hemozoin (Hz) (Slater et al., 1991). More recently, Oliveira et al. demonstrated that this also occurs in

the midgut of the bloodsucking insect *R. prolixus*. The authors showed by transmission electron microscopy (TEM) that large electron-dense aggregates that were similar in appearance to the Hz granules found in *Plasmodium* parasites existed in the lumen of the *R. prolixus* midgut. Finally, their chemical nature was determined, demonstrating the hypothesis of heme detoxification through its conversion to hemozoin in triatomines. It was shown that through this mechanism, these insects can detoxify more than 97% of the heme that is present and that this process occurs in the perimicrovillar membranes, which are extracellular lipid membranes that separate the gut epithelium from the luminal content in hemipterans. This finding is very important, and this process can be considered the first line of defense against the effects of the release of heme via hemoglobin digestion. The sequestration of heme in an insoluble form leads to its elimination in the insect's feces, preventing the heme from crossing the midgut wall and causing oxidative tissue damage (Oliveira et al., 1999; Sterkel et al., 2017). Interestingly, Hz synthesis in the midgut of insects is promoted by a particulate fraction from the intestinal lumen, and the factor responsible for its synthesis is heat labile. To better understand this mechanism, *R. prolixus* were fed with blood supplemented with different concentrations of chloroquine (CLQ) as well as known potent inhibitors of Hz formation. As a result, the heme concentration in the hemolymph increased, which resulted in higher lipid peroxidation. This report reinforces the importance of this mechanism involved in the crystallization of Hz in the *R. prolixus* midgut as a physiological defense against heme toxicity (Oliveira et al., 2000).

Nutritional Availability and Its Impact on Parasite Development

As previously reported, in their natural environment, triatomines go for weeks between feedings, and the complete digestion of a blood meal can take up to 10 days. The influence of starvation on the *T. cruzi*–triatomine interaction has been analyzed by different authors, and a reduction in the number of parasites and the appearance of dead flagellates in starved insects have been reported. In fact, the lack of nutrients affects the population density of *T. cruzi* and, depending on the time interval, results in parasite death. The first dead flagellates can be detected in the rectum after short-term starvation (30 days), while long-term starvation (90 days) can kill up to 99.5% of the *T. cruzi* population in the rectum (Kollien and Schaub, 1998, 2000). Moreover, starvation affects different developmental stages of *T. cruzi* as well as the course of metacyclogenesis differentially. Fifth-instar *R. prolixus* larvae subjected to fasting for different times have been shown to exhibit different rates of differentiation. The lowest percentage of differentiation occurred in a group subjected to 45 days of starvation. This group presented 45% of the normal level of metacyclogenesis, while the others (15 and 30 days of starvation) presented differentiation rates of 85 and 65%, respectively (Garcia et al., 1995).

Kollien and Schaub also demonstrated that when *T. infestans* was parasitized by *T. cruzi*, after a starvation period

of 20 or 30 days, the population of flagellates decreased substantially, and at 60 days after the last feeding (daf), no flagellates were found in the small intestine. The total rectal population was reduced by one-third between 30 and 60 daf, followed by a more significant reduction over the next 30 days, and changes also occurred in different stages, while in regularly fed triatomines, the parasite population in the rectum consisted mainly of equal amounts of epi- and trypomastigotes. The percentage of trypomastigotes seemed to be unaffected by the insect starvation period, and a similar trend was observed on the rectal wall. On the other hand, the percentage of epimastigotes in the rectal lumen and on the rectal wall decreased at 20 daf (from 50 to 15–30%). At ~90 daf, this rate reached 50% on the rectal wall. Interestingly, the percentages of slender intermediate forms varied little during different starvation periods, while drop-like intermediate forms showed a continuous significant increase during the starvation process (ranging from 1 to ~15%). The percentages of spheromastigotes also increased at 60 daf, reaching 22% in the lumen and 18% on the wall. It is important to point that in recently fed bugs that were previously subjected to starvation, spheromastigotes (and other intermediate forms) almost disappear, while epimastigotes dominate (Kollien and Schaub, 1999). This pattern may be associated with the role of spheromastigotes as a stage in the parasite life cycle that develops under stress conditions (Schaub, 1989; Kollien and Schaub, 1998). Feeding the vector at 40 daf induced the appearance of pure populations of trypomastigotes in immediately deposited drops of bug urine and induced metacyclogenesis in epimastigotes. These data emphasize the importance of the feeding status of the vector for the development of different stages of *T. cruzi*.

Interestingly, it has been proposed that blood consumption could regulate epimastigote population density and thereby influence epimastigote differentiation to metacyclic forms, or metacyclogenesis. A study published by Asin and Catalá showed that in *T. infestans*, blood consumption is related to the development of *T. cruzi* epimastigote and metacyclic trypomastigote forms at 28°C. The consumption of at least 120–180 mg of fresh blood ensures the development of the parasite, while a lower amount of consumption impacts this process. However, it does not influence the number of trypomastigotes released in the feces (Asin and Catalá, 1995). Asin also observed that nymphs of *T. infestans* that were fed only once did not possess rectal trypomastigotes and that the total parasitic population declined (Asin, 1992). As mentioned above, triatomines usually consume a large amount of blood in a single feeding, resulting in high hemoglobin ingestion. Garcia et al. demonstrated that when plasma was supplemented with high hemoglobin concentrations and offered to fifth-instar *R. prolixus* nymphs as a meal, there was an increase in the *T. cruzi* metacyclogenesis rate compared to that in insects fed only whole blood or plasma. Therefore, hemoglobin not only has a nutritional effect but is also important in the induction of differentiation (Garcia et al., 1995).

In summary, different natural stresses, such as those caused by temperature changes, the availability of nutrients, or

environmental changes in the redox state of *T. cruzi* habitats inside the insect vector critically influence parasite biology. Myriad adaptations have been selected over time due to the long-term interaction driving coevolution. The consequent exceptional metabolic flexibility of *T. cruzi* is an evolutionary response to the constant challenges it faces in both hosts, but particularly in the insect midgut, which provides a non-homeostatic environment.

CONCLUDING REMARKS

Although several studies have explored the relationship between environmental cues and their impact on the development and biology of a variety of triatomine species (affecting characteristics, such as fertility, mortality, and survival), the way in which parasites respond to these environmental changes has not been explored in depth, especially through *in vitro* experiments, providing little support for discussions of this subject. The purpose of this paper was precisely to collect the main reports in the literature that describe how external factors, such as temperature, the availability of nutritional contents, and consequent oxidative and osmotic stresses may alter the development of *T. cruzi* forms in the insect vector. It has been shown that these stress factors can modify most of the critical processes required for the establishment and transmission of the infection, including the replication of epimastigote forms, the process of metacyclogenesis, the abundance of metacyclic forms and their release in insect feces, the parasitic load, and the parasite composition (percent of the different life cycle stages) in the triatomine gut. It is foreseeable that some issues related to the topics detailed in this review will garner more attention in the literature. The effect of temperature changes on *T. cruzi* development in its vector and transmission to mammals may be important for analyzing possible changes in transmission patterns due to climate change (Paaijmans et al., 2010). Some other types of complex ecological feedback could also be interpreted in this light, such as the possible alterations of the availability and quality of nutritional resources consumed by the insect host (Cahill et al., 2013). Changes in host nutritional status lead to repercussions regarding the dynamics of infection, as they may limit or modify the parasite's access to the nutritional content of the host, upon which it depends to complete its life cycle.

AUTHOR CONTRIBUTIONS

RM and AS conceived the manuscript. RM wrote the first version of the manuscript, produced the figures, and corrected the manuscript. AG and AS worked on the majority of the corrections of the manuscript and the figures. AS prepared the final version of the manuscript.

FUNDING

This work was supported by Fundação de Amparo à Pesquisa do Estado de São Paulo grant 2016/06034-2 (awarded to

AS), Conselho Nacional de Desenvolvimento Científico e Tecnológico (CNPq) grants 301971/2017-0 and 404769/2018-7 (awarded to AS), and Research Council United Kingdom Global Challenges Research Fund under grant agreement A Global Network for Neglected Tropical Diseases (grant MR/P027989/1) (awarded to AS).

REFERENCES

- Almeida-de-Faria, M., Freymüller, E., Colli, W., and Alves, M. J. M. (1999). *Trypanosoma cruzi*: characterization of an intracellular epimastigote-like form. *Exp. Parasitol.* 92, 263–274. doi: 10.1006/expr.1999.4423
- Asin, S. (1992). *Influencia de la temperatura sobre la competencia vectorial de Triatoma infestans Klug, 1834* (Doctoral thesis), Universidad Nacional de Córdoba, Córdoba, Argentina.
- Asin, S., and Catala, S. (1995). Development of *Trypanosoma cruzi* in *Triatoma infestans*: influence of temperature and blood consumption. *J. Parasitol.* 81, 1–7. doi: 10.2307/3283997
- Azambuja, P., Feder, D., and Garcia, E. S. (2004). Isolation of *Serratia marcescens* in the midgut of *Rhodnius prolixus*: impact on the establishment of the parasite *Trypanosoma cruzi* in the vector. *Exp. Parasitol.* 107, 89–96. doi: 10.1016/j.exppara.2004.04.007
- Azambuja, P., Garcia, E. S., and Ratcliffe, N. A. (2005). Gut microbiota and parasite transmission by insect vectors. *Trends Parasitol.* 21, 568–572. doi: 10.1016/j.pt.2005.09.011
- Bennet-Clark, H. C. (1962). Active control of the mechanical properties of insect endocuticle. *J. Insect Physiol.* 8, 627–633. doi: 10.1016/0022-1910(62)90018-5
- Bern, C., Kjos, S., Yabsley, M. J., and Montgomery, S. P. (2011). *Trypanosoma cruzi* and Chagas' disease in the united states. *Clin. Microbiol. Rev.* 24, 655–681. doi: 10.1128/CMR.00005-11
- Brack, C. (1968). Elektronmikroskopische Untersuchungen zum Lebenszyklus von *Trypanosoma cruzi*. *Acta Trop.* 25, 289–356.
- Brener, Z. (1972). A new aspect of *Trypanosoma cruzi* life-cycle in the invertebrate host. *J. Protozool.* 19, 23–27. doi: 10.1111/j.1550-7408.1972.tb03408.x
- Buhaya, M. H., Galvan, S., and Maldonado, R. A. (2015). Incidence of *Trypanosoma cruzi* infection in triatomines collected at Indio Mountains Research Station. *Acta Trop.* 150, 97–99. doi: 10.1016/j.actatropica.2015.07.004
- Cahill, A. E., Aiello-Lammens, M. E., Fisher-Reid, M. C., Hua, X., Karanewsky, C. J., Yeong Ryu, H., et al. (2013). How does climate change cause extinction? *Proc. R. Soc. B Biol. Sci.* 280, 20121890–20121890. doi: 10.1098/rspb.2012.1890
- Castro, D. P., Seabra, S. H., Garcia, E. S., Souza, W., and de Azambuja, P. (2007). *Trypanosoma cruzi*: ultrastructural studies of adhesion, lysis and biofilm formation by *Serratia marcescens*. *Exp. Parasitol.* 117, 201–207. doi: 10.1016/j.exppara.2007.04.014
- Catala, S., Giojalas, L., and Crocco, L. (1992). Temperature effect upon blood consumption in *Triatoma infestans*. *Mem. Inst. Oswaldo Cruz* 87, 473–476. doi: 10.1590/S0074-02761992000400003
- Chagas, C. (1909). Nova tripanozomíaze humana: estudos sobre a morfologia e o ciclo evolutivo do *Schizotrypanum cruzi* n. gen. n. sp. agente etiológico de nova entidade morbida do homem. *Mem. Inst. Oswaldo Cruz* 1, 159–218. doi: 10.1590/S0074-02761909000200008
- Cornet, S., Bichet, C., Larcombe, S., Faivre, B., and Sorci, G. (2014). Impact of host nutritional status on infection dynamics and parasite virulence in a bird-malaria system. *J. Anim. Ecol.* 83, 256–265. doi: 10.1111/1365-2656.12113
- Cupello, M. P., de Souza, C. F., Buchensky, C., Soares, J. B. R. C., Laranja, G. A. T., Coelho, M. G. P., et al. (2011). The heme uptake process in *Trypanosoma cruzi* epimastigotes is inhibited by heme analogues and by inhibitors of ABC transporters. *Acta Trop.* 120, 211–218. doi: 10.1016/j.actatropica.2011.08.011
- De Oliveira, A. B. B., Alevi, K. C. C., Imperador, C. H. L., Madeira, F. F., and de Azeredo-Oliveira, M. T. V. (2018). Parasite–vector interaction of chagas disease: a mini-review. *Am. J. Trop. Med. Hyg.* 98, 653–655. doi: 10.4269/ajtmh.17-0657
- De Souza, W., de Carvalho, T. M. U., and Barrias, E. S. (2010). Review on *Trypanosoma cruzi*: host cell interaction. *Int. J. Cell Biol.* 2010:295394. doi: 10.1155/2010/295394
- Dias, E. (1934). Estudos sobre o *Schizotrypanum cruzi*. *Mem. Inst. Oswaldo Cruz* 28, 1–110. doi: 10.1590/S0074-02761934000100001
- Dias, F. A., Guerra, B., Vieira, L. R., Perdomo, H. D., Gandara, A. C. P., do Amaral, R. J. V., et al. (2015). Monitoring of the parasite load in the digestive tract of *Rhodnius prolixus* by combined qPCR analysis and imaging techniques provides new insights into the trypanosome life cycle. *PLoS Negl. Trop. Dis.* 9:e0004186. doi: 10.1371/journal.pntd.0004186
- Elliot, S. L., Rodrigues J. de O., Lorenzo, M. G., Martins-Filho, O. A., and Guarneri, A. A. (2015). *Trypanosoma cruzi*, etiological agent of Chagas disease, is virulent to its triatomine vector *Rhodnius prolixus* in a temperature-dependent manner. *PLoS Negl. Trop. Dis.* 9:e0003646. doi: 10.1371/journal.pntd.0003646
- Fellet, M. R., Lorenzo, M. G., Elliot, S. L., Carrasco, D., and Guarneri, A. A. (2014). Effects of infection by *Trypanosoma cruzi* and *Trypanosoma rangeli* on the reproductive performance of the vector *Rhodnius prolixus*. *PLoS ONE* 9:e105255. doi: 10.1371/journal.pone.0105255
- Ferreira, R. C., Kessler, R. L., Lorenzo, M. G., Paim, R. M. M., Ferreira, L. L., Probst, C. M., et al. (2016). Colonization of *Rhodnius prolixus* gut by *Trypanosoma cruzi* involves an extensive parasite killing. *Parasitology* 143, 434–443. doi: 10.1017/S0031182015001857
- Flores-Ferrer, A., Marcou, O., Waleckx, E., Dumonteil, E., and Gourbière, S. (2018). Evolutionary ecology of Chagas disease; what do we know and what do we need? *Evol. Appl.* 11, 470–487. doi: 10.1111/eva.12582
- Friend, W. G., Choy, C. T., and Cartwright, E. (1965). The effect of nutrient intake on the development and the egg production of *Rhodnius prolixus* Stahl (Hemiptera: Reduviidae). *Can. J. Zool.* 43, 891–904. doi: 10.1139/z65-092
- Garcia, E. S., and Azambuja, P. (1991). Development and interactions of *Trypanosoma cruzi* within the insect vector. *Parasitol. Today* 7, 240–244. doi: 10.1016/0169-4758(91)90237-1
- Garcia, E. S., Genta, F. A., de Azambuja, P., and Schaub, G. A. (2010). Interactions between intestinal compounds of triatomines and *Trypanosoma cruzi*. *Trends Parasitol.* 26, 499–505. doi: 10.1016/j.pt.2010.07.003
- Garcia, E. S., Gonzalez, M. S., de Azambuja, P., Baralle, F. E., Fraidenraich, D., Torres, H. N., et al. (1995). Induction of *Trypanosoma cruzi* metacyclogenesis in the gut of the hematophagous insect vector, *Rhodnius prolixus*, by hemoglobin and peptides carrying a D-globin sequences. *Exp. Parasitol.* 81, 255–261. doi: 10.1006/expr.1995.1116
- González-Rete, B., Salazar-Schettino, P. M., Bucio-Torres, M. I., Córdoba-Aguilar, A., and Cabrera-Bravo, M. (2019). Activity of the prophenoloxidase system and survival of triatomines infected with different *Trypanosoma cruzi* strains under different temperatures: understanding Chagas disease in the face of climate change. *Parasit. Vectors* 12:219. doi: 10.1186/s13071-019-3477-9
- Gourbière, S., Dorn, P., Tripet, F., and Dumonteil, E. (2011). Genetics and evolution of triatomines: from phylogeny to vector control. *Heredity* 108, 190–202. doi: 10.1038/hdy.2011.71
- Guarneri, A. A., and Lorenzo, M. G. (2017). Triatomine physiology in the context of trypanosome infection. *J. Insect Physiol.* 97, 66–76. doi: 10.1016/j.jinsphys.2016.07.005
- Guhl, F. (2017). Geographical distribution of Chagas disease. *Am. Trypanosom. Chagas Dis.* 2017, 89–112. doi: 10.1016/B978-0-12-801029-7.00005-8
- Jackson, Y., Pinto, A., and Pett, S. (2014). Chagas disease in Australia and New Zealand: risks and needs for public health interventions. *Trop. Med. Int. Health* 19, 212–218. doi: 10.1111/tmi.12235

ACKNOWLEDGMENTS

Despite several initiatives by the current government to diminish the budget of most of Brazilian agencies funding science, the authors would like to acknowledge the efforts made by our scientific community (researchers, students, and staff) to keep science alive in our country.

- Jimenez, V. (2004). Dealing with environmental challenges: mechanisms of adaptation in *Trypanosoma cruzi*. *Res. Microbiol.* 165, 155–165. doi: 10.1016/j.resmic.2014.01.006
- Jurberg, J., and Galvão, C. (2006). Biology, ecology, and systematics of Triatominae (Heteroptera, Reduviidae), vectors of Chagas disease, and implications for human health. *Denisia* 50, 1096–1116.
- Kessler, R. L., Contreras, V. T., Marlière, N. P., Aparecida Guarneri, A., Villamizar Silva, L. H., Mazzarotto, G. A. C. A., et al. (2017). Recently differentiated epimastigotes from *Trypanosoma cruzi* are infective to the mammalian host. *Mol. Microbiol.* 104, 712–736. doi: 10.1111/mmi.13653
- Kollien, A., and Schaub, G. (2000). The development of *Trypanosoma cruzi* in triatominae. *Parasitol. Today* 16, 381–387. doi: 10.1016/S0169-4758(00)01724-5
- Kollien, A. H., Grospietsch, T., Kleffmann, T., Zerbst-Boroffka, I., and Schaub, G. A. (2001). Ionic composition of the rectal contents and excreta of the reduviid bug *Triatoma infestans*. *J. Insect Physiol.* 47, 739–747. doi: 10.1016/S0022-1910(00)00170-0
- Kollien, A. H., and Schaub, G. A. (1998). *Trypanosoma cruzi* in the rectum of the bug *Triatoma infestans*: effects of blood ingestion by the starved vector. *Am. J. Trop. Med. Hyg.* 59, 166–170. doi: 10.4269/ajtmh.1998.59.166
- Kollien, A. H., and Schaub, G. A. (1999). Development of *Trypanosoma cruzi* after starvation and feeding of the vector—a review. *Tokai J. Exp. Clin. Med.* 23, 335–340.
- Lara, F. A., Sant’anna, C., Lemos, D., Laranja, G. A., Coelho, M. G., Reis Salles, I., et al. (2007). Heme requirement and intracellular trafficking in *Trypanosoma cruzi* epimastigotes. *Biochem. Biophys. Res. Commun.* 355, 16–22. doi: 10.1016/j.bbrc.2006.12.238
- Maddrell, S. H. P. (1969). Secretion by the malpighian tubules of *Rhodnius*. The movements of ions and water. *J. Exp. Biol.* 51, 71–97.
- Maddrell, S. H. P. (1972). The mechanisms of insect excretory systems. *Adv. Insect Physiol.* 8, 199–331. doi: 10.1016/S0065-2806(08)60198-8
- Magdaleno, A., Ahn, I. Y., Paes, L. S., and Silber, A. M. (2009). Actions of a proline analogue, L-thiazolidine-4-carboxylic acid (T4C) on *Trypanosoma cruzi*. *PLoS ONE* 4:e4534. doi: 10.1371/journal.pone.0004534
- Marchese, L., Nascimento, J. F., Damasceno, F. S., Bringaud, F., Michels, P. A. M., and Silber, A. M. (2018). The uptake and metabolism of amino acids, and their unique role in the biology of pathogenic trypanosomatids. *Pathogens* 7:36. doi: 10.3390/pathogens7020036
- Merli, M. L., Cirulli, B. A., Menéndez-Bravo, S. M., and Cricco, J. A. (2017). Heme A synthesis and CcO activity are essential for *Trypanosoma cruzi* infectivity and replication. *Biochem. J.* 474, 2315–2332. doi: 10.1042/BCJ20170084
- Merli, M. L., Pagura, L., Hernández, J., Barisón, M. J., Pral, E. F., Silber, A. M., et al. (2016). The *Trypanosoma cruzi* protein TcHTE is critical for heme uptake. *PLoS Negl. Trop. Dis.* 10:e0004359. doi: 10.1371/journal.pntd.0004359
- Neves, D. P. (1971). Influência da temperatura na evolução do *Trypanosoma cruzi* em triatomíneos. *Rev. Inst. Med. Trop. Sao Paulo* 13, 155–161.
- O'Donnell, M. J. (2009). Too much of a good thing: how insects cope with excess ions or toxins in the diet. *J. Exp. Biol.* 212, 363–372. doi: 10.1242/jeb.023739
- Oliveira, M. F., Silva, J. R., Dansa-Petretski, M., de Souza, W., Braga, C. M. S., Masuda, H., et al. (2000). Haemozoin formation in the midgut of the blood-sucking insect *Rhodnius prolixus*. *FEBS Lett.* 477, 95–98. doi: 10.1016/S0014-5793(00)01786-5
- Oliveira, M. F., Silva, J. R., Dansa-Petretski, M., de Souza, W., Lins, U., Braga, C. M., et al. (1999). Haem detoxification by an insect. *Nature* 400, 517–518. doi: 10.1038/22910
- Paaijmans, K. P., Blanford, S., Bell, A. S., Blanford, J. I., Read, A. F., and Thomas, M. B. (2010). Influence of climate on malaria transmission depends on daily temperature variation. *Proc. Natl. Acad. Sci. U.S.A.* 107, 15135–15139. doi: 10.1073/pnas.1006422107
- Paiva-Silva, G. O., Cruz-Oliveira, C., Nakayasu, E. S., Maya-Monteiro, C. M., Dunkov, B. C., Masuda, H., et al. (2006). A heme-degradation pathway in a blood-sucking insect. *Proc. Natl. Acad. Sci. U.S.A.* 103, 8030–8035. doi: 10.1073/pnas.0602224103
- Perez-Molina, J., Perez-Ayala, A., Parola, P., Jackson, Y., Odolini, S., and Lopez-Velez, R. (2011). EuroTravNet: imported Chagas disease in nine European countries, 2008–2009. *Euro Surveill.* 16:19966. doi: 10.2807/ese.16.37.19966-en
- Phillips, N. R. (1960). Experimental studies on the quantitative transmission of *Trypanosoma cruzi*: aspects of the rearing, maintenance and testing of vector material, and of the origin and course of infection in the vector. *Ann. Trop. Med. Parasitol.* 54, 397–414. doi: 10.1080/00034983.1960.11686003
- Rassi, A., de Rezende, J. M., Luquetti, A. O., and Rassi, A. (2010). Clinical phases and forms of Chagas disease. *Am. Trypanosom.* 2010, 709–741. doi: 10.1016/B978-0-12-384876-5.00027-7
- Rolandi, C., and Schilman, P. E. (2018). The costs of living in a thermal fluctuating environment for the tropical haematophagous bug, *Rhodnius prolixus*. *J. Therm. Biol.* 74, 92–99. doi: 10.1016/j.jtherbio.2018.03.022
- Schaub, G. A. (1989). *Trypanosoma cruzi*: quantitative studies of development of two strains in small intestine and rectum of the vector *Triatoma infestans*. *Exp. Parasitol.* 68, 260–273. doi: 10.1016/0014-4894(89)90108-2
- Schipper, H., McClarty, B. M., McRuer, K. E., Nash, R. A., and Penney, C. J. (1980). Tropical diseases encountered in Canada: I. Chagas' disease. *Can. Med. Assoc. J.* 122, 165–169, 171–172.
- Schmitt, T. H., Frezzatti, W. A., and Schreier, S. (1993). Hemin-induced lipid membrane disorder and increased permeability: a molecular model for the mechanism of cell lysis. *Arch. Biochem. Biophys.* 307, 96–103. doi: 10.1006/abbi.1993.1566
- Slater, A. F., Swiggard, W. J., Orton, B. R., Flitter, W. D., Goldberg, D. E., Cerami, A., et al. (1991). An iron-carboxylate bond links the heme units of malaria pigment. *Proc. Natl. Acad. Sci. U.S.A.* 88, 325–329. doi: 10.1073/pnas.88.2.325
- Sterkel, M., Oliveira, J. H. M., Bottino-Rojas, V., Paiva-Silva, G. O., and Oliveira, P. L. (2017). The dose makes the poison: nutritional overload determines the life traits of blood-feeding arthropods. *Trends Parasitol.* 33, 633–644. doi: 10.1016/j.pt.2017.04.008
- Tyler, K. M., and Engman, D. M. (2001). The life cycle of *Trypanosoma cruzi* revisited. *Int. J. Parasitol.* 31, 472–481. doi: 10.1016/S0020-7519(01)00153-9
- Wigglesworth, V. B. (1931). The physiology of excretion in the bloodsucking insect, *Rhodnius prolixus* (Hemiptera, Reduviidae). I. Composition of the urine. *J. Exp. Biol.* 8, 411–451.
- Wolinska, J., and King, K. C. (2009). Environment can alter selection in host–parasite interactions. *Trends Parasitol.* 25, 236–244. doi: 10.1016/j.pt.2009.02.004
- Wood, S. F. (1938). A new locality for *Trypanosoma cruzi* Chagas in California. *Science* 87, 366–367. doi: 10.1126/science.87.2260.366
- Wood, S. F. (1941). New localities for *Trypanosoma cruzi* Chagas in Southwestern United States. *Am. J. Epidemiol.* C34, 1–13. doi: 10.1093/oxfordjournals.aje.a118745
- Wood, S. F. (1943). Observations on vectors of Chagas' disease in the United States. II. Arizona. *Am. J. Trop. Med. Hyg.* 23, 315–320. doi: 10.4269/ajtmh.1943.s1-23.315
- Wood, S. F. (1954). Environmental temperature as a factor in development of *Trypanosoma cruzi* in *Triatoma protracta*. *Exp. Parasitol.* 3, 227–233. doi: 10.1016/0014-4894(54)90021-1
- Woon, S. F. (1942). Observations on vectors of Chagas' disease in the United States. I. California. *Bull. Southern Calif. Acad. Sci.* 41, 61–69.
- World Health Organization (2007). *Reporte Sobre la Enfermedad de Chagas. 17–20 de Abril de 2005, Actualizado en Julio de 2007*, Buenos Aires, Argentina. Geneva: WHO.
- World Health Organization (2014). *Small Bites Big Threats. Chagas. World Health Day*. Retrieved from: <https://www.paho.org/world-health-day-2014/> (accessed April 7, 2014).
- Zuzarte-Luís, V., and Mota, M. M. (2018). Parasite sensing of host nutrients and environmental cues. *Cell Host Microbe* 23, 749–758. doi: 10.1016/j.chom.2018.05.018

Conflict of Interest: The authors declare that the research was conducted in the absence of any commercial or financial relationships that could be construed as a potential conflict of interest.

Copyright © 2020 Melo, Guarneri and Silber. This is an open-access article distributed under the terms of the Creative Commons Attribution License (CC BY). The use, distribution or reproduction in other forums is permitted, provided the original author(s) and the copyright owner(s) are credited and that the original publication in this journal is cited, in accordance with accepted academic practice. No use, distribution or reproduction is permitted which does not comply with these terms.



A CRISPR/Cas9-riboswitch-Based Method for Downregulation of Gene Expression in *Trypanosoma cruzi*

Noelia Lander^{1†}, Teresa Cruz-Bustos^{1†‡} and Roberto Docampo^{1,2*}

¹ Center for Tropical and Emerging Global Diseases, University of Georgia, Athens, GA, United States, ² Department of Cellular Biology, University of Georgia, Athens, GA, United States

OPEN ACCESS

Edited by:

Julius Lukes,
Institute of Parasitology
(CAS), Czechia

Reviewed by:

Eva Gluenz,
University of Oxford, United Kingdom
Drahomíra Faktorová,
Institute of Parasitology
(CAS), Czechia

*Correspondence:

Roberto Docampo
rdocampo@uga.edu

† Present address:

Teresa Cruz-Bustos,
Institute of Parasitology, University of
Veterinary Medicine, Vienna, Austria

‡ These authors have contributed
equally to this work

Specialty section:

This article was submitted to
Parasite and Host,
a section of the journal
Frontiers in Cellular and Infection
Microbiology

Received: 25 November 2019

Accepted: 11 February 2020

Published: 27 February 2020

Citation:

Lander N, Cruz-Bustos T and
Docampo R (2020) A
CRISPR/Cas9-riboswitch-Based
Method for Downregulation of Gene
Expression in *Trypanosoma cruzi*.
Front. Cell. Infect. Microbiol. 10:68.
doi: 10.3389/fcimb.2020.00068

Few genetic tools were available to work with *Trypanosoma cruzi* until the recent introduction of the CRISPR/Cas9 technique for gene knockout, gene knock-in, gene complementation, and endogenous gene tagging. Riboswitches are naturally occurring self-cleaving RNAs (ribozymes) that can be ligand-activated. Results from our laboratory recently demonstrated the usefulness of the *glmS* ribozyme from *Bacillus subtilis*, which has been shown to control reporter gene expression in response to exogenous glucosamine, for gene silencing in *Trypanosoma brucei*. In this work we used the CRISPR/Cas9 system for endogenously tagging *T. cruzi* glycoprotein 72 (TcGP72) and vacuolar proton pyrophosphatase (TcVP1) with the active (*glmS*) or inactive (*M9*) ribozyme. Gene tagging was confirmed by PCR and protein downregulation was verified by western blot analyses. Further phenotypic characterization was performed by immunofluorescence analysis and quantification of growth *in vitro*. Our results indicate that the method was successful in silencing the expression of both genes without the need of glucosamine in the medium, suggesting that *T. cruzi* produces enough levels of endogenous glucosamine 6-phosphate to stimulate the *glmS* ribozyme activity under normal growth conditions. This method could be useful to obtain knockdowns of essential genes in *T. cruzi* and to validate potential drug targets in this parasite.

Keywords: acidocalcisome, CRISPR/Cas9, *glmS*, GP72, riboswitch, *Trypanosoma cruzi*, vacuolar proton pyrophosphatase

INTRODUCTION

Infection by *Trypanosoma cruzi* is the main cause of congestive heart failure in Latin America (Rassi et al., 2000). The disease affects 8–10 million people in the Americas. The FDA approval of a test for these parasites in donated blood (Kessler et al., 2013) emphasizes the relevance of this parasite to human health in the United States, where physicians are largely unaware of the cardiac symptoms of chronic *T. cruzi* infection. Treatment of Chagas disease is limited to drugs with relatively high toxicity and partial efficacy (Urbina and Docampo, 2003). The study of metabolic pathways in these parasites that could be important for their viability but that do not affect their host could result in the finding of specific inhibitors to control the parasites without altering the hosts. A drawback for these studies in *T. cruzi* has been the lack of genetic tools, such as inducible downregulation, which are essential for the demonstration of the essentiality of these metabolic pathways and for the validation of new drug targets.

Few genetic tools were available to work with *T. cruzi* (Docampo, 2011; Burle-Caldas Gde et al., 2015) until the recent introduction of the CRISPR/Cas9 technique for gene knockout

(Peng et al., 2014; Lander et al., 2015; Costa et al., 2018; Romagnoli et al., 2018; Takagi et al., 2019) endogenous gene tagging (Lander et al., 2016b, 2017; Soares Medeiros et al., 2017; Costa et al., 2018), gene complementation (Chiurillo et al., 2017), and gene knock-in (Chiurillo et al., 2019). These studies have been recently reviewed in Lander and Chiurillo (2019).

Control of gene expression can be achieved at the transcriptional, translational or posttranslational levels (Ganesan et al., 2016). In the case of the related trypanosomatid *Trypanosoma brucei*, the fastest method for the generation of conditional mutants is the use of RNA interference (Alibu et al., 2005). This pathway, however, is absent in *T. cruzi* (Darocha et al., 2004). Integration of a tetracycline-regulated extra copy of the gene of interest to allow the knockout of the endogenous alleles in a cell line stably expressing a *tet* repressor and the T7 RNA polymerase (inducible knockout) has also been successfully employed in *T. brucei* (Clayton, 1999). Efforts to develop a similar method for *T. cruzi* have mostly failed until now (Darocha et al., 2004; Burle-Caldas Gde et al., 2015). In contrast to the control of a reporter gene expression over a range of four orders of magnitude in response to tetracycline in *T. brucei*, relatively high expression levels of the gene was detected in *T. cruzi* in the absence of tetracycline and little increase was detected after tetracycline addition [reviewed by (Burle-Caldas Gde et al., 2015)]. Inducible systems using destabilization domains of dihydrofolate reductase (DDD), or the rapamycin binding protein (ddFKBP), were only used to either create suicidal *T. cruzi* strains (Ma et al., 2015), or did not mediate the efficient knockdown of the genes (Burle-Caldas Gde et al., 2015). Inducible expression of dimerizable CRE recombinase (DiCRE system) was also tried in *T. cruzi* but has been only used for removal of exogenous selectable markers from the parasite's genome with limited success (Kangussu-Marcolino et al., 2014).

We recently reported the use of an alternative method for downregulation of gene expression in *T. brucei*, mediated at the mRNA level, using riboswitches (Cruz-Bustos et al., 2018b), which are naturally occurring self-cleaving RNAs (ribozymes) that can be modified to respond to ligands (Winkler et al., 2004). We used the *glmS* gene from *Bacillus subtilis*, which can control reporter gene expression in response to exogenous glucosamine in other eukaryotes, such as *Saccharomyces cerevisiae* (Watson and Fedor, 2011) and *Plasmodium falciparum* (Prommana et al., 2013). The *glmS* gene encodes the enzyme glutamine-fructose 6-phosphate amidotransferase that uses fructose 6-phosphate and glutamine to generate glucosamine 6-phosphate (GlcN6P). A conserved element in the 5'-untranslated region of this gene acts, when transcribed into RNA, as a self-cleaving riboswitch stimulated by glucosamine 6-phosphate (GlcN6P) (Winkler et al., 2004). When this conserved element is inserted in the 5'-UTR or the 3'-UTR of a gene of interest the self-cleaving RNA motif will silence it when in the presence of GlcN6P produced within the cells. Addition of glucosamine to the culture medium stimulates this activity through the endogenous generation of GlcN6P. A mutant *glmS* gene whose RNA has no self-cleaving activity (*M9*) can be used as negative control (Winkler et al., 2004). Tagging only one allele of the gene

of interest (GOI) in *T. brucei* with *glmS* was sufficient to down-regulate gene expression at the mRNA level, and in some cases, produce phenotypic changes (Cruz-Bustos et al., 2018b). Since this technique requires the endogenous tagging of the genes that are targeted for down-regulation, our recent development of C-terminal endogenous tagging of genes in *T. cruzi* using CRISPR/Cas9 (Lander et al., 2016b, 2017) made this approach feasible.

In this work, we report the use of the *glmS* ribozyme for silencing the expression of endogenous genes without the need to add glucosamine to the medium, suggesting that *T. cruzi* produces enough levels of endogenous GlcN6P to stimulate the *glmS* ribozyme activity under normal growth conditions. This method could be useful to validate potential drug targets in this parasite.

RESULTS

Effect of Glucosamine on Growth of Epimastigotes

We first tested whether glucosamine has any effect on parasite growth. **Figure S1** shows the effects of 0–30 mM glucosamine added to a modified SDM-79 medium. This medium, which has been used to grow *T. cruzi* (Hasne et al., 2010), has a known concentration of glucosamine (1 mM) that could be varied to stimulate the riboswitch. We found that 10 mM was the maximum concentration that did not affect growth during the evaluated period and used that concentration in subsequent experiments.

Downregulation of the Expression of *T. cruzi* Glycoprotein 72 (TcGP72)

We first used the CRISPR/Cas9 system (Lander et al., 2016b, 2017) for endogenously tagging *T. cruzi* glycoprotein 72 (TcGP72) with the active (*glmS*) or inactive (*M9*) ribozyme following the strategy shown in **Figure 1**. TcGP72 is a glycoprotein responsible for adhesion of the flagellum to the cell body and is not essential for the parasite survival (Cooper et al., 1993). We co-transfected a specific GP72-3'end-sgRNA/Cas9/pTREX-n construct with a specific DNA donor molecule amplified from the pMOTag-M9/*glmS*-4H vectors (Cruz-Bustos et al., 2018b), as described under Experimental Procedures and grew the cells initially in a modified SDM-79 medium. However, when glucosamine addition was shown to be unnecessary to downregulate TcGP72 expression further experiments were done in regular LIT medium. We obtained G418/hygromycin resistant cells after 3 weeks under selective pressure. Transfectants were analyzed by PCR, using gDNA isolated from them, and a specific primer set to distinguish between the wild type and the tagged cell lines (**Figure 1**). After 21 days in culture it was possible to confirm the presence of the tagged gene (band of 779 bp) in TcGP72-3xHA-*glmS* (*glmS*) and TcGP72-3xHA-M9 (*M9*) transfectants, but not in wild type (WT) parasites (**Figure 2A**). Insertion of *glmS* and *M9* constructs at the 3'UTR of GP72 gene was confirmed by sequencing

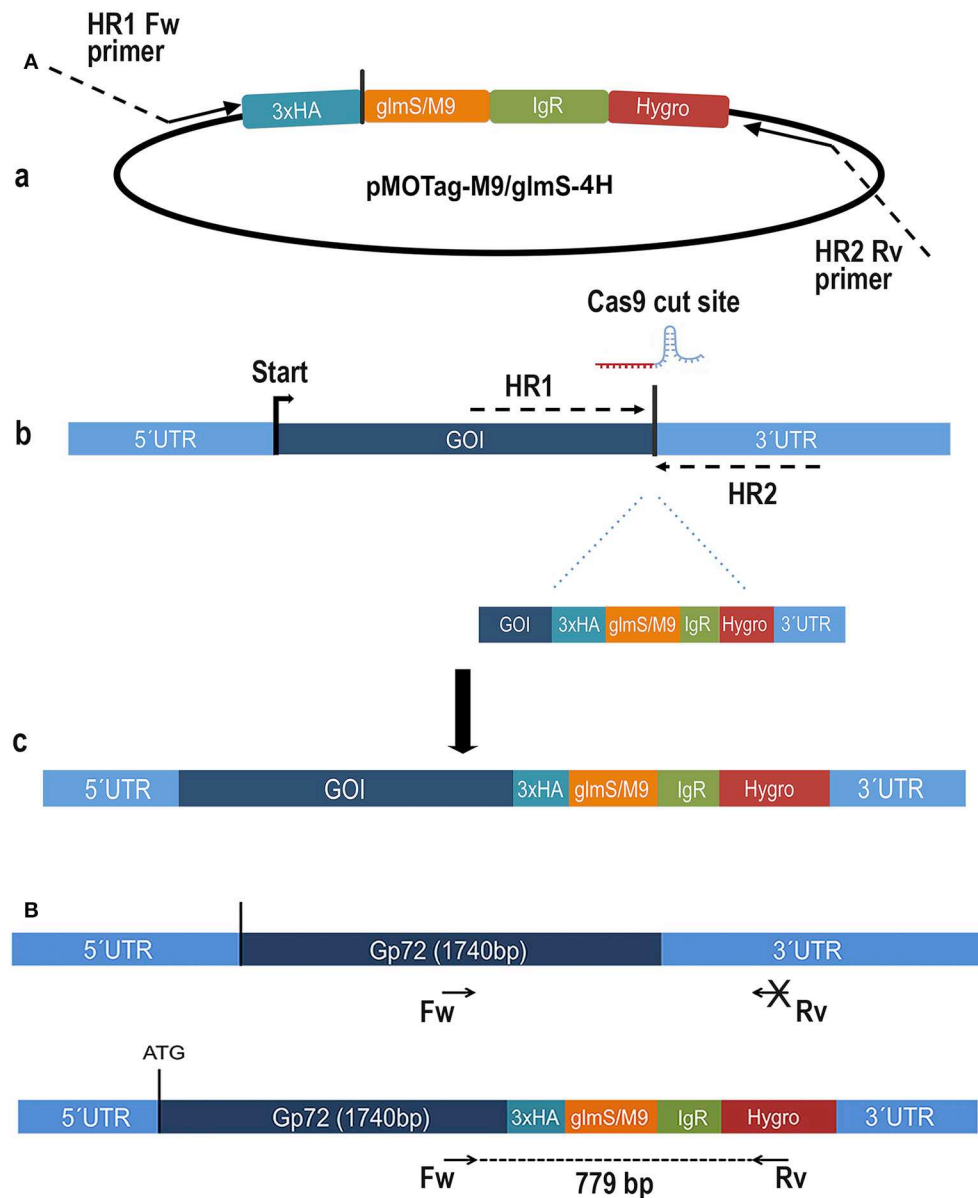


FIGURE 1 | Schematic representation of the strategy used in *Trypanosoma cruzi*. **(A)** pMOTag-4H-M9/glmS vector map. HR1 Fw, and HR2 Rv, ultramers indicate oligonucleotides used to amplify the DNA donor. **(B)** A doubled strand break was produced in the gDNA by Cas9 targeted by the sgRNA downstream of the STOP codon of the gene of interest (GOI), both expressed from 3'-end-sgRNA/Cas9/pTREX-n plasmid. Homologous directed repair was induced co-transfecting epimastigotes with the DNA donor cassette, containing homologous regions to the GOI 3' end (dark blue) and to the GOI 3'UTR (light blue). **(C)** Integration of 3xHA, M9/glmS and antibiotic resistance genes at 3'end of GOI by homologous recombination. **(B)** Diagram representing the positions of the primers (arrows) used to verify the integration of the donor DNA at the 3' end of *TcGP72* ORF.

(Sequences S1, S2, respectively). qRT-PCR showed complete downregulation of *TcGP72* expression (Figure 2B). Western blot analysis using monoclonal antibody WIC 29.26 showed disappearance of the 72-KDa band after 45 days in culture compared to WT and *TcGP72*-3xHA-M9-transfectants (Figure 2C). As reported before (Cooper et al., 1993), this antibody recognizes the glycan epitope in additional proteins. Figure 2D shows the presence of parasites with flagellar detachment and greatly reduced labeling with monoclonal

antibody WIC 29.26. More than 90% of the cells showed this phenotype.

To exclude the possibility of off target effects, we investigated whether an exogenous *TcGP72* gene could complement the *TcGP72* knock down epimastigotes. We found that the exogenous gene (with changes in the PAM sequence to prevent disruption by CRISPR/Cas9) bearing a Ty epitope was targeted to the epimastigote flagellum, as shown in Figure 3A. Western blot analysis showed recovery of the labeling with antibody WIC 29.96

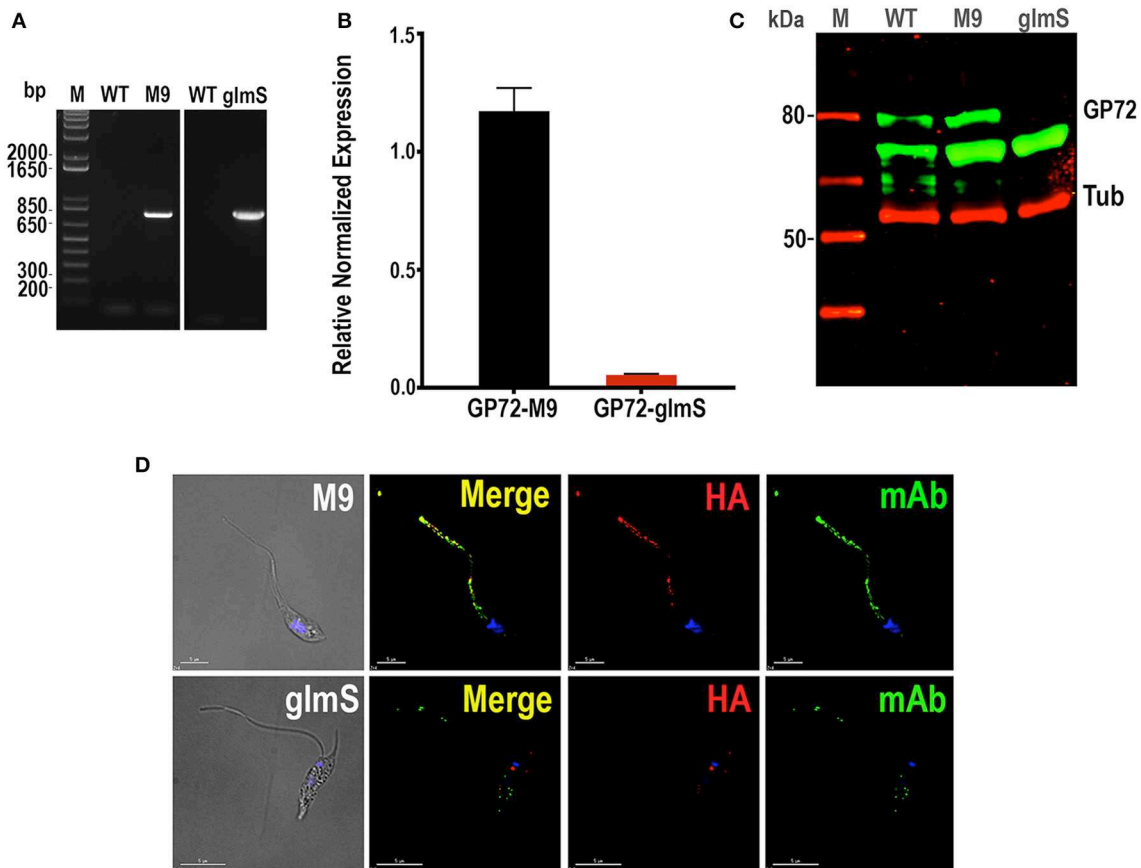


FIGURE 2 | Integration of *glmS*/M9 ribozyme sequences into the *TcGP72* gene. **(A)** PCR analysis using gDNA isolated from WT and *TcGP72*-M9/*glmS* (M9, *glmS*) cell lines. A DNA fragment of 779 bp was amplified in *3xHA-glmS*/M9-tagged epimastigotes, whereas the band is absent in WT cells. **(B)** qRT-PCR shows down-regulation of *TcGP72*. **(C)** Western-blot analysis of *TcGP72*-M9/*glmS* cell lines. Antibody WIC 29.26 labels a band of 72 kDa in *TcGP72*-3xHA-M9- but not in *TcGP72*-3xHA-*glmS*-transfected cells. Anti-tubulin antibody (Tub) was used as loading control. Antibodies are indicated on the right side of the blots, and molecular weights (kDa) are on the left side. **(D)** Immunofluorescence microscopy of *TcGP72*-3xHA-M9- and *TcGP72*-3xHA-*glmS*-transfected epimastigotes. There is co-localization in the flagellum of anti-HA and WIC 29.26 antibodies in *TcGP72*-3xHA-M9-transfected epimastigotes (*merge*) while the flagellum is detached and has little labeling with anti-HA and reduced labeling with WIC 29.26 in *TcGP72*-3xHA-*glmS*-expressing cells. DIC, differential interference contrast microscopy. Scale bars = 5 μ m.

in complemented epimastigotes as compared to *TcGP72*-3xHA-*glmS* transfectants (**Figure 3B**). In conclusion, CRISPR/Cas9-mediated endogenous C-terminal tagging of *T. cruzi* GP72 with *glmS* was successful in silencing the gene without the need to add glucosamine to the medium. These results suggest that *T. cruzi* produces high levels of endogenous GlcN6P and that these levels are sufficient to stimulate the *glmS* ribozyme activity under normal growth conditions.

Downregulation of the Expression of *T. cruzi* Vacuolar Proton Pyrophosphatase (TcVP1)

The *T. cruzi* vacuolar proton pyrophosphatase (TcVP1) is an electrogenic proton pump mainly localized to acidocalcisomes (Scott et al., 1998; Lander et al., 2016b), where it maintains their acidity. In *T. brucei*, RNAi experiments have shown that the enzyme is essential for normal growth of procyclic and

bloodstream forms *in vitro* (Lemerrier et al., 2002). We followed the same procedure used to downregulate the expression of *TcGP72*. Chimeric sgRNA was cloned into *Cas9/pTREX-n* vector and co-transfected with DNA donor containing *glmS* ribozyme sequence or its M9 inactive version into *T. cruzi* epimastigotes. Donor DNAs were amplified from *pMOTag-glmS-4H* and *pMOTag-M9-4H* vectors, respectively (Cruz-Bustos et al., 2018b). Transfectant parasites were obtained after 3 weeks of selection with G418 and hygromycin. We then obtained clonal populations from both *TcVP1*-3xHA-M9 and *TcVP1*-3xHA-*glmS* tagged cell lines by serial dilutions. We confirmed *TcVP1* tagging in mixed and clonal populations by PCR (**Figure 4A**). We chose *TcVP1*-3xHA-M9, clone F9, and *TcVP1*-3xHA-*glmS*, clone E5 for further experiments. TcVP1 downregulation in *glmS*-tagged but not in M9-tagged epimastigotes was confirmed by western blot analysis using monoclonal antibodies anti-TcVP1 in the absence of 10 mM glucosamine (day 0) or at days 1, 2, and

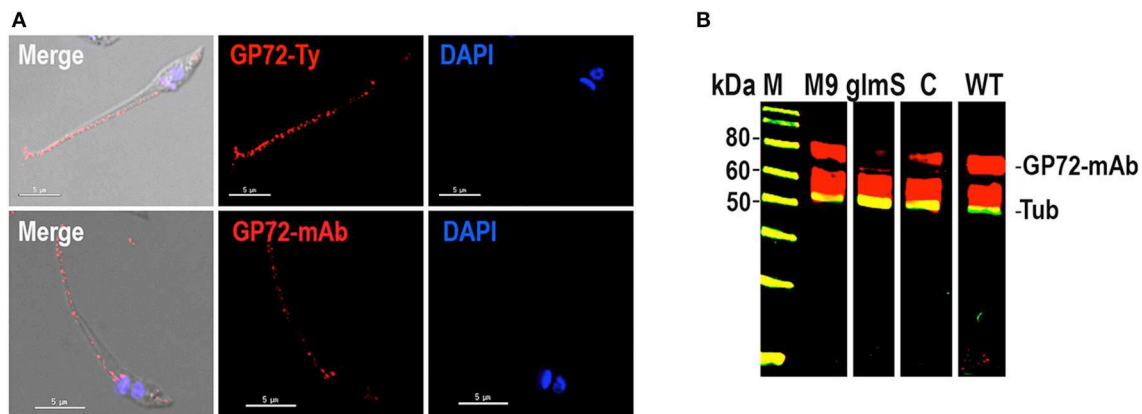


FIGURE 3 | Complementing of *TcGP72-3xHA-glmS*. **(A)** Immunofluorescence microscopy of *TcGP72-3xHA-glmS* epimastigotes complemented with an exogenous copy of *TcGP72* gene. Labeling of the flagellum was detected with anti-Ty and WIC 29.26 antibodies, while no flagellar detachment was observed. Bars = 5 μ m. **(B)** Western-blot analysis of total protein extracts of *TcGP72-3xHA-M9* (M9), *TcGP72-3xHA-glmS* (glmS), *TcGP72-3xHA-glmS* complemented with *TcGP72-Ty* (lane C) and wild type (WT) epimastigotes, using WIC 29.26 antibodies. Anti- α -tubulin antibodies (Tub) were used as a loading control.

3 after addition of glucosamine to the medium (**Figure 4B**). *TcVP1* expression was also evaluated at the RNA level by quantitative RT-PCR under the same conditions (**Figure 4C**). Downregulation of the gene in *TcVP1-glmS* epimastigotes in the absence of glucosamine (day 0) or at days 1, 2, and 3 post-induction (dpi) was confirmed, although basal levels of *TcVP1* expression were detected at all time points in *TcVP1-glmS* cells, relative to *TcVP1-M9* uninduced epimastigotes (day 0). No significant differences were observed in *TcVP1-M9* parasites at days 1, 2, and 3 post induction relative to day 0 (uninduced) (**Figure 4C**). We also evaluated the growth *in vitro* of *TcVP1-M9*- and *TcVP1-glmS*-tagged epimastigotes (**Figures 4D,E**). Growth of *TcVP1-glmS*-expressing epimastigotes in LIT medium was significantly affected as compared with the growth of *TcVP1-M9*-tagged cells but the presence of 10 mM glucosamine did not change the growth rate of these mutants (**Figure 4D**). The growth of these cell lines was then monitored for a longer period (10 days) in LIT medium, including a cell line expressing Cas9 and a scrambled sgRNA as control (*Scrambled*) (**Figure 4E**). Again, the results show a significant lower growth of *TcVP1-glmS*-expressing epimastigotes as compared with those expressing *TcVP1-M9* or a scrambled sgRNA, thus confirming the results observed with downregulation of *TcGP72*.

We induced the differentiation of *TcVP1-glmS* and *TcVP1-M9* epimastigotes to metacyclic forms and infected Vero cells as described in Experimental procedures. Once enough culture-derived trypomastigotes were obtained we used them to test their ability to infect Vero cells and replicate intracellularly as amastigotes. **Figure 5** shows that the ability of *TcVP1-glmS* trypomastigotes to infect tissue-culture cells, but not the amastigote replication, was significantly impaired, as compared with that of *TcVP1-M9* parasites. The presence of added glucosamine had no effect in either invasion or replication, thus confirming the results with epimastigotes in both *TcGP72-glmS* and *TcVP1-glmS* cells. Downregulation of *TcVP1* in the *TcVP1-glmS* but not in the *TcVP1-M9* trypomastigotes used

for the invasion assays was confirmed by western blot analysis (**Figure 5C**).

DISCUSSION

CRISPR/Cas9-mediated endogenous C-terminal tagging of *TcGP72* and *TcVP1* with *glmS*, but not with *M9*, was successful in knocking down the gene expression without the addition of glucosamine to the medium. These results suggest that *T. cruzi* produces high levels of endogenous glucosamine 6-phosphate and that these levels are sufficient to stimulate the *glmS* ribozyme activity under normal growth conditions. In this regard, it has been found that *T. cruzi* (TcCLB.506507.10), as well as *Leishmania major* (LmjF32.3260), possesses an N-acetyl glucosamine 6-phosphate deacetylase (NAGD) that generates glucosamine 6-phosphate while *T. brucei* lacks this enzyme (Naderer et al., 2010). It is tempting to speculate that this enzyme could be involved in the production of high endogenous levels of glucosamine 6-phosphate in *T. cruzi*. However, it is important to indicate that the method, as it has been developed until now, could be useful to obtain knockdowns of essential genes in *T. cruzi*. If the gene is essential, and depending on the ribozyme used, the cells will die (*glmS* transfectants) or survive (*M9* transfectants). This method could then be used to validate the essentiality of potential targets. In addition, as the *glmS* ribozyme acts at the mRNA level, it is possible to detect basal levels of expression in the transfectants, thus allowing the selection of parasites expressing *glmS*-tagged essential genes, as shown in **Figure 4C** for *TcVP1* gene. C-terminal endogenous tagging also facilitates localization studies of the genes of interest.

One advantage of using our previously reported CRISPR/Cas9 methodology (Lander et al., 2016b, 2017) for tagging genes with *glmS* ribozyme, is that the constitutive expression of Cas9 and the sgRNA in the presence of a DNA donor conferring antibiotic resistance, allows tagging both alleles of the gene using a single resistance marker, as previously shown

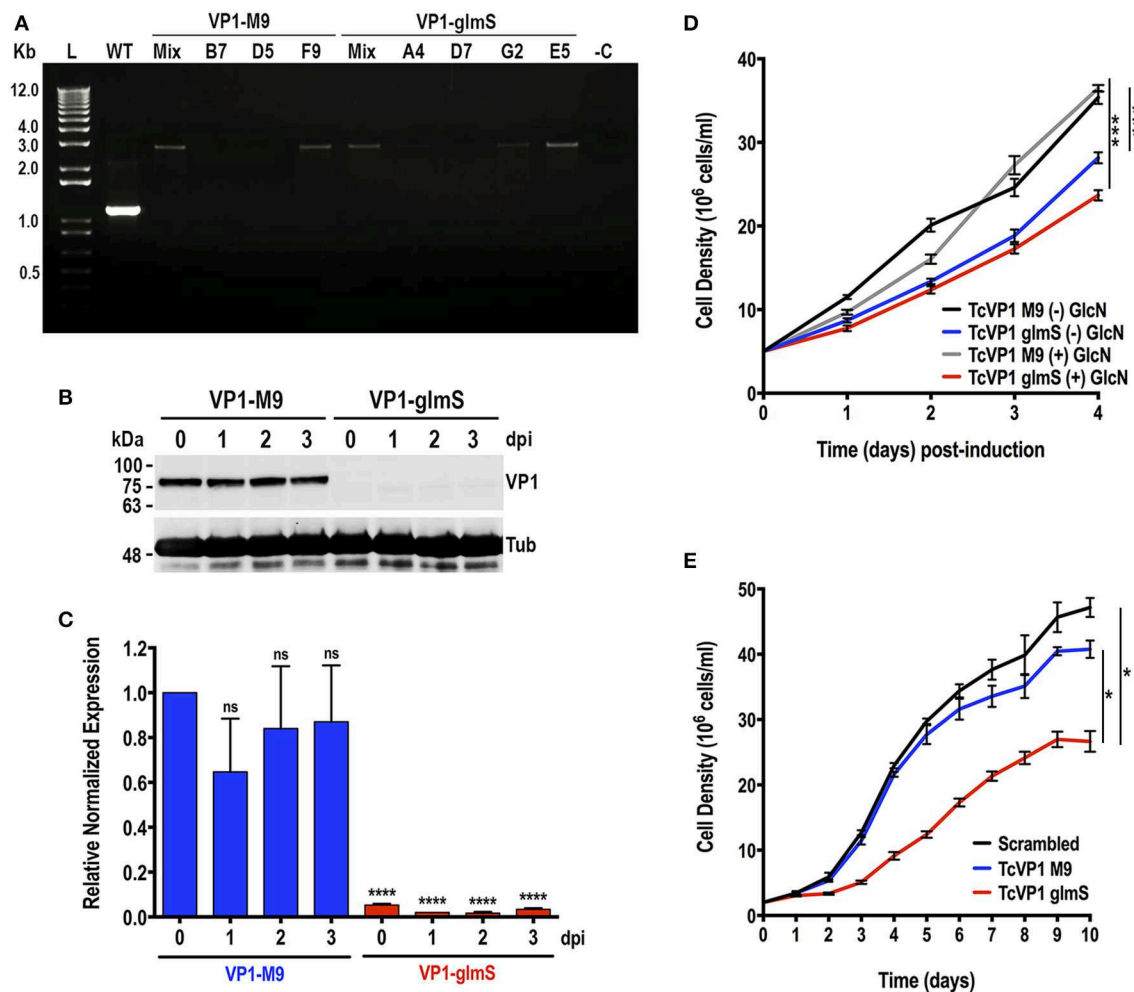


FIGURE 4 | Integration of *glmS*/*M9* ribozyme sequences into the *TcVP1* gene. **(A)** PCR analysis using gDNA isolated from WT and *TcVP1-M9/glmS* mixed (Mix) and clonal populations (*TcVP1-M9*, clones B7, D5, and F9; *TcVP1-glmS*, clones D7, G2, and E5). The primer set used (Table S1, primers 11 and 12) generates a band of 1,144 bp in wild type parasites (WT) and a band of 2,758 bp in *TcVP1*-tagged (*M9* or *glmS*) epimastigotes. Transfectant mixed and clonal populations were analyzed from both tagged versions of *TcVP1*, and in both cases the band of 2,758 bp was detected in the originally transfected cell lines (Mix) and in some of the clones. Clones F9 (*TcVP1-M9*) and E5 (*TcVP1-glmS*) were chosen for further phenotypic analysis. **(B)** Western-blot analysis of *TcVP1-M9* and *TcVP1-glmS* cell lines. Anti *TcVP1* monoclonal antibody labels a band of 85 kDa in *TcVP1-3xHA-M9*- but not in *TcVP1-3xHA-glmS*- epimastigotes. Expression of *TcVP1* was monitored during 3 days after addition of 10 mM glucosamine to the medium (days post induction, dpi). Anti-tubulin antibody (Tub) was used as loading control. Antibodies are indicated on the right side of the blots, and molecular weights (kDa) are on the left side. **(C)** qRT-PCR analysis of *TcVP1-M9* and *TcVP1-glmS* cell lines from 0 to 3 days post induction (dpi). **(D)** Growth *in vitro* of *TcVP1-M9* and *TcVP1-glmS* epimastigotes cultured with [(+) GlcN] or without [(-) GlcN] 10 mM glucosamine. **(E)** Growth *in vitro* of scrambled, *TcVP1-M9* and *TcVP1-glmS* epimastigotes cultured in LIT medium until reaching the stationary phase, without addition of glucosamine. In **(C)**, qRT-PCR data analysis was performed using one-way ANOVA with multiple comparisons ($n = 3$; **** $p < 0.0001$; ns, no significant). In **(D,E)**, one-way ANOVA with multiple comparisons was applied to growth rates calculated from each growth curve ($n = 3$; * $p < 0.05$; *** $p < 0.001$).

(Lander et al., 2015, 2018; Chiurillo et al., 2017, 2019; Cruz-Bustos et al., 2018a; Bertolini et al., 2019). In this way, the downregulation efficiency is significantly improved because only one transfection is necessary to tag and inactivate both alleles of the gene.

It has been reported that in *S. cerevisiae* (Meaux and Van Hoof, 2006) and in *P. falciparum* (Prommana et al., 2013) the ribozyme-cleaved mRNA 5' fragment separated from its polyA tail could be degraded by the 3' exosome. This pathway has also been reported to be active in trypanosomatids (Estevez et al., 2001). When the

glmS ribozyme is in the 5'UTR, mRNA cleavage would separate the mRNA from its 5'cap structure and the de-capped mRNA would be degraded by the 5'-3'-exonucleases, which are also present in trypanosomatids (Li et al., 2006).

Interestingly, our studies revealed that, in contrast to what occurs with TbVP1 in *T. brucei* (Lemerrier et al., 2002), TcVP1 is not essential for the viability of epimastigotes or the infective stages of *T. cruzi*, although is important for normal growth of epimastigotes in rich medium, and for trypomastigote invasion of host cells. TcVP1 is mostly localized to acidocalcisomes where

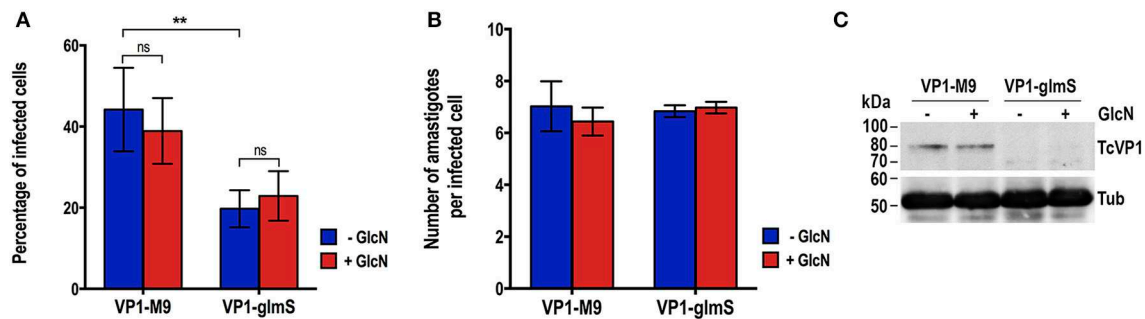


FIGURE 5 | Invasion and intracellular replication of *TcVP1-M9* and *TcVP1-glmS* cell lines. **(A)** *TcVP1-M9* and *TcVP1-glmS* trypomastigote infection of Vero cells. There was a significant difference in the percentage of infected Vero cells but not in the number of intracellular amastigotes per infected host cell observed 48 h post infection **(B)**. Values are mean \pm s.d.; $n = 3$; $**p < 0.01$; ns, not significant (Two-way ANOVA with multiple comparisons test). **(C)** Western-blot analysis of *TcVP1-M9* and *TcVP1-glmS* trypomastigotes. Anti TcVP1 antibody labels an expected band of 85 kDa in *TcVP1-3xHA-M9*- but not in *TcVP1-3xHA-glmS*- epimastigotes. Tissue culture-derived trypomastigotes collected at day 6 post-infection of Vero cells were induced with 10 mM glucosamine (GlcN) overnight at 4°C. After induction, trypomastigotes were used for infection of Vero cells and 1×10^7 trypomastigotes were reserved for protein extraction. Proteins were analyzed by western blot using TcVP1 mAb (1:2,000). Anti-tubulin antibody (Tub) was used as loading control. Antibodies are indicated on the right side of the blots, and molecular weights (kDa) are on the left side.

it contributes to the acidification of the organelle together with a vacuolar proton ATPase (Docampo et al., 1995; Scott et al., 1998).

In conclusion, the CRISPR/Cas9/riboswitch method developed in this work will enable the downregulation of gene expression in *T. cruzi*, and potentially in *Leishmania* spp. in which endogenous gene tagging using CRISPR/Cas9 has been achieved (Lander et al., 2016a,b).

EXPERIMENTAL PROCEDURES

Culture Methods

Trypanosoma cruzi Y strain epimastigotes were cultured in liver infusion tryptose (LIT) medium (Bone and Steinert, 1956) containing 10% heat-inactivated fetal bovine serum at 28°C. The endogenously tagged cell line was maintained in medium containing 250 μ g/ml G418 and 150 μ g/ml of hygromycin. For initial experiments to test the effect of glucosamine, epimastigotes were also cultured in medium SDM-79, without the addition of D-glucosamine and supplemented with hemin (7.5 μ g/mL), 200 μ M putrescine, and 10% heat-inactivated fetal bovine serum (Hasne et al., 2010; Jimenez and Docampo, 2015). Cell growth was determined by counting cells in a Neubauer chamber.

Chemicals and Reagents

The pMOTag4H vector was a gift from Dr. Thomas Seebeck (University of Bern, Bern, Switzerland). Monoclonal antibody WIC 29.26 was a gift from Dr. George A.M. Cross (Rockefeller University). Wild type and M9 mutated *Bacillus subtilis* *glmS* ribozymes were gifts from Dr. Vasant Muralidharan (University of Georgia). Monoclonal antibody BB2 against the *S. cerevisiae* Ty1 virus-like particle was a gift from Dr. R. Drew Etheridge (University of Georgia). Monoclonal antibody against *T. cruzi* vacuolar H⁺-pyrophosphatase (TcVP1) was described before (Seufferheld et al., 2004). GoTaq DNA polymerase and T4 DNA ligase were from Promega. Antarctic phosphatase, restriction enzymes, and Q5 high fidelity DNA polymerase were from

New England Biolabs (Ipswich, MA). Fluoromount-G was from SouthernBiotech (Birmingham, AL). Pierce BCA protein assay, Hygromycin B, BenchMark prestained protein ladder, BenchMark protein ladder, MagicMark™ XP Western Protein Standard, Alexa-conjugated secondary antibodies, and HRP-conjugated secondary antibodies were from Thermo Fisher Scientific. Anti-HA high affinity rat monoclonal antibody (clone 3F10) was purchased from Roche Applied Science. IRDye-conjugated secondary antibodies were from LI-COR Biosciences (Lincoln, NE). Benzonase nuclease was from Novagen (EMD Milli-pore, Billerica, MA). Nitrocellulose membranes were from Bio-Rad. The primers were purchased from Integrated DNA Technologies. TRI[®] reagent, anti-tubulin monoclonal antibody, G418, mammalian cell protease inhibitor mixture (P8340), other protease inhibitors, and all other reagents of analytical grade were from Sigma-Aldrich.

Molecular Constructs

The pMOTag4H vector designed for endogenous C-terminal tagging of *T. brucei* (Oberholzer et al., 2006) was used to construct the template plasmids for DNA donor amplification. This vector contains a 3xHA tag and the hygromycin resistance marker. Wild-type and M9 mutated *Bacillus subtilis* *glmS* ribozyme sequences (Winkler et al., 2004) were used to generate the pMOTag-*glmS*-4H and pMOTag-M9-4H vectors (Addgene plasmids #106378 and #106379) (Cruz-Bustos et al., 2018b). For CRISPR/Cas9-mediated endogenous C-terminal tagging in *T. cruzi* we used the Cas9/pTREX-n vector (Addgene plasmid #68708) (Lander et al., 2015) to clone a specific single guide RNA (sgRNA) sequence targeting the 3' end of *TcGP72* (TcCLB.50956120) and *TcVP1* (TcCLB. 510773.20) genes. The sgRNAs were amplified by PCR (Table S1, primers 1–3), using pUC_sgRNA plasmid as template (Addgene plasmid #68710) (Lander et al., 2015). We co-transfected the GP72-3' end-sgRNA/Cas9/pTREX-n or VP1-3' end-sgRNA/Cas9/pTREX-n construct with the specific DNA donor template for tagging the

3' end of each gene, right upstream the stop codon, with a 3xHA tag sequence and the *glmS/M9* ribozyme amplified from pMOTag-*glmS*-4H and pMOTag-M9-4H vectors, respectively, as previously described (Lander et al., 2016b; Cruz-Bustos et al., 2018b) (Table S1, primers 4–7). sgRNA correct orientation in Cas9/pTREX-n vector was determined by PCR (Table S1, primers 1, 2, and 8) and sequencing using primer 8. Endogenous tagging of *TcVP1* and *TcGP72* was confirmed by PCR (Table S1, primers 9–12). A cell line expressing Cas9 and a scrambled sgRNA (Lander et al., 2015) was used as a control for growth experiments *in vitro*.

Complementation of TcGP72-KO Cells

To revert the phenotype exhibited by *TcGP72-g3xHA-glmS* epimastigotes we used an exogenous *TcGP72* gene to complement the mutants. Following a PCR strategy, we eliminated the PAM sequence (TGG-TGT) specific for the *TcGP72*-sgRNA used to obtain the *TcGP72-g3xHA-glmS* cells, therefore avoiding constitutively expressed Cas9 to target the inserted sequence (Table S1, primers 13 and 14). The PCR product was cloned into pTREX-p vector (Chiurillo et al., 2017), which confers resistance to puromycin, by XbaI and XhoI restriction sites. We also included a C-terminal Ty1 tag in the reverse primer 14 (Table S1) in order to detect the overexpressed protein using anti-Ty1 antibody.

Cell Transfection

Trypanosoma cruzi epimastigotes were grown to a density of $1\text{--}2 \times 10^7$ cells/ml, washed once with cold PBS, pH 7.4, and resuspended in ice-cold Cytomix (120 mM KCl, 0.15 mM CaCl₂, 10 mM K₂HPO₄, 2 mM EDTA, 5 mM MgCl₂, pH 7.6) at a density of 10^8 cells/ml in electroporation buffer. Transfections were carried out in a 4-mm cuvette with 25 µg of plasmid DNA and 25 µg of DNA donor, using the Bio-Rad Gene Pulser Xcell electroporator set at 1.5 kV and 25 µF with three pulses, allowing at least 1 min for cells to recover in ice between pulses, and then incubated at room temperature for 15 min. Parasites were recovered in 5 ml of LIT supplemented with 20% fetal bovine serum at 28°C and after 24 h in culture, geneticin (G418), and hygromycin B were added to a final concentration of 250 and 150 µg/ml, respectively.

Western Blot Analyses

Electrophoresed proteins were transferred to nitrocellulose membranes using a Bio-Rad transblot apparatus for 1 h at 100 V at 4°C. Following transfer, the membrane blots were blocked with 5% non-fat dry milk in PBS containing 0.1% Tween-20 (PBS-T) overnight at 4°C. Blots were probed with primary antibody (WIC 29.26 monoclonal antibody (1:1,000), anti-Ty1 monoclonal antibody (1:1,000), anti *TcVP1* monoclonal antibody (1:2,000) or anti-tubulin monoclonal antibody [1:40,000]) for 1 h, at RT. After washing three times with PBS-T, the blots were incubated with goat anti-rabbit antibody (1:20,000) or goat anti-mouse antibody (1:20,000). The membranes were washed three times with PBS-T, and western blot images were processed and analyzed using the Odyssey infrared system software (LICOR Biosciences) or a ChemiDoc™ Imaging System (Bio-Rad).

Immunofluorescence Analyses

Epimastigotes in log phase were washed once with PBS at room temperature and fixed with 4% paraformaldehyde in PBS for 30 min at room temperature. The cells were allowed to adhere to poly-L-lysine-coated coverslips and then permeabilized for 3 min with 0.3% Triton X-100. Permeabilized cells were blocked with PBS containing 3% BSA, 1% fish gelatin, 50 mM NH₄Cl, and 5% goat serum 1 h at room temperature. Then cells were incubated with the primary antibody (1:100 rat anti-HA tag, 1:500 anti-Ty1 monoclonal antibody and 1:100 mouse WIC 29.26 diluted in PBS (pH 7.4) for 1 h at room temperature. The cells were washed three times with in PBS (pH 7.4) and then incubated for 1 h at room temperature in the dark with Alexa Fluor 488-conjugated goat anti-mouse and Alexa Fluor 546-conjugated goat anti-rat (1:1,000). Following incubation with the secondary antibody, the cells were washed five times in PBS and once in water and then mounted on slides. DAPI (5 µg/ml) was included in the Fluoromount-G mounting medium to stain DNA. Controls were performed as described above using *M9*-tagged epimastigotes. Specimens were imaged using the Delta Vision Elite deconvolution microscope (Applied Precision).

Metacyclogenesis

Trypanosoma cruzi epimastigotes were *in vitro* differentiated into infective metacyclic trypomastigotes by aging in LIT medium for 10 days at 28°C. Cultures were started at 5×10^6 cells/mL and after 10 days, 1.5 mL aged culture was centrifuged at $1,000 \times g$ for 7 min and resuspended in 5 mL RPMI supplemented with 20% FBS fresh. The complement in fresh FBS kills epimastigotes, whereas metacyclic trypomastigotes survive. Cells were examined under the microscope to confirm the presence of about 10% metacyclic trypomastigotes, and used immediately to infect Vero cells as described below.

Host Cell Invasion and Intracellular Replication Assays

Gamma-irradiated (2,000 radiation-absorbed doses) Vero cells (4.5×10^5 cells) were plated onto sterile coverslips in a 12-well plate and incubated overnight at 35°C, 7% CO₂, in RPMI medium plus 10% fresh FBS. Tissue culture-derived trypomastigotes were incubated at 4°C overnight to allow amastigotes to settle from swimming trypomastigotes. Trypomastigotes from the supernatants of these collections were counted and used to infect the coverslips at a 10:1 ratio of parasites to host cells. At 4 h post-infection, coverslips were washed extensively with Hank's balanced salt solution, followed by PBS, pH 7.4, to remove any extracellular parasites. Coverslips were fixed immediately in 4% paraformaldehyde in PBS, pH 7.4, at 4°C for 30 min. Coverslips were washed once with PBS and mounted onto glass slides in Fluoromount-G containing 15 µg/ml DAPI, which stains host and parasite DNA. Coverslips were viewed on an Olympus BX60 microscope to quantify the number of host cells that contained intracellular parasites and the number of intracellular parasites per cell in randomly selected fields. Three hundred host cells were counted per sample in three independent experiments. To quantify amastigote replication, the following modifications were used: host cells were infected at

a ratio of 10 parasites to one host cell, and coverslips were allowed to incubate for 48 h post-infection at 35°C, 7% CO₂, prior to fixation and DAPI staining. Coverslips were mounted onto glass slides and analyzed by fluorescence microscopy. Amastigotes in infected cells were counted using a 100 × objective.

Quantitative Real-Time PCR

Total RNA was isolated from trypanosomes using the TRI[®] reagent (Sigma) by following the manufacturer's instructions. The total RNA was treated with DNase I to remove genomic DNA contamination. cDNA synthesis was accomplished using the iScript cDNA synthesis kit (Bio-Rad) with 100 ng of total RNA used per reaction. Real-time PCR was done using a CFX96 Touch[™] Real-Time PCR Detection System (Bio-Rad) and set up in hard-shell/clear 96-well PCR plates, in a final volume of 10 µl per reaction. The primers for gene amplification are listed in **Table S1** (primers 15–24). Reaction mixtures contained 2 µl of sample DNA (100 ng/µl), 5 µl of a master mix iQ[™] SYBR[®] Green Supermix (Bio-Rad) and 4 µl of nuclease-free water with primers at a final concentration of 300 nM. Activation of polymerase was performed at 95°C for 2 min. PCR cycling conditions included 39 cycles of denaturation at 95°C for 10 s, and annealing and extension at 60°C for 30 s (*GP72* gene) or 55 °C for 45 s (*TcVP1* gene). SYBR Green fluorescent emission was measured at the end of the elongation step. Subsequently, a melting curve program was applied with a continuous fluorescent measurement starting at 65°C and ending at 95°C (ramping rate of 0.1°C/s). In order to normalize the expression of the genes, we used primers for *P0* and *L3* housekeeping genes (**Table S1**, primers 15–18 used for *GP72* normalization) and *α-Tubulin* (**Table S1**, primers 21 and 22 used for *TcVP1* normalization) from *T. cruzi*. Relative quantification normalized to reference genes was performed according to the ΔC_T method and all the assays were performed at least three times.

Statistical Analysis

All values are expressed as means \pm s.d. Significant differences between treatments were compared using the tests indicated in the figure legends. Differences were considered statistically significant at $P < 0.05$, and n refers to the number of independent biological experiments performed. All statistical analyses were conducted using GraphPad Prism 5 (GraphPad Software, San Diego, CA).

REFERENCES

- Alibu, V. P., Storm, L., Haile, S., Clayton, C., and Horn, D. (2005). A doubly inducible system for RNA interference and rapid RNAi plasmid construction in *Trypanosoma brucei*. *Mol. Biochem. Parasitol.* 139, 75–82. doi: 10.1016/j.molbiopara.2004.10.002
- Bertolini, M. S., Chiurillo, M. A., Lander, N., Vercesi, A. E., and Docampo, R. (2019). MICU1 and MICU2 play an essential role in mitochondrial Ca²⁺ uptake, growth, and infectivity of the human pathogen *Trypanosoma cruzi*. *mBio* 10:e00348–e00319. doi: 10.1128/mBio.00348-19
- Bone, G. J., and Steinert, M. (1956). Isotopes incorporated in the nucleic acids of *Trypanosoma mega*. *Nature* 178, 308–309. doi: 10.1038/178308a0
- Burle-Caldas Gde, A., Grazielle-Silva, V., Laibida, L. A., Darocha, W. D., and Teixeira, S. M. (2015). Expanding the tool box for genetic

DATA AVAILABILITY STATEMENT

The raw data supporting the conclusions of this article will be made available by the authors, without undue reservation, to any qualified researcher.

AUTHOR CONTRIBUTIONS

NL, TC-B, and RD designed the experiments and analyzed the data. NL and TC-B conducted the experiments. RD wrote the majority of the manuscript with specific sections contributed by NL and TC-B. RD supervised the work and contributed to the analysis of the experiments.

FUNDING

Funding for his work was provided by the U.S. National Institutes of Health (Grant AI140421 to RD).

ACKNOWLEDGMENTS

We thank Thomas Seebeck for pMOTag4H plasmid, George A. M. Cross for monoclonal antibody WIC 29.26, Vasant Muralidharan for plasmids containing *glmS* and *M9* ribozymes and useful discussions, Drew Etheridge for BB2 monoclonal antibody, and Muthugapatti Kandasamy and the Biomedical Microscopy Core of the University of Georgia for the use of microscopes.

SUPPLEMENTARY MATERIAL

The Supplementary Material for this article can be found online at: <https://www.frontiersin.org/articles/10.3389/fcimb.2020.00068/full#supplementary-material>

Figure S1 | Effect of different glucosamine concentrations on growth of epimastigotes in SDM-79 medium. Values are means \pm s.d. of $n = 3$.

Table S1 | Primers used in this work.

Sequence S1 | *GP72-glmS* locus sequenced with primer 9 (**Table S1**).

Sequence S2 | *GP72-M9* locus sequenced with primer 9 (**Table S1**).

- manipulation of *Trypanosoma cruzi*. *Mol. Biochem. Parasitol.* 203, 25–33. doi: 10.1016/j.molbiopara.2015.10.004
- Chiurillo, M. A., Lander, N., Bertolini, M. S., Storey, M., Vercesi, A. E., and Docampo, R. (2017). Different roles of mitochondrial calcium uniporter complex subunits in growth and infectivity of *Trypanosoma cruzi*. *mBio* 8, e00574–e00517. doi: 10.1128/mBio.00574-17
- Chiurillo, M. A., Lander, N., Bertolini, M. S., Vercesi, A. E., and Docampo, R. (2019). Functional analysis and importance for host cell infection of the Ca²⁺-conducting subunits of the mitochondrial calcium uniporter of *Trypanosoma cruzi*. *Mol. Biol. Cell* 30, 1676–1690. doi: 10.1091/mbc.E19-03-0152
- Clayton, C. E. (1999). Genetic manipulation of kinetoplastida. *Parasitol. Today* 15, 372–378. doi: 10.1016/S0169-4758(99)01498-2
- Cooper, R., De Jesus, A. R., and Cross, G. A. (1993). Deletion of an immunodominant *Trypanosoma cruzi* surface glycoprotein disrupts

- flagellum-cell adhesion. *J. Cell Biol.* 122, 149–156. doi: 10.1083/jcb.122.1.149
- Costa, F. C., Francisco, A. F., Jayawardhana, S., Calderano, S. G., Lewis, M. D., Olmo, F., et al. (2018). Expanding the toolbox for *Trypanosoma cruzi*: a parasite line incorporating a bioluminescence-fluorescence dual reporter and streamlined CRISPR/Cas9 functionality for rapid *in vivo* localisation and phenotyping. *PLoS Negl. Trop. Dis.* 12:e0006388. doi: 10.1371/journal.pntd.0006388
- Cruz-Bustos, T., Potapenko, E., Storey, M., and Docampo, R. (2018a). An intracellular ammonium transporter is necessary for replication, differentiation, and resistance to starvation and osmotic stress in *Trypanosoma cruzi*. *mSphere* 3, e00377–e00317. doi: 10.1128/mSphere.00377-17
- Cruz-Bustos, T., Ramakrishnan, S., Cordeiro, C. D., Ahmed, M. A., and Docampo, R. (2018b). A riboswitch-based inducible gene expression system for *Trypanosoma brucei*. *J. Eukaryot. Microbiol.* 65, 412–421. doi: 10.1111/jeu.12493
- Darocha, W. D., Otsu, K., Teixeira, S. M., and Donelson, J. E. (2004). Tests of cytoplasmic RNA interference (RNAi) and construction of a tetracycline-inducible T7 promoter system in *Trypanosoma cruzi*. *Mol. Biochem. Parasitol.* 133, 175–186. doi: 10.1016/j.molbiopara.2003.10.005
- Docampo, R. (2011). Molecular parasitology in the 21st century. *Essays Biochem.* 51, 1–13. doi: 10.1042/bse0510001
- Docampo, R., Scott, D. A., Vercesi, A. E., and Moreno, S. N. (1995). Intracellular Ca^{2+} storage in acidocalcisomes of *Trypanosoma cruzi*. *Biochem. J.* 310 (Pt 3), 1005–1012. doi: 10.1042/bj3101005
- Estevez, A. M., Kempf, T., and Clayton, C. (2001). The exosome of *Trypanosoma brucei*. *EMBO J.* 20, 3831–3839. doi: 10.1093/emboj/20.14.3831
- Ganesan, S. M., Falla, A., Goldfless, S. J., Nasamu, A. S., and Niles, J. C. (2016). Synthetic RNA-protein modules integrated with native translation mechanisms to control gene expression in malaria parasites. *Nat. Commun.* 7:10727. doi: 10.1038/ncomms10727
- Hasne, M. P., Coppens, I., Soysa, R., and Ullman, B. (2010). A high-affinity putrescine-cadaverine transporter from *Trypanosoma cruzi*. *Mol. Microbiol.* 76, 78–91. doi: 10.1111/j.1365-2958.2010.07081.x
- Jimenez, V., and Docampo, R. (2015). TcPho91 is a contractile vacuole phosphate sodium symporter that regulates phosphate and polyphosphate metabolism in *Trypanosoma cruzi*. *Mol. Microbiol.* 97, 911–925. doi: 10.1111/mmi.13075
- Kangussu-Marcolino, M. M., Cunha, A. P., Avila, A. R., Herman, J. P., and Darocha, W. D. (2014). Conditional removal of selectable markers in *Trypanosoma cruzi* using a site-specific recombination tool: proof of concept. *Mol. Biochem. Parasitol.* 198, 71–74. doi: 10.1016/j.molbiopara.2015.01.001
- Kessler, D. A., Shi, P. A., Avicilla, S. T., and Shaz, B. H. (2013). Results of lookback for chagas disease since the inception of donor screening at New York blood center. *Transfusion* 53, 1083–1087. doi: 10.1111/j.1537-2995.2012.03856.x
- Lander, N., and Chiurillo, M. A. (2019). State-of-the-art CRISPR/Cas9 technology for genome editing in trypanosomatids. *J. Eukaryot. Microbiol.* 66, 981–991. doi: 10.1111/jeu.12747
- Lander, N., Chiurillo, M. A., Bertolini, M. S., Storey, M., Vercesi, A. E., and Docampo, R. (2018). Calcium-sensitive pyruvate dehydrogenase phosphatase is required for energy metabolism, growth, differentiation, and infectivity of *Trypanosoma cruzi*. *J. Biol. Chem.* 293, 17402–17417. doi: 10.1074/jbc.RA118.004498
- Lander, N., Chiurillo, M. A., and Docampo, R. (2016a). Genome editing by CRISPR/Cas9: a game change in the genetic manipulation of protists. *J. Eukaryot. Microbiol.* 63, 679–690. doi: 10.1111/jeu.12338
- Lander, N., Chiurillo, M. A., Storey, M., Vercesi, A. E., and Docampo, R. (2016b). CRISPR/Cas9-mediated endogenous C-terminal tagging of *Trypanosoma cruzi* genes reveals the acidocalcisome localization of the inositol 1,4,5-trisphosphate receptor. *J. Biol. Chem.* 291, 25505–25515. doi: 10.1074/jbc.M116.749655
- Lander, N., Chiurillo, M. A., Vercesi, A. E., and Docampo, R. (2017). Endogenous C-terminal tagging by CRISPR/Cas9 in *Trypanosoma cruzi*. *Bio. Protoc.* 7, 10:21769/BioProtoc 2299. doi: 10.21769/BioProtoc.2299
- Lander, N., Li, Z. H., Niyogi, S., and Docampo, R. (2015). CRISPR/Cas9-induced disruption of paraflagellar rod protein 1 and 2 genes in *Trypanosoma cruzi* reveals their role in flagellar attachment. *mBio* 6, e01012–e01015. doi: 10.1128/mBio.01012-15
- Lemerrier, G., Dutoya, S., Luo, S., Ruiz, F. A., Rodrigues, C. O., Baltz, T., et al. (2002). A vacuolar-type H^{+} -pyrophosphatase governs maintenance of functional acidocalcisomes and growth of the insect and mammalian forms of *Trypanosoma brucei*. *J. Biol. Chem.* 277, 37369–37376. doi: 10.1074/jbc.M204744200
- Li, C. H., Irmer, H., Gudjonsdottir-Planck, D., Freese, S., Salm, H., Haile, S., et al. (2006). Roles of a *Trypanosoma brucei* 5'->3' exoribonuclease homolog in mRNA degradation. *RNA* 12, 2171–2186. doi: 10.1261/rna.291506
- Ma, Y., Weiss, L. M., and Huang, H. (2015). Inducible suicide vector systems for *Trypanosoma cruzi*. *Microbes. Infect.* 17, 440–450. doi: 10.1016/j.micinf.2015.04.003
- Meaux, S., and Van Hoof, A. (2006). Yeast transcripts cleaved by an internal ribozyme provide new insight into the role of the cap and poly(A) tail in translation and mRNA decay. *RNA* 12, 1323–1337. doi: 10.1261/rna.46306
- Naderer, T., Heng, J., and Mcconville, M. J. (2010). Evidence that intracellular stages of *Leishmania major* utilize amino sugars as a major carbon source. *PLoS Pathog.* 6:e1001245. doi: 10.1371/journal.ppat.1001245
- Oberholzer, M., Morand, S., Kunz, S., and Seebeck, T. (2006). A vector series for rapid PCR-mediated C-terminal in situ tagging of *Trypanosoma brucei* genes. *Mol. Biochem. Parasitol.* 145, 117–120. doi: 10.1016/j.molbiopara.2005.09.002
- Peng, D., Kurup, S. P., Yao, P. Y., Minning, T. A., and Tarleton, R. L. (2014). CRISPR-Cas9-mediated single-gene and gene family disruption in *Trypanosoma cruzi*. *mBio* 6, e02097–e02014. doi: 10.1128/mBio.02097-14
- Prommana, P., Uthaiyibull, C., Wongsombat, C., Kamchonwongpaisan, S., Yuthavong, Y., Knuepfer, E., et al. (2013). Inducible knockdown of *Plasmodium* gene expression using the glmS ribozyme. *PLoS ONE* 8:e73783. doi: 10.1371/journal.pone.0073783
- Rassi, A. Jr., Rassi, A., and Little, W. C. (2000). Chagas' heart disease. *Clin. Cardiol.* 23, 883–889. doi: 10.1002/clc.4960231205
- Romagnoli, B. A., Picchi, G. F. A., Hiraiwa, P. M., Borges, B. S., Alves, L. R., et al. (2018). Improvements in the CRISPR/Cas9 system for high efficiency gene disruption in *Trypanosoma cruzi*. *Acta. Trop.* 178, 190–195. doi: 10.1016/j.actatropica.2017.11.013
- Scott, D. A., De Souza, W., Benchimol, M., Zhong, L., Lu, H. G., Moreno, S. N., et al. (1998). Presence of a plant-like proton-pumping pyrophosphatase in acidocalcisomes of *Trypanosoma cruzi*. *J. Biol. Chem.* 273, 22151–22158. doi: 10.1074/jbc.273.34.22151
- Seufferheld, M., Lea, C. R., Vieira, M., Oldfield, E., and Docampo, R. (2004). The H^{+} -pyrophosphatase of *Rhodospirillum rubrum* is predominantly located in polyphosphate-rich acidocalcisomes. *J. Biol. Chem.* 279, 51193–51202. doi: 10.1074/jbc.M406099200
- Soares Medeiros, L. C., South, L., Peng, D., Bustamante, J. M., Wang, W., Bunkofski, M., et al. (2017). Rapid, selection-free, high-efficiency genome editing in protozoan parasites using CRISPR-Cas9 ribonucleoproteins. *mBio* 8, e01788–e01717. doi: 10.1128/mBio.01788-17
- Takagi, Y., Akutsu, Y., Doi, M., and Furukawa, K. (2019). Utilization of proliferable extracellular amastigotes for transient gene expression, drug sensitivity assay, and CRISPR/Cas9-mediated gene knockout in *Trypanosoma cruzi*. *PLoS Negl. Trop. Dis.* 13:e0007088. doi: 10.1371/journal.pntd.0007088
- Urbina, J. A., and Docampo, R. (2003). Specific chemotherapy of chagas disease: controversies and advances. *Trends Parasitol.* 19, 495–501. doi: 10.1016/j.pt.2003.09.001
- Watson, P. Y., and Fedor, M. J. (2011). The glmS riboswitch integrates signals from activating and inhibitory metabolites *in vivo*. *Nat. Struct. Mol. Biol.* 18, 359–363. doi: 10.1038/nsmb.1989
- Winkler, W. C., Nahvi, A., Roth, A., Collins, J. A., and Breaker, R. R. (2004). Control of gene expression by a natural metabolite-responsive ribozyme. *Nature* 428, 281–286. doi: 10.1038/nature02362

Conflict of Interest: The authors declare that the research was conducted in the absence of any commercial or financial relationships that could be construed as a potential conflict of interest.

Copyright © 2020 Lander, Cruz-Bustos and Docampo. This is an open-access article distributed under the terms of the Creative Commons Attribution License (CC BY). The use, distribution or reproduction in other forums is permitted, provided the original author(s) and the copyright owner(s) are credited and that the original publication in this journal is cited, in accordance with accepted academic practice. No use, distribution or reproduction is permitted which does not comply with these terms.



***Trypanosoma cruzi*-Infected Human Macrophages Shed Proinflammatory Extracellular Vesicles That Enhance Host-Cell Invasion via Toll-Like Receptor 2**

André Cronemberger-Andrade¹, Patrícia Xander¹, Rodrigo Pedro Soares², Natália Lima Pessoa², Marco Antônio Campos², Cameron C. Ellis³, Brian Grajeda³, Yifat Ofir-Birin⁴, Igor Correia Almeida³, Neta Regev-Rudzki⁴ and Ana Claudia Torrecilhas^{1*}

OPEN ACCESS

Edited by:

Noelia Lander,
University of Georgia, United States

Reviewed by:

Carlos A. Buscaglia,
National Council for Scientific and
Technical Research
(CONICET), Argentina
Celio Geraldo Freire-de-Lima,
Federal University of Rio de
Janeiro, Brazil

*Correspondence:

Ana Claudia Torrecilhas
ana.torrecilhas@unifesp.br

Specialty section:

This article was submitted to
Parasite and Host,
a section of the journal
Frontiers in Cellular and Infection
Microbiology

Received: 06 November 2019

Accepted: 26 February 2020

Published: 20 March 2020

Citation:

Cronemberger-Andrade A, Xander P, Soares RP, Pessoa NL, Campos MA, Ellis CC, Grajeda B, Ofir-Birin Y, Almeida IC, Regev-Rudzki N and Torrecilhas AC (2020) *Trypanosoma cruzi*-Infected Human Macrophages Shed Proinflammatory Extracellular Vesicles That Enhance Host-Cell Invasion via Toll-Like Receptor 2. *Front. Cell. Infect. Microbiol.* 10:99. doi: 10.3389/fcimb.2020.00099

¹ Departamento de Ciências Farmacêuticas, Universidade Federal de São Paulo (UNIFESP), São Paulo, Brazil, ² Instituto René Rachou/FIOCRUZ – MG, Belo Horizonte, Brazil, ³ Border Biomedical Research Center, Department of Biological Sciences, University of Texas at El Paso (UTEP), El Paso, TX, United States, ⁴ Department of Biomolecular Sciences, Weizmann Institute of Science, Rehovot, Israel

Extracellular vesicles (EVs) shed by trypomastigote forms of *Trypanosoma cruzi* have the ability to interact with host tissues, increase invasion, and modulate the host innate response. In this study, EVs shed from *T. cruzi* or *T. cruzi*-infected macrophages were investigated as immunomodulatory agents during the initial steps of infection. Initially, by scanning electron microscopy and nanoparticle tracking analysis, we determined that *T. cruzi*-infected macrophages release higher numbers of EVs (50–300 nm) as compared to non-infected cells. Using Toll-like-receptor 2 (TLR2)-transfected CHO cells, we observed that pre-incubation of these host cells with parasite-derived EVs led to an increase in the percentage of infected cells. In addition, EVs from parasite or *T. cruzi*-infected macrophages or not were able to elicit translocation of NF- κ B by interacting with TLR2, and as a consequence, to alter the EVs the gene expression of proinflammatory cytokines (TNF- α , IL-6, and IL-1 β), and STAT-1 and STAT-3 signaling pathways. By proteomic analysis, we observed highly significant changes in the protein composition between non-infected and infected host cell-derived EVs. Thus, we observed the potential of EVs derived from *T. cruzi* during infection to maintain the inflammatory response in the host.

Keywords: *Trypanosoma cruzi*, toll-like receptor 2, inflammation, extracellular vesicles, macrophage

INTRODUCTION

Research interest in extracellular vesicles (EVs) and their involvement in cell-cell, cell-pathogen (parasites, viruses, bacteria, and fungi) or pathogen-pathogen communication and modulation processes in infectious and inflammatory diseases has continuously grown in recent years (Campos et al., 2010). The study of EVs has mainly focused on the types of membrane vesicles secreted into the extracellular compartment isolated from different cells, tissues, and biofluids in healthy and pathological conditions. EVs may be divided into exosomes, microvesicles, and apoptotic bodies (Théry et al., 2018; Mathieu et al., 2019; Witwer and Théry, 2019). These types of EVs have

different origins, markers, and sizes (Théry et al., 2002; Tkach and Théry, 2016; van Niel et al., 2018; Mathieu et al., 2019; Witwer and Théry, 2019). EVs are heterogeneous membranous particles from 20 nm to 5 μ m, differing in their biogenesis, molecular composition, biodistribution, and function (Campos et al., 2010; Lässer et al., 2011; Street et al., 2012; Madison et al., 2014). EVs are secreted by either prokaryotic or eukaryotic cells, thus extending their phenotype (Campos et al., 2010; Torrecilhas et al., 2012).

EVs from parasitic protozoa have been demonstrated as important virulence factors (Gonçalves et al., 1991; Trocoli Torrecilhas et al., 2009; Torrecilhas et al., 2012; Marcilla et al., 2014; Nogueira et al., 2015). They function as cell-to-cell effectors in the host-parasite interaction and manipulation of the host immune system (Aline et al., 2004; Bhatnagar et al., 2007; Pope and Lässer, 2013; Regev-Rudzki et al., 2013; Marcilla et al., 2014; Coakley et al., 2015; Ribeiro et al., 2018). EVs isolated from parasitic protozoa contain a wide variety of molecules, including proteins, glycoconjugates, lipids, RNAs, non-transcribed RNAs, and microRNAs (Torrecilhas et al., 2012). In infection-derived inflammatory processes, EVs can induce release of cytokines and nitric oxide. EVs may promote an inflammatory/immunosuppressive response in the host environment, thus affecting the subsequent immunopathological events, resulting in pathogen escape and invasion of the host cells (Silverman and Reiner, 2011; Nogueira et al., 2015). In infective host cell-derived *T. cruzi* trypomastigotes, α -galactosyl (α -Gal)-enriched EVs strongly trigger proinflammatory responses in murine macrophages via Toll-like receptor (TLR2)-dependent pathway, and the proteomic analysis of these EVs revealed the presence of several members of the TS/gp85 superfamily (Nogueira et al., 2015; Ribeiro et al., 2018). In *Leishmania* spp., it has been shown that promastigote-derived EVs contain virulence factors such as GP63 and lipophosphoglycan (LPG), and several molecules involved in the pathogenesis of *Leishmania* (Silverman et al., 2010; Atayde et al., 2015; Barbosa et al., 2018), suggesting that these EVs can contribute in the leishmaniasis infection and disease progression. Moreover, EVs isolated from *Plasmodium*-infected red blood cells (iRBC) transfer genetic material to the host cell and induce parasite gametocytogenesis, demonstrating a mechanism of interaction and communication with host cells as well as between parasites. In malaria, EVs can also mediate cellular communication processes, delivering virulence factors in the circulation and inflammatory infiltrate (Regev-Rudzki et al., 2013). It is known that inflammatory responses occur during *T. cruzi* infection and that this can be reproduced by the parasite EVs (Nogueira et al., 2015). Likewise, Dr Ramirez's group showed that metacyclic-trypomastigotes induce the release of TGF- β coated plasma membrane vesicles from blood macrophages and lymphocytes, which could further increase parasite infectivity (Cestari et al., 2012; Wyllie and Ramirez, 2017; Gavinho et al., 2018; Rossi et al., 2019). However, it is unknown whether EVs released by *T. cruzi*-infected macrophages or EVs isolated from parasite modulate host inflammatory responses and cell invasion.

The invasion of host cells is a key process in *T. cruzi* infection and it has been found that parasite surface molecules play an important role for parasite attachment and entry

in the parasitophorous vacuole (Andrews, 2002). Cell-derived trypomastigotes induce lysosome mobilization, cytoskeleton rearrangements, membrane repair and elevation of Ca^{2+} and cAMP concentrations within the host cell (Tardieux et al., 1992, 1994; Burleigh and Andrews, 1998; Andrews, 2002). In fact, these processes are modulated by parasite EVs that were found to contain the major surface glycoconjugates of the parasite (Ribeiro et al., 2018).

Therefore, in this work, we evaluated whether EV shed by *T. cruzi* infected macrophage modulate inflammatory responses and if EVs from cell-derived trypomastigotes could also modify the cell invasion and the signaling mechanisms involved in this process.

MATERIALS AND METHODS

Ethics Statement

All experimental procedures used in this work were approved by the Ethics Committee on Animal Use (CEUA) of the Federal University of São Paulo, protocol 1073090614.

Cell Lines and Parasite Infection

Tissue culture-derived trypomastigotes (TCT) of the *T. cruzi* Y strain were collected from the culture supernatants after 5 days after infection of LLCMK₂ epithelial cells (monkey kidney epithelial cell line, ATCC® CCL-7™, VA, USA). Cells were maintained in low-glucose DMEM supplemented with 10% fetal bovine serum (FBS) (Invitrogen, CA, USA) at 37°C in a humidified 5% CO₂ atmosphere. THP-1 (human peripheral blood monocyte cell line, ATCC® TIB-202™, VA, USA) cells were cultured in RPMI-1640 medium supplemented with 10% FBS and maintained at 37°C in a humidified 5% CO₂ atmosphere. Cells were tested for *Mycoplasma* contamination by using the polymerase chain reaction (PCR) methodology (Uphoff and Drexler, 2002). The THP-1 monocytes were induced to differentiate into macrophages by the addition of phorbol myristate acetate (50 ng/mL) (Calbiochem, CA, USA) for 24 h in serum-free RPMI 1640. To determine the number of infected cells and the number of intracellular parasites, cells were cultured on circular glass coverslips and subsequently stained with Giemsa.

Isolation and Characterization of EVs

EVs from trypomastigotes (EV-TY) were obtained by incubation of parasites for 2 h in DMEM containing 2% glucose at 37°C and 5% CO₂ and purified by size-exclusion chromatography (SEC), as previously described (Ribeiro et al., 2018). To obtain EVs from THP-1 infected and non-infected macrophages (respectively EV-THP-1inf and EV-THP1) were incubated with *T. cruzi* trypomastigotes at a 1:10 ratio (1 mL) for 4 h at 37°C/5% CO₂ in RPMI 1640 containing 10% ultracentrifuged FBS to remove serum EVs. After infection, the THP-1 macrophages were washed three times with PBS, and then maintained in the same fresh medium for the production of EVs. Controls included THP-1 cells without *T. cruzi* infection. EVs were then recovered at the indicated times by differential ultracentrifugation of culture supernatants. Briefly, the supernatants were submitted to 10 min

at $500 \times g$, followed by 10 min at $3,000 \times g$ and 15 min at $8,000 \times g$ to remove cells and cellular debris. EVs were then pelleted at $100,000 \times g$ for 1 h using a T-890 fixed angle rotor (Thermo Fisher Scientific, MA, USA) as previously described in MISEV guideline (Théry et al., 2018).

The obtained EVs were characterized by NTA analysis to determine concentration and size using NanoSight NS300 (Malvern Instruments, Worcestershire, UK) equipped with a 405 nm laser and coupled to a CCD camera. Data were analyzed using NTA software (version 2.3). Each sample diluted (1:10) in PBS was analyzed in triplicate; and loaded into the instrument for 30 s at 20 frames per second with the camera level set to 14.

Scanning Electron Microscopy (SEM)

THP-1 cells infected or not with *T. cruzi*, and THP-1 cells treated with EV-TY were fixed in a 2.5% glutaraldehyde solution as reported elsewhere (Nogueira et al., 2015). The cells were post fixed with osmium tetroxide, treated with tannic acid, and dehydrated with ethanol. Samples were observed in a Field Emission FEI Quanta 250 FEG scanning electron microscope (FEI, OR, USA).

Immunoblotting

EVs samples containing 10 μ g of protein, quantified by Micro BCA Assay kit (Thermo Fisher Scientific, MA, USA), were resolved by 12% SDS-PAGE and transferred to nitrocellulose membranes using standard procedures. The presence of exosome proteins and parasite surface proteins was evaluated by incubating membranes with primary antibodies against CD63, CD9, MHC II (Thermo Fisher Scientific, MA, USA) and the serum of a rabbit immunized with the extract of *T. cruzi* TCT membranes (Schenkman et al., 1991). Detection was achieved using horseradish peroxidase-conjugated anti-mouse or anti-rabbit (KPL Antibodies Seracare, MA, USA) secondary Abs and visualized with Pierce ECL Western Blotting Substrate (Thermo Fisher Scientific, MA, USA).

CHO Cell Lines

The CHO reporter cell lines (CHO/CD14, CHO/CD14/TLR-2, and CHO/CD14/TLR-4) were generated as described (Lien et al., 1999). These reporter cell lines contain a human CD25 gene reporter under the control of the E-selectin promoter, which contains an NF- κ B-binding site (Delude et al., 1998; Lien et al., 1999 and Campos et al., 2001). All CHO reporter cell lines were grown in Ham's F-12 medium containing 10% FBS, 10 μ g/ml ciprofloxacin, and 400 units/ml hygromycin B. Cells were plated at a concentration of 10^5 /well in 24-well tissue-culture dishes. Cells were incubated with EV-THP-1, EV-THP-1 infected (EV-THP-1 inf) and EV-TY. Medium alone, 100 ng/ml LPS (from *Escherichia coli* serotype 055: B5; Sigma-Aldrich, MI, USA), and UV-killed *Staphylococcus aureus* at a ratio of *S. aureus*/cell of 500:1 (American Type Culture Collection 12.692), were used as controls. After 24 h of stimulation, cells were stained with PE-labeled anti-CD25 (mouse MAb to human CD25, PE conjugate; Caltag Laboratories, CA, USA). The cells were examined by flow cytometry (BD Biosciences, NJ, USA), and analyses were

performed using Cell Quest software (BD Biosciences, NJ, USA) (Campos et al., 2001).

Infection Assays

TLR2- or TLR4-transfected CHO/CD14 cells were grown on 13 mm diameter glass coverslips in a 24-well dish and washed twice with DMEM/F12 medium (with antibiotics). Cells were incubated with culture supernatant or EV-TY (10^5 and 10^6 particles/well) for 30 min, at 37°C , in RPMI-10% FBS. These cells were infected with TCTs (1:10, host cell: parasite ratio), for 1 h at 37°C , and then washed twice with RPMI without FBS. Non-adherent parasites were removed by addition of Lymphoprep (Axis-Shield, Norton, MA) to the cell layers, followed by two washes with PBS. The cells were incubated with RPMI-10% FBS for 18 h, at 37°C , or immediately fixed with methanol and stained with Hoechst fluorescent dye (Molecular Probes, Invitrogen Co., Carlsbad, CA). All experiments were performed in triplicate, and 24 photos of each replicate were made using a digital video-imaging fluorescent inverted microscope (Nikon), enabling the counting of infected and non-infected cells.

Gene Expression

To evaluate the gene expression, quantitative reverse transcriptase polymerase chain reaction (qRT-PCR) was used in THP-1 cells untreated as control, or THP-1 incubated with EV-THP-1 inf, EV-TY (10^8 particles/mL), or infected with trypomastigotes (TY). Total RNA was obtained from macrophages by using TRIzol reagent (Life Technologies, CA, USA). RNA samples were subjected to DNase treatment and cDNA synthesis with the RevertAid First Strand cDNA Synthesis kit (Thermo Fisher Scientific, MA, USA). RNA samples were quantified by UV absorption in a spectrophotometer (Nanodrop 2000c, Thermo Fisher) followed by electrophoresis in 1.5% agarose gels to assess RNA integrity. RNA samples with high quality and integrity were subjected to DNase treatment (RQ1 RNase-free DNase; Promega, Madison, WI, United States) and cDNA synthesis with the RevertAid First Strand cDNA Synthesis kit (Thermo Fisher Scientific, MA, USA). Specific primers for TLR2, TLR4, IL1 β , IL6, TNF- α , STAT1, and STAT3 genes were used to analyze gene expression using RT-qPCR; all sequences were from PrimerBank (<https://pga.mgh.harvard.edu/primerbank/>) (Supplementary Table 1). The expression levels were normalized to those of the GAPDH and Actin-Beta (ACTB) reference genes using the $2^{-\Delta\Delta\text{Ct}}$ cycle threshold method (Schmittgen and Livak, 2008). Differences in the relative expression levels of target genes were determined by comparison between noninfected cells (as reference samples) and the cells infected or treated with EVs. The gene expression from the reference sample was adjusted to be equal to 1.00. All qRT-PCR procedures were developed following the MIQE guidelines (Bustin et al., 2009).

LC-MS/MS and Bioinformatic Analysis

EVs (~ 200 μ g of protein) from uninfected and infected macrophages (EV-THP-1 and EV-THP-1inf) were concentrated in a Speedvac. For LC-MS/MS, the filter-aided sample preparation (FASP) method was used, following the

manufacturer's protocol (Expedeon, San Diego, CA). The samples were reduced by adding 10 mM DTT for 30 min at room temperature (RT) and centrifuging in a spin filter at $14,000 \times g$ for 15 min at rt. After washing twice with 8 M urea in 50 mM Tris-HCl buffer, samples were washed again $2 \times$ with the urea/Tris-HCl buffer and $3 \times$ with 50 mM ammonium bicarbonate. Then, samples were digested with trypsin (Sigma-Aldrich, St. Louis, MO) was performed, as described by Ribeiro et al. (2018). Peptides were eluted from the filter using 0.1% formic acid and subjected to high-resolution LC-MS/MS analysis in a QE Plus Orbitrap (Thermo Fisher Scientific) equipped with a Nanospray Flex Ion Source (Thermo Fisher Scientific). Using a Dionex UltiMate 3000 RSLCnano UHPLC system (Thermo Fisher Scientific), peptides were separated with a PicoFrit column (75- μ m ID \times OD 360 μ m, 25-cm length, New Objective, Woburn, MA) packed in-house with reversed-phase Aqua C18 porous silica (5 μ m, 125 Å, Phenomenex). The column was equilibrated before sample injection at a flow rate of 0.5 μ L/min with 95% solvent A (100% H₂O, 0.1% formic acid) and 5% solvent B (90% acetonitrile, 0.1% formic acid). Samples were then injected onto the C18 column, and the same equilibration phase was run for 10 min. Elution of the peptides was performed using a linear gradient of solvent B up to 35% for 85 min, followed by a 5-min increase to 95%, where the plateau was maintained for 9 min. The column was then re-equilibrated with 5% solvent B for 10 min before injection of the next sample. An automated 2-h run was programmed into the Xcalibur software (Thermo Fisher Scientific), and each sample was analyzed in technical duplicates. Full scan spectra were collected from the 400–1,600 m/z range. Peptides were not excluded based on charge state, and 1 microscan for both full and MS/MS scans were acquired.

The spectra were searched using Proteome Discoverer (PD) 2.1.1.21 (Thermo Fisher Scientific) and filtered via Percolator with an estimated false-discovery rate (FDR) of 1 against sequences from *T. cruzi*, human, bovine, human keratin, and porcine trypsin. Parameters for the database search were as follows: 2 and 1 Da for peptide and fragment mass tolerance, respectively, cysteine carbamidomethylation and methionine oxidation as fixed and variable modifications, respectively. The dataset was further processed through Scaffold Q + 4.8.2 (Proteome Software, Portland, OR), merged, and the probability of their peptide assignments and protein identifications was assessed. Files were exported from Scaffold 4.8.2 for further analysis in Scaffold PerSPECTives (Proteome Software). Only peptides with $\geq 95\%$ probability were accepted. The criteria for human protein identification included detection of at least two uniquely identified peptides and a probability score of $\geq 99\%$. The results were further filtered with the following peptide thresholds: Fisher's exact test (p -value) ≤ 0.001 ; fold change $\geq 50\%$ and $\leq 50\%$. Gene ontology (GO) annotation was carried out using FunRich (version 3.1.3; <http://www.funrich.org/>) with the NCBI database (downloaded on 28 March 2019).

Statistics

All statistical tests were performed using GraphPad Prism version 6 (GraphPad Software, CA, USA). The Mann-Whitney U -test

was used to determine differences between two groups. Analysis of variance (ANOVA) followed by Tukey's post-test was carried out to compare multiple groups. The differences were considered significant when p was < 0.05 .

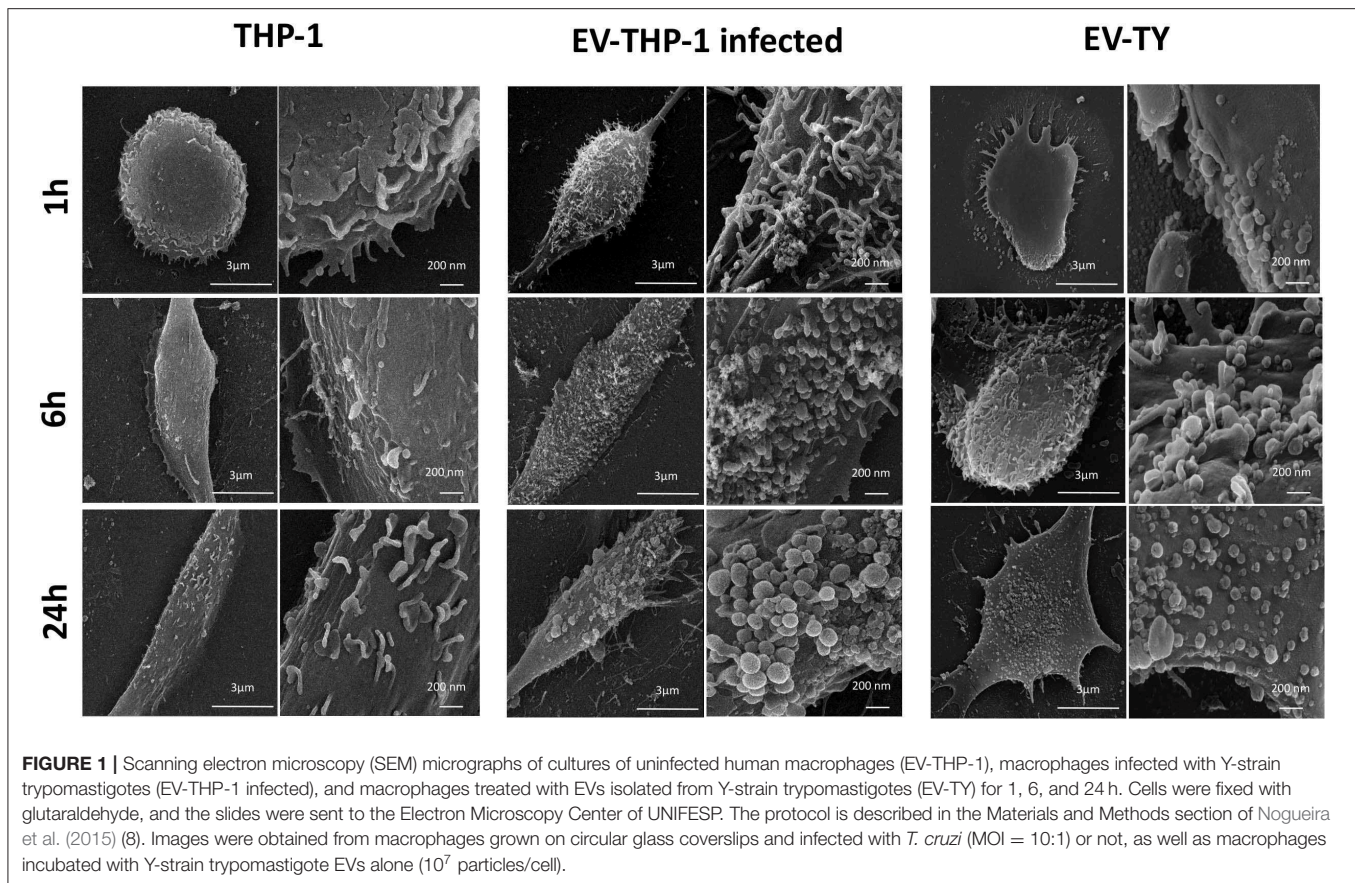
RESULTS

Increased Numbers of EVs Are Released From Macrophages Infected With *T. cruzi*

Scanning electron microscopy (SEM) micrographs of THP-1-derived macrophages uninfected (EV-THP-1), infected (EV-THP-1 inf), or only treated with EVs from trypomastigotes (EV-TY) showed the presence of round-shaped vesicles with the expected size for exosomes (50–100 nm) and ectosomes (100–200 nm) on the surface of their plasma membrane (Figure 1). Compared to uninfected macrophages and those incubated with EV-TY, infected macrophages released a larger number of vesicles. EVs were isolated from the supernatants of THP-1 macrophages through a series of ultracentrifugation steps. The NTA showed a size distribution of 50–200 nm for all EVs (Supplementary Figure 1). The concentration of vesicles was also measured in the same experiment, revealing an increase in vesicle release by infected THP-1 macrophages (EV-THP-inf) (Figure 2A). In the immunoblotting analysis, the exosomal marker proteins CD63 and CD9 and the surface membrane protein MHC II were detected in EV-THP-1 and EV-THP-1 inf samples (Figure 2B). The presence of parasite surface proteins was only found in the EV-TY group (Figure 2B). The increase in EVs released from infected macrophages is related to presence of parasite from 24 to 72 h. (Figure 3A). However, the EVs release did not appear to increase when the number of parasites augment in infected cells (Figure 3B). After that, cells start to lyse and new trypomastigotes are released in the extracellular milieu.

The Interaction of EVs With TLR2 Is Critical for the Induction of NF- κ B Activation and Increase the Susceptibility of Target Cells to *T. cruzi* Infection

Next, we evaluated the importance of the interaction of EVs from *T. cruzi* trypomastigotes with TLRs for the interaction and internalization of the parasite. The CHO reporter cell line contained an inducible NF- κ B-dependent promoter driving the surface expression of CD25 (Campos et al., 2001). CHO cells were incubated with different concentrations of (EV-TY) and with EV-THP-1inf or EV-THP-1. The expression of CD25, which indicates activation of NF- κ B, was measured by flow cytometry. These EVs did not increase the induction of CD25 expression by CHO/CD14 or CHO/CD14/TLR4 cells (Figure 4). Previous studies using wild-type, TLR2- or TLR4-knockout murine macrophages from C57BL/6 mice (WT, TLR2^{-/-}, or TLR4^{-/-} C57BL/6) showed that TLR2 but not in TLR4 was required for production of nitric oxide (NO) or TNF- α following stimulation with EV-TY and activate MAPKs (ERK 1/2, p38 and JNK) (Nogueira et al., 2015). The data presented in Figure 4



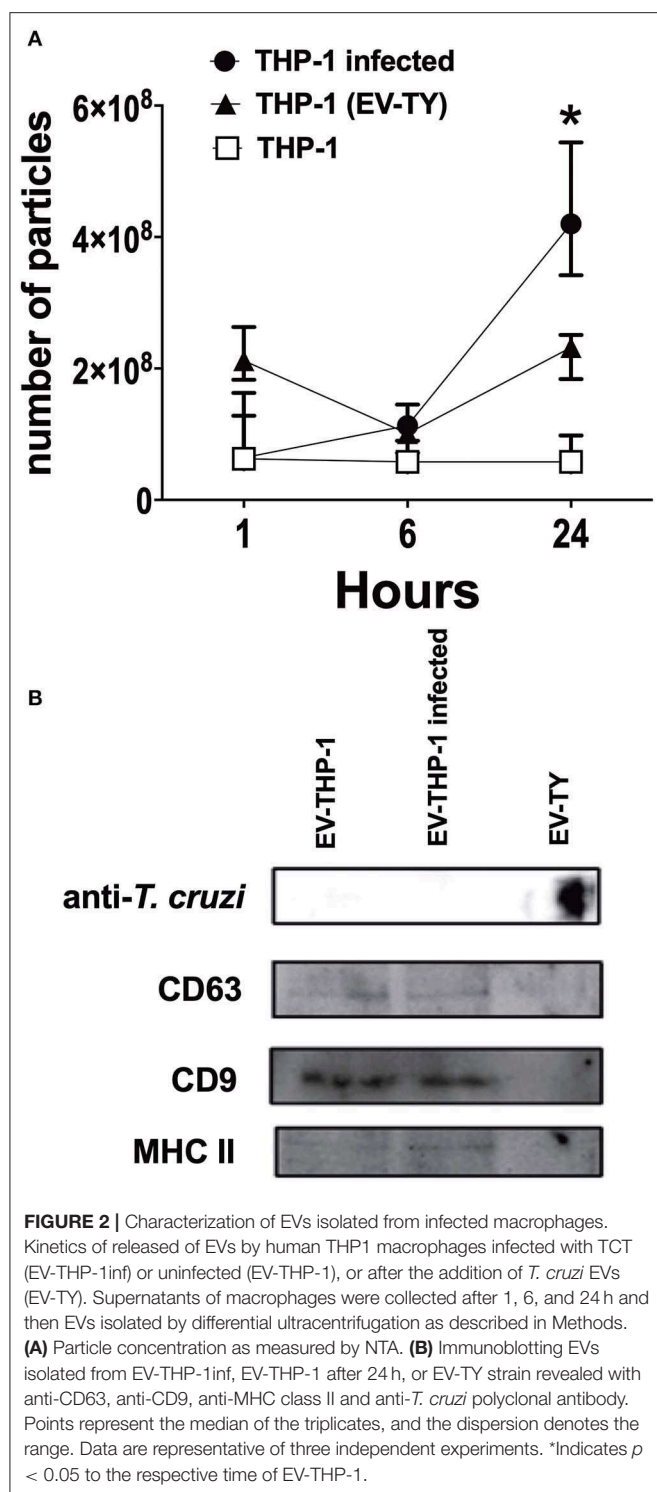
confirmed these previous results showing that the expression of CD25 through the activation of NF- κ B was induced in CHO/CD14/TLR2, but not CHO/CD14/TLR4, exposed to EV-TY. Importantly, EV-THP-1 and EV-THP-1inf were also found to quantitatively promote the expression of CD25 in CHO/CD14/TLR2 cells, but not TLR4 (**Figure 4**), indicating that both EVs derived from *T. cruzi* (EV-TY) and macrophages interact with TLR2, but not TLR4, activating NF- κ B. This result also suggested that induction by macrophage EVs was not due to the presence of parasite molecules, as when we used the same number of particles of non-infected macrophages, the induction was similar. The presence of tGPI-mucins and glycoinositolphospholipids (GIPLs) in the EV-TY was likely responsible for the induction of potent inflammatory responses in macrophages (Almeida et al., 2000; Trocoli Torrecilhas et al., 2009).

The participation of TLR2 in the host-cell infection by *T. cruzi* was then investigated. To test this hypothesis, infection experiments were performed in CHO/CD14 cells, transfected or not with TLR2 or TLR4. Upon prior exposure to culture supernatants of trypanomastigotes or EVs, cells transfected with TLR2, but not TLR4- or non-transfected cells were increase the susceptibility of target cells to *T. cruzi* infection. A remarkable (up to 6–7-fold) increase in percentage of infected cells was observed in TLR2-transfected CHO/CD14 cells exposed either to total shedding or EV-TY (**Figure 5**).

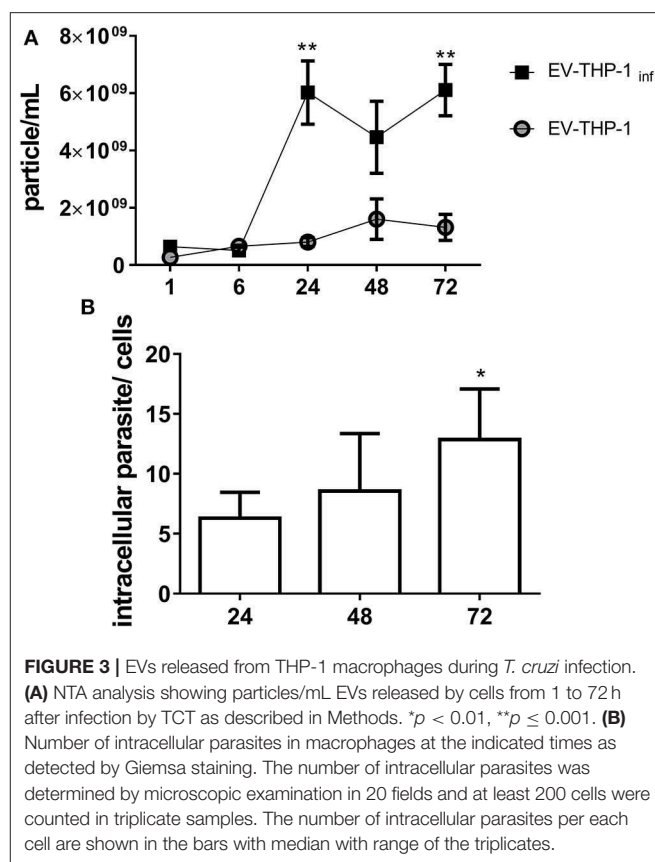
EVs Induce the Differential Expression of TLR2, TLR4, IL-1 β , IL-6, TNF- α and STAT1/STAT3

TLRs are involved in the recognition of *T. cruzi* following the activation of host cells to produce TNF- α , IL-12, and NO (Campos et al., 2004; Koga et al., 2006). Macrophages showed differences in TLR gene expression upon stimulation with EVs and *T. cruzi* infection. We analyzed the gene expression of TLR2, TLR4 by RT-qPCR in macrophages untreated and treated with EV-TY, EV-THP-1control, and EV-THP-1 inf. The gene expression analysis in macrophages treated with EV-THP-1inf and EV-TY revealed alterations in TLR2 and TLR4 (**Figure 6**).

TLR2 expression is essential for proinflammatory cytokine production (Campos and Gazzinelli, 2004). RT-qPCR analysis was performed to assess the changes in gene expression of cytokines and transcription factors. Macrophages, therefore, were incubated with EVs (EV-THP-1 control, EV-THP-1 inf and EV-TY) and also infected with *T. cruzi*. Evaluation of the cytokine gene expression profile revealed an increase in IL-1 β levels after 6 h in both *T. cruzi*-infected cells and in those exposed to EV-THP-1inf (**Figure 6**). There was also an increase in the transcript levels of IL-1 β after 1 h of *T. cruzi* infection. After 24 h of *T. cruzi* infection or stimulation with EV-THP-1 inf, no change in IL-1 β transcript levels was observed, whereas a marked reduction was seen in cells that were treated with EV-TY or EV-THP-1.



After 1 and 6 h of *T. cruzi* infection, the cells showed elevated transcript levels of IL-6. The same result was observed after 1 and 6 h of treatment with EV-TY or EV-THP-1 inf. However, 24 h after the other treatments, there was a reduction in IL-6 gene expression, except for *T. cruzi* infection. In the TNF- α gene expression analysis, elevation of the transcript level was observed



after 1 and 6 h of treatment with EV-THP-1inf and after 6 h of treatment with EV-THP-1. Only *T. cruzi* infection induced the gene expression of TNF- α at 24 h.

Signal transduction through cytokine receptor-binding occurs via the JAK/STAT pathway signaling. We observed the gene expression of STAT1 and STAT3 in the macrophages stimulated with the different EVs. STAT1 and STAT3 gene expression increased only in response to *T. cruzi* infection (Figure 7). Stimulation with the different EVs reduced the gene expression of STAT3 at 1 and 6 h (Figure 7).

EVs Released by Infected Macrophages Have Distinct Contents and Parasite Proteins

We performed mass spectrometry-based proteomic analysis (LC-MS/MS) to determine the content of the EVs purified from uninfected (EV-THP-1) and infected macrophages (EV-THP-1 inf). A total of 123 proteins were found in THP-1-EVs and 89 were found in EV-THP-1 inf, from a total of 154 proteins in both samples (Figure 8A). Using FunRich (version 3.1.3), we compared the list of identified proteins to previously published EV data in the Exocarta database (www.exocarta.org) and found that the majority of the proteins had been previously observed to be present in EVs from different sources (Figure 8B). *T. cruzi*-infected host-cell derived EVs carry proteins from the parasite, as previously described (Ramirez

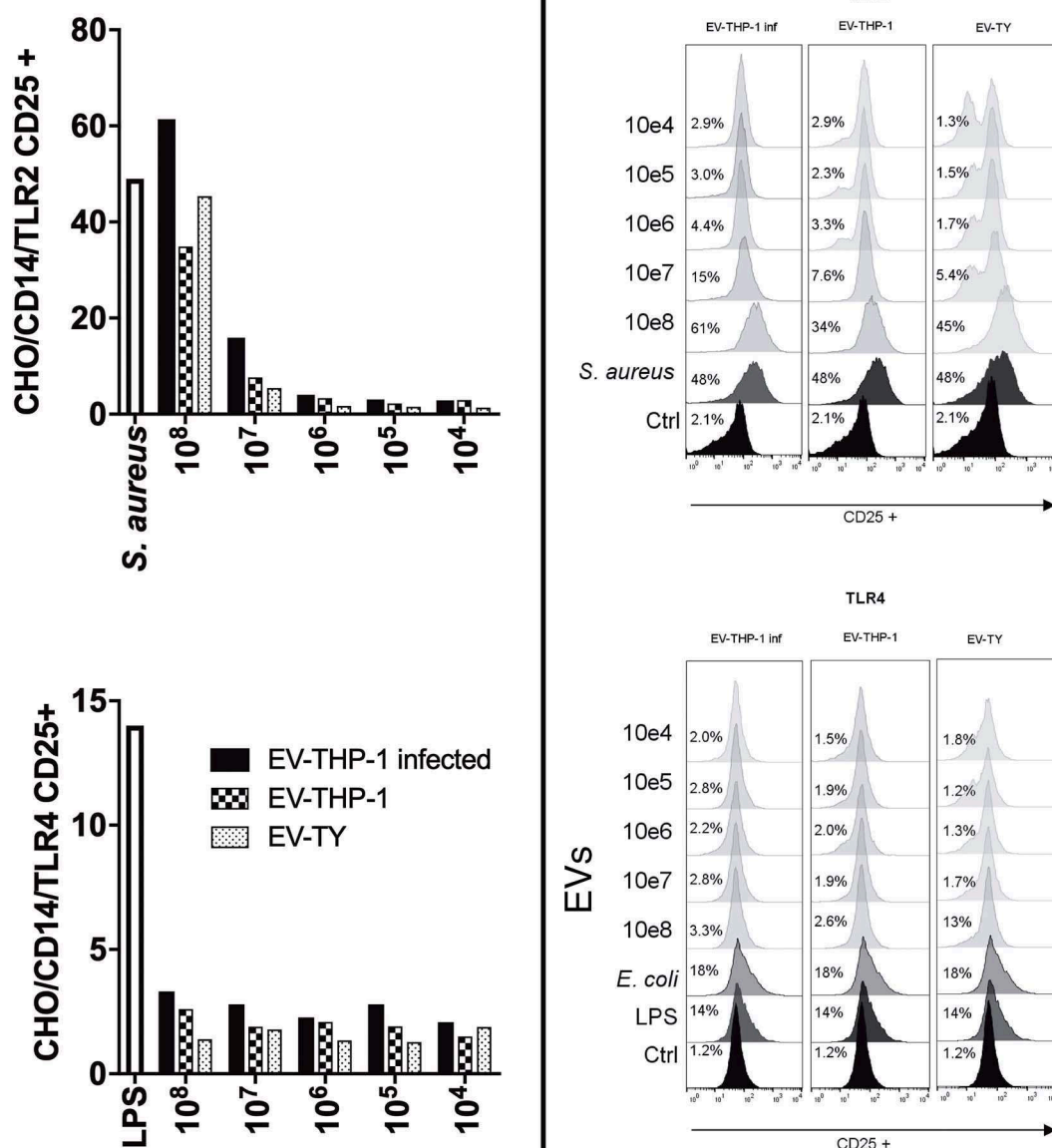


FIGURE 4 | NF- κ B translocation assay using CHO reporter cells transfected with TLR2 or TLR4. Flow cytometry of CD25 expression in CHO cells expressing TLR2 or TLR4 and stimulated with EVs derived from infected or non-infected macrophages or with EVs released by the parasite. Fluorescence was analyzed 24 h after stimulation with EVs on a flow cytometer (FACS) (FACSscan BD). Bars represent the percentages of positive cells. Data are representative of two independent experiments.

et al., 2017). We also looked for *T. cruzi* proteins in EV-THP-1 inf. We found 6 proteins (i.e., HSP60, trypanothione peroxidase, trans-sialidase Group II, flagellar calcium-binding protein, surface protein TolT and paraflagellar rod protein 2) (Supplementary Table 1). We also compared the levels of abundance of the 58 common proteins by calculating their fold change. The abundance of 20 proteins increased and 38 decreased after infection with *T. cruzi* (Supplementary Table 2). Most of the proteins found in EV-THP-1 and EV-THP-1 inf

are involved in binding, immunological and metabolic processes based on GO term annotations (Figure 8C). Moreover, the majority of the proteins in EV-THP-1 and EV-THP-1 inf were localized in exosomes (Figure 8D). Noteworthy, there was a higher percentage of proteins with catalytic activity in EV-THP-1 inf, particularly enzymes such as trans-sialidase (Figure 8E). It is possible that some of these proteins from *T. cruzi* were not directly associated with the EVs obtained from infected macrophages and were released in the culture supernatant of

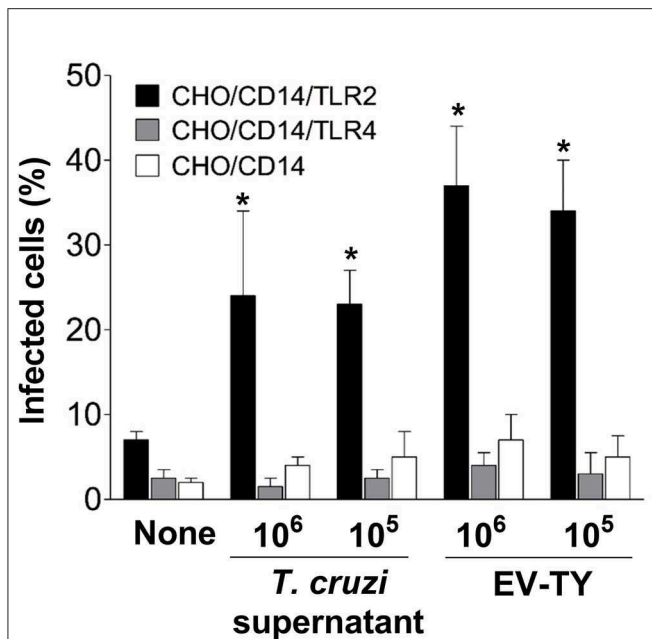


FIGURE 5 | Invasion of TLR2- and TLR4-transfected CHO/CD14 cells with trypomastigotes in the presence or absence of trypomastigotes culture supernatant and EVs isolated from the *T. cruzi* Y strain. Macrophages were preincubated with EVs for 30 min at 37°C in RPMI medium without FCS. Cells were washed with PBS (3×) and Lymphoprep (1×) and then infected with trypomastigotes at a 1:10 ratio (host cell:parasite) for 2 h at 37°C. Cells were then washed (3×) with PBS to remove non-adherent parasites and incubated in RPMI medium with 10% FCS for 24 h at 37°C. Cells were fixed with 100% methanol. Then, the cells were stained with 4',6-diamidino-2-phenylindole (DAPI). The number of infected cells was estimated using an inverted Nikon fluorescence microscope. **p* < 0.01.

the infected cells concomitantly with EV-THP-1 inf production. Furthermore, although unlike, the presence of remaining proteins from the parasites used to infected cells cannot be fully excluded.

DISCUSSION

Macrophages and other mononuclear cells are the host's first line of defense to combat infection of intracellular parasites, such as *T. cruzi*. The release of EVs by *T. cruzi* promotes the activation of murine macrophages (Nogueira et al., 2015). Here, we demonstrate that EVs derived from macrophages infected with *T. cruzi* also modulate the activation of other human THP-1 macrophages to maintain the inflammatory response in the course of infection.

The recognition and response to pathogenic organisms by the immune system is essential for infection control. The expression of TLRs is critical for the response during the early stages of infection for the activation of the immune response. A large number of pathogens express ligands for different TLRs. *T. cruzi* trypomastigote-derived mucin-like glycoproteins (tGPI-mucins) are strong proinflammatory molecules and agonists for the TLR2-TLR6 heterodimer (Campos et al., 2001). *T. cruzi*

also express other glycoconjugates such as GIPLs, which activate TLR4 (Almeida et al., 2000; Oliveira et al., 2004).

In recent years, there has been a growing number of studies showing the capacity of EVs to modulate the immune response, especially in the relationship between parasite and host (Campos et al., 2010; Marcilla et al., 2014). Different strains of *T. cruzi* have been shown to release EVs and promote the activation of macrophages via TLR2 (Nogueira et al., 2015). EVs isolated from macrophages infected with intracellular pathogens (*Mycobacterium bovis* BCG and *M. tuberculosis*) induce a TLR/MyD88-dependent proinflammatory response in naive macrophages (Bhatnagar et al., 2007). In this work, we observed that EVs derived from *T. cruzi*-infected THP-1 human macrophages were able to induce the translocation of NF-κB to the nucleus by interacting with TLR2. EVs released by uninfected THP-1 cells also activated the cells via TLR2. However, the amount of EVs produced by the infected cells was 10-fold higher than that produced by the uninfected cells, showing that the amount of EVs is the prime factor for activation. In addition, uninfected macrophages produce EVs when there is tissue damage, which leads to the activation of these cells or dendritic cells and results in the secretion of TNF-α and other inflammatory mediators through the activation of the p38 MAPK pathway and NF-κB (Thomas and Salter, 2010). Damage-associated molecular pattern molecules (DAMPs) could also be related to the mechanism of action of the EVs described herein. Among the DAMPs, we found heat shock proteins, hyaluronic acid, β-defensin 3 and HMGB1, which are recognized by TLR2 (Scheibner et al., 2006; Funderburg et al., 2007; Curtin et al., 2009).

Internalization and phagocytosis by phagocytic cells such as macrophages are crucial processes for initiation of the killing of intracellular pathogens. *T. cruzi* can invade different mammalian cell types (Yoshida, 2006). It has been demonstrated that metacyclic trypomastigotes can invade cells in a Ca²⁺-dependent manner by exocytosis and the recruitment of host lysosomes to the plasma membrane (Tardieux et al., 1994; Rodríguez et al., 1995). Another mechanism for *T. cruzi* entry in cells independent of lysosome recruitment has been described to occur through the activation of PI3K (Woolsey et al., 2003). Here we observed that macrophages infected with *T. cruzi*, as evaluated by SEM, showed an increase in the number of EVs budding from the plasma membrane after the 24-h culture period. This increase was also confirmed by NTA. The release of EVs can be regulated by changes in intracellular calcium levels. When cells were treated with calcium ionophore (A23187), an increase in the release of EVs was found (Savina et al., 2003). *T. cruzi* infection increases the Ca²⁺ concentration in macrophages (Wilkowsky et al., 1996). Additionally, activated cells release a greater number of particles than non-activated cells (Théry et al., 2009). Thus, the increased release of EVs by infected macrophages is related to an increase in intracellular calcium after *T. cruzi* infection and macrophage activation. The size range of the EVs isolated herein (50–200 nm) corroborates that described in the literature (Raposo and Stoorvogel, 2013; Wang et al., 2015; Hui et al., 2018). EVs can further enhance the parasite's ability to invade the host cells through TLR2 signaling. We observed an increase in the number

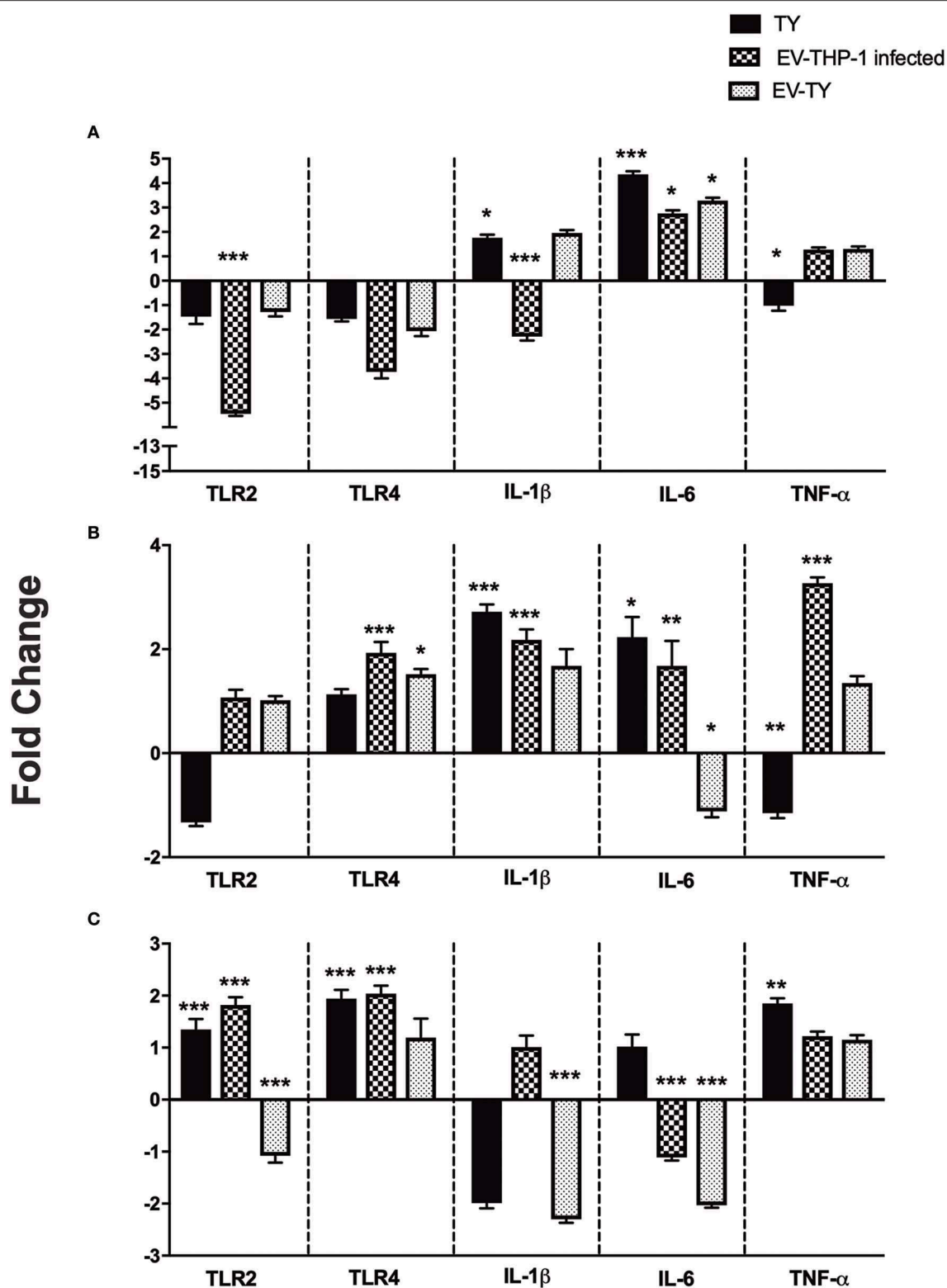


FIGURE 6 | Gene expression levels of TLR2, TLR4, IL-1β, IL-6, and TNF-α proinflammatory cytokines in differentiated THP-1 cells. Relative mRNA expression of TLRs and cytokines were measured after 1 (A), 6 (B), and 24 h (C) of macrophages infected with 5×10^7 /mL trypanomastigotes (TY), or macrophages treated with EV-THP1 inf, EV-TY (both EVs at 10^8 particles/mL). After these treatments, RNA was extracted, and the expression of TLR2, TLR4 and specific cytokines was determined by RT-qPCR. Bars represent the mean of the triplicates, and the dispersion denotes the standard deviation subtracted to THP-1 macrophages maintained in medium. Data are representative of two independent experiments. Statistical analysis with ANOVA, compared to the respective control; * $p < 0.05$; ** $p < 0.01$; and *** $p < 0.001$.

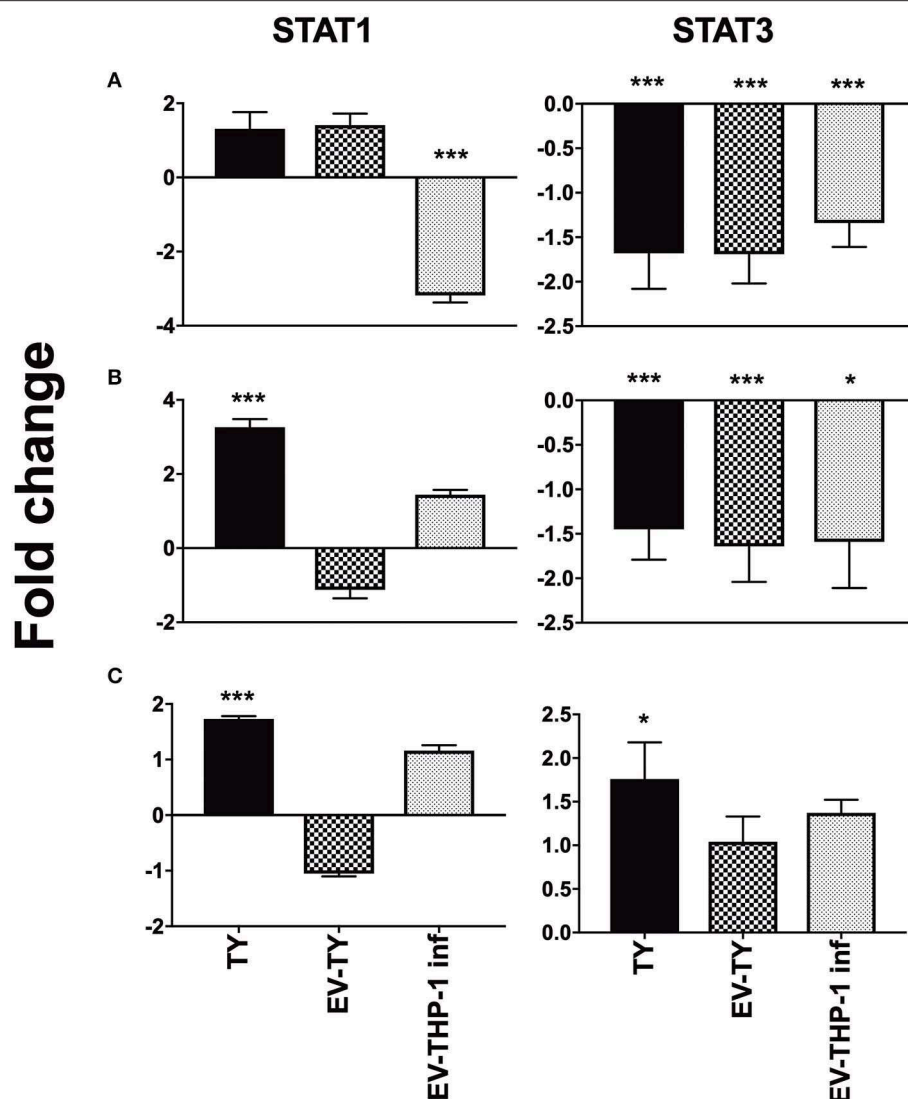


FIGURE 7 | Gene expression of STAT1 and STAT3 in differentiated THP-1 cells. Relative mRNA expression levels of STAT1 and STAT3 transcription factors in macrophages after 1 (A), 6 (B), and 24 h (C) of macrophages infected with 5×10^7 /mL trypomastigotes (TY), or macrophages treated with EV-THP1 inf, EV-TY (both EVs at 10^8 particles/mL). After these treatments, RNA was extracted, and the expression of TLR2, TLR4 and specific cytokines was determined by RT-qPCR. Bars represent the mean of the triplicates, and the dispersion denotes the standard deviation subtracted to THP-1 macrophages maintained in medium. Data are representative of two independent experiments. Statistical analysis with ANOVA, compared to the respective control; * $p < 0.05$; ** $p < 0.01$; *** $p < 0.001$.

of infected cells when they expressed TLR2 and were incubated with parasite-derived EVs (EV-TY). EVs from *T. cruzi* participate in invasion through a mechanism independent of lysosome recruitment. The parasite invasion is associated with activation of PI3K (Wilkowsky et al., 2001). TLR2 activates PI3K during *T. cruzi* infection, leading to Rab5 activation, which is essential for phagosome formation (Maganto-Garcia et al., 2008). The release of EVs by infected macrophages is related to increased parasite replication, which was observed in macrophages infected with *T. cruzi* herein.

Similarly, in mice infected with *Mycobacterium bovis*, an increase in the release of plasma EVs is also related to an increase in the bacterial load (Singh et al., 2012).

We performed proteomic analysis to compare the content of the EVs released from uninfected THP-1 cells and THP-1 cells infected with *T. cruzi*. According to the Exocarta database (www.exocarta.org), all the proteins found in the EVs have previously been identified in different types of cells and body fluids. The infection changed the composition of the EVs from the host cells; 65 proteins were unique to the EV-THP-1 cells, 31 were unique to the EV-THP-1 inf, and the expression of 58 proteins was altered in both EVs (20 proteins increase and 38 decrease).

The EVs isolated from macrophage supernatants showed the presence of the MHC II surface marker and the exosomal markers CD9 and CD63. No *T. cruzi* antigens could be detected by western blotting in EV-THP-1 and the presence

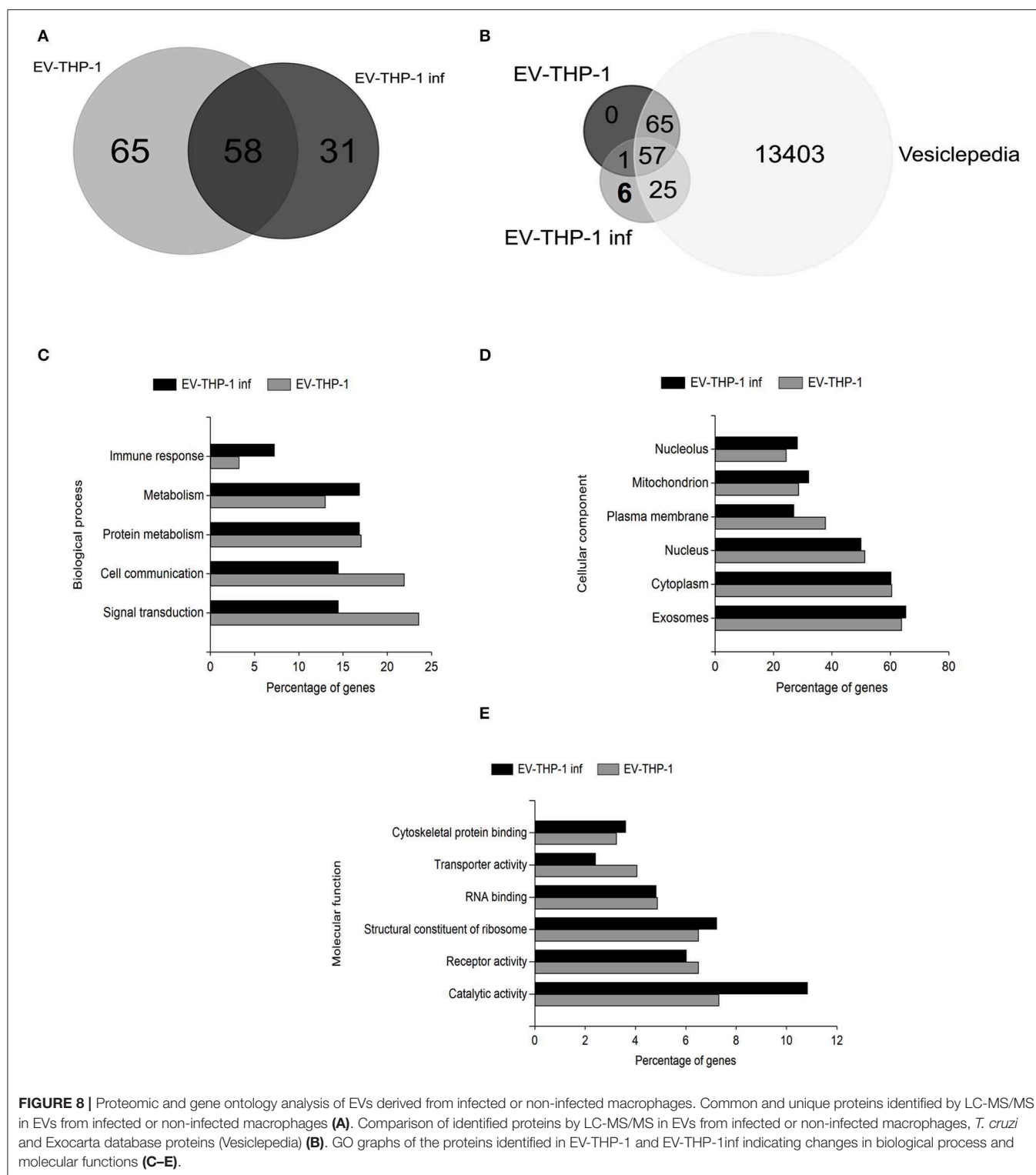


FIGURE 8 | Proteomic and gene ontology analysis of EVs derived from infected or non-infected macrophages. Common and unique proteins identified by LC-MS/MS in EVs from infected or non-infected macrophages (**A**). Comparison of identified proteins by LC-MS/MS in EVs from infected or non-infected macrophages, *T. cruzi* and Exocarta database proteins (Vesiclepedia) (**B**). GO graphs of the proteins identified in EV-THP-1 and EV-THP-1inf indicating changes in biological process and molecular functions (**C–E**).

of plasma membrane glycoproteins expressing α -Gal epitopes (i.e., TcMUCII mucins or tGPI-mucins) of the parasite in the EVs of macrophages infected by *T. cruzi* were not identified by total proteomic analysis. In this analysis only six parasite proteins were found in EVs from macrophages infected with *T.*

cruzi i.e., HSP60, trypanothione peroxidase, trans-sialidase Group II, flagellar calcium-binding protein, surface protein TolT and paraflagellar rod protein 2 (Lobo et al., 2019). These parasite proteins are involved in the recognition of the parasite by host cells, invasion, the adhesion of host cells, metabolism and the

induction of the host immune response (Godsel et al., 1995; Quanquin et al., 1999; Mattos et al., 2014; Urményi et al., 2014; Girard et al., 2018).

Previous studies of EVs derived from macrophages infected with intracellular microorganisms, such as mycobacteria and *Leishmania*, also identified proteins of these intracellular organisms that can be carried by EVs (Giri et al., 2010; Hassani and Olivier, 2013).

A variation in cytokine expression in macrophages stimulated with EVs was observed by RT-qPCR. An increase in IL-1 β expression was evidenced in cells stimulated with TY and EV-THP-1inf at 6 and 24 h. IL-1 β is related to the resistance of the host to infection through stimulation of the IL-1 receptor and activation of the adapter protein MyD88, leading to the production of NO in macrophages (Lima-Junior et al., 2013). Thus, increased IL-1 β production may be important in infection control. In addition, immune activation through TLR2 and NF- κ B receptors by macrophages has been found to rapidly elevate IL-1 β levels (Petersen et al., 2005). Macrophages stimulated with EV-THP-1 and EV-THP-1 inf as well as those infected with *T. cruzi* displayed increased TNF- α expression. TNF- α is a proinflammatory cytokine produced by macrophages and lymphocytes and is important for the control of *T. cruzi* infection. The production of TNF- α by macrophages when stimulated with INF- γ is associated with resistance to infection in mice (Silva et al., 1995). Increased IL-6 production was seen only at 6 h in response to treatment with the EVs of infected macrophages and parasites. Interleukin-6 is a proinflammatory cytokine produced primarily by T cells, dendritic cells and macrophages. It has been reported that IL-6 is not required for a strong Th1 response (Moskowitz et al., 1997) and that in the presence of TGF- β , IL-1 β , and IL-23 cause the differentiation of Th0 lymphocytes into Th17 lymphocytes (Acosta-Rodriguez et al., 2007; Zhou et al., 2007).

The cytokine expression profile observed after stimulation with EVs released by infected cells demonstrates the modulation of the proinflammatory conditions caused by the release of these EVs. This cytokine expression profile also occurs in response to EVs from *Leishmania amazonensis*-infected macrophages, which promote the production of the inflammatory cytokines IL-12, IL-1 β , and TNF- α (Cronemberger-Andrade et al., 2014). The production of TNF- α , IL-1 β and IL-6 by macrophages is associated with the M1 type phenotype. M1 macrophages are responsible for polarizing the Th1 immune response, producing IL-12 and maintaining a low production level of IL-10. The main stimuli that favor the activation and polarization in M1 macrophages are LPS and IFN- γ (Mantovani et al., 2004). It has recently been demonstrated that plasma-isolated EVs from chronic Chagas disease patients promote increased regulation of genes related to the proinflammatory response in macrophages (Chowdhury et al., 2017). In addition, the composition of the EVs isolated from the plasma of mice and patients revealed them to be of cardiac, lymphocyte, and macrophage origin (Chowdhury et al., 2017) thus demonstrating the importance of the potential modulation and activation of macrophages in the chronic phase of Chagas disease.

Signal transduction through IFN- γ receptors is mediated by the phosphorylation of JAK and STAT1. The activation of

STAT1 is important for the production of a proinflammatory response. In STAT1 knockout mice, an increase in mortality was found due to increased numbers of parasites found in the blood and tissues (Kulkarni et al., 2015). We did not observe regulation by this mechanism after stimulation with the different EVs. STAT3 phosphorylation induces transcription of the gene encoding SOCS-3 (He et al., 2003). In macrophages infected with *M. tuberculosis*, NF- κ B activation was found to be inhibited, and SOCS-3 expression was found to be induced as a mechanism of inflammatory response evasion (Nair et al., 2011; Hillmer et al., 2016). The production of IL-10 leads to increased expression of SOCS-3 and STAT3 in *T. cruzi*-infected cardiomyocytes due to the inactivation of NF- κ B and ERK/MAPK (Hovsepian et al., 2013). In the analysis of STAT3 expression, we observed a reduction in expression at 1 and 6 h and an increase only at 24 h after *T. cruzi* infection. The EVs released by infected or non-infected macrophages, as well as the parasite-derived EVs, modulated the response of macrophages favoring the maintenance of a proinflammatory response. It was previously shown that *T. cruzi* GIPLs were not able to activate STAT1 or STAT3 (Stahl et al., 2013). However, in that study the authors did not evaluate tGPI-mucins, which have much stronger proinflammatory than GIPLs (Almeida et al., 2000; Campos et al., 2001). Therefore, we conclude that tGPI-mucins (or TcMUCII mucins), which are present in trypomastigote-derived EVs (Ribeiro et al., 2018), and/or other molecules expressed on the surface of the parasite and the EVs (EV-TY) there from -TY may be involved in the activation of these transcription factors.

In summary, our results indicate that signaling through EVs during *T. cruzi* infection is essential in host-parasite interactions. After infection, increased amounts of EVs are released from infected macrophages that interact with TLR2 and stimulate the translocation of NF- κ B. As a result of this interaction and activation, proinflammatory cytokines (TNF- α , IL-6, and IL-1 β) are produced and maintain the inflammatory response generated by *T. cruzi* infection. In addition, human macrophage-derived EVs carry parasite proteins, which could be the reason for their increased ability to induce inflammatory responses.

DATA AVAILABILITY STATEMENT

All datasets generated for this study are included in the article/**Supplementary Material**.

ETHICS STATEMENT

All experimental procedures used in this work were approved by the Ethics Committee on Animal Use (CEUA) of the Federal University of São Paulo, protocol 1073090614.

AUTHOR CONTRIBUTIONS

AC-A, PX, IA, YO-B, NR-R, and AT conceived and designed the experiments. AC-A, PX, YO-B, and AT performed most

experiments. NP and MC assisted in NF- κ B translocation assay. IA, CE, and BG performed the proteomic analysis. AC-A, PX, YO-B, and AT wrote the manuscript. AC-A, PX, RS, YO-B, IA, NR-R, and AT contributed to final manuscript. All the authors reviewed the manuscript.

FUNDING

This work was supported by the FAPESP (2016-01917-3) and doctoral fellowship from CNPq and CAPES. IA was partially supported by the grant No. 2G12MD007592 from the National Institute of General Medical Sciences (NIGMS). We are grateful to the Biomolecule Analysis Core Facility (BACF) at UTEP/BBRC, funded by NIGMS grant No. 2G12MD007592, for the access to the LC-MS instrument.

ACKNOWLEDGMENTS

We thank all colleagues from Laboratório de Imunologia Celular & Bioquímica de fungos e protozoários (LICBf), Departamento

de Ciências Farmacêuticas, UNIFESP who provided helpful technical advice and expertise that greatly assisted the research.

SUPPLEMENTARY MATERIAL

The Supplementary Material for this article can be found online at: <https://www.frontiersin.org/articles/10.3389/fcimb.2020.00099/full#supplementary-material>

Supplementary Figure 1 | Size distribution of EVs from macrophages. Kinetics of released EVs isolated from THP-1 cells (differentiated to macrophages) infected or uninfected with *T. cruzi* and or treated with *T. cruzi* EVs. Supernatants from infected or not macrophages and from macrophages incubated with *T. cruzi* EVs were collected after 1, 6, and 24 h and then isolated by ultracentrifugation.

Supplementary Table 1 | Proteins identified by LC-MS/MS in EVs derived from uninfected (THP-1) and infected (THP-1 infected) macrophages.

Supplementary Table 2 | Table containing sequences of the primers selected for the gene expression analysis of human macrophages stimulated with EVs derived from infected or non-infected macrophages and infected with *T. cruzi* strain Y trypomastigotes.

REFERENCES

- Acosta-Rodriguez, E. V., Napolitani, G., Lanzavecchia, A., and Sallusto, F. (2007). Interleukins 1 β and 6 but not transforming growth factor- β are essential for the differentiation of interleukin 17-producing human T helper cells. *Nat. Immunol.* 8, 942–949. doi: 10.1038/ni1496
- Aline, F., Bout, D., Amigorena, S., Roingeard, P., and Dimier-Poisson, I. (2004). Toxoplasma gondii antigen-pulsed-dendritic cell-derived exosomes induce a protective immune response against *T. gondii* infection. *Infect. Immun.* 72, 4127–4137. doi: 10.1128/IAI.72.7.4127-4137.2004
- Almeida, I. C., Camargo, M. M., Procópio, D. O., Silva, L. S., Mehlert, A., Travassos, L. R., et al. (2000). Highly purified glycosylphosphatidylinositols from *Trypanosoma cruzi* are potent proinflammatory agents. *EMBO J.* 19, 1476–1485. doi: 10.1093/emboj/19.7.1476
- Andrews, N. W. (2002). Lysosomes and the plasma membrane. *J. Cell Biol.* 158, 389–394. doi: 10.1083/jcb.200205110
- Atayde, V. D., Aslan, H., Townsend, S., Hassani, K., Kamhawi, S., and Olivier, M. (2015). Exosome secretion by the parasitic protozoan *Leishmania* within the sand fly midgut. *Cell Rep.* 13, 957–967. doi: 10.1016/j.celrep.2015.09.058
- Barbosa, F. M. C., Dupin, T. V., Toledo, M. D. S., Reis, N. F. D. C., Ribeiro, K., Cronemberger-Andrade, A., et al. (2018). Extracellular vesicles released by *Leishmania (Leishmania) amazonensis* promote disease progression and induce the production of different cytokines in macrophages and B-1 cells. *Front. Microbiol.* 9:3056. doi: 10.3389/fmicb.2018.03056
- Bhatnagar, S., Shinagawa, K., Castellino, F. J., and Schorey, J. S. (2007). Exosomes released from macrophages infected with intracellular pathogens stimulate a proinflammatory response *in vitro* and *in vivo*. *Blood* 110, 3234–3244. doi: 10.1182/blood-2007-03-079152
- Burleigh, B. A., and Andrews, N. W. (1998). Signaling and host cell invasion by *Trypanosoma cruzi*. *Curr. Opin. Microbiol.* 1, 461–465. doi: 10.1016/S1369-5274(98)80066-0
- Bustin, S. A., Benes, V., Garson, J. A., Hellems, J., Huggett, J., Kubista, M., et al. (2009). The MIQE guidelines: minimum information for publication of quantitative Real-Time PCR experiments. *Clin. Chem.* 55, 611–622. doi: 10.1373/clinchem.2008.112797
- Campos, F. M. F., Franklin, B. S., Teixeira-Carvalho, A., Filho, A. L. S., de Paula, S. C. O., Fontes, C. J., et al. (2010). Augmented plasma microparticles during acute *Plasmodium vivax* infection. *Malar. J.* 9:327. doi: 10.1186/1475-2875-9-327
- Campos, M. A., Almeida, I. C., Takeuchi, O., Akira, S., Valente, E. P., Procópio, D. O., et al. (2001). Activation of Toll-like receptor-2 by glycosylphosphatidylinositol anchors from a protozoan parasite. *J. Immunol.* 167, 416–423. doi: 10.4049/jimmunol.167.1.416
- Campos, M. A., Closel, M., Valente, E. P., Cardoso, J. E., Akira, S., Alvarez-Leite, J. I., et al. (2004). Impaired production of proinflammatory cytokines and host resistance to acute infection with *Trypanosoma cruzi* in mice lacking functional myeloid differentiation factor 88. *J. Immunol.* 172, 1711–1718. doi: 10.4049/jimmunol.172.3.1711
- Campos, M. A., and Gazzinelli, R. T. (2004). *Trypanosoma cruzi* and its components as exogenous mediators of inflammation recognized through Toll-like receptors. *Mediators Inflamm.* 13, 139–143. doi: 10.1080/09511920410001713565
- Cestari, I., Ansa-Addo, E., Deolindo, P., Inal, J. M., and Ramirez, M. I. (2012). *Trypanosoma cruzi* immune evasion mediated by host cell-derived microvesicles. *J. Immunol.* 189, 1942–1952. doi: 10.4049/jimmunol.1102053
- Chowdhury, I. H., Koo, S.-J., Gupta, S., Liang, L. Y., Bahar, B., Silla, L., et al. (2017). Gene expression profiling and functional characterization of macrophages in response to circulatory microparticles produced during *Trypanosoma cruzi* infection and chagas disease. *J. Innate Immun.* 9, 203–216. doi: 10.1159/000451055
- Coakley, G., Maizels, R. M., and Buck, A. H. (2015). Exosomes and other extracellular vesicles: the new communicators in parasite infections. *Trends Parasitol.* 31, 477–489. doi: 10.1016/j.pt.2015.06.009
- Cronemberger-Andrade, A., Aragão-França, L., de Araujo, C. F., Rocha, V. J., da Cruz Borges-Silva, M., Pereira Figueira, C., et al. (2014). Extracellular vesicles from *Leishmania*-infected macrophages confer an anti-infection cytokine-production profile to naïve macrophages. *PLoS Negl. Trop. Dis.* 8:e3161. doi: 10.1371/journal.pntd.0003161
- Curtin, J. F., Liu, N., Candolfi, M., Xiong, W., Assi, H., Yagiz, K., et al. (2009). HMGB1 mediates endogenous TLR2 activation and brain tumor regression. *PLoS Med.* 6:e10. doi: 10.1371/journal.pmed.100010
- Delude, R. L., Yoshimura, A., Ingalls, R. R., and Golenbock, D. T. (1998). Construction of a lipopolysaccharide reporter cell line and its use in identifying mutants defective in endotoxin, but not TNF- α , signal transduction. *J. Immunol.* 161, 3001–3009.
- Funderburg, N., Lederman, M. M., Feng, Z., Drage, M. G., Jadlowsky, J., Harding, C. V., et al. (2007). Human -defensin-3 activates professional antigen-presenting cells via Toll-like receptors 1 and 2. *Proc. Natl. Acad. Sci. U.S.A.* 104, 18631–18635. doi: 10.1073/pnas.0702130104

- Gavinho, B., Rossi, I. V., Evans-Osses, I., Inal, J., and Ramirez, M. I. (2018). A new landscape of host-protozoa interactions involving the extracellular vesicles world. *Parasitology* 12, 1521–1530. doi: 10.1017/S0031182018001105
- Girard, M. C., Acevedo, G. R., López, L., Ossowski, M. S., Piñeyro, M. D., Grosso, J. P., et al. (2018). Evaluation of the immune response against *Trypanosoma cruzi* cytosolic trypanothione peroxidase in human natural infection. *Immunology* 155, 367–378. doi: 10.1111/imm.12979
- Giri, P. K., Kruh, N. A., Dobos, K. M., and Schorey, J. S. (2010). Proteomic analysis identifies highly antigenic proteins in exosomes from *M. tuberculosis*-infected and culture filtrate protein-treated macrophages. *Proteomics* 10, 3190–3202. doi: 10.1002/pmic.200900840
- Godsel, L. M., Tibbetts, R. S., Olson, C. L., Chaudoir, B. M., and Engman, D. M. (1995). Utility of recombinant flagellar calcium-binding protein for serodiagnosis of *Trypanosoma cruzi* infection. *J. Clin. Microbiol.* 33, 2082–2085.
- Gonçalves, M. F., Umezawa, E. S., Katzin, A. M., de Souza, W., Alves, M. J., Zingales, B., et al. (1991). *Trypanosoma cruzi*: shedding of surface antigens as membrane vesicles. *Exp. Parasitol.* 72, 43–53. doi: 10.1016/0014-4894(91)90119-H
- Hassani, K., and Olivier, M. (2013). Immunomodulatory impact of leishmania-induced macrophage exosomes: a comparative proteomic and functional analysis. *PLoS Negl. Trop. Dis.* 7:e2185. doi: 10.1371/journal.pntd.0002185
- He, B., You, L., Uematsu, K., Matsangou, M., Xu, Z., He, M., et al. (2003). Cloning and characterization of a functional promoter of the human SOCS-3 gene. *Biochem. Biophys. Res. Commun.* 301, 386–391. doi: 10.1016/S0006-291X(02)03071-1
- Hillmer, E. J., Zhang, H., Li, H. S., and Watowich, S. S. (2016). STAT3 signaling in immunity. *Cytokine Growth Factor Rev.* 31, 1–15. doi: 10.1016/j.cytogfr.2016.05.001
- Hovsepian, E., Penas, F., Siffo, S., Mirkin, G. A., and Goren, N. B. (2013). IL-10 inhibits the NF- κ B and ERK/MAPK-mediated production of pro-inflammatory mediators by up-regulation of SOCS-3 in *Trypanosoma cruzi*-infected cardiomyocytes. *PLoS ONE* 8:e79445. doi: 10.1371/journal.pone.0079445
- Hui, W. W., Hercik, K., Belsare, S., Alugubelly, N., Clapp, B., Rinaldi, C., et al. (2018). *Salmonella enterica* Serovar Typhimurium alters the extracellular proteome of macrophages and leads to the production of proinflammatory exosomes. *Infect. Immun.* 86:e00386–e00317 doi: 10.1128/IAI.00386-17
- Koga, R., Hamano, S., Kuwata, H., Atarashi, K., Ogawa, M., Hisaeda, H., et al. (2006). TLR-dependent induction of IFN- β mediates host defense against *Trypanosoma cruzi*. *J. Immunol.* 177, 7059–7066. doi: 10.4049/jimmunol.177.10.7059
- Kulkarni, M. M., Varikuti, S., Terrazas, C., Kimble, J. L., Satoskar, A. R., and McGwire, B. S. (2015). Signal transducer and activator of transcription 1 (STAT-1) plays a critical role in control of *Trypanosoma cruzi* infection. *Immunology* 145, 225–231. doi: 10.1111/imm.12438
- Lässer, C., Alikhani, V. S., Ekström, K., Eldh, M., Paredes, P. T., Bossios, A., et al. (2011). Human saliva, plasma and breast milk exosomes contain RNA: uptake by macrophages. *J. Transl. Med.* 9:9. doi: 10.1186/1479-5876-9-9
- Lien, E., Sellati, T. J., Yoshimura, A., Flo, T. H., Rawadi, G., Finberg, R. W., et al. (1999). Toll-like receptor 2 functions as a pattern recognition receptor for diverse bacterial products. *J. Biol. Chem.* 274, 33419–33425. doi: 10.1074/jbc.274.47.33419
- Lima-Junior, D. S., Costa, D. L., Carregaro, V., Cunha, L. D., Silva, A. L. N., Mineo, T. W. P., et al. (2013). Inflammasome-derived IL-1 β production induces nitric oxide-mediated resistance to Leishmania. *Nat. Med.* 19, 909–915. doi: 10.1038/nm.3221
- Lobo, M., Balouz, V., Melli, L., Carlevaro, G., Cortina, M. E., Cámara, M., et al. (2019). Molecular and antigenic characterization of *Trypanosoma cruzi* TolT proteins. *PLoS Negl. Trop. Dis.* 13:e0007245. doi: 10.1371/journal.pntd.0007245
- Madison, M. N., Roller, R. J., and Okeoma, C. M. (2014). Human semen contains exosomes with potent anti-HIV-1 activity. *Retrovirology* 11:102. doi: 10.1186/s12977-014-0102-z
- Maganto-Garcia, E., Punzon, C., Terhorst, C., and Fresno, M. (2008). Rab5 activation by Toll-like receptor 2 is required for *Trypanosoma cruzi* internalization and replication in macrophages. *Traffic* 9, 1299–1315. doi: 10.1111/j.1600-0854.2008.00760.x
- Mantovani, A., Sica, A., Sozzani, S., Allavena, P., Vecchi, A., and Locati, M. (2004). The chemokine system in diverse forms of macrophage activation and polarization. *Trends Immunol.* 25, 677–686. doi: 10.1016/j.it.2004.09.015
- Marcilla, A., Martin-Jaurar, L., Treliis, M., de Menezes-Neto, A., Osuna, A., Bernal, D., et al. (2014). Extracellular vesicles in parasitic diseases. *J. Extracell. Vesicles* 3:25040. doi: 10.3402/jev.v3.25040
- Mathieu, M., Martin-Jaurar, L., Lavieu, G., and Théry, C. (2019). Specificities of secretion and uptake of exosomes and other extracellular vesicles for cell-to-cell communication. *Nat. Cell Biol.* 1, 9–17. doi: 10.1038/s41556-018-0250-9
- Mattos, E. C., Tonelli, R. R., Colli, W., and Alves, M. J. M. (2014). The Gp85 surface glycoproteins from *Trypanosoma cruzi*. *Subcell. Biochem.* 74, 151–180. doi: 10.1007/978-94-007-7305-9_7
- Moskowitz, N. H., Brown, D. R., and Reiner, S. L. (1997). Efficient immunity against Leishmania major in the absence of interleukin-6. *Infect. Immun.* 65, 2448–2450. doi: 10.1128/IAI.65.6.2448-2450.1997
- Nair, S., Pandey, A. D., and Mukhopadhyay, S. (2011). The PPE18 protein of mycobacterium tuberculosis Inhibits NF- κ B-mediated proinflammatory cytokine production by upregulating and phosphorylating suppressor of cytokine signaling 3 protein. *J. Immunol.* 186, 5413–5424. doi: 10.4049/jimmunol.1000773
- Nogueira, P. M., Ribeiro, K., Silveira, A. C. O., Campos, J. H., Martins-Filho, O. A., Bela, S. R., et al. (2015). Vesicles from different *Trypanosoma cruzi* strains trigger differential innate and chronic immune responses. *J. Extracell. Vesicles* 4:28734. doi: 10.3402/jev.v4.28734
- Oliveira, A.-C., Peixoto, J. R., de Arruda, L. B., Campos, M. A., Gazzinelli, R. T., Golenbock, D. T., et al. (2004). Expression of functional TLR4 confers proinflammatory responsiveness to *Trypanosoma cruzi* glycoinositolphospholipids and higher resistance to infection with *T. cruzi*. *J. Immunol.* 173, 5688–5696. doi: 10.4049/jimmunol.173.9.5688
- Petersen, C. A., Krumholz, K. A., and Burleigh, B. A. (2005). Toll-like receptor 2 regulates interleukin-1 β -dependent cardiomyocyte hypertrophy triggered by *Trypanosoma cruzi*. *Infect. Immun.* 73, 6974–6980. doi: 10.1128/IAI.73.10.6974-6980.2005
- Pope, S. M., and Lässer, C. (2013). *Toxoplasma gondii* infection of fibroblasts causes the production of exosome-like vesicles containing a unique array of mRNA and miRNA transcripts compared to serum starvation. *J. Extracell. Vesicles* 2:22484. doi: 10.3402/jev.v2i0.22484
- Quanquin, N. M., Galaviz, C., Fouts, D. L., Wrightsman, R. A., and Manning, J. E. (1999). Immunization of mice with a Tola-like surface protein of *Trypanosoma cruzi* generates CD4(+) T-cell-dependent parasitocidal activity. *Infect. Immun.* 67, 4603–4612. doi: 10.1128/IAI.67.9.4603-4612.1999
- Ramirez, M. I., Deolindo, P., de Messias-Reason, I. J., Arigi, E. A., Choi, H., Almeida, I. C., et al. (2017). Dynamic flux of microvesicles modulate parasite-host cell interaction of *Trypanosoma cruzi* in eukaryotic cells. *Cell. Microbiol.* 19:e12672. doi: 10.1111/cmi.12672
- Raposo, G., and Stoorvogel, W. (2013). Extracellular vesicles: exosomes, microvesicles, and friends. *J. Cell Biol.* 200, 373–383. doi: 10.1083/jcb.201211138
- Regev-Rudski, N., Wilson, D. W., Carvalho, T. G., Sisquella, X., Coleman, B. M., Rug, M., et al. (2013). Cell-cell communication between malaria-infected red blood cells via exosome-like vesicles. *Cell* 153, 1120–1133. doi: 10.1016/j.cell.2013.04.029
- Ribeiro, K. S., Vasconcellos, C. I., Soares, R. P., Mendes, M. T., Ellis, C. C., Aguilera-Flores, M., et al. (2018). Proteomic analysis reveals different composition of extracellular vesicles released by two *Trypanosoma cruzi* strains associated with their distinct interaction with host cells. *J. Extracell. Vesicles* 7:1463779. doi: 10.1080/20013078.2018.1463779
- Rodríguez, A., Rioult, M. G., Ora, A., and Andrews, N. W. (1995). A trypanosome-soluble factor induces IP3 formation, intracellular Ca²⁺ mobilization and microfilament rearrangement in host cells. *J. Cell Biol.* 129, 1263–1273. doi: 10.1083/jcb.129.5.1263
- Rossi, I. V., Gavinho, B., and Ramirez, M. I. (2019). Isolation and characterization of extracellular vesicles derived from *Trypanosoma cruzi*. *Methods Mol. Biol.* 89–104. doi: 10.1007/978-1-4939-9148-8_7
- Savina, A., Furlán, M., Vidal, M., and Colombo, M. I. (2003). Exosome release is regulated by a Calcium-dependent mechanism in K562 Cells. *J. Biol. Chem.* 278, 20083–20090. doi: 10.1074/jbc.M301642200
- Scheibner, K. A., Lutz, M. A., Boodoo, S., Fenton, M. J., Powell, J. D., and Horton, M. R. (2006). Hyaluronan fragments act as an endogenous danger signal by engaging TLR2. *J. Immunol.* 177, 1272–1281. doi: 10.4049/jimmunol.177.2.1272

- Schenkman, S., Pontes de Carvalho, L., and Nussenzweig, V. (1991). *Trypanosoma cruzi* trans-sialidase and neuraminidase activities can be mediated by the same enzymes. *J. Exp. Med.* 2, 567–575. doi: 10.1084/jem.175.2.567
- Schmittgen, T. D., and Livak, K. J. (2008). Analyzing real-time PCR data by the comparative C_T method. *Nat. Protoc.* 3, 1101–1108. doi: 10.1038/nprot.2008.73
- Silva, J. S., Vespa, G. N., Cardoso, M. A., Aliberti, J. C., and Cunha, F. Q. (1995). TNF- α mediates resistance to *Trypanosoma cruzi* infection in mice by inducing nitric oxide production in infected gamma interferon-activated macrophages. *Infect. Immun.* 63, 4862–4867. doi: 10.1128/IAI.63.12.4862-4867.1995
- Silverman, J. M., Clos, J., DeOliveira, C. C., Shirvani, O., Fang, Y., Wang, C., et al. (2010). An exosome-based secretion pathway is responsible for protein export from *Leishmania* and communication with macrophages. *J. Cell Sci.* 123, 842–852. doi: 10.1242/jcs.056465
- Silverman, J. M., and Reiner, N. E. (2011). Exosomes and other microvesicles in infection biology: organelles with unanticipated phenotypes. *Cell. Microbiol.* 13, 1–9. doi: 10.1111/j.1462-5822.2010.01537.x
- Singh, P. P., Smith, V. L., Karakousis, P. C., and Schorey, J. S. (2012). Exosomes isolated from mycobacteria-infected mice or cultured macrophages can recruit and activate immune cells *in vitro* and *in vivo*. *J. Immunol.* 189, 777–785. doi: 10.4049/jimmunol.1103638
- Stahl, P., Ruppert, V., Meyer, T., Schmidt, J., Campos, M. A., Gazzinelli, R. T., et al. (2013). Trypomastigotes and amastigotes of *Trypanosoma cruzi* induce apoptosis and STAT3 activation in cardiomyocytes *in vitro*. *Apoptosis* 18, 653–663. doi: 10.1007/s10495-013-0822-x
- Street, J. M., Barran, P. E., Mackay, C. L., Weidt, S., Balmforth, C., Walsh, T. S., et al. (2012). Identification and proteomic profiling of exosomes in human cerebrospinal fluid. *J. Transl. Med.* 10:5. doi: 10.1186/1479-5876-10-5
- Tardieux, I., Nathanson, M. H., and Andrews, N. W. (1994). Role in host cell invasion of *Trypanosoma cruzi*-induced cytosolic-free Ca^{2+} transients. *J. Exp. Med.* 179, 1017–1022. doi: 10.1084/jem.179.3.1017
- Tardieux, I., Webster, P., Ravesloot, J., Boron, W., Lunn, J. A., Heuser, J. E., et al. (1992). Lysosome recruitment and fusion are early events required for trypanosome invasion of mammalian cells. *Cell* 71, 1117–1130. doi: 10.1016/S0092-8674(05)80061-3
- Théry, C., Ostrowski, M., and Segura, E. (2009). Membrane vesicles as conveyors of immune responses. *Nat. Rev. Immunol.* 9, 581–593. doi: 10.1038/nri2567
- Théry, C., Witwer, K. W., Aikawa, E., Alcaraz, M. J., Anderson, J. D., Andriantsitohaina, R., et al. (2018). Minimal information for studies of extracellular vesicles 2018 (MISEV2018): a position statement of the international society for extracellular vesicles and update of the MISEV2014 guidelines. *J. Extracell. Vesicles* 7:1535750. doi: 10.1080/20013078.2018.1535750
- Théry, C., Zitvogel, L., and Amigorena, S. (2002). Exosomes: composition, biogenesis and function. *Nat. Rev. Immunol.* 2, 569–579. doi: 10.1038/nri855
- Thomas, L. M., and Salter, R. D. (2010). Activation of macrophages by P2X7-induced microvesicles from myeloid cells is mediated by phospholipids and is partially dependent on TLR4. *J. Immunol.* 185, 3740–3749. doi: 10.4049/jimmunol.1001231
- Tkach, M., and Théry, C. (2016). Communication by extracellular vesicles: where we are and where we need to go. *Cell* 6, 1226–1232. doi: 10.1016/j.cell.2016.01.043
- Torreilhas, A. C., Schumacher, R. I., Alves, M. J. M., and Colli, W. (2012). Vesicles as carriers of virulence factors in parasitic protozoan diseases. *Microbes Infect.* 14, 1465–1474. doi: 10.1016/j.micinf.2012.07.008
- Trocoli Torreilhas, A. C., Tonelli, R. R., Pavanelli, W. R., da Silva, J. S., Schumacher, R. I., de Souza, W., et al. (2009). *Trypanosoma cruzi*: parasite shed vesicles increase heart parasitism and generate an intense inflammatory response. *Microbes Infect.* 11, 29–39. doi: 10.1016/j.micinf.2008.10.003
- Uphoff, C. C., and Drexler, H. G. (2002). Comparative PCR analysis for detection of mycoplasma infections in continuous cell lines. *In Vitro Cell Dev. Biol. Anim.* 38, 79–85. doi: 10.1290/1071-2690(2002)038<0079:CPAFDO>2.0.CO;2
- Urményi, T. P., Silva, R., and Rondinelli, E. (2014). The heat shock proteins of *Trypanosoma cruzi*. *Subcell. Biochem.* 74, 119–135. doi: 10.1007/978-94-007-7305-9_5
- van Niel, G., D'Angelo, G., and Raposo, G. (2018). Shedding light on the cell biology of extracellular vesicles. *Nat. Rev. Mol. Cell Biol.* 19, 213–228. doi: 10.1038/nrm.2017.125
- Wang, J., Yao, Y., Wu, J., and Li, G. (2015). Identification and analysis of exosomes secreted from macrophages extracted by different methods. *Int. J. Clin. Exp. Pathol.* 8, 6135–6142.
- Wilkowsky, S. E., Barbieri, M. A., Stahl, P., and Isola, E. L. (2001). *Trypanosoma cruzi*: phosphatidylinositol 3-kinase and protein kinase B activation is associated with parasite invasion. *Exp. Cell Res.* 264, 211–218. doi: 10.1006/excr.2000.5123
- Wilkowsky, S. E., Wainszelbaum, M. J., and Isola, E. L. D. (1996). *Trypanosoma cruzi*: participation of intracellular Ca^{2+} during metacyclic trypomastigote-macrophage interaction. *Biochem. Biophys. Res. Commun.* 222, 386–389. doi: 10.1006/bbrc.1996.0753
- Witwer, K. W., and Théry, C. (2019). Extracellular vesicles or exosomes? On primacy, precision, and popularity influencing a choice of nomenclature. *J. Extracell. Vesicles* 1:1648167. doi: 10.1080/20013078.2019.1648167
- Woolsey, A. M., Sunwoo, L., Petersen, C. A., Brachmann, S. M., Cantley, L. C., and Burleigh, B. A. (2003). Novel PI 3-kinase-dependent mechanisms of trypanosome invasion and vacuole maturation. *J. Cell Sci.* 116, 3611–3622. doi: 10.1242/jcs.00666
- Wyllie, M. P., and Ramirez, M. I. (2017). Microvesicles released during the interaction between *Trypanosoma cruzi* TcI and TcII strains and host blood cells inhibit complement system and increase the infectivity of metacyclic forms of host cells in a strain-independent process. *Pathog. Dis.* 75. doi: 10.1093/femspd/ftx077
- Yoshida, N. (2006). Molecular basis of mammalian cell invasion by *Trypanosoma cruzi*. *An. Acad. Bras. Cienc.* 78, 87–111. doi: 10.1590/S0001-37652006000100010
- Zhou, L., Ivanov, I. I., Spolski, R., Min, R., Shenderov, K., Egawa, T., et al. (2007). IL-6 programs T_H -17 cell differentiation by promoting sequential engagement of the IL-21 and IL-23 pathways. *Nat. Immunol.* 8, 967–974. doi: 10.1038/ni1488

Conflict of Interest: The authors declare that the research was conducted in the absence of any commercial or financial relationships that could be construed as a potential conflict of interest.

Copyright © 2020 Cronemberger-Andrade, Xander, Soares, Pessoa, Campos, Ellis, Grajeda, Ofir-Birin, Almeida, Regev-Rudski and Torreilhas. This is an open-access article distributed under the terms of the Creative Commons Attribution License (CC BY). The use, distribution or reproduction in other forums is permitted, provided the original author(s) and the copyright owner(s) are credited and that the original publication in this journal is cited, in accordance with accepted academic practice. No use, distribution or reproduction is permitted which does not comply with these terms.



***Trypanosoma brucei* and *Trypanosoma cruzi* DNA Mismatch Repair Proteins Act Differently in the Response to DNA Damage Caused by Oxidative Stress**

Viviane Grazielle-Silva^{1,2}, Tehseen Fatima Zeb², Richard Burchmore², Carlos Renato Machado¹, Richard McCulloch^{2*} and Santuza M. R. Teixeira^{1*}

¹ Departamento de Bioquímica e Imunologia, Universidade Federal de Minas Gerais, Belo Horizonte, Brazil, ² The Wellcome Centre for Integrative Parasitology, Institute of Infection, Immunity and Inflammation, University of Glasgow, Glasgow, United Kingdom

OPEN ACCESS

Edited by:

Martin Craig Taylor,
University of London, United Kingdom

Reviewed by:

Jennifer Surtees,
University at Buffalo, United States
Veronica Jimenez,
California State University, Fullerton,
United States

*Correspondence:

Richard McCulloch
Richard.mcculloch@glasgow.ac.uk
Santuza M. R. Teixeira
santuzat@ufmg.br

Specialty section:

This article was submitted to
Parasite and Host,
a section of the journal
Frontiers in Cellular and Infection
Microbiology

Received: 13 October 2019

Accepted: 23 March 2020

Published: 16 April 2020

Citation:

Grazielle-Silva V, Zeb TF,
Burchmore R, Machado CR,
McCulloch R and Teixeira SMR (2020)
Trypanosoma brucei and
Trypanosoma cruzi DNA Mismatch
Repair Proteins Act Differently in the
Response to DNA Damage Caused by
Oxidative Stress.
Front. Cell. Infect. Microbiol. 10:154.
doi: 10.3389/fcimb.2020.00154

MSH2, associated with MSH3 or MSH6, is a central component of the eukaryotic DNA Mismatch Repair (MMR) pathway responsible for the recognition and correction of base mismatches that occur during DNA replication and recombination. Previous studies have shown that MSH2 plays an additional DNA repair role in response to oxidative damage in *Trypanosoma cruzi* and *Trypanosoma brucei*. By performing co-immunoprecipitation followed by mass spectrometry with parasites expressing tagged proteins, we confirmed that the parasites' MSH2 forms complexes with MSH3 and MSH6. To investigate the involvement of these two other MMR components in the oxidative stress response, we generated knockout mutants of MSH6 and MSH3 in *T. brucei* bloodstream forms and MSH6 mutants in *T. cruzi* epimastigotes. Differently from the phenotype observed with *T. cruzi* MSH2 knockout epimastigotes, loss of one or two alleles of *T. cruzi* *msh6* resulted in increased susceptibility to H₂O₂ exposure, besides impaired MMR. In contrast, *T. brucei* *msh6* or *msh3* null mutants displayed increased tolerance to MNNG treatment, indicating that MMR is affected, but no difference in the response to H₂O₂ treatment when compared to wild type cells. Taken together, our results suggest that, while *T. cruzi* MSH6 and MSH2 are involved with the oxidative stress response in addition to their role as components of the MMR, the DNA repair pathway that deals with oxidative stress damage operates differently in *T. brucei*.

Keywords: *Trypanosoma cruzi*, *Trypanosoma brucei*, DNA Mismatch Repair, MSH2, MSH6, oxidative stress

INTRODUCTION

Chagas disease (or American trypanosomiasis) and African Sleeping Sickness (or Human African trypanosomiasis—HAT) are two important endemic and neglected zoonoses caused by parasites of the trypanosomatidae family, respectively called *Trypanosoma cruzi* and *Trypanosoma brucei*. About 6–7 million people worldwide are estimated to be infected with *T. cruzi*. Although Chagas disease is endemic in Latin American countries, it has become a global health concern due to migration flows to Europe, United States, Canada and Japan (Antinori et al., 2017; WHO, 2019a).

Besides infecting humans, *T. brucei* infects animals, including cattle, causing a form of the disease named Nagana (or African Animal Trypanosomiasis-AAT) that has a major economic impact for the livestock industry in east and southern Africa (Isaac et al., 2017). Human African Trypanomiasis is caused by *Trypanosoma brucei gambiense* or *Trypanosoma brucei rhodesiense* and is frequently fatal if not treated (WHO, 2019b).

Both parasites have digenetic life cycles that involve an invertebrate host—a triatomine bug infected with *T. cruzi*, or a tsetse fly infected with *T. brucei*—and a mammalian host. Inside the digestive tract of the triatomine bug, *T. cruzi* multiplies as epimastigotes before differentiating into infective, non-replicative metacyclic trypomastigotes. After a blood meal, metacyclic trypomastigotes are expelled with the vector's feces. During a bite, eliminated parasites can enter the bloodstream when the host scratches the skin area, or through mouth mucosa, eyes and nose. Although less frequent, human infection may also happen by non-vectorial routes such as ingestion of contaminated food, blood transfusion, organ transplantation, or during pregnancy from contaminated mothers (Cevallos and Hernández, 2014; Santana et al., 2019). Circulating trypomastigotes can invade different cell types, where they replicate as intracellular replicative amastigotes that burst the cell and are released into the bloodstream with the potential to infect new cells (Brener, 1973). Similar to *T. cruzi*, *T. brucei* has a complex life cycle in which it has to adapt to the host bloodstream and different compartments of the tsetse fly, such as the midgut after a blood meal and then the salivary gland before transmission to a new mammalian host. Two replicative forms are most readily cultured *in vitro*: procyclic form (PCF), found in the insect vector, and bloodstream form (BSF) present in the mammalian host. Because of this experimental accessibility, most genetic analyses have focused on *T. brucei* BSF and PCF (Matthews, 2005).

To maintain their genome integrity, while adapting to survive in distinct and often hostile environments, trypanosomatids rely on various DNA repair pathways that act in response to different types of DNA damage (Machado-Silva et al., 2016). One such pathway is the DNA Mismatch Repair (MMR) pathway, which is the main pathway, widely conserved from prokaryotes to eukaryotes, that corrects replication errors that escape the proofreading activity of replicative DNA Polymerases (Li, 2008). Besides recognizing non-Watson-Crick base pairing, MMR also acts on insertion/deletion loops (IDLs), as well as on DNA damage caused by endogenous agents such reactive oxygen species (ROS) derived from cell metabolism, hydrolytic and oxidative reactions with water or exogenous sources, for example UV and ionizing radiations, alkylating agents, and crosslinking agents (Edelbrock et al., 2013). In eukaryotes, MMR initiates by the recognition of DNA mispairing by the partially redundant MSH2-MSH6 (MutS α) and MSH2-MSH3 (MutS β) heterodimers, which are homologous to the bacterial MutS homodimer. MutS α recognizes single base pair mismatches and 1–2 base insertion/deletion loops (IDLs), while MutS β primarily recognizes larger IDLs. When MSH2-MSH6 or MSH2-MSH3 binds to mispaired bases, a ring is formed around the DNA, with the DNA binding domain of MSH6 or MSH3 making contact with both the mispaired base and adjacent sites of the DNA.

This binding results in DNA bending (Kumar et al., 2011), which works as a “double check” before DNA repair is initiated (LeBlanc et al., 2018). In addition to their DNA binding domains, MSH proteins also have an ATP binding domain. ATP activation is required for downstream events leading to DNA repair. The lesion detected by MSH proteins is repaired through enzymatic complexes that make an endonucleolytic cut on the newly synthesized strand. The ATP-activated MSH complex recruits MLH/PMS heterodimers that are homologs of bacterial MutL proteins. Together with accessory factors including PCNA, RFC, RPA, and exonuclease 1 (ExoI), MLH/PMS initiate the excision of the error-containing strand. Upon removal, the segment is re-synthesized by DNA polymerase delta and ligation by DNA ligase I restores a corrected DNA duplex (Kim et al., 2018).

Besides their primary role in MMR, eukaryotic MMR proteins are involved in diverse cellular processes such as homologous recombination (HR) (Spies and Fishel, 2015), triplet repeat expansion (Iyer et al., 2015), somatic hypermutation of immunoglobulins (Pilzecker and Jacobs, 2019) and cell signaling (Gupta and Heinen, 2019). MMR proteins activate cell cycle checkpoints and cell death pathways in response to certain DNA lesions, an additional role in the DNA damage response that can trigger cell cycle arrest and apoptosis (Li et al., 2016). Because of their importance in genome maintenance, mutations that cause loss of function in different MMR genes have been associated with predisposition to various types of cancer (Lee et al., 2016).

Genome sequence analyses revealed that *T. cruzi* and *T. brucei* possess a complete set of MMR proteins, indicating that these organisms have a functional MMR pathway composed of homologs of MSH2, MSH3, and MSH6 (originally named MSH8 in *T. brucei*) (Bell et al., 2004), MLH1 and PMS1 (Passos-Silva et al., 2010). However, no homolog for MSH1, which is the MutS homolog involved with the repair of mitochondrial DNA, including oxidative damage (Kaniak et al., 2009; Pogorzala et al., 2009; Foyer, 2018), has been identified in these organisms. We have previously investigated the role of the MSH2 and MLH1 components of the MMR pathway in *T. cruzi* and *T. brucei* by generating knockout mutants in different life cycle forms of these parasites (Bell and McCulloch, 2003; Machado-Silva et al., 2008; Campos et al., 2011; Grazielle-Silva et al., 2015). Because *T. cruzi* and *T. brucei* are exposed to several sources of oxidative stress during their life cycle and, among the different antioxidant defense mechanisms these parasites have evolved to protect genomic and mitochondrial DNA from oxidative lesions is the MMR pathway, we began investigating the role of MSH2 in response to the oxidative stress in both parasites (Machado-Silva et al., 2016). *T. brucei* *msh2* null mutants show increased tolerance to MNNG exposure, a phenotype characteristic of MMR impaired cells (Bell et al., 2004; Grazielle-Silva et al., 2015). In addition, in *T. brucei* bloodstream forms, the lack of TbMSH2 resulted in increased susceptibility to H₂O₂ exposure (Machado-Silva et al., 2008; Campos et al., 2011). Complementation of the TbMSH2 null mutant with *T. cruzi* MSH2 restores the oxidative stress response, but not MMR impairment as suggested by the response to MNNG treatment and microsatellite instability (MSI) assays (Machado-Silva et al., 2008). These experiments provided the first line of evidence indicating that *T. cruzi* MSH2

acts in response to the oxidative stress in a pathway or a signaling process that is independent of canonical MMR pathway. To better investigate this new role of MSH2 in response to oxidative damage in DNA, we have also tested a *T. brucei* *mlh1* null mutant, which showed impaired MMR, but no defect in the oxidative stress response (Bell et al., 2004; Machado-Silva et al., 2008; Grazielle-Silva et al., 2015). *T. cruzi* heterozygous *msh2* knockout mutants have increased susceptibility to oxidative stress caused by H_2O_2 and accumulate more 8-oxo-guanine in genomic and mitochondrial DNA after H_2O_2 exposure (Campos et al., 2011) but, surprisingly, deletion of the two *msh2* alleles in *T. cruzi* epimastigotes resulted in increased tolerance to oxidative damage caused by H_2O_2 . Similarly, *msh2* knockout generated in *T. brucei* PCF also presented increased tolerance to H_2O_2 treatment. These results have led us to propose that an adaptation mechanism to cope with the loss of MSH2 took place in the insect stages of these mutant parasites, i.e., *T. brucei* PCF and *T. cruzi* epimastigotes, allowing them to deal with the oxidative stress in the absence of this protein (Grazielle-Silva et al., 2015). Here, we investigate the involvement of other MMR components in the oxidative stress response by analyzing the effect of various DNA damaging treatments on *T. brucei* and *T. cruzi* *msh3* or *msh6* knockout cell lines. Our main goal was to verify whether the previously observed response to oxidative stress involving MSH2 is part of a DNA damage response that works independently of MMR, or if other MMR proteins act together with MSH2 to repair oxidative damage in a non-canonical DNA repair pathway.

METHODOLOGY

Parasite Cultures

T. brucei cultures of the Lister 427 strain bloodstream (BSF) form were maintained at 37°C, 5% CO_2 in HMI-9 (GIBCO) medium supplemented with 20% fetal bovine serum (GIBCO). Cell passages were performed every 48 h, with population density maintained between 1×10^5 and 2×10^6 cells/mL. Epimastigotes of the CL Brener clone of *T. cruzi* were maintained in logarithmic growth phase at 28°C in liver infusion tryptose (LIT) medium supplemented with 10% fetal bovine serum (GIBCO) and penicillin (10,000 U/mL)/Streptomycin (10,000 µg/mL) (GIBCO) as described (Camargo, 1964). Metacyclic trypomastigotes, obtained after metacyclogenesis of epimastigote cultures maintained in LIT medium for 15–20 days, were used to infect Vero cells cultured in high-glucose DMEM medium (GIBCO) supplemented with 5% fetal bovine serum (GIBCO) and penicillin (10,000 U/mL)/Streptomycin (10,000 µg/mL) (GIBCO).

Plasmid Constructs to Generate Knockout and Tagged Parasites

Knockout constructs prepared to delete *msh3* (TritrypDB Tb427tmp.160.3760) or *msh6* (TritrypDB Tb427.10.6410) in *T. brucei* BSF cells have minor changes in their designs relative to those used before for *msh2* and *mlh1* knockout (Grazielle-Silva et al., 2015). The knockout constructs were generated by PCR-amplifying the 5' and 3' UTRs of the gene of interest from *T. brucei* Lister 427 genomic DNA. PCR amplified fragments

containing the 5' and 3' UTRs from *msh3* and *msh6* were cloned into the knockout construct. These constructs were linearized with *SacI* and *XhoI* and used for transfection of *T. brucei* BSF as described below. *T. brucei* BSF and PCF were also transfected with constructs to tag MSH2 and MSH6 C-terminally in their endogenous locus. Primers complementary to the C-terminal region of *msh2* CDS were used to generate an amplicon that was cloned into the plasmid pNAT12^{myc} (Alsford and Horn, 2008) resulting in the *msh2* CDS fused to 12 repeats of the c-myc epitope. Similarly, primers complementary to a C-terminal region of *msh6* CDS were designed to generate a fragment with the *msh6* CDS in frame with six repeats of the hemagglutinin (HA) epitope derived from the *T. brucei* pTbMCM-HA plasmid (Tiengwe et al., 2012).

To generate *T. cruzi* epimastigotes with the two *msh6* alleles deleted, we used a donor plasmid containing the Neomycin phosphotransferase gene (Neo) or Hygromycin B phosphotransferase gene (Hygro) flanked by intergenic sequences of the *HX1* and *GAPDH* regions derived from the pROCK_GFP vector (DaRocha et al., 2004). To generate the donor sequence named TcMSH6_HX1_Neo_GAPDH_MSH6, *Tcmsh6* coding region previously cloned in the pCR[®] TOPO 2.1 (Thermo Fisher Scientific) was digested with *SacII* and *XmnI* and ligated with T4 DNA ligase into the construct named HX1_Neo_GAPDH (Grazielle-Silva et al., 2015). The donor sequence MSH6_HX1_Neo_GAPDH_MSH6 was PCR-amplified and used together with the ribonucleoprotein (RNP) complex formed by recombinant Cas9 (rCAS9) and two sgRNAs that recognizes the 5' and 3' portions of *Tcmsh6* CDS for transfection of *T. cruzi* CL Brener clone. To generate parasites resistant to Neomycin and Hygromycin in which the two alleles of *Tcmsh6* were deleted, another round of transfection was performed using the RNP complex described above and the donor sequence named MSH6_HX1_Hygro_GAPDH_MSH6. The donor sequence with the Hygro gene was constructed after digesting the Topo_HX1_Hygro_GAPDH plasmid, in which the insert was cloned in the reverse orientation, with *KpnI* and *EcoRV*. The fragment of interest was cloned in the pGEM_TcMSH6 vector previously digested with *Clal* and *KpnI*. This construction was designed in a way that HX1_Hygro_GAPDH disrupts *Tcmsh6* CDS.

To generate *T. cruzi* *msh6* knockouts complemented with *msh6*, two knockout clones (cl1 and cl2) were transfected with the pTREX plasmid (Vazquez and Levin, 1999) containing the MSH6 fused to an HA tag and the puromycin resistance gene. A PCR fragment with the *msh6* CDS and six in frame repeats of the HA epitope and the restriction enzymes *SpeI* and *XhoI* was cloned into the pTREX_GFP-PAC plasmid digested with *XbaI* and *XhoI*. Three days after transfection the parasite populations growing in medium with 15 µg/mL of puromycin were tested by Western blot and treatments with MNNG and H_2O_2 .

To evaluate the cellular localization of MSH6, *T. cruzi* epimastigotes were transfected with a modified version of pTREX plasmid (Vazquez and Levin, 1999) to express MSH6 fused to the monomeric red fluorescent protein (mRFP). The *msh6* CDS without the stop codon was amplified with primers that also added the restriction sites for *XbaI* and *SmaI* to the

PCR fragment. After digestion, this fragment was cloned into pTREX_mRFP giving origin to pTREX_MSH6_mRFP. To C-terminally tag MSH6 at its endogenous locus, primers were generated against a C-terminal region of *msh6* CDS excluding the stop codon. This fragment was cloned into pCR[®] TOPO 2.1 (Thermo Fisher Scientific) in frame with the six repeats of the HA epitope derived from the *T. brucei* pTbMCM-HA plasmid (Tiengwe et al., 2012). As a selective marker, neomycin resistance gene derived from the pROCK_Neo plasmid (DaRocha et al., 2004) was also cloned in the same pCR[®] TOPO 2.1 (Thermo Fisher Scientific) vector. The construct was linearized with *KpnI* and used to transfect *T. cruzi* epimastigotes.

Primers used to generate knockout constructions, plasmids to express tagged proteins and to evaluate the correct insertion of knockout constructions in the genome are listed in **Supplementary Table 1**.

***T. brucei* Transfection**

Transfection of *T. brucei* BSF was performed using the AMAXA Nucleofactor kit (Amaya Biosystems) and the X-001 programme. Cultures were grown to a density of 1×10^6 cells/mL and around 4×10^7 cells were used per transfection with 5–10 μ g of linearized DNA, as previously described (Burkard et al., 2007).

***T. cruzi* Transfection With Recombinant Cas9**

Transfection to generate *T. cruzi* knockout cells using the CRISPR/Cas9 system were performed as previously described (Burle-Caldas et al., 2018). Briefly, Cas9/sgRNAs RNP complex plus a donor sequence composed of *Tcmsh6* CDS replaced by the resistance gene construction HX1_Neo_GAPDH (named MSH6_HX1_Neo_GAPDH_MSH6) were used to transfect *T. cruzi* epimastigotes from the CL Brener cloned strain. Recombinant Cas9 derived from *Staphylococcus aureus* and two sgRNAs that were transcribed *in vitro* formed the ribonucleoprotein (RNP) complex that was transfected together with the donor cassette with the Tb-BSF buffer (Schumann Burkard et al., 2011) and the Amaya Nucleofactor (Lonza) program U-033. After one pulse, parasites were cultivated in LIT medium with 200 μ M G418 (GIBCO). After selection of G418 resistant parasites, another round of transfection was performed as described above using the donor sequence MSH6_HX1_Hygro_GAPDH_MSH6 and selection with 200 μ M Hygromycin B (Thermo Fisher).

Cellular Localization

T. cruzi expressing MSH6 fused to mRFP or to 6x HA epitopes were fixed with 4% paraformaldehyde for 5 min, permeabilized with 0.1% Triton X-100 for 10 min, blocked with 1% BSA, 0.2% Tween 20 for 1 h at room temperature and incubated with 1:500 anti-HA antiserum (Roche) for 1 h. After washing with PBS, nuclei were stained with 1 μ g/mL of DAPI (Molecular Probes/ Life Technologies) for 5 min and cover slides mounted with prolong gold anti-fade solution (Molecular Probes/Life Technologies). Images were acquired with a 100x objective in the fluorescence microscope Olympus BX60 microscope using Q-color 5 digital camera and Qcapture Pro 6.0 software

and with Nikon Eclipse Ti Tecnai G2-12 SpiritBiotwin FEI (120kV) at the Centro de Aquisição e Processamento de Imagens (CAPI-ICB/UFMG).

Immunoprecipitation of MMR Components

Pulldown of TbMSH2 with c-myc tag was performed as described (Tiengwe et al., 2012). Briefly, 10^9 cells of *T. brucei* BSF or PCF co-expressing TbMSH2 fused to c-myc tag (TbMSH2::myc) and MSH6 fused to HA tag (MSH6::HA) were lysed in lysis buffer (50 mM Hepes [pH7.55]; 100 mM NaCl; 1 mM EDTA [pH8.0]; 10% glycerol; 1% Triton X-100) for 2 h at 4°C and incubated with anti-myc antibody (Milipore) previously bound to Dynabeads M-280 Sheep Anti-Mouse IgG (ThermoFisher) for 2 h at 4°C. After five washing steps with wash buffer (50 mM Hepes [pH7.55]; 100 mM LiCl; 1 mM EDTA [pH8.0]; 1 mM EGTA; 0.7% Na Deoxycolate; 1% NP-40) and one step washing with TE wash buffer (10 mM Tris [pH8.0], 1 mM EDTA [pH8.0]; 50 mM NaCl), beads were collected using a magnetic rack and bound protein with its binding partners released in elution buffer (50 mM Tris [pH8.0], 10 mM EDTA [pH8.0]; 1% SDS). Samples (input and pulldown) were analyzed by SDS-polyacrylamide gel electrophoresis and Western blotting with anti-myc antibody against the pulled down TbMSH2 and with anti-HA antibody against TbMSH6.

T. cruzi immunoprecipitation was performed after lysing epimastigotes WT and transfected parasites co-expressing MSH6 fused to HA tag (MSH6::HA) and MSH2 fused to c-myc tag (MSH2::myc) in RIPA buffer (0.5 mM Tris-HCl pH 8.; 15 mM NaCl; 0.1% NP-40, 0.05% Deoxicolato de sódio, 0.01% SDS). After lysis, cell extracts were centrifuged $8,200 \times g$ for 10 min and the supernatant incubated with EZview Red Anti-HA Affinity Gel (Sigma—Aldrich) at 4°C under soft agitation for 16 h. Ten percentage of cell lysate (input fraction) were transferred to a new tube and saved for further western blot analysis. After incubation period beads were centrifuged $8,200 \times g$ for 1 min and unbound proteins, present in the supernatant, transferred to new tube. Beads were washed five times with lysis buffer and bound proteins eluted in elution buffer (62.5 mM Tris-HCl pH 6.8; 10% glycerol; 2% SDS; 5% β -mercaptoethanol; 0.002% bromophenol blue). Samples were analyzed by SDS-polyacrylamide gel electrophoresis and Western blotting with anti-HA antibody against the pulled down TcMSH6 and with anti-myc antibody against TcMSH2.

Parasite Treatment With Genotoxic Agents

T. brucei BSF cultures were inoculated in HMI-9 medium (Hirumi and Hirumi, 1994) at density of 1×10^5 cells/mL. The conversion of Alamar blue to fluorescent Resazurin (Räz et al., 1997) was used to determine the sensitivity of *T. brucei* WT cells and *Tbmsh3* and *Tbmsh6* mutants toward MNNG. Briefly, 200 μ L of 1×10^5 cells/mL cultures were plated on polystyrene 96 well-plates in the presence of medium containing doubling dilutions of MNNG from 400 to 0.39 μ M. After 48 h, 20 μ L of Resazurin (0.125 mg/mL) was added to each well. Cultures were allowed to grow for another 24 h and then florescence was measured using luminescence spectrometer (LS 55, Perkin Elmer) at an emission wavelength of 590 nm. IC50 values was calculated using Prism

(GraphPad). For treatment with H₂O₂ BSF cells were diluted to 1×10^6 cells/mL in HMI-9 medium and incubated with 100 μ M H₂O₂ (VWR) at 37°C, 5% CO₂ for 72 h. After growth, cell density was measured using a haematocytometer.

WT *T. cruzi* epimastigotes and *msh6* mutants in the exponential growth phase were counted and diluted to 1×10^7 cells/mL in LIT medium in the absence or presence of 5 μ M MNNG (Tokyo chemical industry Ltd). After 72 h cell densities were determined by counting live cells with a haematocytometer using Erythrosin B exclusion and plotted as the percentage survival of the MNNG treated cells relative to untreated cultures. For treatment with H₂O₂, *T. cruzi* epimastigotes were incubated in 100 μ M H₂O₂ for 30 min in PBS 1x, after which H₂O₂ containing PBS was removed and cells allowed to grow in LIT medium for 72 h. Cell viability was determined with a haematocytometer using Erythrosin B exclusion and plotted as percentage survival of the treated cells relative to untreated. Similar to described above, *T. cruzi msh6* knockouts transfected with pTREX_MSH6::HA_PAC were treated with 5 μ M MNNG and 100 μ M H₂O₂. 72 h after drug incubation cell numbers were determined with a haematocytometer using Erythrosin B exclusion and plotted as the percentage survival.

DNA Sequencing

Two different clones of *T. cruzi msh6* CDS amplified by PCR and cloned in the pCR[®] TOPO 2.1 (Thermo Fisher Scientific) were selected for DNA sequencing by capillary electrophoresis using an ABI Prism 3730 Genetic Analyzer (Applied Biosystems). Four different primers were used to cover the complete *msh6* sequence.

Cell Infection

Vero cells were infected with *T. cruzi* metacyclic trypomastigotes and maintained at 37 °C in a humidified atmosphere containing 5% CO₂ until trypomastigotes were released in the supernatant. These trypomastigotes were counted using a haemocytometer and an equal number of WT and two *msh6* null mutant clones were used to infect Vero cells or macrophages harvest from Balb/C mice after thioglycollate injection, previously adhered to 13 mm glass coverslips inside 24 wells-plates. At a MOI of 5 parasites per cell, trypomastigotes were allowed to infect cells for 2 h after which non-internalized trypomastigotes were removed. Time points 24 and 48 h after infection were fixed and stained with panoptic. Five hundred uninfected and infected cells counted in random fields. Intracellular amastigotes of infected cells were also counted. The data was represented by the infection index = percentage of infected cells \times mean number of parasites per infected cells.

Statistical Analyses

Statistical analyses in this work were performed using the GraphPad Prism version 7.00 for Mac OS X, GraphPad Software, La Jolla California USA, www.graphpad.com. Data are presented as mean plus standard deviation, and all experiments were repeated at least three times. Results were analyzed for significant differences using ANOVA followed by Bonferroni post-test. Statistical tests used are described at each figure legend. The level of significance was set at $P < 0.05$.

RESULTS

MSH2 Forms Heterodimers With MSH3 and MSH6

Previous studies have shown that *T. cruzi* and *T. brucei* MSH2 are involved in the oxidative stress response to DNA damage (Grazielle-Silva et al., 2015). To investigate the mechanisms behind this additional role of MSH2 we searched for proteins that may interact with MSH2 by tagging *T. brucei* MSH2 with the myc epitope and performing immunoprecipitation. As shown in **Figure 1A**, *T. brucei* MSH2::myc forms a complex with MSH6 in BSFs co-expressing HA-tagged MSH6. Protein bands identified after SDS-PAGE of the immunoprecipitated fraction obtained from cells co-expressing MSH2::myc and MSH6::HA, but not from WT BSFs, were sent for protein sequencing and identification using mass spectrometry. As shown in **Figure 1B**, the two major bands present in the immunoprecipitated pellet were identified as MSH2 and MSH3. Similarly, PCFs expressing MSH2 with the myc epitope were used for immunoprecipitation with anti-myc antibody as shown on western blot in **Figure 1C**. Mass spectrometry analyses of the proteins present in the two bands shown in **Figure 1D** showed that, in transfected PCF parasites, but not in WT cells, MSH3 co-immunoprecipitated with myc-tagged MSH2 (**Figure 1D**). **Supplementary Table 2** shows identified proteins and peptide sequences obtained after mass spectrometry. Similar to the data obtained in *T. brucei*, immunoprecipitation of cell extracts from *T. cruzi* epimastigotes co-expressing MSH6::HA and MSH2::myc showed the presence of the MSH2-MSH6 complex (**Figure 1E**). In conclusion, these analyses showed that MSH2 forms a complex with both MSH3 and MSH6 in *T. brucei* BSFs. In *T. brucei* PCFs we identified a complex containing MSH2 and MSH3, and in *T. cruzi* epimastigotes MSH2 was found to interact with MSH6.

T. brucei msh6 and *msh3* Null Mutants Present a Similar Response to Oxidative Stress When Compared to Wild Type Parasites

The first step during DNA error recognition by the eukaryotic MMR is performed by heterodimers formed between MSH2 and MSH6, named MutS α , or MSH2 and MSH3, named MutS β . We showed that both complexes are formed in *T. brucei* and, as described previously, that MSH2 is involved in the response to oxidative damage in DNA. Since we have also evidences indicating that MSH2 works independently from downstream effector proteins, like MLH1, in the response to oxidative damage (Grazielle-Silva et al., 2015), it is possible that such activity is part of a non-canonical MMR pathway. To test the possibility that MSH2 is the only protein of the MMR pathway responsible for the recognition of oxidative damage, we generated *T. brucei* BSF and PCF mutants with deleted *msh3* or *msh6*. *Tbmsh6* and *Tbmsh3* knockouts were obtained by disrupting their coding sequences (CDS) with constructs containing blasticidin or puromycin drug resistance genes flanked by tubulin and actin intergenic regions to provide SL addition and poly-A processing

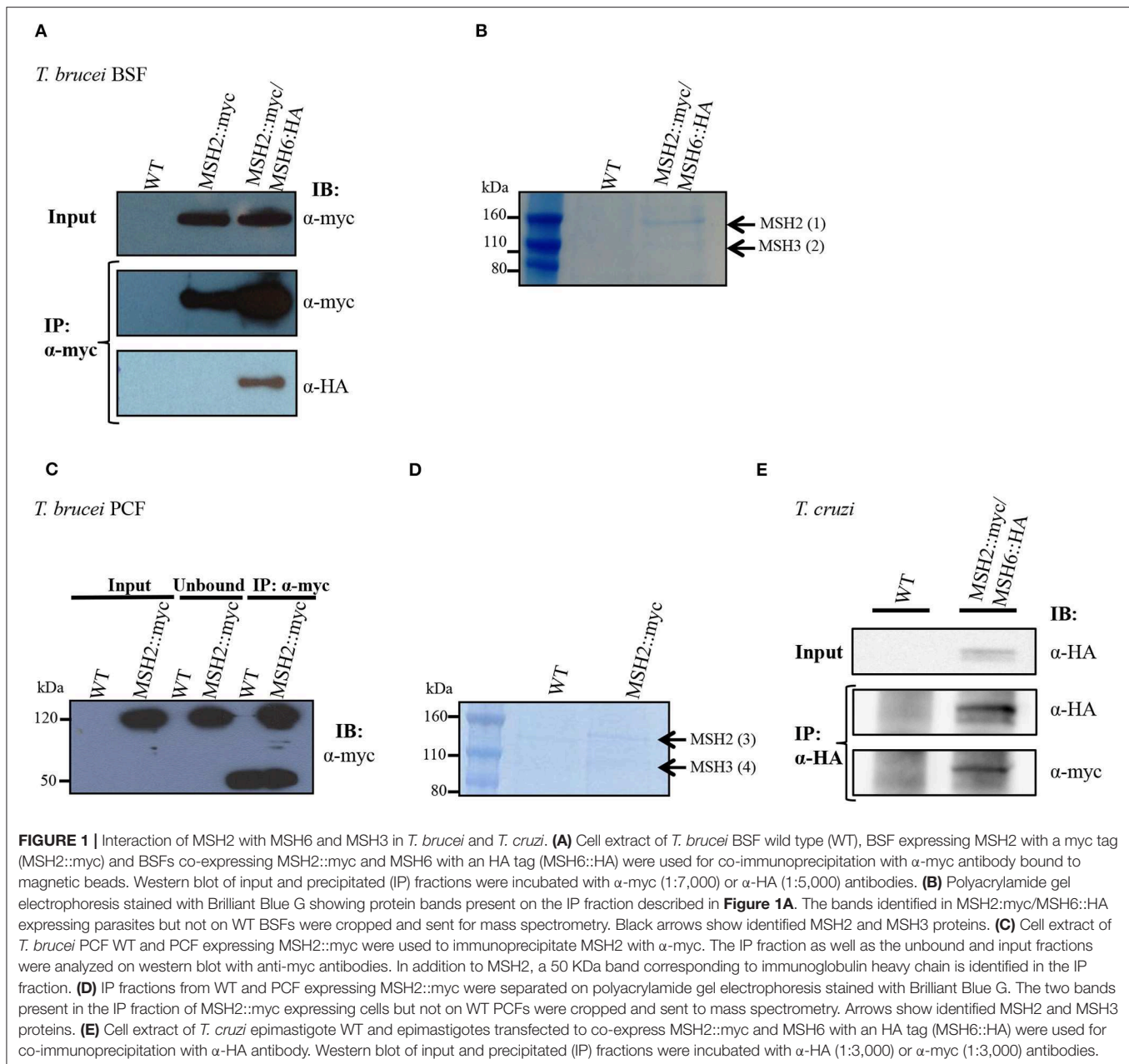
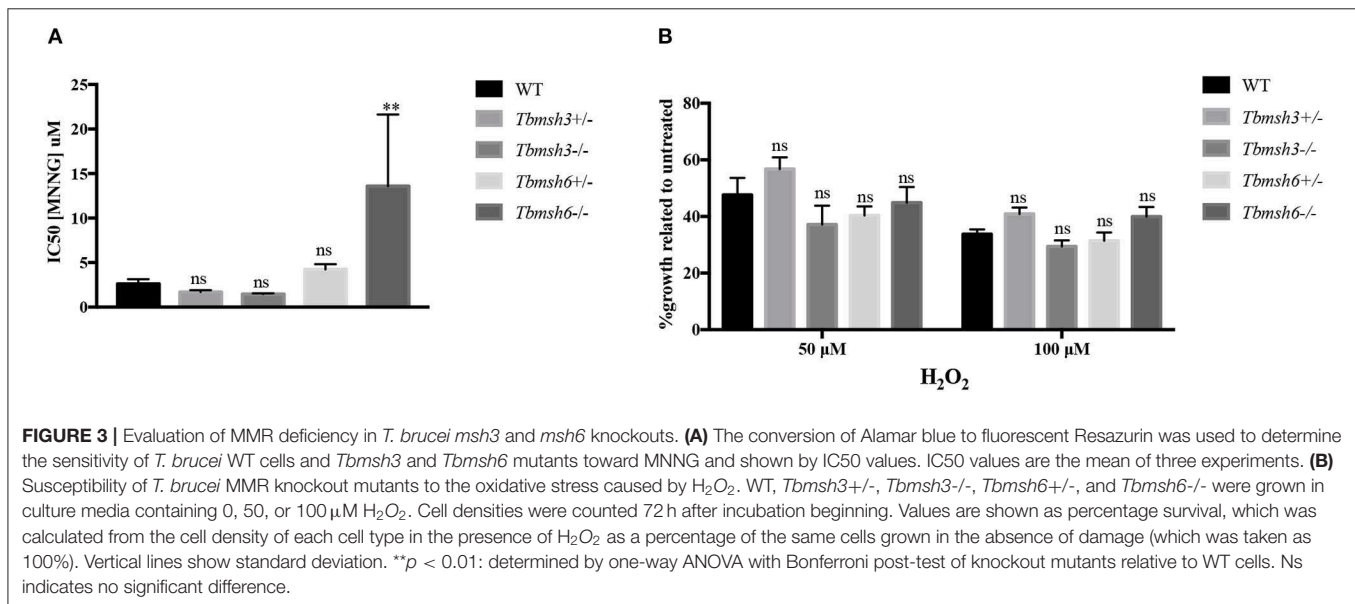
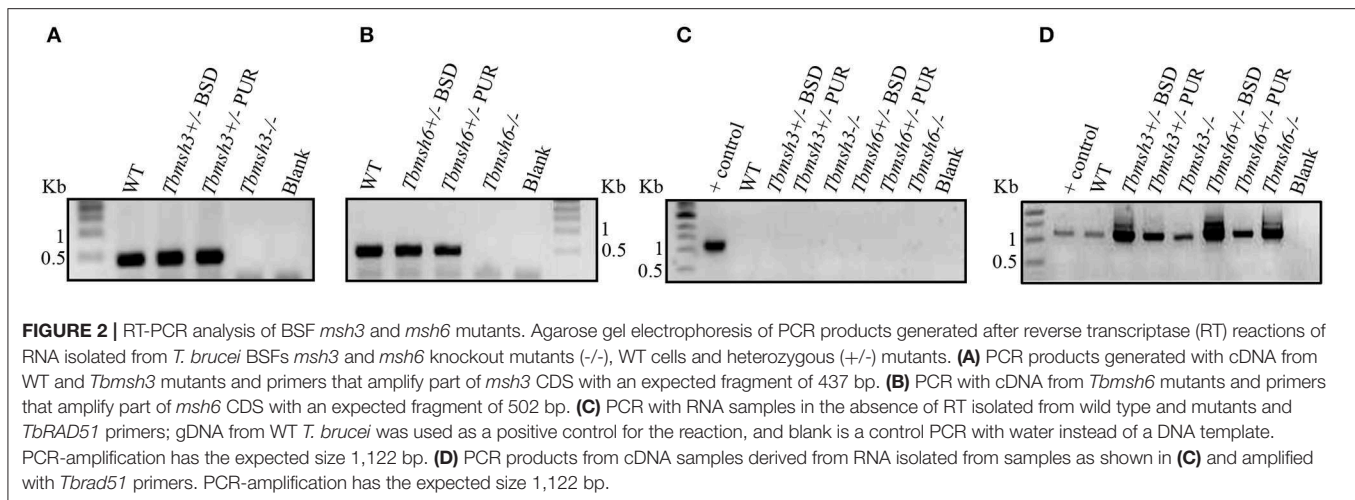


FIGURE 1 | Interaction of MSH2 with MSH6 and MSH3 in *T. brucei* and *T. cruzi*. **(A)** Cell extract of *T. brucei* BSF wild type (WT), BSF expressing MSH2 with a myc tag (MSH2::myc) and BSFs co-expressing MSH2::myc and MSH6 with an HA tag (MSH6::HA) were used for co-immunoprecipitation with α-myc antibody bound to magnetic beads. Western blot of input and precipitated (IP) fractions were incubated with α-myc (1:7,000) or α-HA (1:5,000) antibodies. **(B)** Polyacrylamide gel electrophoresis stained with Brilliant Blue G showing protein bands present on the IP fraction described in **Figure 1A**. The bands identified in MSH2::myc/MSH6::HA expressing parasites but not on WT BSFs were cropped and sent for mass spectrometry. Black arrows show identified MSH2 and MSH3 proteins. **(C)** Cell extract of *T. brucei* PCF WT and PCF expressing MSH2::myc were used to immunoprecipitate MSH2 with α-myc. The IP fraction as well as the unbound and input fractions were analyzed on western blot with anti-myc antibodies. In addition to MSH2, a 50 kDa band corresponding to immunoglobulin heavy chain is identified in the IP fraction. **(D)** IP fractions from WT and PCF expressing MSH2::myc were separated on polyacrylamide gel electrophoresis stained with Brilliant Blue G. The two bands present in the IP fraction of MSH2::myc expressing cells but not on WT PCFs were cropped and sent to mass spectrometry. Arrows show identified MSH2 and MSH3 proteins. **(E)** Cell extract of *T. cruzi* epimastigote WT and epimastigotes transfected to co-express MSH2::myc and MSH6 with an HA tag (MSH6::HA) were used for co-immunoprecipitation with α-HA antibody. Western blot of input and precipitated (IP) fractions were incubated with α-HA (1:3,000) or α-myc (1:3,000) antibodies.

signals. After transfection, clones resistant to blasticidin and puromycin were tested by PCR to confirm gene disruption (**Supplementary Figure 1**). As shown in **Figure 2**, PCR analyses of cDNAs generated from RNA isolated from WT and drug resistant parasites using primers that bind specifically to the *Tbmsh3* or *Tbmsh6* CDSs showed no expression of *msh3* or *msh6* mRNAs in knockout parasites (**Figures 2A,B**). PCR reactions performed with RNA samples that were not previously incubated with Reverse Transcriptase generated no products, except with control DNA (**Figure 2C**). To attest the quality of the cDNAs produced from all samples, the *Tbrad51* CDS was amplified with specific primers, generating the expected PCR products (**Figure 2D**).

A phenotype frequently associated with MMR impairment is increased tolerance to MNNG exposure (de Wind et al., 1995). Using the alamar blue assay to determine cell viability after treatment of WT and *T. brucei* knockout mutants with MNNG, we showed that, while *Tbmsh6* null mutants are more resistant to MNNG exposure compared to WT cells, *Tbmsh3* null mutants have no alteration regarding tolerance to MNNG (**Figure 3A**).

To verify whether *Tbmsh3* or *Tbmsh6* null mutants respond differently to oxidative stress, *T. brucei* WT BSF and *Tbmsh6* or *Tbmsh3* mutants were grown in culture media containing 0, 50, or 100 μM H₂O₂ and parasite survival determined 72 h later. As shown in **Figure 3B**, distinct from the results previously described with *Tbmsh2* null mutants (Machado-Silva et al., 2008;



Grazielle-Silva et al., 2015), no changes in the susceptibility to H₂O₂ of *Tbmsh3* or *Tbmsh6* knockout cells were observed when compared to WT parasites.

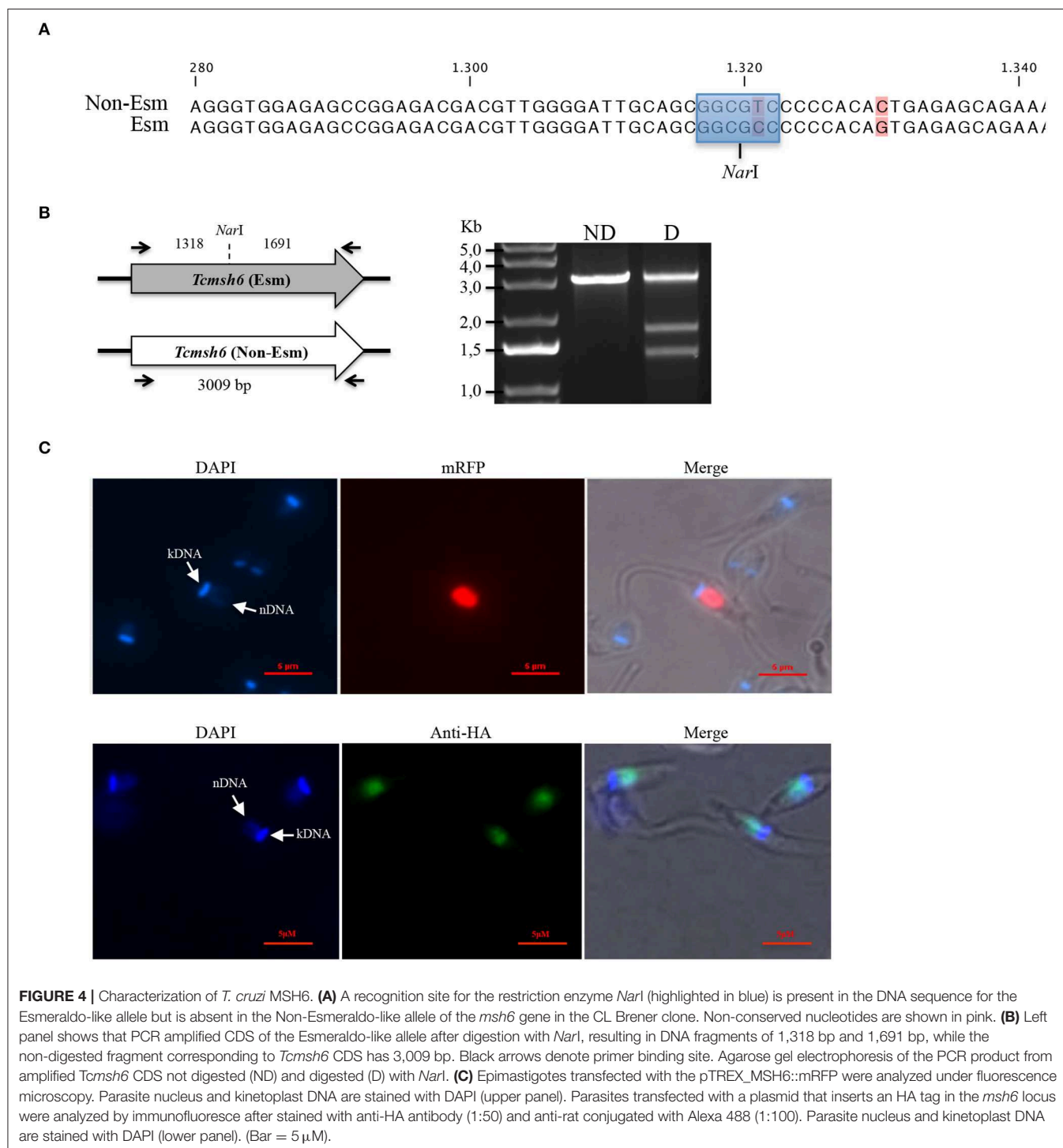
T. cruzi MSH6, Encoded by a Heterozygous Single-Copy Gene, Localizes to the Nucleus

Analyses of the *T. cruzi* and *T. brucei* genomes have shown that *msh6* is present as a single-copy gene in both parasites (Berriman et al., 2005; El-Sayed et al., 2005). Because CL Brener, the *T. cruzi* reference strain, is a hybrid strain, most genes have been assigned to one of the two haplotypes, named Esmeraldo and Non-Esmeraldo, that compose the CL Brener genome (El-Sayed et al., 2005). When we searched for *msh6* in the CL Brener genome database (available at <https://tritrypdb.org>) we identified only one sequence annotated as belonging to the non-Esmeraldo haplotype. However, during our initial attempts to generate a

Tcmsh6 null mutant using donor sequences with homology to *Tcmsh6* flanking a drug resistance marker, we observed that only clones with a single deleted allele were generated. This result prompted us to investigate whether the CL Brener genome contains two alleles instead, with sequences that are different enough to prevent homologous recombination with the same donor sequence. To test this hypothesis, we amplified the *msh6* locus using primers annealing at the beginning and the end of *msh6* CDS and cloned the PCR product into pCR® TOPO 2.1 (Thermo Fisher Scientific). By sequencing plasmid DNA from different clones, we verified that the DNA sequence for *Tcmsh6* currently annotated in the *T. cruzi* CL Brener genome database represents a hybrid between the Esmeraldo-like and Non-Esmeraldo-like alleles (**Supplementary Figure 2A**), a frequent error that occurred during the assembly process (Daniella Bartholomeu, personal communication). Based on the PCR sequences, we concluded that the *Tcmsh6* has two alleles that

present 94.2% homology at the nucleotide level and the translated product generates two distinct protein isoforms presenting 96.9% amino acid identity (**Supplementary Figure 2B**). To confirm the results from our sequence analyses, we digested the PCR products corresponding to *Tcmsh6* CDSs with the enzyme *NarI*. As shown in the upper panel of **Figure 4A**, according to its sequence, the Esmeraldo-like *msh6* allele has the *NarI* restriction site whereas

the non-Esmeraldo allele cannot be digested by *NarI*. Agarose gel electrophoresis of the digested products showed two fragments with 1,318 and 1,691 bp corresponding to the Esmeraldo-like allele, and one fragment with the expected size (3,009 bp) of the non-digested Non-Esmeraldo-like allele (**Figure 4B**). Thus, contrary to the data currently available in the CL Brener genome database, this *T. cruzi* strain contains two distinct *msh6* alleles,



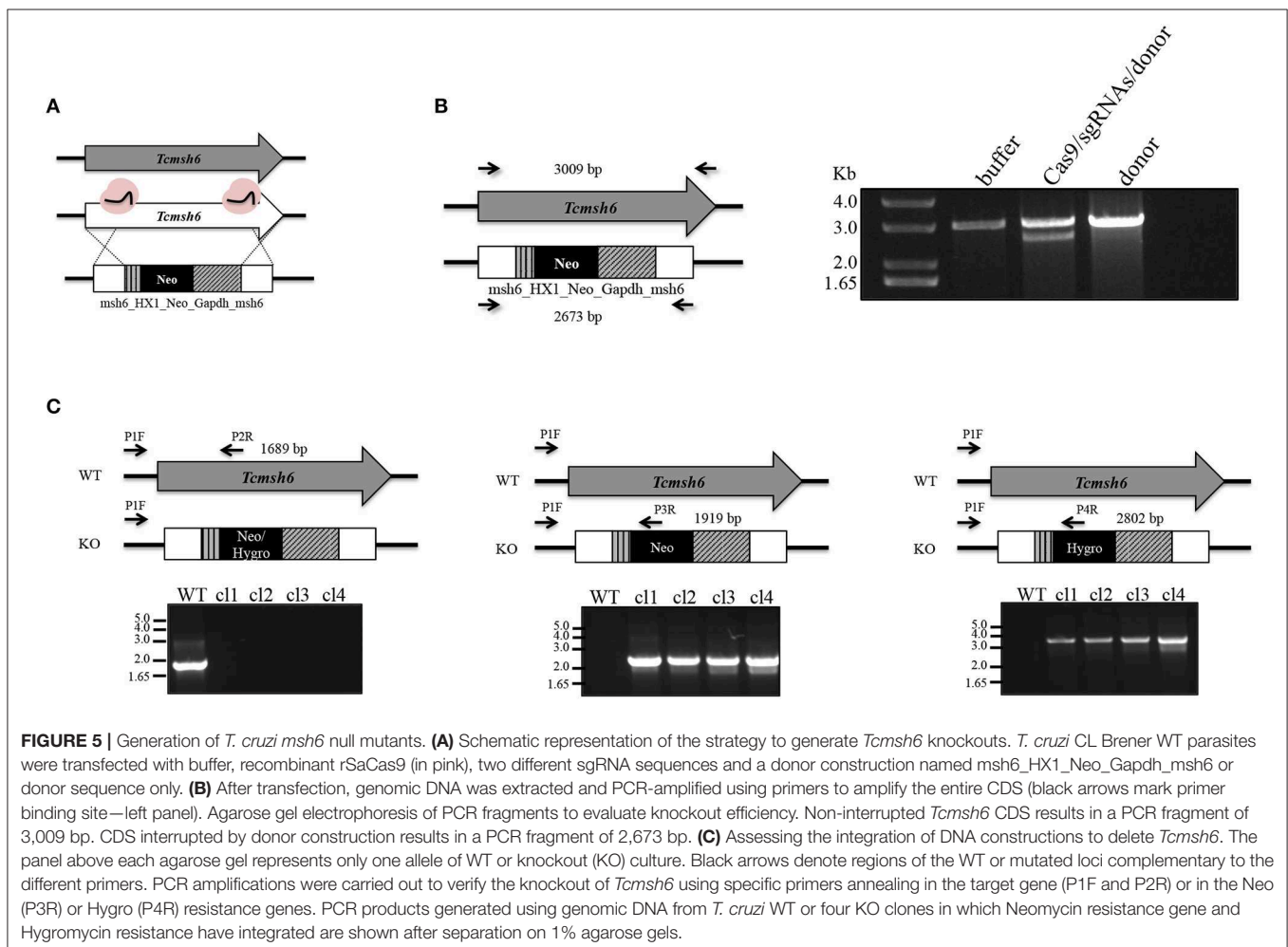
which can be distinguished by the presence/absence of a *NarI* restriction site.

By expressing TcMSH6 ectopically as a C-terminal fusion with monomeric Red Fluorescence Protein (mRFP), we were able to verify that, similar to *T. cruzi* and *T. brucei* MSH2 (Grazielle-Silva et al., 2015), TcMSH6 has a nuclear localization (Figure 4C, upper panel). We confirmed the MSH6 nuclear localization by generating *T. cruzi* epimastigotes expressing the protein with an HA tag inserted in the endogenous *msh6* locus (Figure 4C, lower panel). Using western blot, we showed that TcMSH6 fused to an HA tag is expressed in epimastigotes as a protein with the expected molecular weight of 117.4 kDa (Supplementary Figure 3). Thus, identical nuclear localization of TcMSH6 was observed using two different approaches, i.e., by ectopically expressing the protein fused to mRFP using an episomal vector or by expressing a HA-tagged protein inserted in its endogenous genomic locus.

T. cruzi *msh6* Null Mutants Display Impaired MMR and Increased Susceptibility to Hydrogen Peroxide

To initiate the mismatch repair mechanism, MSH2 must form a heterodimer with MSH6 or MSH3. To verify if *T. cruzi*

MSH2 works as a dimer with MSH6 in response to the oxidative stress, we generated *msh6* knockout cell lines using the CRISPR/Cas9 protocol. Recently, a *T. cruzi* gene editing protocol using recombinant Cas9 derived from *Staphylococcus aureus* (rSaCas9) expressed in *Escherichia coli* was described (Soares Medeiros et al., 2017; Burle-Caldas et al., 2018). We transfected epimastigotes with two sgRNAs complexed with rSaCas9 together and a donor sequence fragment. As shown in Figure 5A, the donor fragment contains *msh6* sequences and the Neomycin phosphotransferase gene (Neo^R) flanked by intergenic sequences that provide trans-splicing and poly-A addition sites (HX1_Neo_Gapdh cassette), as well as sequences corresponding to 5' and 3' regions of the *msh6* gene. After transfection DNA from G418 resistant parasites was verified by PCR analyses. While *Tcmsh6* coding sequence has 3,009 base pairs (bp), when the *msh6* CDS is replaced by the Neo^R cassette, the PCR product using the same primer pair generated a smaller fragment with 2,673 bp (Figure 5B). Figure 5B also showed that without G418 drug selection, in the absence of the Cas9 RNP, no parasites with disrupted *msh6* gene were generated. After transfection with the Cas9 RNP and donor DNA, only clones with one allele disrupted were generated. To disrupt the second allele, we performed a second round of transfection of one heterozygous mutant



cloned cell line that is G418 resistant. PCR analyses of DNA extracted from four double resistant cloned cell lines showed that the 3.009 pb fragment was replaced by the Hygromycin cassette, which has 3.520 bp and contains the hygromycin resistance gene flanked by trans-splicing and poly-A addition signals (HX1_Hygro_Gapdh cassette) as well as 5' and 3' *msh6* sequences. As shown in **Figure 5C** the correct insertion of the Neo^R and Hyg^R cassettes, interrupting both *msh6* alleles, was confirmed by PCR-amplification with primers annealing in the *msh6* 5' UTR and CDS (P1F–P2R, see left panel), in the *msh6* 5' UTR and in the Neo^R gene (P3R or P4R, see middle panel) and in the *msh6* 5' UTR and the HygR gene (P1F and P2R, right panel). The PCR-amplified *msh6* fragment of 1,689 bp was observed only in WT parasites but not in the four *Tcmsh6* null mutants cell lines. On the other hand, PCR fragments amplified with the *msh6* and NeoR primer of 1.919 bp and with the *msh6* and HygroR of 2,802 bp were only detected with DNA from transfected cloned cell lines and not with DNA from WT parasites (**Figure 5C**).

To evaluate if TcMSH6 knockout affects the MMR capacity of the mutant cell lines, parasites were treated with MNNG

and compared with treated WT cells. As shown in **Figure 6A**, a significant increase in the tolerance to MNNG treatment was observed in all *msh6* mutants, including the *Tcmsh6* heterozygous (*Tcmsh6*^{+/−}) and null mutants (*Tcmsh6*^{−/−}), compared to WT parasites. To ask if the phenotype observed with *Tcmsh2* null mutants in response to treatment with H₂O₂ is also observed in *Tcmsh6* mutants, we compared the growth of WT cells and two cloned heterozygous mutants, as well as two cloned homozygous *msh6* mutants, after treatment for 30 min with 100 μM H₂O₂ and incubating in LIT medium for 72 h. As shown in **Figure 6B** *Tcmsh6*^{+/−} and *Tcmsh6*^{−/−} mutants are more susceptible to the treatment with H₂O₂ than WT cells. To analyze the reversion of the *msh6* knockout phenotype, we transfected two *Tcmsh6*^{−/−} cloned cell lines with the pTREX vector containing the complete *msh6* coding region fused to an HA tag. Western blot analyses with anti-HA antibody showed the expression of MSH6::HA in cell extracts derived from transfected cultures (**Supplementary Figure 4**). Although no significant differences in the tolerance to MNNG were observed, both MSH6 re-expresser cell lines showed reversion of the susceptibility to H₂O₂ treatment (**Figures 6C, D**).

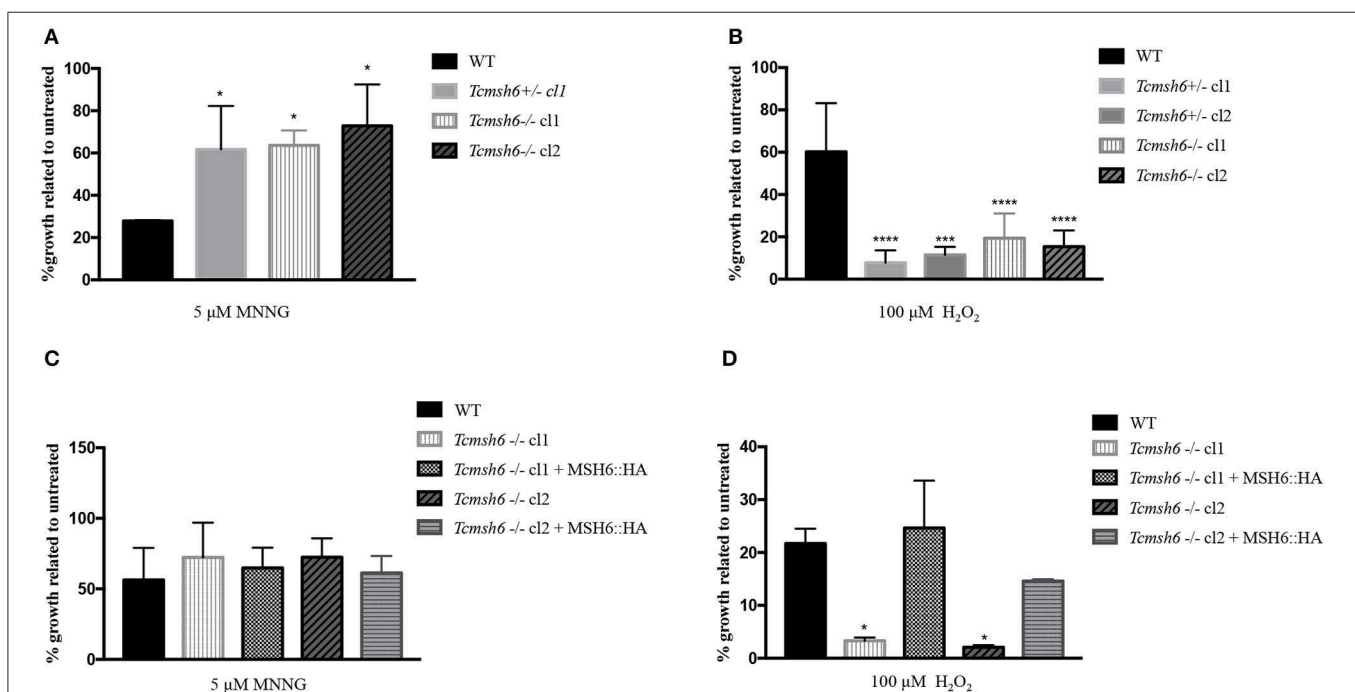


FIGURE 6 | Evaluation of susceptibility of *T. cruzi* *msh6* mutants to N-methyl-N'-nitro-N-nitrosoguanidine (MNNG) and H₂O₂. **(A)** *T. cruzi* WT and MSH6 mutants (*Tcmsh6*^{+/−} and *Tcmsh6*^{−/−}) were grown in culture medium with 0 μM or 5 μM MNNG. Cell viability was measured after 72 h and is plotted as the percentage survival of the MNNG treated cells relative to untreated cultures. Vertical lines indicate standard deviation. The graph represents the average of two independent experiments performed in duplicate. **(B)** *T. cruzi* epimastigote cells wild type (WT), *Tcmsh6*^{+/−} (clones 1 and 2) and *Tcmsh6*^{−/−} (clones 1 and 2) mutants were incubated in the presence or absence of H₂O₂ 100 μM for 30 min in PBS 1x and then allowed to grow in LIT medium for 72 h, after which cell viability was determined and plotted as percentage survival of the treated cells relative to untreated. **(C)** *T. cruzi* WT, *Tcmsh6*^{−/−} and *Tcmsh6*^{−/−} transfected to express MSH6::HA were grown in culture medium with 0 μM or 5 μM MNNG. Cell viability was measured after 72 h and is plotted as the percentage survival of the MNNG treated cells relative to untreated cultures. Vertical lines indicate standard deviation. The graph represents the average of two independent experiments, each performed in duplicate. **(D)** *T. cruzi* WT, *Tcmsh6*^{−/−} and *Tcmsh6*^{−/−} transfected to express MSH6::HA mutants were incubated in the presence or absence of 100 μM H₂O₂ for 30 min in PBS 1x and then allowed to grow in LIT medium for 72 h, after which cell viability was determined and plotted as percentage survival of the treated cells relative to untreated. Data represent the average of three independent experiments, each performed in duplicate. Vertical lines show standard deviation. *****p* < 0.0001, ****p* < 0.001, **p* < 0.1: determined by one-way ANOVA with Bonferroni post-test of mutants relative to wild type cells.

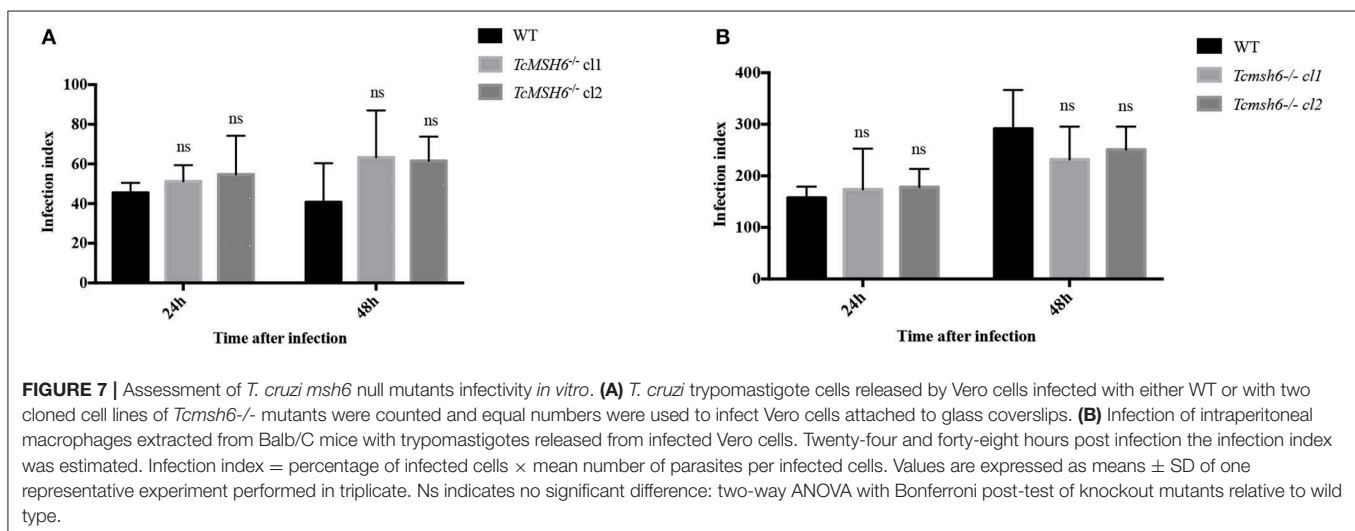
Because we observed that *msh6* mutants are more sensitive to H_2O_2 treatment, we investigated whether deletion of *msh6* gene affects parasite intracellular survival and amastigote multiplication. Different from *T. brucei*, *T. cruzi* has a part of its life cycle as an intracellular amastigote stage, which must cope with the generation of ROS by infected cells (Paiva et al., 2018). We investigated the role of MSH6 in response to the oxidative stress generated by two different cell types: epithelial cells and intraperitoneal macrophages extracted from BALB/c mice. Both cell types, previously attached to a glass coverslip, were infected with equal numbers of WT and *Tcmsh6*^{-/-} trypomastigotes released from infected Vero cells. As shown in **Figure 7** no differences in the infection index were observed between the WT and *Tcmsh6*^{-/-} after infection of Vero cells (**Figure 7A**) or macrophages (**Figure 7B**). **Supplementary Figure 5** shows that, for infected Vero cells, we observed no differences in the number of infected cells (**Supplementary Figure 5A**) or in the number of intracellular amastigotes per infected cells at 24 h or 48 h post-infection (**Supplementary Figure 5B**). Similarly, no differences in the number of infected macrophages (**Supplementary Figure 5C**), or in the number of intracellular parasites per infected macrophages (**Supplementary Figure 5D**), were observed between WT and *Tcmsh6*^{-/-} mutants.

DISCUSSION

We have shown previously that the response to oxidative DNA damage works differently in *T. brucei* and *T. cruzi*, and that this response is dependent on the life cycle stage of each parasite. A summary of the responses, to the two genotoxic agents, observed in the different *T. brucei* and *T. cruzi* knockout mutants is provided in **Supplementary Table 3**. In *T. brucei*, MSH2 appears to be directly involved with the response to H_2O_2 exposure, since loss of MSH2 in BSFs resulted in increased sensitivity to the oxidative agent, whereas MSH2 loss in PCF cells resulted in increased tolerance to H_2O_2 . Increased tolerance to H_2O_2 exposure was also seen in *T. cruzi* epimastigote MSH2

null mutants, which also showed increased survival in ROS-producing macrophages, compared with WT parasites. Similar to the phenotype observed in other eukaryotes, loss of MSH2 resulted in impaired MMR, both in *T. brucei* and *T. cruzi* mutants, as demonstrated by the increased tolerance to the alkylator MNNG. Because altered H_2O_2 tolerance was not observed in *T. brucei* BSF or PCF cells lacking MLH1, a protein that acts downstream from MSH2 in the MMR pathway, we hypothesized that MSH2 displays a dual role, one as an MMR component and a second role as a factor involved in the response to oxidative stress, in a way that is independent of MLH1. We have also hypothesized that the increased oxidative resistance of *msh2* null mutants generated in procyclic *T. brucei* and in *T. cruzi* epimastigotes may be due to adaptation of the insect stages of these parasites to MSH2 loss. This hypothesis is corroborated by the necessity of having a gradual process to obtain *T. cruzi* epimastigotes mutants with both *msh2* alleles deleted. We have also speculated that the differences observed in the phenotypic outcomes observed in *T. brucei* MSH2 mutants generated in PCFs may be explained by the greater burden of oxidative stress that the parasites are submitted during their insect life cycle stages (Grazielle-Silva et al., 2015).

Here we asked whether the role played by *T. brucei* and *T. cruzi* MSH2 in the oxidative stress response is MMR-independent or if MSH2 acts together with other MMR proteins in a non-canonical pathway. Toward that, we generated *T. brucei* BSF mutants with deleted *msh3* or *msh6*, and *T. cruzi* epimastigotes *msh6* null mutants. As indicated above, studies with *T. brucei* *mlh1* knockout cell lines have already indicated that this MMR protein is not involved in the oxidative stress response (Grazielle-Silva et al., 2015). Initially, co-immunoprecipitation assays followed by mass spectrometry showed that *T. brucei* MSH2 physically interacts with MSH3 and MSH6 in both BSF and PCF forms, though no other proteins were identified in the co-immunoprecipitation complex that contains MSH2. We also showed that, MSH2 interacts with MSH6 in *T. cruzi* epimastigotes. We have repeated the co-immunoprecipitation assay after treatment with MNNG or



H₂O₂, but no novel interactions with MSH2 could be identified (data not shown).

In contrast to *msh3* knockout parasites, *T. brucei msh6* null mutants, but not the heterozygous mutants, showed impaired MMR, since tolerance to MNNG was increased in *msh6*^{-/-} BSFs compared to WT BSF, similar to previous observation in BSF *msh2*^{-/-} mutants (Bell and McCulloch, 2003). O⁶meG lesions can be formed after DNA alkylation by MNNG and attempts to repair this damage leads to futile repair cycles that ends up signaling or causing cell death (Gupta et al., 2018). A similar phenotype was observed with *T. cruzi msh6* null mutants after MNNG treatment. These results thus indicate that the absence of MSH6 results in non-functional MMR in both parasites. Although we showed that MSH3 is a binding partner to MSH2 in both *T. brucei* BSFs and PCFs, MSH3 does not seem to be involved in the response to this alkylating damage. What substrates the *T. brucei* MSH2-MSH3 heterodimer acts on remain to be determined.

After showing evidence that the lack of MSH6 affects the MMR pathway in both parasites, we showed that in *T. brucei* BSFs, MSH3, and MSH6 seems not to be involved in the oxidative stress response, using the same experimental conditions applied previously with *msh2* null mutants. The effect of disrupting *msh3* and *msh6* genes in PCFs still needs to be verified. Also, to test the hypothesis that *T. brucei* MSH2 is involved in the response to oxidative DNA damage in a way that is independent of other MMR components, a double mutant *Tbmsh6*^{-/-}*msh3*^{-/-} needs to be generated to compare the differences in the response to H₂O₂ treatment with WT parasites. With a double *msh3/msh6* mutant, we would be able to exclude the possibility that, in the absence of MSH6, MSH2 may still form a complex with MSH3 and provide a role in tackling oxidative stress.

Nevertheless, the lack of sensitivity of *msh6* null mutants to oxidative damage adds detail to our hypothesis that MSH2 may provide a unique function in this role, as initially shown by our previous studies showing that *T. brucei* BSF *msh2* null mutants complemented with *T. cruzi msh2* have restored their capacity to respond to oxidative stress response, but have not restored MMR function (Machado-Silva et al., 2008).

The results obtained with the analyses of *T. brucei* mutants are in sharp contrast with the effect of disrupting the *msh6* gene in *T. cruzi* epimastigotes, which showed a clear effect on the susceptibility to H₂O₂ treatment. Besides increased susceptibility to oxidative stress, *T. cruzi msh6*^{-/-} mutants display increased resistance to MNNG, suggesting impaired MMR. Although we were able to demonstrate that re-expressing MSH6 causes the sensitivity to H₂O₂ to be reverted, we do not see a significant reversion of the tolerance to MNNG, which may due to an imbalanced expression of MSH6 and altered dynamics of MSH2-MSH6 function during MMR. The effect observed with *T. cruzi msh6* mutants is in line with the expected role of MSH6 as a MSH2 partner during the initial steps of the MMR. However, because in *T. cruzi* epimastigotes *msh2* knockouts presented an increased tolerance to H₂O₂ treatment, whereas MSH6 deficient cells were more sensitive to the same treatment, the role of MSH6 as a MSH2 partner in the response to oxidative stress is unclear. The fact that re-expression of MSH6 in the *msh6* knockout mutants reverts the H₂O₂ susceptibility further corroborates its

role as a component of the DNA repair machinery involved with the oxidative stress response. It is possible that the generation of *T. cruzi msh6* deletions with the highly efficient CRISPR/Cas9 protocol makes it impossible for an adaptation process that we speculated that may have resulted from the *msh2* disruption obtained with the classical HR-based protocol, which has a slower selection of drug resistant parasites. Thus, in contrast to the *msh2* mutants, the rapid generation of *msh6*^{-/-} may not have allowed the mutated parasites to adapt their metabolism to cope with the oxidative stress response in the absence of a MMR protein (Grazielle-Silva et al., 2015). Recent evidence suggests that an oxidative environment is favorable for intracellular parasite survival and infection (Paiva et al., 2018). The parasite has an arsenal of enzymes to assure infection and keeps homeostasis while going into different redox environments inside the hosts (Mesías et al., 2019). How this plasticity is achieved is still unclear. Long-term cultivation of *T. cruzi* induces mutational events. This frequency is increased when parasites are cultivated in sub-lethal doses of H₂O₂ (Torres-Silva et al., 2018). In trypanosomatids, MMR proteins might have an additional role in recognizing DNA oxidative damage and act as signaling molecules. It is possible that after long-term cultivation of *T. cruzi msh6*^{-/-} in sub-lethal doses of H₂O₂ parasites adapted to the oxidative stress, such as *T. cruzi msh2*^{-/-} could be obtained. It should be also considered that, since MSH2 forms pairs with MSH3 or MSH6, the formation of the heterodimer may be required for the stability of MSH2 and loss of MSH6 could lead to a destabilization and a direct impact on the levels of MSH2 protein. Consequently, in a model where the oxidative damage response mechanism requires MSH2 independently of other MMR proteins, the lack of MSH6 may have an indirect effect by reducing MSH2 half-life. Taken together, our data suggest that MSH2, but not MSH6, has a predominant role in the oxidative stress response in *T. cruzi*. The observation showing no differences in the survival rates after infection of two different cell types with *T. cruzi msh6*^{-/-}, whereas a clear difference was observed when macrophages were infected with *msh2* mutants compared to WT parasites (Grazielle-Silva et al., 2015), also points toward a distinct role between these two MMR components in the oxidative stress response of *T. cruzi*.

With the current data, one cannot conclude whether *T. cruzi* MSH6 acts together with MSH2 to recognize oxidative damage, or if MSH6 acts by maintaining the stability of the MutSα heterodimer, which may be also important for *T. brucei* MSH2. In a scenario of a non-canonical MMR function in the oxidative stress response it is also possible that, even though MSH6 in *T. cruzi* is also involved in the oxidative stress response, by recognizing DNA damage through MutSα heterodimer, MSH2 may have a more predominant role with the recruitment of proteins related to damage signaling, such as ATR (Wang and Qin, 2003; Stojic et al., 2004; Yan et al., 2014). In *Leishmania major* has been demonstrated that ATR is involved in the oxidative stress response (da Silva et al., 2018). Clearly, the involvement of other signaling molecules in the oxidative stress response in *T. cruzi* and *T. brucei* needs to be further investigated. Although it is not surprising that the oxidative stress response works differently in *T. cruzi* and *T. brucei*, since these parasites

have diverged around 100 million years ago (Stevens et al., 1999), the additional studies needed to clarify this response in these two important human pathogens may still bring new interesting surprises.

DATA AVAILABILITY STATEMENT

The raw data supporting the conclusions of this article will be made available by the authors, without undue reservation, to any qualified researcher.

ETHICS STATEMENT

The animal study was reviewed and approved by Comissão de Ética no USO de Animais - CEUA - UFMG.

AUTHOR CONTRIBUTIONS

VG-S, TZ, CM, RM, and ST conceived and designed the experiments. VG-S, TZ performed the experiments. VG-S, TZ, RB, CM, RM, and ST analyzed the data. RB, CM, RM, and ST contributed reagents, materials and analysis tools. VG-S, RM and ST wrote the paper.

FUNDING

This study was supported, in Brazil, by Fundação de Apoio à Pesquisa do Estado de Minas Gerais (FAPEMIG), the Conselho

Nacional de Desenvolvimento Científico e Tecnológico (CNPq), the Coordenação de Aperfeiçoamento de Pessoal de Nível Superior (Capes, grant number 8320/12-8 and 1785670 to VG-S), and the Instituto Nacional de Ciência e Tecnologia de Vacinas (INCTV). In the UK, this work was supported by the Biotechnology and Biological Sciences Research Council (BBSRC [BB/K006495/1, BB/M028909/1, BB/N016165/1]) and the Wellcome Center for Integrative Parasitology is supported by core funding from the Wellcome Trust [104111].

ACKNOWLEDGMENTS

The authors wish to thank Craig Lapsley and Renata Barbosa Peixoto for technical support and DNA sequencing, Rafael André Ferreira for helping with macrophage infections, Suzanne McGill for helping with Mass Spectrometry analysis, as well as João Luiz Cunha and Daniella Bartholomeu for helpful discussion regarding *T. cruzi* genome annotation. Microscopy analyses were done at Centro de Aquisição e Processamento de Imagens (CAPI-ICB/UFMG).

SUPPLEMENTARY MATERIAL

The Supplementary Material for this article can be found online at: <https://www.frontiersin.org/articles/10.3389/fcimb.2020.00154/full#supplementary-material>

REFERENCES

- Alsford, S., and Horn, D. (2008). Single-locus targeting constructs for reliable regulated RNAi and transgene expression in *Trypanosoma brucei*. *Mol. Biochem. Parasitol.* 161, 76–79. doi: 10.1016/j.molbiopara.2008.05.006
- Antinori, S., Galimberti, L., Bianco, R., Grande, R., Galli, M., and Corbellino, M. (2017). Chagas disease in Europe: a review for the internist in the globalized world. *Eur. J. Intern. Med.* 43, 6–15. doi: 10.1016/j.ejim.2017.05.001
- Bell, J. S., Harvey, T. I., Sims, A.-M., and McCulloch, R. (2004). Characterization of components of the mismatch repair machinery in *Trypanosoma brucei*. *Mol. Microbiol.* 51, 159–173. doi: 10.1046/j.1365-2958.2003.03804.x
- Bell, J. S., and McCulloch, R. (2003). Mismatch repair regulates homologous recombination, but has little influence on antigenic variation, in *Trypanosoma brucei*. *J. Biol. Chem.* 278, 45182–45188. doi: 10.1074/jbc.M308123200
- Berriman, M., Ghedin, E., Hertz-Fowler, C., Blandin, G., Renaud, H., Bartholomeu, D. C., et al. (2005). The genome of the African trypanosome *Trypanosoma brucei*. *Science* 309, 416–422. doi: 10.1126/science.1112642
- Brener, Z. (1973). Biology of *Trypanosoma cruzi*. *Annu. Rev. Microbiol.* 27, 347–382. doi: 10.1146/annurev.mi.27.100173.002023
- Burkard, G., Fragoso, C. M., and Roditi, I. (2007). Highly efficient stable transformation of bloodstream forms of *Trypanosoma brucei*. *Mol. Biochem. Parasitol.* 153, 220–223. doi: 10.1016/j.molbiopara.2007.02.008
- Burle-Caldas, G. A., Soares-Simões, M., Lemos-Pechnicki, L., DaRocha, W. D., and Teixeira, S. M. R. (2018). Assessment of two CRISPR-Cas9 genome editing protocols for rapid generation of *Trypanosoma cruzi* gene knockout mutants. *Int. J. Parasitol.* 48, 591–596. doi: 10.1016/j.ijpara.2018.02.002
- Camargo, E. P. (1964). Growth and differentiation in *trypanosoma cruzi*. I. origin of metacyclic trypanosomes in liquid media. *Rev. Inst. Med. Trop.* 6, 93–100.
- Campos, P. C., Silva, V. G., Furtado, C., Machado-Silva, A., Darocha, W. D., Peloso, E. F., et al. (2011). *Trypanosoma cruzi* MSH2: functional analyses on different parasite strains provide evidences for a role on the oxidative stress response. *Mol. Biochem. Parasitol.* 176, 8–16. doi: 10.1016/j.molbiopara.2010.11.001
- Cevallos, A. M., and Hernández, R. (2014). Chagas' disease: pregnancy and congenital transmission. *Biomed. Res. Int.* 2014:401864. doi: 10.1155/2014/401864
- da Silva, R. B., Machado, C. R., Rodrigues, A. R. A., and Pedrosa, A. L. (2018). Selective human inhibitors of ATR and ATM render *Leishmania* major promastigotes sensitive to oxidative damage. *PLoS ONE* 13:e0205033. doi: 10.1371/journal.pone.0205033
- DaRocha, W. D., Silva, R. A., Bartholomeu, D. C., Pires, S. F., Freitas, J. M., Macedo, A. M., et al. (2004). Expression of exogenous genes in *Trypanosoma cruzi*: improving vectors and electroporation protocols. *Parasitol. Res.* 92, 113–120. doi: 10.1007/s00436-003-1004-5
- de Wind, N., Dekker, M., Berns, A., Radman, M., and te Riele, H. (1995). Inactivation of the mouse Msh2 gene results in mismatch repair deficiency, methylation tolerance, hyperrecombination, and predisposition to cancer. *Cell* 82, 321–330. doi: 10.1016/0092-8674(95)90319-4
- Edelbrock, M. A., Kaliyaperumal, S., and Williams, K. J. (2013). Structural, molecular and cellular functions of MSH2 and MSH6 during DNA mismatch repair, damage signaling and other noncanonical activities. *Mutat. Res.* 743–744, 53–66. doi: 10.1016/j.mrfmmm.2012.12.008
- El-Sayed, N. M., Myler, P. J., Bartholomeu, D. C., Nilsson, D., Aggarwal, G., Tran, A.-N., et al. (2005). The genome sequence of *Trypanosoma cruzi*, etiologic agent of Chagas disease. *Science* 309, 409–415. doi: 10.1126/science.1112631
- Foyer, C. H. (2018). Reactive oxygen species, oxidative signaling and the regulation of photosynthesis. *Environ. Exp. Bot.* 154, 134–142. doi: 10.1016/j.envexpbot.2018.05.003
- Grazielle-Silva, V., Zeb, T. F., Bolderson, J., Campos, P. C., Miranda, J. B., Alves, C. L., et al. (2015). Distinct phenotypes caused by mutation of MSH2 in *Trypanosoma* insect and mammalian life cycle forms are associated with

- parasite adaptation to oxidative stress. *PLoS Negl. Trop. Dis.* 9:e0003870. doi: 10.1371/journal.pntd.0003870
- Gupta, D., and Heinen, C. D. (2019). The mismatch repair-dependent DNA damage response: mechanisms and implications. *DNA Repair* 78, 60–69. doi: 10.1016/j.dnarep.2019.03.009
- Gupta, D., Lin, B., Cowan, A., and Heinen, C. D. (2018). ATR-Chk1 activation mitigates replication stress caused by mismatch repair-dependent processing of DNA damage. *Proc. Natl. Acad. Sci. U.S.A.* 115, 1523–1528. doi: 10.1073/pnas.1720355115
- Hirumi, H., and Hirumi, K. (1994). Axenic culture of African trypanosome bloodstream forms. *Parasitol. Today* 10, 80–84. doi: 10.1016/0169-4758(94)90402-2
- Isaac, C., Ohiole, J. A., Ebhodaghe, F., Igbinosa, I. B., and Eze, A. A. (2017). Animal African Trypanosomiasis in Nigeria: a long way from elimination/eradication. *Acta Trop.* 176, 323–331. doi: 10.1016/j.actatropica.2017.08.032
- Iyer, R. R., Pluciennik, A., Napierala, M., and Wells, R. D. (2015). DNA triplet repeat expansion and mismatch repair. *Annu. Rev. Biochem.* 84, 199–226. doi: 10.1146/annurev-biochem-060614-034010
- Kaniak, A., Dzierzbicki, P., Rogowski, A. T., Malc, E., Fikus, M., and Ciesla, Z. (2009). Msh1p counteracts oxidative lesion-induced instability of mtDNA and stimulates mitochondrial recombination in *Saccharomyces cerevisiae*. *DNA Repair* 8, 318–329. doi: 10.1016/j.dnarep.2008.11.004
- Kim, D., Fishel, R., and Lee, J.-B. (2018). Coordinating multi-protein mismatch repair by managing diffusion mechanics on the DNA. *J. Mol. Biol.* 430, 4469–4480. doi: 10.1016/j.jmb.2018.05.032
- Kumar, C., Piacente, S. C., Sibert, J., Bukata, A. R., O'Connor, J., Alani, E., et al. (2011). Multiple factors insulate Msh2-Msh6 mismatch repair activity from defects in Msh2 domain I. *J. Mol. Biol.* 411, 765–780. doi: 10.1016/j.jmb.2011.06.030
- LeBlanc, S. J., Gauer, J. W., Hao, P., Case, B. C., Hingorani, M. M., Weninger, K. R., et al. (2018). Coordinated protein and DNA conformational changes govern mismatch repair initiation by MutS. *Nucleic Acids Res.* 46, 10782–10795. doi: 10.1093/nar/gky865
- Lee, K., Tosti, E., and Edelman, W. (2016). Mouse models of DNA mismatch repair in cancer research. *DNA Repair* 38, 140–146. doi: 10.1016/j.dnarep.2015.11.015
- Li, G.-M. (2008). Mechanisms and functions of DNA mismatch repair. *Cell Res.* 18, 85–98. doi: 10.1038/cr.2007.115
- Li, Z., Pearlman, A. H., and Hsieh, P. (2016). DNA mismatch repair and the DNA damage response. *DNA Repair* 38, 94–101. doi: 10.1016/j.dnarep.2015.11.019
- Machado-Silva, A., Cerqueira, P. G., Grazielle-Silva, V., Gadelha, F. R., Peloso, E., de Figueiredo Peloso, E., et al. (2016). How *Trypanosoma cruzi* deals with oxidative stress: antioxidant defence and DNA repair pathways. *Mutat. Res. Rev. Mutat. Res.* 767, 8–22. doi: 10.1016/j.mrrrev.2015.12.003
- Machado-Silva, A., Teixeira, S. M. R., Franco, G. R., Macedo, A. M., Pena, S. D. J., McCulloch, R., et al. (2008). Mismatch repair in *Trypanosoma brucei*: heterologous expression of MSH2 from *Trypanosoma cruzi* provides new insights into the response to oxidative damage. *Gene* 411, 19–26. doi: 10.1016/j.gene.2007.12.021
- Matthews, K. R. (2005). The developmental cell biology of *Trypanosoma brucei*. *J. Cell. Sci.* 118, 283–290. doi: 10.1242/jcs.01649
- Mesías, A. C., Garg, N. J., and Zago, M. P. (2019). Redox balance keepers and possible cell functions managed by Redox homeostasis in *Trypanosoma cruzi*. *Front. Cell Infect. Microbiol.* 9:435. doi: 10.3389/fcimb.2019.00435
- Paiva, C. N., Medei, E., and Bozza, M. T. (2018). ROS and *Trypanosoma cruzi*: fuel to infection, poison to the heart. *PLoS Pathog.* 14:e1006928. doi: 10.1371/journal.ppat.1006928
- Passos-Silva, D. G., Rajão, M. A., Nascimento de Aguiar, P. H., Vieira-da-Rocha, J. P., Machado, C. R., and Furtado, C. (2010). Overview of DNA repair in *Trypanosoma cruzi*, *Trypanosoma brucei*, and leishmania major. *J. Nucleic Acids* 2010:840768. doi: 10.4061/2010/840768
- Pilzecker, B., and Jacobs, H. (2019). Mutating for good: DNA damage responses during somatic hypermutation. *Front. Immunol.* 10:438. doi: 10.3389/fimmu.2019.00438
- Pogorzala, L., Mookerjee, S., and Sia, E. A. (2009). Evidence that msh1p plays multiple roles in mitochondrial base excision repair. *Genetics* 182, 699–709. doi: 10.1534/genetics.109.103796
- Ráz, B., Iten, M., Grether-Bühler, Y., Kaminsky, R., and Brun, R. (1997). The Alamar blue assay to determine drug sensitivity of African trypanosomes (*T.b. rhodesiense* and *T.b. gambiense*) in vitro. *Acta Trop.* 68, 139–147. doi: 10.1016/s0001-706x(97)00079-x
- Santana, R. A. G., Guerra, M. G. V. B., Sousa, D. R., Couceiro, K., Ortiz, J. V., Oliveira, M., et al. (2019). Oral transmission of *Trypanosoma cruzi*, Brazilian Amazon. *Emerging Infect. Dis.* 25, 132–135. doi: 10.3201/eid2501.180646
- Schumann Burkard, G., Jutzi, P., and Roditi, I. (2011). Genome-wide RNAi screens in bloodstream form trypanosomes identify drug transporters. *Mol. Biochem. Parasitol.* 175, 91–94. doi: 10.1016/j.molbiopara.2010.09.002
- Soares Medeiros, L. C., South, L., Peng, D., Bustamante, J. M., Wang, W., Bunkofski, M., et al. (2017). Rapid, selection-free, high-efficiency genome editing in protozoan parasites using CRISPR-Cas9 Ribonucleoproteins. *MBio* 8:e01788-17. doi: 10.1128/mBio.01788-17
- Spies, M., and Fishel, R. (2015). Mismatch repair during homologous and homeologous recombination. *Cold Spring Harb. Perspect. Biol.* 7:a022657. doi: 10.1101/cshperspect.a022657
- Stevens, J. R., Noyes, H. A., Dover, G. A., and Gibson, W. C. (1999). The ancient and divergent origins of the human pathogenic trypanosomes, *Trypanosoma brucei* and *T. cruzi*. *Parasitology* 118, 107–116. doi: 10.1017/s0031182098003473
- Stojic, L., Mojas, N., Cejka, P., Di Pietro, M., Ferrari, S., Marra, G., et al. (2004). Mismatch repair-dependent G2 checkpoint induced by low doses of SN1 type methylating agents requires the ATR kinase. *Genes Dev.* 18, 1331–1344. doi: 10.1101/gad.294404
- Tiengwe, C., Marcello, L., Farr, H., Gadelha, C., Burchmore, R., Barry, J. D., et al. (2012). Identification of ORC1/CDC6-interacting factors in *Trypanosoma brucei* reveals critical features of origin recognition complex architecture. *PLoS ONE* 7:e32674. doi: 10.1371/journal.pone.0032674
- Torres-Silva, C. F., Repolés, B. M., Ornelas, H. O., Macedo, A. M., Franco, G. R., Junho Pena, S. D., et al. (2018). Assessment of genetic mutation frequency induced by oxidative stress in *Trypanosoma cruzi*. *Genet. Mol. Biol.* 41, 466–474. doi: 10.1590/1678-4685-GMB-2017-0281
- Vazquez, M. P., and Levin, M. J. (1999). Functional analysis of the intergenic regions of TcP2beta gene loci allowed the construction of an improved *Trypanosoma cruzi* expression vector. *Gene* 239, 217–225. doi: 10.1016/s0378-1119(99)00386-8
- Wang, Y., and Qin, J. (2003). MSH2 and ATR form a signaling module and regulate two branches of the damage response to DNA methylation. *Proc. Natl. Acad. Sci. U.S.A.* 100, 15387–15392. doi: 10.1073/pnas.2536810100
- WHO (2019a). *Chagas Disease (American trypanosomiasis)*. Available online at: [https://www.who.int/news-room/fact-sheets/detail/chagas-disease-\(american-trypanosomiasis\)](https://www.who.int/news-room/fact-sheets/detail/chagas-disease-(american-trypanosomiasis)) (accessed October 12, 2019).
- WHO (2019b). *Trypanosomiasis, Human African (Sleeping Sickness)*. Available online at: [https://www.who.int/news-room/fact-sheets/detail/trypanosomiasis-human-african-\(sleeping-sickness\)](https://www.who.int/news-room/fact-sheets/detail/trypanosomiasis-human-african-(sleeping-sickness)) (accessed October 12, 2019).
- Yan, S., Sorrell, M., and Berman, Z. (2014). Functional interplay between ATM/ATR-mediated DNA damage response and DNA repair pathways in oxidative stress. *Cell. Mol. Life Sci.* 71, 3951–3967. doi: 10.1007/s00018-014-1666-4

Conflict of Interest: The authors declare that the research was conducted in the absence of any commercial or financial relationships that could be construed as a potential conflict of interest.

Copyright © 2020 Grazielle-Silva, Zeb, Burchmore, Machado, McCulloch and Teixeira. This is an open-access article distributed under the terms of the Creative Commons Attribution License (CC BY). The use, distribution or reproduction in other forums is permitted, provided the original author(s) and the copyright owner(s) are credited and that the original publication in this journal is cited, in accordance with accepted academic practice. No use, distribution or reproduction is permitted which does not comply with these terms.



GCN2-Like Kinase Modulates Stress Granule Formation During Nutritional Stress in *Trypanosoma cruzi*

Amaranta Muniz Malvezzi¹, Mirella Aricó¹, Normanda Souza-Melo¹, Gregory Pedroso dos Santos¹, Paula Bittencourt-Cunha¹, Fabiola Barbieri Holetz² and Sergio Schenkman^{1*}

¹ Departamento de Microbiologia, Imunologia e Parasitologia, Escola Paulista de Medicina, Universidade Federal de São Paulo, São Paulo, Brazil, ² Instituto Carlos Chagas, Fundação Oswaldo Cruz-Fiocruz, Curitiba, Brazil

OPEN ACCESS

Edited by:

Noelia Lander,
University of Georgia, United States

Reviewed by:

Alejandra Schoijet,
CONICET Instituto de Investigaciones
en Ingeniería Genética y Biología
Molecular Dr. Héctor N. Torres
(INGEBI), Argentina

Ronald Drew Etheridge,
University of Georgia, United States

*Correspondence:

Sergio Schenkman
sschenkman@unifesp.br

Specialty section:

This article was submitted to
Parasite and Host,
a section of the journal
Frontiers in Cellular and Infection
Microbiology

Received: 11 November 2019

Accepted: 20 March 2020

Published: 16 April 2020

Citation:

Malvezzi AM, Aricó M, Souza-Melo N, dos Santos GP, Bittencourt-Cunha P, Holetz FB and Schenkman S (2020) GCN2-Like Kinase Modulates Stress Granule Formation During Nutritional Stress in *Trypanosoma cruzi*. *Front. Cell. Infect. Microbiol.* 10:149. doi: 10.3389/fcimb.2020.00149

The integrated stress response in eukaryotic cells is an orchestrated pathway that leads to eukaryotic Initiation Factor 2 alpha subunit (eIF2 α) phosphorylation at ser51 and ultimately activates pathways to mitigate cellular damages. Three putative kinases (*Tck1*, *Tck2*, and *Tck3*) are found in the *Trypanosoma cruzi* genome, the flagellated parasite that causes Chagas disease. These kinases present similarities to other eukaryotic eIF2 α kinases, exhibiting a typical insertion loop in the kinase domain of the protein. We found that this insertion loop is conserved among kinase 1 of several *T. cruzi* strains but differs among various Kinetoplastidae species, suggesting unique roles. Kinase 1 is orthologous of GCN2 of several eukaryotes, which have been implicated in the eIF2 α ser51 phosphorylation in situations that mainly affects the nutrients levels. Therefore, we further investigated the responses to nutritional stress of *T. cruzi* devoid of *Tck1* generated by CRISPR/Cas9 gene replacement. In nutrient-rich conditions, replicative *T. cruzi* epimastigotes depleted of *Tck1* proliferate as wild type cells but showed increased levels of polysomes relative to monosomes. Upon nutritional deprivation, the polysomes decreased more than in *Tck1* depleted line. However, eIF2 α is still phosphorylated in *Tck1* depleted line, as in wild type parasites. eIF2 α phosphorylation increased at longer incubations times, but KO parasites showed less accumulation of ribonucleoprotein granules containing ATP-dependent RNA helicase involved in mRNA turnover (DHH1) and Poly-A binding protein (PABP1). Additionally, the formation of metacyclic-trypomastigotes is increased in the absence of *Tck1* compared to controls. These metacyclics, as well as tissue culture trypomastigotes derived from the *Tck1* knockout line, were less infective to mammalian host cells, although replicated faster inside mammalian cells. These results indicate that GCN2-like kinase in *T. cruzi* affects stress granule formation, independently of eIF2 α phosphorylation upon nutrient deprivation. It also modulates the fate of the parasites during differentiation, invasion, and intracellular proliferation.

Keywords: GCN2, eIF2 α , *Trypanosoma cruzi*, *Tck1*, phosphorylation, stress-granules, CRISPR/Cas9

INTRODUCTION

The formation of the ternary complex is the first step of the cap-dependent translation initiation process and comprises the eukaryotic initiation factor 2 (eIF2), the methionine-tRNAⁱ and a GTP molecule. eIF2 is a heterotrimeric complex that includes the eIF2 α subunit, which can be phosphorylated at Ser 51; eIF2 β , which binds to tRNA^{met}, mRNA and others initiation factors; and eIF2 γ that binds to the GTP and possesses GTPase activity (Hinnebusch and Lorsch, 2012). This complex scans the mRNA to find the AUG initiation codon and delivers the methionine for protein synthesis initiation (Jennings and Pavitt, 2014). For this, the ternary complex associates with the 40S minor ribosomal subunit and other translation factors such as eIF1, eIF1A, eIF3, and eIF5 to form the 43S pre-initiation complex. This complex binds to the mRNA cap region pre-activated by the eIF4F trimer, with the participation of the poly-A binding protein, eIF4B, eIF4H, and eIF3. Once bound near the cap, the 43S complex initiates mRNA scanning from the 5'-3' direction until the recognition of the AUG initiation codon, which causes the hydrolysis of eIF2-linked GTP through its GTPase activity by eIF5, a GTPase-activating protein. eIF2-GDP is then released by the action of eIF5B ensuing translation elongation. In order to begin a new phase of translation initiation, the eIF2B protein converts GDP to GTP through its guanine nucleotide exchange factor activity (Gordiyenko et al., 2014).

Translation initiation is regulated through decreasing the levels of eIF2-GTP and by eIF4F complex availability. For the eIF2, phosphorylation of the α subunit at serine 51 results in an increased affinity of eIF2-eIF2B, preventing the GDP-GTP exchange (Jennings and Pavitt, 2014). This results in protein translation inhibition due to the unavailability of active ternary complex (Sudhakar et al., 2000). Four protein kinases were described as acting on eIF2 α phosphorylation in eukaryotes. The protein kinase named General Control Non-repressible 2 (GCN2), which is activated in the presence of uncharged tRNAs and nutritional stress (Dever and Hinnebusch, 2005); the Heme Regulated Inhibitor (HRI) kinase, which acts in response to low level of intracellular heme (Chen and London, 1995); the RNA-dependent protein kinase (PKR), which is activated in response to viral infections (Garcia et al., 2007); and PKR-like endoplasmic reticulum kinase (PERK), activated in response to elevated levels of misfolded proteins (Ron and Harding, 2012). Since a large variety of stress stimuli ultimately lead to eIF2 α phosphorylation, this pathway was denominated as the Integrated Stress Response. This pathway is crucial for cell survival, acting like a hub leading to eIF2 α phosphorylation, reducing translation globally, and activating the translation of a particular subset of mRNAs that can revert the initial harm and restore regular levels of translation (Holcik and Sonenberg, 2005). In this scenario, selective mRNA translation occurs preferentially when small reading phases near the initiation codon are present and these proteins act modulating the stress response (Palam et al., 2011).

Trypanosomatids, a group of several protozoan parasites display unique gene expression control, characterized mainly by post-transcriptional regulation (Clayton, 2019). It is particularly relevant the control of mRNA stability due to the presence

of several RNA binding proteins (Kolev et al., 2014; Harvey et al., 2018) and the formation of RNA granules (Cassola, 2011; Guzikowski et al., 2019), operating to cope with the environmental changes during the parasite life cycle. It is less known whether the regulation of translation initiation through eIF2 α is also relevant for parasite adaptation. In Trypanosomatids, eIF2 α has an N-terminal extension so the conserved Ser 51 corresponds to the amino acid threonine 169, as described in *Trypanosoma brucei* (Moraes et al., 2007), *Trypanosoma cruzi* (Tonelli et al., 2011), *Leishmania* species (Cloutier et al., 2012). Furthermore, three kinases that could potentially phosphorylate eIF2 α have been identified (Moraes et al., 2007). In *T. cruzi* these kinases are called Tck1, Tck2, and Tck3. Tck2, which has a topology similar to PERK, had been previously characterized and found in the endosomal compartment of *T. cruzi* (da Silva Augusto et al., 2015), as the homolog of *T. brucei* (Moraes et al., 2007). Tck2 was found to be activated by heme deprivation and gene knockouts showed decreased growth and impaired infectious capacity. The K2 homolog in *Leishmania infantum* is in the endoplasmic reticulum and is required for the intracellular amastigotes' growth (Chow et al., 2011). Tck3 has not yet been characterized, but its ortholog in *T. brucei* has been described and shown to be related to programmed stress-induced cell death (Goldshmidt et al., 2010) by inducing the TATA binding protein phosphorylation (Hope et al., 2014). In *Leishmania donovani*, the K1 (LdeK1) was demonstrated to phosphorylate eIF2 α under starvation (Rao et al., 2016). The substantial importance of GCN2 homologs in phosphorylating eIF2 α and modulating the stress response has also been demonstrated in other protozoan parasites. In *P. falciparum* the GCN2 ortholog was implicated in managing the proper response during amino acid starvation (Fennell et al., 2009) but surprisingly this kinase is not required for the parasite to enter in the hibernation mode during nutritional stress (Babbitt et al., 2012). In *T. gondii*, the GCN2-like ortholog enables extracellular viability and knockouts parasites present fitness defects (Konrad et al., 2011). It was recently shown that upon arginine deprivation, GCN2 induces eIF2 α phosphorylation and upregulation of arginine transporters (Augusto et al., 2019). All these studies establish GCN2 at the center of the nutritional stress response in these parasites, modulating a myriad of pathways to avoid cell death, but its role in *T. cruzi* had not yet been established. We hypothesized that Tck1 can also be activated in response to nutritional stress and amino acid deficiency. To test this, we generated Tck1 depleted parasites by gene replacement using CRISPR/Cas9 tools and evaluated its role in nutritional stress responses and importance for its life cycle progression.

MATERIALS AND METHODS

The procedures used in this work were approved by the "Comite de Ética em Pesquisa da Universidade Federal de São Paulo" under protocol 266629/2015. All methods were performed in accordance with the relevant guidelines and regulations approved by the Universidade Federal de São Paulo that follows the Brazilian Animal Practice and Ethics legislation.

Primer Design

The gene sequences were taken from the TriTrypDB website [http://tritrypdb.org] (Aslett et al., 2010). Single guide RNAs (sgRNA) were obtained by *in vitro* transcription as described (Peng et al., 2014). Briefly, the oligonucleotide TcK1-Primer sgRNA48 and sgRNAThr169/2 were designed to contain the T7 RNA polymerase promoter followed by the proto-spacer region of 20 nucleotides and the Cas9 PAM site. These sites were chosen based on the EuPATGDT tool (http://grna.ctegd.uga.edu/) to present the best combination of score, absence of off-targets and the best location for mutation insertion (Table S1). To generate the sgRNA template, the oligonucleotides and a common reverse primer were employed to amplify by PCR a portion of the pUC-sgRNA template plasmid (Lander et al., 2015). The blasticidin resistance DNA sequence flanked by homologous regions to the TcK1 gene was used as DNA repair donor. For the donor production the forward primer (TcK1-Primer Forward for the donor) was designed containing 80 nucleotides corresponding to the 5' sequence immediately upstream the TcK1 ATG start codon plus 20 initial nucleotides of blasticidin coding region (BSD) from plasmid pTrex-b-NLS-hSpCas9 (a gift from Rick Tarleton obtained from Addgene, plasmid # 62543). The reverse primer (TcK1-Primer Reverse for the donor) contained the 20 final nucleotides of the BSD sequence and 80 nucleotides homologous to the sequence of the TcK1 gene downstream to the PAM site (Lander et al., 2015). The donor for the eIF2 α T169A mutant was the oligonucleotide eIF2Donnorv2, which contained an indicator BssHII restriction site. The total DNA of the generated eIF2 α T169A mutant parasites were amplified by PCR using primers to eIF2 α and the product digested with BssHII and the correct substitution confirmed by DNA sequencing.

In vitro Transcription for sgRNA Generation and Donor DNA Generation

For *in vitro* transcription, the sgRNA template generated by PCR was used as scaffold for the reactions using the MEGAShortscript Kit (Thermo Fisher Scientific) according to the manufacturer instructions. After the transcription reactions, the RNA was extracted with 1:1 phenol/chloroform and recovered by precipitation overnight at -20°C by the addition of 100% ethanol and ammonium sulfate to 0.3 M. The samples were centrifuged at 13,000 g for 15 min at 4°C , the supernatant was discarded, and the RNA pellet was resuspended in 20 μL of RNase free water and stored at -80°C . This final product was used later as sgRNA for transfection of parasites. To produce the donor for TcK1, a conventional PCR was performed using the TcK1-Primer Forward for the donor and TcK-Primer Reverse for the donor to amplify the blasticidin (BSD) coding region from the plasmid pTrex-b-NLS-hSpCas9 (Lander et al., 2015). The donor for the eIF2 α T169A mutant (eIF2Donnorv2) was chemically synthesized.

Generation of Mutated Parasites

Trypanosoma cruzi wild type Y epimastigotes were cultured in medium containing liver and infusion tryptose (LIT) supplemented with 10% fetal bovine serum at 28°C . The parasites expressing Cas9 were generated by transfection with plasmid

pTrex-Cas9-Neo (Lander et al., 2015), selected and maintained in the same medium supplemented with 200 $\mu\text{g}/\text{mL}$ Geneticin G418. For transfection, 4×10^7 exponentially growing Y-Cas9 epimastigotes were collected and centrifuged at 2,000 g for 5 min, parasites were washed in 1 mL of electroporation buffer (5 mM KCl, 0.15 mM CaCl_2 , 90 mM Na_2HPO_4 , 50 mM HEPES, 50 mM Mannitol) (Pacheco-Lugo et al., 2017) and resuspended in 100 μL of electroporation buffer, along with 50 μL containing 2 μg of purified sgRNA and 25 μg of purified PCR fragments containing the BSD sequence. Parasites were transfected in 2 mm cuvettes using AMAXA Nucleofactor II apparatus, with two pulses of X-014 program. Subsequently, parasites were transferred to bottles with fresh LIT medium supplemented with 10% fetal bovine serum and maintained at 28°C for recovery. After 18 h, BSD (100 $\mu\text{g}/\text{mL}$) was added for selection of TcK1 knockout parasites. After transfection and recovery time, cultures were evaluated by PCR genotyping to confirm the insertion of the desired resistance marker and TcK1 gene disruption. PCRs of the samples to determine the presence of the TcK1 gene were made using the primers 5K1fowApal (P1) and TcK1KDRevXho (P2) and the correct insertion of BSD with primers BSDfow (P3) and BSDRev (P4). To test for the elimination of TcK1 ORF, we used the primers CDSK1FowNdeI (P5) and 1TcK1KDRevXhoI (P2). For the generation of eIF2 α in which the threonine 169 was replaced by alanine, the same transfection procedure was used, but without antibiotic selection, as the donor was the oligonucleotide eIF2Donnorv2.

Western Blot

Parasites were collected by centrifugation ($2,000 \times g$ for 5 min), washed in PBS and resuspended in TDB buffer [5 mM KCl, 80 mM NaCl, 1 mM MgSO_4 , 20 mM Na_2HPO_4 , 2 mM NaH_2PO_4 , 20 mM glucose (pH 7.4) containing EDTA-free Complete-C protease inhibitor and PhoSTOP (Sigma-Aldrich)] and lysed by three freeze and thaw cycles in liquid nitrogen and at 37°C . For the differential solubilization experiments, 5×10^7 washed parasites were resuspended in 100 mL of 50 mM Tris-HCl (pH 7.6), 50 mM NaCl, 5 mM MgCl_2 , 0.1% Nonidet-P40, 1 mM β -mercaptoethanol, EDTA-free Complete-C protease inhibitors at 4°C . After 10 min, the lysates were centrifuged 10 min at 10,000 g and the supernatant, corresponding to the soluble fraction transferred to a new tube. The insoluble precipitate was then resuspended in 100 μL of the same buffer. For both types of lysates 5XSDS-sample buffer was added and the samples boiled for 5 min before fractionation by 10% SDS-PAGE and transference to nitrocellulose membranes. After transfer, membranes were incubated in 10 mM Tris-HCl, pH 7.4, 0.15 M NaCl (TBS) containing 5% BSA and 0.05% Tween-20 for 2 h for blocking and then incubated 2–12 h in the same buffer with the primary antibodies. After three washes of 10 min each with TBS containing 0.05% Tween-20, bound antibodies were detected by 1-h incubation in washing buffer with the α -rabbit or α -mouse IgG coupled to IRDye 800 and IRDye 680 (LI-COR Biosciences) antibodies, respectively, three 10-min washes, and acquisition using an Odyssey Fc System (LI-COR Biosciences). Rabbit antibodies directed to *T. cruzi* eIF2 α phosphorylated at Thr 169 were generated as previously described (Tonelli et al.,

2011). Specific antibodies were re-purified by sequential affinity chromatography on peptides NH₃YTEI[^PT]RIRIRAIGKC-amide and NH₃YTEIRIRIRAIGKC-amide (GeneScript) both coupled to SulfoLink[®] Coupling Resin (Thermo Fisher Scientific). Elution from the first column was achieved by using 50 mM glycine pH 2.8 buffer, followed by neutralization by adding 2 M Tris-HCl pH 9.0 and the second column was only used to adsorb non-phospho-specific antibodies. α -T. cruzi eIF2 α antibodies that recognize the full protein was obtained by immunizing mice with the T. cruzi recombinant protein cloned in pET28a and expressed in E. coli BL21 as described previously (da Silva Augusto et al., 2015). Antibodies to the T. cruzi PABP1 and T. brucei biphosphate aldolase proteins were generated by immunizing rabbits with the respective recombinant proteins cloned in pET28a, expressed in E. coli and purified in Ni²⁺-agarose columns. α -PABP1 antibodies were further purified by adsorption on the recombinant protein transferred to nitrocellulose membranes. α -tubulin was obtained from Sigma-Aldrich (T-6074).

Immunofluorescence

Trypanosoma cruzi cultures at log growth phase (0.8 and 1×10^7 cells/mL) were used for the immunofluorescence assays. Parasite cultures were centrifuged, washed twice in PBS and then resuspended in 4% PFA in PBS. After 30 min, the cells were washed in PBS twice and then resuspended in PBS to 5×10^4 cells/mL. About 10 μ l of the sample was distributed into an 8-well slide and allowed to dry at room temperature. The cells were then rehydrated in PBS and permeabilized for 5 min in PBS containing 0.1% Triton X-100, washed twice and incubated for 1 h at room temperature with blocking solution (5% BSA in PBS). After blocking, the slides were incubated with the primary α -DHH1 antibody diluted 1: 100 in blocking solution. The antibodies were prepared in mice by using the recombinant protein generated as described (Costa et al., 2018). The serum was precipitated with 30% ammonium sulfate and resuspended in the original volume in PBS. After three consecutive washes with PBS-T (PBS with 0.1% Tween 20) the slides were incubated 1 h with the mouse α -IgG Alexa 594 (Thermo Fisher Scientific) with 20 μ g/mL of Hoechst DNA marker for 1 h. Following three washes in PBS-T the slides were mounted, and images were taken using $\times 100$ plan Apo-oil objective (NA 1.4) in an Olympus (BX-61) microscope equipped with a Hamamatsu Orca R2 CCD camera. Acquisitions were made through the Z-axis in 0.2 μ m sections. Image analyses were done using Autoquant 2.2 (Media Cybernetics). For quantification of the DHH1 granules after immunofluorescence, the parasites from several photos were taken in randomly chosen fields at 100x magnification and in different focal planes for Z series composition. The total number of granules was manually quantified at the maximum projection for a least 100 parasites of each strain.

Polysome Profile

The polysome profile was generated using the method previously described (Holetz et al., 2007). Briefly, cycloheximide (100 μ g/mL) was added to exponentially growing parasites (1×10^9) and cells were kept at 28°C for 10 min before incubation

on ice for another 10 min. For analysis of parasites subjected to nutritional stress, the same number of parasites was incubated in Triatoma Artificial Urine medium [TAU, 0.19 M NaCl, 0.017 M KCl, 2 mM CaCl₂, 2 mM MgCl₂, 8 mM potassium phosphate (pH 6.8)] for 1 h at a concentration of 10^9 parasites/mL prior to treatment with the same proportion of cycloheximide (200 μ g/ 10^7 parasites). Afterwards, the parasites were centrifuged for 5 min at 2,000 g at 4°C, washed in ice-cold PBS containing 100 μ g/mL cycloheximide and resuspended in 450 μ L of TKM buffer (10 mM Tris-HCl, pH 7.4, 300 mM KCl, 10 mM MgCl₂ and 100 μ g/mL cycloheximide) containing 10 μ M E-64, 1 mM PMSF, 0.2 mg/mL heparin.

Parasites were lysed by adding 50 μ l of 10% NP-40, 2 M sucrose in TKM buffer by gentle mixing. The lysates were centrifuged for 5 min at 10,000 g at 4°C and the supernatant was transferred to the top of a previously prepared sucrose gradient from 15 to 55% sucrose in TKM buffer using a gradient generator (Gradient Master, Biocomp). Samples were ultracentrifuged at 39,000 r.p.m. for 3:00 h in a Beckman SW41 rotor at 4°C and fractions collected and analyzed by continuous injection of 62% sucrose at 0.6 mL/minute using the Econo Gradient Pump (Bio-Rad) followed by absorbance detector analysis at 254 nm.

Metacyclogenesis

For epimastigote differentiation, parasites were washed and resuspended in TAU medium to 1×10^9 parasites/mL and incubated for 1 h at 28°C. After this initial incubation period, the parasites were diluted 100x in TAU medium containing 10 mM glucose, 2 mM L-aspartic acid, 50 mM L-glutamic acid and 10 mM L-proline (TAU3AAG) and 10 mL incubated in laid down 25 cm² tissue culture flasks at 28°C for 5 days. Alternatively, 1 volume of epimastigotes exponentially growing cultures ($2-4 \times 10^7$ /mL) were incubated with 3 volumes of Grace's Insect Media (Thermo Fisher Scientific) at 28°C for 5 days. After the differentiation period, the number of parasites was counted by using a Neubauer chamber and the differentiation rate assessed by staining with Giemsa solution. Aliquots of the differentiated parasites were also used for cell infection experiments to obtain tissue culture trypomastigote forms.

Parasite Infection

The trypomastigotes were maintained in human U-2 OS osteosarcoma cells (ATCC) plated a day before infection in 75 cm² flask incubated at 37°C in low glucose DMEM (Thermo-Fischer Scientific) supplemented with 10% fetal bovine serum (SFB), 59 mg/mL penicillin and 133 mg/mL streptomycin in a CO₂ incubator. The cells were initially infected with cultures incubated with DEAE-cellulose to obtain purified metacyclic-trypomastigotes (Yoshida, 1983). For the next round of infections, we used tissue culture-derived trypomastigotes (TCTs) released from the infected cells. To quantify parasite infection, we performed infections of 3×10^4 U-2 OS cells seeded in 96-well plates containing 100 μ L of medium. The next day, 1.5×10^6 trypomastigotes in 50 μ L of medium corresponding to a multiplicity of infection of 25 TCTs per cell were added and plates incubated for 6 h at 37°C. Afterwards, the media were removed, wells were washed with PBS and fresh medium was

added. The plates were incubated for 72 h in a CO₂ incubator for better detection of the amastigotes nests and after this period, the cells were fixed with 4% paraformaldehyde in PBS and stained with Draq5 (Biostatus). Then, the plates were scanned using a High Content Imaging System In Cell Analyzer 2200 (GE) at 20X magnification and the acquired images analyzed by using the In Cell Investigator Software 1.6 (GE). Five images of each well were acquired and analyzed for determination of the infection ratio. Three different sets of infections were performed, enabling the analyses of thousands of cells. Non-infected cells were used as negative controls.

Sequence and Statistical Analyses

Sequences were analyzed through blast, and after *in silico* translation of the predicted open reading frame, the domains were identified by Pfam (El-Gebali et al., 2019) and HHpred Analyses (Zimmermann et al., 2018). Multiple sequence alignment was generated by the Muscle method (Edgar, 2004). For the phylogenetic analysis, the sequences were downloaded from TriTryp.org and the translated sequences corresponding to the kinase domain of the proteins aligned by 8 iterations using the MUSCLE program included in the Geneious 11.1.15 software. Phylogenetic trees were generated by PHYML also included in the Geneious package. Graphic and statistical analysis were performed using Prism 7 (GraphPad).

RESULTS

In silico Identification of *T. cruzi* GCN2

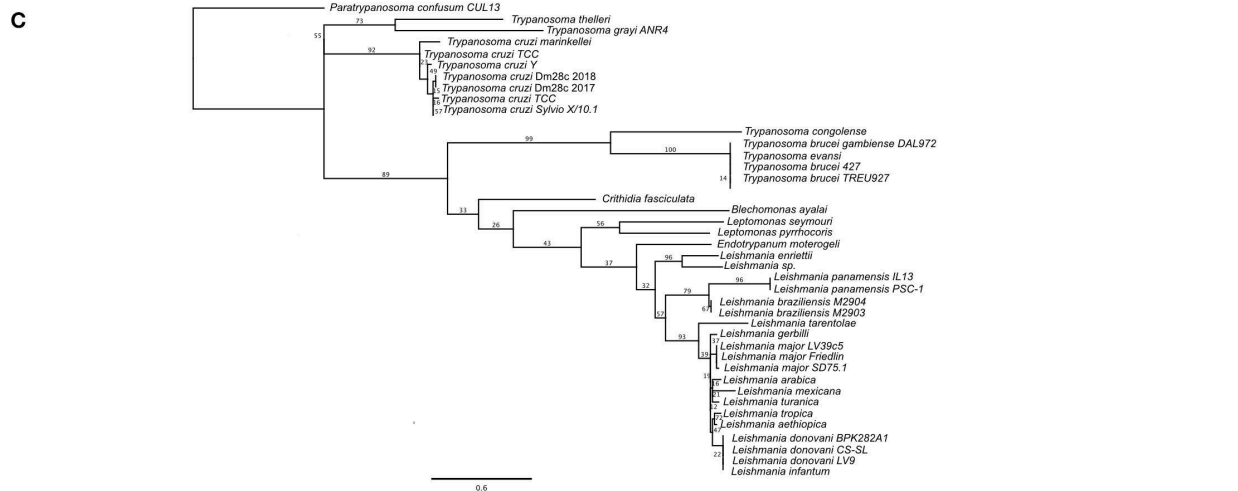
The prediction of the TcK1 protein comprises the relevant domains for the GCN2 signature (Figure 1A). Pfam analysis identified the RWD (RING finger-containing proteins, WD-repeat-containing proteins, and yeast DEAD (DEXD)-like helicases) and kinase domains. The RWD domain was found located in the N-terminal portion (AA^{28–136}). In mammals and yeast this sequence binds to GCN1 regulatory protein being important for GCN2 full activation (Dever and Hinnebusch, 2005; Castilho et al., 2014). As was reported for *L. donovani* (Rao et al., 2016), *P. falciparum* (Fennell et al., 2009), and *T. gondii* (Konrad et al., 2014), TcK1 also lacks the pseudo-kinase domain. HHpred analysis identified another hallmark characteristic in the TcK1 sequence, the presence of the HisRS-like domain (AA^{698–1090}) in the C-terminal portion (CTD), despite its low level of sequence conservation. This domain resembles the HistRNA synthetase domain but lacks significant residues to be enzymatically active although it was shown to bind to uncharged tRNA and to act during GCN2 activation (Wek et al., 1995). The kinase domain (KD) (AA^{277–641}) includes all of the eleven subdomains characteristic of protein kinases (Hanks and Hunter, 1995; Olsen et al., 1998) and the typical eIF2 α kinase insertion (denoted by the gray box), which varies in size in different organisms (Ramirez et al., 1992) (Figure 1B). This insertion presents little conservation even among the trypanosomatids analyzed (8.3% identical sites). Little is known about the role of this insertion in the kinase domain, although works have demonstrated its importance for heme binding and activation of HRI (Rafie-Kolpin et al., 2000; Pakos-Zebrucka et al., 2016).

The insert was also found to increase the binding of PERK to the eIF2 substrate (Marciniak et al., 2006). Most of the conserved residues among general protein kinases (Hanks and Hunter, 1995), indicated by green squares in Figure 1B, are identical or highly similar, with exception of the Ala²⁸⁷ that replaces the conserved Gly residue in the Gly-rich P-loop at the ATP binding motif in *T. cruzi* as in the other trypanosomatids. There are, however, subtle differences in residues more specific for eIF2 α protein kinases (Padyana et al., 2005), indicated by arrows in Figure 1B, specifically the L492F and A510G substitutions, also found in other trypanosomatids. Nevertheless, other substitutions such as S617R and R635P are not conserved in any of the protozoa parasites. Actually, the subdomains IX–XI present a lower level of conservation in kinases and seem to be less important for kinase activity. It is also important to highlight the conservation of the Thr⁵⁴⁸ and Ser⁵⁵³ residues, the latter of which is substituted to a threonine in yeast, *Drosophila* and mammals. These residues correspond to one of the two threonine residues involved in the autophosphorylation of PKR in the activation loop, which is relevant for substrate recognition (Romano et al., 1998; Dey et al., 2005).

A phylogenetic tree based on the amino acid sequence of the KD indicates a clear separation of at least three distinct groups of GCN2 in Trypanosomatids following the expected speciation based on ribosomal small subunit analysis, with the most distant species being *Paratrypanosoma confusum* (Figure 1C). All *Leishmania* species forms one of the three groups. Although presenting very few amino acid substitutions, the separation of the subgenus *Leishmania* from *Viannia* can be detected. The tree also correlates quite well with the separation between the *T. cruzi* and *T. brucei* clades. Interestingly, the inserts in the KD were conserved among each species group, suggesting possible differences between the enzymatic function in the parasites (Figure S1). However, we found no evidence of episodic diversifying selection in the phylogeny considering the insert in the KD of all Kinetoplastidae species sequenced so far by using adaptive branch-site REL test for episodic diversification (aBSREL, <http://datamonkey.org/absrel>), suggesting that the differences observed in each species might represent a random event during the evolution. In *T. cruzi* for example, the inserts, although conserved, contain 3 silent mutations in the third base and 4 non-silent mutations.

Generation of *T. cruzi* Depleted From TcK1 Gene

To better understand the role of TcK1 in *T. cruzi*, we generated parasites in which the TcK1 was interrupted by insertion of the BSD resistance encoding gene by using the CRISPR/Cas9 system (Figure 2A). In this approach, the donor DNA was obtained by PCR using as a template a BSD resistance gene flanked by sequences homologous to the TcK1 gene. The donor DNA was generated by PCR and inserted into epimastigotes parasites expressing the Cas9 enzyme, already resistant to geneticin G418 together with the sgRNA, which was synthesized by *in vitro* transcription. We obtained parasites resistant to G418 and BSD 3 weeks after transfection. Expected insertion of BSD disrupting the targeted gene was verified by PCR using primers P1 and P2.



(Continued)

FIGURE 1 | the HisRS-like domain despite its low sequence conservation. The black boxes indicate the typical insertion in the kinase domain of eIF2 α kinases. The panel also indicates CTD domain, and the pseudo-kinase (Ψ KD). The numbers indicate the position of each domain. **(B)** Sequence alignment of the kinase domain of TcK1 in comparison with GCN2 of model organisms that have been already characterized. Identical residues are indicated in black shades and similar residues are in light gray. The bars on the top with roman numerals correspond to the eleven subdomains characteristic of the GCN2 kinases. Asterisks indicates the residues that undergo auto phosphorylation in eIF2 α kinases in the VIII subdomain. Green squares indicate residues conserved in Ser/Thr protein kinases and arrows the residues maintained in eIF2 α protein kinases. The positions of the P-loop, hinge, catalytic loop and activation loop are indicated by thin bars. The sequence for the TcK1 from the Y strain was obtained from Trityp.org from the nucleotide sequence NMZ001000706.1:2,035.5,676. The other sequences were downloaded from GenBank with the following accession numbers: *Toxoplasma gondii*: AED01979.1; *T. brucei*: XP_828792.1; *Saccharomyces cerevisiae*: DAA12123.1; *Plasmodium falciparum*: XP_001348597.1; *Leishmania donovani*: AKG62099.1; *Homo sapiens*: Q9P2K8.3; *Drosophila melanogaster*: AGB96521.1 **(C)** Phylogenetic tree of the amino acid sequences corresponding to the kinase domain of the homologous of GCN2 of the indicated Kinetoplastidae species. The tree was generated with PHYML using the LG substitution model and 100 bootstraps (Guindon et al., 2010). The access numbers for these sequences are shown in **Table S2**.

It was possible to verify that the band size increased for the TcK1 gene locus, compatible with the insertion event (**Figure 2B**). The presence of the correct insertion of the BSD and absence of the TcK1 ORF were also evaluated by PCR using primers P3/P4 and P1/P2, respectively (**Figure 2B**).

Parasites Depleted of TcK1 Gene Show Increased Polysome Levels

We found that epimastigotes parasites lacking TcK1 gene showed similar growth rates compared to control lineages when maintained under standard culture conditions. Apparently, neither the replication capacity nor the morphology was affected in the epimastigotes (see 3.5 and 3.6 topics). Considering the role of TcK1 in performing eIF2 α phosphorylation during nutritional starvation and the possible inhibition of translation initiation stage, we performed experiments to analyze the polysome profile of the TcK1 depleted strain in normal and in starved parasites. The experiments were performed using samples prepared from control and mutated parasites grown in LIT medium compared to both parasite lines subjected to incubation in TAU medium for 1 h. We observed that the polysome amounts, particularly the ones containing more than 4 ribosomal subunits were consistently enriched in the TcK1 depleted line compared to the control line (**Figure 3**). Upon starvation, the levels of polysome decreased 5 times in the control line and 4 times in the TcK1-KO. These results suggest that GCN2 homolog in *T. cruzi* could be involved in the translation control.

Parasites With Mutated TcK1 Are Still Able to Phosphorylate eIF2 α Under Nutrient Deprivation

To gain more information about the role of TcK1, we examined the levels of eIF2 α phosphorylation after nutritional stress in both control and mutated parasites. For that, we used an α -phospho-eIF2 α labeling that was specific for the phosphorylated protein at threonine 169, as demonstrated in the *T. cruzi* line expressing a mutated version of eIF2 α in which the threonine 169 was replaced by alanine showed no labeling (**Figure 4A**). Surprisingly, both cell lines showed a progressive increased phosphorylation levels of eIF2 α after incubation in TAU medium from 1 to 8 h (**Figure 4B**). Interestingly, in this experiment, we noticed that the eIF2 α phosphorylation diminished progressively in rich medium when the growing parasites were diluted in fresh medium in both control and mutated cells, with a more pronounced decrease in the TcK1-KO cells (see LIT 8 h points),

possibly explaining the increased amounts of polysomes in these cells. A quantitative analysis of phosphorylation is shown in **Figure 4C**. This finding suggests that other eIF2 α kinases are able to phosphorylate eIF2 α under nutritional depletion, mainly at longer incubation periods. In addition, TcK1 seems to affect the low level of phosphorylation in rich medium.

TcK1 Depleted Line Show Reduction of Stress Granules Formation Under Starvation

It has been found that mRNAs can be stored in granules containing RNA binding proteins in unfavorable scenarios such as during nutrient scarcity (Guzikowski et al., 2019). At the same time, translation is inhibited. Thus, taking into account this context, and the fact that GCN2 is involved in stress granule formation (Panas et al., 2016), we investigated the formation of RNA granules in TcK1-KO line during nutritional stress through immunofluorescence. As a marker for granule formation, we used the antibody against DHH1 protein, a protein already well-described as part of the P-body granules (processing bodies) in higher eukaryotes (Aulas et al., 2017; Guzikowski et al., 2019). DHH1 has also been identified in trypanosomatids as part of granules (Kramer et al., 2008, 2010; Holetz et al., 2010). In Y strain epimastigotes, DHH1 labeled small dots distributed over the entire cytosol in both control and in mutated TcK1 (**Figure 5A**). The labeling excluded the nucleus and the mitochondrion, as well as other intracellular organelles. After incubation for 1, 2, and 6 h in TAU medium, the labeling appeared progressively more intense in discrete regions of the cytosol in control cells. Within 1 h of nutritional stress, α -DHH1 labeling detected very small granules located in the perinuclear area with a small decrease in the cytoplasmic signal. Within 6 h, all cells showed large granules, concomitant with decreased cytoplasmic signal (**Figure 5B**). This pattern was not so evident in TcK1-KO parasites, in which <10% of the cells present evident granules in the first h. Therefore, we performed a quantitative analysis 6 h after the stress, which showed a significant decrease in the number of granules in the K1-mutated parasites (**Figure 5C**). To remove small granules in these analyses the images were modified to include threshold that clearly showed a decrease in the large granules in the line in which TcK1 was modified (**Figure S2**). Importantly, the number of granules identified was very similar in the non-transfected Y and Cas9 transfected parasites. These results suggest that TcK1 depletion disturbed DHH1 granule formation in *T. cruzi*.

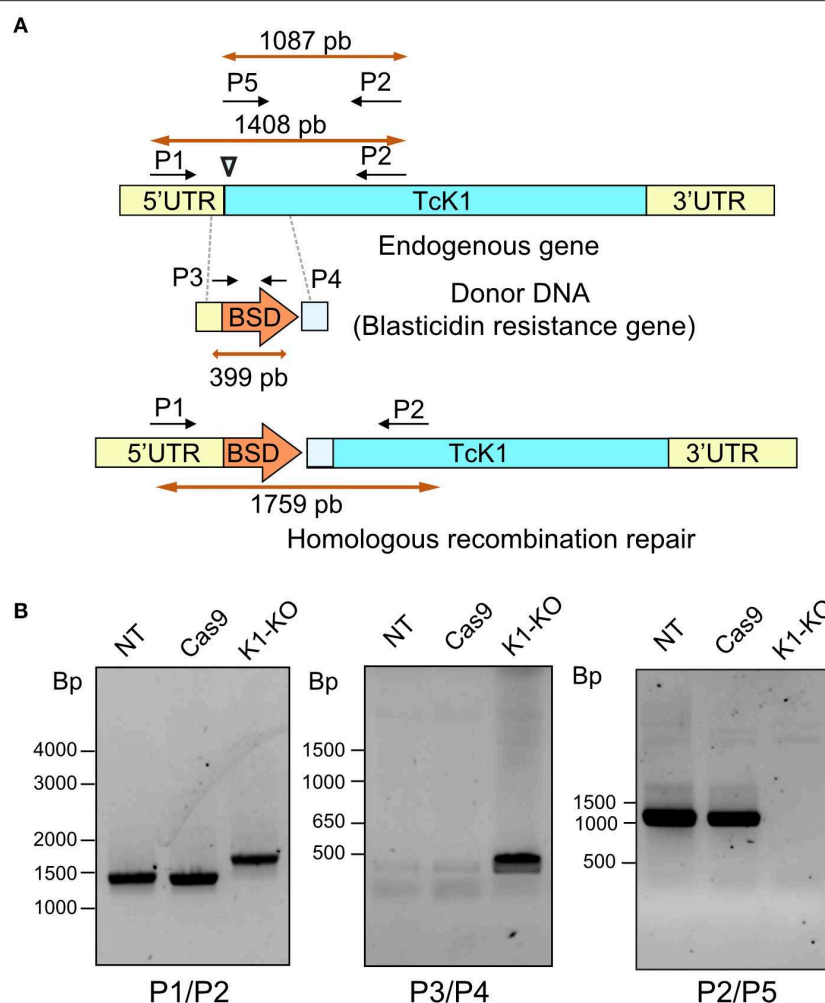


FIGURE 2 | (A) Illustrative diagram of the approach used to generate TcK1 knockout. A PAM site (inverted triangle) was chosen in the begin of the TcK1 ORF (blue) (Top). The donor DNA sequence was prepared comprising the BSD resistance gene and homologous sequences to the TcK1 5'UTR (yellow) and to the ORF immediately after the PAM site (light blue) to favor the repair by homologous recombination (Middle). The bottom diagram denotes the correct integration of the donor DNA to generate the TcK1 interrupted ORF. P1 and P2 represent the pair of primers used to amplify the TcK1 gene corresponding to the N-terminal sequence of the protein and P3 and P4 primers used to amplify the BSD sequence. P5 indicates the position of the primer that aligns with the removed region of TcK1 gene. **(B)** *T. cruzi* genomic DNA was isolated and genotyped by PCR using a combination of primers to amplify the endogenous genes of TcK1 (P1 and P2), the BSD integration (P3 and P4) and to detect the original ORF of TcK1 (P5 and P2). The numbers on the left of each gel stained with ethidium bromide represent the migration of DNA size markers.

Stress granules are large ribonucleoprotein complex that include proteins involved in translation initiation as eukaryotic initiation factors 4E, 4G and 3 as well as poly-A binding proteins (Anderson and Kedersha, 2006). The same set of proteins were also found in *T. brucei* RNA granules induced upon stress (Fritz et al., 2015). In addition, these granules contained eIF2 subunits and GCN1, a protein known to regulate the GCN2 (Castilho et al., 2014), the homolog of TcK1. Therefore, to confirm the participation of TcK1 in the stress granule formation in *T. cruzi*, we measured the amount of poly-A binding protein 1 (PABP1) in insoluble materials that contained RNA granules. The measurements were made in wild type and TcK1-KO incubated in control or stress conditions. As shown in **Figure 6A**, soluble PABP1 levels decreased in parasites incubated in TAU for 6 h in

control parasites compared to TcK1-KO in two independent experiments. More important, the expected increase in the granules of control cells incubated in TAU was reduced in TcK1-KO parasites. Similar results were obtained in at least 3 independent experiments (**Figure 6B**), supporting the notion that the absence of the kinase diminished the stress granules. Interestingly, in both cases, cells presented a double band that disappear after incubation in TAU, which can be related to its phosphorylation state.

Tck1 Affects Metacyclogenesis and Host Cell Infection

Because nutritional stress (Romaniuk et al., 2018), and eIF2 α phosphorylation (Tonelli et al., 2011) have previously been associated with parasite differentiation, we investigated the

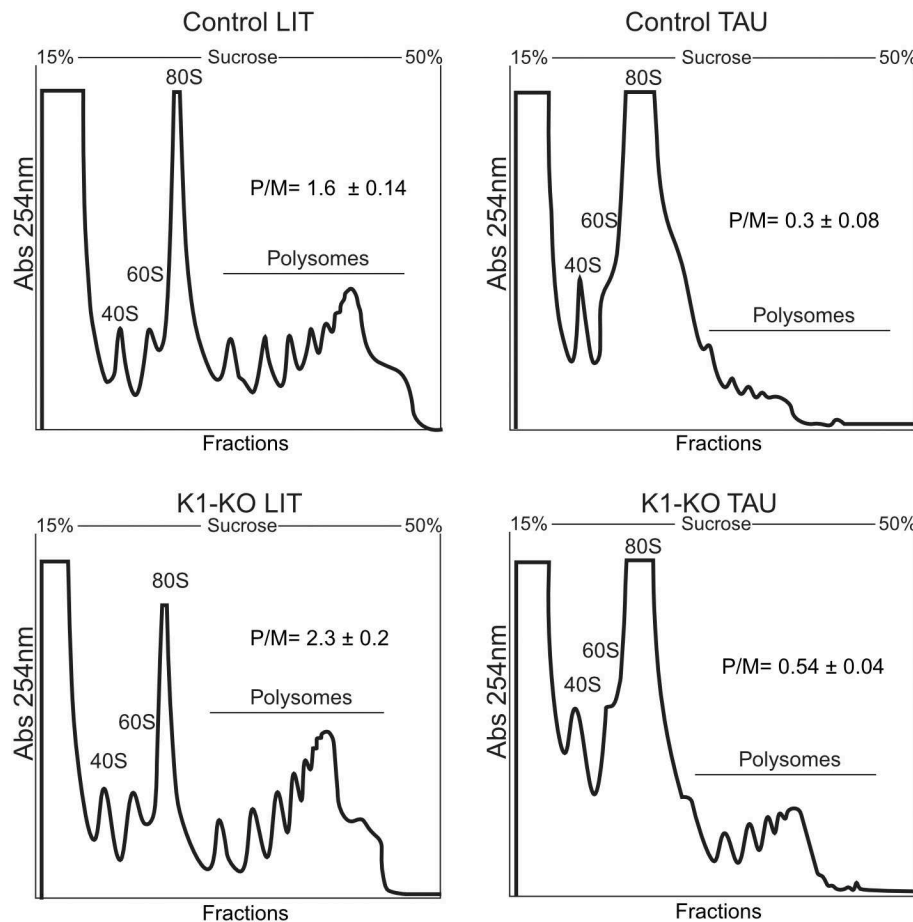


FIGURE 3 | Polysome profile analysis of control and *TcK1* depleted parasites (*TcK1*-KO). Epimastigotes were cultivated in LIT medium and incubated in LIT or in TAU medium for 1 h. The parasites extracts were prepared as described in Methods and fractionated by ultracentrifugation through a 15–55% sucrose gradient. The fractions were collected from the top to bottom and the amount of RNA estimated by the absorbance at 254 nm. In each panel it is indicated the migrating position of the 40S, 60S, 80S and the polysomal fractions. The amount of polysomes relative to the 80S (P/M) was estimated by measuring the area under each peak in triplicate samples.

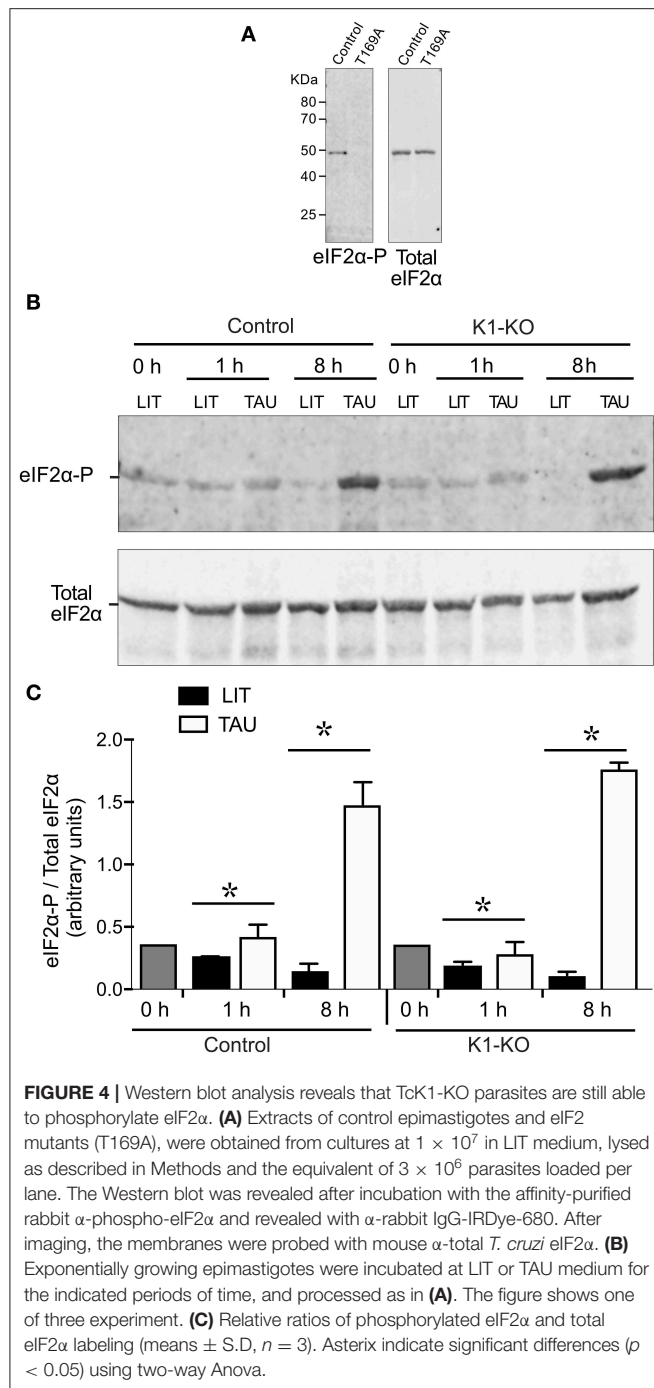
effects of *TcK1* absence on parasite metacyclogenesis. As mentioned above, no growth effect was found by comparing control and mutated cell lines (**Figure 7A**). However, *TcK1*-KO showed an increased differentiation from epimastigotes to metacyclic-trypomastigotes compared to control parasites when induced to differentiate in TAU medium followed by incubation in TAU3AGG (**Figure 7B**). Similar results were observed when the differentiation was induced in Grace's medium.

Next, the obtained metacyclics were used to infect mammalian cells and to generate cell-derived trypomastigotes. When trypomastigotes were probed for their infection capacity, we found a large decrease (more than 90%) in the infectivity of the *TcK1*-KO compared to the control parasites (**Figure 7C**). Interestingly, the number of obtained trypomastigotes from the infected cells was similar in both cases. Indeed, after 72 h, the number of intracellular parasites was even higher in mutated cell lines, suggesting that although less infective, the cell line lacking *TcK1* replicated faster in mammalian cells.

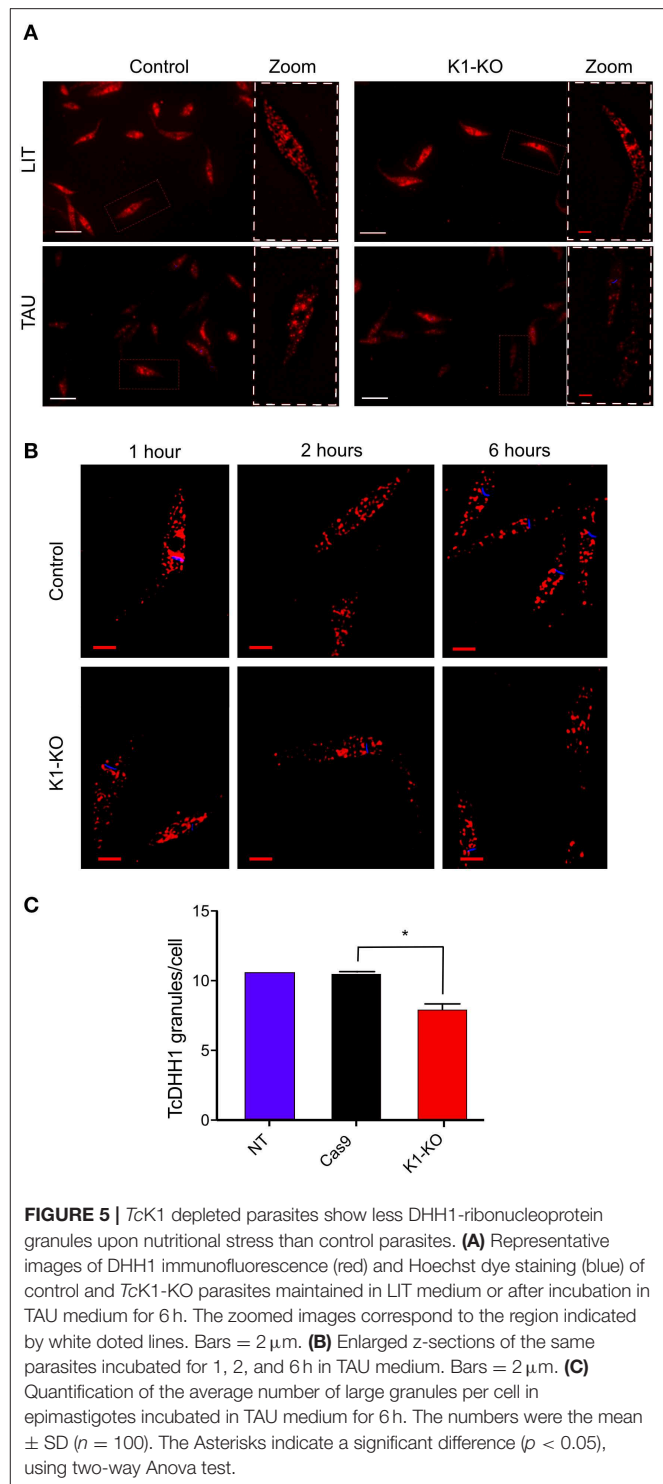
DISCUSSION

We characterized the *T. cruzi* GCN2 homolog, named *TcK1*. This protein kinase was found highly conserved through different Kinetoplastidae. We found that *TcK1* presents the main characteristics of eIF2 α protein kinases. The most divergent region was the insertion of the kinase domain, postulated to make a loop involved in the substrate recognition. Nevertheless, these inserts were conserved in Kinetoplastidae species and our phylogenetic analysis indicated a non-selective pattern in each case, suggesting a random evolution, not necessarily related to the enzymatic role, or substrate recognition.

Through genome editing with CRISPR/Cas9, we provided evidence that *TcK1* is not the main protein kinase involved in the eIF2 α phosphorylation under nutrient deprivation, differently to what has been shown in many organisms, including *L. donovani* (Rao et al., 2016). Nevertheless, the absence of *TcK1* decreased the formation of DHH1-containing granules under nutritional stress, possibly related to the action

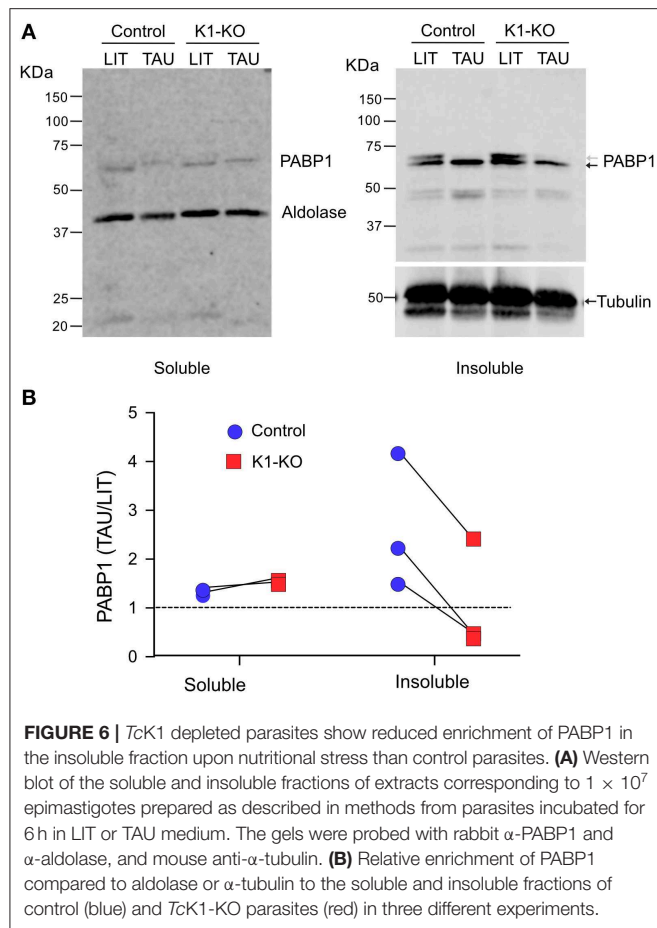


through a different mechanism, as shown for translation arrest induced by TIA-1 and TIAR proteins in human cells (Damgaard and Lykke-Andersen, 2011). At the same time, less insoluble PABP1 was found when parasites were incubated under nutritional stress. Finally, we found that in absence of TcK1 the capacity of parasite differentiation, mammalian cell invasion and proliferation in the host was largely affected, all suggesting that TcK1 modifies the expression



of proteins relevant at the different moments of the parasite life cycle.

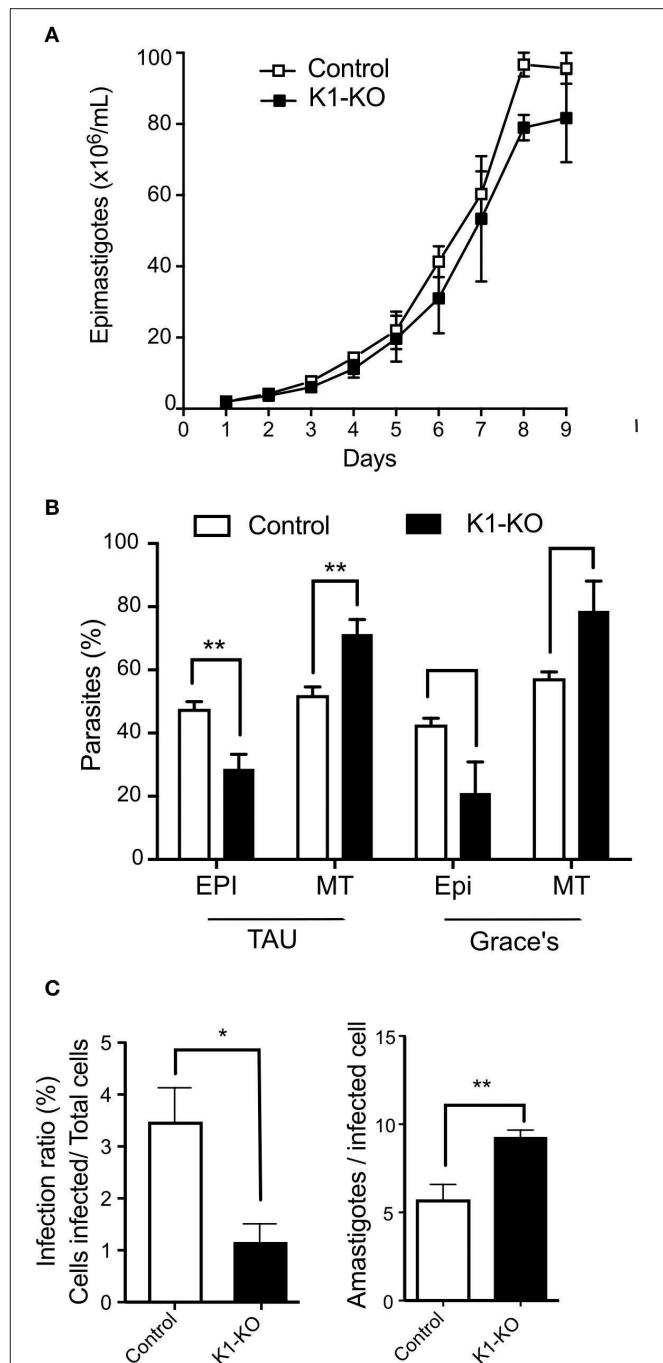
We depleted the TcK1 gene by the insertion of the BSD sequence at the beginning of the TcK1 gene. The same drug resistance approach has been used to generated gene depletions



in other Trypanosomatids (Lander et al., 2015; Beneke et al., 2017). In our case, the correct insertion and the absence of the *TcK1* gene were confirmed by PCR reactions. The obtained epimastigotes had no morphological and proliferation changes when maintained in rich medium and indicated the kinase absence is well-tolerated by replicating epimastigotes. As we observed eIF2 α phosphorylation in starved *TcK1*-depleted parasites, it was clear that other kinases such as *TcK2*, or even *TcK3* could phosphorylate eIF2 α in these conditions.

Our results showed that cells lacking *TcK1* still presented polysomes when submitted to nutritional stress, indicating that it has a direct effect on translation initiation. This appeared to occur independently of eIF2 α phosphorylation as its levels were still detected in proliferating parasites. This contrasts with the effect of eIF2 α T169A mutant observed previously, which had the same polysome levels and sustained the polysome levels upon incubation in TAU medium (Tonelli et al., 2011). However, a more evident decrease in eIF2 α phosphorylation seen at 8 h after cell inoculation in fresh medium as shown in the quantification in **Figure 4B**, suggested that this effect occurs through eIF2 α phosphorylation.

More relevant was that we noticed that *TcK1*-depleted parasites showed reduced amounts of DHH1 granules upon



(Continued)

FIGURE 7 | the mean \pm SD of three independent experiments. **(C)**

Trypomastigotes of control and TcK1-KO lines (7.5×10^5) in a volume of 0.1 mL obtained from the supernatant of infected cells were used to infect U2-OS cells (3×10^4) seed a day before in 96 wells plates. After 6 h, the parasites were removed, the wells were washed, and one-half of the wells fixed with 4% *p*-formaldehyde in PBS and the other half incubated with fresh medium for 72 h, before washing and fixation. The number of intracellular parasites was then quantified by imaging the fluorescent parasites per cell both labeled with Draq5. The values are means \pm SD of three independent experiments, each one corresponding to values of 5 wells. Asterisks indicate $p < 0.01$ (*) or 0.05 (**) calculated using the Student *t*-test.

full starvation. This result was confirmed by decreased levels of PABP1 found in granules. It is known that DHH1 prevents the binding of the ternary complex to the 5' end of the mRNA to form the 43S pre-initiation complex, inducing the decapping and mRNA degradation (Zeidan et al., 2018). DHH1 was also proposed to sense codon usage during translation elongation (Radhakrishnan et al., 2016), which is shown to perform a key control in *T. brucei* protein translation (Jeacock et al., 2018). PABP1 was found to interact with several components of SG in *T. cruzi* and its differential accumulation could be a direct, or indirect action of TcK1 activity due to its phosphorylation state (de Melo Neto et al., 2018). Therefore, our findings suggested TcK1 could have a role in controlling the gene expression in *T. cruzi*. In fact, the differences in the differentiation of epimastigotes to metacyclics, invasion capability of trypomastigotes and proliferation of amastigotes, could be attributed to differences in protein expression between control and mutated cells (Holetz et al., 2010).

The increased metacyclogenesis observed in the TcK1-KO compared to controls contrast with our previous results showing that the T169A mutant had reduced differentiation (Tonelli et al., 2011). These different phenotypes may be explained because eIF2 α remains phosphorylated in TcK1-KO under nutritional stress when metacyclogenesis was induced. As metacyclogenesis was inhibited in the TcK2 knockouts (da Silva Augusto et al., 2015), we can speculate that TcK1 mutant has additional functions, which would promote increased differentiation.

Our results did not explain how TcK1 affected the DHH1 granule formation, but it could be related to the increased polysome levels. It is widely known that the formation of stress granules (SG) is associated with dramatic changes in gene expression coupled to differential translation, mRNA processing and mRNP granules formation (Guzikowski et al., 2019). Indeed, in some situations, it seems that there is a balance between the amount of mRNA engaged in translation with polysome formation, and the levels of SG formation. Furthermore, the composition of the different SG changes in different conditions (Guzikowski et al., 2019). SG and also P-bodies are rapidly formed in response to stress, as fast as the levels of mRNAs disengage from translation (Kershaw and Ashe, 2017). The composition of these granules varies but some components overlap in both granules, as is the case of DHH1 protein (Guzikowski et al., 2019). In agreement with our findings, the formation of SG may occur independently of

eIF2 α phosphorylation but through the action of GCN2. This protein kinase affects a myriad of cellular processes (Castilho et al., 2014). For example, situations that affect translation initiation via the eIF4F complex can lead to SG formation independently of eIF2 α phosphorylation (Mahboubi and Stochaj, 2017). There is a crosstalk between the GCN2 pathway and other pathways involved in stress responses to nutrient starvation to avoid cell death, involving TOR (Cherkasova and Hinnebusch, 2003) and Snf1 (Cherkasova et al., 2010) kinases in yeast. In permanently activated GCN2, both P-bodies and SG were highly increased after nutritional stress, specifically under glucose deprivation. The granules became larger, brighter and more frequent in cells expressing constitutively active GCN2 compared to control during glucose deprivation in yeasts (Buchan et al., 2008). Aulas and colleagues vastly explored the effect of diverse stressful stimuli on SG formation in knockout cells of all 4 eIF2 α kinases in HAP1 cells and its effect on eIF2 α phosphorylation (Aulas et al., 2017). Surprisingly, the levels of phospho-eIF2 α were not altered, except under UV-stress in GCN2 depleted cells, where it was abolished. Furthermore, GCN2 was shown to induce autophagy that clear the SG (Battu et al., 2018).

In conclusion, our findings demonstrate the role of the *T. cruzi* ortholog of GCN2, TcK1, in controlling several steps of *T. cruzi* life cycle through modulating the formation of SG. It does not perform its canonical function and does not affect the levels of phosphorylated eIF2 α under nutritional stress. TcK1 may have other potential substrates that have yet to be identified but may be related to the phenotypes observed. The elucidation of the mechanism by which TcK1 modulates the formation of SG, as well as their role in the parasite, may help to understand the intricate regulatory network in this and other trypanosomes.

DATA AVAILABILITY STATEMENT

The raw data supporting the conclusions of this article will be made available by the authors, without undue reservation, to any qualified researcher.

ETHICS STATEMENT

The animal study was reviewed and approved by the Comit  de  tica em Pesquisa da Universidade Federal de S o Paulo under protocol 266629/2015.

AUTHOR CONTRIBUTIONS

AM designed and characterized the TcK1-KO line, performed the polysome analyses, quantified the DHH1 RNP structures and wrote the paper. NM help designed the mutations, performed the metacyclogenesis and infections experiments and analysis, and discussed the results. GS generated and verified the *T. cruzi* lineage expressing Cas9 and helped in the characterization of the TcK1 mutation. MA performed DNA analysis experiments, growth curves, and maintained the parasite. FH helped with

the polysome experiments and stress granule analyses. PB-C performed the Western blots using the α -phospho eIF2 α antibodies and helped in the writing of the manuscript. SS obtained the funds, conducted the work strategy, analyzed the data, performed the phylogenetic analysis, and wrote the paper.

FUNDING

This work was funded through grants from Fundação de Amparo à Pesquisa do Estado de São Paulo (FAPESP, 2015/20031-0), Conselho Nacional de Desenvolvimento Científico e Tecnológico (CNPq 445655/2014-3 and INCTV-CNPq to SS). AM and NM by a FAPESP postdoctoral fellowships (2017/02496-4 and 2017/02416-0), GS has a FAPESP Ph.D. fellowship

(2018/07766-2), and MA an undergraduate fellowship from CNPq (PIBIC-Unifesp).

ACKNOWLEDGMENTS

We thank the technical help of Claudio Rogerio Oliveira from Hospital S. Paulo, and Claudeci Medeiros for their excellent technical support during this work.

SUPPLEMENTARY MATERIAL

The Supplementary Material for this article can be found online at: <https://www.frontiersin.org/articles/10.3389/fcimb.2020.00149/full#supplementary-material>

REFERENCES

- Anderson, P., and Kedersha, N. (2006). RNA granules. *J. Cell Biol.* 172:803–808. doi: 10.1083/jcb.200512082
- Aslett, M., Aurrecochea, C., Berriman, M., Brestelli, J., Brunk, B. P., Carrington, M., et al. (2010). TriTrypDB: a functional genomic resource for the Trypanosomatidae. *Nucleic Acids Res.* 38, D457–D462. doi: 10.1093/nar/gkp851
- Augusto, L., Amin, P. H., Wek, R. C., and Sullivan, W. J. (2019). Regulation of arginine transport by GCN2 eIF2 kinase is important for replication of the intracellular parasite *Toxoplasma gondii*. *PLoS Pathog.* 15:e1007746. doi: 10.1371/journal.ppat.1007746
- Aulas, A., Fay, M. M., Lyons, S. M., Achorn, C. A., Kedersha, N., Anderson, P., et al. (2017). Stress-specific differences in assembly and composition of stress granules and related foci. *J. Cell Sci.* 130, 927–937. doi: 10.1242/jcs.199240
- Babbitt, S. E., Altenhofen, L., Cobbold, S. A., Istvan, E. S., Fennell, C., Doerig, C., et al. (2012). *Plasmodium falciparum* responds to amino acid starvation by entering into a hibernatory state. *Proc. Natl. Acad. Sci. U.S.A.* 109, E3278–E3287. doi: 10.1073/pnas.1209823109
- Battu, S., Afroz, S., Giddaluru, J., Naz, S., Huang, W., Khumukcham, S. S., et al. (2018). Amino acid starvation sensing dampens IL-1 β production by activating riboclustering and autophagy. *PLoS Biol.* 16:e2005317. doi: 10.1371/journal.pbio.2005317
- Beneke, T., Madden, R., Makin, L., Valli, J., Sunter, J., and Gluenz, E. (2017). A CRISPR Cas9 high-throughput genome editing toolkit for kinetoplastids. *R Soc. Open Sci.* 4:170095. doi: 10.1098/rsos.170095
- Buchan, J. R., Muhrad, D., and Parker, R. (2008). P bodies promote stress granule assembly in *Saccharomyces cerevisiae*. *J. Cell Biol.* 183, 441–455. doi: 10.1083/jcb.200807043
- Cassola, A. (2011). RNA granules living a post-transcriptional life: the trypanosomes' case. *Curr. Chem. Biol.* 5, 108–117. doi: 10.2174/2212796811105020108
- Castilho, B. A., Shanmugam, R., Silva, R. C., Ramesh, R., Himme, B. M., and Sattlegger, E. (2014). Keeping the eIF2 alpha kinase Gcn2 in check. *Biochim. Biophys. Acta.* 1843, 1948–1968. doi: 10.1016/j.bbamcr.2014.04.006
- Chen, J. J., and London, I. M. (1995). Regulation of protein synthesis by heme-regulated eIF-2 alpha kinase. *Trends Biochem. Sci.* 20, 105–108. doi: 10.1016/S0968-0004(00)88975-6
- Cherkasova, V., Qiu, H., and Hinnebusch, A. G. (2010). Snf1 promotes phosphorylation of the alpha subunit of eukaryotic translation initiation factor 2 by activating Gcn2 and inhibiting phosphatases Glc7 and Sit4. *Mol. Cell. Biol.* 30, 2862–2873. doi: 10.1128/MCB.00183-10
- Cherkasova, V. A., and Hinnebusch, A. G. (2003). Translational control by TOR and TAP42 through dephosphorylation of eIF2 α kinase GCN2. *Genes Dev.* 17, 859–872. doi: 10.1101/gad.1069003
- Chow, C., Cloutier, S., Dumas, C., Chou, M. N., and Papadopolou, B. (2011). Promastigote to amastigote differentiation of *Leishmania* (2018/07766-2), and MA an undergraduate fellowship from CNPq (PIBIC-Unifesp).
- Clayton, C. (2019). Regulation of gene expression in trypanosomatids: living with polycistronic transcription. *Open Biol.* 9:190072. doi: 10.1098/rsob.190072
- Cloutier, S., Laverdiere, M., Chou, M.-N., Boilard, N., Chow, C., and Papadopolou, B. (2012). Translational control through eIF2 α phosphorylation during the *Leishmania* differentiation process. *PLoS ONE* 7:e35085. doi: 10.1371/journal.pone.0035085
- Costa, J. F. D., Ferrarini, M. G., Nardelli, S. C., Goldenberg, S., Avila, A. R., and Holetz, F. B. (2018). *Trypanosoma cruzi* XRNA granules colocalise with distinct mRNP granules at the nuclear periphery. *Mem. Inst. Oswaldo Cruz.* 113:e170531. doi: 10.1590/0074-02760170531
- da Silva Augusto, L., Moretti, N. S., Ramos, T. C., de Jesus, T. C., Zhang, M., Castilho, B. A., et al. (2015). A membrane-bound eIF2 alpha kinase located in endosomes is regulated by heme and controls differentiation and ROS levels in *Trypanosoma cruzi*. *PLoS Pathog.* 11:e1004618. doi: 10.1371/journal.ppat.1004618
- Damgaard, C. K., and Lykke-Andersen, J. (2011). Translational coregulation of 5'TOP mRNAs by TIA-1 and TIAR. *Genes Dev.* 25, 2057–2068. doi: 10.1101/gad.17355911
- de Melo Neto, O. P., da Costa Lima, T. D. C., Merlo, K. C., Romao, T. P., Rocha, P. O., Assis, L. A., et al. (2018). Phosphorylation and interactions associated with the control of the *Leishmania* Poly-A Binding Protein 1 (PABP1) function during translation initiation. *RNA Biol.* 15, 739–755. doi: 10.1080/15476286.2018.1445958
- Dever, T. E., and Hinnebusch, A. G. (2005). GCN2 whets the appetite for amino acids. *Mol. Cell.* 18, 141–142. doi: 10.1016/j.molcel.2005.03.023
- Dey, M., Cao, C., Dar, A. C., Tamura, T., Ozato, K., Sicheri, F., et al. (2005). Mechanistic link between PKR dimerization, autophosphorylation, and eIF2 α substrate recognition. *Cell* 122, 901–913. doi: 10.1016/j.cell.2005.06.041
- Edgar, R. C. (2004). MUSCLE: multiple sequence alignment with high accuracy and high throughput. *Nucleic Acids Res.* 32, 1792–1797. doi: 10.1093/nar/gkh340
- El-Gebali, S., Mistry, J., Bateman, A., Eddy, S. R., Luciani, A., Potter, S. C., et al. (2019). The Pfam protein families database in 2019. *Nucleic Acids Res.* 47, D427–D432. doi: 10.1093/nar/gky995
- Fennell, C., Babbitt, S., Russo, I., Wilkes, J., Ranford-Cartwright, L., Goldberg, D. E., et al. (2009). PfeIK1, a eukaryotic initiation factor 2 α kinase of the human malaria parasite *Plasmodium falciparum*, regulates stress-response to amino-acid starvation. *Malar. J.* 8:99. doi: 10.1186/1475-2875-8-99
- Fritz, M., Vanselow, J., Sauer, N., Lamer, S., Goos, C., Siegel, T. N., et al. (2015). Novel insights into RNP granules by employing the trypanosome's microtubule skeleton as a molecular sieve. *Nucleic Acids Res.* 43, 8013–8032. doi: 10.1093/nar/gkv731

- Garcia, M. A., Meurs, E. F., and Esteban, M. (2007). The dsRNA protein kinase PKR: virus and cell control. *Biochimie* 89, 799–811. doi: 10.1016/j.biochi.2007.03.001
- Goldshmidt, H., Matas, D., Kabi, A., Carmi, S., Hope, R., and Michaeli, S. (2010). Persistent ER stress induces the spliced leader RNA silencing pathway (SLS), leading to programmed cell death in *Trypanosoma brucei*. *PLoS Pathogens* 6:e1000731. doi: 10.1371/journal.ppat.1000731
- Gordiyenko, Y., Schmidt, C., Jennings, M. D., Matak-Vinkovic, D., Pavitt, G. D., and Robinson, C. V. (2014). eIF2B is a decameric guanine nucleotide exchange factor with a γ 2epsilon2 tetrameric core. *Nat. Commun.* 5:3902. doi: 10.1038/ncomms4902
- Guindon, S., Dufayard, J. F., Lefort, V., Anisimova, M., Hordijk, W., and Gascuel, O. (2010). New algorithms and methods to estimate maximum-likelihood phylogenies: assessing the performance of PhyML 3.0. *System Biol.* 59, 307–321. doi: 10.1093/sysbio/syq010
- Guzikowski, A. R., Chen, Y. S., and Zid, B. M. (2019). Stress-induced mRNP granules: form and function of processing bodies and stress granules. *Wiley Interdiscip. Rev. RNA* 10:e1524. doi: 10.1002/wrna.1524
- Hanks, S. K., and Hunter, T. (1995). Protein kinases 6. The eukaryotic protein kinase superfamily: kinase (catalytic) domain structure and classification. *FASEB J.* 9, 576–596. doi: 10.1096/fasebj.9.8.7768349
- Harvey, R. F., Smith, T. S., Mulroney, T., Queiroz, R. M. L., Pizzinga, M., Dezi, V., et al. (2018). Trans-acting translational regulatory RNA binding proteins. *Wiley Interdiscip. Rev. RNA* 9:e1465. doi: 10.1002/wrna.1465
- Hinnebusch, A. G., and Lorsch, J. R. (2012). The mechanism of eukaryotic translation initiation: new insights and challenges. *Cold Spring Harb. Perspect. Biol.* 4:a011544. doi: 10.1101/cshperspect.a011544
- Holcik, M., and Sonenberg, N. (2005). Translational control in stress and apoptosis. *Nat. Rev. Mol. Cell Biol.* 6, 318–327. doi: 10.1038/nrm1618
- Holetz, F. B., Alves, L. R., Probst, C. M., Dallagiovanna, B., Marchini, F. K., Manque, P., et al. (2010). Protein and mRNA content of TcDHH1-containing mRNPs in *Trypanosoma cruzi*. *FEBS J.* 277, 3415–3426. doi: 10.1111/j.1742-4658.2010.07747.x
- Holetz, F. B., Correa, A., Avila, A. R., Nakamura, C. V., Krieger, M. A., and Goldenberg, S. (2007). Evidence of P-body-like structures in *Trypanosoma cruzi*. *Biochem. Biophys. Res. Commun.* 356, 1062–1067. doi: 10.1016/j.bbrc.2007.03.104
- Hope, R., Ben-Mayor, E., Friedman, N., Voloshin, K., Biswas, D., Matas, D., et al. (2014). Phosphorylation of the TATA-binding protein activates the spliced leader silencing pathway in *Trypanosoma brucei*. *Sci. Signal.* 7:ra85. doi: 10.1126/scisignal.2005234
- Jeacock, L., Faria, J., and Horn, D. (2018). Codon usage bias controls mRNA and protein abundance in trypanosomatids. *Elife* 7. doi: 10.7554/eLife.32496.020
- Jennings, M. D., and Pavitt, G. D. (2014). A new function and complexity for protein translation initiation factor eIF2B. *Cell Cycle* 13, 2660–2665. doi: 10.4161/15384101.2014.948797
- Kershaw, C. J., and Ashe, M. P. (2017). Untangling P-bodies: dissecting the complex web of interactions that enable tiered control of gene expression. *Mol. Cell.* 68, 3–4. doi: 10.1016/j.molcel.2017.09.032
- Kolev, N. G., Ullu, E., and Tschudi, C. (2014). The emerging role of RNA-binding proteins in the life cycle of *Trypanosoma brucei*. *Cell. Microbiol.* 16, 482–489. doi: 10.1111/cmi.12268
- Konrad, C., Wek, R. C., and Sullivan, W. J. (2011). A GCN2-like eukaryotic initiation factor 2 kinase increases the viability of extracellular *Toxoplasma gondii* parasites. *Eukaryotic Cell.* 10, 1403–1412. doi: 10.1128/EC.05117-11
- Konrad, C., Wek, R. C., and Sullivan, W. J. (2014). GCN2-like eIF2 α kinase manages the amino acid starvation response in *Toxoplasma gondii*. *Int. J. Parasitol.* 44, 139–146. doi: 10.1016/j.ijpara.2013.08.005
- Kramer, S., Queiroz, R., Ellis, L., Hoheisel, J. D., Clayton, C., and Carrington, M. (2010). The RNA helicase DHH1 is central to the correct expression of many developmentally regulated mRNAs in trypanosomes. *J. Cell Sci.* 123, 699–711. doi: 10.1242/jcs.058511
- Kramer, S., Queiroz, R., Ellis, L., Webb, H., Hoheisel, J. D., Clayton, C., et al. (2008). Heat shock causes a decrease in polysomes and the appearance of stress granules in trypanosomes independently of eIF2(α) phosphorylation at Thr169. *J. Cell Sci.* 121, 3002–3014. doi: 10.1242/jcs.031823
- Lander, N., Li, Z. H., Niyogi, S., and Docampo, R. (2015). CRISPR/Cas9-induced disruption of paraflagellar rod protein 1 and 2 genes in *Trypanosoma cruzi* reveals their role in flagellar attachment. *MBio* 6:e01012–15. doi: 10.1128/mBio.01012-15
- Mahboubi, H., and Stochaj, U. (2017). Cytoplasmic stress granules: dynamic modulators of cell signaling and disease. *Biochim. Biophys. Acta Mol. Basis Dis.* 1863, 884–895. doi: 10.1016/j.bbdis.2016.12.022
- Marciniak, S. J., Garcia-Bonilla, L., Hu, J., Harding, H. P., and Ron, D. (2006). Activation-dependent substrate recruitment by the eukaryotic translation initiation factor 2 kinase PERK. *J. Cell Biol.* 172, 201–209. doi: 10.1083/jcb.200508099
- Moraes, M. C., Jesus, T. C., Hashimoto, N. N., Dey, M., Schwartz, K. J., Alves, V. S., et al. (2007). Novel membrane-bound eIF2 α kinase in the flagellar pocket of *Trypanosoma brucei*. *Eukaryotic Cell.* 6, 1979–1991. doi: 10.1128/EC.00249-07
- Olsen, D. S., Jordan, B., Chen, D., Wek, R. C., and Caverer, D. R. (1998). Isolation of the gene encoding the *Drosophila melanogaster* homolog of the *Saccharomyces cerevisiae* GCN2 eIF-2 α kinase. *Genetics* 149, 1495–1509.
- Pacheco-Lugo, L., Diaz-Olmos, Y., Saenz-Garcia, J., Probst, C. M., DaRocha, W. D. (2017). Effective gene delivery to *Trypanosoma cruzi* epimastigotes through nucleofection. *Parasitol. Int.* 66, 236–239. doi: 10.1016/j.parint.2017.01.019
- Padyana, A. K., Qiu, H., Roll-Mecak, A., Hinnebusch, A. G., and Burley, S. K. (2005). Structural basis for autoinhibition and mutational activation of eukaryotic initiation factor 2 α protein kinase GCN2. *J. Biol. Chem.* 280, 29289–29299. doi: 10.1074/jbc.M504096200
- Pakos-Zebrucka, K., Koryga, I., Mnich, K., Lujic, M., Samali, A., and Gorman, A. M. (2016). The integrated stress response. *EMBO Rep.* 17, 1374–1395. doi: 10.15252/embr.201642195
- Palam, L. R., Baird, T. D., and Wek, R. C. (2011). Phosphorylation of eIF2 facilitates ribosomal bypass of an inhibitory upstream ORF to enhance CHOP translation. *J. Biol. Chem.* 286, 10939–10949. doi: 10.1074/jbc.M110.216093
- Panas, M. D., Ivanov, P., and Anderson, P. (2016). Mechanistic insights into mammalian stress granule dynamics. *J. Cell Biol.* 215, 313–323. doi: 10.1083/jcb.201609081
- Peng, D., Kurup, S. P., Yao, P. Y., Minning, T. A., and Tarleton, R. L. (2014). CRISPR-Cas9-mediated single-gene and gene family disruption in *Trypanosoma cruzi*. *MBio* 6:e02097–14. doi: 10.1128/mBio.02097-14
- Radhakrishnan, A., Chen, Y. H., Martin, S., Alhusaini, N., Green, R., and Collier, J. (2016). The DEAD-box protein Dhh1p couples mRNA decay and translation by monitoring codon optimality. *Cell* 167:e129. doi: 10.1016/j.cell.2016.08.053
- Rafie-Kolpin, M., Chefalo, P. J., Hussain, Z., Hahn, J., Uma, S., Matts, R. L., et al. (2000). Two heme-binding domains of heme-regulated eukaryotic initiation factor-2 α kinase. N terminus and kinase insertion. *J. Biol. Chem.* 275, 5171–5178. doi: 10.1074/jbc.275.7.5171
- Ramirez, M., Wek, R. C., Vazquez de Aldana, C. R., Jackson, B. M., Freeman, B., and Hinnebusch, A. G. (1992). Mutations activating the yeast eIF-2 α kinase GCN2: isolation of alleles altering the domain related to histidyl-tRNA synthetases. *Mol. Cell. Biol.* 12, 5801–5815. doi: 10.1128/MCB.12.12.5801
- Rao, S. J., Meleppattu, S., and Pal, J. K. (2016). A GCN2-like eIF2 α kinase (LdeK1) of *Leishmania donovani* and its possible role in stress response. *PLoS ONE* 11:e0156032. doi: 10.1371/journal.pone.0156032
- Romaniuk, M. A., Frasca, A. C., and Cassola, A. (2018). Translational repression by an RNA-binding protein promotes differentiation to infective forms in *Trypanosoma cruzi*. *PLoS Pathog.* 14:e1007059. doi: 10.1371/journal.ppat.1007059
- Romano, P. R., Garcia-Barrio, M. T., Zhang, X., Wang, Q., Taylor, D. R., Zhang, F., et al. (1998). Autophosphorylation in the activation loop is required for full kinase activity *in vivo* of human and yeast eukaryotic initiation factor 2 α kinases PKR and GCN2. *Mol. Cell. Biol.* 18, 2282–2297. doi: 10.1128/MCB.18.4.2282
- Ron, D., and Harding, H. P. (2012). Protein-folding homeostasis in the endoplasmic reticulum and nutritional regulation. *Cold Spring Harb. Perspect. Biol.* 4:1–13. doi: 10.1101/cshperspect.a013177
- Sudhakar, A., Ramachandran, A., Ghosh, S., Hasnain, S. E., Kaufman, R. J., and Ramaiah, K. V. (2000). Phosphorylation of serine 51 in initiation factor 2 α (eIF2 α) promotes complex formation between eIF2 α (P) and eIF2B and causes inhibition in the guanine nucleotide exchange activity of eIF2B. *Biochemistry* 39, 12929–12938. doi: 10.1021/bi000862

- Tonelli, R. R., Augusto Ld, S., Castilho, B. A., and Schenkman, S. (2011). Protein synthesis attenuation by phosphorylation of eIF2 α Is required for the differentiation of *Trypanosoma cruzi* into infective forms. *PLoS ONE* 6:e27094. doi: 10.1371/journal.pone.0027904
- Wek, S. A., Zhu, S., and Wek, R. C. (1995). The histidyl-tRNA synthetase-related sequence in the eIF-2 α protein kinase GCN2 interacts with tRNA and is required for activation in response to starvation for different amino acids. *Mol Cell Biol.* 15, 4497–4506. doi: 10.1128/MCB.15.8.4497
- Yoshida, N. (1983). Surface antigens of metacyclic trypomastigotes of *Trypanosoma cruzi*. *Infect. Immun.* 40, 836–839.
- Zeidan, Q., He, F., Zhang, F., Zhang, H., Jacobson, A., and Hinnebusch, A. G. (2018). Conserved mRNA-granule component Scd6 targets Dhh1 to repress translation initiation and activates Dcp2-mediated mRNA decay *in vivo*. *PLoS Genet.* 14:e1007806. doi: 10.1371/journal.pgen.1007806
- Zimmermann, L., Stephens, A., Nam, S. Z., Rau, D., Kubler, J., Lozajic, M., et al. (2018). A completely reimplemented MPI bioinformatics toolkit with a new HHpred server at its core. *J. Mol. Biol.* 430, 2237–2243. doi: 10.1016/j.jmb.2017.12.007

Conflict of Interest: The authors declare that the research was conducted in the absence of any commercial or financial relationships that could be construed as a potential conflict of interest.

Copyright © 2020 Malvezzi, Aricó, Souza-Melo, dos Santos, Bittencourt-Cunha, Holetz and Schenkman. This is an open-access article distributed under the terms of the Creative Commons Attribution License (CC BY). The use, distribution or reproduction in other forums is permitted, provided the original author(s) and the copyright owner(s) are credited and that the original publication in this journal is cited, in accordance with accepted academic practice. No use, distribution or reproduction is permitted which does not comply with these terms.



Precision Health for Chagas Disease: Integrating Parasite and Host Factors to Predict Outcome of Infection and Response to Therapy

Santiago J. Martinez^{1,2}, Patricia S. Romano^{1*} and David M. Engman^{2,3,4*}

¹ Laboratorio de Biología de *Trypanosoma cruzi* y la célula hospedadora—Instituto de Histología y Embriología “Dr. Mario H. Burgos,” (IHEM-CONICET- Universidad Nacional de Cuyo), Mendoza, Argentina, ² Department of Pathology and Laboratory Medicine, Cedars Sinai Medical Center, Los Angeles, CA, United States, ³ Department of Pathology and Laboratory Medicine, University of California, Los Angeles, Los Angeles, CA, United States, ⁴ Departments of Pathology and Microbiology-Immunology, Northwestern University, Chicago, IL, United States

OPEN ACCESS

Edited by:

Julius Lukes,
Institute of Parasitology
(ASCR), Czechia

Reviewed by:

John Kelly,
University of London, United Kingdom
Michael Alexander Miles,
University of London, United Kingdom

*Correspondence:

Patricia S. Romano
promano@fcm.uncu.edu.ar
David M. Engman
dme953@gmail.com

Specialty section:

This article was submitted to
Parasite and Host,
a section of the journal
Frontiers in Cellular and Infection
Microbiology

Received: 27 November 2019

Accepted: 16 April 2020

Published: 08 May 2020

Citation:

Martinez SJ, Romano PS and
Engman DM (2020) Precision Health
for Chagas Disease: Integrating
Parasite and Host Factors to Predict
Outcome of Infection and Response
to Therapy.
Front. Cell. Infect. Microbiol. 10:210.
doi: 10.3389/fcimb.2020.00210

Chagas disease, caused by the infection with the protozoan parasite *Trypanosoma cruzi*, is clinically manifested in approximately one-third of infected people by inflammatory heart disease (cardiomyopathy) and, to a minor degree, gastrointestinal tract disorders (megaesophagus or megacolon). Chagas disease is a zoonosis transmitted among animals and people through the contact with triatomine bugs, which are found in much of the western hemisphere, including most countries of North, Central and South America, between parallels 45° north (Minneapolis, USA) and south (Chubut Province, Argentina). Despite much research on drug discovery for *T. cruzi*, there remain only two related agents in widespread use. Likewise, treatment is not always indicated due to the serious side effects of these drugs. On the other hand, the epidemiology and pathogenesis of Chagas disease are both highly complex, and much is known about both. However, it is still impossible to predict what will happen in an individual person infected with *T. cruzi*, because of the highly variability of parasite virulence and human susceptibility to infection, with no definitive molecular predictors of outcome from either side of the host-parasite equation. In this Minireview we briefly discuss the current state of *T. cruzi* infection and prognosis and look forward to the day when it will be possible to employ precision health to predict disease outcome and determine whether and when treatment of infection may be necessary.

Keywords: chagas disease, *Trypanosoma cruzi*, therapy, outcome of infection, precision health

Trypanosoma cruzi AND CHAGAS DISEASE

Chagas disease, American trypanosomiasis, is caused by infection with the protozoan parasite *Trypanosoma cruzi* which displays a complex life cycle involving human and animal hosts as reservoirs of disease and triatomine insects of the Reduviidae family as vectors. Although the route of infection was originally felt to be restricted to contamination of the wound or mucous membrane with *T. cruzi*-contaminated excreta of hematophagous insects, other forms of transmission are also important, including oral infection through consumption of food and drink contaminated with the parasite, blood transfusion, organ transplantation, and congenital infection (Moncayo, 2003; Coura, 2014; Dolhun and Antes, 2016; Alarcón de Noya et al., 2017). Although 6–7 million infected individuals live in the Americas (WHO, 2020), migration of *T. cruzi*-infected people throughout

the world, many of whom are unaware of being infected, has contributed to the globalization of the disease (Steverding, 2014). Of the 238,000 infected people which are believed to reside in the United States, mostly immigrants from South America (Meymandi et al., 2017), 30,000 are found in Los Angeles, where Dr. Sheba Meymandi oversees a large Chagas clinic and a Center of Excellence for Chagas Disease (Meymandi, 2020). A few dozen cases of vector-borne transmission have been documented in the United States, although infection is widespread in wild animals throughout the southern half of the country (Montgomery et al., 2016; Kruse et al., 2019). The lack of an effective vaccine against *T. cruzi*, and the moderate effectiveness and toxicity of first-line drugs aggravate the situation (Schaub et al., 2011; Nunes et al., 2013; Rodríguez-Morales et al., 2015). Considering these aspects of epidemiology, continued surveillance of insects and wild animals, continued screening of the blood supply, and perhaps implementing screening of women of childbearing age will help to reduce transmission of *T. cruzi* through various routes.

In the human host, *T. cruzi* trypomastigotes, the infective forms of the parasite, can enter a wide variety of host cells. Trypomastigotes then differentiate into amastigotes which replicate in the cytoplasm and differentiate back to trypomastigotes again, which lyse the host cell membrane and exit the cell to continue the infectious cycle in the human. Cardiac and smooth muscle tissues are preferential cellular targets of *T. cruzi*. The adverse sequelae of infection described below depend on the tissues and organs involved, which is a highly variable and unpredictable factor. Chagas disease is highly complex. While traditionally considered as having acute, indeterminate (chronic-asymptomatic) and chronic (symptomatic) phases, this illness is highly heterogeneous and best considered to be a unique illness for each patient (Bonney et al., 2019). Most infected individuals live normal lives and eventually die of causes other than Chagas disease, completely unaware of their lifelong infection, whereas around 30% of infected people develops clinical manifestations. The acute phase of *T. cruzi* infection, lasting 4–8 weeks, often has no associated symptoms, despite the fact that the parasite is replicating and spreading throughout the body (Bastos et al., 2010; De Bona et al., 2018). In the case of vector transmission, it is possible to see Romaña's sign around 5% of the time, when parasites deposited by the triatomine on the face enter the conjunctiva, leading to periorbital inflammation and edema. Chagoma, an inflammatory skin lesion at the site of the insect bite, is also occasionally observed (Bastos et al., 2010). In most cases, however, acute infection is not recognized due to the non-specificity of signs and symptoms (fever, anorexia, and/or flu-like symptoms like body ache). In very rare cases acute infection leads to sudden death, due to parasitization of the cardiac conduction system and a fatal dysrhythmia. In most people, parasite-specific adaptive immunity develops, keeping overall tissue parasitosis and blood parasitemia at very low levels for life. In contrast, approximately one-third of infected individuals develop cardiomyopathy or, to a lesser degree, mega disease of the esophagus or colon, occurring many years after infection. Disease pathogenesis is extremely complex with multiple known and proposed mechanisms of tissue-specific damage. Current data highlight the persistence of parasites in

cardiac tissue as a key factor to disease progression, whether by anti-parasite immunity, autoimmunity or other mechanisms, suggesting that reduction of parasitosis through trypanocidal treatment is key to combatting the illness (Hyland et al., 2007; Viotti et al., 2009; Bastos et al., 2010; Bocchi et al., 2017; Bonney et al., 2019). We have recently reviewed pathogenesis (Bonney et al., 2019) and will not discuss this further in this review.

TREATMENT OF *Trypanosoma cruzi* INFECTION

Current Treatment for Chagas Disease

Trypanosoma cruzi infection is treated with Benznidazole (BNZ) or Nifurtimox (NFX), nitroimidazole compounds that have been used for decades. The approach currently practiced by most is to treat all acutely infected individuals, newborns with congenital infection, and anyone under 50 years of age. Further, all immunocompromised individuals such as those with HIV/AIDS or other immunosuppressive disorders or treatments, should be treated to prevent reactivation of chronic infection, normally maintained at very low levels by effective adaptive immunity (Pinazo et al., 2013). BNZ is administered to adults a dose of 5–8 mg/kg/day for 60 days. Children's doses are somewhat higher because they are more tolerant to the drugs and show quicker resolution of the common hepatic and renal toxicity upon drug cessation. Adults over 50 years of age with chronic *T. cruzi* infection should be considered individually, balancing the potential benefits and risks based. BNZ treatment is contraindicated for pregnant women and people with significant hepatic and renal illness (WHO, 2020). NFX is recommended as a second line drug, only in the cases of BNZ failure and in the absence of neurological and psychiatric disorders. NFX is administered at 8–10 mg/kg/day for 90 days in adults, and at 15–20 mg/kg/day for 90 days in children (Bern et al., 2007).

Although there are cases in which BNZ has been found to be more effective than NFX, both in the laboratory and in patients, the reasons for these differences are not known (Olivera et al., 2017; Crespillo-Andújar et al., 2018). Limitations of BNZ monotherapy includes the lower probability of parasitological cure in cases of chronic infection in contrast to the high probability of parasitological cure in the acute phase when treatment is maintained for the entire 60 day treatment period (Meymandi et al., 2018). It is also possible that BNZ-resistant *T. cruzi* clones emerge after partial treatment (Hughes and Andersson, 2017). Finally, the relatively short half-life of the drug (about 12 h), the low penetration of some tissues (Perin et al., 2017) and the occasional serious side effects are additional limitations. These adverse side effects are well-known, and include allergic dermatitis, peripheral neuropathy, anorexia, weight loss, and insomnia (Castro and Diaz de Toranzo, 1988). When they do develop, these side effects occur early in treatment and often become intolerable, causing patients to abort treatment; this can occur in up to 40% of individuals (Castro and Diaz de Toranzo, 1988; Castro et al., 2006; Viotti et al., 2009).

There have been a number of attempts to improve BNZ and NFX therapy, both to increase efficacy and to reduce toxicity,

by decreasing the daily dose, giving the drug intermittently, or preemptively treating potential side effects (Bastos et al., 2010; Álvarez et al., 2016; Morillo et al., 2017; Rassi et al., 2017; Cardoso et al., 2018). During the last decade, two important randomized clinical trials were conducted to evaluate the capacity of BNZ to modulate the evolution of Chagas heart disease in adult patients with established cardiomyopathy—the BENEFIT study (Morillo et al., 2015) and the TRAENA trial (Riarte, 2012). Both used a dose of 5 mg/kg/day of BNZ or placebo for 60 days and patient follow up over 5–10 years. Both found that BNZ was able to significantly reduce parasitemia and parasite-specific serum antibodies. However, these trials also showed that BNZ did not significantly reduce progression of clinical cardiac disease through 5 years of follow-up. Additional studies confirmed the low efficacy of BNZ to prevent progression of cardiomyopathy in patients with documented heart disease (Rassi and Rassi, 2010; Rassi et al., 2017). What these trials did not address is the potential benefit of therapy to indeterminate patients. Can drug treatment prevent the development of cardiomyopathy in chronically infected people with no cardiac disease? A retrospective study addressed this directly and showed that treatment with BNZ prevents the development of ECG alterations and decreases parasite-specific antibody titers in indeterminate patients (Fragata-Filho et al., 2016). Taken together, and considering additional studies (Villar et al., 2014; Pérez-Molina et al., 2015), these data suggest that trypanocidal therapy benefits acutely infected individual and chronically infected people who have not yet developed clinical heart disease.

Approaches to Improve Treatment of Chagas Disease

Research on new treatments involves two main strategies: a search for new candidate drugs that are more effective and less toxic to replace BNZ, and a search for adjunctive agents that can either increase the efficacy of BNZ/NFX or reduce their doses to prevent adverse effects. Typically, compounds tested for efficacy as monotherapy are also tested in combination with BNZ/NFX.

The main approaches to preclinical drug discovery for *T. cruzi* drugs involve seven main groups of inhibitors: (1) inhibitors of ergosterol biosynthesis (e.g., posaconazole and other antifungal azoles), (2) trypanothione metabolism (amiodarone and dronedarone), (3) pyrophosphate metabolism (biphosphonates), (4) cruzipain inhibitors (K777 and derivatives), (5) calcium metabolism (amiodarone, dronedarone), (6) protein and purine synthesis inhibitors, and (7) compounds that impair the redox metabolism (nitroaromatic compounds like BNZ, NFX and fexinidazole). Unfortunately, only a few clinical trials for treatment are ongoing or were performed recently for these candidates (Apt, 2010; Sales Junior et al., 2017).

Inhibitors of ergosterol biosynthesis affect the production of the parasite cell membrane and show trypanocidal effects, similar to what they do in fungi. For *T. cruzi*, a number of antifungals drugs have been found to have good *in vitro* and *in vivo* efficacy (Bustamante et al., 2014; Molina et al., 2014; Torrico et al., 2018), both as single agents and in combination with BNZ.

Posaconazole, for example, demonstrated trypanocidal activity particularly in combination with BNZ (Bustamante et al., 2014). However, in clinical trials, no advantage was observed with the combined therapy vs. BNZ monotherapy (Morillo et al., 2017). In addition, posaconazole showed no curative effects in patients on its own (Molina et al., 2014). Ravuconazole and E-1224, a ravuconazole prodrug with better drug absorption and bioavailability, are antifungal azoles with potent *in vitro* activity against *T. cruzi*. However, E-1224 failed to show sustained efficacy 1 year after treatment in comparison with BNZ and presented some safety issues at high doses (Torrico et al., 2018).

Besides antifungals azoles, the most advanced candidates in clinical trials are amiodarone and fexinidazole, which have ongoing or completed Phase II clinical studies, respectively. One advantage of amiodarone is its potential dual role in patients with cardiomyopathy since it is an antiarrhythmic drug as well as a potent and selective anti-*T. cruzi* agent (Benaïm and Paniz Mondolfi, 2012). Dronedarone, a derivative of amiodarone developed to reduce thyroid toxicity, showed a better profile at a lower dose, and will hopefully be tested in a clinical trial soon (Benaïm et al., 2012).

The Drugs for Neglected Diseases initiative (DNDi) has actively chosen to investigate nitroaromatic compounds. Their investigations have proved fruitful, resulting in a trypanosomatid portfolio that contains several agents. The DNDi portfolio published in December 2019 lists fexinidazole as in a Phase IIa clinical trial, whereas new BNZ regimens are in Phase IIb/III. Fexinidazole can induce high levels of parasitological cure in mice infected with BNZ-susceptible, partially resistant and resistant *T. cruzi* strains in acute and chronic experimental Chagas models (Bahia et al., 2012). These and other data have encouraged DNDi to include fexinidazole in clinical studies. In addition, the BENDITA (Benznidazole New Doses Improved Treatment & Associations) trial showed that a BNZ 2-week treatment course for adult patients with chronic Chagas disease displayed similar efficacy and significantly fewer side effects than the standard treatment duration of 8 weeks, when compared to placebo (DNDi, 2019). DNDi will now continue to work with national programs, partners, and health ministries of endemic countries to confirm these results and encourage the necessary steps to register the new regimen.

Other interesting strategies in preclinical studies are nanoparticle therapy and natural compounds. Considering that a major disadvantage of BNZ is its high toxicity, recent work has employed nanotechnology to attempt deliver this drug in an effective but safe way. The development of nanoparticles for drug delivery is an area of great promise. The earliest particles investigated were liposomal formulations of BNZ, which were developed to target the drug to the liver (Morilla et al., 2004). Since that time a variety of particles have been tested, including polymethacrylate interpolyelectrolyte complexes (García et al., 2018) and the amphipathic poloxamer P188 (Scalise et al., 2016). While these formulations were tested in different *in vitro* and *in vivo* systems, they show great promise in delivering BNZ and other trypanocidal agents to parasites and parasitized cells at lower effective BNZ doses with lower associated toxicity.

Natural compounds constitute a newer but nonetheless active area of Chagas drug discovery. Many plants extract display trypanocidal properties, with some demonstrating activity more potent than BNZ or NFX. Like other drugs, natural trypanocides can be useful either as independent agents, or through enhancing the activities of BNZ or NFX by enhancing their uptake by host cells, killing of intracellular amastigotes, or reducing toxicity. Drug repurposing is also being applied to *T. cruzi* as it is to many infectious and non-infectious diseases (Bellera et al., 2015). Some effective drugs can come from unlikely places, like agents used in cancer chemotherapy (Epting et al., 2017), antivirals, antibiotics, and cardiac medicines (Bellera et al., 2015).

Despite much research by hundreds of researchers over several decades, we still do not have an agent or regimen that is superior to BNZ/NFX for the treatment of *T. cruzi* infection. Several candidates showed good trypanocidal activity *in vitro*, but fail preclinical or clinical trials. There are many factors determining the outcome of infection and susceptibility of the parasite to treatment beyond what can be measured through typical studies. In the rest of this Mini Review we discuss other aspects of the host-pathogen interaction that impact the outcome of infection and treatment, which should be considered in whether, when and how to treat infection.

OUTCOME OF *T. cruzi* INFECTION AND EFFICACY OF TREATMENT DEPEND ON MANY FACTORS

It is difficult to extrapolate the results of *in vitro* tests to *in vivo* animal studies and even harder to extend those results to humans. Besides being human, people are highly heterogeneous genetically, and physiologically and respond to most challenges and interventions, including infections and drug treatments, with great variation; this can lead to treatment failures (Francisco et al., 2015). Although success of any treatment can be measured by the reduction of parasitemia and even of parasite-specific serum antibodies, success is ultimately measured by reduction in the development of long-term sequelae such as cardiomyopathy and megacolon. As mentioned above, treatment with intermittent low doses of BNZ in patients with established chagasic cardiomyopathy significantly reduced parasitemia, but not progression of cardiomyopathy (Morillo et al., 2015). Also *T. cruzi* displays a high degree of genetic and pathogenetic heterogeneity and are commonly present as mixtures of distinct parasite clones in a single infected triatomine or infected host (Pronovost et al., 2018). However, it is theoretically possible to predict the outcome of infection—subclinical for life, cardiomyopathy, mega disease—if we knew more about the genetic and physiologic basis of parasite virulence (broadly defined) and host susceptibility (also broadly defined). We are a long way from this understanding today. Variability in host physiologic factors such as nutrition, immune status, existence of coinfections, etc., further complicate the issue. The balance among host genetics, host physiology and parasite genetics determine outcome of infection and response to treatment. A number of these are discussed below. The reader should keep in

mind that these factors are ultimately based in large part on the genetics of host and parasite, which makes a systems approach to Chagas disease management possible in the future.

Epidemiology

In the absence of other information, epidemiologic data can be of modest help in predicting the outcome of *T. cruzi* infection. Information about patient origin, possible form of transmission (insect, congenital, oral), presence of other conditions such as immunosuppressive states such as cancer, HIV coinfection, or treatment with immunosuppressive drugs, may inform patient management. Clearly, infected individuals who are immunocompromised need treatment. Other aspects of the infection, such as the location where infection takes place, and by extension the characteristics of the human and parasite populations, can be useful. An estimated two-thirds of infected Brazilians are infected with the TcII strain of *T. cruzi* (Brenière et al., 2016; Zingales, 2018), one of seven discrete typing units (DTU) TcI-TcVI, plus TcBat (Zingales et al., 2009; Lima et al., 2015). Some of these DTUs can be identified serologically (Bhattacharyya et al., 2019). TcII strains, represented by the common laboratory strain Y, generally exhibit high virulence and may produce mega disease as well as cardiac disease in chronic infection (De Oliveira et al., 2008; Oliveira et al., 2017). In contrast, people from Argentina and Bolivia frequently are infected with TcV strains and frequently develop cardiomyopathy (Zuñiga et al., 1997; Messenger et al., 2015; Quebrada Palacio et al., 2018; Zingales, 2018). Other DTUs such as TcI (e.g., Colombian) or TcVI (e.g., Tulahuen) have a tendency not to cause clinical disease and are often used in chronic indeterminate mouse models of infection (Chandra et al., 2002; Santana et al., 2014). Unfortunately, the DTU system alone is not sufficient to predict disease outcome or response to therapy since there is no single outcome associated with any given DTU. No physician would withhold drug treatment in an acutely infected individual simply based on the fact that they may be infected with one particular *T. cruzi* strain or another.

Parasite Virulence

Virulence is a complex term in its own right. It is important to carefully define at each use. Virulence could be the capacity of *T. cruzi* to invade host cells, replicate, and emerge after host cell lysis. This leads to high parasitemia in experimental animals. It could refer to tissue tropism, with some tissue infections being more harmful to the host than others. Virulence might refer to the ability of the parasite to kill its host. At some level, considering the parasite alone, virulence is based on genetic elements. Virulence may be conferred by specific parasite surface proteins or secreted proteins that signal host cells, facilitating parasite entry and replication. Molecules from trans-sialidase and cruzipain families are well-established virulence factors of *T. cruzi* and validated targets for drug discovery. Cruzipain also participates in the modulation of the host cell immunity, highlighting the key role of the host response in the establishment and outcome of *T. cruzi* infection (Guiñazú et al., 2004; San Francisco et al., 2017). High virulence is usually defined as the ability to cause high parasitemia and/or tissue parasitosis and/or

death of experimental animals (Sales-Campos et al., 2015). This is based in part on the ability to invade and/or replicate in host cells more rapidly than do low virulence isolates. Low virulence strains are more likely to cause low-level chronic infection that may never cause clinical disease (Cardillo et al., 2015). As mentioned above, the commonly used high-virulence Y strain of *T. cruzi* causes death in young C57BL/6 mice between 14 and 21 days post-infection in conjunction with maximal parasitemia (Casassa et al., 2019). By contrast, the K98 strain causes chronic infection. It should be emphasized that virulence is equally influenced by the host (Ferreira et al., 2018), as discussed in more detail below.

Tissue Tropism

Another characteristic of *T. cruzi* is differential tissue tropism. Some isolates of this parasite have a propensity to infect certain tissues over others. This may be due to specific affinity for certain host cell surface molecules, preferential ability to replicate in some cells better than others, or specific attraction to an organ-specific vascular bed. If a person becomes infected with a myotropic strain, it is more likely that cardiac pathology or skeletal myositis will develop. On the contrary, a pantropic strain may affect many organs and promote development of megaesophagus or megacolon. Tropism can be ascertained by *in vitro* testing using different cell lines. A strain with cellular myotropism will prefer H9C2 cardiac myoblasts or human skeletal myoblasts (Jorge et al., 1986; Mirkin et al., 1997; Aridgides et al., 2013), while a pantropic strain will not have a preference, for example affecting kidney cells and embryonic fibroblasts equally (Piras et al., 1982; Jorge et al., 1986; Medina et al., 2018). Information about the tropism of parasite clone or clones could potentially be important in guiding treatment decisions, including a decision not to treat. The challenge of course is to determine potential tropism or other characteristics of a clone without having isolated and cultured parasites for laboratory study. There may be ways to do this in the future using a combination of advanced imaging and molecular approaches (see below). In the meantime, it is really not possible to predict the tissue tropism of a strain based on the region of origin or DTU.

Drug Resistance

The differential resistance of *T. cruzi* to BNZ among isolates has been documented (Bustamante et al., 2014; Abegg et al., 2017; Vieira et al., 2018). This intrinsic resistance in some strains could explain why some patients receiving the same BNZ treatment show parasitological cure while others do not. Similar to virulence, the capacity of parasites to resist or be susceptible to a drug is genetically determined by the presence of specific factors. The *T. cruzi* Colombian and V-10 strains are highly resistant to BNZ, while the Y and Dm28c strains are partially resistant and the CL strain is highly sensitive (Filardi and Brener, 1984; Bahia et al., 2012; Reigada et al., 2019). Somewhat paradoxically, intracellular replication of some strains is enhanced by the presence of BNZ and the associated production of reactive oxygen species (Paiva et al., 2018). Several have proposed that different *T. cruzi* DTU have different resistance to BNZ and NFX (Cencig et al., 2012; Teston et al., 2013). Some DTU are

more resistant to BNZ than others, although even within a single DTU there can be variability in BNZ sensitivity (Quebrada Palacio et al., 2018). Interestingly, parasite strains of different DTUs do show common BNZ susceptibility and resistance patterns (Revollo et al., 2019). Clearly there can be much greater refinement in genetic characterization of *T. cruzi* than the DTU system but it is a measure that has shown great utility in many studies. However, data from genotyping could be used to predict the susceptibility of an isolate to drug treatment. As mentioned above and discussed below, the challenge is to be able to genotype or phenotype parasites without isolating them, since in many chronically-infected patients circulating parasites are rare or absent. As a relatively crude measure of *T. cruzi* sensitivity to BNZ, quantitative PCR to detect parasite DNA in blood before and after BNZ treatment is the best we have at the moment (Britto et al., 1999; Maffey et al., 2012; Barros et al., 2017; Rodrigues-dos-Santos et al., 2018). It is also possible that parasite dormancy may play a role in drug resistance (Sánchez-Valdéz et al., 2018).

Host Factors in Parasite Susceptibility and Resistance

As in many diseases, the outcome of *T. cruzi* infection is determined not only by the pathogen, but also by the host. We tend to focus on immunity but there are other intrinsic (innate) factors that may also contribute to susceptibility and resistance. These known and unknown attributes are bundled in the vague term “genetic factors.” Beyond the genetic factors there is also host nutritional status, possible presence of coinfections, and other environmental factors that may influence outcome. This concept is best exemplified by the finding that most *T. cruzi*-infected individuals have no clinical signs or symptoms of infection—ever. Regarding host genetic background, T lymphocytes in chronic patients with no clinical disease have a high frequency of CD4⁺ and CD8⁺ T cells expressing HLA-DR and CD45RO (Dutra et al., 1994), with little to no costimulatory CD28 (Dutra et al., 1996; Menezes et al., 2004; Albareda et al., 2006). This profile positively correlates with the expression of the regulatory cytokine IL-10 (Menezes et al., 2004) and also with the presence of CTLA-4, a costimulatory molecule which leads to T cell modulation (Souza et al., 2007). Since CD8⁺ T cell destruction of parasitized cells can lead to tissue inflammation and clinical disease, it is possible that immunoregulatory mechanisms in these patients prevent pathology and facilitate lifelong indeterminate, subclinical disease. The balance between proinflammatory and anti-inflammatory immune responses is central to the outcome of infection. Although a pro-inflammatory adaptive immune response is necessary to control *T. cruzi*, immunoregulation is necessary later on to prevent tissue destruction and possible subsequent autoimmune damage (Bonney and Engman, 2015). In this way, IL-10 plays an essential modulating role in controlling disease development. The ability to express IL-10 at sufficiently high levels may be genetically determined and may influence disease outcome. Studies in experimental models of *T. cruzi* infection demonstrate the influence of host immune response in the outcome of infection. BALB/c mice, which

develop a Th2-skewed response upon *T. cruzi* infection, are hypersensitive to infection and do not survive the acute phase. In contrast, C57BL/6 mice, which develop Th1 immunity through the IL-12/IFN- γ /iNOS axis, control the parasite and show low parasitemia and mortality during the acute phase (Michailowsky et al., 2001).

TOWARD PRECISION HEALTH MANAGEMENT OF CHAGAS DISEASE

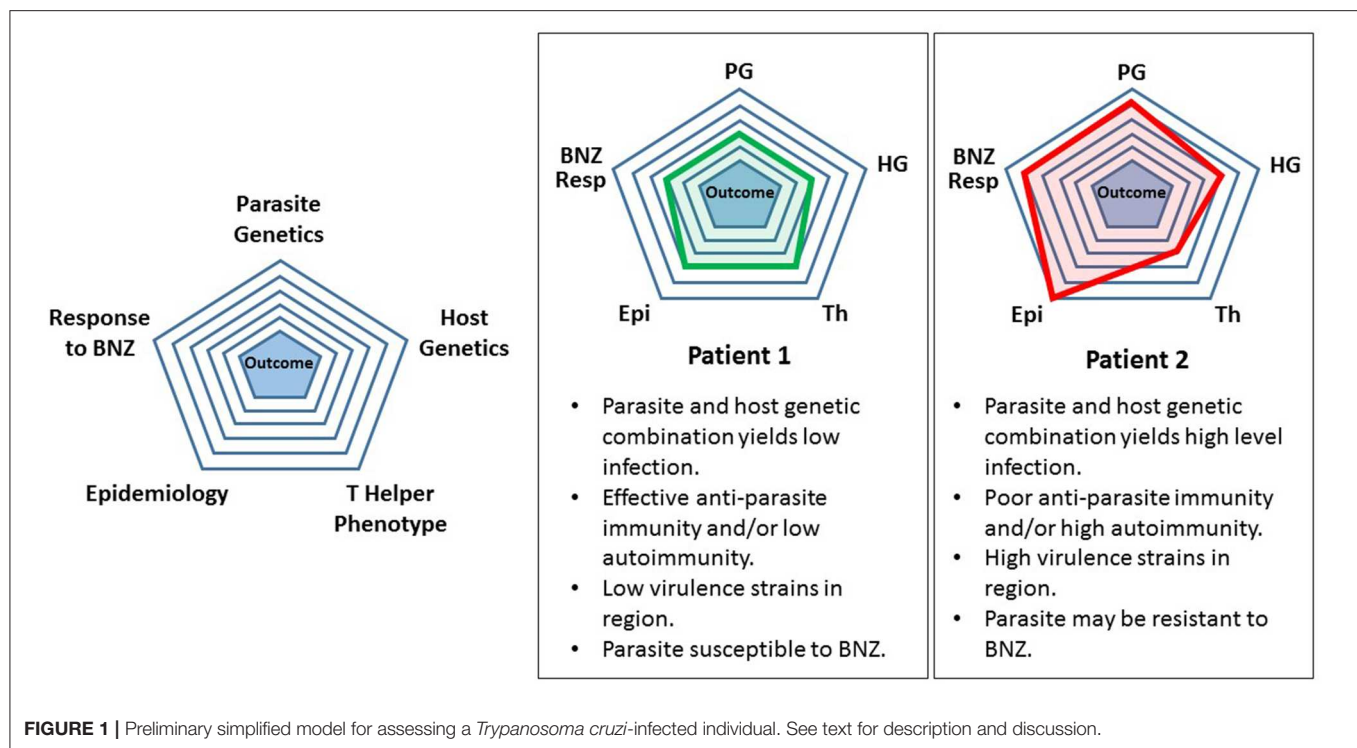
As described above, *T. cruzi* infection and Chagas disease are highly complex. At the present time, no single factor or combination of factors can predict disease outcome or response to therapy in an infected individual. The assignment of *T. cruzi* strains to DTUs and the assessment of a person's HLA haplotype and other immunogenetics are starting points. In chronic infection it is often not possible to isolate parasites for analysis and, even if successful, the parasite isolated may not represent all parasite clones present in the patient, which might have different pathogenic potential. Detection of parasites in chronically infected individuals is most frequently accomplished by PCR (Schijman et al., 2011) and this method has also been used to monitor the effect of therapy on parasite persistence (Morillo et al., 2015; Sulleiro et al., 2019). Unfortunately, the sensitivity of PCR is problematic—only 60% in the large BENEFIT Trial of several thousand patients (Morillo et al., 2015). Although there are many possible reasons for this, a likely reason is suboptimal sampling. Perhaps a proteomic approach would be better and recent work detecting *T. cruzi* antigens in circulating immune complexes from infected individuals is promising (Ohyama et al., 2016). A major breakthrough in patient management would be the ability to assess the distribution of parasites in the body, much as is done today with nuclear medicine scans for cancer. We can do this in mice employing bioluminescent imaging of engineered luminescent parasites (Hyland et al., 2008) but obviously this is not possible in patients. Interestingly the infection in mice is highly dynamic with migration of parasite foci around the body over time (Lewis et al., 2014). Development of approaches to image parasites in an infected person to determine location(s) and burden would enhance the care of Chagas patients if these are found to be linked to organ-specific dysfunction. Another would be the detection of parasite-free *T. cruzi* DNA in blood or body fluids, much as is done today for circulating tumor cell DNA. In this way it is theoretically possible to genotype all parasite clones in an infected individual, perhaps quantitatively, by next generation sequencing (NGS), in the absence of circulating parasites. This is an active area of investigation in a number of laboratories (Domagalska and Dujardin, 2020).

A more refined genetic analysis of *T. cruzi* than the DTU system will no doubt emerge through large scale NGS whole exome or genome analysis of parasites and integration of this information with detailed clinical information and patient outcomes, including response to treatment. In this way, the complex interplay between parasite and host genetics that ultimately determines the outcome of infection might emerge.

This may not happen tomorrow, but it is a major goal of the medical field as applied to many diseases, both infectious and otherwise. Unfortunately genome wide association studies have not been successful in identifying gene polymorphisms associated with disease progression (Deng et al., 2013). Regarding drug treatment, a comprehensive, systems approach to parasite and host will essentially allow a pharmacogenomic approach to treatment, much as is done today for personalized treatment decisions for cancer, arrhythmias and pain management (Wang et al., 2011).

How will this happen? Until now, associations between biological data and biological behaviors were deduced from simultaneous consideration of small numbers of data features from a laboratory experiment or clinical trial. This limitation has hindered our understanding of polygenic diseases like diabetes and coronary heart disease. The advent of machine learning now allows the simultaneous analysis of hundreds or even thousands of features across a very large number of biological samples employing supercomputing to identify relationships among the features (Rajkomar et al., 2019). For some applications, the machine needs to be “trained,” for example by “learning” the associations of histologic images with cancer types. If all goes well with the training, the computer can then type the cancer with high accuracy (Esteve et al., 2017; Gertych et al., 2019). Extending the histology example further, there is information in a complex image like tissue histology that reflects underlying genetic modifications, such as DNA methylation, and machine learning can identify those subtleties in a way that the human eye never could (Zheng et al., 2020). This approach can also be applied to molecular data *de novo* for gene discovery (Wood et al., 2018). Ultimately, the promise of precision health will be realized by the application machine learning to a wider variety of data features and, for Chagas disease, this means clinical data, basic patient information, including demographics, baseline genome sequence, behavioral and physiological data and, of course, genomic information of the parasite clone(s) infecting the person. We believe that it is only a matter of time when this will be science and not just science fiction.

As an intermediate step between the present and future, we propose a highly simplistic theoretical approach to categorizing *T. cruzi* infection and treatment. Refinement of this model over time by adding levels of sophistication might eventually yield a useful tool for patient management. For example, considering five attributes derived from host or parasite it is possible to generate a pictorial representation of the infection (**Figure 1**). This is based loosely on the modeling of Santi-Rocca (Santi-Rocca et al., 2017). Each attribute—parasite genetics, host genetics, T helper phenotype, epidemiology, and response to BNZ can be “scored” from 1 to 5, with 1 corresponding to the lowest level of a particular attribute and 5 the highest. When applied to two different infections, Patient 1 having a low-level, chronic infection with no clinical disease and Patient 2 having significant cardiomyopathy, a pictorial representation of the infection can be generated. The attributes are listed below each patient in clockwise order from the top. Clearly this is so simplistic that it is not useful today. These attributes are not really “scorable” in this way and do not correlate in the manner



shown in these examples. However, simplistic, this approach does give a preliminary glimpse into a future analytic scheme that shows how specific features of host and parasite might contribute the ultimate outcome of infection and responsiveness to treatment.

In terms of refinement, the field really does need to move beyond studies of laboratory strains to analyze strains present in patients and insects in a systematic and non-biased way through NGS. It is possible that the DTU structure will have value over time since if nothing else DTU by definition reflects the genetic relatedness of strains. We foresee a day when genotyping of the strain(s) present in each patient will become part of the standard workup of *T. cruzi* infection and that NGS genotyping of circulating parasite DNA will solve this problem. The premise underlying this entire discussion is that, ultimately, disease outcome and response to therapy can be predicted based on the genotypes of parasite and host, both as independent factors and in combination. The latter notion is based on the well-known fact that an individual parasite strain shows differential virulence depending on the host, and that an individual host has different disease outcome depending on the parasite strain. This complexity is challenging but no more so than in many other polygenetic diseases affecting millions.

CONCLUSION

Since its discovery more than 100 years ago (Chagas, 1909), Chagas disease has proven to be a major clinical and public

health challenge due to the extreme heterogeneity in the outcome of infection, the wide range of mammalian hosts and reservoirs, the large geographic range of its triatomine insect vectors, worldwide migration of infected individuals, and paucity of drugs. While we have discussed the potential future for disease diagnosis, prognosis and patient management, the ultimate solution is the development of an effective and curative treatment having low toxicity. Better yet, a safe and effective vaccine that provides sterilizing immunity or even immunity sufficient to minimize the parasite burden to prevent clinical disease. Science and medicine are developing rapidly and we are hopeful that someday *T. cruzi* and Chagas disease will be considered manageable infections, much like the viral and bacterial infections that were previously deadly and now are managed through vaccination and effective drug treatments.

AUTHOR CONTRIBUTIONS

All authors listed have made a substantial, direct and intellectual contribution to the work, and approved it for publication.

FUNDING

This work was funded in part by NIH grants R01-HL075822 and GM93359. SM was supported by a Wood-Whelan Fellowship from the International Union of Biochemistry and Molecular Biology.

REFERENCES

- Abegg, C. P., de Abreu, A. P., da Silva, J. L., de Araújo, S. M., Gomes, M. L., Ferreira, É. C., et al. (2017). Polymorphisms of blood forms and in vitro metacyclogenesis of *Trypanosoma cruzi* I, II, and IV. *Exp. Parasitol.* 176, 8–15. doi: 10.1016/j.exppara.2017.02.013
- Alarcón de Noya, B., Ruiz-Guevara, R., Noya, O., Castro, J., Ossenkopp, J., Díaz-Bello, Z., et al. (2017). Long-term comparative pharmacovigilance of orally transmitted Chagas disease: first report. *Exp. Rev. Anti. Infect. Ther.* 15, 319–325. doi: 10.1080/14787210.2017.1286979
- Albareda, M. C., Laucella, S. A., Alvarez, M. G., Armenti, A. H., Bertochi, G., Tarleton, R. L., et al. (2006). *Trypanosoma cruzi* modulates the profile of memory CD8⁺ T cells in chronic Chagas' disease patients. *Int. Immunol.* 18, 465–471. doi: 10.1093/intimm/dxh387
- Álvarez, M. G., Hernández, Y., Bertocchi, G., Fernández, M., Lococo, B., Ramírez, J. C., et al. (2016). New scheme of intermittent benznidazole administration in patients chronically infected with *Trypanosoma cruzi*: a pilot short-term follow-up study with adult patients. *Antimicrob. Agents Chemother.* 60, 833–837. doi: 10.1128/AAC.00745-15
- Apt, W. (2010). Current and developing therapeutic agents in the treatment of Chagas disease. *Drug Des. Devel. Ther.* 4, 243–253. doi: 10.2147/DDDT.S8338
- Aridigides, D., Salvador, R., and Pereiraperrin, M. (2013). *Trypanosoma cruzi* hijacks TrkC to enter cardiomyocytes and cardiac fibroblasts while exploiting TrkA for cardioprotection against oxidative stress. *Cell. Microbiol.* 15, 1357–1366. doi: 10.1111/cmi.12119
- Bahia, M. T., de Andrade, I. M., Martins, T. A. F., Nascimento, Á. F., da S. do, Diniz, L., de, F., et al. (2012). Fexinidazole: a potential new drug candidate for chagas disease. *PLoS Negl. Trop. Dis.* 6:e1870. doi: 10.1371/journal.pntd.0001870
- Barros, J. H. S., Xavier, S. C. C., Bilac, D., Lima, V. S., Dario, M. A., and Jansen, A. M. (2017). Identification of novel mammalian hosts and Brazilian biome geographic distribution of *Trypanosoma cruzi* TcIII and TcIV. *Acta Trop.* 172, 173–179. doi: 10.1016/j.actatropica.2017.05.003
- Bastos, C. J. C., Aras, R., Mota, G., Reis, F., Dias, J. P., de Jesus, R. S., et al. (2010). Clinical outcomes of thirteen patients with acute chagas disease acquired through oral transmission from two urban outbreaks in Northeastern Brazil. *PLoS Negl. Trop. Dis.* 4:e711. doi: 10.1371/journal.pntd.0000711
- Bellera, C. L., Balcazar, D. E., Vanrell, M. C., Casassa, A. F., Palestro, P. H., Gavernet, L., et al. (2015). Computer-guided drug repurposing: identification of trypanocidal activity of clofazimine, benidipine and saquinavir. *Eur. J. Med. Chem.* 93, 338–348. doi: 10.1016/j.ejmech.2015.01.065
- Benaïm, G., Hernandez-Rodriguez, V., Mujica-Gonzalez, S., Plaza-Rojas, L., Silva, M. L., Parra-Gimenez, N., et al. (2012). In vitro anti-*Trypanosoma cruzi* activity of dronedarone, a novel amiodarone derivative with an improved safety profile. *Antimicrob. Agents Chemother.* 56, 3720–3725. doi: 10.1128/AAC.00207-12
- Benaïm, G., and Paniz Mondolfi, A. E. (2012). The emerging role of amiodarone and dronedarone in Chagas disease. *Nat. Rev. Cardiol.* 9, 605–609. doi: 10.1038/nrcardio.2012.108
- Bern, C., Montgomery, S. P., Herwaldt, B. L., Rassi, A., Marin-Neto, J. A., Dantas, R. O., et al. (2007). Evaluation and treatment of chagas disease in the United States: a systematic review. *J. Am. Med. Assoc.* 298, 2171–2181. doi: 10.1001/jama.298.18.2171
- Bhattacharyya, T., Murphy, N., and Miles, M. A. (2019). *Trypanosoma cruzi* lineage-specific serology: New rapid tests for resolving clinical and ecological associations. *Futur. Sci. OA* 5:FSO422. doi: 10.2144/fsoa-2019-0103
- Bocchi, E. A., Bestetti, R. B., Scanavacca, M. I., Cunha Neto, E., and Issa, V. S. (2017). Chronic chagas heart disease management: from etiology to cardiomyopathy treatment. *J. Am. Coll. Cardiol.* 70, 1510–1524. doi: 10.1016/j.jacc.2017.08.004
- Bonney, K. M., and Engman, D. M. (2015). Autoimmune pathogenesis of Chagas heart disease: looking back, looking ahead. *Am. J. Pathol.* 185, 1537–1547. doi: 10.1016/j.ajpath.2014.12.023
- Bonney, K. M., Luthringer, D. J., Kim, S. A., Garg, N. J., and Engman, D. M. (2019). Pathology and pathogenesis of chagas heart disease. *Annu. Rev. Pathol.* 14, 421–447. doi: 10.1146/annurev-pathol-020117-043711
- Brenière, S. F., Waleckx, E., and Barnabé, C. (2016). Over six thousand *Trypanosoma cruzi* strains classified into discrete typing units (DTUs): attempt at an Inventory. *PLoS Negl. Trop. Dis.* 10:e0004792. doi: 10.1371/journal.pntd.0004792
- Britto, C., Cardoso, A., Silveira, C., Macedo, V., and Fernandes, O. (1999). Polymerase chain reaction (PCR) as a laboratory tool for the evaluation of the parasitological cure in chagas disease after specific treatment. *Medicina.* 59, 176–178.
- Bustamante, J. M., Craft, J. M., Crowe, B. D., Ketchie, S. A., and Tarleton, R. L. (2014). New, combined, and reduced dosing treatment protocols cure *trypanosoma cruzi* infection in mice. *J. Infect. Dis.* 209, 150–162. doi: 10.1093/infdis/jit420
- Cardillo, F., Pinho, R. T., Antas, P. R. Z., and Mengel, J. (2015). Immunity and immune modulation in *Trypanosoma cruzi* infection. *Pathog. Dis.* 73:ftv082. doi: 10.1093/femspd/ftv082
- Cardoso, C. S., Ribeiro, A. L. P., Oliveira, C. D. L., Oliveira, L. C., Ferreira, A. M., Bierrenbach, A. L., et al. (2018). Beneficial effects of benznidazole in Chagas disease: NIH SaMi-Trop cohort study. *PLoS Negl. Trop. Dis.* 12:e0006814. doi: 10.1371/journal.pntd.0006814
- Casassa, A. F., Vanrell, M. C., Colombo, M. I., Gottlieb, R. A., and Romano, P. S. (2019). Autophagy plays a protective role against *Trypanosoma cruzi* infection in mice. *Virulence* 10, 151–165. doi: 10.1080/21505594.2019.1584027
- Castro, J. A., deMecca, M. M., and Bartel, L. C. (2006). Toxic side effects of drugs used to treat Chagas' disease (American Trypanosomiasis). *Hum. Exp. Toxicol.* 25, 471–479. doi: 10.1191/0960327106het653oa
- Castro, J. A., and Diaz de Toranzo, E. G. (1988). Toxic effects of nifurtimox and benznidazole, two drugs used against American trypanosomiasis (Chagas' disease). *Biomed. Environ. Sci.* 1, 19–33.
- Cencig, S., Coltel, N., Truyens, C., and Carlier, Y. (2012). Evaluation of benznidazole treatment combined with nifurtimox, posaconazole or AmBisome® in mice infected with *Trypanosoma cruzi* strains. *Int. J. Antimicrob. Agents* 40, 527–532. doi: 10.1016/j.ijantimicag.2012.08.002
- Chagas, C. (1909). Nova trypanosomíase humana. Estudo sobre a morfologia e o ciclo evolutivo do Schizotripanum cruzi n. gen. Sp, agente etiológico de nova entidade mórbida do homem. *Mem. Inst. Oswaldo Cruz* 1, 159–218. doi: 10.1590/S0074-02761909000200008
- Chandra, M., Tanowitz, H. B., Petkova, S. B., Huang, H., Weiss, L. M., Wittner, M., et al. (2002). Significance of inducible nitric oxide synthase in acute myocarditis caused by *Trypanosoma cruzi* (Tulahuen strain). *Int. J. Parasitol.* 32, 897–905. doi: 10.1016/S0020-7519(02)00028-0
- Coura, J. R. (2014). The main sceneries of Chagas disease transmission. The vectors, blood and oral transmissions - A comprehensive review. *Mem. Inst. Oswaldo Cruz* 110, 277–282. doi: 10.1590/0074-0276140362
- Crespillo-Andújar, C., Chamorro-Tojeiro, S., Norman, F., Monge-Maillo, B., López-Vélez, R., and Pérez-Molina, J. A. (2018). Toxicity of nifurtimox as second-line treatment after benznidazole intolerance in patients with chronic Chagas disease: when available options fail. *Clin. Microbiol. Infect.* 24, 1344.e1–1344.e4. doi: 10.1016/j.cmi.2018.06.006
- De Bona, E., Lidani, K. C. F., Bavia, L., Omidian, Z., Gremski, L. H., Sandri, T. L., et al. (2018). Autoimmunity in chronic chagas disease: a road of multiple pathways to cardiomyopathy? *Front. Immunol.* 9:1842. doi: 10.3389/fimmu.2018.01842
- De Oliveira, G. M., De Melo Medeiros, M., Da Silva Batista, W., Santana, R., Araújo-Jorge, T. C., and De Souza, A. P. (2008). Applicability of the use of charcoal for the evaluation of intestinal motility in a murine model of *Trypanosoma cruzi* infection. *Parasitol. Res.* 102, 747–750. doi: 10.1007/s00436-007-0829-8
- Deng, X., Sabino, E. C., Cunha-Neto, E., Ribeiro, A. L., Ianni, B., Mady, C., et al. (2013). Genome wide association study (GWAS) of chagas cardiomyopathy in trypanosoma cruzi seropositive subjects. *PLoS ONE* 8:e79629. doi: 10.1371/journal.pone.0079629
- DNDi (2019). *The BENDITA Study: A Phase II Study to Assess Safety, Tolerability, and Efficacy of Different Benznidazole Regimens, Alone and in Combination with Fosravuconazole*. Available online at: https://www.dndi.org/wp-content/uploads/2019/03/2page_BenditastudyOverview_ENG.pdf.
- Dolhun, E. P., and Antes, A. W. (2016). A case of cardboard boxes likely facilitating the biting of a patient by *Trypanosoma cruzi*-infected Triatomine bugs. *Am. J. Trop. Med. Hyg.* 95, 1115–1117. doi: 10.4269/ajtmh.16-0455
- Domagalska, M. A., and Dujardin, J. C. (2020). Next-generation molecular surveillance of TriTryp diseases. *Trends Parasitol.* 36, 356–367. doi: 10.1016/j.pt.2020.01.008

- Dutra, W. O., Martins-filho, O. A., Canado, J. R., Pinto-dias, J. C., Brenner, Z., Freeman, G. L., et al. (1994). Activated T and B lymphocytes in peripheral blood of patients with Chagas' disease. *Int. Immunol.* 6, 499–506. doi: 10.1093/intimm/6.4.499
- Dutra, W. O., Martins-Filho, O. A., Cançado, J. R., Pinto-Dias, J. C., Brenner, Z., Gazzinelli, G., et al. (1996). Chagasic patients lack CD28 expression on many of their circulating T lymphocytes. *Scand. J. Immunol.* 43, 88–93. doi: 10.1046/j.1365-3083.1996.d01-9.x
- Epting, C. L., Emmer, B. T., Du, N. Y., Taylor, J. M., Makanji, M. Y., Olson, C. L., et al. (2017). Cell cycle inhibition to treat sleeping sickness. *MBio* 8:e01427–17. doi: 10.1128/mBio.01427-17
- Esteva, A., Kuprel, B., Novoa, R. A., Ko, J., Swetter, S. M., Blau, H. M., et al. (2017). Dermatologist-level classification of skin cancer with deep neural networks. *Nature* 542, 115–118. doi: 10.1038/nature21056
- Ferreira, B. L., Ferreira, É. R., de Brito, M. V., Salu, B. R., Oliva, M. L. V., Mortara, R. A., et al. (2018). BALB/c and C57BL/6 mice cytokine responses to *Trypanosoma cruzi* infection are independent of parasite strain infectivity. *Front. Microbiol.* 9:553. doi: 10.3389/fmicb.2018.00553
- Filardi, L. S., and Brenner, Z. (1984). A rapid method for testing *in vivo* the susceptibility of different strains of *Trypanosoma cruzi* to active chemotherapeutic agents. *Mem. Inst. Oswaldo Cruz* 79, 221–225. doi: 10.1590/S0074-02761984000200008
- Fragata-Filho, A. A., França, F. F., Fragata, C., da, S., Lourenço, A. M., Faccini, C. C., et al. (2016). Evaluation of parasiticide treatment with benznidazole in the electrocardiographic, clinical, and serological evolution of Chagas disease. *PLoS Negl. Trop. Dis.* 10:e0004508. doi: 10.1371/journal.pntd.0004508
- Francisco, A. F., Lewis, M. D., Jayawardhana, S., Taylor, M. C., Chatelain, E., and Kelly, J. M. (2015). Limited ability of posaconazole to cure both acute and chronic *Trypanosoma cruzi* infections revealed by highly sensitive *in vivo* imaging. *Antimicrob. Agents Chemother.* 59, 4653–4661. doi: 10.1128/AAC.00520-15
- García, M. C., Martinelli, M., Ponce, N. E., Sanmarco, L. M., Aoki, M. P., Manzo, R. H., et al. (2018). Multi-kinetic release of benznidazole-loaded multiparticle drug delivery systems based on polymethacrylate interpolyelectrolyte complexes. *Eur. J. Pharm. Sci.* 120, 107–122. doi: 10.1016/j.ejps.2018.04.034
- Gertych, A., Swiderska-Chadaj, Z., Ma, Z., Ing, N., Markiewicz, T., Cierniak, S., et al. (2019). Convolutional neural networks can accurately distinguish four histologic growth patterns of lung adenocarcinoma in digital slides. *Sci. Rep.* 9:1483. doi: 10.1038/s41598-018-37638-9
- Guiñazú, N., Pellegrini, A., Giordanengo, L., Aoki, M. P., Rivarola, H. W., Cano, R., et al. (2004). Immune response to a major *Trypanosoma cruzi* antigen, cruzipain, is differentially modulated in C57BL/6 and BALB/c mice. *Microbes Infect.* 6, 1250–1258. doi: 10.1016/j.micinf.2004.07.010
- Hughes, D., and Andersson, D. I. (2017). Evolutionary trajectories to antibiotic resistance. *Annu. Rev. Microbiol.* 71, 579–596. doi: 10.1146/annurev-micro-090816-093813
- Hyland, K. V., Asfaw, S. H., Olson, C. L., Daniels, M. D., and Engman, D. M. (2008). Bioluminescent imaging of *Trypanosoma cruzi* infection. *Int. J. Parasitol.* 38, 1391–400. doi: 10.1016/j.ijpara.2008.04.002
- Hyland, K. V., Leon, J. S., Daniels, M. D., Gias, N., Woods, L. M., Bahk, T. J., et al. (2007). Modulation of autoimmunity by treatment of an infectious disease. *Infect Immun* 75, 3641–3650. doi: 10.1128/IAI.00423-07
- Jorge, T. C. A., Barbosa, H. S., Moreira, A. L., De Souza, W., and Meirelles, M. N. L. (1986). The interaction of myotropic and macrophagotropic strains of *Trypanosoma cruzi* with myoblasts and fibers of skeletal muscle. *Zeitschrift für Parasitenkd. Parasitol. Res.* 72, 577–584. doi: 10.1007/BF00925477
- Kruse, C. S., Guerra, D. A., Gelillo-Smith, R., Vargas, A., Krishnan, L., and Stigler-Granados, P. (2019). Leveraging technology to manage Chagas disease by tracking domestic and sylvatic animal hosts as sentinels: a systematic review. *Am. J. Trop. Med. Hyg.* 101, 1126–1134. doi: 10.4269/ajtmh.19-0050
- Lewis, M. D., Fortes Francisco, A., Taylor, M. C., Burrell-Saward, H., Mclatchie, A. P., Miles, M. A., et al. (2014). Bioluminescence imaging of chronic *Trypanosoma cruzi* infections reveals tissue-specific parasite dynamics and heart disease in the absence of locally persistent infection. *Cell. Microbiol.* 16, 1285–1300. doi: 10.1111/cmi.12297
- Lima, L., Espinosa-Álvarez, O., Ortiz, P. A., Trejo-Varón, J. A., Carranza, J. C., Pinto, C. M., et al. (2015). Genetic diversity of *Trypanosoma cruzi* in bats, and multilocus phylogenetic and phylogeographical analyses supporting Tcbat as an independent DTU (discrete typing unit). *Acta Trop.* 151, 166–177. doi: 10.1016/j.actatropica.2015.07.015
- Maffey, L., Cardinal, M. V., Ordóñez-Krasnowski, P. C., Lanati, L. A., Lauricella, M. A., Schijman, A. G., et al. (2012). Direct molecular identification of *Trypanosoma cruzi* discrete typing units in domestic and peridomestic triatoma infestans and triatoma sordida from the Argentine Chaco. *Parasitology* 139, 1570–1579. doi: 10.1017/S0031182012000856
- Medina, L., Castillo, C., Liempi, A., Herbach, M., Cabrera, G., Valenzuela, L., et al. (2018). Differential infectivity of two *Trypanosoma cruzi* strains in placental cells and tissue. *Acta Trop.* 186, 35–40. doi: 10.1016/j.actatropica.2018.07.001
- Menezes, C. A. S., Rocha, M. O. C., Souza, P. E. A., Chaves, A. C. L., Gollob, K. J., and Dutra, W. O. (2004). Phenotypic and functional characteristics of CD28+ and CD28- cells from chagasic patients: distinct repertoire and cytokine expression. *Clin. Exp. Immunol.* 137, 129–138. doi: 10.1111/j.1365-2249.2004.02479.x
- Messenger, L. A., Miles, M. A., and Bern, C. (2015). Between a bug and a hard place: *Trypanosoma cruzi* genetic diversity and the clinical outcomes of Chagas disease. *Expert Rev. Anti. Infect. Ther.* 13, 995–1029. doi: 10.1586/14787210.2015.1056158
- Meymandi, S., Hernandez, S., Park, S., Sanchez, D. R., and Forsyth, C. (2018). Treatment of Chagas disease in the United States. *Curr. Treat. Options Infect. Dis.* 10, 373–388. doi: 10.1007/s40506-018-0170-z
- Meymandi, S. K. (2020). *Center of Excellence for Chagas Disease*. Available online at: www.chagasus.org.
- Meymandi, S. K., Forsyth, C. J., Soverow, J., Hernandez, S., Sanchez, D., Montgomery, S. P., et al. (2017). Prevalence of Chagas disease in the Latin American-born population of Los Angeles. *Clin. Infect. Dis.* 64, 1182–1188. doi: 10.1093/cid/cix064
- Michailowsky, V., Silva, N. M., Rocha, C. D., Vieira, L. Q., Lannes-Vieira, J., and Gazzinelli, R. T. (2001). Pivotal role of interleukin-12 and interferon- γ axis in controlling tissue parasitism and inflammation in the heart and central nervous system during *Trypanosoma cruzi* infection. *Am. J. Pathol.* 159, 1723–1733. doi: 10.1016/S0002-9440(10)63019-2
- Mirkin, G. A., Celentano, A. M., Malchiodi, E. L., Jones, M., and González Cappa, S. M. (1997). Different *Trypanosoma cruzi* strains promote neuromyopathic damage mediated by distinct T lymphocyte subsets. *Clin. Exp. Immunol.* 107, 328–334. doi: 10.1111/j.1365-2249.1997.267-ce1166.x
- Molina, I., Gómez i Prat, J., Salvador, F., Treviño, B., Sulleiro, E., Serre, N., et al. (2014). Randomized trial of posaconazole and benznidazole for chronic Chagas' disease. *N. Engl. J. Med.* 370, 1899–1908. doi: 10.1056/NEJMoa1313122
- Moncayo, A. (2003). Chagas disease: current epidemiological trends after the interruption of vectorial and transfusional transmission in the Southern Cone countries. *Mem. Inst. Oswaldo Cruz* 98, 577–591. doi: 10.1590/S0074-02762003000500001
- Montgomery, S. P., Parise, M. E., Dotson, E. M., and Bialek, S. R. (2016). What do we know about Chagas disease in the United States? *Am. J. Trop. Med. Hyg.* 95, 1225–1227. doi: 10.4269/ajtmh.16-0213
- Morilla, M. J., Montanari, J. A., Prieto, M. J., Lopez, M. O., Petray, P. B., and Romero, E. L. (2004). Intravenous liposomal benznidazole as trypanocidal agent: increasing drug delivery to liver is not enough. *Int. J. Pharm.* 278, 311–318. doi: 10.1016/j.ijpharm.2004.03.025
- Morillo, C. A., Marin-Neto, J. A., Avezum, A., Sosa-Estani, S., Rassi, A., Rosas, F., et al. (2015). Randomized trial of benznidazole for chronic Chagas' cardiomyopathy. *N. Engl. J. Med.* 373, 1295–1306. doi: 10.1056/NEJMoa1507574
- Morillo, C. A., Waskin, H., Sosa-Estani, S., del Carmen Bangher, M., Cuneo, C., Milesi, R., et al. (2017). Benznidazole and posaconazole in eliminating parasites in asymptomatic *T. cruzi* carriers. *J. Am. Coll. Cardiol.* 69, 939–947. doi: 10.1016/j.jacc.2016.12.023
- Nunes, M. C. P., Dones, W., Morillo, C. A., Encina, J. J., and Ribeiro, A. L. (2013). Chagas disease: an overview of clinical and epidemiological aspects. *J. Am. Coll. Cardiol.* 62, 767–776. doi: 10.1016/j.jacc.2013.05.046
- Ohshima, K., Huy, N. T., Yoshimi, H., Kishikawa, N., Nishizawa, J. E., Roca, Y., et al. (2016). Proteomic profile of circulating immune complexes in chronic Chagas disease. *Parasite Immunol.* 38, 609–617. doi: 10.1111/pim.12341
- Oliveira, M. T., de Branquinho, R. T., Alessio, G. D., Mello, C. G. C., Nogueira-de-Paiva, N. C., Carneiro, C. M., et al. (2017). TcI, TcII and TcVI

- Trypanosoma cruzi* samples from Chagas disease patients with distinct clinical forms and critical analysis of *in vitro* and *in vivo* behavior, response to treatment and infection evolution in murine model. *Acta Trop.* 167, 108–120. doi: 10.1016/j.actatropica.2016.11.033
- Olivera, M. J., Forj, J. A., and Olivera, A. J. (2017). Therapeutic drug monitoring of benzimidazole and nifurtimox: a systematic review and quality assessment of published clinical practice guidelines. *Rev. Soc. Bras. Med. Trop.* 50, 748–755. doi: 10.1590/0037-8682-0399-2016
- Paiva, C. N., Medei, E., and Bozza, M. T. (2018). ROS and *Trypanosoma cruzi*: Fuel to infection, poison to the heart. *PLoS Pathog.* 14:e1006928. doi: 10.1371/journal.ppat.1006928
- Pérez-Molina, J. A., Perez, A. M., Norman, F. F., Monge-Maillo, B., and López-Vélez, R. (2015). Old and new challenges in Chagas disease. *Lancet Infect. Dis.* 15, 1347–1356. doi: 10.1016/S1473-3099(15)00243-1
- Perin, L., Moreira da Silva, R., Fonseca, K., da, S., Cardoso, J. M. de, O., Mathias, F. A. S., et al. (2017). Pharmacokinetics and tissue distribution of benzimidazole after oral administration in mice. *Antimicrob. Agents Chemother.* 61:e02410–16. doi: 10.1128/AAC.02410-16
- Pinazo, M.-J., Espinosa, G., Cortes-Lletget, C., Posada, E., de, J., Aldasoro, E., et al. (2013). Immunosuppression and Chagas disease: a management challenge. *PLoS Negl. Trop. Dis.* 7:e1965. doi: 10.1371/journal.pntd.0001965
- Piras, M. M., Piras, R., and Henriquez, D. (1982). Changes in morphology and infectivity of cell culture-derived trypomastigotes of *Trypanosoma cruzi*. *Mol. Biochem. Parasitol.* 6, 67–81. doi: 10.1016/0166-6851(82)90066-4
- Pronovost, H., Peterson, A. C., Chavez, B. G., Blum, M. J., Dumontel, E., and Herrera, C. P. (2018). Deep sequencing reveals multiclonality and new discrete typing units of *Trypanosoma cruzi* in rodents from the southern United States. *J. Microbiol. Immunol. Infect.* 21:S1684–1182(18)30097-5. doi: 10.1016/j.jmii.2018.12.004
- Quebrada Palacio, L. P., González, M. N., Hernandez-Vasquez, Y., Perrone, A. E., Parodi-Talice, A., Bua, J., et al. (2018). Phenotypic diversity and drug susceptibility of *Trypanosoma cruzi* TcV clinical isolates. *PLoS ONE* 13:e0203462. doi: 10.1371/journal.pone.0203462
- Rajkomar, A., Dean, J., and Kohane, I. (2019). Machine learning in medicine. *N. Engl. J. Med.* 380, 1347–1358. doi: 10.1056/NEJMr1814259
- Rassi A. Jr., Marin Neto, J. A., and Rassi, A. (2017). Chronic Chagas cardiomyopathy: a review of the main pathogenic mechanisms and the efficacy of aetiological treatment following the BENznidazole Evaluation for Interrupting Trypanosomiasis (BENEFIT) trial. *Mem. Inst. Oswaldo Cruz* 112, 224–235. doi: 10.1590/0074-02760160334
- Rassi, A., and Rassi, A. (2010). Predicting prognosis in patients with Chagas disease: why are the results of various studies so different? *Int. J. Cardiol.* 145, 64–65. doi: 10.1016/j.ijcard.2009.04.034
- Reigada, C., Sayé, M., Valera-Vera, E., Miranda, M. R., and Pereira, C. A. (2019). Repurposing of terconazole as an anti *Trypanosoma cruzi* agent. *Heliyon* 5:e01947. doi: 10.1016/j.heliyon.2019.e01947
- Revollo, S., Oury, B., Vela, A., Tibayrenc, M., and Sereno, D. (2019). In vitro benzimidazole and nifurtimox susceptibility profile of *trypanosoma cruzi* strains belonging to discrete typing units tci, tcii, and tcv. *Pathogens* 8:197. doi: 10.3390/pathogens8040197
- Riarte, A. R. (2012). Estudio TRAENA: Evaluación de potenciales biomarcadores de eficacia terapéutica informativo N° 2. Plataforma de información clínica en enfermedad de Chagas.
- Rodrigues-dos-Santos, Í., Melo, M. F., de Castro, L., Hasslocher-Moreno, A. M., do Brasil, P. E. A. A., Silvestre de Sousa, A., et al. (2018). Exploring the parasite load and molecular diversity of *Trypanosoma cruzi* in patients with chronic Chagas disease from different regions of Brazil. *PLoS Negl. Trop. Dis.* 12:e0006939. doi: 10.1371/journal.pntd.0006939
- Rodríguez-Morales, O., Monteón-Padilla, V., Carrillo-Sánchez, S. C., Rios-Castro, M., Martínez-Cruz, M., Carabarin-Lima, A., et al. (2015). Experimental vaccines against chagas disease: a journey through history. *J. Immunol. Res.* 2015:489758. doi: 10.1155/2015/489758
- Sales Junior, P. A., Molina, I., Fonseca Murta, S. M., Sánchez-Montalvá, A., Salvador, F., Corrêa-Oliveira, R., et al. (2017). Experimental and clinical treatment of chagas disease: a review. *Am. J. Trop. Med. Hyg.* 97, 1289–1303. doi: 10.4269/ajtmh.16-0761
- Sales-Campos, H., Kappel, H. B., Andrade, C. P., Lima, T. P., Castilho, A., De Giraldo, L. E. R., et al. (2015). *Trypanosoma cruzi* DTU TcII presents higher blood parasitism than DTU TcI in an experimental model of mixed infection. *Acta Parasitol.* 60, 435–441. doi: 10.1515/ap-2015-0060
- San Francisco, J., Barria, I., Gutiérrez, B., Neira, I., Muñoz, C., Sagua, H., et al. (2017). Decreased cruzipain and gp85/trans-sialidase family protein expression contributes to loss of *Trypanosoma cruzi* trypomastigote virulence. *Microbes Infect.* 19, 55–61. doi: 10.1016/j.micinf.2016.08.003
- Sánchez-Valdéz, F. J., Padilla, A., Wang, W., Orr, D., and Tarleton, R. L. (2018). Spontaneous dormancy protects *trypanosoma cruzi* during extended drug exposure. *Elife* 7:e34039. doi: 10.7554/eLife.34039
- Santana, R. A., Magalhães, L. K., Magalhães, L. K., Prestes, S., Maciel, M., da Silva, G. A., et al. (2014). *Trypanosoma cruzi* strain TcI is associated with chronic Chagas disease in the Brazilian Amazon. *Parasit. Vectors* 7:267. doi: 10.1186/1756-3305-7-267
- Santi-Rocca, J., Fernandez-Cortes, F., Chillón-Marinas, C., González-Rubio, M.-L., Martín, D., Gironès, N., et al. (2017). A multi-parametric analysis of *Trypanosoma cruzi* infection: common pathophysiologic patterns beyond extreme heterogeneity of host responses. *Sci. Rep.* 7:8893. doi: 10.1038/s41598-017-08086-8
- Scalise, M. L., Arrúa, E. C., Rial, M. S., Esteve, M. I., Salomon, C. J., and Fichera, L. E. (2016). Promising efficacy of benzimidazole nanoparticles in acute *Trypanosoma cruzi* murine model: *in-vitro* and *in-vivo* studies. *Am. J. Trop. Med. Hyg.* 95, 388–393. doi: 10.4269/ajtmh.15-0889
- Schaub, G. A., Meiser, C. K., and Balczun, C. (2011). “Interactions of *Trypanosoma cruzi* and Triatomines” in *Progress in Parasitology*, ed M. Heinz (Berlin; Heidelberg: Springer Berlin Heidelberg), 155–178. doi: 10.1007/978-3-642-21396-0_9
- Schijman, A. G., Bisio, M., Orellana, L., Sued, M., Duffy, T., Mejia Jaramillo, A. M., et al. (2011). International study to evaluate PCR methods for detection of *Trypanosoma cruzi* DNA in blood samples from Chagas disease patients. *PLoS Negl. Trop. Dis.* 5:e931. doi: 10.1371/journal.pntd.0000931
- Souza, P. E. A., Rocha, M. O. C., Menezes, C. A. S., Coelho, J. S., Chaves, A. C. L., Gollob, K. J., et al. (2007). *Trypanosoma cruzi* infection induces differential modulation of costimulatory molecules and cytokines by monocytes and T cells from patients with indeterminate and cardiac Chagas’ disease. *Infect. Immun.* 75, 1886–1894. doi: 10.1128/IAI.01931-06
- Steveding, D. (2014). The history of Chagas disease. *Parasit. Vect.* 7:317. doi: 10.1186/1756-3305-7-317
- Sulleiro, E., Muñoz-Calderon, Q., and Schijman, A. G. (2019). Role of nucleic acid amplification assays in monitoring treatment response in chagas disease: usefulness in clinical trials. *Acta Trop.* 199:105120. doi: 10.1016/j.actatropica.2019.105120
- Teston, A. P. M., Monteiro, W. M., Reis, D., Bossolani, G. D. P., Gomes, M. L., de Araújo, S. M., et al. (2013). In vivo susceptibility to benzimidazole of *Trypanosoma cruzi* strains from the western Brazilian Amazon. *Trop. Med. Int. Heal.* 18, 85–95. doi: 10.1111/tmi.12014
- Torrico, F., Gascon, J., Ortiz, L., Alonso-Vega, C., Pinazo, M. J., Schijman, A., et al. (2018). Treatment of adult chronic indeterminate Chagas disease with benzimidazole and three E1224 dosing regimens: a proof-of-concept, randomised, placebo-controlled trial. *Lancet Infect. Dis.* 18, 419–430. doi: 10.1016/S1473-3099(17)30538-8
- Vieira, G. A. L., Silva, M. T. A., da Regasini, L. O., Cotinguiba, F., Laure, H. J., Rosa, J. C., et al. (2018). *Trypanosoma cruzi*: analysis of two different strains after piplartine treatment. *Braz. J. Infect. Dis.* 22, 208–218. doi: 10.1016/j.bjid.2018.02.009
- Villar, J. C., Perez, J. G., Cortes, O. L., Riarte, A., Pepper, M., Marin-Neto, J. A., et al. (2014). Trypanocidal drugs for chronic asymptomatic *Trypanosoma cruzi* infection. *Cochrane Database Syst. Rev.* 27:CD003463. doi: 10.1002/14651858.CD003463.pub2
- Viotti, R., Vigliano, C., Lococo, B., Alvarez, M. G., Petti, M., Bertocchi, G., et al. (2009). Side effects of benzimidazole as treatment in chronic Chagas disease: fears and realities. *Expert Rev. Anti. Infect. Ther.* 7, 157–163. doi: 10.1586/14787210.7.2.157
- Wang, L., McLeod, H. L., and Weinshilboum, R. M. (2011). Genomics and drug response. *N. Engl. J. Med.* 364, 1144–1153. doi: 10.1056/NEJMr1010600
- WHO (2020). Chagas disease (*American trypanosomiasis*). Available online at: <https://www.who.int/chagas/en/>
- Wood, D. E., White, J. R., Georgiadis, A., Van Emburgh, B., Parpart-Li, S., Mitchell, J., et al. (2018). A machine learning approach for somatic

- mutation discovery. *Sci. Transl. Med.* 10:eaar7939. doi: 10.1126/scitranslmed.aar7939
- Zheng, H., Momeni, A., Cedoz, P.-L., Vogel, H., and Gevaert, O. (2020). Whole slide images reflect DNA methylation patterns of human tumors. *NPJ Genomic Med.* 5:11. doi: 10.1038/s41525-020-0120-9
- Zingales, B. (2018). *Trypanosoma cruzi* genetic diversity: something new for something known about Chagas disease manifestations, serodiagnosis and drug sensitivity. *Acta Trop.* 184, 38–52. doi: 10.1016/j.actatropica.2017.09.017
- Zingales, B., Andrade, S., Briones, M., Campbell, D., Chiari, E., Fernandes, O., et al. (2009). A new consensus for *Trypanosoma cruzi* intraspecific nomenclature: second revision meeting recommends TcI to TcVI. *Mem. Inst. Oswaldo Cruz* 104, 1051–1054. doi: 10.1590/S0074-02762009000700021
- Zuñiga, C., Palau, T., Penin, P., Gamallo, C., and Diego, J. A. (1997). Protective effect of *Trypanosoma rangeli* against infections with a highly virulent strain of *Trypanosoma cruzi*. *Trop. Med. Int. Heal.* 2, 482–487. doi: 10.1111/j.1365-3156.1997.tb00171.x
- Conflict of Interest:** The authors declare that the research was conducted in the absence of any commercial or financial relationships that could be construed as a potential conflict of interest.

Copyright © 2020 Martinez, Romano and Engman. This is an open-access article distributed under the terms of the Creative Commons Attribution License (CC BY). The use, distribution or reproduction in other forums is permitted, provided the original author(s) and the copyright owner(s) are credited and that the original publication in this journal is cited, in accordance with accepted academic practice. No use, distribution or reproduction is permitted which does not comply with these terms.



Trypanosoma cruzi Promotes Transcriptomic Remodeling of the JAK/STAT Signaling and Cell Cycle Pathways in Myoblasts

Lindice M. Nisimura¹, Laura L. Coelho², Tatiana G. de Melo³, Paloma de Carvalho Vieira⁴, Pedro H. Victorino⁵, Luciana R. Garzoni², David C. Spray⁶, Dumitru A. Iacobas⁷, Sanda Iacobas⁸, Herbert B. Tanowitz^{9†} and Daniel Adesse^{4*}

¹ Laboratório de Pesquisa em Apicomplexa, Instituto Carlos Chagas, Fundação Oswaldo Cruz, Curitiba, Brazil, ² Laboratório de Inovações em Terapias, Ensino e Bioprodutos, Instituto Oswaldo Cruz, Fundação Oswaldo Cruz, Rio de Janeiro, Brazil, ³ Laboratório de Ultraestrutura Celular, Instituto Oswaldo Cruz, Fundação Oswaldo Cruz, Rio de Janeiro, Brazil, ⁴ Laboratório de Biologia Estrutural, Instituto Oswaldo Cruz, Fundação Oswaldo Cruz, Rio de Janeiro, Brazil, ⁵ Laboratório de Neurogênese, Instituto de Biofísica Carlos Chagas Filho, Universidade Federal do Rio de Janeiro, Rio de Janeiro, Brazil, ⁶ Dominick P. Purpura Department of Neuroscience, Albert Einstein College of Medicine, New York, NY, United States, ⁷ Personalized Genomics Laboratory, Center for Computational Systems Biology, Prairie View A&M University, Prairie View, TX, United States, ⁸ Department of Pathology, New York Medical College, Valhalla, NY, United States, ⁹ Department of Pathology, Albert Einstein College of Medicine, New York, NY, United States

OPEN ACCESS

Edited by:

Nobuko Yoshida,
Federal University of São Paulo, Brazil

Reviewed by:

Sergio Schenkman,
Federal University of São Paulo, Brazil
Manuel Fresno,
Autonomous University of
Madrid, Spain

*Correspondence:

Daniel Adesse
adesse@ioc.fiocruz.br

[†]In memoriam

Specialty section:

This article was submitted to
Parasite and Host,
a section of the journal
Frontiers in Cellular and Infection
Microbiology

Received: 08 November 2019

Accepted: 30 April 2020

Published: 17 June 2020

Citation:

Nisimura LM, Coelho LL, Melo TG, Vieira PC, Victorino PH, Garzoni LR, Spray DC, Iacobas DA, Iacobas S, Tanowitz HB and Adesse D (2020) Trypanosoma cruzi Promotes Transcriptomic Remodeling of the JAK/STAT Signaling and Cell Cycle Pathways in Myoblasts. Front. Cell. Infect. Microbiol. 10:255. doi: 10.3389/fcimb.2020.00255

Chagas disease is responsible for more than 10,000 deaths per year and about 6 to 7 million infected people worldwide. In its chronic stage, patients can develop mega-colon, mega-esophagus, and cardiomyopathy. Differences in clinical outcomes may be determined, in part, by the genetic background of the parasite that causes Chagas disease. *Trypanosoma cruzi* has a high genetic diversity, and each group of strains may elicit specific pathological responses in the host. Conflicting results have been reported in studies using various combinations of mammalian host—*T. cruzi* strains. We previously profiled the transcriptomic signatures resulting from infection of L6E9 rat myoblasts with four reference strains of *T. cruzi* (Brazil, CL, Y, and Tulahuen). The four strains induced similar overall gene expression alterations in the myoblasts, although only 21 genes were equally affected by all strains. *Cardiotrophin-like cytokine factor 1 (Clcf1)* was one of the genes found to be consistently upregulated by the infection with all four strains of *T. cruzi*. This cytokine is a member of the interleukin-6 family that binds to glycoprotein 130 receptor and activates the JAK/STAT signaling pathway, which may lead to muscle cell hypertrophy. Another commonly upregulated gene was tyrosine 3-monooxygenase/tryptophan 5-monooxygenase activation protein theta (*Ywhaq*, 14-3-3 protein Θ), present in the Cell Cycle Pathway. In the present work, we reanalyzed our previous microarray dataset, aiming at understanding in more details the transcriptomic impact that each strain has on JAK/STAT signaling and Cell Cycle pathways. Using Pearson correlation analysis between the expression levels of gene pairs in biological replicas from each pathway, we determined the coordination between such pairs in each experimental condition and the predicted protein interactions between the significantly altered genes by each strain. We found that although these highlighted genes were similarly affected by all four strains, the downstream genes or their interaction partners

were not necessarily equally affected, thus reinforcing the idea of the role of parasite background on host cell transcriptome. These new analyses provide further evidence to the mechanistic understanding of how distinct *T. cruzi* strains lead to diverse remodeling of host cell transcriptome.

Keywords: Chagas disease, myoblasts, cell cycle, JAK-STAT pathway, *Clcf1*, *Ywhaq*

INTRODUCTION

Chagas disease (CD) is caused by the protozoan *Trypanosoma cruzi* and affects about 6 to 7 million people worldwide (WHO, 2019). The cardiac form of CD (Mukherjee et al., 2003; Goldenberg et al., 2009; Soares et al., 2010; Adesse et al., 2011) is the main clinical manifestation, which can be observed in more than 30% of chronically infected people, whereas another 10% develop digestive, neurological, or mixed alterations (Rassi et al., 2010, 2012; WHO, 2019). These diverse presentations might in part be explained by genetic differences between strains of *T. cruzi*, which have been classified into six discrete typing units (DTUs) (Andrade and Magalhaes, 1997; Zingales et al., 2009). This classification is based on distinct ecological, epidemiological, natural, and experimental infection features of the parasite, but clinical manifestations are not strictly associated with the specific *T. cruzi* DTUs (Zingales et al., 2012). In order to understand the variations in CD severity and tissue specificity, there is a need to identify key molecular biomarkers and to correlate the gene expression profiles of *T. cruzi* strains with CD pathogenicity.

We previously compared gene expression profiles in a rat myoblast cell line (L6E9) infected with four different strains of *T. cruzi* (Brazil, Y, CL, and Tulahuen) (Adesse et al., 2010a). That study identified up regulation of *cardiotrophin-like cytokine factor 1* (*Clcf1*) by all four strains of *T. cruzi*. *Clcf1* belongs to the interleukin (IL)-6 family of cytokines that have the glycoprotein gp130 as a common signal-transducing receptor and is involved in cell differentiation, survival, apoptosis, and proliferation through activation of Janus kinase (JAK). JAKs in turn, activate signal transducer and activator of transcription (STAT) factors (Gorshkova et al., 2016). CLCF1 has been reported to induce hypertrophy and survival of cardiomyocytes *in vitro* (Sheng et al., 1996; Latchman, 1999) through gp130 and STAT3 pathway activation (Kunisada et al., 1998). Plasma levels of CLCF1 are correlated with severity of hypertrophy in patients with hypertrophic cardiomyopathy or hypertension (Monserrat et al., 2011; Song et al., 2014). In acute experimental CD, rats infected with *T. cruzi* (Sylvio X10/7 strain, TcI) revealed cardiac overexpression of CLCF1 and gp130 (Chandrasekar et al., 1998). These data could explain in part why the predominant DTUs in our previous study (TcI and TcII) are associated with cardiac manifestation of CD.

STAT proteins include STAT1–4, –5a, –5b, and –6 and have been shown to play an important role in cytokine signaling. These proteins are tyrosine phosphorylated by

JAKs following the binding of cytokine to its receptor. Upon tyrosine phosphorylation, STAT proteins form homodimers or heterodimers and rapidly translocate to the nucleus and induce gene expression. Recent evidence has demonstrated the necessity of STAT3 in cell growth and transformation (Zong et al., 2000; Ponce et al., 2013; Stahl et al., 2013). The JAK/STAT pathway is involved in cell cycle regulation, and it has been shown that myoblast proliferation involves this pathway (Sorensen et al., 2018; Steyn et al., 2019). JAK1 and STAT1 induce cell proliferation and reduce myogenic differentiation (Sun et al., 2007). Additionally, phosphorylation of JAK2–STAT5 has been shown to protect skeletal muscle in acute aerobic exercise (Consitt et al., 2008).

Regarding *T. cruzi* infection, STAT3 phosphorylation induces cardiomyocyte protection against apoptosis through increased expression of anti-apoptotic factor Bcl-2 (Ponce et al., 2012). Cell cycle was modulated distinctly in cells infected with the Dm28c (type I) and the Y and CL-Brener *T. cruzi* stocks (type II), and there were different levels of apoptosis induction by each strain. Moreover, *T. cruzi* infection provoked variable apoptosis rates in distinct host cell types (cardiomyocytes, fibroblasts, and macrophages) (de Souza et al., 2003).

In this context, transcriptomic analyses may be expected to elucidate associations between the DTUs and prediction of the pathogenesis of *T. cruzi* strains. In the present study, we focus on determination of the transcriptomic impact of each strain on JAK/STAT signaling and cell cycle pathways. Novel bioinformatics tools were used to reanalyze the data generated by microarray analysis of L6E9 cells infected with four distinct strains of *T. cruzi* (Brazil, CL, Y, and Tulahuen).

METHODS

Experimental Design

For microarrays analyses, rat skeletal myoblast L6E9 were used as described in Adesse et al. (2010a). Before reaching confluency, cells were dissociated with trypsin/EDTA in phosphate-buffered saline (PBS) and plated for experiments. Trypomastigotes of *Trypanosoma cruzi* were isolated from supernatants of infected Vero cells and used at a multiplicity of infection (MOI) of 10. Twenty-four hours after infection, cultures were washed twice with Ringer's saline solution and fresh supplemented medium was added. Medium was replaced daily and cultures were kept up to 72 h post infection.

Microarray

Microarray data were obtained from our previous publication (Adesse et al., 2010a), and the experimental design and procedures are described in brief as follows. Cell culture dishes containing the L6E9 rat myoblast cell line were infected with trypomastigote forms of *T. cruzi* (Y, CL Brener, Tulahuen, and Brazil strains) (see Adesse et al., 2010a, for details). Total RNA was harvested 72 h post infection using TRIzol reagent (Invitrogen, Carlsbad, CA), following the protocol indicated by the manufacturer. Microarray analysis was performed using the protocol optimized in our laboratory according to the standards of the Microarray Gene Expression Data Society. Differently labeled RNA samples from biological replicas of control (uninfected cells cultured for the same duration) or infected with one strain at a time were co-hybridized (“multiple yellow” strategy) with rat oligonucleotide arrays printed by Duke University. The abundance of host cell transcripts was considered as significantly altered after infection if the absolute fold change was >1.5 -fold and the *P*-value of the heteroscedastic *t*-test (two-sample, unequal variance) was >0.05 . Experimental details and raw and processed expression data have been deposited and are publically available at <https://www.ncbi.nlm.nih.gov/geo/query/acc.cgi?acc=GSE18175>.

Expression Coordination Analysis

As previously described (Iacobas et al., 2008a), the gene networks in uninfected control L6E9 myocytes and those infected with each of the four strains (Brazil, CL, Tulahuen, or Y strain) were established by calculating pairwise Pearson correlation coefficients of the (\log_2) expression levels of each pair of pathway genes in the biological replicas. Two genes were considered as synergistically expressed if their expression levels increased and decreased together (positive covariance) in a set of similar samples or as antagonistically expressed (negative covariance) when they manifest opposite tendencies and as independently expressed when their expressions are not correlated (close to zero covariance). In the case of four biological replicas, the ($p < 0.05$) cut-off for synergism is a pairwise Pearson correlation coefficient $\rho > 0.90$, for antagonism $\rho < -0.90$, and for independence $|\rho| < 0.05$. To illustrate, **Supplementary Figure 1** presents examples of synergistically (*Antxr1*), antagonistically (*Dus3l*), and independently (*Golim4*) expressed genes with *Clcf1* in control L6E9 rat myoblasts.

“See-Saw” Partners of Key Genes

For each gene of interest and each experimental condition, we determined the coordination profile, defined as the set of Pearson correlation coefficients between the expression levels within biological replicas of that gene and each other gene. We then identified the gene pairs with very similar or opposite coordination profiles in each condition, termed “see-saw” partners, both in recognition of the appearance of the graphs and to denote the strength of their synergistic and antagonistic relationships (Iacobas et al., 2007a,b, 2008a,b; Spray and Iacobas, 2007).

Pathway Analysis

On the basis of our initial analyses of genes whose expression was altered by infection with different *T. cruzi* strains, we selected the following gene pathways for further analysis using the Kyoto Encyclopedia of Genes and Genomes (KEGG): a) JAK/STAT Signaling Pathway (<http://www.kegg>.

TABLE 1 | Top 30 upregulated genes by Brazil strain-infected L6E9 cells at 72 hpi.

Gene name	Gene symbol	Fold change
Erythroid spectrin beta	LOC314251	35.5
Transmembrane protease, serine 11d	Tmprss11d	20.9
4-Hydroxyphenylpyruvic acid dioxygenase	Hpd	11.9
IQ motif and Sec7 domain 3	Iqsec3	10.2
DNA-damage inducible transcript 3	Ddit3	9.3
One cut domain, family member 1	Onecut1	9.3
Olfactory receptor 1751 (predicted)	Olr1751_predicted	9.3
Olfactory receptor 135 (predicted)	Olr135_predicted	8.9
Cut-like 1 (<i>Drosophila</i>)	Cutl1	
Proprotein convertase subtilisin/kexin type 7	Pcsk7	6.9
Olfactory receptor 3 (predicted)	Olr3_predicted	5.9
Amiloride binding protein 1 (amine oxidase, copper-containing)	Abp1	5.7
Arylacetamide deacetylase (esterase)	Aadac	5.5
EGF-like domain 7	Egfl7	5.5
Similar to 60S ribosomal protein L29 (P23) (predicted)	RGD1566397_predicted	5.5
Similar to RIKEN cDNA 0610012D17 (predicted)	RGD1564702_predicted	5.4
Similar to 60S ribosomal protein L23a	LOC291686	5.2
Potassium channel, subfamily K, member 2	Kcnk2	5.1
Cdc2-related kinase, arginine/serine-rich	Crks	5.1
PITPNM family member 3 (predicted)	Pitpmn3_predicted	5.0
Ras association (RalGDS/AF-6) domain family 3 (predicted)	Rassf3_predicted	5.0
Similar to DIP13 beta (predicted)	RGD1563028_predicted	4.9
Similar to ribosomal protein L13 (predicted)	RGD1563194_predicted	4.6
Similar to BTB and CNC homology 1, basic leucine zipper transcription factor 2 (predicted)	RGD1562865_predicted	4.5
Elastin	Eln	4.4
RT1 class I, CE15	RT1-CE15	4.4
Adaptor-related protein complex 3, mu 2 subunit	Ap3m2	4.4
Rhesus blood group-associated C glycoprotein	Rhcg	4.3
FYVE and coiled-coil domain containing 1 (predicted)	Fyco1_predicted	4.3

jp/kegg-bin/show_pathway?org_name=rno&mapno=04630&mapscale=1.0&show_description=hide) and b) Cell Cycle Pathway (http://www.kegg.jp/kegg-bin/show_pathway?org_name=rno&mapno=04110&mapscale=1.0&show_description=hide).

TABLE 2 | Top 30 downregulated genes by Brazil strain-infected L6E9 cells at 72 hpi.

Gene name	Gene symbol	Fold change
Solute carrier family 39 (metal ion transporter), member 6	Slc39a6	−2.8
Glycoprotein (transmembrane) nmb	Gpnmb	−2.5
Tropomyosin 4	Tpm4	−2.5
Parkinson disease (autosomal recessive, early onset) 7	Park7	−2.4
ATP-binding cassette, sub-family E (OABP), member 1	Abce1	−2.4
Keratin 25D	Krt25d	−2.4
Proteasome (prosome, macropain) 28 subunit, beta	Psme2	−2.3
Similar to hypothetical protein MGC40499 (predicted)	RGD1307636_predicted	−2.3
Milk fat globule-EGF factor 8 protein	Mfge8	−2.3
Macoilin	LOC313618	−2.3
NADPH oxidase 3	Nox3	−2.3
Similar to RIKEN cDNA 9630046K23	RGD1306248	−2.3
Xylulokinase homolog (<i>Haemophilus influenzae</i>)	Xylb	−2.2
Similar to A disintegrin-like and metalloprotease (repolysin type) with thrombospondin type 1 motif, 2 (predicted)	RGD1565950_predicted	−2.2
COP9 (constitutive photomorphogenic) homolog, subunit 4 (<i>Arabidopsis thaliana</i>)	Cops4	−2.1
Ankyrin repeat domain 1 (cardiac muscle)	Ankrd1	−2.1
Gasdermin domain containing 1 (predicted)	Gsdmdc1_predicted	−2.1
Similar to mKIAA1011 protein	LOC366669	−2.1
Similar to RIKEN cDNA 1500016L11 (predicted)	RGD1305050_predicted	−2.1
Ribosomal protein L28	Rpl28	−2.1
Thymoma viral proto-oncogene 1	Akt1	−2.1
SEC24 related gene family, member A (<i>Saccharomyces cerevisiae</i>) (predicted)	Sec24a_predicted	−2.0
Adaptor protein complex AP-2, alpha 2 subunit	Ap2a2	−2.0
Guanosine diphosphate dissociation inhibitor 1	Gdi1	−2.0
Similar to hypothetical protein MGC25461 (predicted)	RGD1306717_predicted	−2.0
Matrix metalloproteinase 14 (membrane-inserted)	Mmp14	−2.0
Rho GTPase activating protein 27	Arhgap27	−2.0
Voltage-dependent anion channel 2	Vdac2	−1.9
C1q and tumor necrosis factor-related protein 1	C1qtnf1	−1.9

RESULTS

Differential Alterations in Predicted Protein–Protein Interactions (PPI) in L6E9 Myoblasts Infected With Distinct *Trypanosoma cruzi* Strains

In our previous paper (Adesse et al., 2010a), randomly selected genes were presented among those that were significantly altered

TABLE 3 | Top 30 upregulated genes by CL strain-infected L6E9 cells at 72 hpi.

Gene name	Gene symbol	Fold change
Similar to protein phosphatase 1, regulatory (inhibitory) subunit 1C; thymocyte ARPP; DNA segment, Chr 9, Brigham and Women's Genetics 1012 expressed	RGD1307215	43.5
Calcium/calmodulin-dependent protein kinase I gamma	Camk1g	29.6
Chemokine (C-X-C motif) ligand 10	Cxcl10	20.8
5-Methyltetrahydrofolate-homocysteine methyltransferase	Mtr	16.5
Olfactory receptor 813 (predicted)	Olr813_predicted	9.9
Transmembrane protease, serine 11d	Tmprss11d	9.6
ATP-binding cassette, sub-family G (WHITE), member 3	Abcg3	7.7
Nuclear receptor subfamily 4, group A, member 1	Nr4a1	6.2
Peptidyl arginine deiminase, type I	Padi1	4.3
Pericentriolar material 1	Pcm1	4.3
ATPase, H ⁺ transporting, lysosomal V0 subunit A isoform 4 (predicted)	Atp6v0a4_predicted	3.7
Clasp homolog (<i>Xenopus laevis</i>) (predicted)	Clspn_predicted	3.6
Mitochondrial trans-2-enoyl-CoA reductase	Mecr	3.5
Checkpoint kinase 1 homolog (<i>Schizosaccharomyces pombe</i>)	Chek1	3.5
Similar to RIKEN cDNA 6530401L14 gene	RGD1309107	3.4
Radial spokehead-like 2 (predicted)	Rshl2_predicted	3.4
UDP-glucose ceramide glucosyltransferase-like 1	Ugcgl1	3.4
Glutamate receptor, ionotropic, N-methyl d-aspartate 2B	Grin2b	3.4
Similar to RIKEN cDNA 4921513E08 (predicted)	RGD1305153_predicted	3.2
Similar to RIKEN cDNA 2700097O09 (predicted)	RGD1304624_predicted	3.2
Similar to RIKEN cDNA A530088I07 gene	LOC311984	3.1
Leucine rich repeat protein 3, neuronal	Lrrn3	3.1
Erythroid spectrin beta	LOC314251	3.1
DNA-damage inducible transcript 3	Ddit3	3.1
Peroxisomal biogenesis factor 11c (predicted)	Pex11c_predicted	3.1
Potassium channel tetramerization domain containing 1	Kctd1	3.1
Similar to hypothetical protein FLJ31846 (predicted)	RGD1306118_predicted	3.1
ATH1, acid trehalase-like 1 (yeast) (predicted)	Ath1_predicted	3.0
Interleukin-21 receptor	Il21r	3.0
Similar to pseudouridylate synthase-like 1	LOC362681	3.0

by each strain of *Trypanosoma cruzi*. We now listed the 30 genes most downregulated and upregulated genes by each strain (Tables 1–8). Whereas the fold changes of the most strongly downregulated genes were similar (about -4 - to -2 -fold), fold

changes of upregulated genes were as high as 13- to 54-fold in the various *T. cruzi* strains. The Y strain was the least disruptive for the transcriptome because fold changes of the 30 most strongly upregulated genes were notably lower than for the other strains.

TABLE 4 | Top 30 downregulated genes by CL strain-infected L6E9 cells at 72 hpi.

Gene name	Gene symbol	Fold change
V-maf musculoaponeurotic fibrosarcoma oncogene homolog (avian)	Maf	-3.1
Glycoprotein (transmembrane) nmb	Gpnmb	-2.8
T-cell immunomodulatory protein	Cda08	-2.6
Succinate-Coenzyme A ligase, ADP-forming, beta subunit (predicted)	Suc1a2_predicted	-2.6
OMA1 homolog, zinc metalloproteinase (<i>Saccharomyces cerevisiae</i>) (predicted)	Oma1_predicted	-2.4
Similar to CG9996-PA	LOC300173	-2.3
Regenerating islet-derived 1	Reg1	-2.3
Phosphotriesterase related	Pter	-2.2
Similar to myosin, light polypeptide 6, alkali, smooth muscle and non-muscle (predicted)	RGD1559821_predicted	-2.1
Syndecan 1	Sdc1	-2.1
Pyruvate dehydrogenase kinase, isoenzyme 2	Pdk2	-2.0
Aminoacidate-semialdehyde dehydrogenase-phosphopantetheinyl transferase (predicted)	Aasdhpt_predicted	-2.0
Matrix metalloproteinase 14 (membrane-inserted)	Mmp14	-1.9
Solute carrier family 27 (fatty acid transporter), member 1	Slc27a1	-1.8
Similar to phosphatidylglycerophosphate synthase (predicted)	RGD1305052_predicted	-1.8
UDP-Gal:betaGlcNAc beta 1,4-galactosyltransferase, polypeptide 5 (predicted)	B4galt5_predicted	-1.8
Spondin 2, extracellular matrix protein	Spon2	-1.8
Spastic paraplegia 21 homolog (human)	Spg21	-1.8
C1q and tumor necrosis factor-related protein 1	C1qtnf1	-1.8
Neuropathy target esterase like 1	Ntel1	-1.8
Similar to 60S ribosomal protein L35 (predicted)	RGD1562863_predicted	-1.8
Carnitine palmitoyltransferase 1a, liver	Cpt1a	-1.8
Gametogenetin-binding protein 1	Ggnbp1	-1.8
F-box and leucine-rich repeat protein 3	Fbxl3	-1.7
Homer homolog 3 (<i>Drosophila</i>)	Homer3	-1.7
Phospholipase C, gamma 1	Plcg1	-1.7
DEAH (Asp-Glu-Ala-His) box polypeptide 16	Dhx16	-1.7
Similar to C530044N13Rik protein	RGD1306568	-1.7
Similar to CG4768-PA (predicted)	RGD1309748_predicted	-1.7
UDP-N-acetylglucosamine pyrophosphorylase 1-like 1 (predicted)	Uap111_predicted	-1.7

TABLE 5 | Top 30 upregulated genes by Tulahuen strain-infected L6E9 cells at 72 hpi.

Gene name	Gene symbol	Fold change
Calcium/calmodulin-dependent protein kinase I gamma	Camk1g	57.6
Chemokine (C-X-C motif) ligand 10	Cxcl10	35.9
Similar to Set alpha isoform	LOC317165	20.2
Erythroid spectrin beta	LOC314251	20.2
Similar to protein phosphatase 1, regulatory (inhibitory) subunit 1C; thymocyte ARPP; DNA segment, Chr 9, Brigham and Women's Genetics 1012 expressed	RGD1307215	19.1
Vacuolar protein sorting 37C (yeast) (predicted)	Vps37c_predicted	14.5
5-Methyltetrahydrofolate-homocysteine methyltransferase	Mtr	13.7
ATP-binding cassette, sub-family G (WHITE), member 3	Abcg3	12.2
Similar to BCL6 co-repressor-like 1 (predicted)	RGD1566108_predicted	10.1
Transmembrane protease, serine 11d	Tmprss11d	9.7
Interleukin-21 (predicted)	Il21_predicted	9.4
Matrix metalloproteinase 15 (predicted)	Mmp15_predicted	7.8
Activin A receptor type II-like 1	Acvr1	7.6
Olfactory receptor 3 (predicted)	Olr3_predicted	7.4
Oncomodulin	Ocm	7.1
Olfactory receptor 889 (predicted)	Olr889_predicted	6.9
Seminal vesicle secretion 1	Svs1	6.7
Olfactory receptor 859 (predicted)	Olr859_predicted	6.7
Olfactory receptor 155 (predicted)	Olr155_predicted	6.1
Arylacetamide deacetylase (esterase)	Aadac	5.8
Homeo box, msh-like 3	Msx3	5.7
4-hydroxyphenylpyruvic acid dioxygenase	Hpd	5.5
Beta-1,3-glucuronyltransferase 1 (glucuronosyltransferase P)	B3gat1	5.4
CD4 antigen	Cd4	5.4
Cut-like 1 (<i>Drosophila</i>)	Cutl1	5.4
BMP and activin membrane-bound inhibitor, homolog (<i>Xenopus laevis</i>)	Bambi	5.3
Similar to hypothetical protein FLJ31846 (predicted)	RGD1306118_predicted	5.2
Slit homolog 3 (<i>Drosophila</i>)	Slit3	5.2
Eyes absent 2 homolog (<i>Drosophila</i>)	Eya2	5.1
PDZ domain containing 6 (predicted)	Pdzk6_predicted	5.0

TABLE 6 | Top 30 downregulated genes by Tulahuen strain-infected L6E9 cells at 72 hpi.

Gene name	Gene symbol	Fold change
Procollagen, type XVI, alpha 1	Col16a1	−4.7
Solute carrier family 16 (monocarboxylic acid transporters), member 1	Slc16a1	−3.8
Inositol 1,4,5-triphosphate receptor 3	Itpr3	−3.7
Matrix metalloproteinase 11	Mmp11	−3.5
Exocyst complex component 7	Exoc7	−3.4
V-abl Abelson murine leukemia viral oncogene homolog 1	Abl1	−3.3
Dermatopontin (predicted)	Dpt_predicted	−3.2
Guanosine monophosphate reductase 2	Gmpr2	−3.2
Discoidin domain receptor family, member 1	Ddr1	−3.2
Tetraspanin 5	Tspan5	−3.2
Olfactory receptor 865 (predicted)	Olr865_predicted	−3.1
Similar to hypothetical protein (predicted)	RGD1561605_predicted	−3.1
Protein phosphatase 1 (formerly 2C)-like (predicted)	Ppm1l_predicted	−3.0
Bcl2 modifying factor	Bmf	−2.9
IAP promoted placental gene (predicted)	lpp_predicted	−2.9
AE binding protein 1 (predicted)	Aebp1_predicted	−2.9
Ectonucleoside triphosphate diphosphohydrolase 1	Entpd1	−2.9
Troponin T2, cardiac	Tnnt2	−2.9
Spondin 2, extracellular matrix protein	Spon2	−2.9
Phospholipase D2	Pld2	−2.9
Signal recognition particle receptor ("docking protein")	Srpr	−2.9
Similar to late endosomal/lysosomal Mp1 interacting protein (p14) (predicted)	RGD1562501_predicted	−2.9
Tripeptidyl peptidase I	Tpp1	−2.8
A disintegrin and metalloproteinase domain 33 (predicted)	Adam33_predicted	−2.8
Similar to RIKEN cDNA 2010012005 (predicted)	RGD1311783_predicted	−2.8
F-box protein 38 (predicted)	Fbxo38_predicted	−2.8
NADH dehydrogenase (ubiquinone) 1 beta subcomplex 3 (predicted)	Ndufb3_predicted	−2.8
RNA binding motif protein 4 (predicted)	Rbm4_predicted	−2.8
RAB8B, member RAS oncogene family	Rab8b	−2.8
Spastin (predicted)	Spast_predicted	−2.8

TABLE 7 | Top 30 upregulated genes by Y strain-infected L6E9 cells at 72 hpi.

Gene name	Gene symbol	Fold change
Oncomodulin	Ocm	13.5
Syntaxin binding protein 5 (tomosyn)	Stxbp5	11.8
Similar to hypothetical protein FLJ31846 (predicted)	RGD1306118_predicted	8.9
ATP-binding cassette, sub-family G (WHITE), member 3	Abcg3	8.4
Ankyrin repeat and SOCS box-containing protein 3 (predicted)	Asb3_predicted	6.3
Slit homolog 3 (<i>Drosophila</i>)	Slit3	5.5
Elastin	Eln	5.1
Zinc finger protein 13 (predicted)	Zfp13_predicted	4.6
BMP and activin membrane-bound inhibitor, homolog (<i>Xenopus laevis</i>)	Bambi	4.5
FYVE and coiled-coil domain containing 1 (predicted)	Fyco1_predicted	4.4
Interleukin-21 (predicted)	Il21_predicted	4.4
Galactose mutarotase	Galm	4.3
Presenilin 2	Psen2	3.8
Pericentriolar material 1	Pcm1	3.7
Guanylate cyclase activator 2a (guanylin)	Guca2a	3.5
PDZ domain containing 6 (predicted)	Pdzk6_predicted	3.3
5-Methyltetrahydrofolate-homocysteine methyltransferase	Mtr	3.2
Similar to transcription factor (p38 interacting protein)	RGD1307812	3.1
UDP-glucose ceramide glucosyltransferase-like 1	Ugcgl1	3.1
Similar to protein phosphatase 1, regulatory (inhibitory) subunit 1C; thymocyte ARPP; DNA segment, Chr 9, Brigham and Women's Genetics 1012 expressed	RGD1307215	3.0
Eyes absent 2 homolog (<i>Drosophila</i>)	Eya2	3.0
Pregnancy-specific beta 1-glycoprotein	LOC292668	2.9
Ets variant gene 4 (E1A enhancer binding protein, E1AF) (predicted)	Etv4_predicted	2.9
Transferrin receptor	Tfrc	2.9
Similar to RIKEN cDNA 2700097009 (predicted)	RGD1304624_predicted	2.9
Jumonji domain containing 3 (predicted)	Jmjd3_predicted	2.9
Similar to hypothetical protein FLJ10342 (predicted)	RGD1307791_predicted	2.8
RNA pseudouridylation synthase domain containing 2 (predicted)	Rpusd2_predicted	2.8
Transmembrane protein 12	Tmem12	2.8
Oxidoreductase NAD-binding domain containing 1 (predicted)	Oxnad1_predicted	2.7

We used the STRING platform to predict protein–protein interaction (PPI) networks and subsequently applied K-means algorithm to determine clusters of genes with a similar expression profile (**Figure 1**). The clusters that were generated

were then analyzed by Pathvisio software (Kutmon et al., 2015), in order to determine their molecular function; these clusters and their associated functions are shown in **Figure 1**.

TABLE 8 | Top 30 downregulated genes by Y strain-infected L6E9 cells at 72 hpi.

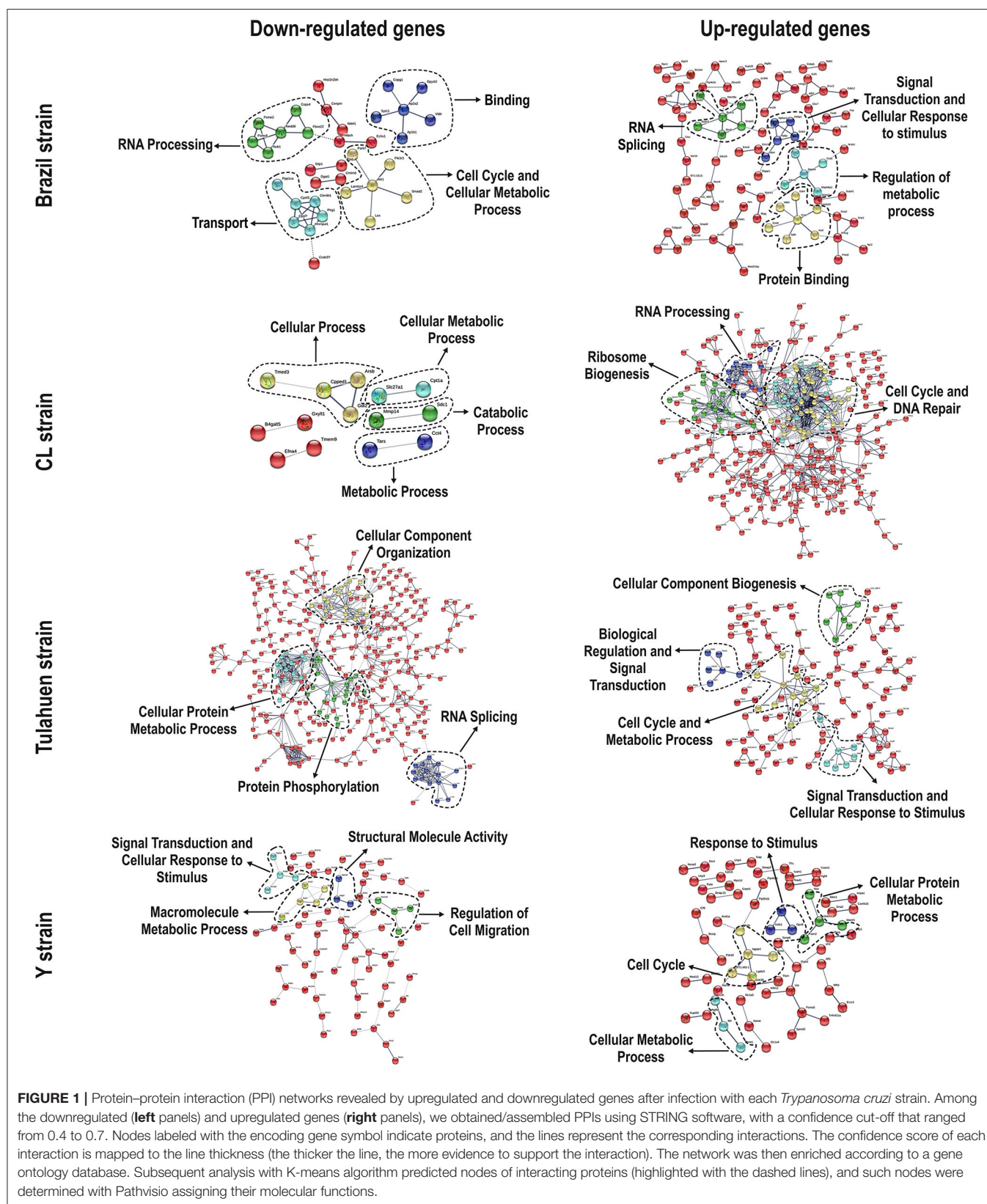
Gene name	Gene symbol	Fold change
Actin, alpha 1, skeletal muscle	Acta1	−4.8
Similar to cDNA sequence BC019755 (predicted)	RGD1306601_predicted	−3.3
Cytochrome P450, family 2, subfamily d, polypeptide 22	Cyp2d22	−2.9
Cadherin 15	Cdh15	−2.9
Cytochrome P450, family 26, subfamily b, polypeptide 1	Cyp26b1	−2.8
Olfactory receptor 865 (predicted)	Olr865_predicted	−2.7
Ankyrin repeat domain 1 (cardiac muscle)	Ankrd1	−2.7
Similar to nuclease sensitive element binding protein 1	LOC367118	−2.7
Acyl-CoA synthetase long-chain family member 3	Acsl3	−2.6
Dispatched homolog 1 (<i>Drosophila</i>) (predicted)	Disp1_predicted	−2.6
Carbonic anhydrase 3	Ca3	−2.6
Inhibitor of growth family, member 3	Ing3	−2.6
C-fos-induced growth factor	Figf	−2.6
Naked cuticle 2 homolog (<i>Drosophila</i>) (predicted)	Nkd2_predicted	−2.5
Inhibitor of DNA binding 4	Id4	−2.4
Cytidine 5'-triphosphate synthase (predicted)	Ctps_predicted	−2.4
Similar to Eso3 protein (predicted)	RGD1562476_predicted	−2.3
Cysteine and glycine-rich protein 2	Csrp2	−2.3
RAC/CDC42 exchange factor	Geft	−2,26947
Similar to DNA segment, Chr 8, ERATO Doi 82, expressed (predicted)	RGD1311793_predicted	−2.3
Stanniocalcin 2	Stc2	−2.2
Family with sequence similarity 3, member C	Fam3c	−2.2
Cohen syndrome homolog 1 (predicted)	Cohh1_predicted	−2.2
Guanosine monophosphate reductase	Gmpr	−2.2
Similar to RIKEN cDNA 9630046K23	RGD1306248	−2.2
Unc-51-like kinase 1	Ulk1	−2.2
DnaJ (Hsp40) homolog, subfamily A, member 4	Dnaja4	−2.2
Ephrin B1	Efnb1	−2.1
Dermatopontin (predicted)	Dpt_predicted	−2.1
Testis expressed gene 264 homolog (mouse)	Tex264	−2.1

Among 111 downregulated genes, the Brazil strain affected the “RNA processing,” “binding,” “transport,” and “cell cycle and cellular metabolic process” pathways, and 377 upregulated genes involved “RNA splicing,” “signal transduction and cellular response to stimulus,” “regulation of metabolic process,” and “protein binding.” The CL strain downregulated the expression

of 53 genes, but only nine interactions were found among 14 regulated genes, belonging to the “cellular process,” “cellular metabolic process,” “catabolic process,” and “metabolic process” categories. Regarding the 764 genes of the L6E9 cells that were upregulated by the CL, we found a total of 884 interactions that could be grouped into three main biological processes: “ribosome biogenesis,” “RNA processing,” and “cell cycle and DNA repair.” By contrast, analysis of the Tulahuen-infected samples revealed that most of the 1,144 differentially expressed genes (DEGs) were downregulated (761 genes), which formed 494 interactions. Such interactions were grouped into four main clusters: “cellular component organization,” “RNA splicing,” “protein phosphorylation,” and “cellular protein metabolic process,” each with 22, 15, 22, and 18 genes, respectively. The remaining 383 DEGs by the Tulahuen strain were all upregulated and generated 146 interactions with four main biological processes: “cellular component biogenesis,” “biological regulation and signal transduction,” “signal transduction and cellular response to stimulus,” and “cell cycle and metabolic process” (Figure 1). Finally, we analyzed the DEGs from the Y strain-infected samples. We found a total of 68 and 44 predicted interactions when looking at 150 downregulated and 276 upregulated genes, respectively. Among the biological processes found among the downregulated network, we found “signal transduction and cellular response to stimulus,” “structural molecule activity,” “regulation of cell migration,” and “macromolecule metabolic process”; and in the upregulated genes, the “cell cycle,” “response to stimulus,” “cellular protein process,” and “cellular metabolic process” were found (Figure 1).

Trypanosoma cruzi Strains Differentially Alter the Expression of JAK/STAT Signaling Pathway Members

As previously described, all four strains of *T. cruzi* induced upregulation of the *Clcf1* transcript in infected rat myoblasts by 2.2-, 2.3-, 1.8-, and 2.3-fold by the Brazil, CL, Tulahuen, and Y strains, respectively. Because this cytokine is one of the known activators of the JAK/STAT signaling pathway, we investigated whether other genes in such pathway might be altered by all four strains, which would validate JAK/STAT activation as a hallmark of *T. cruzi* infection. Using KEGG pathway database, we highlighted which genes were significantly upregulated or downregulated by each parasite strain (Figure 2). We found that the CL strain, an isolate from the southern part of Brazil (TcVI), had the highest impact on JAK/STAT signaling pathway, inducing alteration in 37% of the 30 genes detected by the arrays. The Tulahuen strain, a Chilean isolate (also TcVI), altered 30% of the genes, whereas the Brazil and Y strains showed fewer pathway elements altered (3/30:10% and 5/30: 17%, respectively). In initial steps of this signaling cascade, the Brazil and CL strains upregulated only *Clcf1* expression, whereas the Tulahuen strain also induced overexpression of IL-11 (1.7-fold), IL-21 (9.4-fold), and colony stimulating factor 3 receptor (2.3-fold). The Y strain also led to increased expression of IL-21 transcript (4.4-fold). Concerning the membrane receptors that trigger JAK/STAT signaling, we found that the Brazil and



Tulahuen strains both induced upregulation of prolactin receptor (Prlr, 3.5- and 3.9-fold, respectively). Cells infected with the CL strain showed increased expression of IL-3 (1.9-fold) and IL-21

(3.0-fold) receptors, as well as IFN- α receptor 1 (IfnaR1, 1.8-fold). The Y strain also increased the expression of IL-21 receptor (2.5-fold). Other constituents of this pathway were altered by the Y

and CL strains: PIAS4 was upregulated by 1.6- and 2.0-fold, respectively. Conversely, the Tulahuen strain downregulated expression of *protein inhibitor of STAT1 and STAT3* (PIAS1 and PIAS3) by 1.7- and 2.5-fold, respectively (Figure 2).

Distinct Modulation in Cell Cycle Pathway by *Trypanosoma cruzi* Strains

JAK/STAT pathway activation may lead to changes in cell cycle components, and one of these (*Tyrosine 3-Monooxygenase/Tryptophan 5-Monooxygenase Activation Protein Theta*; *Ywhaq*) was one of the few genes found to be upregulated by all four strains studied (Adesse et al., 2010a). In addition, three out of the four strains used in this work led to increased expression of *Cyclin D1* (*Ccnd1*), a major player in the cell cycle pathway, as has also been previously reported (Bouzahzah et al., 2008). Thus, we investigated how *T. cruzi* altered the cell cycle pathway by using KEGG templates (Figure 3), and the findings are described below.

The cell cycle pathway was most altered by the CL and Tulahuen strains showing 22% (12 of 55 analyzed spots) and 27% (15/55 spots) altered genes, respectively. The Brazil strain (TcI) and Y strain (isolated from São Paulo state, Brazil, TcII) had an impact on these two pathways, although to a lesser extent, affecting eight and five of the 55 measured genes, respectively. Specific Cell Cycle Pathway genes whose expression was altered following infection are described below.

In the Brazil strain, upregulated genes included *cyclin-dependent kinase inhibitor 1B* (*Cdkn1b*, 2.3-fold); *ATM serine/threonine kinase* (*ATM*, 2.9-fold); *checkpoint kinase 1 homolog* (*Chek1*, 2.3-fold), and *MAD2 (mitotic arrest deficient, homolog)-like 1* (*Mad2l1*, 1.8-fold). Downregulated genes include *SMAD family member 2* (*SMAD2*, -1.5-fold) and *cell division cycle 7* (*Cdc7*, -1.8-fold). Whereas the theta polypeptide of tyrosine 3-monooxygenase/tryptophan 5-monooxygenase activation protein (*Ywhaq*) was upregulated (2.9-fold), the zeta polypeptide (*Ywhaz*) was downregulated (-1.9-fold) (Figure 3A).

In the CL strain, upregulated genes included *Cyclin D1* (*CycD*, 2.0-fold), *histone deacetylase 1* (*HDAC1*, 1.6-fold), *cyclin dependent kinase 2* (*Cdk2*, 2.0-fold), *proliferating cell nuclear antigen* (*PCNA*, 1.8-fold), *growth arrest and DNA-damage-inducible beta* (*Gadd45b*, 2.1-fold), *Checkpoint kinase 1 homolog* (*Chek1*, 3.5-fold), *protein kinase, membrane associated tyrosine/threonine 1* (*Pkmyt1*, 1.8-fold), *MAD2 (mitotic arrest deficient, homolog)-like 1 (yeast)* (*Mad2l1*, 1.9-fold), *anaphase promoting complex subunit 2* (*Anapc2*, 1.8-fold), and *cell division cycle 20* (*Cdc20*, 2.9-fold). Regarding the members of the 14-3-3 complex, CL infection upregulated the *theta polypeptide* (*Ywhaq*, 2.9-fold) (Figure 3B).

The Tulahuen strain was very disruptive for cell cycle genes, with 27% significantly altered. Upregulated genes included *S-phase kinase-associated protein 1* (*Skp1a*, 2-fold),

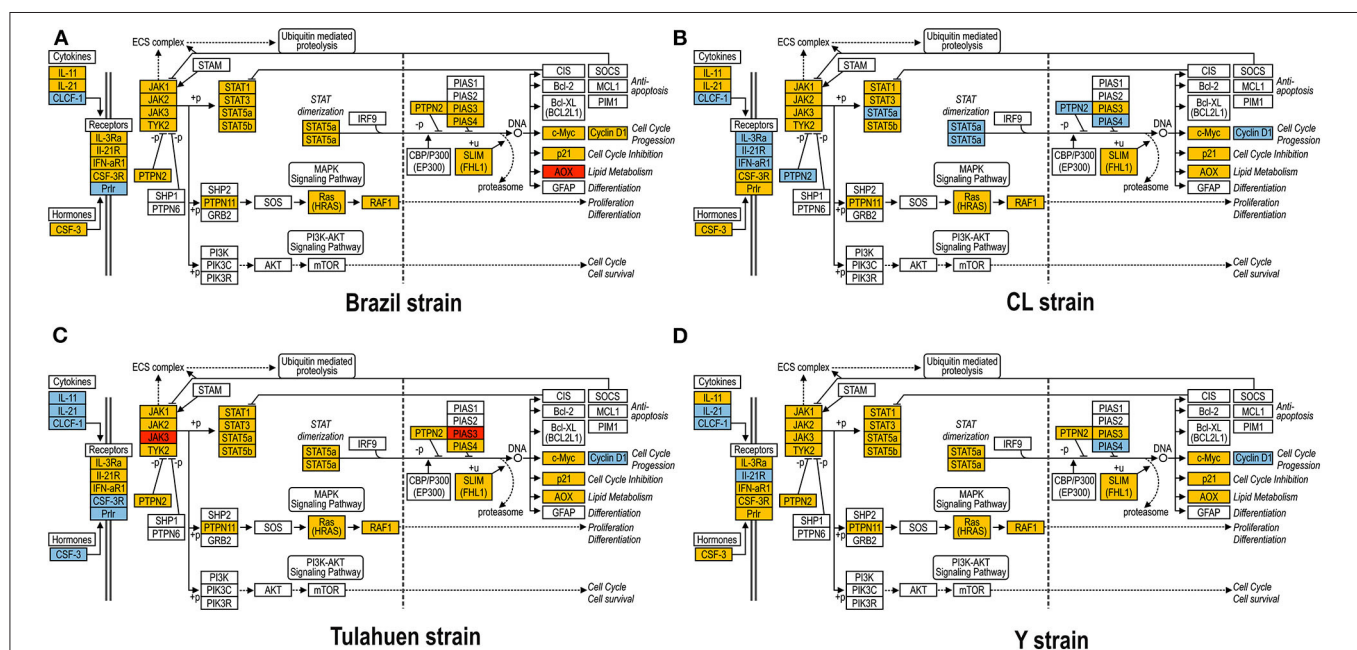
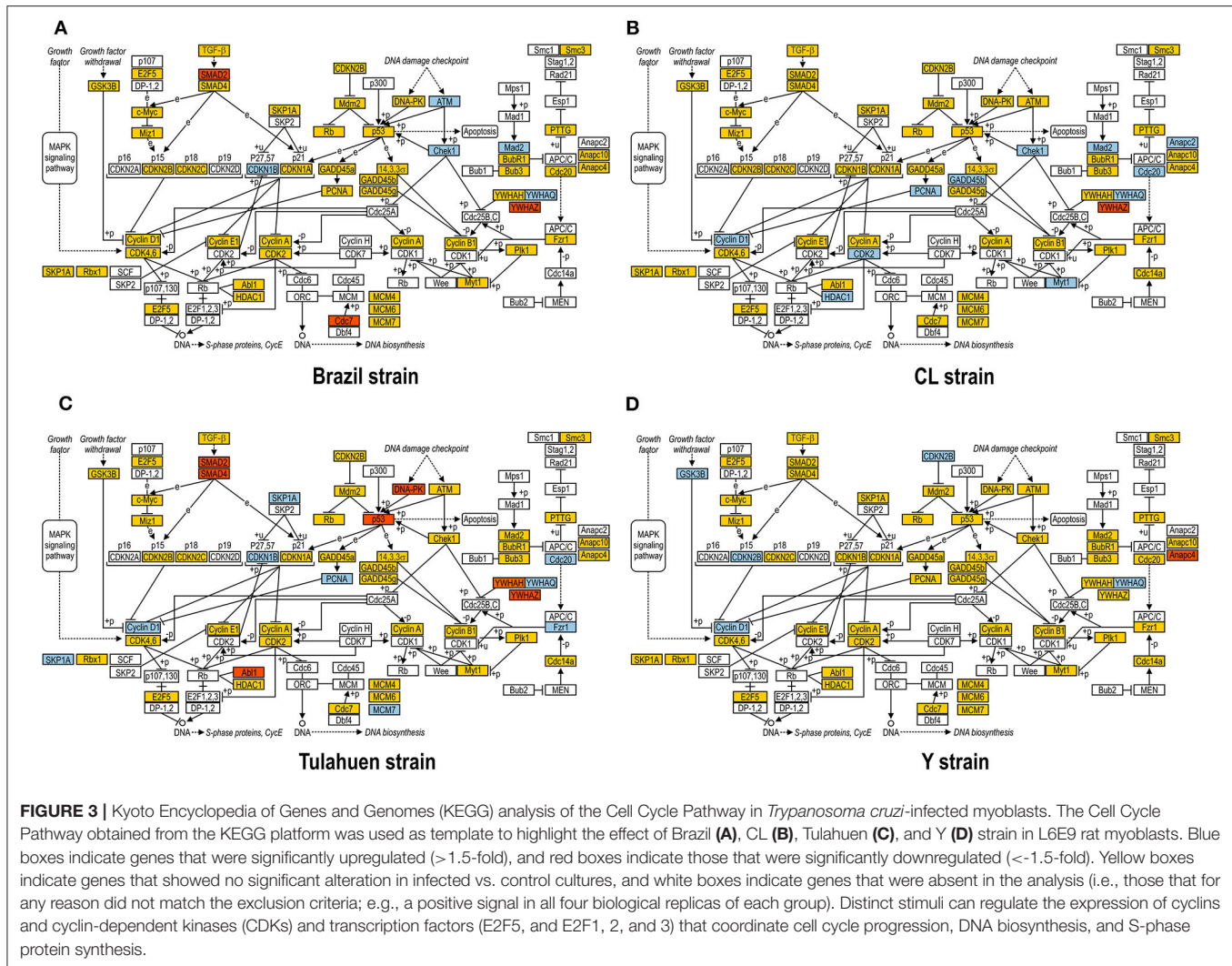


FIGURE 2 | Kyoto Encyclopedia of Genes and Genomes (KEGG) analysis of the JAK/STAT Pathway in *Trypanosoma cruzi*-infected myoblasts. The JAK/STAT Pathway obtained from the KEGG platform was used as template to highlight the effect of Brazil (A), CL (B), Tulahuen (C), and Y (D) strain in L6E9 rat myoblasts. Blue boxes indicate significant upregulation (>1.5-fold), and red boxes indicate significant downregulation (<-1.5-fold). Yellow boxes indicate genes that showed no significant alteration in infected vs. control cultures, whereas white boxes indicate genes that were absent in the analysis (i.e., those that for any reason did not match the exclusion criteria; e.g., a positive signal in all four biological replicates of each group). Extracellular ligands such as IL-6 family of cytokines bind to membrane receptors, including IL-3R and IL-21R, which in turn activate members of the JAK/STAT pathway or, alternatively, of the MAPK signaling pathway. STATs translocate to cell nucleus and activate transcription of genes that can activate cell cycle, apoptosis, or cell differentiation.



CyclinD1 (*Ccnd1*, 2-fold), cyclin-dependent kinase inhibitor 1B (*Cdkn1b*, 1.7-fold), minichromosome maintenance deficient 2 mitotin (*MCM2*, 1.5-fold), *fizzy/cell division cycle 20 related 1* (*Fzr1*, 2.3-fold), *cell division cycle 20 homolog* (*Cdc20*, 1.8-fold), *proliferating cell nuclear antigen* (*PCNA*, 1.6-fold). Downregulated genes included MAD homolog 2 (*SMAD2*, -1.9-fold), MAD homolog 4 (*SMAD4*, -1.7-fold), V-abl Abelson murine leukemia viral oncogene homolog 1 (*Abl1*, -3.3-fold), *protein kinase, DNA activated, catalytic polypeptide* (*Prkdc*, -1.8-fold), and *tumor protein p53* (*tp53*, -1.9-fold). Three members of the *tyrosine 3-monooxygenase/tryptophan 5-monooxygenase activation protein* were affected by the Tulahuen strain infection: downregulated the *eta* (*Ywhah*, -1.8-fold) and *zeta* (*Ywhaz*, -1.8-fold), and upregulated the *theta* (*Ywhaq*, 1.8-fold) (Figure 3C).

The Y strain was the least disruptive for the cell cycle pathway, leading to upregulation of *glycogen synthase kinase 3 beta* (*Gsk3b* 1.5-fold), *cyclin-dependent kinase inhibitor 2B* (*Cdkn2b*, 1.7-fold), *Ywhaq* (2.6-fold), and downregulation of *anaphase promoting complex subunit 4* (*Anapc4*, -1.6-fold) (Figure 3D).

Expression Coordination

The pathway expression analysis shown in Figures 2, 3 provides information on whether genes within a pathway are individually affected by a treatment or condition but does not indicate whether expression of genes within a pathway is coordinately expressed. To examine this issue, we used pairwise Pearson coefficients to determine whether expression differences in individual samples were correlated with one another, possibly indicating that the encoded proteins may be functionally interlinked (Spray and Iacobas, 2007, Figure 4).

From these measurements, we determined the number of gene pairs with significant pairwise Pearson correlation coefficients, with synergistic correlations shown in blue and antagonistic in red in Figures 4A,B. Graphical representation of the coordination interactions (synergistic and antagonistic) of genes in the JAK/STAT and Cell Cycle pathways are shown in Figures 4C,D, respectively.

In the non-infected control group, the JAK/STAT signaling pathway had 16 synergistic and six antagonistic coordination. Samples obtained for each of the four strains exhibited higher

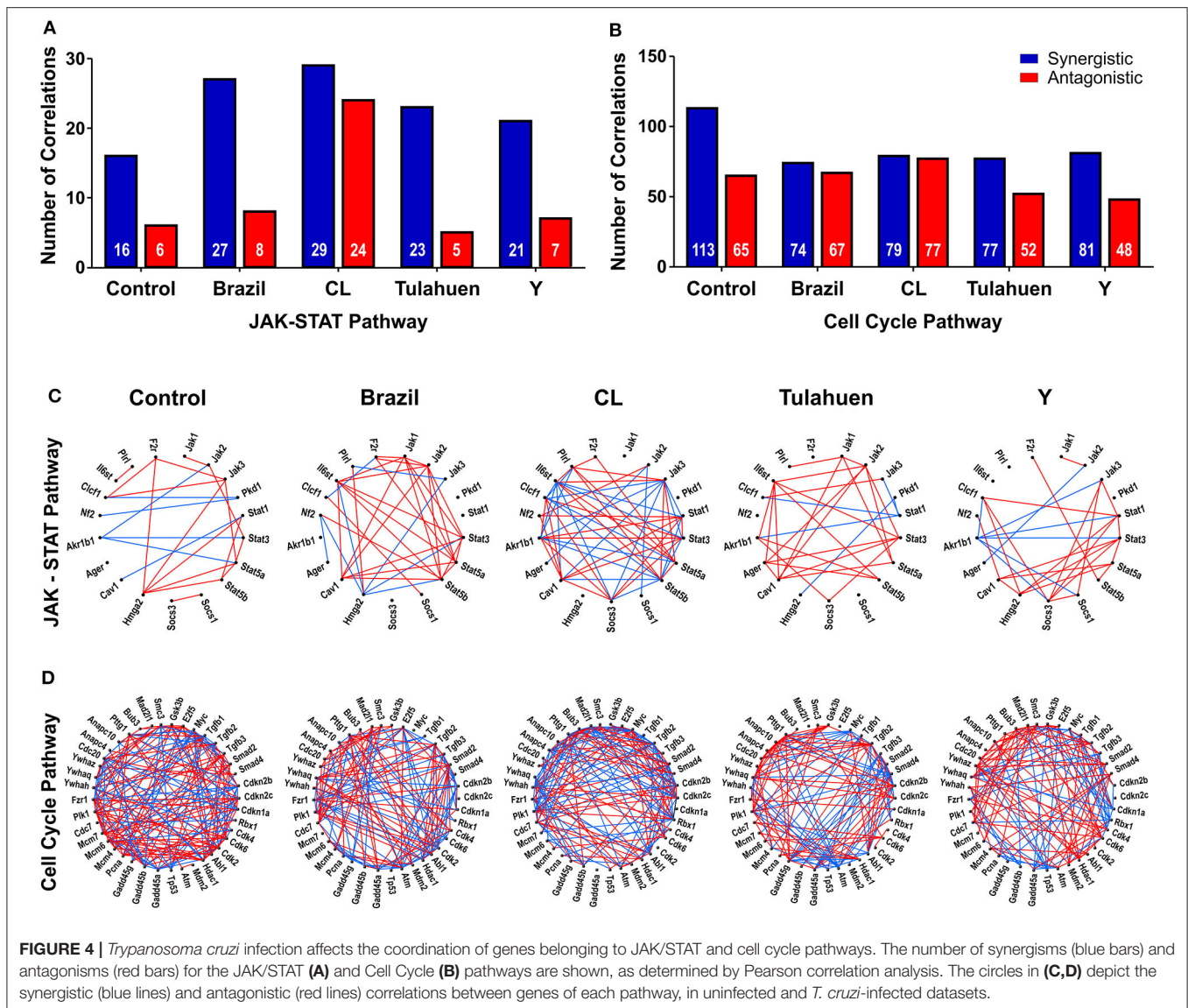


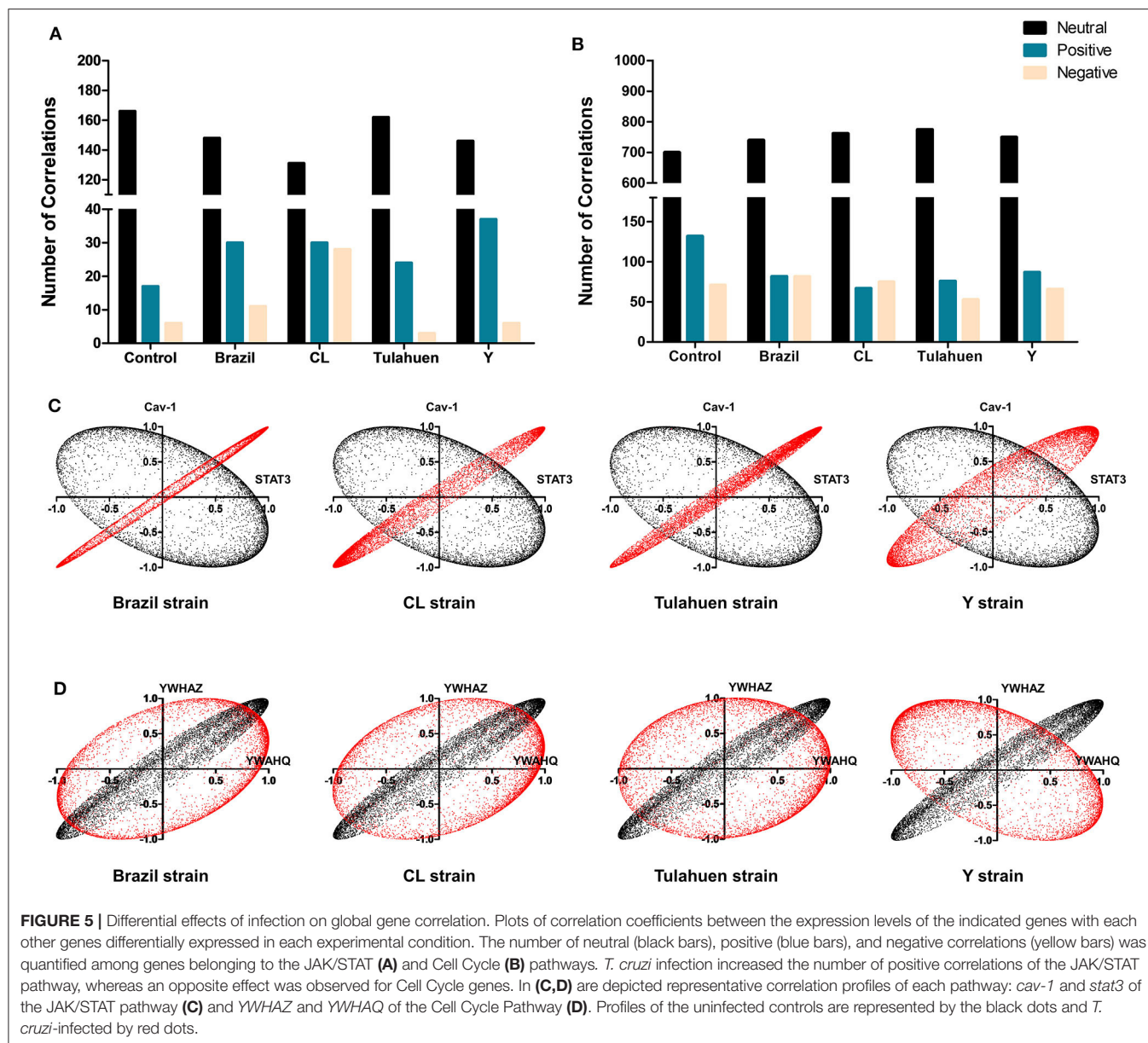
FIGURE 4 | *Trypanosoma cruzi* infection affects the coordination of genes belonging to JAK/STAT and cell cycle pathways. The number of synergisms (blue bars) and antagonisms (red bars) for the JAK/STAT (A) and Cell Cycle (B) pathways are shown, as determined by Pearson correlation analysis. The circles in (C,D) depict the synergistic (blue lines) and antagonistic (red lines) correlations between genes of each pathway, in uninfected and *T. cruzi*-infected datasets.

numbers of synergisms (27, 29, 23, and 21 for Brazil, CL, Tulahuen, and Y, respectively); antagonistic correlations for the Brazil, Tulahuen, and Y strains were similar to those of control (six antagonisms each) (Figure 4A). The CL strain induced a much higher number of antagonisms (24) (Figures 4A,C).

In the Cell Cycle Pathway, the control group showed 113 synergisms and 65 antagonisms. In contrast to what was observed in gene coordination in the JAK/STAT signaling pathway, *T. cruzi* infection by all strains resulted in fewer synergisms (ranging from 74 to 81, Figures 4B–D).

Additionally, we determined whether infection by each of the *T. cruzi* strains altered the number of correlations of the JAK/STAT (Figure 5A) and Cell Cycle genes (Figure 5B) with all other genes quantified on the arrays. Overall, the number of neutral correlations was fairly constant for genes in both pathways, and negative correlations were similar except for a larger number in the CL genes in the JAK/STAT pathway. By

contrast, the number of positive associations was higher in all infected than uninfected groups for JAK/STAT and lower in all infected groups for the Cell Cycle Pathway. To illustrate the effect that *T. cruzi* infection had on coordination between members of the JAK/STAT pathway, we show in Figure 5C the coordination profile between STAT3 and caveolin-1. In the control condition (shown in black), these two genes had a neutral profile (corresponding to a broad ellipse covering all quadrants of the graph), which was altered to a variably narrow but significantly positive profile in each of the infected conditions (shown in red). An example of conversion of a coordination of Cell Cycle genes from a positive coordination under control conditions to a neutral profile in infected cells is shown in Figure 5D. Uninfected cultures displayed a positive profile (black dots) for the *Ywhaq* and *Ywhaz* pair of genes. In infected samples from each strain (shown in red), the coordination changed to a neutral profile.



DISCUSSION

Trypanosoma cruzi infection results in CD that has different clinical forms that include asymptomatic, cardiac, digestive, and neurological features (WHO, 2019). These diverse outcomes may be related to the environment, host, and parasite genetic variability (Lewis et al., 2016) and by a combination of all these variables. *T. cruzi* genetic isolates are currently divided into six DTUs according to genetic, biochemical, and/or biological markers (Zingales et al., 2009); and strains from TcII, TcV, or TcVI were associated with chronic infection (Zingales, 2018). Here, we reanalyzed data from a previously published transcriptomic profiling of the infection of rat myoblasts by four *T. cruzi* strains, in order to further understand the impact that infection has on JAK/STAT signaling and cell

cycle pathways and to understand the different outcomes of infection.

One of the few genes showing increased expression increased by all four strains of *T. cruzi* was *Clcf1* (Adesse et al., 2010a). CLCF1 belongs to the IL-6 cytokine family that includes IL-6, IL-11, ciliary neurotrophic factor (CNTF), leukemia inhibitory factor (LIF), oncostatin M (OSM), cardiotrophin 1 (CT-1), and IL-27.

Cytokines and growth factors commonly mediate their actions through the JAK/STAT pathway, which is associated with such cellular functions as inflammation, apoptosis, and cell-cycle control (Barry et al., 2007). IL-6 and IL-10 induce STAT3 activity (Barry et al., 2007). In Tulahuen strain infection, IL-6/pSTAT3 protects cardiomyocytes through upregulation of anti-apoptotic factor Bcl-2 (Ponce et al., 2012), thus maintaining

the survival of the host cell that is beneficial for parasite persistence. IL-10/STAT3 signaling induces the SOCS-3 gene reducing tissue damage inducers such as pro-inflammatory factors nitric oxide synthase (NOS2) and tumor necrosis factor (TNF)- α in *T. cruzi* RA strain-infected cardiomyocytes culture (Hovsepian et al., 2013).

IFNs activate predominantly STAT1 and STAT2 (Barry et al., 2007). IFN γ /STAT1 signaling protected fibroblasts against CL Brener and Y infection by inhibition of amastigote growth (Stahl et al., 2014) that could explain the higher *T. cruzi* (Brazil strain) replication and dissemination in STAT1 knockout mice (Kulkarni et al., 2015). Interestingly, infection of STAT6- but not STAT4-knockout mice with this same (Brazil) strain resulted in decreased parasitemia, inflammation, and mortality when compared with wild-type mice (Tarleton et al., 2000). Therefore, different ways of modulating this pathway may induce different clinical aspects of the infection.

Our results showed that three out of four isolates of *T. cruzi* that were tested had nodules of predicted PPI of Cell Cycle process within their upregulated genes and that one (Brazil) had such interactions among the downregulated genes. Regarding the pairwise coordination profiling of genes belonging to the cell cycle pathway, we verified an overall reduction of synergistic interactions induced by all four strains. Accordingly, infection of L6E9 myoblasts by the Brazil strain led to no significant alteration of cyclin D1 promoter activity or cyclin D1 protein stability in infected cultures (Bouzahzah et al., 2008).

It is well-documented that *T. cruzi* affects host cell proliferation (Bouzahzah et al., 2006; Droguett et al., 2017; Duran-Rehbein et al., 2017). Curiously, one work that utilized the Y strain of *T. cruzi* showed that late mitotic genes were downregulated in infected cultures of vascular smooth muscle cells and fibroblasts (Costales et al., 2009), indicating defects in cytokinesis. This finding reinforces the fact that host cell or even host animal background plays a complimentary role on the course of infection. This seems to be the case of vascular smooth cells that were shown to have increased proliferation when infected by the Tulahuen strain of this parasite (Hassan et al., 2006).

Interestingly, our study showed that infected cultures had a decrease in the number of neutral correlations in JAK/STAT-related genes and an increase in the number of positive profiles. We exemplified this phenomenon with the correlation of caveolin-1 and STAT3. Caveolins are implicated in transcytosis of macromolecules, cholesterol transport, and signal transduction (Li et al., 2005). Knockout mice for caveolin-1, caveolin-2, and caveolin-3 develop hypertrophic cardiomyopathy with increase in fibrosis (Park et al., 2002; Cohen et al., 2003; Augustus et al., 2008). Experimental CD in mice also affects caveolins (Adesse et al., 2010b), with subsequent activation of MAPK signaling pathways (Huang et al., 2003), thus leading to remodeling of heart tissue.

The tyrosine 3-monooxygenase/tryptophan 5-monooxygenase activation proteins are a family of molecular chaperones commonly referred to as 14-3-3 proteins. The family consists of seven transcripts in mammals: 14-3-3 β (YWHAB),

14-3-3 γ (YWHAG), 14-3-3 ϵ (YWHAH), 14-3-3 ζ (YWHAZ), 14-3-3 η (YWHAH), 14-3-3 θ (YWHAQ), and 14-3-3 σ also known as stratifin (SFN) (MacKay et al., 2011). YWHAH for instance has a well-established cardioprotective role in cases of cardiac overload. Mice with a dominant mutation in 14-3-3 proteins display reduced survival, left ventricular fraction, and fraction shortening (Thandavarayan et al., 2011; Sreedhar et al., 2016). The fact that 14-3-3 transcripts are altered in myoblasts infected with *T. cruzi* reinforces the idea that 14-3-3 proteins may contribute to cardiomyocyte apoptosis, inflammation, fibrosis, and hypertrophy observed in cardiac forms of Chagas chronic disease.

In summary, the bioinformatic tools used in this work allowed the further description of the differential impact of *T. cruzi* genetic background on host cell transcriptome, as a good predictor of biological outcomes. Although *Clcf-1* and *Ywhaq* were equally altered in the infected L6E9 cells, their network ensemble was in fact composed of different transcripts, which may lead to variations in the degrees of activations in these molecular pathways. These observations are important to deepen the understanding of how CD can present multiple pathologies, according to parasite background, combined with host diversity and environmental aspects. Such variability should be taken in consideration when proposing chemotherapeutic or immunomodulatory approaches to control of this disease.

DATA AVAILABILITY STATEMENT

The raw datasets generated in this study can be found in NCBI, accession number GSE18175.

AUTHOR CONTRIBUTIONS

DA, LG, DS, HT, and DI conceptualized the study. DA, DI, and DS contributed to methodology, resources, and funding acquisition. PCV, PHV, LN, TM, and LC helped with the validation. SI, DI, and TM did the formal analysis. DA, LN, PCV, PHV, LC, and TM carried out the investigation. DA and LN contributed to data curation and writing the original draft. DA, LG, DS, and DI wrote, reviewed, and edited the manuscript. DA was responsible for the visualization and project administration. DA, DI, DS, and HT supervised the study. All authors contributed to the article and approved the submitted version.

FUNDING

This work was supported by Conselho Nacional de Pesquisa e Desenvolvimento Tecnológico (CNPq, grant Numbers: 401772/2015-2 and 444478/2014-0) and Fundação Oswaldo Cruz (Fiocruz), through the INOVA Fiocruz program, grant number 3231984391 for DA. DI was supported by the Chancellor's Research Initiative (CRI) funding for the Center for Computational Systems Biology at the Prairie View A&M University. DS was supported by NIH grant number NS092466.

ACKNOWLEDGMENTS

The authors thank Mrs. Heloisa Diniz from the Department of Image Production and Processing (Serviço de Produção e Tratamento de Imagem—IOC) at the Oswaldo Cruz Institute for help in generating the schematic images presented in **Figures 1–4**. They also thank Dr. Helene Santos Barbosa (Laboratory of Structural Biology, IOC) for providing equipment, laboratory facility, and some reagents.

REFERENCES

- Adesse, D., Goldenberg, R. C., Fortes, F. S., Iacobas, D. A., Iacobas, S., Huang, H., et al. (2011). Gap junctions and chagas disease. *Adv. Parasitol.* 76, 63–81. doi: 10.1016/B978-0-12-385895-5.00003-7
- Adesse, D., Iacobas, D. A., Iacobas, S., Garzoni, L. R., Meirelles Mde, N., Tanowitz, H. B., et al. (2010a). Transcriptomic signatures of alterations in a myoblast cell line infected with four distinct strains of *Trypanosoma cruzi*. *Am. J. Trop. Med. Hyg.* 82, 846–854. doi: 10.4269/ajtmh.2010.09-0399
- Adesse, D., Lisanti, M. P., Spray, D. C., Machado, F. S., Meirelles Mde, N., Tanowitz, H. B., et al. (2010b). *Trypanosoma cruzi* infection results in the reduced expression of caveolin-3 in the heart. *Cell Cycle* 9, 1639–1646. doi: 10.4161/cc.9.8.11509
- Andrade, S. G., and Magalhaes, J. B. (1997). Biodemes and zymodemes of *Trypanosoma cruzi* strains: correlations with clinical data and experimental pathology. *Rev. Soc. Bras. Med. Trop.* 30, 27–35. doi: 10.1590/S0037-86821997000100006
- Augustus, A. S., Buchanan, J., Gutman, E., Rengo, G., Pestell, R. G., Fortina, P., et al. (2008). Hearts lacking caveolin-1 develop hypertrophy with normal cardiac substrate metabolism. *Cell Cycle* 7, 2509–2518. doi: 10.4161/cc.7.16.6421
- Barry, S. P., Townsend, P. A., Latchman, D. S., and Stephanou, A. (2007). Role of the JAK-STAT pathway in myocardial injury. *Trends Mol. Med.* 13, 82–89. doi: 10.1016/j.molmed.2006.12.002
- Bouzahzah, B., Nagajyothi, F., Desruisseaux, M. S., Krishnamachary, M., Factor, S. M., Cohen, A. W., et al. (2006). Cell cycle regulatory proteins in the liver in murine *Trypanosoma cruzi* infection. *Cell Cycle* 5, 2396–2400. doi: 10.4161/cc.5.20.3380
- Bouzahzah, B., Yurchenko, V., Nagajyothi, F., Hulit, J., Sadofsky, M., Braunstein, V. L., et al. (2008). Regulation of host cell cyclin D1 by *Trypanosoma cruzi* in myoblasts. *Cell Cycle* 7, 500–503. doi: 10.4161/cc.7.4.5327
- Chandrasekar, B., Melby, P. C., Pennica, D., and Freeman, G. L. (1998). Overexpression of cardiotrophin-1 and gp130 during experimental acute chagasic cardiomyopathy. *Immunol. Lett.* 61, 89–95. doi: 10.1016/S0165-2478(97)00167-3
- Cohen, A. W., Park, D. S., Woodman, S. E., Williams, T. M., Chandra, M., Shirani, J., et al. (2003). Caveolin-1 null mice develop cardiac hypertrophy with hyperactivation of p42/44 MAP kinase in cardiac fibroblasts. *Am. J. Physiol. Cell Physiol.* 284, C457–474. doi: 10.1152/ajpcell.00380.2002
- Consitt, L. A., Wideman, L., Hickey, M. S., and Morrison, R. F. (2008). Phosphorylation of the JAK2-STAT5 pathway in response to acute aerobic exercise. *Med. Sci. Sports Exerc.* 40, 1031–1038. doi: 10.1249/MSS.0b013e3181690760
- Costales, J. A., Daily, J. P., and Burleigh, B. A. (2009). Cytokine-dependent and-independent gene expression changes and cell cycle block revealed in *Trypanosoma cruzi*-infected host cells by comparative mRNA profiling. *BMC Genomics* 10:252. doi: 10.1186/1471-2164-10-252
- de Souza, E. M., Araujo-Jorge, T. C., Bailly, C., Lansiaux, A., Batista, M. M., Oliveira, G. M., et al. (2003). Host and parasite apoptosis following *Trypanosoma cruzi* infection in *in vitro* and *in vivo* models. *Cell Tissue Res.* 314, 223–235. doi: 10.1007/s00441-003-0782-5
- Droguett, D., Carrillo, I., Castillo, C., Gomez, F., Negrete, M., Liempi, A., et al. (2017). *Trypanosoma cruzi* induces cellular proliferation in the trophoblastic

SUPPLEMENTARY MATERIAL

The Supplementary Material for this article can be found online at: <https://www.frontiersin.org/articles/10.3389/fcimb.2020.00255/full#supplementary-material>

Supplementary Figure 1 | Examples of genes synergistically (*Antxr1* = ANTXR cell adhesion molecule 1), antagonistically (*Dus3l* = dihydrouridine synthase 3-like), and independently (*Golim4* = golgi integral membrane protein 4) expressed genes with *Cicf1* (cardiotrophin-like cytokine factor 1) in control L6E9 rat myoblasts. Numbers in brackets are the Pearson correlation coefficients.

- cell line BeWo. *Exp. Parasitol.* 173, 9–17. doi: 10.1016/j.exppara.2016.12.005
- Duran-Rehbein, G. A., Vargas-Zambrano, J. C., Cuellar, A., Puerta, C. J., and Gonzalez, J. M. (2017). Induction of cellular proliferation in a human astrocytoma cell line by a *Trypanosoma cruzi*-derived antigen: a mechanism of pathogenesis? *Cell. Mol. Biol.* 63, 23–27. doi: 10.14715/cmb/2017.63.1.5
- Goldenberg, R. C., Iacobas, D. A., Iacobas, S., Rocha, L. L., da Silva de Azevedo Fortes, F., Vairo, L., et al. (2009). Transcriptomic alterations in *Trypanosoma cruzi*-infected cardiac myocytes. *Microbes Infect.* 11, 1140–1149. doi: 10.1016/j.micinf.2009.08.009
- Gorshkova, E. A., Nedospasov, S. A., and Shilov, E. S. (2016). Evolutionary plasticity of IL-6 cytokine family. *Mol. Biol.* 50, 918–926. doi: 10.1134/S0026893316060066
- Hassan, G. S., Mukherjee, S., Nagajyothi, F., Weiss, L. M., Petkova, S. B., de Almeida, C. J., et al. (2006). *Trypanosoma cruzi* infection induces proliferation of vascular smooth muscle cells. *Infect. Immun.* 74, 152–159. doi: 10.1128/IAI.74.1.152-159.2006
- Hovsepian, E., Penas, F., Siffo, S., Mirkin, G. A., and Goren, N. B. (2013). IL-10 inhibits the NF-kappaB and ERK/MAPK-mediated production of pro-inflammatory mediators by up-regulation of SOCS-3 in *Trypanosoma cruzi*-infected cardiomyocytes. *PLoS ONE* 8:e79445. doi: 10.1371/journal.pone.0079445
- Huang, H., Petkova, S. B., Cohen, A. W., Bouzahzah, B., Chan, J., Zhou, J. N., et al. (2003). Activation of transcription factors AP-1 and NF-kappa B in murine chagasic myocarditis. *Infect. Immun.* 71, 2859–2867. doi: 10.1128/IAI.71.5.2859-2867.2003
- Iacobas, D. A., Fan, C., Iacobas, S., and Haddad, G. G. (2008a). Integrated transcriptomic response to cardiac chronic hypoxia: translation regulators and response to stress in cell survival. *Funct. Integr. Genomics* 8, 265–275. doi: 10.1007/s10142-008-0082-y
- Iacobas, D. A., Iacobas, S., and Spray, D. C. (2007a). Connexin43 and the brain transcriptome of newborn mice. *Genomics* 89, 113–123. doi: 10.1016/j.ygeno.2006.09.007
- Iacobas, D. A., Iacobas, S., and Spray, D. C. (2007b). Connexin-dependent transcellular transcriptomic networks in mouse brain. *Prog. Biophys. Mol. Biol.* 94, 169–185. doi: 10.1016/j.pbiomolbio.2007.03.015
- Iacobas, D. A., Iacobas, S., Urban-Maldonado, M., Scemes, E., and Spray, D. C. (2008b). Similar transcriptomic alterations in Cx43 knockdown and knockout astrocytes. *Cell Commun. Adhes.* 15, 195–206. doi: 10.1080/15419060802014222
- Kulkarni, M. M., Varikuti, S., Terrazas, C., Kimble, J. L., Satoskar, A. R., and McGwire, B. S. (2015). Signal transducer and activator of transcription 1 (STAT-1) plays a critical role in control of *Trypanosoma cruzi* infection. *Immunology* 145, 225–231. doi: 10.1111/imm.12438
- Kunisada, K., Tone, E., Fujio, Y., Matsui, H., Yamauchi-Takahara, K., and Kishimoto, T. (1998). Activation of gp130 transduces hypertrophic signals via STAT3 in cardiac myocytes. *Circulation* 98, 346–352. doi: 10.1161/01.CIR.98.4.346
- Kutmon, M., van Iersel, M. P., Bohler, A., Kelder, T., Nuner, N., Pico, A. R., et al. (2015). PathVisio 3: an extendable pathway analysis toolbox. *PLoS Comput. Biol.* 11:e1004085. doi: 10.1371/journal.pcbi.1004085

- Latchman, D. S. (1999). Cardiotrophin-1 (CT-1): a novel hypertrophic and cardioprotective agent. *Int. J. Exp. Pathol.* 80, 189–196. doi: 10.1046/j.1365-2613.1999.00114.x
- Lewis, M. D., Francisco, A. F., Taylor, M. C., Jayawardhana, S., and Kelly, J. M. (2016). Host and parasite genetics shape a link between *Trypanosoma cruzi* infection dynamics and chronic cardiomyopathy. *Cell. Microbiol.* 18, 1429–1443. doi: 10.1111/cmi.12584
- Li, J., Scherl, A., Medina, F., Frank, P. G., Kitsis, R. N., Tanowitz, H. B., et al. (2005). Impaired phagocytosis in caveolin-1 deficient macrophages. *Cell Cycle* 4, 1599–1607. doi: 10.4161/cc.4.11.2117
- MacKay, R. K., Colson, N. J., Dodd, P. R., and Lewohl, J. M. (2011). Differential expression of 14-3-3 isoforms in human alcoholic brain. *Alcohol. Clin. Exp. Res.* 35, 1041–1049. doi: 10.1111/j.1530-0277.2011.01436.x
- Monserat, L., Lopez, B., Gonzalez, A., Hermida, M., Fernandez, X., Ortiz, M., et al. (2011). Cardiotrophin-1 plasma levels are associated with the severity of hypertrophy in hypertrophic cardiomyopathy. *Eur. Heart J.* 32, 177–183. doi: 10.1093/eurheartj/ehq400
- Mukherjee, S., Belbin, T. J., Spray, D. C., Iacobas, D. A., Weiss, L. M., Kitsis, R. N., et al. (2003). Microarray analysis of changes in gene expression in a murine model of chronic chagasic cardiomyopathy. *Parasitol. Res.* 91, 187–196. doi: 10.1007/s00436-003-0937-z
- Park, D. S., Woodman, S. E., Schubert, W., Cohen, A. W., Frank, P. G., Chandra, M., et al. (2002). Caveolin-1/3 double-knockout mice are viable, but lack both muscle and non-muscle caveolae, and develop a severe cardiomyopathic phenotype. *Am. J. Pathol.* 160, 2207–2217. doi: 10.1016/S0002-9440(10)61168-6
- Ponce, N. E., Cano, R. C., Carrera-Silva, E. A., Lima, A. P., Gea, S., and Aoki, M. P. (2012). Toll-like receptor-2 and interleukin-6 mediate cardiomyocyte protection from apoptosis during *Trypanosoma cruzi* murine infection. *Med. Microbiol. Immunol.* 201, 145–155. doi: 10.1007/s00430-011-0216-z
- Ponce, N. E., Carrera-Silva, E. A., Pellegrini, A. V., Cazorla, S. I., Malchiodi, E. L., Lima, A. P., et al. (2013). *Trypanosoma cruzi*, the causative agent of Chagas disease, modulates interleukin-6-induced STAT3 phosphorylation via gp130 cleavage in different host cells. *Biochim. Biophys. Acta* 1832, 485–494. doi: 10.1016/j.bbdis.2012.12.003
- Rassi, A. Jr., Rassi, A., and Marcondes de Rezende, J. (2012). American trypanosomiasis (Chagas disease). *Infect. Dis. Clin. North Am.* 26, 275–291. doi: 10.1016/j.idc.2012.03.002
- Rassi, A. Jr., Rassi, A., and Marin-Neto, J. A. (2010). Chagas disease. *Lancet* 375, 1388–1402. doi: 10.1016/S0140-6736(10)60061-X
- Sheng, Z., Pennica, D., Wood, W. I., and Chien, K. R. (1996). Cardiotrophin-1 displays early expression in the murine heart tube and promotes cardiac myocyte survival. *Development* 122, 419–428.
- Soares, M. B., de Lima, R. S., Rocha, L. L., Vasconcelos, J. F., Rogatto, S. R., dos Santos, R. R., et al. (2010). Gene expression changes associated with myocarditis and fibrosis in hearts of mice with chronic chagasic cardiomyopathy. *J. Infect. Dis.* 202, 416–426. doi: 10.1086/653481
- Song, K., Wang, S., Huang, B., Luciano, A., Srivastava, R., and Mani, A. (2014). Plasma cardiotrophin-1 levels are associated with hypertensive heart disease: a meta-analysis. *J. Clin. Hypertens.* 16, 686–692. doi: 10.1111/jch.12376
- Sorensen, J. R., Fuqua, J. D., Deyhle, M. R., Parmley, J., Skousen, C., Hancock, C., et al. (2018). Preclinical characterization of the JAK/STAT inhibitor SGI-1252 on skeletal muscle function, morphology, and satellite cell content. *PLoS ONE* 13:e0198611. doi: 10.1371/journal.pone.0198611
- Spray, D. C., and Iacobas, D. A. (2007). Organizational principles of the connexin-related brain transcriptome. *J. Membr. Biol.* 218, 39–47. doi: 10.1007/s00232-007-9049-5
- Sreedhar, R., Arumugam, S., Thandavarayan, R. A., Giridharan, V. V., Karuppagounder, V., Pitchaimani, V., et al. (2016). Depletion of cardiac 14-3-3 β protein adversely influences pathologic cardiac remodeling during myocardial infarction after coronary artery ligation in mice. *Int. J. Cardiol.* 202, 146–153. doi: 10.1016/j.ijcard.2015.08.142
- Stahl, P., Ruppert, V., Meyer, T., Schmidt, J., Campos, M. A., Gazzinelli, R. T., et al. (2013). Trypomastigotes and amastigotes of *Trypanosoma cruzi* induce apoptosis and STAT3 activation in cardiomyocytes *in vitro*. *Apoptosis* 18, 653–663. doi: 10.1007/s10495-013-0822-x
- Stahl, P., Ruppert, V., Schwarz, R. T., and Meyer, T. (2014). *Trypanosoma cruzi* evades the protective role of interferon-gamma-signaling in parasite-infected cells. *PLoS ONE* 9:e110512. doi: 10.1371/journal.pone.0110512
- Steyn, P. J., Dzobo, K., Smith, R. I., and Myburgh, K. H. (2019). Interleukin-6 induces myogenic differentiation via JAK2-STAT3 signaling in mouse C2C12 myoblast cell line and primary human myoblasts. *Int. J. Mol. Sci.* 20:E5273. doi: 10.3390/ijms20215273
- Sun, L., Ma, K., Wang, H., Xiao, F., Gao, Y., Zhang, W., et al. (2007). JAK1-STAT1-STAT3, a key pathway promoting proliferation and preventing premature differentiation of myoblasts. *J. Cell Biol.* 179, 129–138. doi: 10.1083/jcb.200703184
- Tarleton, R. L., Grusby, M. J., and Zhang, L. (2000). Increased susceptibility of Stat4-deficient and enhanced resistance in Stat6-deficient mice to infection with *Trypanosoma cruzi*. *J. Immunol.* 165, 1520–1525. doi: 10.4049/jimmunol.165.3.1520
- Thandavarayan, R. A., Giridharan, V. V., Sari, F. R., Arumugam, S., Veeraveedu, P. T., Pandian, G. N., et al. (2011). Depletion of 14-3-3 protein exacerbates cardiac oxidative stress, inflammation and remodeling process via modulation of MAPK/NF- κ B signaling pathways after streptozotocin-induced diabetes mellitus. *Cell. Physiol. Biochem.* 28, 911–922. doi: 10.1159/000335805
- WHO (2019). *Chagas' Disease (American trypanosomiasis) Factsheet*. Available online at: <http://www.who.int/mediacentre/factsheets/fs340/en/index.html> (accessed March 11, 2020).
- Zingales, B. (2018). *Trypanosoma cruzi* genetic diversity: something new for something known about Chagas disease manifestations, serodiagnosis and drug sensitivity. *Acta Trop.* 184, 38–52. doi: 10.1016/j.actatropica.2017.09.017
- Zingales, B., Andrade, S. G., Briones, M. R., Campbell, D. A., Chiari, E., Fernandes, O., et al. (2009). A new consensus for *Trypanosoma cruzi* intraspecific nomenclature: second revision meeting recommends TcI to TcVI. *Mem. Inst. Oswaldo Cruz* 104, 1051–1054. doi: 10.1590/S0074-02762009000700021
- Zingales, B., Miles, M. A., Campbell, D. A., Tibayrenc, M., Macedo, A. M., Teixeira, M. M., et al. (2012). The revised *Trypanosoma cruzi* subspecific nomenclature: rationale, epidemiological relevance and research applications. *Infect. Genet. Evol.* 12, 240–253. doi: 10.1016/j.meegid.2011.12.009
- Zong, C. S., Chan, J., Levy, D. E., Horvath, C., Sadowski, H. B., and Wang, L. H. (2000). Mechanism of STAT3 activation by insulin-like growth factor I receptor. *J. Biol. Chem.* 275, 15099–15105. doi: 10.1074/jbc.M000089200

Conflict of Interest: The authors declare that the research was conducted in the absence of any commercial or financial relationships that could be construed as a potential conflict of interest.

Copyright © 2020 Nisimura, Coelho, de Melo, Vieira, Victorino, Garzoni, Spray, Iacobas, Iacobas, Tanowitz and Adesse. This is an open-access article distributed under the terms of the Creative Commons Attribution License (CC BY). The use, distribution or reproduction in other forums is permitted, provided the original author(s) and the copyright owner(s) are credited and that the original publication in this journal is cited, in accordance with accepted academic practice. No use, distribution or reproduction is permitted which does not comply with these terms.

Advantages of publishing in Frontiers



OPEN ACCESS

Articles are free to read
for greatest visibility
and readership



FAST PUBLICATION

Around 90 days
from submission
to decision



HIGH QUALITY PEER-REVIEW

Rigorous, collaborative,
and constructive
peer-review



TRANSPARENT PEER-REVIEW

Editors and reviewers
acknowledged by name
on published articles

Frontiers

Avenue du Tribunal-Fédéral 34
1005 Lausanne | Switzerland

Visit us: www.frontiersin.org

Contact us: info@frontiersin.org | +41 21 510 17 00



REPRODUCIBILITY OF RESEARCH

Support open data
and methods to enhance
research reproducibility



DIGITAL PUBLISHING

Articles designed
for optimal readership
across devices



FOLLOW US

@frontiersin



IMPACT METRICS

Advanced article metrics
track visibility across
digital media



EXTENSIVE PROMOTION

Marketing
and promotion
of impactful research



LOOP RESEARCH NETWORK

Our network
increases your
article's readership